

**Approaches to pseudotype DNA and RNA viruses
of veterinary interest for use as tools in cell
tropism and immune response studies**

By CECILIA DI GENOVA

A thesis submitted in partial fulfilment of the
requirements of the University of Kent and the
University of Greenwich for the Degree of
Doctor of Philosophy in the subject of
Pharmacy

Medway School of Pharmacy
Universities of Kent and Greenwich at Medway
Central Avenue, Chatham, Kent, ME4 4TB

MARCH 2022

DECLARATION

I certify that this work has not been accepted in substance for any degree, and is not concurrently being submitted for any degree other than that of the Doctor of Philosophy being studied at the Universities of Greenwich and Kent. I also declare that this work is the result of my own investigations except where otherwise identified by references and that I have not plagiarised the work of others.

PhD Student ----- Cecilia Di Genova

----- Date

PhD Supervisor ----- Simon Scott

----- Date

Ai miei genitori,

le mie colonne.

ACKNOWLEDGMENTS

I would like to extend my gratitude to my supervisors, Dr. Simon Scott and Dr. Nigel Temperton, for the learning experience and guidance during my PhD to become a better scientist. And to believe I could stepover to become a postdoc during the first wave of pandemic.

To Dr. Stéphane Pronost who warmly welcomed me in his laboratory at LABÉO, and for the exciting projects I could investigate under his supervision. And to Dr. Romain Paillot for the collaboration, ideas and discussions.

To the real postdocs: Kelly, Joanne, Diego, Martin and Dips, who I admired for their frenetic pace but always there to give precious advice.

To the *Norman* experience which gave a hint to my PhD life: Gabrielle for the help to settle into the lab and the friendship, Erika for the patience and *les mesdames* of the office, Camille and Flora and the other PhD students at LABÉO.

To Alessia, Giulia and Miguel with whom I have shared this very wavy journey since the start.

To Aiste for the kindness and the “last of us” of the PhD office for the smiles: Stephanie and Maria.

To Luke with whom the future holds something great.

Finally, to my parents, who I dedicate this work, for the constant support and understanding during the hard times despite the long way home.

ABSTRACT

Pseudotype viruses (PVs) provide an alternative platform to wild type viruses since they mimic their receptor binding and entry processes and are able to interact with the host immune response. For this thesis, a PV system was developed to conduct experimental research on a DNA and RNA viruses of veterinary interest.

Equid herpesvirus 1 (EHV-1) is a DNA virus of the *Herpesviridae* family representing a significant welfare issue in horses and a great impact on the equine industry. EHV-1 entry mechanism is complicated by the presence of twelve glycoproteins on the viral envelope. To investigate EHV-1 entry, a simplified lentiviral PV system was generated including gB, gD, gH and gL able to transduce target cell lines demonstrating that the four essential entry glycoproteins of EHV-1 are not only required but also sufficient for cell entry. Successful generation of an EHV-1 PV permitted the development of a PV neutralisation assay (PVNA). Feasibility of the PVNA was first tested by measuring the level of neutralising antibodies in EHV-1 experimentally infected horses in a longitudinal manner and secondly by detecting an immune response in vaccinated horses. The performance of the assay was compared with a conventional EHV-1 virus neutralisation (VN) assay, showing a good correlation.

Furthermore, PVs routinely require -80°C for long term storage and a dry ice cold-chain during transport which can impede dissemination and utilisation in other laboratories. Consequently, freeze-drying (lyophilisation) of EHV-1 PVs was investigated to address this issue. PVs were lyophilised and pellets either reconstituted immediately or stored under various temperature conditions at different timepoints. The recovery and functionality of these lyophilised PVs was compared with standard frozen aliquots in titration and neutralisation tests.

Influenza viruses are RNA viruses of the *Orthomyxoviridae* family and some novel Influenza A viruses that circulate among avian species pose a concern to public health. Partial genomic RNA sequences from an apparently novel strain (denoted Kz52) close to the H9 subtype were isolated from a dead *Aythya farina* near the Caspian Sea in Kazakhstan. Different approaches were attempted to generate Kz52 PV for the future perspective to develop a PVNA system for screening and sero-surveillance studies in wild birds. Despite the challenges in generating the PV system, here we show the ability of Kz52 HA to cross-react to antibodies suggesting the potential of Kz52 HA to trigger an immune response.

CONTENTS

| | | |
|---------|--|----|
| 1 | INTRODUCTION..... | 1 |
| 1.1 | Herpesviruses..... | 1 |
| 1.1.1 | Equid herpesviruses..... | 1 |
| 1.1.2 | Equid herpesvirus 1 (EHV-1)..... | 3 |
| 1.1.2.1 | Background history..... | 3 |
| 1.1.2.2 | EHV-1 genome structure..... | 3 |
| 1.1.2.3 | EHV-1 glycoproteins..... | 4 |
| 1.1.3 | EHV-1 lifecycle..... | 6 |
| 1.1.3.1 | Attachment and entry..... | 6 |
| 1.1.3.2 | Replication..... | 7 |
| 1.1.3.3 | Egress..... | 8 |
| 1.1.4 | Latency and reactivation..... | 9 |
| 1.1.5 | Epidemiology and transmission..... | 10 |
| 1.1.6 | Pathogenesis..... | 11 |
| 1.1.7 | EHV-1 and the host immune response..... | 14 |
| 1.1.7.1 | Innate immune response..... | 14 |
| 1.1.7.2 | Adaptive immune response..... | 15 |
| 1.1.8 | Vaccines..... | 16 |
| 1.1.9 | Laboratory diagnosis..... | 17 |
| 1.1.9.1 | Serology..... | 18 |
| 1.2 | Influenza viruses..... | 22 |
| 1.2.1 | Classification and nomenclature..... | 22 |
| 1.2.2 | Structure..... | 23 |
| 1.2.2.1 | Haemagglutinin (HA)..... | 25 |
| 1.2.2.2 | Neuraminidase (NA)..... | 28 |
| 1.2.2.3 | M2 ion-channel..... | 28 |
| 1.2.3 | Lifecycle..... | 29 |
| 1.2.3.1 | Attachment and entry..... | 29 |
| 1.2.3.2 | RNA and protein production..... | 29 |
| 1.2.3.3 | Assembly and release..... | 30 |
| 1.2.4 | Evolution of Influenza virus: antigenic drift and antigenic shift..... | 31 |
| 1.2.5 | Ecology and transmission..... | 32 |
| 1.2.6 | Immune response..... | 33 |
| 1.2.6.1 | Innate immune response..... | 33 |

| | | |
|---------|--|----|
| 1.2.6.2 | Adaptive immune response | 34 |
| 1.2.7 | Surveillance and serology | 35 |
| a. | Haemagglutination inhibition (HI) | 35 |
| b. | Single radial haemolysis (SRH) | 36 |
| c. | ELISA..... | 36 |
| d. | Virus neutralisation (VN)..... | 37 |
| 1.3 | Pseudotype viruses | 38 |
| 1.3.1 | Pseudotype virus neutralisation assay..... | 40 |
| 1.4 | Thesis aims and structure | 41 |
| 2. | MATERIALS AND METHODS | 42 |
| 2.1 | Molecular biology | 42 |
| 2.1.1 | Expression vectors | 42 |
| 2.1.2 | Gene design..... | 44 |
| 2.1.3 | Gene synthesis | 44 |
| 2.1.4 | Cloning into expression vector and screening | 45 |
| 2.1.5 | Ligation..... | 46 |
| 2.1.6 | Transformation | 47 |
| 2.1.7 | Glycerol stocks | 48 |
| 2.1.8 | Plasmid DNA purification | 48 |
| 2.1.9 | Measure of nucleic acid concentration..... | 48 |
| 2.1.10 | Sequencing..... | 48 |
| 2.1.11 | Polymerase Chain Reaction for colony screening..... | 49 |
| 2.1.12 | Agarose gel electrophoresis..... | 51 |
| 2.1.13 | SDS-Polyacrylamide Gel Electrophoresis | 51 |
| 2.2 | Cell culture | 53 |
| 2.2.1 | Cell lines and maintenance | 53 |
| 2.2.2 | Freezing and thawing of cell lines..... | 53 |
| 2.3 | Pseudotype virus (PV) generation | 54 |
| 2.3.1 | Generation of lentiviral particles | 54 |
| 2.4 | Pseudotype virus (PV) titration..... | 55 |
| 2.5 | Pseudotype virus neutralisation assay (PVNA) | 56 |
| 2.6 | Statistical analysis of PV titration and PVNA data | 57 |
| 3 | EHV-1 PSEUDOTYPE VIRUS GENERATION AND OPTIMISATION..... | 58 |
| 3.1 | INTRODUCTION..... | 58 |
| 3.2 | MATERIALS AND METHODS | 60 |
| 3.2.1 | Gene sequences and synthesis | 60 |

| | | |
|---------|---|-----|
| 3.2.2 | Cloning strategy, plasmid amplification and purification | 60 |
| 3.2.3 | Cell lines and maintenance | 62 |
| 3.2.4 | EHV-1 PV generation | 62 |
| 3.2.5 | EHV-1 PV titration | 63 |
| 3.2.6 | TCID ₅₀ assay | 64 |
| 3.2.7 | SDS-Polyacrylamide Gel Electrophoresis | 65 |
| 3.2.8 | Data analysis | 65 |
| 3.3 | RESULTS..... | 65 |
| 3.3.1 | Molecular biology | 65 |
| 3.3.1.1 | Cloning of EHV-1 gB, gD, gH and gL genes | 65 |
| 3.3.1.2 | Colony screen of EHV-1 gB, gC, gD, gH and gL..... | 67 |
| 3.3.1.3 | Verification of EHV-1 gB, gC, gD, gH and gL genes in pCAGGS | 70 |
| 3.3.1.4 | Sequencing of EHV-1 gB, gC, gD, gH and gL plasmid DNA | 71 |
| 3.3.2 | EHV-1 PV generation..... | 75 |
| 3.3.3 | EHV-1 PV titration | 75 |
| 3.3.4 | EHV-1 PV optimisation | 78 |
| 3.3.5 | EHV-1 gC entry function investigation | 81 |
| 3.3.6 | Target cell entry study | 83 |
| 3.3.7 | TCID ₅₀ | 87 |
| 3.3.8 | SDS-Polyacrylamide Gel Electrophoresis | 87 |
| 3.4 | DISCUSSION..... | 87 |
| 4 | DEVELOPMENT OF AN EHV-1 PSEUDOTYPE VIRUS NEUTRALISATION ASSAY | 92 |
| 4.1 | INTRODUCTION..... | 92 |
| 4.2 | MATERIALS AND METHODS | 93 |
| 4.2.1 | Sera samples | 93 |
| 4.2.2 | EHV-1 PV neutralisation assay | 94 |
| 4.2.3 | Data analysis | 94 |
| 4.3 | RESULTS..... | 95 |
| 4.3.1 | EHV-1 PV neutralisation assay | 95 |
| 4.3.1.1 | Preliminary EHV-1 PV neutralisation test | 95 |
| 4.3.1.2 | EHV-1 PV in a longitudinal antibody neutralisation study | 97 |
| 4.3.2 | Correlation of antibody titres | 101 |
| 4.4 | DISCUSSION..... | 103 |
| 5 | EHV-1 PSEUDOTYPE VIRUS LYOPHILISATION AND BIOLOGICAL STABILITY TESTING... | 107 |
| 5.1 | INTRODUCTION..... | 107 |
| 5.2 | MATERIALS AND METHODS | 108 |

| | | |
|---------|---|-----|
| 5.2.1 | EHV-1 PV concentration..... | 108 |
| 5.2.2 | EHV-1 PV lyophilisation and storage..... | 108 |
| 5.2.3 | Lyophilised EHV-1 PV titration | 109 |
| 5.2.4 | Cytotoxicity test | 109 |
| 5.2.5 | Lyophilised EHV-1 PV neutralisation assay | 109 |
| 5.2.6 | Data analysis | 110 |
| 5.3 | RESULTS..... | 110 |
| 5.3.1 | Impact of lyophilisation on EHV-1 PV titre..... | 110 |
| 5.3.2 | Impact of storage on lyophilised EHV-1 PV titre..... | 111 |
| 5.3.3 | Application of lyophilised EHV-1 PV..... | 113 |
| 5.4 | DISCUSSION..... | 115 |
| 6 | APPLICATION OF THE PSEUDOTYPE VIRUS NEUTRALISATION ASSAY TO DETERMINE THE IMMUNE STATUS OF HORSES POST EHV-1 VACCINATION AND TRANSDUCTION TESTING OF EHV-1 PSEUDOTYPE VIRUS | 119 |
| 6.1 | INTRODUCTION..... | 119 |
| 6.2 | MATERIALS AND METHODS | 122 |
| 6.2.1 | Cell lines and maintenance | 122 |
| 6.2.2 | EHV-1 PV titration | 123 |
| 6.2.2.1 | EHV-1 PV titration on xCELLigence RTCA..... | 123 |
| 6.2.2.2 | EHV-1 PV titration on Incucyte® RTCA..... | 124 |
| 6.2.3 | EHV-1 PV neutralisation assay | 125 |
| 6.2.3.1 | Sera samples | 125 |
| 6.2.4 | Flow cytometry | 126 |
| 6.2.5 | Data analysis | 127 |
| 6.3 | RESULTS..... | 127 |
| 6.3.1 | EHV-1 PV titration | 127 |
| 6.3.1.1 | EIV PV titre comparison on SPARK® (Tecan) and GloMax® (Promega) luminometers..... | 127 |
| 6.3.1.2 | SPARK® (Tecan) luminometer reading mode test..... | 128 |
| 6.3.1.3 | EHV-1 PV titration on SPARK® (Tecan) luminometer..... | 129 |
| 6.3.1.4 | EHV-1 PV titration on xCELLigence and Incucyte® RTCA | 130 |
| 6.3.2 | EHV-1 PV transduction assessment by flow cytometry | 134 |
| 6.3.3 | EHV-1 PV neutralisation assay | 138 |
| 6.3.3.1 | EHV-1 PV input assessment | 138 |
| 6.3.3.2 | IC ₅₀ threshold value..... | 139 |
| 6.3.3.3 | Validation of EHV-1 PV neutralisation assay for the detection of an immune response in vaccinated horses..... | 140 |

| | | |
|----------|---|-----|
| 6.4 | DISCUSSION..... | 145 |
| 7 | APPROACHES TO PSEUDOTYPE LENTIVIRUS PARTICLES WITH THE HA OF A NOVEL SUBTYPE OF INFLUENZA VIRUS STRAIN FOR USE AS A TOOL FOR CELL TROPISM AND DIAGNOSTIC STUDIES..... | 149 |
| 7.1 | INTRODUCTION..... | 149 |
| 7.2 | MATERIALS AND METHODS | 151 |
| 7.2.1 | Kz52 haemagglutinin (HA) gene sample | 151 |
| 7.2.2 | Recovery project | 152 |
| 7.2.3 | Cloning into expression plasmid | 153 |
| 7.2.4 | High-fidelity Polymerase Chain Reaction..... | 153 |
| 7.2.5 | 3D modelling | 154 |
| 7.2.6 | Plasmids | 155 |
| 7.2.7 | Site Directed Mutagenesis in-house protocol..... | 155 |
| 7.2.8 | Site Directed Mutagenesis QuikChange™ protocol | 156 |
| 7.2.9 | Sequencing of plasmid DNA..... | 158 |
| 7.2.10 | Cell lines and maintenance | 159 |
| 7.2.11 | Influenza PV generation..... | 159 |
| 7.2.12 | Influenza VSV PV generation..... | 160 |
| 7.2.13 | Influenza PV titration | 160 |
| 7.2.13.1 | Addition of Trypsin (TPCK-treated)..... | 161 |
| 7.2.14 | Influenza VSV PV titration..... | 161 |
| 7.2.15 | Influenza PV neutralisation assay | 161 |
| 7.2.16 | SDS-Polyacrylamide Gel Electrophoresis | 162 |
| 7.2.17 | Immunofluorescence | 162 |
| 7.2.18 | SYBR-Green Product-Enhanced Reverse Transcriptase | 163 |
| 7.2.19 | Enzyme-Linked Immunosorbent Assay..... | 164 |
| 7.2.19.1 | Influenza PV concentration and purification | 165 |
| 7.2.19.2 | Indirect Enzyme-Linked Immunosorbent Assay..... | 165 |
| 7.2.20 | Data analysis | 166 |
| 7.3 | RESULTS..... | 166 |
| 7.3.1 | Chromatogram and sequence analysis | 166 |
| 7.3.2 | Sequence alignment with H9 haemagglutinin (HA)..... | 168 |
| 7.3.3 | 3D modelling | 169 |
| 7.3.4 | Molecular cloning and analysis of the Kz52 haemagglutinin (HA) gene..... | 170 |
| 7.3.4.1 | Cloning of Influenza HA genes into pI.18 or pCAGGS | 170 |
| 7.3.4.2 | Site Directed Mutagenesis | 181 |

| | | |
|---------|---|-----|
| 7.3.5 | Attempts to generate functional Kz52 PV particles..... | 197 |
| 7.3.5.1 | Effect of Trypsin (TPCK-treated) at different incubation times | 201 |
| 7.3.5.2 | Effect of KLK-5, TMPRSS3 and TMPRSS6 proteases..... | 203 |
| 7.3.5.3 | Target cell entry study | 204 |
| 7.3.5.4 | Site Directed Mutagenesis | 207 |
| 7.3.5.5 | Influenza PV generated with HA and NA combination | 217 |
| 7.3.5.6 | Influenza VSV PV titre | 218 |
| 7.3.6 | Influenza PV neutralisation assay | 219 |
| 7.3.7 | SDS-Polyacrylamide Gel Electrophoresis | 220 |
| 7.3.8 | Immunofluorescence of HA in producer cells..... | 221 |
| 7.3.9 | Influenza PV application in an Enzyme-linked immunosorbent assay..... | 226 |
| 7.3.10 | Quality control of lentiviral PV | 228 |
| 7.4 | DISCUSSION..... | 229 |
| 8 | CONCLUSIONS AND FUTURE WORK | 236 |
| 9 | REFERENCES | 241 |
| 10 | APPENDIX..... | 302 |
| 10.1 | APPENDIX CHAPTER 3 | 302 |
| 10.2 | APPENDIX CHAPTER 6 | 309 |
| 10.3 | APPENDIX CHAPTER 7 | 314 |

ABBREVIATIONS

| | |
|--------------------|--|
| A | adenine |
| ACE2 | Angiotensin-converting enzyme 2 |
| AHV | asinine herpesvirus |
| AIV | avian influenza virus |
| ALV | avian leukosis virus |
| AmpR | ampicillin resistance |
| AmpR PRO | promoter |
| APHA | Animal and Plant Health Agencies |
| BDHL | EHV-1 PV generated using the gB, gD, gH and gL GP plasmids |
| BDL | EHV-1 PV generated using the gB, gD and gL GP plasmids |
| BH | EHV-1 PV generated using the gB and gH GP plasmids |
| BHK | baby hamster kidney cells |
| BHL | EHV-1 PV generated using the gB, gH and gL GP plasmids |
| BLASTP | protein BLAST |
| CDC | Centers for Disease Control and Prevention |
| CEF | Chicken embryonic fibroblasts |
| CF | complement fixing |
| CHO-K1 | Chinese Hamster Ovary cells |
| CI | cell index |
| CI _n | normalised cell index |
| CNS | Central nervous system |
| CO | codon optimisation |
| CPE | cytopathic effect |
| cRNA | complimentary RNA |
| CTL | cytotoxic T lymphocyte |
| CTRL | control |
| D | aspartic acid |
| DC | dendritic cells |
| ddH ₂ O | double distilled water |
| DEF | Duck embryonic fibroblasts |
| DHL | EHV-1 PV generated using the gD, gH and gL GP plasmids |
| DMEM | Dulbecco's Modified Eagle Medium |

| | |
|------------------|--|
| DMSO | dimethyl sulfoxide |
| DNA | deoxyribonucleic acid |
| dpi | days post infection |
| dsDNA | double-stranded DNA |
| E.derm or CCL57 | equine dermal cells |
| EBOV | ebolavirus |
| ECCD | European Community Commission Directive |
| EDTA | Ethylenediaminetetraacetic acid |
| EEC | equine endothelial cells |
| EEO | low electroendosmosis |
| EFSA | European Food Safety Authority |
| EHM | equine herpesvirus myeloencephalopathy |
| EHV | equid herpesvirus |
| EIV | equine influenza virus |
| ELISA | enzyme-linked immunosorbent assay |
| EMEM | Eagle's Minimum Essential Medium |
| emGFP | emerald green fluorescence protein |
| <i>env</i> | HIV-1 envelope gene |
| ETIF or VP16-E | EHV-1 tegument transactivator protein or α -trans-inducing factor |
| exNA | exogenous neuraminidase |
| F-12 | Ham's F-12 Nutrient Mixture |
| FACS | fluorescence-activated single cell sorting |
| FBS | foetal bovine serum |
| FEI | Fédération Équestre Internationale |
| FHK-Tcl3 | Foetal Horse Kidney cells |
| FLW | Firefly luciferase |
| FW | forward |
| G | guanine |
| <i>gag - pol</i> | HIV-1 core structural proteins and reverse transcriptase |
| GFP | green fluorescence protein |
| GHV | gazelle herpesvirus |
| GP | glycoprotein |
| gX | glycoprotein X (referred to EHV-1 glycoprotein) |
| HA | haemagglutinin |

| | |
|--------------------|--|
| HA0 | HA precursor protein |
| HA1 and HA2 | HA subunits 1 and 2 |
| HACS | HA cleavage site |
| HAT | human airway trypsin-like protease |
| hCMV | human cytomegalovirus |
| HEF | haemagglutinin-esterase-fusion |
| HEK | human embryonic kidney cells |
| HEPES | 4-(2-hydroxyethyl)-1-piperazineethanesulfonic acid |
| HI | hemagglutination inhibition |
| HIV-1 | human immunodeficiency virus type 1 |
| HPAI | Highly Pathogenic Avian influenza |
| hRSV | Human Respiratory syncytial virus |
| HSV | herpes simplex virus |
| HveC | herpesvirus entry mediator C or Nectin-1 |
| HVEM | herpesvirus entry mediator |
| IC ₅₀ | half-maximal inhibitory concentration |
| ICPO | infected cell polypeptide 0 |
| ICTV | International Committee on Taxonomy of Viruses |
| IE | immediate early or α gene |
| IFN- γ | interferon type II or γ |
| IgX | immunoglobulin X |
| IL-2 | interleukin-2 |
| IL-4 | interleukin-4 |
| INF α/β | interferon type I |
| IR ₆ | inverted repeat gene |
| IR _L | internal repeat long sequence |
| IR _S | internal repeat short sequence |
| JEV | Japanese encephalitis virus |
| K | lysine |
| KLK-5 | kallikrein-5 |
| KyD | Kentucky D |
| LAT | latency-associated transcript |
| LB | Luria-Bertani |
| L-glut | L-glutamine |

| | |
|----------------------|--|
| LPAI | Low Pathogenic Avian influenza |
| M&M | Materials and methods |
| M1 | matrix-1 proteins |
| M2 | matrix-2 proteins or membrane ion channel |
| MBG H ₂ O | DNase-free water |
| MCS | multiple cloning site |
| MDBK | Madin-Darby bovine kidney cells |
| MDCK I & II | Madin-Darby Canine Kidney cells |
| MEM/EBSS | Minimum Essential Medium with Earle's balanced salts solution |
| MHC-I/MHC-II | major histocompatibility complex class I or II |
| ML | maximum likelihood |
| MLST | Multi Locus Sequence Typing |
| MLV | Modified live vaccines |
| MN | microneutralisation |
| MOI | Multiplicity of infection |
| mRNA | messenger RNA |
| N | asparagine |
| NA | neuraminidase |
| NIBSC | National Institute for Biological Standards and Control |
| NJ | neighbour-joining |
| NK | neutrophils natural killer |
| NP | nucleoprotein |
| NPC | nucleopore complex |
| NS1 | non-structural proteins 1 |
| NS2 or NEP | non-structural proteins 2 or nuclear export proteins |
| OD | Optical density |
| OIE | World Organization for Animal Health |
| ON | overnight |
| ORF | open reading frame |
| P/S | penicillin/streptomycin |
| p8.91 | HIV core plasmid |
| PA | polymerase acid proteins of the heterotrimeric polymerase complex |
| PB1 and PB2 | polymerase basic proteins of the heterotrimeric polymerase complex |
| PBMC | peripheral blood mononuclear cells |

| | |
|-------------|---|
| PBS | phosphate-buffered saline |
| PBS-T | PBS-0.05%Tween® 20 |
| PCR | polymerase chain reaction |
| PDL | Poly-D-lysine |
| PEG | polyethylene glycol |
| PEI | polyethylenimine |
| PFA | paraformaldehyde |
| PRNT | plaque reduction neutralisation test |
| pUC ORI | pUC origin of replication |
| PV | pseudotype virus |
| PVNA | pseudotype virus neutralisation assay |
| PVNT | pseudotype virus neutralisation test |
| qPCR | quantitative PCR |
| R | arginine |
| RAVV | Ravn virus |
| RBC | red blood cells |
| RBS | receptor binding site |
| RDE | receptor-destroying enzyme |
| REs | restriction enzymes |
| Rev | reverse |
| RK13 | rabbit kidney cells |
| RLU | relative luminescence unit |
| RNA | ribonucleic acid |
| RPM | revolutions per minute |
| RRE | HIV-1 Rev response element |
| RSV | Rous sarcoma virus |
| RT | room temperature |
| RT-activity | reverse transcriptase activity |
| RTCA | real-time cell analysis technology |
| RT-PCR | reverse transcription PCR |
| SA | sialic acid |
| SARS-CoV-2 | Severe acute respiratory syndrome coronavirus 2 |
| SDM | site-directed mutagenesis |
| SDS | Tris-glycine-sodium dodecyl Sulphate |

| | |
|------------------------|--|
| SDS-PAGE | SDS-polyacrylamide gel electrophoresis |
| SFFV | spleen focus forming virus promoter |
| SG-PERT | SYBR Green product-enhanced reverse transcriptase assay |
| SN | supernatant |
| SOC | super optimal broth with catabolite repression |
| SRH | single radial hemolysis |
| ssRNA | single-stranded RNA |
| TAE | tris-acetate- ethylenediaminetetraacetic acid buffer |
| TCID ₅₀ | 50% Tissue Culture Infectious Dose |
| TMB | 3,3',5,5'-tetramethylbenzidine |
| TMPRSS2 | transmembrane serine protease 2 |
| TMPRSS3 | transmembrane serine protease 3 |
| TMPRSS4 | transmembrane serine protease 4 |
| TMPRSS6 | transmembrane serine protease 6 |
| TNS | Trypsin Neutralising Solution |
| TPCK-trypsin | L-tosylamido-2-phenyl ethyl chloromethyl ketone treated trypsin |
| TR _L or LTR | terminal repeat long sequence |
| TR _S | terminal repeat short sequence |
| UK | United Kingdom |
| U _L | unique long region |
| U _S | unique short region |
| Vero | African green monkey kidney cells |
| VN | virus neutralising |
| VP | viral particles |
| VPU | Viral Pseudotype Unit |
| vRNA | viral RNA |
| vRNPs | viral ribonucleoprotein complexes |
| VRS | Virology Research Services |
| VSV | vesicular stomatitis virus |
| WHO | World Health Organisation |
| WPRE | Woodchuck Hepatitis Virus Posttranscriptional Regulatory Element |
| WT | wild type |
| Ψ | packaging signal sequence |

FIGURES

| | |
|--|----|
| Figure 1: Schematic illustration of EHV-1 genome and functional ORFs..... | 4 |
| Figure 2: Schematic illustration of EHV-1 virion..... | 5 |
| Figure 3: Schematic of EHV-1 lytic lifecycle..... | 9 |
| Figure 4: Schematic of EHV-1 pathogenesis..... | 14 |
| Figure 5: VN assay..... | 20 |
| Figure 6: Example of nomenclature of Influenza virus..... | 23 |
| Figure 7: Structure of an Influenza virion..... | 24 |
| Figure 8: HACS in LPAI and HPAI viruses in poultry..... | 27 |
| Figure 9: Schematic of Influenza virus lifecycle..... | 31 |
| Figure 10: Significant interspecies transmission of Influenza A virus..... | 33 |
| Figure 11: Visual example of plaques in a PRNT..... | 37 |
| Figure 12: Visual example of CPE in a MN..... | 38 |
| Figure 13: Principle of PVNA..... | 41 |
| Figure 14: pI.18 plasmid map..... | 43 |
| Figure 15: pCAGGS plasmid map..... | 43 |
| Figure 16: Lentiviral packaging vectors for PV generation..... | 44 |
| Figure 17: PV titration set-up in 96-well plate..... | 56 |
| Figure 18: PVNA set-up in 96-well plate..... | 57 |
| Figure 19: EHV-1 PV generation..... | 63 |
| Figure 20: Pseudotype TCID ₅₀ titration set-up in 96-well plate..... | 64 |
| Figure 21: Plasmid maps of pMX-EHV-1 gB, gD, gH and gL..... | 66 |
| Figure 22: RE digests of EHV-1 GP genes in pMX..... | 66 |
| Figure 23: Gel extraction of EHV-1 GP genes from pMX..... | 67 |
| Figure 24: Colony screen of EHV-1 gB clones..... | 68 |
| Figure 25: Colony screen of EHV-1 gH clones..... | 68 |
| Figure 26: Colony screen of EHV-1 gD clones..... | 69 |
| Figure 27: Colony screen of EHV-1 gL clones..... | 69 |
| Figure 28: Colony screen of EHV-1 gC clones..... | 70 |
| Figure 29: Control digestion of EHV-1 GPs into pCAGGS..... | 71 |
| Figure 30: Control digestion of EHV-1 gC into pCAGGS..... | 71 |
| Figure 31: Alignment summary of EHV-1 gB gene sequences..... | 72 |
| Figure 32: EHV-1 gB gene (strain 2010-203) aligned with EHV-1 gB FW, gB Rev, gB INT FW and gB INT Rev sequences..... | 72 |

| | |
|---|-----|
| Figure 33: EHV-1 gB gene (strain 2010-203) aligned with EHV-1 gB FW, gB Rev, gB INT FW and gB INT Rev sequences.. | 72 |
| Figure 34: Alignment summary of EHV-1 gD gene sequences. | 72 |
| Figure 35: EHV-1 gD gene (strain 2010-203) aligned with EHV-1 gD FW and gD Rev sequences. | 73 |
| Figure 36: EHV-1 gD gene (strain 2010-203) aligned with EHV-1 gD FW and gD Rev sequences. | 73 |
| Figure 37: Alignment summary of EHV-1 gH gene sequences. | 73 |
| Figure 38: EHV-1 gH gene (strain 2010-203) aligned with EHV-1 gH FW, gH Rev, gH INT FW and gH INT Rev sequences. | 73 |
| Figure 39: EHV-1 gH gene (strain 2010-203) aligned with EHV-1 gH FW, gH Rev, gH INT FW and gH INT Rev sequences. | 74 |
| Figure 40: Alignment summary of EHV-1 gL gene sequence. | 74 |
| Figure 41: EHV-1 gL gene (strain 2010-203) aligned with EHV-1 gL FW sequence only. | 74 |
| Figure 42: EHV-1 gL gene (strain 2010-203) aligned with EHV-1 gL FW sequence only. | 74 |
| Figure 43: Alignment summary of EHV-1 gC gene sequences. | 75 |
| Figure 44: EHV-1 gC gene (strain 2009-87) aligned with EHV-1 gC FW and gC Rev sequences. | 75 |
| Figure 45: EHV-1 gC gene (strain 2009-87) aligned with EHV-1 gC FW and gC Rev sequences. | 75 |
| Figure 46: Green HEK293T/17 cells transduced with EHV-1 PV. | 77 |
| Figure 47: Titration results of EHV-1 PV. | 78 |
| Figure 48: Titration results of EHV-1 PV optimisation. | 80 |
| Figure 49: Titration results of EHV-1 PV optimisation. | 81 |
| Figure 50: Titration results of EHV-1 PV optimisation. | 82 |
| Figure 51: Green target cells transduced with EHV-1 PV and EIV PV. | 84 |
| Figure 52: Titration results of target cell entry study. | 86 |
| Figure 53: TCID ₅₀ titres in HEK293T target cells. | 87 |
| Figure 54: Timeline of study. | 94 |
| Figure 55: Preliminary PVNT (EHV-1 PV). | 96 |
| Figure 56: Preliminary PVNT (EIV PV). | 96 |
| Figure 57: EHV-1 Pseudotype virus neutralisation assay. | 98 |
| Figure 58: Individual PVNA (A and B). | 99 |
| Figure 59: Individual PVNA (C and D). | 100 |
| Figure 60: Correlation EHV-1 VN and ppNT50. | 102 |
| Figure 61: Correlation xCELLNT50 and ppNT50. | 103 |

| | |
|---|-----|
| Figure 62: Correlation xCELLNT50 and EHV-1 VN..... | 103 |
| Figure 63: Titration results of EHV-1 PV immediately resuspended after lyophilisation. | 110 |
| Figure 64: Titration results of impact of storage (1 week) on lyophilised EHV-1 PV. | 112 |
| Figure 65: Titration results of impact of storage (4 weeks) on lyophilised EHV-1 PV. | 113 |
| Figure 66: PVNA (lyophilised EHV-1 PV)..... | 114 |
| Figure 67: PVNA (lyophilised EIV PV)..... | 114 |
| Figure 68: PVNA (lyophilised EIV PV)..... | 115 |
| Figure 69: PBMC study design..... | 126 |
| Figure 70: PV titration comparison between GloMax® (Promega) and SPARK® (Tecan) Luminometers. | 128 |
| Figure 71: PV titration on SPARK® (Tecan) Luminometer using either an orbital shaking mode or no shaking..... | 129 |
| Figure 72: PV titration on xCELLigence RTCA on HEK293T cells. | 132 |
| Figure 73: PV titration on xCELLigence RTCA on CCL57 cells. | 132 |
| Figure 74: PV titration on xCELLigence RTCA on RK13 cells..... | 133 |
| Figure 75: PV titration on xCELLigence RTCA on MDCK II cells..... | 133 |
| Figure 76: Flow cytometry analysis of equine PBMC. | 135 |
| Figure 77: Flow cytometry analysis of equine PBMC..... | 136 |
| Figure 78: Flow cytometry analysis of HEK293T cells. | 137 |
| Figure 79: Flow cytometry analysis of HEK293T cells. | 137 |
| Figure 80: PVNT for PV input assessment. | 138 |
| Figure 81: Graphical summary of IC ₅₀ values for threshold assessment. | 139 |
| Figure 82: Graphical summary of the IC ₅₀ values of a panel of sera samples collected from EHV-1 vaccinated pregnant mares (Group G). | 141 |
| Figure 83: Graphical summary of the IC ₅₀ values of a panel of sera samples collected from primary EHV-1 vaccinated horses (Group P). | 142 |
| Figure 84: Graphical summary of the IC ₅₀ values of a panel of sera samples collected from horses already EHV-1 vaccinated (Group R)..... | 143 |
| Figure 85: Correlation xCELLNT ₅₀ and ppNT ₅₀ | 145 |
| Figure 86: Phylogenetic tree of Kz52 HA. | 151 |
| Figure 87: Alignment summary pre-recovery project..... | 167 |
| Figure 88: Alignment summary post-recovery project. | 167 |
| Figure 89: BLASTP alignment between Kz52 HA and H9..... | 168 |
| Figure 90: 3D model structures..... | 169 |
| Figure 91: Gradient PCR for CO Kz52 cloning primers..... | 171 |

| | |
|--|-----|
| Figure 92: High-fidelity PCR amplification product of CO Kz52. | 172 |
| Figure 93: Colony screen of pl.18-WT Kz52 clones. | 173 |
| Figure 94: Colony screen of pCAGGS-WT Kz52 clones. | 173 |
| Figure 95: Colony screen of pl.18-CO Kz52 clones. | 174 |
| Figure 96: Colony screen of pCAGGS-CO Kz52 clones. | 174 |
| Figure 97: Colony screen of pCAGGS-H9 clones. | 175 |
| Figure 98: Control digestion of WT Kz52 HA into pl.18. | 175 |
| Figure 99: Control digestion of WT Kz52 HA into pCAGGS. | 176 |
| Figure 100: Control digestion of CO Kz52 HA into pCAGGS. | 176 |
| Figure 101: Control digestion of H9 HA into pCAGGS. | 177 |
| Figure 102: Alignment summary of WT Kz52 HA gene sequences. | 177 |
| Figure 103: WT Kz52 HA gene clone was sequenced using flanking pl.18 FW primer. | 178 |
| Figure 104: WT Kz52 HA gene clone was sequenced using flanking pl.18 Rev primer. | 178 |
| Figure 105: Alignment summary of WT Kz52 HA gene sequences. | 178 |
| Figure 106: WT Kz52 HA gene clone was sequenced using flanking pCAGGS FW primer. | 178 |
| Figure 107: WT Kz52 HA gene clone was sequenced using flanking pCAGGS Rev primer. | 178 |
| Figure 108: Alignment summary of CO Kz52 HA gene sequences. | 179 |
| Figure 109: CO Kz52 HA gene clone was sequenced using flanking pl.18 FW primer. | 179 |
| Figure 110: CO Kz52 HA gene clone was sequenced using flanking pl.18 Rev primer. | 179 |
| Figure 111: Alignment summary of CO Kz52 HA gene sequences. | 179 |
| Figure 112: CO Kz52 HA gene clone was sequenced using flanking pCAGGS FW primer. | 179 |
| Figure 113: CO Kz52 HA gene clone was sequenced using flanking pCAGGS Rev primer. | 180 |
| Figure 114: Alignment summary of H9 HA gene sequences. | 180 |
| Figure 115: H9 HA gene clone was sequenced using flanking pl.18 and pCAGGS FW primers. | 180 |
| Figure 116: H9 HA gene clone was sequenced using flanking pl.18 and pCAGGS Rev primers. | 180 |
| Figure 117: Amplification product of mutant WT Kz52 HA E337 in pl.18. | 182 |
| Figure 118: Amplification product of mutant CO Kz52 HA E337 in pl.18. | 182 |
| Figure 119: Alignment summary of mutant WT Kz52 HA gene E337S sequences. | 183 |
| Figure 120: Mutant WT Kz52 HA gene E337S clone was sequenced using flanking pl.18 FW and Rev primers. | 183 |
| Figure 121: Alignment summary of mutant CO Kz52 HA gene E337S sequences. | 183 |

| | |
|---|-----|
| Figure 122: Mutant CO Kz52 HA gene E337S clone was sequenced using flanking pl.18 FW and Rev primers. | 183 |
| Figure 123: Amplification product of mutants WT and CO Kz52 HA PARSSR in pl.18. | 184 |
| Figure 124: Alignment summary of mutant WT Kz52 HA gene PARSSR sequences. | 184 |
| Figure 125: Mutant WT Kz52 HA gene PARSSR clone was sequenced using flanking pl.18 FW and Rev primers. | 185 |
| Figure 126: Alignment summary of mutant CO Kz52 HA gene PARSSR sequences. | 185 |
| Figure 127: Mutant CO Kz52 HA gene PARSSR clone was sequenced using flanking pl.18 FW and Rev primers. | 185 |
| Figure 128: High-fidelity PCR amplification product of mutant CO Kz52 HA (PARSSR).... | 186 |
| Figure 129: Colony screen of pCAGGS-WT Kz52 mutant clones (PARSSR)..... | 187 |
| Figure 130: Colony screen of pCAGGS-CO Kz52 mutant clones (PARSSR)..... | 187 |
| Figure 131: Control digestion of mutant WT Kz52 HA gene (PARSSR) into pCAGGS..... | 188 |
| Figure 132: Control digestion of mutant CO Kz52 HA gene (PARSSR) into pCAGGS. | 188 |
| Figure 133: Alignment summary of mutant WT Kz52 HA gene (PARSSR) sequences..... | 189 |
| Figure 134: Mutant WT Kz52 HA gene (PARSSR) clone was sequenced using flanking pCAGGS FW primer. | 189 |
| Figure 135: Mutant WT Kz52 HA gene (PARSSR) clone was sequenced using flanking pCAGGS Rev primer..... | 189 |
| Figure 136: Alignment summary of mutant CO Kz52 HA gene (PARSSR) sequences..... | 189 |
| Figure 137: Mutant CO Kz52 HA gene (PARSSR) clone was sequenced using flanking pCAGGS FW primer. | 190 |
| Figure 138: Mutant CO Kz52 HA gene (PARSSR) clone was sequenced using flanking pCAGGS Rev primer..... | 190 |
| Figure 139: Amplification product of mutants H9 HA PIKETR in pl.18..... | 190 |
| Figure 140: Alignment summary of mutant H9 HA gene PIKETR sequences. | 191 |
| Figure 141: Mutant H9 HA gene PIKETR clone was sequenced using flanking pl.18 FW and Rev primers..... | 191 |
| Figure 142: Control digestion of mutant H9 HA gene (PIKETR) into pCAGGS. | 192 |
| Figure 143: Alignment summary of mutant H9 HA gene (PIKETR) sequences..... | 192 |
| Figure 144: Mutant H9 HA gene (PIKETR) clone was sequenced using flanking pCAGGS FW primer. | 193 |
| Figure 145: Mutant H9 HA gene (PARSSR) clone was sequenced using flanking pCAGGS Rev primer. | 193 |
| Figure 146: Amplification product of mutants WT and CO Kz52 HA and H9 HA PARKKR in pl.18. | 194 |
| Figure 147: Alignment summary of mutant WT Kz52 HA gene PARKKR sequences..... | 194 |

| | |
|---|-----|
| Figure 148: Mutant WT Kz52 HA gene PARKKR clone was sequenced using flanking pl.18 FW and Rev primers. | 194 |
| Figure 149: Alignment summary of mutant CO Kz52 HA gene PARKKR sequences..... | 195 |
| Figure 150: Mutant CO Kz52 HA gene PARKKR clone was sequenced using flanking pl.18 FW and Rev primers. | 195 |
| Figure 151: Alignment summary of mutant H9 HA gene PARKKR sequences. | 195 |
| Figure 152: Mutant H9 HA gene PARKKR clone was sequenced using flanking pl.18 FW and Rev primers. | 195 |
| Figure 153: Amplification product of mutants WT and CO Kz52 HA KOZAK in pl.18..... | 196 |
| Figure 154: Alignment summary of mutant WT Kz52 HA gene Kozak sequences. | 196 |
| Figure 155: Mutant WT Kz52 HA gene Kozak clone was sequenced using flanking pl.18 FW and Rev primers. | 197 |
| Figure 156: Alignment summary of mutant CO Kz52 HA gene Kozak sequences. | 197 |
| Figure 157: Mutant WT Kz52 HA gene Kozak clone was sequenced using flanking pl.18 FW and Rev primers. | 197 |
| Figure 158: Green HEK293T/17 cells transduced with GFP Kz52 PVs..... | 199 |
| Figure 159: Titration results of WT Kz52 HA in pl.18 and pCAGGS..... | 201 |
| Figure 160: Titration results of CO Kz52 HA in pl.18 and pCAGGS. | 201 |
| Figure 161: TPCK-trypsin titration of WT Kz52 HA in pl.18 and pCAGGS. | 202 |
| Figure 162: TPCK-trypsin titration of CO Kz52 HA in pl.18 and pCAGGS. | 202 |
| Figure 163: Contribution of KLK-5, TMPRSS3 and TMPRSS6 proteases for WT KZ52 PVs. | 203 |
| Figure 164: Contribution of KLK-5, TMPRSS3 and TMPRSS6 proteases for CO KZ52 PVs. | 204 |
| Figure 165: Titration results of WT and CO Kz52 HA in pl.18 on MDCK I. | 205 |
| Figure 166: Titration results of WT and CO Kz52 HA in pl.18 on MDCK II. | 205 |
| Figure 167: Titration results on HEK293T expressing ACE2 and TMPRSS2..... | 207 |
| Figure 168: Sequence alignment of H9 HA and Kz52 HA. | 208 |
| Figure 169: Amino acid motif and conservation of the hemagglutinin cleavage site..... | 208 |
| Figure 170: Titration results of mutants WT and CO Kz52 E337S HA in pl.18. | 208 |
| Figure 171: TPCK-trypsin titration of mutants WT and CO Kz52 E337S HA in pl.18. | 209 |
| Figure 172: Titration results of mutants WT and CO Kz52 E337S HA in pl.18 on MDCK I. | 210 |
| Figure 173: Titration results of mutants WT and CO Kz52 E337S HA in pl.18 on MDCK II. | 210 |
| Figure 174: Titration results of mutant WT Kz52 HA PARSSR in pl.18 and pCAGGS..... | 211 |
| Figure 175: Titration results of mutant CO Kz52 HA PARSSR in pl.18 and pCAGGS. | 212 |
| Figure 176: Green HEK293T/17 cells transduced with H9 HA PIKETR PVs. | 213 |
| Figure 177: Titration results of mutant H9 HA PIKETR in pl.18. | 214 |

| | |
|--|-----|
| Figure 178: Titration results of mutant H9 HA PIKETR in pl.18. | 214 |
| Figure 179: Titration results of mutant H9 HA PIKETR in pl.18 and pCAGGS in DEF cells. | 215 |
| Figure 180: Green HEK293T/17 cells transduced with mutant GFP H9 HA PARKK PV..... | 216 |
| Figure 181: Titration results of mutant H9 HA PARKKR in pl.18..... | 216 |
| Figure 182: Titration results of HA and NA PV combinations..... | 218 |
| Figure 183: Titration results of vPVs..... | 219 |
| Figure 184: PVNT (H9 PV)..... | 220 |
| Figure 185: Titration results of concentrated PVs for SDS-PAGE. | 221 |
| Figure 186: SDS-PAGE results..... | 221 |
| Figure 187: Immunofluorescence at 20x on ZOE™..... | 223 |
| Figure 188: Immunofluorescence at 20x on ZEISS LSM. | 224 |
| Figure 189: Immunofluorescence at 63x on ZEISS LSM. | 225 |
| Figure 190: Standard curve obtained with known amounts of BSA. | 226 |
| Figure 191: Indirect ELISA results. | 227 |
| Figure 192: Standard curve obtained with recombinant HIV-1 RT..... | 228 |
| Figure 193: Reverse transcriptase activity | 228 |
| | |
| Appendix Figure 1: Flow chart - Subcloning gB from pMA in pCAGGS.. Error! Bookmark not defined. | |
| Appendix Figure 2: Flow chart - Subcloning of gD and gL from pMA and gH from pMK in pCAGGS..... | 305 |
| Appendix Figure 3: Flow chart - Cloning of gC in pCAGGS. Error! Bookmark not defined. | |
| Appendix Figure 4: RTCA PV titration on HEK293T/17 cells. | 309 |
| Appendix Figure 5: RTCA PV titration on CCL57 cells..... | 310 |
| Appendix Figure 6: RTCA PV titration on RK13 cells. | 311 |
| Appendix Figure 7: RTCA PV titration on MDCK II cells. | 312 |
| Appendix Figure 8: Flow chart – Cloning of WT Kz52 HA gene into pl.18 vector..... | 315 |
| Appendix Figure 9: Flow chart – Subcloning of WT Kz52 HA gene into pCAGGS vector.. | 317 |
| Appendix Figure 10: Flow chart – Cloning of CO Kz52 HA gene into pl.18 vector. Error! Bookmark not defined. | |
| Appendix Figure 11: Flow chart – Subcloning of CO Kz52 HA gene into pCAGGS vector. | 321 |
| Appendix Figure 12: Flow chart – Subcloning of H9 HA gene into pCAGGS vector. Error! Bookmark not defined. | |
| Appendix Figure 13: BLASTN tree..... | 324 |

Appendix Figure 14: Green HEK293T/17, DEF, MDCK I & II cells transduced with Influenza H9 PVs..... 327

TABLES

| | |
|---|------------|
| Table 1: Equid herpesviruses. | 2 |
| Table 2: Function of EHV-1 envelope glycoproteins. | 6 |
| Table 3: The Influenza genome structure encoding for different viral proteins. | 25 |
| Table 4: Conventional RE digestion reaction volumes. | 45 |
| Table 5: FastDigest® RE digestion reaction volumes. | 46 |
| Table 6: Ligation reaction volumes. | 47 |
| Table 7: Sequencing primers. | 49 |
| Table 8: pCAGGS NT primers for amplification and screening purposes. | 50 |
| Table 9: Colony screen PCR program. | 51 |
| Table 10: Sequencing primers designed for EHV-1 gB and gH. | 61 |
| Table 11: Length of EHV-1 GP genes. | 67 |
| Table 12: Record of green HEK293T/17 cells transduced with EHV-1 PVs. | 83 |
| Table 13: LogIC₅₀ and IC₅₀ values. | 96 |
| Table 14: LogIC₅₀ and IC₅₀ values. | 97 |
| Table 15: Statistical analysis of PVNA. | 101 |
| Table 16: Comparison of EHV-1 PVNA and VN. | 102 |
| Table 17: LogIC₅₀ and IC₅₀ values. | 114 |
| Table 18: LogIC₅₀ and IC₅₀ values (lyophilised EIV PV). | 115 |
| Table 19: Target cells per titration assay. | 124 |
| Table 20: RTCA xCELLigence and Incucyte® programmes | 125 |
| Table 21: Record of EHV-1 PVs titre. | 130 |
| Table 22: LogIC₅₀ and IC₅₀ values. | 139 |
| Table 23: Comparison of EHV-1 PVNA and VN. | 144 |
| Table 24: Primer sequences for CO Kz52 cloning. | 153 |
| Table 25: Gradient PCR program. | 154 |
| Table 26: QuikChange™ PCR reaction volumes. | 157 |
| Table 27: phCMV1 sequencing primers. | 158 |
| Table 28: MS2 primer sequences. | 163 |
| Table 29: SG-PERT master mix reaction volumes. | 164 |
| Table 30: SG-PERT cycle conditions. | 164 |
| Table 31: Main antigenic sites. | 169 |
| Table 32: LogIC₅₀ and IC₅₀ values. | 220 |

| | |
|---|------------|
| Table 33: HA plasmid intake. | 226 |
| Table 34: Protein quantification of concentrated purified samples obtained with Pierce™ BCA assay..... | 226 |
| | |
| Appendix Table 1: Record of green target cells transduced with combination of EHV-1 PVs. | 308 |
| Appendix Table 2: Supplementary information..... | 313 |
| Appendix Table 3: Primers sequences used for SDM PCR (cleavage site). | 325 |
| Appendix Table 4: Primers sequences used for SDM PCR (Kozak sequence). | 326 |

1 INTRODUCTION

1.1 Herpesviruses

Herpesviruses belong to the *Herpesviridae* family and as of 2021 about 115 species are recognised by the International Committee on Taxonomy of Viruses (ICTV) (Walker *et al.*, 2021). The etymology of the name attributed to this family of viruses derives from ancient Greek history. The word '*herpes*' derives from '*herpein*' which means 'to creep' in Greek, as to describe the spreading of skin lesions, a typical characteristic of the disease (Beswick, 1962). Herpesviruses are large viruses (200-250 nm in diameter) possessing a linear, double-stranded DNA (dsDNA) genome (125-245 kbp) enclosed into an icosahedral capsid (about 125 nm in diameter). This capsid is in turn surrounded by a protein-rich tegument and an external double lipid layer, derived from the host plasma membrane, constituting the envelope onto which a various number of proteins and glycoproteins (GPs) are inserted (Davison and Clements, 2010). On the basis of their distinct biological characteristic and genomic features, Herpesviruses have been divided into three subfamilies: *Alphaherpesviridae*, *Betaherpesviridae* and *Gammaherpesviridae* (Roizman, 1996; Minson *et al.*, 2000). A peculiarity of alphaherpesviruses is the ability to establish latency within the host at the neuronal level after primary infection (Bloom, 2016). At this stage, the host is asymptomatic but still able to spread the infection and shed virions once the virus reactivates. Reactivation of latent virus has been linked to events of emotional or physical stress, leading to virus replication and production of lesions (Szpara, Kobilier and Enquist, 2010; Nicoll, Proença and Efstathiou, 2012; Grinde, 2013). Herpesviruses are able to infect a wide range of hosts from all group members both vertebrates (such as mammals, birds, reptiles and fish) and invertebrates (such as molluscs) (Le Deuff *et al.*, 1994; Davison, 2002). Infection is generally host-specific, and it has been proven from phylogenetic studies that herpesviruses have co-evolved with their hosts, and are thus well adapted to them (Davison, 2002). However, despite the co-evolutionary principles, some herpesviruses may not be strictly host-specific and are able to infect other species often with fatal outcomes in non-definitive hosts (Greenwood *et al.*, 2012; Azab *et al.*, 2018).

1.1.1 Equid herpesviruses

In the *Equidae* family, nine equid herpesviruses (EHVs) have been identified (Table 1). The horse (*Equus caballus*) represents the natural host of EHV-1, EHV-2, EHV-3, EHV-4 and EHV-5 (Ostlund, 1993). The donkey (*Equus asinus*) is the natural host of EHV-6, EHV-7 and EHV-8,

formerly known as asinine herpesvirus (AHV) 1 (AHV-1), AHV-2 and AHV-3 respectively (Browning, Ficorilli and Studdert, 1988). The zebra (*Equus grevyi*) is the natural host of EHV-9 also known as gazelle herpesvirus (GHV) 1 (GHV-1) because it was first isolated from Thomson's gazelles (*Gazella thomsoni*) (Fukushi *et al.*, 1997; Abdelgawad *et al.*, 2016). To date, all EHV-9s isolated belong either to the *Alphaherpesviridae* or *Gammaherpesviridae* subfamilies according to the latest taxonomic classification (Davison *et al.*, 2009; Maclachlan *et al.*, 2017). The *Alphaherpesviridae* subfamily include EHV-1, EHV-3, EHV-4, EHV-6, EHV-8 and EHV-9 all belonging to the *Varicellovirus* genus, characterised by lytic infections (Davison, 2007; Bloom, 2016). On the other hand, the *Gammaherpesviridae* subfamily including EHV-2, EHV-5 belonging to the *Percavirus* genus and EHV-7 not yet assigned to a genus in the subfamily, do not give rise to lytic infection upon cell entry (Marenzoni *et al.*, 2015). Among EHV-9s, EHV-1 is considered the most severe EHV as its infection is associated not only to respiratory disease, but also to abortion, perinatal death and neurological disorders, including myeloencephalopathy known as Equine Herpesvirus Myeloencephalopathy (EHM) (Wilson, 1997; Lunn *et al.*, 2009).

| Host Species | Taxonomy Name | Other Name | Subfamily | Genus |
|-----------------------|---------------|-------------------------------|-----------|-----------------------|
| <i>Equus caballus</i> | EHV-1 | Equine abortion virus; EHM | α | <i>Varicellovirus</i> |
| | EHV-2 | Equine cytomegalovirus | γ | <i>Percavirus</i> |
| | EHV-3 | Equine coital exanthema virus | α | <i>Varicellovirus</i> |
| | EHV-4 | Equine rhinopneumonitis virus | α | <i>Varicellovirus</i> |
| | EHV-5 | Equine cytomegalovirus | γ | <i>Percavirus</i> |
| <i>Equus asinus</i> | EHV-6 | AHV-1 | α | <i>Varicellovirus</i> |
| | EHV-7 | AHV-2 | γ | Unassigned |
| | EHV-8 | AHV-3 | α | <i>Varicellovirus</i> |
| <i>Equus grevyi</i> | EHV-9 | GHV-1 | α | <i>Varicellovirus</i> |

Table 1: Equid herpesviruses. Modified from Paillot *et al.*, 2008.

1.1.2 Equid herpesvirus 1 (EHV-1)

1.1.2.1 Background history

EHV-1 was first associated with contagious epizootic abortion of pregnant mares in 1932 by observing the disease in mares inoculated with materials of aborted fetuses (Dimock and Edwards, 1932). Only later was the abortive virus was grown in *ex vivo* tissues and laboratory animals highlighting the pathological changes occurring (Anderson and Goodpasture, 1942; Randall *et al.*, 1953). Similar reproductive disorders plus respiratory disfunctions were documented in Hungary nearly a decade later (Manninger and Csontons, 1941), leading to the proposed association of viral abortion with equine influenza infections (Manninger, 1949; Doll, Wallace and Richards, 1954). However, later in 1963 this abortive virus was assigned as a member of the herpes group thanks to higher resolution at electron microscopy (Plummer and Waterson, 1963).

1.1.2.2 EHV-1 genome structure

In 1992, Telford *et al.* sequenced the full linear dsDNA genome of EHV-1 (150223 bp) from a purified clone of EHV-1 strain Ab4, also highlighting features of the genomic structure. As such, the genome structure is divided into a unique long (U_L, 112870 bp) and unique short (U_S, 11861 bp) regions both flanked by an inverted internal and terminal repeat sequences (IR_L/TR_L, 32bp and IR_S/TR_S, 12714 bp respectively) of different sizes (Henry *et al.*, 1981; Whalley, Robertson and Davison, 1981; Telford *et al.*, 1992). The genome contains 80 open reading frames (ORFs) encoding for 76 unique proteins, with four ORFs (ORF 64, 65, 66 and 67) duplicated at the TR_S (Telford *et al.*, 1992; Crabb and Studdert, 1993; Allen *et al.*, 2004). EHV-1 ORFs are tightly arranged showing little interposing or overlaps among them and few cases of exon splicing (Allen *et al.*, 2004; Figure 1). This gene disposition is typical among other sequenced alphaherpesviruses, especially EHV-4 which shares homologous genes with a degree of amino acids sequence identity ranging from 54.9 – 96.4 % (Telford *et al.*, 1992; Telford *et al.*, 1998). For instance, five genes (ORF 1, 2, 67, 71 and 75) in EHV-1 and EHV-4 genomes have no structural homologues when compared to other herpes sequences up to now (Allen *et al.*, 2004; Fukushi, Yamaguchi and Yamada, 2012). The functions of these genes have not been elucidated yet despite a few *in vitro* studies demonstrated their contribution to immune evasion and virus propagation (Sun *et al.*, 1996; Ma *et al.*, 2012; Hussey *et al.*, 2014), but they are believed to have had a major role during evolution and mechanisms of adaptation to the horse, their natural host (Allen *et al.*, 2004).

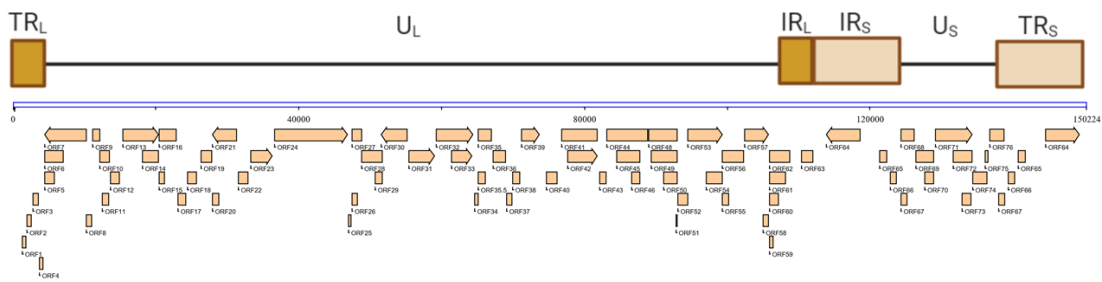


Figure 1: Schematic illustration of EHV-1 genome and functional ORFs. Upper diagram: EHV-1 genome structure is divided into a U_L and U_S regions (black lines) both flanked by an inverted internal and terminal repeat sequences (IR_L/TR_L as dark yellow rectangles and IR_S/TR_S as light brown rectangles) of different sizes. Designed with BioRender. **Bottom diagram:** Functional ORFs. The EHV-1 genome was imported from GenBank accession number: NC_001491.2 and generated with DNADynamo version 1.556 software (BlueTractor).

1.1.2.3 EHV-1 glycoproteins

The EHV-1 dsDNA genome is enclosed in an icosahedral nucleocapsid (100-110 nm in diameter) composed of six viral proteins (from ORFs 22, 25, 35, 42, 43 and 56) (Perdue *et al.*, 1974; Allen *et al.*, 2004). The structure and arrangement of capsids are similar across all herpesviruses (Baines, 2011; Brown and Newcomb, 2011), with 162 capsomers of which 12 pentons and 150 hexons, contribute to the overall structure, plus 12 portal proteins disposed in a ring permit passage of the viral DNA into the capsid (Newcomb *et al.*, 1989; Baker *et al.*, 1990; Paillot *et al.*, 2008). The tegument layer which resides in between the nucleocapsid and the envelope, is composed of twelve viral proteins (from ORFs 11, 12, 13, 14, 15, 23, 24, 40, 46, 49, 51, and 76) including enzymes involved during early stages of infection and essential to initiate viral replication (Batterson, Furlong and Roizman, 1983; Coulter *et al.*, 1993; Allen *et al.*, 2004; Paillot *et al.*, 2008). The viral envelope is the outer layer formed by patches of modified host cell membrane which surrounds the nucleocapsid and the tegument (Riaz *et al.*, 2017). Embedded on its surface there are twelve viral glycoproteins: glycoprotein (g) B (gB), gC, gD, gE, gG, gH, gI, gK, gL, gM and gN which are preserved across all alphaherpesviruses and are therefore named according to the HSV-1 nomenclature, plus gp2 which homologues have only been found in EHV-4 and EHV-8 (AHV-3) (Paillot *et al.*, 2008; Osterrieder and Van de Walle, 2010; Ren *et al.*, 2012; Figure 2).

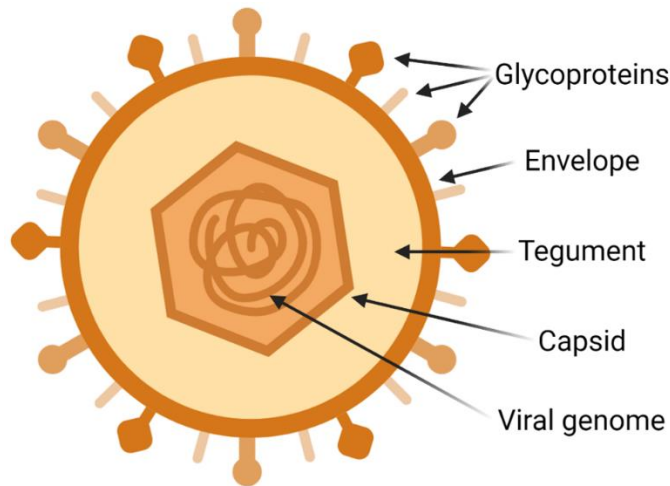


Figure 2: Schematic illustration of EHV-1 virion. Twelve glycoproteins are embedded on the envelope surface. A tegument layer resides below it with the dsDNA genome enclosed in the capsid. Designed with BioRender.

EHV-1 GPs play a crucial role in the infection process including viral attachment and entry by fusion of the viral envelope with the membrane of the susceptible host cells, cell to cell spread, egress, pathogenicity and promotion of inflammation as an immunologic response to infection (Osterrieder and Van de Walle, 2010; Ren *et al.*, 2012; Table 2). In the *Alphaherpesviridae* subfamily four glycoproteins (gB, gD, gH and gL) are required of viral entry, cell fusion and assembly of infectious virions (Cai *et al.*, 1988; Cai, Gu and Person, 1988; Highlander *et al.*, 1988; Huff *et al.*, 1988; Johnson and Ligas, 1988; Ligas and Johnson, 1988; Forrester *et al.*, 1992; Hutchinson *et al.*, 1992; Roop, Hutchinson and Johnson, 1993; Balan *et al.*, 1994; Davis-Poynter *et al.*, 1994; Wilson, Davis-Poynter and Minson, 1994; Heldwein and Krummenacher, 2008). The same glycoproteins were also found to be critical determinants for viral growth *in vitro* thus essential for infection (Ren *et al.*, 2012). The conserved gB, gH and gL performs as a fusion machinery during the fusion process by binding to entry receptors defining the cell tropism (Chowdary *et al.*, 2010; Eisenberg *et al.*, 2012). gB and gD are essential to viral penetration and cell-to-cell spread (Wellington, Love and Walley, 1996; Neubauer *et al.*, 1997b; Csellner *et al.*, 2000). Deletion of either gB, gD or gH did not permit entry of HSV-1 (Cai, Gu and Person, 1988; Desai, Schaffer and Minson, 1988; Ligas and Johnson, 1988). Viral attachment was observed in EHV-1 mutants lacking gD, however penetration of the susceptible host cell was not detected (Whittaker *et al.*, 1992). gH and gL are often referred as the gH-gL heterodimer since their strong interactions contribute to folding of the virion structure and create a tight complex (Chowdary *et al.*, 2010). In several HSV-1 studies, even in the absence of gB, the gH-gL heterodimer was able

to initiate the fusogenic process, suggesting a determining fusion role of gH (Subramanian and Geraghty, 2007; Galdiero *et al.*, 2008). gL is also necessary to process and incorporate gH onto the external layer of the host cell from which the viral envelope will derive. In an HSV-1 study, the surface envelope of mutants lacking gL was absent of both gH and gL (Roop, Hutchinson and Johnson, 1993). Other glycoproteins have also demonstrated active roles in EHV-1 viral entry and replication *in vitro* or *in vivo* such as gC (Neubauer *et al.*, 1997a; Osterrieder, 1999; Csellner *et al.*, 2000) or gK (Azab and El-Sheikh, 2012).

| Envelope GP | Function | Reference |
|-------------|--|-----------------------------------|
| gB | virus penetration and cell-to-cell spread | Neubauer <i>et al.</i> , 1997 |
| gC | attachment and egress | Osterrieder, 1999 |
| gD | virus entry and cell-cell fusion | Csellner <i>et al.</i> , 2000 |
| gE | cell-to-cell spread | Matsumura <i>et al.</i> , 1998 |
| gG | immunomodulatory (chemokine-binding) | Von Einem <i>et al.</i> , 2007 |
| gH | cell-to-cell spread | Azab, Zajic and Osterrieder, 2012 |
| gI | cell-to-cell spread | Matsumura <i>et al.</i> , 1998 |
| gK | virus penetration and cell-to-cell spread | Neubauer and Osterrieder, 2004 |
| gL | unclear - processing of gH in HSV-1 (Roop, Hutchinson and Johnson, 1993) | |
| gM | virus penetration and cell-to-cell spread | Osterrieder <i>et al.</i> , 1996 |
| gN | Processing of gM | Rudolph <i>et al.</i> , 2002 |
| gp2 | egress | Rudolph and Osterrieder, 2002 |

Table 2: Function of EHV-1 envelope glycoproteins. Modified from Paillot *et al.*, 2008.

1.1.3 EHV-1 lifecycle

1.1.3.1 Attachment and entry

EHV-1 is able to infect a large range of host cell types such as epithelial cells in the respiratory tract, endothelial cells of inner organs, mononuclear cells of lymphoid organs and peripheral blood mononuclear cells (PBMC) and cells of the nervous system (Osterrieder and Van de Walle, 2010). Cells are infected by direct contact with an infectious viral particle or by contact

with an infected cell (cell-to-cell spread) (Paillot *et al.*, 2008). As observed in many other alphaherpesviruses, EHV-1 infection is initiated by an unstable binding of gB and gC to heparan sulphate moieties rich in glycosaminoglycans on the host cell surface (Osterrieder, 1999; Frampton *et al.*, 2005). gD then interacts specifically with one of the cell surface receptors and triggers conformational changes, enabling interactions between gB and gH-gL and leading to viral entry (Sugahara *et al.*, 1997; Whitbeck *et al.*, 1997; Osterrieder, 1999; Csellner *et al.*, 2000; Spear, 2004; Frampton *et al.*, 2005; Azab *et al.*, 2010; Sasaki *et al.*, 2011). The major entry receptors across alphaherpesviruses are Nectin-1, known as herpesvirus entry mediator (Hve) C (HveC), and herpesvirus entry mediator (HVEM) known as HveA (Frampton *et al.*, 2005). The equine Major Histocompatibility Complex I (MHC-I) was identified as a unique EHV-1 entry receptor facilitating virus entry into equine dermal cells and equine brain microvascular endothelial cells (Kurtz *et al.*, 2010; Sasaki *et al.*, 2011). The same receptor strategy is exploited by EHV-4 (Azab *et al.*, 2014). Other receptors might be involved in EHV-1 entry as the virus is able to enter other cell types despite blocking of the MHC-I receptor with antibodies (Sasaki *et al.*, 2011). EHV-1 entry into the cell occurs by either viral envelope fusion with host plasma membrane (non-endocytic pathway) or by endocytosis, followed by the release of the EHV-1 nucleocapsid and tegument proteins into the cells to activate infection (Frampton *et al.*, 2007). The ability to reach the nucleus of the cell resides in the dynein motor protein which transports the nucleocapsid along microtubules, a typical mechanism found in other alphaherpesviruses. Especially in neurons in which the site of entry can be located far from the cell body, infection of alphaherpesviruses is facilitated by the microtubule-mediated transport through the axon to the nucleus (Sodeik, Ebersold and Helenius, 1997; Paillot *et al.*, 2008; Kukhanova, Korovina and Kochetkov, 2014). Once the nucleus is reached, the nucleocapsid directly binds to the nucleopore complex (NPC) and the viral genome is released into the nucleus while the capsid is left in the cytoplasm (Whittaker and Helenius, 1998; Ojala *et al.*, 2000).

1.1.3.2 Replication

Once the viral genome enters the nucleus, a series of temporally and sequentially ordered events takes place during transcription and replication of its genome, leading towards assembly of the progeny virus (van Lint and Knipe, 2009; Kukhanova, Korovina and Kochetkov, 2014). Three groups of regulatory genes coordinate transcription of EHV-1 genes: immediate early (IE) or α genes, early or β genes, and the late or γ genes (Gray *et al.*, 1987a). The EHV-1 tegument transactivator protein (ETIF), also known as VP16-E and homologue of HSV-1 α -

trans-inducing factor (α -TIF), triggers a signal cascade mechanism which activates α genes synthesised *ex novo* by cellular RNA polymerase II (Gray *et al.*, 1987a; Gray *et al.*, 1987b; Harty *et al.*, 1989; Kim, Holden and O'Callaghan, 1997; Garko-Buczynski *et al.*, 1998; von Einem *et al.*, 2006; van Lint and Knipe, 2009). α genes are necessary to promote expression of β and γ genes (Garko-Buczynski *et al.*, 1998). β genes encode proteins required to stimulate viral DNA replication (van Lint and Knipe, 2009), while the late genes encode for viral structure proteins, in particular those encoding for assembly of progeny virion particles (van Lint and Knipe, 2009; Kukhanova, Korovina and Kochetkov, 2014).

1.1.3.3 Egress

The viral nucleocapsid is assembled in the nucleus of the host cell, first as a precursor capsid, named procapsid, in the presence of scaffolding proteins of the tegument and free of the viral genome (Perdue *et al.*, 1976; Lee, Irmiere and Gibson, 1988; Rixon *et al.*, 1988; Mettenleiter, Klupp and Granzow, 2006; Paillot *et al.*, 2008; van Lint and Knipe, 2009). Once the procapsid has been formed, it is then filled with the viral dsDNA genome under the activity of a terminase enzyme, consisting of three subunit proteins (Yang, Homa and Baines, 2007). This stage marks the maturation of the procapsid into capsid surrounded by tegument proteins and acquires a primary envelope from budding through the inner nuclear membrane of the host cell (envelopment) (Mettenleiter, 2002). This first envelopment process is followed by a de-envelopment in which the newly formed nucleocapsid loses this nuclear envelope acquired from the first envelopment by direct fusion between the enveloped nucleocapsid and the outer nuclear membrane of the host cell (Mettenleiter, Klupp and Granzow, 2006). During the release of the "naked" nucleocapsid into the cytoplasm, new tegument proteins are acquired and once in the cytoplasm finalisation of the viral tegument occurs (Mettenleiter, 2002). A secondary envelopment occurs in the cytoplasmic compartments of the host cell at the trans-Golgi network incorporating all the viral glycoproteins contributing to the structural integrity of the matured virion (Mettenleiter, 2006; Mettenleiter, Klupp and Granzow, 2006; Johnson and Baines, 2011). The mature virus particle enclosed in a cellular vesicle is transported towards the plasma membrane and released into the extracellular space by direct vesicle-plasma membrane fusion (Whittaker and Helenius, 1998; Mettenleiter, Klupp and Granzow, 2009). Alternatively, the mature virion can infect adjacent cells via virus-induced fusion, escaping from neutralising antibodies of the host immune system (van Lint and Knipe, 2009). According to many studies, EHV-1 gB, gD and gH-gL heterodimer are involved in cell-to-cell fusion (Stokes *et al.*, 1996; Wellington,

Love and Walley, 1996; Csellner *et al.*, 2000). The mechanism is probably facilitated by additional glycoproteins such as gI, gE (Flowers and O’Callaghan, 1992; Matsumura *et al.*, 1998) gM and gK (Osterrieder *et al.*, 1996b; Wellington, Love and Whalley, 1996; Cselner *et al.*, 2000; Neubauer and Osterrieder, 2004). Infection of cells results in their lysis due to viral cytopathic effects following the replication cycle of EHV-1 virions (van Lint and Knipe, 2009; Figure 3).

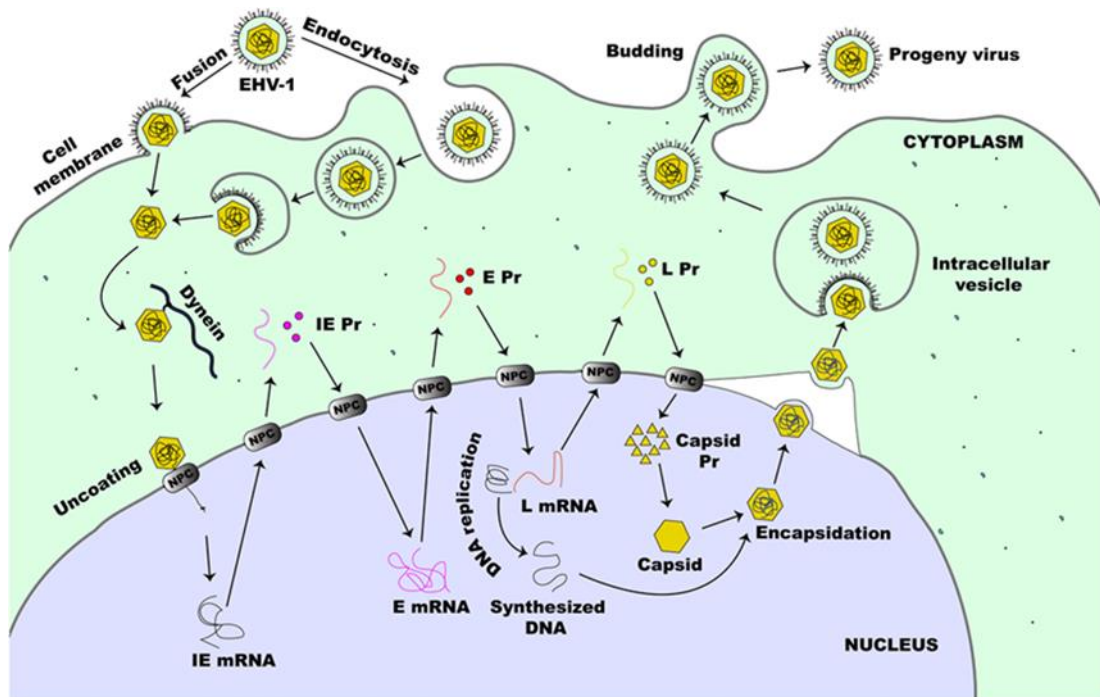


Figure 3: Schematic of EHV-1 lytic lifecycle. Source: Oladunni, Horohov and Chambers, 2019.

1.1.4 Latency and reactivation

A peculiarity of EHV-1, as all herpesviruses, is the establishment of ‘permanent residence’ within the cells of the susceptible host once primary infection occurs in the epithelium of the respiratory upper tract. During this latency the infected horse appears asymptomatic, showing no virus shedding or active cell-associated viremia (Allen *et al.*, 2004; Paillot *et al.*, 2008). At the genomic level, EHV-1 gene expression is suppressed resulting in inability to synthesise viral factors and no presence of active viral particles (Allen *et al.*, 2004; Paillot *et al.*, 2008). The preferred EHV-1 latent site occurs at the sensory neuron bodies in the trigeminal ganglia (Slater *et al.*, 1994b; Baxi *et al.*, 1995), although other studies have confirmed latency in circulating lymphocytes and draining lymph nodes in the lymphoid tissues (Welch *et al.*, 1992; Edington, Welch and Griffiths, 1994; Slater *et al.*, 1994b; Chesters

et al., 1997; Carvalho *et al.*, 2000; Allen, 2006; Allen *et al.*, 2008; Pusterla *et al.*, 2010). The prevalent site of EHV-1 latency was observed in CD5⁺/CD8⁺ T lymphocytes (about 80%), while findings in CD5⁺/CD8⁻/CD4⁻ cells represents a smaller sub-population (about 20%) (Smith *et al.*, 1998). The ability to establish a cycle of latent life-long presence in its host and then, once reactivated, spread to other susceptible horses appears as an intentional biological behaviour of survival and propagation. The only viral transcript expressed during latent EHV-1 form is the latency-associated transcript (LAT) a viral RNA transcribed from the α gene (Baxi *et al.*, 1995; Chesters *et al.*, 1997; Paillot *et al.*, 2008). How EHV-1 latency is dictated by molecular, physiological and immunological pathways has not been fully elucidated yet. However, from HSV studies, LAT seems likely to promote latency but has no role in its maintenance or in reactivating the latent virus (Javier *et al.*, 1988; Sedarati *et al.*, 1989; Steiner *et al.*, 1989). The initiation of latency might be triggered by a faulty activation of the α gene by HSV-1 VP16 (homologous protein to VP16-E) (Efstathiou and Preston, 2005). Reactivation of EHV-1 from latency is often associated with stressful events such as handling, transport, movement and weaning as much as that observed with corticosteroid or immunosuppressant administrations (Burrows and Goodridge, 1984; Edington, Bridges and Huckle, 1985; Edington, Welch and Griffiths, 1994; Slater *et al.*, 1994b) suggesting periodic virus shedding from asymptomatic horses with latent EHV-1 infection. Interleukin-2 (IL-2) has been shown to modulate EHV-1 latency (Smith *et al.*, 1998), same as the EHV-1 thymidine kinase gene (Field and Wildy, 1978; Becker *et al.*, 1984; Efstathiou *et al.*, 1989; Slater *et al.*, 1994b). It is presumed that reactivation of EHV-1 goes through a cascade of gene expression activated by the infected cell polypeptide 0 (ICP0) a cellular factor as it occurs in HSV (Paillot *et al.*, 2008). Reactivation of latent EHV-1 is not always associated to the appearance of typical clinical signs (i.e. mucus discharge, abortion, viremia etc), but it can also occur silently and meanwhile the horses are actively shedding the virus in the environment (Edington, Bridges and Huckle, 1985).

1.1.5 Epidemiology and transmission

EHV-1 is an ubiquitous pathogen across the worldwide horse population. It is believed that infection occurs during early stages of the horse life. According to Allen (2002), the infection rate is between 80 and 90% below the two years of age, however this estimate includes infection by the EHV-1 closest relative: EHV-4. Clinically, both EHV-1 and EHV-4 are associated with respiratory disease, but EHV-1 epizootics are much more serious because the virus can cause reproductive and neurological issues (Wagner *et al.*, 1992). Moreover,

complications arise by the fact that EHV-1 as well as EHV-4 establish a latent stage within their natural host employed as a survival technique to persist and disseminate within the equine population, and evade the host immune system (Whitley and Gnann, 1993). Reactivation of the latent virus happens periodically to sustain the biological cycle of the virus with shedding and clinical manifestation of the disease. Importantly, neurological pathologies have been associated with EHV-1 reactivation events leading to outbreaks (Pusterla *et al.*, 2021; Vereecke *et al.*, 2021). EHV-1 is able to infect susceptible hosts by direct contact with an infected horse (symptomatic or asymptomatic) through nasopharyngeal droplets (horizontal transmission) or indirectly through contact of infected material rich in infectious viral particles such as aborted foetus, placenta tissue or personnel as well as inanimate objects (fomite transmission) (Allen *et al.*, 2004; Lunn *et al.*, 2009). Foals are extremely subjected to EHV-1 infection especially within their first month of life through horizontal transmission facilitated by the close contact between the foal and the infected mares since pregnancy and partum represent a stressful event causing reactivation of the latent virus in the mare (Gilkerson *et al.*, 1999). To identify and differentiate the type of EHV involved, the PCR could be employed as a sensitive and rapid technique (Sharma *et al.*, 1992; Wagner *et al.*, 1992; Kirisawa *et al.*, 1993). There is a high antigenic cross-reactivity between natural infection by EHV-1 and EHV-4, and these cross-reactivity responses hinder the possibility of defining an annual record of EHV-1 infection. These overlapping results are due to the lack of a type specific antibody test complicating sero-epidemiological studies (Patel and Heldens, 2005). Nonetheless, Crabb, Nagesha and Studdert (1992) demonstrated it was possible to differentiate antibodies between EHV-1 and EHV-4 in polyclonal equine sera by a type specific antibody response elicited to the gG envelope protein of the two EHV types. The difference resides in the carboxyl domain of gG determining its antigenic features and therefore permitting differentiation between the unique humoral response elicited in the horse of the two EHV-1 and EHV-4 (Crabb, Nagesha and Studdert, 1992; Crabb and Studdert, 1993).

1.1.6 Pathogenesis

EHV-1 infection first takes place in the nasal and mucosal epithelial cells in the respiratory upper tract facilitated by the absence of a protective mucosal immunity (Patel, Edington and Mumford, 1982; Kydd *et al.*, 1994; Rusli *et al.*, 2014). Following active replication, the virus breaches the epithelial layer of the respiratory upper tract and the draining lymph nodes followed by an acute inflammation response. In addition, cell necrosis is clinically exhibited by pyrexia and nasal discharge associated with shedding of infectious particles (Paillot *et al.*,

2008). The seriousness of the respiratory infection depends on several factors such as age, immune status and health condition of the infected horse. For instance, when young naïve horses get infected might manifest more severe clinical signs, while older horses previously exposed to EHV-1 infection could have reduced symptoms (Allen, 2002; Allen *et al.*, 2004). Hygiene in the animal environment also influences the progression of the disease (Mumford and Rossdale, 1980). From the primary site of infection, EHV-1 spreads systemically by infecting mucosal monocytes reaching the deep connective tissue of the respiratory tract (Kydd *et al.*, 1994; Gryspeerdt *et al.*, 2010; Vandekerckhove *et al.*, 2010), as well as the basal membrane establishing in the lymphatic and reticuloendothelial system by infecting leucocytes and endothelial cells in the blood and lymphatic vessels within four to six days post infection (Kydd *et al.*, 1994; Gryspeerdt *et al.*, 2010) in which EHV-1 replicates and amplifies its progeny provoking a cell-associated viremia that could last nine to fourteen days (Patel, Edington and Mumford, 1982; Dutta and Myrup, 1983; Scott, Dutta and Myrup, 1983; Edington, Bridges and Patel, 1986). At this stage, EHV-1 is able to disseminate to further locations invading the uterus in pregnant mares or the central nervous system establishing its third site of infection with the high risk to cause two concerning clinical outcome such as abortion or EHM (Mumford *et al.*, 1994; Slater *et al.*, 1994a; Allen *et al.*, 2004; Figure 4). The severity of the disease is most likely associated to the strain of the virus. Indeed, despite all EHV-1 strains are potentially inducing the respiratory form, depending on the outcome of the disease (either abortion or EHM), EHV-1 is described as either non-neuropathogenic (known as abortigenic) or neuropathogenic (known as paralytic) respectively (Allen and Breathnach, 2006; Nugent *et al.*, 2006). Comparison studies between two EHV-1 strains, Ab4 a neuropathogenic strain (Crowhurst, Dickinson and Burrows, 1981) and V592 a non-neuropathogenic strain (Mumford *et al.*, 1994; Smith *et al.*, 2000) demonstrated consistent differences in pathogenicity. This distinction is due to the viral DNA polymerase encoded by ORF30, in which a point mutation at nucleotide 2254 substitutes the base adenine (A) to guanine (G) (A→G₂₂₅₄) resulting in a change of the amino acid in position 752 from asparagine (N) to aspartic acid (D) (N→D₇₅₂) (Nugent *et al.*, 2006; Goodman *et al.*, 2007; Van de Walle *et al.*, 2009). Nugent *et al.*, (2003; 2006) found a significant association of the mutation with the development of EHM in the horse ($p < 0.0001$), suggesting an important function role of the amino acid position in the DNA polymerase. Nevertheless, virus strains without the N→D₇₅₂ mutation have been isolated in several outbreaks with horses suffering with neurological signs (Goehring *et al.*, 2006; Nugent and Paillot, 2009; van Galen *et al.*, 2015; Garvey *et al.*, 2019; Dunuwille *et al.*, 2020; Pusterla *et al.*, 2020; Sutton *et al.*, 2020; Vereecke

et al., 2021). For instance, during the 2021 EHV-1 outbreak in Valencia (Spain), the virus did not belong to the so-called neuropathogenic strain but to other viruses circulating for several years in Europe (Sutton *et al.*, 2021; Vereecke *et al.*, 2021) suggesting that there are no specific neuropathogenic EHV-1 virus strains, and that any strain can lead to respiratory, reproductive and neurological signs. The N→D₇₅₂ mutation also showed good employment in the diagnostic sector by real time PCR (RT-PCR) able to distinguish neuropathogenic and non-neuropathogenic EHV-1 strains using allelic discrimination and correlates to different intensities of associated viremia in PBMC (Allen, 2006; Allen, 2007). *In vivo* studies demonstrated that the neuropathogenic EHV-1 strains produce active levels of viremia, contributing to its magnitude and longer-lasting duration, compared to the one provoked by non-neuropathogenic strain, thus associated with higher levels of virulence (Allen and Breathnach, 2006; Allen, 2006). Other factors might be involved in regulating the virulence levels such as the induction of an inflammatory response in the host or structural changes of viral components. Upregulation of specific inflammatory genes following infection of endothelial cells might induce a raised magnitude of vasculitis provoking associated damages to the nervous tissue, thus contributing to a higher risk to develop of EHM (Johnstone *et al.*, 2016). EHV-1 strains gaining amino acids mutations leading to glycoprotein structural changes may be more advantaged in terms of their cycle (attachment, entry or other functions glycoprotein dependent). As such they might show more efficient replication and able to induce important damages contributing to the level of severity of the disease.

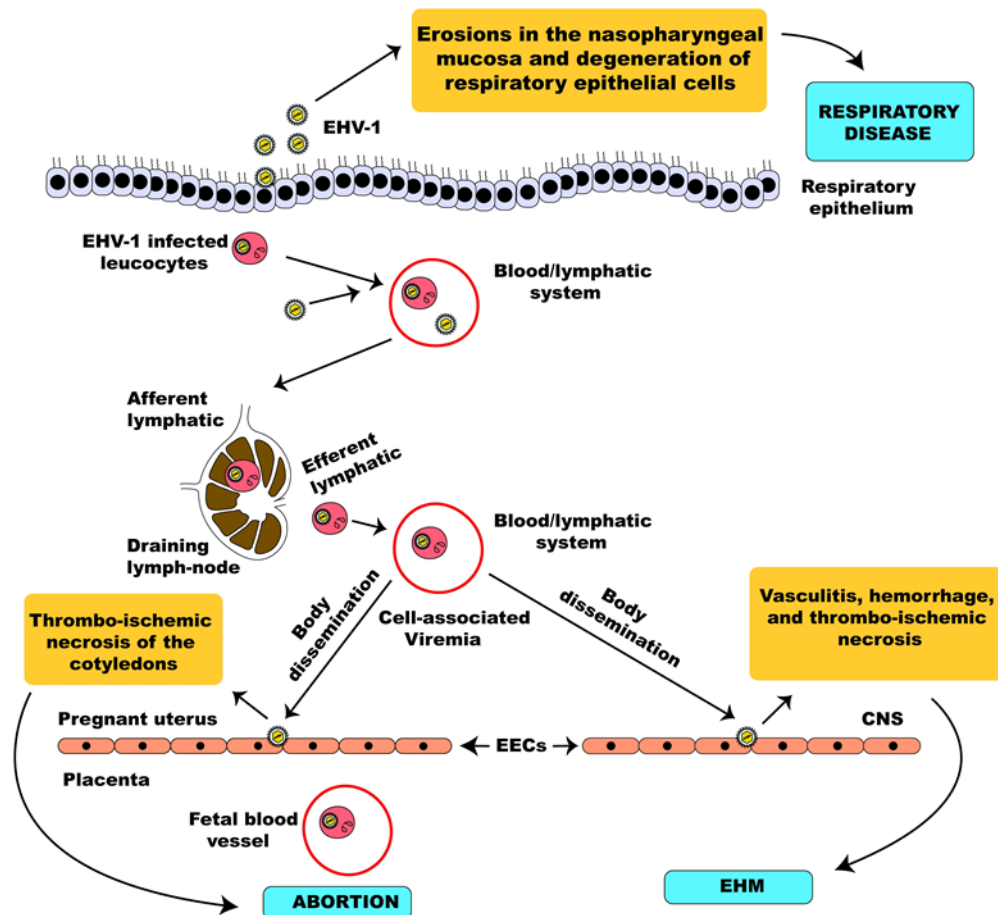


Figure 4: Schematic of EHV-1 pathogenesis. Source: Oladunni, Horohov and Chambers, 2019.

1.1.7 EHV-1 and the host immune response

Understanding how the host responds to EHV-1 infection would be a valuable tool to develop diagnostic resources and effective immunotherapies. However, it is not fully clear how EHV-1 interact with the host immune system. Therefore, further insights would be useful.

1.1.7.1 Innate immune response

It was shown during early stages of EHV-1 infection how the host immune system reacts by activating an inflammatory response with a predominance of cytokines (Kydd *et al.*, 1994; Johnstone *et al.*, 2016). An increase of the percentage of neutrophils accompanied by a decrease of macrophages and lymphocytes was observed in the respiratory tract as a first response to EHV-1 infection following inflammation of the lung tissue and lysis of leucocytes (Kydd, Hannant and Mumford, 1996). Furthermore, a significant increase of CD8⁺ T lymphocytes was detected at the bronchioalveolar level as well as an increase of the interferon type I (INF α/β) was reported in nasal secretions and serum samples from EHV-1 experimentally infected ponies (Edington, Bridges and Griffiths, 1989). The active role of

INF α / β immunomodulates both the innate and the adaptive immune response (Edington, Bridges and Griffiths, 1989).

1.1.7.2 Adaptive immune response

Following this first upregulation of pro-inflammatory cytokines, an adaptive immune response is triggered which focuses on eliminating the viral particles but depending on its magnitude it might be counterproductive and induce disease pathology (Paillot *et al.*, 2008). In any case, immunity to EHV-1 is short-lived and its duration has also been at the centre of debates since horses are still susceptible to re-infections even after vaccination (van der Meulen *et al.*, 2006). The presence of virus neutralising (VN) and complement fixing (CF) antibodies are used in serology to demonstrate exposure to EHV-1 infection. However, due to pre-existing antibodies to either EHV-1 or EHV-4 as the result of prior infection or vaccination, serology is less useful as a diagnostic tool (Balasuriya, Crossley and Timoney, 2015). EHV-1 specific antibodies have been detected within two weeks after EHV-1 infection and different isotypes have been recognised: IgGa, IgGb, IgGc, IgGd, IgG(T) and IgM (Sugiura *et al.*, 1994; Paillot *et al.*, 2008; Wagner *et al.*, 2015; Perkins *et al.*, 2019), and their response is specific to the viral envelope glycoproteins' epitopes (Allen and Yeargan, 1987; Crabb, Allen and Studdert, 1991; Packiarajah *et al.*, 1998; Perkins *et al.*, 2019). VN were found more durable than CF antibodies (approximately one year compared to three months), however the level of protection from infection is controversial. Despite the presence of circulating VN antibodies and mucosal antibodies of the IgA isotype promote protection of the respiratory upper tract during the initial respiratory infection and reduce the amount and duration of nasopharyngeal viral shedding (Mumford *et al.*, 1987; Hannant *et al.*, 1993), their potential is limited once a cell-associated viremia is established as they are not able to reach the intracellular level. During this stage, as for other intracellular pathogens, the activation of a cytotoxic T lymphocyte (CTL) response by interferon (IFN) γ (IFN- γ) plays an important role in eliminating virus-infected cells. IFN- γ is a well-known cell-mediated marker used to measure human immune response to herpesvirus infections which has found application in veterinary studies (Breathnach *et al.*, 2005; Paillot *et al.*, 2005; Paillot *et al.*, 2006). IFN- γ promotes antigen presentation to cells of the adaptive immune response and the synthesis of T helper 1 lymphocytes, thus contributing to increase cell-mediated immunity. Protection from clinical signs of the pathology caused by EHV-1 has been shown to correlate to the frequency and levels of circulating CTLs. Less clinical signs and higher levels of EHV-1 specific circulating CTL were found in adult ponies which had higher chances of being previously

exposed to EHV-1 compared to findings in younger ponies in which an EHV-1 specific CTL response was lower (O'Neill *et al.*, 1999; Paillot *et al.*, 2007). Higher frequencies of EHV-1 specific CTL precursors were also observed by inducing repeated exposures to EHV-1 (O'Neill *et al.*, 1999). These findings suggest the potential of EHV-1 specific CTL precursors or memory cell activation after subsequent stimulations from infection or vaccination during the host lifecycle or by reactivation of latent EHV-1. Therefore, the CTL response of cell mediated immunity may find useful application to test efficacy of EHV-1 vaccines for horses (Paillot *et al.*, 2008).

1.1.8 Vaccines

Vaccination alongside proper hygiene and management measures remains a good control practice to fight EHV-1 infection, although its effectiveness has not completely proven to provide a reasonable level of protection against EHV-1 disease especially when cell-associated viremia has been identified leading to abortion or EHM (Allen *et al.*, 2004). Indeed, a good vaccine candidate should contribute to stimulating the whole host immune system, awakening both the humoral and cellular immune response able to protect from EHV-1 infection, the further development of the respiratory disease and potentially preventing the dissemination of EHV-1 within the host system and then eventual shedding in the environment to other susceptible horses. The vaccines currently available on the market can be grouped into two, either as modified live or inert vaccines. Modified live vaccines (MLV) include artificially attenuated virus generated by deletion of the IR6 protein (ORF 67) (Osterrieder *et al.*, 1996a), meanwhile the latter are based on inactivated virus, known as killed whole virus vaccines, and are at the most frequent commercialised vaccines (Ma, Azab and Osterrieder, 2013). Inactivated vaccines are able to provide variable levels of protection by first inducing VN antibodies which promote protection of the respiratory upper tract during the initial respiratory infection and reduce the amount and duration of nasopharyngeal viral shedding thus reducing clinical respiratory symptoms (Mumford *et al.*, 1987; Hannant *et al.*, 1993). MLV vaccines are considered better immunomodulators of both humoral and cell mediated immunity after administration compared to whole inactivated ones (Ma, Azab and Osterrieder, 2013). However, no vaccine to date has been able to stimulate the cellular immune response enough to significantly hinder the intracellular life cycle of the virus and so protect against EHV-1 re-infection following latency and sequela infection. Pregnant mares are under a strict vaccination protocol with administration at the 5th, 7th and 9th month of gestation, but the induction of the humoral immune response does

not efficiently protect from abortion despite the satisfactory response detected with high levels of VN antibodies in the mare (Mumford *et al.*, 1994). Development of new vaccines is focussed on improving the induced immune response, providing strong protection and alleviation of the severity of clinical signs, and reduce viral shedding. The new MLV vaccines are based on the current circulating strains thus more similar genetically to the epidemic EHV-1 strains, but attenuation of targeted genes associated to virulence has not been fully optimised creating a matter of safety concern (Ma, Azab and Osterrieder, 2013). Subunit proteins vaccines have specific gene deletions aiming to lower their virulence (i.e. α gene, viral glycoproteins) or immune evasion. However, this category has not led to a satisfactory immune response but only partial protection, despite their safety (Neubauer *et al.*, 1997a; Matsumura *et al.*, 1998; Tsujimura *et al.*, 2009; Ma, Azab and Osterrieder, 2013). Lastly, recombinant vaccines expressing viral glycoproteins or other viral genes remains questionable in terms of efficacy. A case study demonstrated a recombinant vaccine expressing EHV-1 α gene (ORF 64) induced protection from clinical signs and cell-associated viremia, but the level of VN antibodies was low and did not prevent abortion or EHM occurred (Soboll *et al.*, 2010). Nevertheless, to help reduce the severity of EHV-1 related clinical manifestation it is still recommended to vaccinate horses which are likely to be at risk of exposure to EHV-1 infection (World Organisation for Animal Health – OIE Terrestrial Manual, 2018).

1.1.9 Laboratory diagnosis

When clinical signs appear following an EHV-1 infection, it is difficult to give a precise diagnosis of the disease pathogen since other viral equine infections (e.g. influenza, adenovirus) might manifest a similar outcome, at least regarding the respiratory form. Thus, PCR is considered a valuable diagnostic tool to immediately identify and detect EHV-1 genomic material extracted from either clinical or pathological samples (nasal swabs, nasal discharges, aborted foetus, placenta, brain, spinal cord, infected cell culture or paraffin-embedded tissues) (Ballagi-Pordany *et al.*, 1990; Borchers and Slater, 1993; Kirisawa *et al.*, 1993; Lawrence *et al.*, 1994; Mackie *et al.*, 1996). RT-PCR is more sensitive compared to the classic PCR as it is capable to discriminate neurological from non-neurological EHV-1 strains by allelic discrimination of viral nucleic acid in position 2254 (ORF30) either A_{2254} or G_{2254} (Allen, 2007; Smith *et al.*, 2012). Nonetheless, the genetic outcome is often but not always directly correlated to the clinical manifestation of EHM. PCR is not able to determinate replicative ability of the virus. As such, it is recommended to combine PCR with virus isolation,

considered the gold standard technique to diagnose EHV-1. *In vitro* isolation of the virus occurs using various cell lines of different origin such as equine (endothelial cells; EEC), rabbit (rabbit kidney; RK13), non-human primate (African green monkey kidney; Vero) or cattle (Madin-Darby bovine kidney; MDBK) (Allen *et al.*, 2004; Rybachuk, 2009). A typical cytopathic effect (CPE) caused by infection can be observed. Cells appear clustering together, enlarged, rounded and herpetic, detaching easily from the surface (Allen *et al.*, 2004). For epidemiological studies (Sutton *et al.*, 2020) it is therefore useful to combine the two diagnostic techniques to characterise EHV-1. Positive EHV-1 infection has been demonstrated by direct detection of the viral antigen using immunofluorescence (Allen, 2002) or by observation of histopathological lesions via immunohistochemistry (Allen *et al.*, 2004).

1.1.9.1 Serology

Diagnosis of EHV-1 infection is also possible by serology using either virus neutralisation (VN) (Thomson *et al.*, 1976), complement fixation (CF) (Thomson *et al.*, 1976) or enzyme-linked immunosorbent assay (ELISA) (Crabb *et al.*, 1995). Demonstration of a humoral antibody response to EHV-1 by serological assay is one method to demonstrate exposure to EHV-1. However due to cross-reactivity of antibodies among EHV-1 especially EHV-4 as a result of prior infections or vaccination, a type-specific diagnosis is difficult to obtain (Hartley *et al.*, 2005; Balasuriya, Crossley and Timoney, 2015). Nevertheless, serology is employed for seroprevalence surveys (Gilkerson *et al.*, 1999; Gilkerson, Love and Whalley, 2000; Pusterla *et al.*, 2009; Dunowska *et al.*, 2015; El Brini *et al.*, 2021), to monitor the response to vaccination (Bresgen *et al.*, 2012; Bnnai *et al.*, 2019; Warda *et al.*, 2021; Abousenna *et al.*, 2022) and occasionally as an adjunct to inconclusive PCR results and during an outbreak situation to confirm or exclude recent virus circulation as recommended by the European Food Safety Authority (EFSA; EFSA, 2022). EHV-1 can be serologically detected by screening paired sera samples collected from suspected cases during the acute and convalescent stages of infection against type-specific antigen able to demonstrate seroconversion or a greater increase of 4-fold rise in antibody titre that is the highest dilution of serum which neutralisation/binding is detected (OIE Terrestrial Manual, 2018). Currently there are neither standardised laboratory protocols to perform serological tests nor reagents recognised as standards, thus direct comparison of serological results among laboratories is problematic due to the frequent variables (Balasuriya, Crossley and Timoney, 2015).

a. Virus neutralisation test

A virus neutralisation (VN) or serum neutralisation test is based on the ability to detect the specific neutralising IgG immune response to EHV-1 (Thomson *et al.*, 1976). On the other hand, the IgG response to EHV-4 reacts to both EHV-1 and EHV-4 induced by cross-reactive antibodies towards common epitopes on both viruses (Balasuriya, Crossley and Timoney, 2015). For EHV-1, the IgG immune response starts from 8 to 10 days post infection (dpi) with peaks around 30 to 40 dpi, and persists for more than 9 months (Thomson *et al.*, 1976). Because the VN levels are detectable some time after the acute phase of EHV-1 infection, seroconversion is assessed by serological surveys demonstrating seroconversion or a significant increase (4-fold rise) in VN antibody titres from paired samples collected 14 to 28 days apart (OIE Terrestrial Manual, 2018; Figure 5). At present a VN titre to confer protection has not been assessed yet because the currently available vaccines do not provide complete protection as they especially stimulate high titres of circulating antibodies and are unlikely to stimulate cytotoxic effector lymphocytes (Soboll *et al.*, 2006). Nevertheless, inactivated virus vaccines can stimulate high titres of serum VN antibody, which were demonstrated to reduce the amount and duration of virus shedding and prime the mucosal compartment (Breathnach *et al.*, 2001; Kydd *et al.*, 2006), as well as protect animals from clinical disease and reduce the amount and the duration of viral excretion by the respiratory route (Di Francesco *et al.*, 2020). Several studies have shown contradictory results with respect to the type specificity of antibody detection by use of VN (Burrows, Goodridge and Denyer, 1984; Mumford and Bates, 1984; Edington and Bridges, 1990). It has been reported that assay conditions and the virus strains can markedly influence the sensitivity and type specificity of the VN tests (van Maanen, de Boe-Luijtzte and Terpstra, 2000). Assay variation between laboratories may be inherent in the strains of viruses used and the antigenic relatedness of EHV-1 and EHV-4 strains. Furthermore, the susceptibility of different cell types or even the same cell type in different laboratories may influence the VN assay results of antibody titers against EHV-1 or EHV-4 (Hartley *et al.*, 2005).

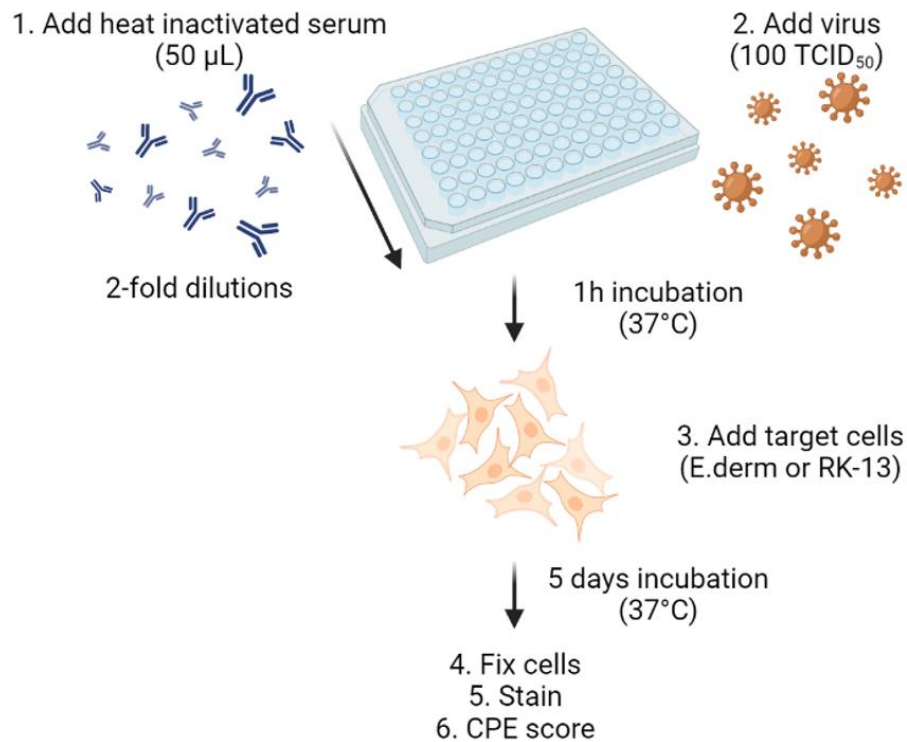


Figure 5: VN assay. Schematic following the World Organisation for Animal Health method (OIE Terrestrial manual, 2018). Designed with BioRender.

b. Complement fixation test

The CF test is based on an antibody-antigen reaction resulting in fixation of serum complement. If the sample contains desired antibodies or antigens, the antibody-antigen complex will be formed in the sample after the addition of a complementary reactant (usually guinea pig serum), and the haemolytic indicator system will not be able to react to the added complement since it already gets fixed with the antibody-antigen complex, thus resulting in no haemolysis of red blood cells (RBC). Complement fixing antibodies generally occur early after EHV-1 infection and persist for a limited time only. Thus, this test is not employed for sero-epidemiological studies. CF measures a high specific IgM response to EHV-1 which permits discrimination among EHV-1 only in primary infections. However, similarly to the VN assay, contradictory results with respect to the type specificity of antibody detection by use of CF assay have been shown in several studies (Burrows, Goodridge and Denyer, 1984; Mumford and Bates, 1984; Edington and Bridges, 1990). It has been reported that assay conditions and the virus strains can markedly influence the sensitivity and type specificity of the CF tests in terms of non-specific haemolysis (van Maanen, de Boe-Luijtzte and Terpstra, 2000; Bannai *et al.*, 2013). The presence of IgM antibodies is detected from 4 to 5 dpi with peaks around 20 to 30 dpi and decreases to undetectable levels within 60 to 80 dpi (Thomson

et al., 1976). Current acute or recent EHV-1 infection is suspected if high CF antibody titres are observed. Nonetheless, seroconversion is assessed similarly to VN by demonstrating seroconversion or a significant increase (4-fold rise) in CF antibody titres from paired samples collected 14 to 28 days apart (OIE Terrestrial Manual, 2018). The CF test is not as used as the VN assay for routine detection of EHV-1. However, CF assay is widely accepted method of detecting antibody to EHV-1 (or EHV-4) (OIE Terrestrial Manual, 2018) and it has been employed to investigate the response to EHV-1 vaccination (Kydd, Watrang and Hannant, 2003; Bannai *et al.*, 2013).

c. ELISA

ELISA is an easier technique to perform compared to VN and CF and is used for high throughput screening of many sera samples for EHV-1 antibodies. The most widely approach is the indirect ELISA (Dutta, Talbot and Myrup, 1983) and here described. First, the multiwell plate is coated with EHV-1 antigen. Once the protein-binding site is blocked in the coated wells, the diluted primary antibody (sera or monoclonal antibodies) is then added. After incubation, a conjugated secondary antibody is added which is able to recognise the primary antibodies. Following further incubation, an appropriate substrate solution is added and the assay is measured using an appropriate plate reader. The ELISA readings are eventually converted to antibody titer in serum (Sugiura *et al.*, 1997; Warda *et al.*, 2021). As for VN assay, it measures the IgG response, and as such is subjected to cross-reactivity between EHV-1 and EHV-4 antibodies (Balasuriya, Crossley and Timoney, 2015). A type-specific ELISA was developed based on the ability to discriminate between EHV-1 and EHV-4 IgG antibodies specific to antibodies specific to the variable region at the C terminus of gG epitope (Crabb and Studdert, 1993; Crabb *et al.*, 1995). Many epidemiologic studies used this latter technique to differentiate horses infected with EHV-1 from those with serum antibodies against EHV-4 (Hartley *et al.*, 2005; Goodman *et al.*, 2006; Hussey *et al.*, 2011; El Brini *et al.*, 2021). A further experimental ELISA was able to discriminate a specific humoral response induced by peptide antigens derived from a unique immunodominant region of EHV-1 gE (Andoh *et al.*, 2013) and EHV-4 gG (Lang *et al.*, 2013). Further validation of this technique could permit its use as a valuable cost-effective alternative and reliable tool for serological EHV-1/EHV-4 diagnosis and could be accepted as a routine test (Lang *et al.*, 2013) including seroprevalence studies (Abdelgawad *et al.*, 2015). Nonetheless, seroconversion is assessed similarly to VN and CF assays by demonstrating seroconversion or a significant increase (4-

fold rise) in ELISA-detectable antibodies from paired samples collected 14 to 28 days apart (OIE Terrestrial Manual, 2018).

1.2 Influenza viruses

1.2.1 Classification and nomenclature

Influenza viruses belong to the *Orthomyxoviridae* family, as assigned by the ICTV (Walker *et al.*, 2021), and to Group V in the Baltimore classification system (Baltimore, 1971) since they possess a segmented negative sense single-stranded RNA (ssRNA) genome. Four influenza types, A, B, C and D can be distinguished on the basis of internal protein, antigenic and phylogenetic characteristics. Type A can infect a wide range of avian and mammalian species, including humans (Webster *et al.*, 1992), while type B circulates only among humans and seals (Osterhaus *et al.*, 2000) with a few reported cases in horses, dogs and pigs (Chang *et al.*, 1976; Kawano *et al.*, 1978; Ran *et al.*, 2015). Types A and B are associated with seasonal influenza, whereas only A produces pandemics among humans, such as the one in 1918 leading to more than 50 million deaths (Taubenberger and Morens, 2006; Khanna *et al.*, 2013) and recurring outbreaks among avians (Guan and Smith, 2013), pigs (Ouchi *et al.*, 1996), dogs (Voorhees *et al.*, 2017), horses (Olguin-Perglione *et al.*, 2020) and seals (Zohari *et al.*, 2014). Type C can produce mild diseases in humans (Crescenzo-Chaigne, Barbezange, van der Werf, 2008) and found in pigs (Guo *et al.*, 1983), dogs (Ohwada *et al.*, 1987) and dromedary camels (Salem *et al.*, 2017). Type D was first isolated in pigs in 2011 (Hause *et al.*, 2013) and later its host range extended to cattle (Hause *et al.*, 2014) and small ruminants (Quast *et al.*, 2015). No human has been detected with type D, however serological findings suggest that it can infect humans (White *et al.*, 2016) thus representing a potential threat to human health. Influenza A viruses are classified into subtypes defined by their envelope glycoproteins haemagglutinin (HA) and neuraminidase (NA) based on antigenic (Tumová and Schild, 1972) and phylogenetic (Röhm *et al.*, 1996) characteristics. To date there are 16 HA and 9 NA avian influenza subtypes, some of which are also seen in mammals (Kawaoka *et al.*, 1990; Röhm *et al.*, 1996; Fouchier *et al.*, 2005), plus two bat derived subtypes, H17 and H18 based solely on isolated RNA sequences (Tong *et al.*, 2012; Tong *et al.*, 2013). The different HA subtypes are grouped into two lineages based on phylogenetic similarity: Group 1 (H1, H2, H5, H6, H8, H9, H11, H12, H13, H16, H17 and H18) and Group 2 (H3, H4, H7, H10, H14 and H15). Also, the NA subtypes are grouped into two lineages: Group 1 (N2, N3, N6, N7 and N9) and Group 2 (N1, N4, N5 and N8) with N10 and N11 not yet assigned (Wu *et al.*, 2014). The reservoir for Type A viruses is migratory, often aquatic birds, which can infect other birds including

domestic poultry (Webster et al., 1992). Influenza A viruses are further classified in Highly Pathogenic Avian influenza (HPAI) and Low Pathogenic Avian influenza (LPAI) depending on the pathological phenotypes and biological properties (OIE Terrestrial Manual, 2021). HPAI causes devastating losses in the poultry industry worldwide and pose a great concern for initiating a new pandemic due to repeated zoonotic transmissions to humans (Gohrbandt *et al.*, 2011). On the other hand, LPAI results in a subclinical outcomes or mild disease for example leading to drops in egg production, delays in growth, or exacerbation of underlying conditions or other disease (Suarez, 2010). The current nomenclature of influenza virus strains follows a specific order reported separated by forward slashes starting with influenza type, followed by the common or scientific name of the host species (when not human), the geographical origin where first isolated, the isolate number, and the year of isolation. Furthermore, for influenza A virus, the HA and NA subtypes are also reported in parentheses (World Health Organization – WHO, 1980; Figure 6).

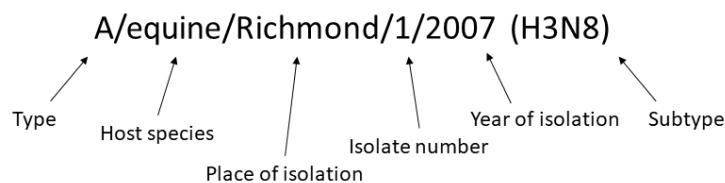


Figure 6: Example of nomenclature of Influenza virus. Designed with Microsoft® PowerPoint™.

1.2.2 Structure

Influenza virions are pleomorphic (varying in size from spherical to filament shapes), enveloped particles (80 – 170 nm) where the envelope is acquired during viral budding and thus composed of materials of cellular host origin organised in a single lipid bilayer (Gerl *et al.*, 2012). The envelope includes three different proteins: two spike glycoproteins, HA and NA (Laver and Kilbourne, 1966), in a 4:1 ratio respectively (Webster, Laver and Kilbourne, 1968) and the transmembrane ion-channel M2 (Zebedee and Lamb, 1988; Figure 7). This is the case for influenza A and B, while in influenza C and D the two major glycoproteins are replaced by a single unit known as haemagglutinin-esterase-fusion (HEF) protein, which possess HA and NA activity (Rosenthal *et al.*, 1998). Beneath the lipid envelope, the core is organised with the matrix proteins (M1), the non-structural proteins (NS1 and NS2 known as nuclear export proteins or NEPs), and the viral ribonucleoprotein complexes (vRNPs)

enclosing the influenza ssRNA genome. This genome is tightly associated in a stoichiometric manner to the nucleoprotein (NP) by opposite charge attraction and to the heterotrimeric polymerase complex, consisting of the polymerase basic proteins (PB1 and PB2) and the polymerase acid protein (PA) (Compans, Content and Duesberg 1972; Heggeness *et al.*, 1982; Ruigrok and Baudin, 1995). The genome is structured into eight different individual segments of viral RNA (vRNA) each of them encoding for one or more proteins for a total of 17 (Vasin *et al.*, 2014; Table 3).

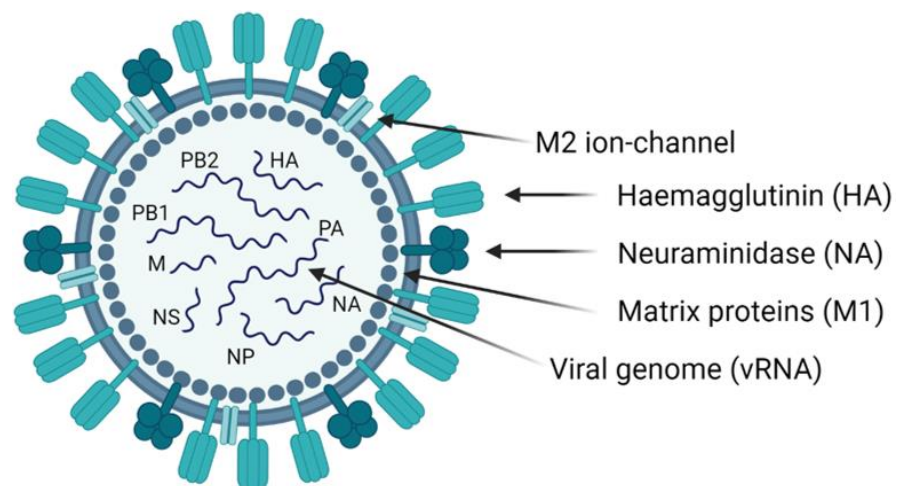


Figure 7: Structure of an Influenza virion. On its surface, three major envelope glycoproteins reside: HA, NA and M2 ion-channel. Underlying the lipid envelope: M1 and eight vRNA segments. Designed with BioRender.

| vRNA segment | Protein | Function |
|--------------|-----------|---|
| 1 | PB2 | vRNP subunit involved in host-mRNA cap recognition |
| 2 | PB1 | vRNP subunit involved in RNA chain elongation |
| | PB1-N40 | Maintain balance between PB1 and PB1-F2 |
| | PB1-F2 | Virulence factor and pro-apoptotic activity |
| 3 | PA | vRNP subunit involved in cap-snatching mechanism |
| | PA-X | Modulates host response and viral virulence |
| | PA-N155 | Not clear yet, but maybe involved in viral replication |
| | PA-N182 | |
| 4 | HA | Surface glycoprotein involved in receptor binding and membrane fusion |
| 5 | NP | Major component of vRNP involved in nuclear RNA transport |
| 6 | NA | Surface glycoprotein with sialidase activity |
| 7 | M1 | Membrane protein involved in nuclear export of vRNP |
| | M2 | Membrane ion channel for proton conductance |
| | M42 | M2 function in M2-null viruses |
| 8 | NS1 | Modulate virus-host interaction |
| | NS2 (NEP) | Nuclear export of vRNP |
| | NS3 | Not clear yet, but maybe involved in adaptation to new host |

Table 3: The Influenza genome structure encoding for different viral proteins. Adapted from Vasin *et al.*, 2014.

1.2.2.1 Haemagglutinin (HA)

HA is a trimer composed of three identical polypeptide chains, each of them has a rod-like shape structure: a globular head essential for the receptor binding and a stalk region responsible for the envelope-endosome fusion (Wilson, Skehel and Wiley, 1981; Weis *et al.*, 1988). Viral attachment occurs via the HA receptor binding site (RBS) to the host cellular receptor of sialic (N-acetylneuraminic) acids (Suzuki *et al.*, 2000). Depending on the HA affinity and specificity for sialic acid, the host range and infection site are different. Generally, the HA of avian origin binds to α -2,3 linked sialic acids while mammal viruses have higher affinity to α -2,6 sialic acids (Rogers and Paulson, 1983). Interestingly, equine influenza viruses

preferentially bind to α -2,3 linked sialic acids (Connor *et al.*, 1994), meanwhile pigs are susceptible to both avian and mammalian influenza viruses since the pig trachea contains both α -2,3 and α -2,6 sialic acids (Rogers and Paulson, 1983; Ito *et al.*, 1998). The epithelial cells of the human respiratory tract present both sialic acids, but the distribution is different. α -2,6 sialic acids are typical of the bronchi (ciliated and non-ciliated cells), whereas α -2,3 sialic acids are also found in the alveoli level (ciliated cells). Therefore, human influenza viruses infect predominantly the upper respiratory system (Matrosovich, Stech and Klenk, 2009). Not all influenza A HAs bind to canonical sialic acids. H17 and H18 glycoproteins exhibited on bat influenza particles do not, due to specific structural features in the putative RBS (Tong *et al.*, 2013). Instead, H17 and H18 entry is mediated by MHC class II proteins (Giotis *et al.*, 2019; Karakus *et al.*, 2019). HA also mediates envelope-endosome fusion during infection. In the endosome a pH-mediated structural change of the HA exposes a α -helix fusion peptide present in the stalk region facilitating the fusion of the HA with the endosomal membrane (Daniels *et al.*, 1985; Bullough *et al.*, 1994).

1.2.2.1.1 Haemagglutinin (HA) activation

HA is synthesised as a precursor protein, HA0, and its synthesis is subjected to post-translational modification such as glycosylation and palmitoylation which regulate HA folding and expression (Veit and Schmidt, 1993; Brassard and Lamb, 1997; Hebert *et al.*, 1997; Chen, Takeda and Lamb, 2005). HA0 has also to be cleaved at a distinct arginine (R) or lysine (K) – glycine peptide bond by a host cell protease into the subunits HA1 and HA2 to gain its fusion capacity (Chen *et al.*, 1998). Cleavage of HA0 is a prerequisite for a conformational change at low pH in the endosome that triggers membrane fusion with the viral envelope and is, therefore essential for viral infectivity and spread (Chen *et al.*, 1998; Steinhauer, 1999; Kido *et al.*, 2008). HA activation could occur at different time points of the viral life cycle: it could occur during synthesis and assemble when HA is transported to the plasma membrane or during budding and release of the progeny virus or at a very late stage upon attachment and entry into the host cell (Böttcher-Friebertshäuser, Klenk and Garten 2013). HA activation is also dictated depending on the cellular localisation of the protease. Indeed, activation could occur during HA synthesis if the protease is expressed intracellularly or during HA production or viral entry when protease expression is on the plasma membrane (Böttcher-Friebertshäuser *et al.*, 2010; Zmora and Pöhlmann, 2014). Bacterial infections, which could occur concomitant or secondary to influenza infection, proved to facilitate activation and spread of the virus. For instance, HA activation was detected *in vitro* and *in vivo* following

certain strains of *Staphylococcus aureus* infection since secretions of bacterial proteases have been shown ability to cleave HA (Tashiro *et al.*, 1987; Tashiro *et al.*, 2011; Böttcher-Friebertshäuser, Klenk and Garten 2013). Depending on the amino acids sequence at the cleavage site, HAs vary in their susceptibility to different host cell proteases (Baron *et al.*, 2013). The HA cleavage site (HACS) permits classification of avian influenza viruses (AIV), as different forms impact virulence, into LPAI and HPAIV. LPAI contain a monobasic HACS, usually a single arginine (R) or rarely a lysine (K) which is cleaved by tissue-restricted proteases only such as found in the respiratory or intestinal tract. Trypsin-like proteases of the Serine family such as HAT, TMPRSS2 and TMPRSS4 cleave HA with monobasic specificity (Klenk and Garten, 1994), thereby limiting spread in the infected host. HPAIV carry a polybasic HACS characterised by several arginines and lysines in a R-X-R/K-R consensus sequence leading to proteolytic activation by the protease furin which is ubiquitous in many cell types. This different type of activation results in very broad, non-restricted organ tropism and a highly pathogenic phenotype in poultry (Thomas, 2002; Horimoto and Kawaoka, 2005; Figure 8).

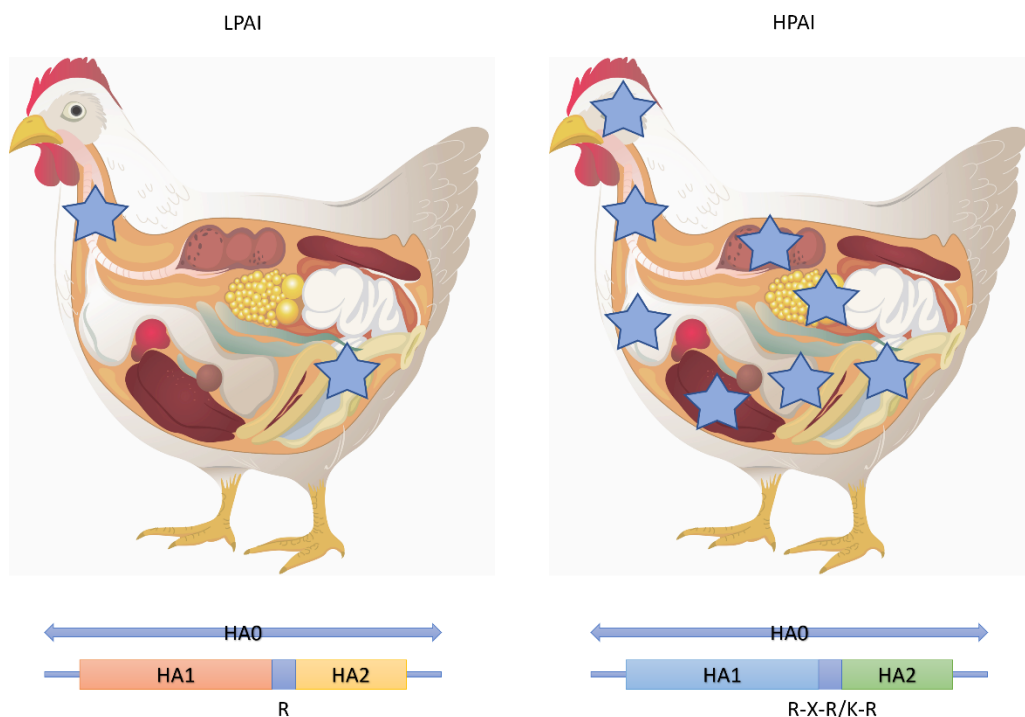


Figure 8: HACS in LPAI and HPAI viruses in poultry. Designed with Microsoft® PowerPoint™ (adapted from Horimoto and Kawaoka, 2005).

1.2.2.2 Neuraminidase (NA)

NA is a mushroom-shaped tetramer composed by four identical polypeptide chains, each of them with a rod-like shape structure similar to HA (Gottschalk, 1957). NA is a sialidase involved in viral progeny release by cleaving sialic acid bonds between the virus and infected cells (Webster and Laver, 1967; Palese *et al.*, 1974). Only recently it was found that NA is involved in the viral entry process by influencing viral binding to the receptor showed *in vitro* by a decrease in infection of cells in the presence of NA inhibitor drugs (Matrosovich *et al.*, 2004) or by aiding virus penetration through the mucus layer to reach the inner epithelia level in the lung showed by inhibiting the NA cleavage of the substrate with bead-bound mucins (Cohen *et al.*, 2013). Further studies suggested the role in viral entry correlated with NA mutations close to the active site associated with sialic acid receptor binding activity (Lin *et al.*, 2010; Gulati *et al.*, 2013; Hooper and Bloom, 2013; Mohr, Deng and McKimm-Breschkin, 2015). N10 and N11 of the H17 and H18 subtypes do not possess sialidase activity although they maintain a similar structure to the other NAs (García-Sastre, 2012; Sun *et al.*, 2013; Zhu *et al.*, 2013). Since NA plays an essential role in the pathogenicity of influenza viruses, it represents an interesting target for various antiviral drugs, such as oseltamivir, which inhibits NA enzymatic activity by imitating its substrate, thus preventing release of viral progeny particles from producer cells (Kim *et al.*, 1997).

1.2.2.3 M2 ion-channel

The third envelope protein of viral origin is M2. This protein is a tetramer composed by four identical monomers, tightly associated by disulphide bonds, in which three domains can be identified (N-terminal ectodomain, acid transmembrane segment and cytoplasmic tail) (Lamb, Zebedee and Richardson, 1985; Holsinger and Alams, 1991). The M2 protein is an ion channel allowing a selective and regulated conductance of protons in an inward direction (from the extracellular to the intracellular domain) through the viral envelope (Pinto, Holsinger and Lamb, 1992; Mould *et al.*, 2000; Venkataraman, Lamb and Pinto, 2005) and has numerous functions during the influenza virus replication cycle due to its pH regulation: viral uncoating, stabilisation of HA, viral particle assembly and membrane scission (Sakaguchi, Leser and Lamb, 1996; Baudin *et al.*, 2001; Chen *et al.*, 2008; Hong and DeGrado, 2012; Stauffer *et al.*, 2014).

1.2.3 Lifecycle

1.2.3.1 Attachment and entry

The first step of influenza infection is initiated by the HA RBS interaction with the host cell surface glycoconjugates rich in terminal sialic acid residues (Weis *et al.*, 1988; Gamblin and Skehel, 2010; Hamilton, Whittaker and Daniel, 2012). This interaction triggers endocytosis of the virion either via a clathrin-dependent manner (Roy *et al.*, 2000; Chen and Zhuang, 2008) or via macropinocytosis (Sieczkarski and Whittaker, 2002; de Vries *et al.*, 2011). Once inside the endosome, the acid environment contributes to conformational changes of the previously cleaved HA structure by exposing the fusion peptide and thus facilitating its insertion into the endosome membrane (White, Helenius and Gething, 1982; Yoshimura and Ohnishi, 1984; Bullough *et al.*, 1994). This viral strategy permits escape from degradation by lysosomal hydrolytic enzymes (Starin, Raaben and Brummelkamp, 2018). The activation of the M2 ion channel contributes to acidification of the inner environment by pumping hydrogen ions from the endosome to the virion, weakening the M1–vRNPs interactions (Lakadamyali *et al.*, 2003; Pinto and Lamb, 2006). The dissociation from M1 accompanied with generation of pores from fusion of the membranes permits the release of genetic materials into the host cytoplasm (Martin and Helenius, 1991; Bui, Whittaker and Helenius, 1998). The vRNPs are then actively transported into the nucleus through the nuclear pore complex by importin- α/β heterodimer (O’Neill *et al.*, 1995; Görlich *et al.*, 1996).

1.2.3.2 RNA and protein production

Once in the nucleus, transcription and replication of the influenza genome occur in a two-step manner modulated by the viral heterotrimeric polymerase complex (PB1, PB2 and PA) (Fodor, 2013; Pflug *et al.*, 2017). Transcription leads to the production of capped and polyadenylated viral messenger RNA (mRNA) (Plotch *et al.*, 1981). PB2 ‘cap snatches’ from the cellular mRNA and PA cleaves it into 8-14 nucleotides to be used as primer during transcription (Dias *et al.*, 2009; Guilligay *et al.*, 2008; Yuan *et al.*, 2009). Then PB1 starts to elongate the cap structure from negative sense vRNA template mediated by the viral RNA polymerase (Robertson, Schubert and Lazzarini 1981). During splicing of mRNA to derive more mRNAs, host cell proteins are usually exploited together with viral factors (Lamb and Lai, 1982; Lamb and Lai, 1984). The new mRNA leaves the nucleus for the cytoplasm to be translated by the host cell ribosomes allowing synthesis of NPs, M1 and NS2 viral polymerase proteins which are then imported into the nucleus (Jorba, Coloma and Ortín, 2009). Several other mRNAs encode for the viral envelope proteins (HA, NA and M2) which are synthesised by ribosomes associated to the host cell endoplasmic reticulum. From here, they are

trafficked in vesicles to the Golgi apparatus, in which maturation and post translational modifications occur, and finally to the host cell plasma membrane (Rodriguez-Boulan, Paskiet and Sabatini 1983; Doms *et al.*, 1993). Following this initial phase of transcription, the viral polymerase starts the replication of the vRNA by copying it into positive strand complimentary RNA (cRNA) which is then used as a template for the synthesis of new negative sense vRNA (Fodor, 2013; Pflug *et al.*, 2017). It is not clear how the production of dinucleotide structures occurs, whether by the viral polymerase or by cellular enzymes. Nevertheless, these dinucleotide structures are then exploited by the viral polymerase to start replication (Fodor 2013). Furthermore, recent studies have shown that the vRNA replication process is mediated by newly synthesised polymerases (Fodor 2013). Once the replication mechanism is finished, the new vRNA exits through the nuclear pores mediated by association to the newly synthesised M1 and NS2 (Cros and Palese, 2003).

1.2.3.3 Assembly and release

Once in the cytoplasm, all the newly synthesised virion components assemble to generate a viral particle (Rodriguez-Boulan, Paskiet and Sabatini 1983). In order to be infectious, the particle has to incorporate all eight vRNA segments (Noda *et al.*, 2006). Thus, the packaging mechanism has been demonstrated as a selective process (Fujii *et al.*, 2003). In addition, the virion particle prepares for budding and scission from the plasma membrane. Budding is promoted by a significant curvature of the membrane apparently induced by the expression of HA and NA on one side of the membrane (Varghese, Laver and Colman, 1983; Chen *et al.*, 2007), while M2 contribute to bending the membrane and facilitating scission (Rossman *et al.*, 2010). Progeny viral release is mediated by the sialidase activity of NA by removing glycosidic bonds on SA, and by removing local SA residues it prevents HA binding of the new virions to the cell surface (Gottschalk, 1957; Webster and Laver, 1967; Palese and Compans, 1976; Figure 9).

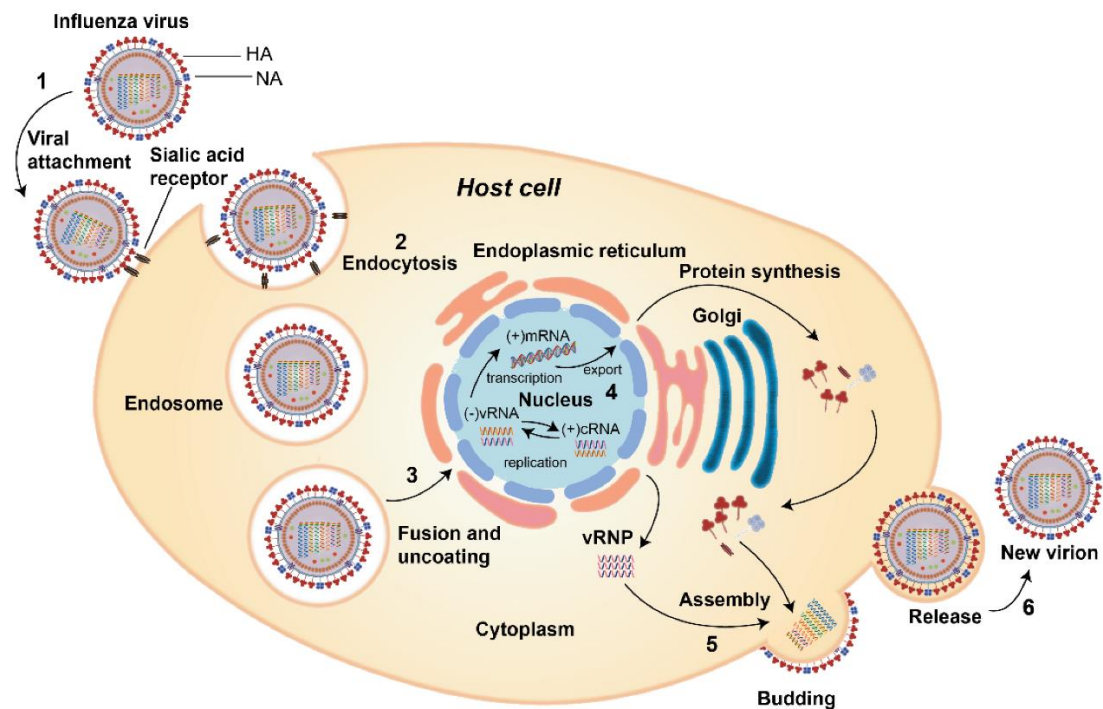


Figure 9: Schematic of Influenza virus lifecycle. Source: Nuwarda, Alharbi and Kayser, 2021.

1.2.4 Evolution of Influenza virus: antigenic drift and antigenic shift

Influenza virus is a constantly evolving pathogen with the ability to evade the host adaptive immune response, especially the antibody response. This mechanism of evolution is mostly associated to changes of the two major surface glycoproteins, HA and NA, against which antibodies are primarily directed (Virelizier, 1975). When minor genetic mutations occur in the HA and NA of known influenza A, B and C strains that code for antibody-binding sites, this is referred as ‘antigenic drift’ (Webster, 1999). The biological mechanism at the basis of this antigenic changes is due to the low fidelity and lack of proofreading ability of the vRNA dependent RNA polymerase enzyme, estimated to be one error per genome replicated (Steinhauer, Domingo and Holland, 1992; Drake, 1993). The immune system becomes less effective in mounting an effective response against new strains of virus that have specific antigenic mutations thus making it easier for the virus to infect and spread in the host. As a result of the different antigenic properties, seasonal flu vaccine composition must be reviewed every year to keep up with evolving strains (de Jong *et al.*, 2000). A second evolutionary form of the antigenic change of AIV is ‘antigenic shift’. This is a result of the combination of two or more different virus strains within the same cell that exchange genetic materials creating a new subtype which can then infect the immunologically naïve human population and potentially leading to a pandemic (Webster, Laver and Kilbourne, 1968). Very

often, swine is the host in which both avian and mammalian influenza viruses mix, adapt and reassort since they express both the α -2,3 and α -2,6 sialic acids on their respiratory epithelium (Ito *et al.*, 1998). Understanding the effects of switching combinations of genomic segments during reassortment is therefore critical for uncovering the sudden emergence of influenza viruses with increased pathogenicity (Verhagen *et al.*, 2017). Although the high prevalence of LPAI viruses among the bird populations, there is a widespread concern for genomic reassortment and the potential yield of a new highly pathogenic strain that can 'spillover' and spread to human population (Macken, Webby and Bruno, 2006).

1.2.5 Ecology and transmission

Influenza virus is able to infect a wide range of hosts, however, aquatic wild birds of the order *Anseriformes* and *Charadriiformes* are the natural reservoir of AIV (Webster *et al.*, 1992; Olsen *et al.*, 2006). Evidence of this comes from direct virus isolation of all HA and NA subtypes of both LPAI and HPAI (Stallknecht and Shane, 1988). Further evolution studies demonstrated a limited evolution within the reservoir suggesting a balanced adaptation of the virus to its natural host (Bean *et al.*, 1992; Webster *et al.*, 1992; Reid *et al.*, 2003). Indeed, it appears that there is a host specificity associated with exclusive restriction factors in many subtypes e.g. H13 and H16 being a notable example (Tønnessen *et al.*, 2013). Transmission of the pathogen to domestic birds is associated to seasonal migration of wild birds causing variable morbidity and mortality rates depending on the infection pathogenicity potential (Munster *et al.*, 2005; Alexander, 2006; Hill *et al.*, 2016). When reassortment events among vRNA of different subtypes occur and the mutation is associated with replication success, there is a high chance of spillover events of the new viruses to infect humans (Runstadler *et al.*, 2013; Verhagen, Herfst and Fouchier, 2015; Lee *et al.*, 2017). It is not clearly understood which factors determine such host preference. Nevertheless, AIV has also adapted to other mammalian host species as a result of several mutations at the RBS site of the HA impacting the tropism of the virus (Obenauer *et al.*, 2006; Herfst *et al.*, 2012; Zaraket, Bridges and Russel, 2013; Linster *et al.*, 2014; Figure 10). Therefore, constant surveillance of AIV evolution is essential to better understand its transmission route and to implement biosecurity measures to prevent and minimise the risk of transmission to domestic poultry and mammals, humans included.

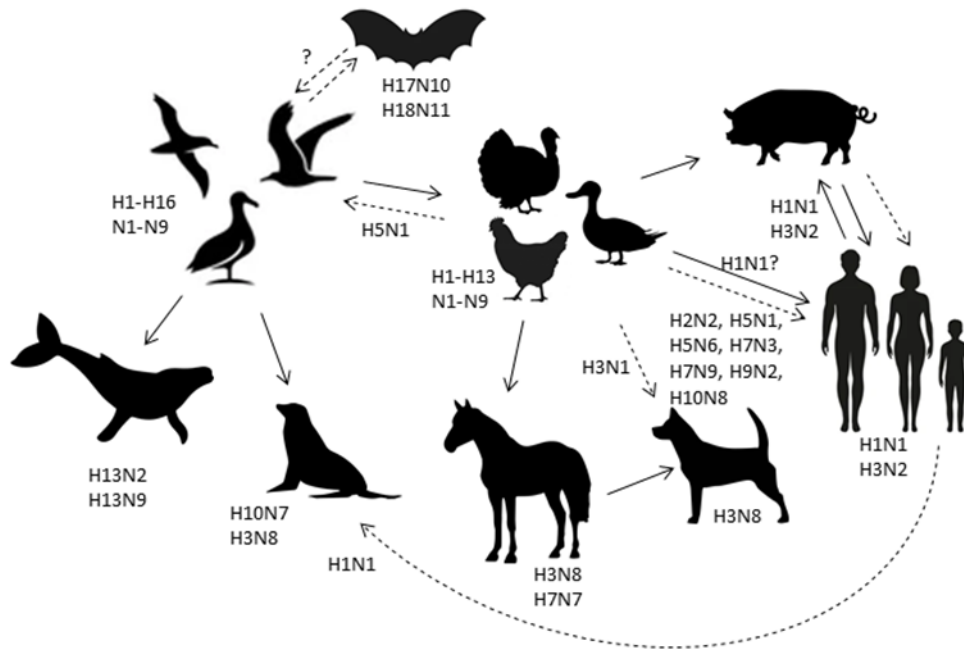


Figure 10: Significant interspecies transmission of Influenza A virus. Solid arrows represent direct transmission events that have been established in the host species, while dashed arrows represent sporadic or limited infection of subtypes where sustained transmission in the new host has not been detected. Bat influenza viruses are distinct to the bat species and origin of transmission has still to be elucidated. Designed with Microsoft® PowerPoint™ (adapted from Joseph *et al.*, 2017 and Yang, Schountz and Ma, 2021).

1.2.6 Immune response

Following infection of influenza virus, a series of mechanisms are activated by the host immune response to limit the invasion of the pathogen, contain its replication and eliminate the virus.

1.2.6.1 Innate immune response

The first barrier the virus faces is the host innate immune response which then induces activation of the adaptive immune response. Once at the primary site of infection, receptors of the mucosa respiratory epithelium detect the invading pathogen limiting its spread and recognise pathogen-associated molecular patterns inducing expression and secretion of type I IFNs and pro-inflammatory cytokines by infected cells. The release of these products initiates the innate immune response by recruiting immune cells such as macrophages, neutrophils natural killer (NK) and dendritic cells (DCs) to the site of infection (Wareing *et al.*, 2004; Veckman *et al.*, 2006; Wareing *et al.*, 2007). The alveolar macrophages actively clear pathogens and infected cells, and also produce type I IFN during RNA virus infection,

contributing to maintain the lung homeostasis (Trapnell and Whitsett, 2002; Kumagai *et al.*, 2007). Neutrophils phagocytose infected cells limiting the spread of influenza virus. However, they can lead to pulmonary immunopathology if recruited excessively (Brandes *et al.*, 2013). NK cells have cytotoxic activity towards infected cells by releasing granules containing perforin and granzyme as well as regulate the levels of IFN- γ and IL-2 (He *et al.*, 2004; Hwang *et al.*, 2012; Cooper *et al.*, 2018) influencing the evolution of infection and if uncontrolled inducing lung tissue damage (Abdul-Careem *et al.*, 2012; Zhou, Juang and Kane, 2013). DCs represent a link between the innate and adaptive immunity since they play a crucial role in presenting viral antigens to the MHC class I and II proteins, activating the adaptive immune response (Jung and Lee, 2020).

1.2.6.2 Adaptive immune response

CD4⁺ T cells recognise viral antigens presented by MHC class II and migrate from the lymph node to the lung differentiating into T helper 1 and 2 cells contributing to the production of IFN and cytokines (in particular IL-4) respectively (Brown *et al.*, 2006). Activation of CD4⁺ T cells also influence CD8⁺ T cells responses and promote activation of B cell antibody production (Tamura and Kurata 2004; Sant *et al.*, 2007). CD8⁺ T cells recognise the viral antigen presented by MHC class I and migrate to the site of infection where they lyse infected cells by releasing granules containing perforin and granzyme (Kreijtz, Fouchier and Rimmelzwaan, 2011) and secrete IFN- γ and TNF- α (Krammer *et al.*, 2018; Schmidt and Varga, 2018; Kim *et al.*, 2019). If re-infection occurs, memory CD8⁺ T cells respond more efficiently compared to naïve T cells (Tamura and Kurata, 2004). B cells specific to influenza activate and differentiate into antibody-producing cells. Immunoglobulins are able to specifically recognise the major influenza glycoproteins, in particular HA and NA, and neutralise the virus by binding and inactivation. Production of the IgA isotope occurs mainly in the upper respiratory tract, while IgG and IgM are found predominantly in the lungs and lower respiratory tract (Tamura and Kurata, 2004). Antibodies directed to HA mainly bind to HA globular head and neutralise the virus by interfering directly with virus attachment and entry into the host cell (Hensley *et al.*, 2009; Neu, Dunand and Wilson, 2016; Angeletti *et al.*, 2017). Antibodies directed to NA are able to block viral replication by interfering with viral progeny release and shedding (Kreijtz, Fouchier and Rimmelzwaan, 2011; Van de Sandt, Kreijts and Rimmelzwaan, 2012).

1.2.7 Surveillance and serology

Surveillance of influenza viruses is an efficient and necessary strategy to identify and control the pathogen in its natural host population to eventually recognise new threats (Fouchier, Osterhaus and Brown, 2003). AIV infection often remain in their subclinical form or produce mild symptoms constrained to the respiratory or intestinal tract of wild aquatic birds, associated to LPAI (Webster and Rott, 1987). However, considering the ability of evolution of influenza virus, concerning LPAI subtypes related to H5 and H7 could mutate into HPAI causing a devastating series of events associated to high mortality of domestic birds and related economical losses to the poultry industry, but also a potential risk to human health (Macken, Webby and Bruno, 2006; Dugan *et al.*, 2008; Capua and Munoz, 2013). Surveillance can be carried out either by direct detection of the causative agent or indirectly through measurement of antibodies against influenza virus. This latter method allows demonstration of seroconversion (usually a four-fold increase in antibody titre) and thus detection of infection (present or past) despite no symptoms are shown. More importantly, detection of antibodies against the HA has been correlated with the presence of protective immunity since they are able to interfere with the virus entry process (Brandenburg *et al.*, 2013). Therefore, serology is a valuable tool not only to assess many aspects of influenza surveillance, but also as a diagnostic examination of the infection and development and evaluation of influenza vaccines candidates (OIE Terrestrial Manual, 2021). Below is a brief description of the current serological assays employed for clinical evaluation of influenza virus by detecting the presence of antibodies directed to the influenza HA within blood sera samples.

a. Haemagglutination inhibition (HI)

The HI assay is considered the golden standard for influenza A subtyping and antigenic characterisation and is recommended by both the OIE (OIE Terrestrial Manual, 2021) and the EU via the European Community Commission Directive (ECCD, 2006). The assay was developed in the 1940s and is based on the ability of influenza virus to bind to the sialic acid expressed on the surface of red blood cells (RBC) causing agglutination. Thus, antibodies are measured indirectly by assessing their ability to block HA binding to target receptors resulting in an inhibition of agglutination thus the viral infectivity (Hirst, 1941). HI is measured following a two-fold serial dilution of serum at a fixed amount of virus. Serum has to be pre-treated to avoid non-specific inhibitors binding to the HA which would result in false positive results. This is done by a receptor-destroying enzyme (RDE) treatment followed by heat

inactivation to clear any RDE residual activity and serum complement (OIE Terrestrial Manual, 2021). The HI assay is officially recognised by the European Medicines Agency (EMA) to use in vaccine evaluation studies in line with the OIE recommendations (EMA, 2016). An HI titre of $\geq 1:40$ is considered to be the protective threshold value in humans (Cox, 2013). Meanwhile in horses, a mean HI titre of $\geq 1:64$ is required to induce clinical protection against equine influenza in accordance with EMA (EMA, 2014) and the European Pharmacopoeia (European Directorate for the Quality of Medicines and Healthcare – EDQM, 2017). Despite the assay being widely employed, recurring issues of inter-laboratory variability are reported, particularly due to the source of RBC which is challenging to standardise which can affect results. Therefore, it is imperative to use an internal reference standard in order to improve results for integrity studies (Katz, Hancock and Xu, 2011).

b. Single radial haemolysis (SRH)

SRH was developed in 1975 on the basis of the ability of antibodies to immunodiffuse towards an antigen mediated by the complement in an agarose gel creating a zone of haemolysis (RBC lysis). Therefore, antibody presence, mainly IgG, is determined indirectly by a complement-mediated lysis of RBC (Russell, McCahon and Beare, 1975; Schild, Pereira and Chakraverty, 1975). Pre-treatment and dilution of serum are not necessary, unlike HI. SRH is measured by determining the diameter of the lysis zone by subtracting from the area of the well the area of the zone (OIE Terrestrial Manual, 2021). The SRH is considered on the same merit as the HI assay to assess immunogenicity of influenza vaccines (EMA, 2016). In fact, a good correlation between the HI titre and SRH results have been observed, and little inter-laboratory variability has been reported (Yamagishi *et al.*, 1982; Wood *et al.*, 1994; Wang *et al.*, 2017). An SRH zone area of 25 mm² are defined as protective titre in humans (Cox, 2013) or 150 mm² to confer protection in horses in accordance with EMA (EMA, 2014) and EDQM (EDQM, 2017). However, it is not possible to evaluate the presence of antibody of the IgA subclass because they do not fix to complement (Russell, McCahon and Beare, 1975).

c. ELISA

ELISA detects different class-specific antibodies (IgA, IgG and IgM) able to bind influenza virus proteins, in particular the HA, in a serum sample via a colorimetric reaction. Because it detects the binding, it does not give information on biological neutralisation activity (Katz, Hancock and Xu, 2011). Moreover, it is not able to distinguish among influenza subtypes

(Hammond, Smith and Noble, 1980). Many ELISA approaches have been developed, but the most common remains the indirect ELISA (as described in Section 1.1.9.1.). Briefly, the multiwell plate is coated with the HA. Once the protein-binding site is blocked in the coated wells, the diluted primary antibody (sera or monoclonal antibodies) is then added. After incubation, a conjugated secondary antibody is added which is able to recognise the primary antibodies. Following further incubation, an appropriate substrate solution is added and the assay is measured using an appropriate plate reader.

d. Virus neutralisation (VN)

Finally, the VN assay measures the ability of antibodies to inhibit virus entry and/or block viral replication within cells. Various modified techniques based on the VN assay have been developed, but the general principle is to assess neutralising antibody activity by reduction of viral infectivity (Kida *et al.*, 1985; Zambon, 1998; Skehel and Wiley, 2000). For example, plaque reduction neutralisation test (PRNT) is based on the ability of the neutralising antibodies to reduce the formation of lysis plaques on a target cell monolayer which are normally generated when the virus is entering and infecting the cells. Plaques appear as clear regions of infected cells and, depending on the virus, the appearance could be clearer or more turbid (Figure 11). First, diluted serum and virus are incubated to permit antibody attachment (if present). Subsequently, target cells are added. Following further incubation, a layer of substrate typically agarose is placed on top of the assay for the purpose to limit the spread of viral progeny that would eventually occur after infection. The substrate is eventually removed, and cells fixed and stained with crystal violet. Thereafter, plaques are counted and neutralisation is assessed by the reduced number of plaques compared to the control represented by unbound virus (Cooper, 1961; Hartley 1963).

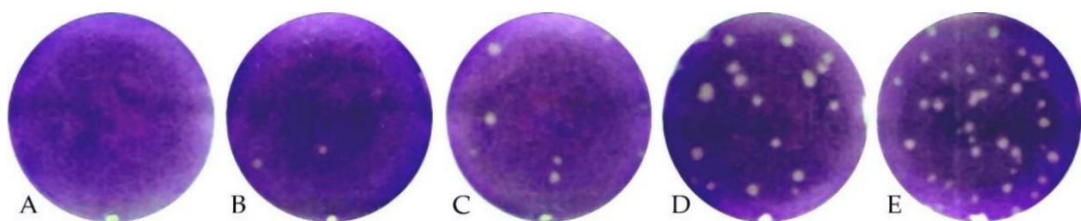


Figure 11: Visual example of plaques in a PRNT. Serial dilutions of the serum from 1/8 (A) to 1/128 (E) show a steady increase in plaques. Source: Hartlaub *et al.*, 2021.

A further assay more commonly employed is Microneutralisation (MN) in which neutralisation is assessed on the ability of antibodies to avoid a generalised cytopathic effect (CPE) in mammalian cell culture visualised by morphological changes of the cells as the virus replicates (Figure 12) or by measuring the quantity of virus within the supernatant (Okuno *et al.*, 1990; OIE Terrestrial Manual, 2021). Significant inter-laboratory variability is shown due to the lack of a standardised reference protocol and differences in assay readouts and ranges (Katz, Hancock and Xu, 2011).

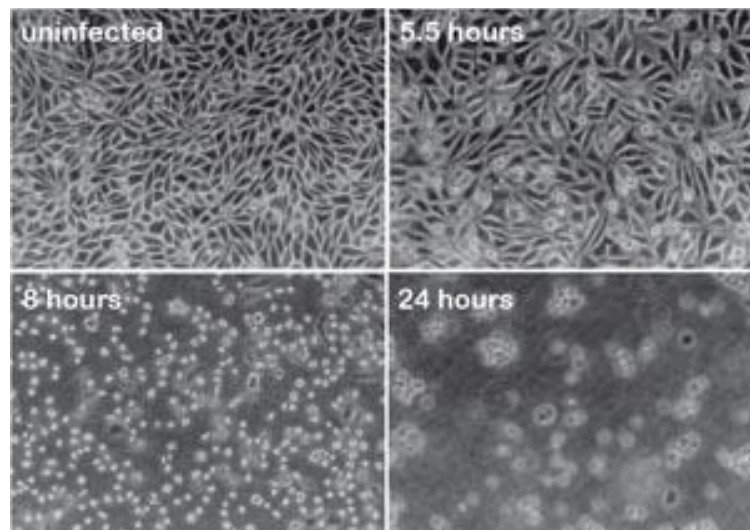


Figure 12: Visual example of CPE in a MN. The upper left panel shows uninfected cells, and the other panels show the cells at the indicated times after infection. As the virus replicates, infected cells round up and detach from the cell culture plate. Source: Racaniello, 2009.

1.3 Pseudotype viruses

Rubin (1965) first observed that the tropism of a non-replicative Rous sarcoma virus (RSV) was led by the outer glycoprotein of avian leukosis virus (ALV) expressed on its surface, determining the cellular host range as well as the typical neoplastic lesions. This natural mixing phenomenon gave rise to ideas of engineering viruses for many purposes. Pseudotype viruses (PVs) have seen major applications in research and as diagnostic tools for basic and clinical virology studies. Several virus families have been pseudotyped. This has permitted understanding of the functions of single gene products and interactions with host cell receptors (Deng *et al.*, 1997; Chan *et al.*, 2000; Cormier *et al.*, 2004; Wang *et al.*, 2004; Reignier *et al.*, 2006; Funke *et al.*, 2008; Shelton *et al.*, 2013), and to evaluate vaccines and host immune responses (Alberini *et al.*, 2009; Wright *et al.*, 2009; Zhao *et al.*, 2013; Pegu *et al.*, 2014), therapeutics and antivirals (Su *et al.*, 2008; Aljofan *et al.*, 2009; Yu *et al.*, 2012;

Both *et al.*, 2013; Madrid *et al.*, 2013; Basu *et al.*, 2014). PVs are chimeric virus particles which typically consist of the 'core' representing the genome encased in the protein nucleocapsid of one virus (e.g. a lentivirus), contained in the host cell membrane-derived 'envelope' acquired during budding from the host cell. At the same time the envelope is studded with proteins of the study virus (e.g. HA for influenza viruses or GPs for herpesviruses or Spike for coronaviruses). Expression of these proteins on the virion surface allows the resultant particles to mimic certain aspects of the native virus lifecycle, such as target cell entry and eliciting of immune responses (Temperton, Wright and Scott, 2015). Notably however, PVs are replicative defective particles able to self-assemble but not to replicate or give rise to a new progeny since some viral elements of the genome are removed preventing so. Instead, a foreign gene replaces this genetic material. Because of this, PVs enable the study of highly pathogenic viruses such as H5 or H7 influenza, without the need for high containment, representing a safer alternative to study compared with infectious wild-type virus (Temperton *et al.*, 2007; Molesti *et al.*, 2012). The viral cores employed to generate a pseudotype system are primarily from the *Retroviridae* family (e.g. lentivirus or gammaretrovirus) or *Rhabdoviridae* family (e.g. rhabdovirus). The lentiviral human immunodeficiency virus (HIV) type 1 (HIV-1) core is the most common due to its ability to integrate into the host cell genome, and unlike gammaretroviruses it can infect both dividing and non-dividing cells. Retroviral vectors have been well established for influenza pseudotyping (Del Rosario *et al.*, 2021) and other RNA viruses such as Ebola virus (Wool-Lewis and Bates, 1998), Lassa virus (Radoshitzky *et al.*, 2007), Hepatitis C virus (Bartosch, Dubuisson and Cosset, 2003), Vesicular stomatitis virus (Naldini *et al.*, 1996) or SARS-CoV-2 (Di Genova *et al.*, 2021). While for DNA viruses, only an herpesvirus PV has been generated so far employing a VSV system (Rogalin and Heldwein, 2016). The foreign gene, usually a transfer or reporter gene, is inserted into the genome. The packaging signals upstream the gene are used to pack into capsids. The relatively straightforward manipulation of PVs, compared with native study viruses, has made them a considerable tool in gene therapy for their ability to transfer therapeutic genes into specific target cell types (Zufferey *et al.*, 1997). Integration of a reporter gene permits direct quantification of the viral particles. Thus, reporter gene expression in target cells indicates successful transduction (Demaison *et al.*, 2002). The method of quantification depends on the reporter gene expressed (e.g. green fluorescent protein or firefly luciferase) and the available equipment (e.g. flow cytometer, epifluorescence microscope or luminometer). On the other hand, their entry may be inhibited by antibodies or certain antivirals, thus representing an alternative to wildtype

viruses in neutralisation or antiviral screening assays, quantifiable by measuring the reduction of the reporter expression in susceptible target cells.

1.3.1 Pseudotype virus neutralisation assay

Pseudotype virus neutralisation assay (PVNA) offers a potential alternative to current serological assays to detect the presence of functional neutralising antibodies within sera samples. Typically, firefly luciferase is used as reporter. Thus, the principle of the assay is based on the reduction of luminescence from target cells emitted indicating the presence of neutralising antibodies targeting the envelope glycoprotein able to inhibit viral infectivity. A small amount of serum (generally 5 μ L) is serially diluted and incubated with a fixed amount of PV to allow antibody binding before target cells are added. If transduction activity is detected that is the PV able to enter cells and not neutralised the PV particle will transduce cells and the reporter gene will be expressed following integration of the viral genome. On the other hand, if neutralising antibodies are present in the serum, then PV entry is hindered resulting in lower expression of the reporter signal (Figure 13). The reduction of the signal is extrapolated to calculate the antibody effect reported as IC_{50} as the reciprocal of the serum dilution by which 50% of PVs are neutralised. In influenza studies, PVNA have demonstrated good correlations with traditional serological assay (Molesti *et al.*, 2013; Kinsley *et al.*, 2020) and higher sensitivity to detect specific HA-antibodies rather wild-type viruses (Temperton *et al.*, 2007; Wang *et al.*, 2008), therefore providing a valuable platform to assess antibody responses to natural infections or vaccination efficacy, including for emerging diseases (Kemenesi *et al.*, 2021). However, reproducibility is a recurrent issue which needs to be assessed (Carnell *et al.*, 2015). Therefore, the importance of validation and standardisation of the method are necessary to minimise variability among research groups.

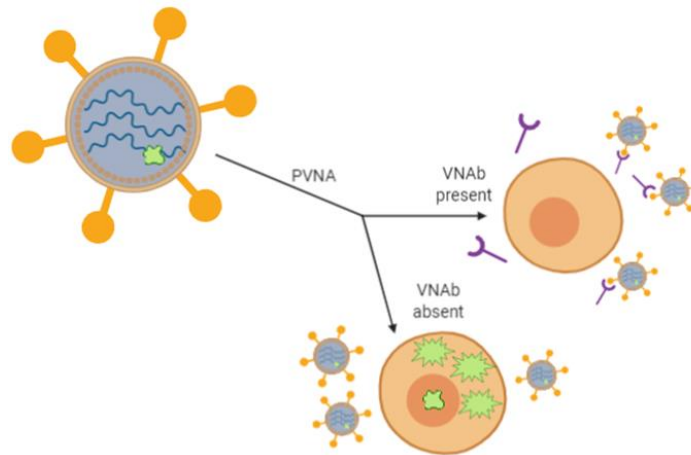


Figure 13: Principle of PVNA. In the presence of neutralising antibodies, the reporter gene signal is reduced, meanwhile in absence of neutralising antibodies the reporter gene signal is maximal. Designed with BioRender.

1.4 Thesis aims and structure

The primary purpose of these studies was to generate pseudotyped particles employing the lentiviral system of a DNA and RNA virus of veterinary interest and their further application in a neutralisation assay to assess the presence of neutralising antibodies from different sera panels. Since no DNA PV has been pseudotyped before employing the lentiviral system, it was necessary to first develop adequate plasmid vectors expressing the GPs to permit entry and optimise a protocol to generate EHV-1 PV (Chapter 3.). Subsequently, evaluate its performance in a neutralisation assay and establish its use (Chapter 4.) and finally assess its functionality after lyophilisation to ease transport barriers (Chapter 5.). This latter consideration was assessed for the purpose to export the newly functional EHV-1 PV to our research collaborators at LABÉO (France) where the PV system would have been employed for further applications exploiting the advanced technologies available at the host platform (Chapter 6.). The second project was focussed on the generation of pseudotype lentivirus particles with the HA of a novel subtype of influenza virus strain. One of the challenges was to generate the Influenza PV for use as a tool for cell tropism and diagnostic studies. Therefore, different approaches were carried out to investigate the expression of the HA gene and evaluate its functionality as an immune antigen (Chapter 7.).

2. MATERIALS AND METHODS

In this chapter the general Materials and Methods will be described. For more accurate Materials and Methods each chapter will provide the related info.

2.1 Molecular biology

2.1.1 Expression vectors

To produce a safe and efficient pseudotype particle that will not induce pathogenicity, a suitable platform must be chosen that will permit a co-transfection system to work. pI.18 or pCAGGS (Niwa, Yamamura and Miyazaki, 1991) plasmids, both available in-house at the Viral Pseudotype Unit (VPU; University of Kent, UK), were used to clone the glycoprotein (GP) genes used in this project thesis. pCAGGS was a kind gift of Dr. Graham Simmons (Vitalant Research Institute, San Francisco, USA). Both plasmids are high-copy number, ampicillin resistant pUC-based plasmids which permits robust mammalian gene expression in various eukaryotic cell lines by virtue of the human cytomegalovirus immediate-early gene promoter and enhancer (Figures 14 and 15). The production of all lentiviral PVs in this study was dependent on plasmid p8.91, which encodes the HIV *gag-pol* genes and facilitates viral particle formation. p8.91, originally called pCMVΔR8.91 (Zufferey *et al.*, 1997), is a second generation plasmid expressing the HIV *gag* and *pol* encoding for HIV-1 core proteins under a human cytomegalovirus (CMV) promoter substituting the LTR-based promotion. The packaging signal sequence (Ψ) as well as the accessory protein genes (*vif*, *vpr*, *vpu* and *nef*) and HIV-1 envelope (*env*) gene have been also deleted to avoid packaging of genome core proteins into the new progeny and so their replication (Naldini *et al.*, 1996; Figure 16 upper diagram). Due to the low copy nature of p8.91, the plasmid DNA was produced and purified via industrial processes by GenScript® (GenScript Biotech, CloneArk Plasmid Preparation: Plasmid: p8.91). On receipt, the lyophilised product was resuspended to the required concentration using molecular biology grade, DNase-free water (MBG H₂O; Sigma-Aldrich®, Merck, #W4502). To facilitate direct quantification of functional PV particle concentration, a reporter gene was incorporated into particles. This was either the firefly luciferase (FLW), encoded by pCSFLW, provided by Dr. Nigel Temperton (University of Kent, UK) or the emerald green fluorescence protein (emGFP) encoded by pCSemGW, kindly provided by Dr. Greg Towers (University College London, UK). The reporter gene is expressed by a self-inactivating second generation plasmid containing the Ψ , LTRs and RRE which permit incorporation of the construct into the PV genome and under a SFFV promoter and WPRE which permit integration and expression into the host cell genome respectively. pCSFLW

derives from pCSGW (Demaison *et al.*, 2002) by substitution of the reporter gene (Figure 16 bottom diagram).

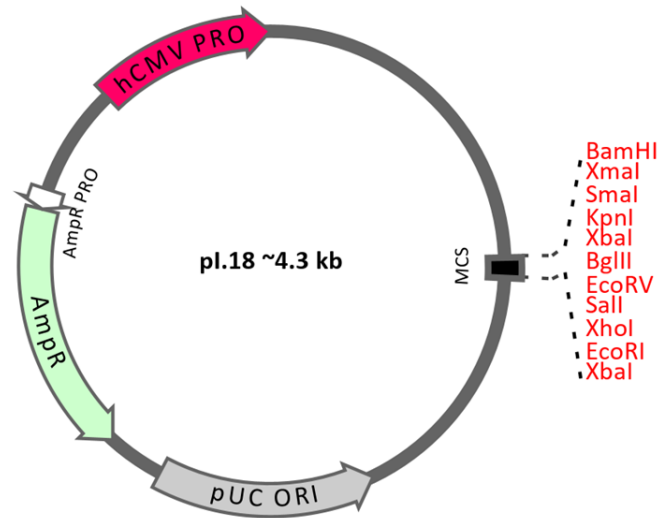


Figure 14: pl.18 plasmid map. The plasmid map was generated with DNADynamo version 1.556 software (BlueTractor). The hCMV promoter is highlighted in red, permitting gene expression in mammalian cells. The gene is cloned into the restriction enzyme sites within the multiple cloning site (MCS) highlighted in red. The ampicillin resistance (AmpR) gene is highlighted in green, driven by its own promoter (AmpR PRO) highlighted in white, mediates resistance during cloning experiments. The pUC origin of replication (pUC ORI) is highlighted in grey allows plasmid amplification in bacterial cells.

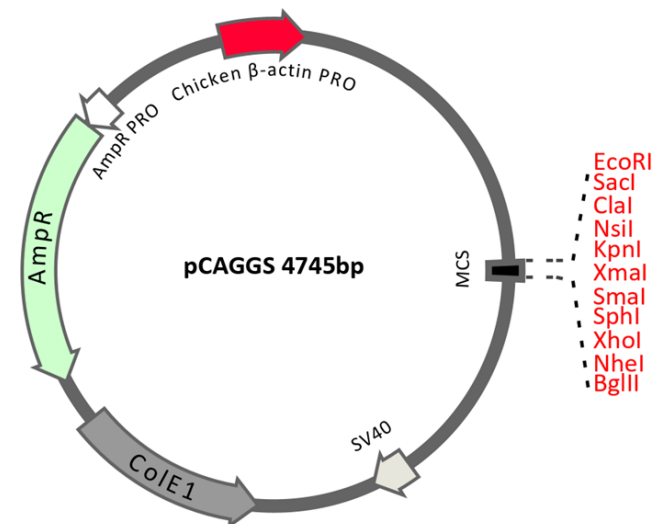


Figure 15: pCAGGS plasmid map. The plasmid map was generated with DNADynamo version 1.556 software (BlueTractor). The chicken β -actin promoter is highlighted in red, permitting gene expression in mammalian cells. The gene is cloned into the restriction enzyme sites within the multiple cloning site (MCS) highlighted in red. The ampicillin resistance (AmpR) gene is highlighted in green, driven by its own promoter (AmpR PRO) highlighted in white, mediates resistance during cloning experiments. The ColE1 origin of replication is highlighted in dark grey allows plasmid amplification in bacterial cells.

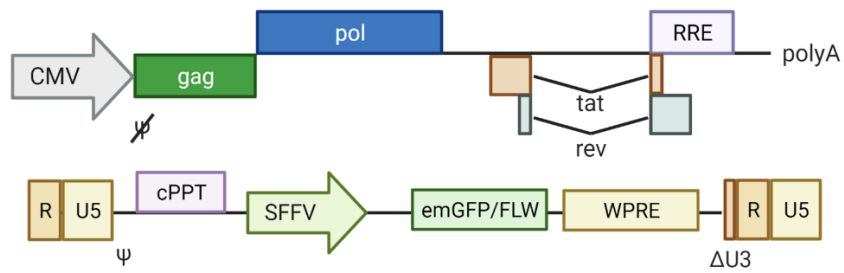


Figure 16: Lentiviral packaging vectors for PV generation. Upper diagram: p8.91 plasmid for HIV-1 expression of gag and pol genes for expression of core proteins and polymerase, protease and integrase. **Bottom diagram:** lentiviral vector coding for emGFP or FLW reporter genes to assemble into PVs. Designed with BioRender (adapted from Zufferey et al., 1997 and Demaison et al., 2002).

2.1.2 Gene design

DNA sequences of the study genes of this thesis were provided by partner collaborators of each project. For successful cloning into the multiple cloning site (MCS) of expression plasmids, one or more restriction sites were carefully chosen (avoiding those represented internally) and incorporated at the 5' and 3' end of the synthesised open reading frames – upstream of the start codon ATG or downstream the stop codon TAA, TAG or TGA respectively. In addition, a six-nucleotide Kozak consensus sequence (successfully used previously) was included between the restriction site and the starting codon ATG to aid the initiation of the translational process. A detailed cloning strategy is described into the Materials and Methods of Chapter 3. and 7. represented as Flow Charts in the Appendix Figures 1-3.

2.1.3 Gene synthesis

The GP genes were synthesised by GeneArt™ (Invitrogen™, Thermo Fisher Scientific) either as 'gene strings' (DNA fragments) or subcloned into pMX series vector (plasmid series owned by GeneArt™) where X represents the antibiotic resistance gene i.e. pMA for ampicillin resistant plasmid; pMK for kanamycin resistant plasmid. The pMX vector series is based on pUC cloning vectors, minus promoter sequences (thus biosafety level 1) as assured by the manufacturer. Codon Optimisation (CO) was also an option to be requested to enhance the translational efficiency of the gene of interest once subcloned into expression vectors, which could increase the envelope protein expression and possibly pseudotype titres. On receipt, the lyophilised product was resuspended in MBG H₂O to a final concentration of 100 ng/μL,

mixed well and incubated 30 minutes at room temperature (RT) to resuspend before storing in -20°C.

2.1.4 Cloning into expression vector and screening

Standard or FastDigest® restriction enzymes (REs; Thermo Scientific™, Thermo Fisher Scientific) were used for cloning and screening purposes. Tables 4 and 5 indicate the usual quantity of DNA used per reaction as well as the appropriate REs and restriction digest buffer. DNA volumes and MBG H₂O were adjusted depending on the original DNA concentrations (500 ng per reaction). The reaction mixture was then incubated in a heat block at the optimal reaction temperature depending on the conventional REs used for a maximum of 2 hours. On the other hand, FastDigest® reactions were incubated at +37°C for 20 minutes. 1 µL of 6X DNA Loading Dye (Thermo Scientific™, Thermo Fisher Scientific, #R0611) was added to 4 µL of samples when running digest reactions on an agarose gel to verify correct digest. As an alternative to adding loading dye, the universal FastDigest® Green buffer (Thermo Scientific™, Thermo Fisher Scientific, #B72) was used.

| Reagent | Plasmid DNA/PCR product |
|------------------------------|--|
| DNA | 500 ng |
| 10x Buffer | 2 µl |
| Enzyme | 1 µl (0.5 µL if potential star activity) |
| Sterile H ₂ O | x µl |
| <i>Total reaction volume</i> | 20 µl |

Table 4: Conventional RE digestion reaction volumes.

| Reagent | Plasmid DNA/PCR product |
|------------------------------|-------------------------|
| DNA | 500 ng |
| FastDigest® Green buffer | 1 µl |
| FastDigest® Enzyme 1 | 0.5 µl |
| FastDigest® Enzyme 2 | 0.5 µl |
| Sterile H ₂ O | x µl |
| <i>Total reaction volume</i> | 10 µl |

Table 5: FastDigest® RE digestion reaction volumes.

2.1.5 Ligation

Following digestion of the genomic DNA (GP gene of study) and the backbone plasmid for cloning, the gene insert and the vector were ligated at a 1:1, 1:3 or 1:5 molar ratio using 5 units of T4 DNA Ligase (Thermo Scientific™, Thermo Fisher Scientific, #EL0011) in 10X T4 DNA Ligase Buffer and adjusted volume of MBG H₂O, in a total volume of 10 µL. For blunt-end ligation, polyethylene glycol (PEG 4000; Thermo Fisher) was added to increase the ligation efficiency. The general formula to calculate the amount of insert to include in the ligation reaction is shown below along with Table 6 for reaction volumes used. To determine the presence of any re-ligated or undigested (mainly circular) vector DNA, a vector only (no insert) control reaction was also set up. The reactions were then incubated at RT for 48-72 hours before being transformed into chemically induced competent DH5α *Escherichia coli* cells.

General formula for volume DNA in 1:1 molar ratio = $\frac{\text{Insert size (kb)}}{\text{vector size (kb)}} \times \text{linear vector DNA}$

| Reagent | Volume |
|------------------------------|---|
| Linear vector DNA | 25-50 ng |
| Insert DNA | 1:1 to 1:5 molar ratio over vector |
| 10X T4 DNA Ligase Buffer | 1 μ l |
| T4 DNA Ligase 5U | 0.7 μ l |
| 50% PEG 4000 Solution | 1 μ L (only to add if blunt-ligation) |
| Sterile H ₂ O | x μ l |
| <i>Total reaction volume</i> | 10 μ l |

Table 6: Ligation reaction volumes.

2.1.6 Transformation

For plasmid amplification or cloning (following ligation reactions) purposes, transformation was carried out using Subcloning Efficiency™ DH5 α Competent Cells (Invitrogen™, Thermo Fisher Scientific, #18265017). A classic heat-shock transformation protocol was followed and here described. An aliquot containing 12.5 μ L or 25 μ l of DH5 α competent cells was thawed for 5 minutes from -80°C storage on ice to maintain cell viability. Then 1 μ l or 2.5 μ L respectively (0.5-10 ng) of DNA was added by stirring gently to the cells. After a further incubation on ice for 30 minutes, the cells including the DNA mix were heat-shocked at +42°C in an AccuBlock™ Digital Dry Bath (Labnet International, #D1100-230 V) for 30 seconds and then placed for 5 minutes on ice to allow cells to recover. 200 μ L of SOC medium (Invitrogen™, Thermo Fisher Scientific, #15544034) was added to obtain maximum transformation efficiency. After 1 hour at +37°C at 225 revolutions per minute (RPM) in a New Brunswick™ Incubator Shaker (Eppendorf UK Ltd, model: Classic C25KC), 50 μ L of SOC/bacteria was plated onto LB Agar (Fisher Scientific™, Thermo Fisher Scientific, #BP1425) plates with the appropriate antibiotic selection (100 μ g/mL of ampicillin or 50 μ g/mL of kanamycin) and incubated overnight (ON) in a dry incubator (Genlab, model: INC/75). The following day, single colonies were picked either for colony screening or for plasmid amplification. In the latter case, colonies were inoculated in 5 mL LB Broth with the addition of the appropriate antibiotic solution and incubated ON at +37°C with shaking as before.

2.1.7 Glycerol stocks

To store and maintain plasmid clones for future use, a glycerol stock was prepared by mixing 800 μL of the ON grown bacterial culture in 200 μL of 80% (v/v) glycerol (Sigma-Aldrich®, Merck, #G5516) for a final stock 15% stock to be kept at -80°C . Plasmid DNA from the remaining culture was purified.

2.1.8 Plasmid DNA purification

DNA plasmid purification was performed using Monarch® Plasmid Miniprep Kit (New England Biolabs, #T1010) to isolate plasmid DNA from transformed bacterial cells. The ON culture was pelleted at 6800 g for 3 minutes in a tabletop Pico™ 17 Microcentrifuge (Thermo Scientific™, Thermo Fisher Scientific, #75002401) then the manufacturer's guidelines were followed and DNA was finally eluted in 30 μL of MBG H₂O warmed to $+70^{\circ}\text{C}$ to increase the DNA yield. All amplified and purified DNA was stored at -20°C for further experiments (DNA transfection for PV production).

2.1.9 Measure of nucleic acid concentration

The concentration and purity of DNA was determined by ultraviolet visible spectrophotometry at an absorbance ratio of 260/280 nm using NanoDrop™ 2000 Spectrophotometer (Thermo Scientific™, Thermo Fisher Scientific, model: NanoDrop™ 2000). MBG H₂O was used as a blank control before loading 1 μL of sample for assessment.

2.1.10 Sequencing

5 μL of 100 ng/ μL DNA plasmid was mixed with an equal volume of 5 pmol/ μL of either forward (FW) or reverse (Rev) primer (pI.18 or pCAGGS sequencing primer details are reported in Table 7) were sent for Sanger sequencing performed at Eurofins (former GATC Biotech Ltd London) and carried out in a LightRUN™ system. Sequencing was conducted to check the correct orientation of the insert, if any mutation event had taken place during the cloning process or to check if the correct mutation was incorporated during site-directed mutagenesis (SDM).

| Primer ID | Primer sequence (5' to 3') | Features | Designed by |
|-----------|-----------------------------------|--|--|
| pl.18 | FW 5'-ggtagggcagtgtagtct-3' | Anneals upstream the MCS of pl.18 plasmid in position 1134-1153 | Dr. Nigel Temperton (University of Kent, UK) |
| | Rev 5'-gcgaggatgtcacctgatgg-3' | Anneals downstream the MCS of pl.18 plasmid in position 1430-1449 | |
| pl.18 int | FW 5'-tctttctgcagtcaccgtccttg-3' | Anneals upstream the MCS of pl.18 plasmid (closer than pl.18 FW) in position 1230-1253 | Dr. Simon Scott (University of Kent, UK) |
| | Rev 5'-cccacgtcactattgtatactct-3' | Anneals downstream the MCS of pl.18 plasmid (closer than pl.18 Rev) in position 1317-1339 | |
| pCAGGS | FW 5'-ttcggcttctggcgtgtga-3' | Anneals upstream the MCS of pCAGGS plasmid (closer than pCAGGS NT FW) in position 1527-1545 | Dr. Edward Wright (University of Sussex, UK) |
| | Rev 5'-cagaagtcagatgctcaagg-3' | Anneals downstream the MCS of pCAGGS plasmid (closer than pCAGGS NT Rev) in position 1742-1761 | |

Table 7: Sequencing primers.

2.1.11 Polymerase Chain Reaction for colony screening

A colony PCR was carried out to identify positive clones with the correct size insert. Individual colonies were picked from either 1:1, 1:3 or 1:5 LB agar plates using a sterile pipette tip and first transferred onto a grid LB agar plate (incubated ON as usual) before remaining cells were

placed into a PCR microtube (Greiner Bio-One, #683201) containing 10 µL of MBG H₂O for 5 minutes. If present, a colony was also picked from the vector only (no insert) LB agar plate for negative control purposes. MBG H₂O was included as control to check the presence of any contamination from DNA carry-over. Then the PCR microtubes were heated for 3 minutes at +94°C in a Mastercycler® (Eppendorf UK Ltd, model: Mastercycler® ep Gradient) thermal cycler to lyse the bacterial cells. Once cooled down to RT, 5 µL of lysed cell mixture was added to a PCR mix consisting of 12.5 µL 2X DreamTaq Green PCR Master Mix (Thermo Scientific™, Thermo Fisher Scientific, #K1081), 0.5 µL FW and Rev primer (0.2 µM) and adjusted volume of MBG H₂O to make a final volume of 25 µL. FW and Rev primers were chosen accordingly to permit the amplification of the DNA region/gene within the arms of the backbone vector either pl.18 int (as described in Table 7) or pCAGGS NT here below reported in Table 8.

| Primer ID | Primer sequence (5' to 3') | Features | Designed by |
|--------------|---------------------------------|--|---|
| pCAGGS NT | FW 5'-ttctccatctccagcctcggg-3' | Anneals upstream the MCS of pCAGGS plasmid in position 1064-1084 | Dr. Nigel Temperton (University of Kent, UK) |
| | Rev 5'-cccatatgtccttccgagtga-3' | Anneals downstream the MCS of pCAGGS plasmid in position 1506-1526 | |

Table 8: pCAGGS NT primers for amplification and screening purposes.

20 ng of a positive control DNA was also included to the colony screening to ensure the performance of the PCR reaction. The DNA mixture was then placed in a thermocycler and the following program (Table 9) followed for amplification:

| Step | Temperature | Time | Cycles |
|----------------------------|-------------|-------------------------------|--------|
| Initial denaturation phase | 94°C | 2 minutes | |
| Denaturation | 94°C | 30 seconds | 30 |
| Annealing phase | 51°C | 1 minute | |
| Extension phase | 72°C | 2 minutes (30 seconds per Kb) | |
| Final extension | 72°C | 5 minutes | |

Table 9: Colony screen PCR program.

The PCR products were verified on an agarose gel to identify which clones were positive for gene insertion. The positive clones were then picked from the master grid LB agar plate and grown ON in 5 mL of LB broth growth media for plasmid purification and glycerol stocks as described in Sections 2.1.7. and 2.1.8.

2.1.12 Agarose gel electrophoresis

For analytical purposes, DNA reactions were loaded onto a 1% (w/v) agarose (Fisher Scientific™, Thermo Fisher Scientific, #BP1356) gel containing 1X Tris-Acetate-Ethylenediaminetetraacetic acid (EDTA) buffer (TAE; 50X Stock solution, Fisher Scientific™, Thermo Fisher Scientific, #BP1332) and stained with 10000X SYBR® Safe DNA Gel Stain (Invitrogen™, Thermo Fisher Scientific, #S33102). If required, samples were loaded after addition of 1 µL of 6X DNA Loading Dye. For DNA gel extraction, gels were prepared with 1% (w/v) low electroendosmosis (EEO) agarose (Sigma-Aldrich®, Merck, #A5093). The gel was placed in a sized gel tank in 1X TAE buffer and run in a Consort™ power supply (Merck, model: Consort™ EV231) at 80 V for 40 minutes. Images of the DNA migration patterns were first observed on a trans illuminator (UVIttec, #BXT-26.MX) before being acquired in a G:Box gel imager (Syngene, model: G:Box iChemi XT Imaging System) and GeneSnap software (Syngene). At times, images were taken with a Samsung A6 camera due to faulty imager machinery.

2.1.13 SDS-Polyacrylamide Gel Electrophoresis

Sodium dodecyl sulphate-polyacrylamide gel electrophoresis (SDS-PAGE) was employed to investigate either the molecular weight of the GP or to verify whether the envelope HA was present on the produced PV. Tris-glycine-sodium dodecyl Sulphate (SDS) buffer was used as

running buffer for SDS-polyacrylamide gel electrophoresis (SDS-PAGE). It was prepared by dissolving the components in double distilled water (ddH₂O) to a concentration of 250 mM Tris base (Fisher Scientific™, Thermo Fisher Scientific, #BP152-1), 1.92 M glycine (Sigma-Aldrich®, Merck, #G7126), and 1% (w/v) SDS (Sigma-Aldrich®, Merck, #L6026) for a final pH 8.3 and stored at RT. 2 mL of harvested PV were low speed centrifuged at 3000 g at +4°C for 24 hours in a bench top refrigerated microcentrifuge (VWR International Ltd, model: Micro Star 17R, #521-1647). 1.95 mL of supernatant was then removed and discarded, making sure not to disrupt the pelleted virus, and 100 µL of cold OptiMEM® (kept at +4°C) were added to the tube. Samples were incubated ON at +4°C to permit particle resuspension and stored at -80°C before preparing samples for SDS-PAGE. Samples were prepared by adding 10 µL of sample, 2.5 µL of 4X Laemmli buffer (Bio-Rad, #1610747) and 27.5 µL of phosphate-buffered saline (PBS; PAN Biotech, UK, #P04-36500) to a final volume of 40 µL. All samples were boiled in a heat block at +95°C for 5 minutes before mixing them briefly and loading them on an Any kD™ Mini-PROTEAN® TGX™ Precast Protein Gel (Bio-Rad, #4569034). 5 µL of Precision Plus Protein™ Dual Color Standards (Bio-Rad, #1610374) was loaded on the gel to aid estimation of sample protein molecular weight. The gel was run in a Mini-PROTEAN Tetra Cell (Bio-Rad, #1658005EDU) with Tris-Glycine-SDS running buffer for 5 minutes at 50 V and then at 150 V until the loading dye reached the bottom of the gel (approximately 1 hour). The gel was then transferred to a container and treated with fixing solution for 30 minutes on a platform rocker (VWR International Ltd, model: SKD1807-E) in the dark. The fixing solution was prepared by dissolving components in ddH₂O to a concentration of 50% (v/v) methanol (CH₄O; Fisher Scientific™, Thermo Fisher Scientific, #M/3900/17) and 7% (v/v) acetic acid (CH₃CO₂H; Sigma-Aldrich®, Merck, #33209). Fixing solution was discarded and replaced with fixing solution followed by a second incubation for 30 minutes. Gels were stained with a solution prepared with 0.1 % (w/v) Coomassie Brilliant Blue G-250 (Fisher Scientific™, Thermo Fisher Scientific, #BP100), 40% (v/v) ethanol (CH₃CH₂OH; Honeywell, #32221) and 10% (v/v) glacial acetic acid (Fisher Scientific™, Thermo Fisher Scientific, #A/0360/PB17), and incubated ON in the dark. The next day gels were destained with a solution containing 10% (v/v) methanol and 7% (v/v) glacial acetic acid until bands were visible and background staining was minimal.

2.2 Cell culture

All cell culture procedures were performed under a MSC-Advantage™ Class II Biological Safety Cabinet (Thermo Scientific™, Thermo Fisher Scientific, #51028226) and using a HERAcCell™ 150i humidified CO₂ Incubator (Thermo Scientific™, Thermo Fisher Scientific, #51026280) for incubations at +37°C at 5% CO₂.

2.2.1 Cell lines and maintenance

Human Embryonic Kidney (HEK) 293T/17 cells were purchased from American Type Culture Collection (ATCC®, #CRL-11268) and used for both production and entry target of PVs. HEK293T/17 were maintained in Dulbecco's Modified Eagle Medium (DMEM; PAN Biotech, UK, #P04-04510) added with 10% Foetal Bovine Serum (FBS; PAN Biotech, UK, #P40-37500HI) and 1% Penicillin/Streptomycin (P/S; PAN Biotech, UK, #P06-07100) – referred as 'complete medium' – in T75 flasks (Thermo Scientific™, Thermo Fisher Scientific, #156499) at +37°C 5% CO₂. Sub-culturing of cells was processed by removing the medium and detachment of the cell layer by EDTA-Trypsin (PAN Biotech, UK, #P10-040100). Cells were then resuspended in fresh complete medium and seeded at the adequate density for maintenance of the cell line.

2.2.2 Freezing and thawing of cell lines

Cells were frozen when 80% confluence was reached. Briefly, cells were detached using trypsin and resuspended in fresh complete medium which also neutralise the trypsin. Cells were then centrifuged at 500 RPM for 5 minutes in Rotor 6M centrifuge (ELMI, #CM-6MT) and the pellet gently resuspended in freezing medium which is complete medium added with 10% (v/v) of dimethyl sulfoxide (DMSO; VWR International Ltd, #282164K). Cells were then transferred to cryovials (1 mL/cryovial) (Corning, #430915) and kept in CoolCell™ LX Cell Freezing Container (Corning, #432002) for 24 hours at -80°C before placing in a microtube storage box (VWR International Ltd, #525-0925P) at -80°C. When cells were required, a T75 or T25 flask (Thermo Scientific™, Thermo Fisher Scientific, #156367) with the appropriate amount of complete medium was first placed in the incubator for 30 minutes to reach the desired temperature and adjust the pH. Afterwards, the whole content of an aliquot of frozen cells was added to the flask, gently rocked and placed back to the incubator. The next day, the existing medium was replaced with fresh complete medium to remove any residue of DMSO. Before being used in experiments, cells were passaged at least twice once

confluence permitted so. If a T25 was initially used, then cells were transferred to a T75 at the first passage.

2.3 Pseudotype virus (PV) generation

The protocol described below in this section will provide general information of how to generate a PV with lentiviral core. Due to the diversity of the PVs in this thesis, the specific PV generation protocols are given in the Materials and Methods of Chapter 3. and 7.

2.3.1 Generation of lentiviral particles

Production of PV was performed by co-transfection of p8.91 for HIV *gag* and *pol* expression, pCSFLW or pCSemGW for reporter gene expression (described in Section 2.1.1.) and the GP of interest plasmid for GP expression into the producer cell line HEK293T/17 using polyethylenimine (PEI; Sigma-Aldrich®, Merck, #408727) transfection reagent at 1 mg/ml (pH 7). On day 1, HEK293T/17 cells were seeded from a confluent T75 flask into a 6-well Nunc™ Cell Culture Treated Multidishes (Thermo Scientific™, Thermo Fisher Scientific, #140675) containing 2 mL of complete medium per well to get a desired amount of 400000 cells/well. Cells were manually counted using a FastRead 102™ counting slide (Immune Systems, #BVS100) following manufacturer's instructions under the light microscope (Medline scientific, #Inverso-TC100). Cells were then incubated at +37°C 5% CO₂. On day 2, a DNA mix of 500 ng of p8.91, 750 ng of either pCSFLW or pCSemGW and 500 ng of GP expression plasmid were combined in a tube with 100 µL of OptiMEM™ GlutaMAX™ Supplement (Gibco™, Thermo Fisher Scientific, #51985-034). In a separate tube, 17.5 µL of PEI was carefully added to 100 µL of OptiMEM™ by pipetting just below the surface and the solution was mixed by gently tapping the tube to the surface. Both DNA mix-OptiMEM™ and PEI-OptiMEM™ tubes were incubated for 5 minutes at RT. Afterwards, the whole content of the PEI-OptiMEM™ tube was added to the DNA mix-OptiMEM™ solution and incubated for 20 minutes at RT with frequent gently mixing of the tube. In the meantime, the cell culture medium of HEK293T/17 cells was replaced from each well with 2 mL of fresh complete medium. To avoid detaching the adherent cell, culture medium was added slowly to one side of the well. At the completion of the incubation time, the DNA mix-PEI-OptiMEM™ solution was distributed dropwise around each well of the plate. Plate was gently rocked to ensure an even dispersal and returned to the incubator at +37°C 5% CO₂. On day 3, HEK293T/17 cell culture medium was replaced from each well with 2 mL of fresh complete medium once

again making sure not to disrupt the cell layer. On day 4, the first harvest of PV was collected (identified in this thesis as 48h) from the transfected cells. This was done by filtering the supernatant in a 0.45 µm filter, cellulose acetate (STARLAB, #E4780-1453) with the aid of a syringe (Fisher Scientific™, Thermo Fisher Scientific, #14955457). Eventually for a second harvest PV (identified in this thesis as 72h), 2 mL of fresh complete medium was added to each well and collected on Day 5 following the same procedure of Day 4. Therefore, the second harvest of PV was collected by filtering the supernatant with the aid of syringe.

2.4 Pseudotype virus (PV) titration

PV entry functionality was assessed by titration for PVs expressing either an emGFP or FLW reporter gene. A 1:2 fold serial dilution was performed across a clear Nunc™ MicroWell™ 96-Well, Nunclon Delta-Treated, Flat-Bottom Microplates (Thermo Scientific™, Thermo Fisher Scientific, #161093) for emGFP or white for FLW expressing PVs (Thermo Scientific™, Thermo Fisher Scientific, #136101) starting with 100 µL of PV in the first row down the plate and discarding the last 50 µL. 50 µL of complete medium was added in each well (Figure 17). Then 50 µL of target cells (1×10^4 cells/mL) were added per well. A PV bearing no envelope GP (Δ env) and cell only controls were added to the plate to identify the PV functionality threshold and the luminescence background respectively. A known high titre PV was included as positive control to ensure the performance of the assay. The plate was incubated for 48h at +37°C at 5% CO₂ before reading. For emGFP expressing PVs, green emGFP-expressing cells were manually counted with the aid of a tally counter under a fluorescent microscope (Nikon, model: Eclipse TS100) and the reported numbers in the results were collected from the first wells of each PV dilution. Images of green emGFP-expressing cells were taken at a 20x ZOE™ Fluorescent Cell Imager (Bio-Rad, #1450031). For FLW expressing PVs, Bright Glo™ luciferase assay system (BG; Promega, #E2650) was employed to read the relative luminescence per unit (RLU). Briefly, BG was mixed with PBS in a 50:50 ratio and 25 µL/well added to the 96-well plate previously aspirated with VACUSIP (INTEGRA, #159000). After 5 minutes incubation, the 96-well plate was read on a GloMax® Navigator Microplate Luminometer (Promega, model: GloMax® Navigator).

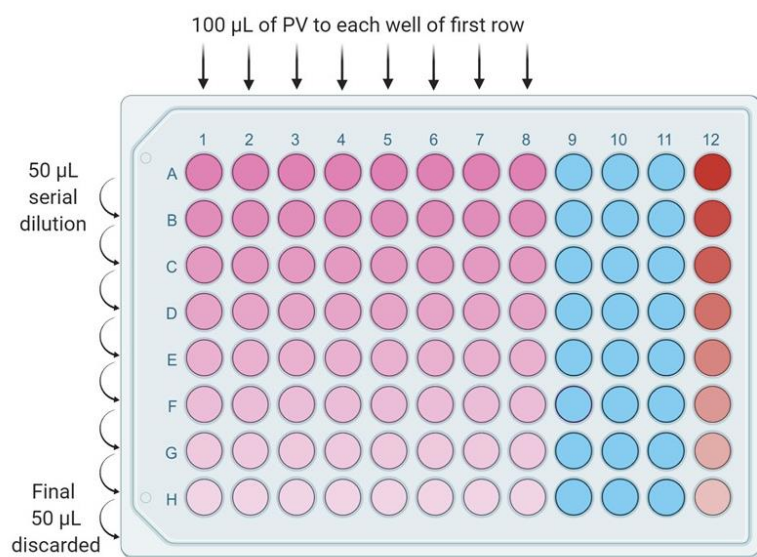


Figure 17: PV titration set-up in 96-well plate. 100 µL of PV supernatant is added to each well of row A and serially diluted down till row H by taking 50 µL from row A to row B and so on till the end of plate. At this point the final 50 µL is discarded. Δenv PV control is indicated in red (column 12), and cell only controls are indicated in blue (columns 9-11). Designed with BioRender.

2.5 Pseudotype virus neutralisation assay (PVNA)

5 µL of heat-inactivated sera was serially diluted in a 1:2 fold in 50 µL in a 96-well white plate. FBS (free of study virus specific antibodies) and sera from a known infected or vaccinated subject (antibodies against the native virus) were included in the assay and serially diluted as well since representing a valuable negative and positive controls respectively. Moreover, a PV only (no sera) and cell only (no PV) controls were included in the plate as they would represent the 0% and 100% neutralisation against the PV. 1×10^6 RLU/mL input of PV (previously titrated as described in Section 2.4.) diluted in the same target cells medium was added to the wells, excluding the cell only ones. The plate was briefly centrifuged at 400 RPM for 30 seconds and incubated for 1 hour at +37°C to allow the priming binding of the antibody to the antigen. After this time, 1×10^4 target cells/well were added to each well in plate in 50 µL, which was then incubated for 48 hours at +37°C at 5% CO₂ before luminescence was read on GloMax® luminometer as described in Section 2.4. A schematic representation of a PVNA is reported in Figure 18 below.

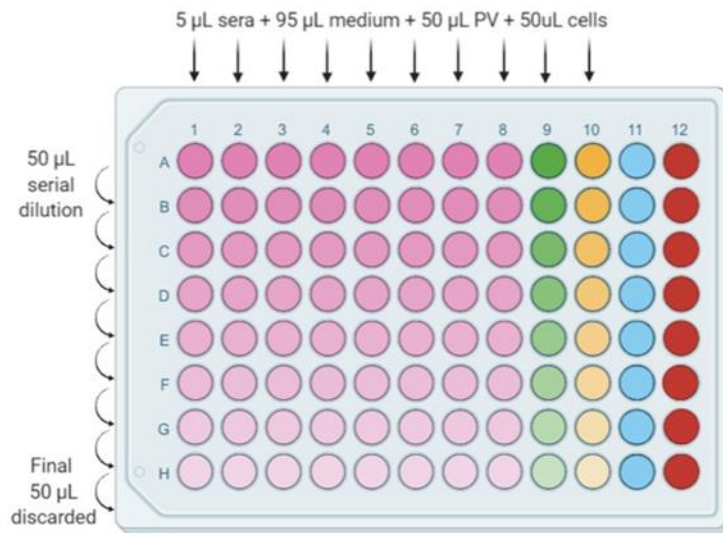


Figure 18: PVNA set-up in 96-well plate. 5 µL of sera is added to 95 µL of medium to each well of row A and serially diluted down till row H by taking 50 µL from row A to row B and so on till the end of plate. At this point the final 50 µL is discarded. Heat-inactivated sera is indicated in pink (column 1-8), FBS is indicated in green (column 9), and positive control sera is indicated in yellow (column 10). 50 µL of PV is added to rows 1-10 and 12. Plate is incubated for 1 hour at +37°C and subsequently 50 µL of cells are added to the whole plate. PV only control is indicated in red (column 12), and cell only controls are indicated in blue (column 11). Designed with BioRender.

2.6 Statistical analysis of PV titration and PVNA data

PV titres obtained at each of a range of dilution points (n=8) were expressed as RLU/mL and the arithmetic mean was first calculated using Microsoft® Excel™ 365 software (Microsoft® Windows). Subsequently, data results were plotted using GraphPad Prism® version 5 software (GraphPad) and when two data sets were compared an unpaired t-test was used (p<0.005). PVNAs were analysed using a non-linear regression method. Firstly, the raw RLU data were converted to a percentage neutralisation value considering 100% neutralisation to the cell only RLU value mean and 0% neutralisation to the PV only RLU value mean. Data were normalised and plotted on a neutralisation percentage scale and the reciprocal of the serum dilution which induces 50% neutralisation or IC₅₀ was calculated.

3 EHV-1 PSEUDOTYPE VIRUS GENERATION AND OPTIMISATION

3.1 INTRODUCTION

Equid herpesviruses (EHVs) are enveloped DNA viruses predominantly infecting members of the *Equidae* family worldwide. To date, nine EHVs have been identified and mostly cause respiratory diseases (Paillot *et al.*, 2008). However, among these, EHV-1 is considered the most concerning as its infection is associated not only to respiratory disease, but also to abortion, perinatal death and stillbirth and neurological disorders, including myeloencephalopathy known as Equine Herpesvirus Myeloencephalopathy (EHM) (Edington, Bridges and Patel, 1986; Edington, Smyth and Griffiths, 1991; Allen, 2002; Paillot *et al.*, 2008). Thus, infection create a significant impact on the equine welfare and economic losses within the horse industry. Infection rates fluctuate between 80 and 90% in the first two years of age of the horse. However, this estimate includes infection by the EHV-1 closest relative, EHV-4 (Allen, 2002). Challenges arise to define EHV-1 annual incidence considering the virus ability to establish latency within the host, as well as EHV-4. EHV-1 belongs to the *Alphaherpesviridae* subfamily and its high incidence of infection is believed to mostly occur during early stages of the horse life followed by latency within the host nervous system. Latency has been exploited by the virus to adapt and co-evolve to the natural host allowing long-term survival and evasion of the immune system (Allen *et al.*, 2004). EHV-1 transmission occurs through direct contact between horses, infectious materials such as aerosol or nasal excretion droplets, fomites, aborted foetus or placenta (Dayaram, Seeber and Greenwood, 2021). Primary infections occur in the respiratory epithelium and cell entry occurs by interaction between specific viral envelope glycoproteins and cell receptors (Patel, Edington and Mumford, 1982; Kydd *et al.*, 1994). EHV-1 exhibits a complex array of 12 glycoproteins on its surface envelope, but it is unclear precisely which are important for virus cell entry and eventual roles in host immune responses (Osterrieder and Van de Walle, 2010). Similarly to what is observed in many other alphaherpesviruses, four glycoproteins (gB, gD, gH and gL) are required for EHV-1 entry (Campadelli-Fiume and Menotti, 2007; Frampton *et al.*, 2007; Kurtz *et al.*, 2010; Sasaki *et al.*, 2011; Azab and Osterrieder, 2012), with gD being highly conserved among alphaherpesviruses and demonstrated to define EHV-1 cellular host range (Azab and Osterrieder, 2012). Pseudotype viruses offer a valuable tool to study viral entry of susceptible cells by relatively easy manipulation of different combinations of candidate envelope glycoprotein genes. Their inability to replicate allows researchers to focus solely on entry processes to identify the virus-cell receptor interaction and to study specific aspect of

the viral binding mechanism (Temperton, Wright and Scott, 2015). The system can be employed to study solo envelope glycoproteins (e.g. HA for influenza virus or Spike glycoprotein for coronaviruses) (Wang *et al.*, 2004; Ferrara *et al.*, 2012; Di Genova *et al.*, 2021) or combined with others (e.g. HA and NA for influenza virus) (Temperton *et al.*, 2007). Successful transduction of the PV into a target cell line should be followed by optimisation of the PV generation protocol to enhance viral titre. If a high titre is generated, less volume of PV is needed to obtain a fixed input to add in plate assays (such as PVNA) and at the same time it would allow consistency of the results by using the same PV batch especially in large scale studies. The term 'PV batch' refers to the volume of PV collected on the same day from the producer cell line supernatant harvested. To investigate the contribution of EHV-1 glycoproteins in entry, this amenable PV system may prove useful. To date, no EHV-1 PV system has been established. However, Rogalin and Heldwein (2016) generated an HSV-1 PV system incorporating four entry glycoproteins employing a VSV core. Most of EHV-1 gene encoding for glycoproteins are homologous among alphaherpesviruses. Thus, EHV-1 glycoproteins are appointed after their homologous in HSV-1, the prototype of alphaherpesviruses (Seyboldt, Granzow and Osterrieder, 2000). In the *Alphaherpesviridae* subfamily, four glycoproteins (gB, gD, gH and gL) are required for viral entry, cell fusion and assembly of infectious virions. More precisely, EHV-1 gB and gD are essential virus components for EHV-1 infectivity involved in virus penetration, virus release and direct cell-to-cell spread (Neubauer *et al.*, 1997b; Csellner *et al.*, 2000). EHV-1 gH and gL, although minor components, are co-associated in a heterodimer and studies suggest their role in viral infection, including cell-to-cell spread (Granzow *et al.*, 2001; Azab, Zajic and Osterrieder, 2012). Therefore, the purpose of this study was to determine which of the 12 EHV-1 glycoproteins are involved in receptor attachment and entry by generating an EHV-1 pseudotype lentiviral system including gB, gD, gH and gL by first testing equal masses of the glycoprotein encoding plasmids, and then by testing different combinations for optimisation purposes. EHV-1 gC is often mentioned as a mediator of EHV-1 entry, driving its attachment into cells through direct envelope-plasma fusion (Neubauer *et al.*, 1997b; Osterrieder 1999; Csellner *et al.*, 2000). To further verify the importance of EHV-1 gC in entry, the glycoprotein encoding plasmid was added to the system or substituting one of the other four glycoproteins. Compared to other EHV-1s or to HSV, EHV-1 is capable to infect a wide range of host cells (Whalley *et al.*, 2007). Tropism is mostly towards epithelial and endothelial cells, but not restricted to those. A range of target cells were investigated to investigate the ability of EHV-1 PV transduction and select the best target.

3.2 MATERIALS AND METHODS

3.2.1 Gene sequences and synthesis

The full length EHV-1 gB, gD, gH and gL gene sequences (ORF 33, 72, 39 and 62 respectively) were kindly provided by Dr. Stéphane Pronost and Dr. Romain Paillot (LABÉO, Saint-Contest, France) obtained from an EHV-1 strain isolated from organs of an aborted horse foetus during a significant EHV-1 outbreak in Normandy (France) in 2010. The strain is recognised as EHV-1 2010.203 after the year and the sample ID they were isolated and belongs to the Multi Locus Sequence Typing (MLST) group 10. These glycoprotein (GP) gene sequences were aligned with the respective homologues in the reference EHV-1 strains; Ab4 (GenBank accession number: AY665713.1) (Telford *et al.*, 1992) and V592 (GenBank accession number: AY464052.1) (Tearle *et al.*, 2003) to verify the correct size in terms of nucleotide length. Next, a molecular strategy was designed for cloning the GP genes into the pCAGGS expression plasmid, by adding restriction enzymes at both 5' and 3' end plus the Kozak consensus sequence GCCACC to initiate the translation process upstream the ATG codon start (Kozak, 1987). The cloning strategy is described in detail in the next Section 3.2.2. and in the Flow Charts in Appendix Figures 1 and 2 for each EHV-1 GP gene. The EHV-1 GP genes were custom synthesised via GeneArt™ (Thermo Fisher) based on the sequences provided to the company, and cloned into their in-house pMX plasmids. The gB, gD and gH genes were cloned into pMA (ampicillin resistant plasmid) while the gL gene was cloned into pMK (kanamycin resistant plasmid). The full length of EHV-1 gC gene sequence (ORF 16) was once again kindly provided by Dr. Stéphane Pronost and Dr. Romain Paillot (LABÉO, Saint-Contest, France). The gC sequence of our study was not obtained from the same 2010 EHV-1 strain used for the other GPs as not available, but from EHV-1 strain Suffolk/87/2009 (GenBank accession number: KU206443.1). However, the gC sequence belongs to the same MLST cluster of the initial 2010 EHV-1 strain (MLST group 10) and no point mutation detected at the amino acids level after aligning gC sequences available on GenBank database. In this project, EHV-1 gC reference sequence is identified as 2009-87. The cloning strategy into pCAGGS vector is described in the next Section 3.2.2. However, in this case the custom synthesised gene fragment it was provided as a lyophilised DNA pellet rather than a pMX clone.

3.2.2 Cloning strategy, plasmid amplification and purification

The EHV-1 gB, gD, gH and gL genes were subcloned from pMX vector series into an in-house pCAGGS expression plasmid previously used to produce functional pseudotypes (Carnell, 2017). The gel-purified gB gene fragment was ligated into pCAGGS using a blunt strategy with

the 3' *XbaI* (restriction site filled with Klenow fragment to fill in the recessed 3' termini of dsDNA) and 5' *XhoI* restriction enzymes. gD, gH and gL were digested with *KpnI* and *XhoI* restriction enzymes. The gC gene fragment ('String') was delivered dried and resuspended in MBG H₂O following the manufacturer's instructions to get 100 ng/μL as final DNA stock. It was digested with *EcoRI* and *BglII* restriction enzymes. A schematic representation of the cloning strategy is shown in the Flow Chart in Appendix Figure 3. All DNA fragments (except gC) were gel extracted with the aid of a scalpel and QIAquick Gel Extraction Kit (QIAGEN, #28704), while all plasmids were prepared and purified as described in Section 2.1.8. To verify whether the correct DNA sequence was inserted into pCAGGS and that no mutation occurred during the process, miniprep purified plasmid clone DNA was sent for Sanger sequencing using pCAGGS FW and Rev primers as described in Table 7 in Section 2.1.10. To verify the whole length of EHV-1 gB and gH, internal FW and Rev primers had to be designed accordingly using Eurofins PCR primer design tool (<https://eurofinsgenomics.eu/en/ecom/tools/pcr-primer-design/>). Primers were synthesised by Eurofins salt free purified in a 10 nmol synthesis scale and delivered lyophilised. Primer sequences are reported in Table 10.

| Primer ID | Primer sequence (5' to 3') | Features |
|-----------------|----------------------------------|--|
| EHV-1 gB INT | FW 5'-gagataacatcatgcaccacg-3' | Anneals downstream the ATG codon start of EHV-1 gB gene sequence in position 716-736 |
| | Rev 5'-aagggtcaagtttagttcaacg-3' | Anneals downstream the ATG codon start of EHV-1 gB gene sequence in position 2235-2256 |
| EHV-1 gH INT | FW 5'-acttacataagccccttgcc-3' | Anneals downstream the ATG codon start of EHV-1 gH gene sequence in position 646-666 |
| | Rev 5'-cgatgcgagagtttagaatcc-3' | Anneals downstream the ATG codon start of EHV-1 gH gene sequence in position 1898-1918 |

Table 10: Sequencing primers designed for EHV-1 gB and gH.

3.2.3 Cell lines and maintenance

HEK293T/17 cells were used for pseudotype virus (PV) production, titration and neutralisation protocols. Maintenance of this cell line is described in Section 2.2.1. Other cell lines were employed to test their efficacy as optimal target cells for EHV-1 PV entry. Equine Dermal fibroblasts (E.Derm; ATCC®, #CCL-57) and RK13 (ATCC®, #CCL-37) were a kind gift from Dr. Stéphane Pronost and Dr. Romain Paillot (LABÉO, Saint-Contest, France). E.Derm were maintained in DMEM added with 20% FBS and 1% P/S, while RK13 were grown in special Minimum Essential Medium with Earle's balanced salts solution (MEM/EBSS; HyClone™, Cytiva, #SH30024.01) added with 10% FBS and 1% P/S. Chinese Hamster Ovary cells (CHO-K1; ATCC®, #CCL-61) were a kind gift from Dr. Giada Mattiuzzo (National Institute for Biological Standards and Control; NIBSC, UK) and were maintained in special Ham's F-12 Nutrient Mixture (F-12; Gibco™, Thermo Fisher Scientific, #11765054) added with 10% FBS and 1% P/S. Foetal Horse Kidney cells (FHK-Tcl3; Andoh *et al.*, 2009; Mahmoud *et al.*, 2013) were a kind gift from Dr. Ken Maeda (The National Institute of Infectious Diseases, Tokyo, Japan). Baby hamster kidney (BHK) cells were a kind gift from Dr. Edward Wright (University of Sussex, UK). FHK-Tcl3, BHK, Madin-Darby Canine Kidney (MDCK I & II; ATCC®, #CRL-2935 and ATCC®, #CRL-2936 respectively) and African green monkey kidney cells (Vero; ATCC®, #CCL-81) were grown in DMEM added with 10% FBS and 1% P/S. All the cell lines described were maintained at +37°C in 5% CO₂ environment in a humidified incubator.

3.2.4 EHV-1 PV generation

PV generation was attempted following the PV generation protocol as described in Section 2.3.1., but using a six-plasmid system transfection for EHV-1. Briefly, 4×10^5 HEK293T/17 cells/well were cultured in a 6-well dish the day before the DNA transfection. The following day, 100 µL of OptiMEM™ was mixed with the DNA plasmid preps: 250 ng of each of the 4 GP gene plasmids (gB, gD, gH and gL in pCAGGS), 750 ng of the reporter gene plasmid (pCSemGW or pCSFLW) and 500 ng of the lentiviral HIV core plasmid (p8.91). For optimisation purposes, the EHV-1 GP plasmids was tested in a range of equal masses of 150 ng, 250 ng or 500 ng or in different combinations between 100 ng or 250 ng. An extra tube with 100 µL of OptiMEM™ was mixed with 1 mg/mL of PEI solution employed as transfection reagent. Both mixtures were left to incubate at room temperature for 5 minutes and subsequently the PEI-OptiMEM™ was added to the DNA mix-OptiMEM™. Following incubation at room temperature for 20 minutes with frequent gentle mixing of the components, the transfection mix was added dropwise to the adherent cells and incubated

at +37°C for 24 hours. The day after, the cell culture media was substituted with 2 mL of fresh cell culture media. 48 hours post-transfection, the supernatant was collected and put through using a 0.45 µm syringe filter for immediate PV titration or stored at -80°C until next use. An additional collection at 72 hours post transfection was performed by adding 2 mL of fresh media to the adherent cells, then harvested as before. A schematic representation of the six-plasmid EHV-1 PV generation is reported in Figure 19 below.

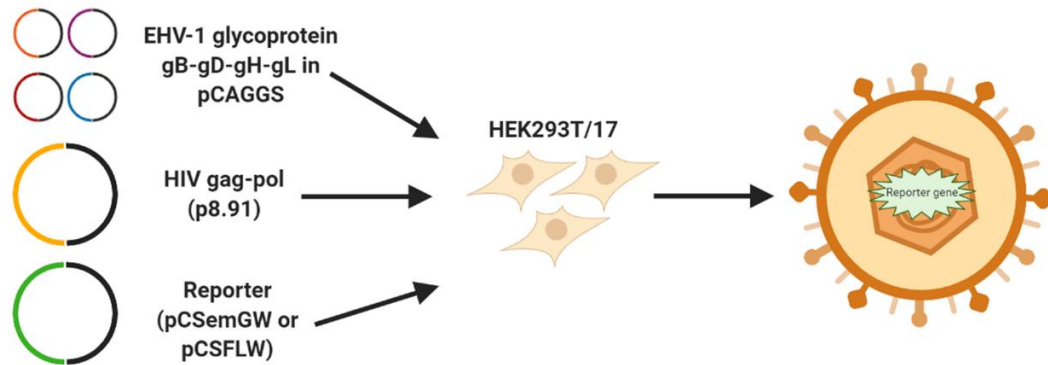


Figure 19: EHV-1 PV generation. Schematic of transient transfection of six plasmids into HEK293T/17. Designed with BioRender.

To investigate whether gC is involved in EHV-1 entry, the gC gene plasmid was added as an extra GP to the six-plasmid system creating a new seven-plasmid system or replacing either gB, gD, gH or gL separately. For optimisation purposes the EHV-1 gC gene plasmid was transfected either at 100 ng or 250 ng.

3.2.5 EHV-1 PV titration

In order to assess the functionality of the newly produced EHV-1 PVs, a GFP titration was first employed on different target cells to evaluate the ability for PV particles to enter cells. If successful, a titration using FLW-expressing EHV-1 PV was used to measure luminescence (in Relative Light Units) emitted as a measure of functional PV particles in the harvested supernatants. PV titration was performed as described in Section 2.4. A PV bearing no envelope glycoproteins (Δenv), and cell only controls were added to the plate to define background luminescence. An equine influenza PV (EIV PV) containing both the haemagglutinin (HA) and neuraminidase (NA) from the Florida clade 2 equine influenza virus strain A/equine/Richmond/1/07 (H3N8) (GenBank accession number: KF559336.1) was included as a further positive control. The EIV PV was generated following the Influenza PV

protocol as described in Section 7.2.11. The cell culture plates were incubated for 48 hours at +37°C at 5% CO₂ before reading either under a Nikon fluorescent microscope for GFP expressing PVs or GloMax® Luminometer for FLW expressing PVs.

3.2.6 TCID₅₀ assay

The 50% Tissue Culture Infectious Dose (TCID₅₀) is used as indicator of viral infectivity and permits PV input normalisation and PV titre results comparison between research groups. In a white 96-well plate, 25 µL of EHV-1 PV and 25 µL of EIV PV supernatants (s/n) were added to the wells in the first column each in 4 replicates. 100 µL of complete cell culture media was added to the rest of the plate. A 5-fold dilution series was performed across the plate until column 11, since column 12 was designed to contain the negative control represented by the cell only (no PV). 100 µL of 2x10⁴ target cells were added to each well and the plate subsequently incubated at +37°C at 5% CO₂ for 48 hours before luminescence was read at the GloMax® Luminometer. A schematic representation of a TCID₅₀ is reported in Figure 20 below.

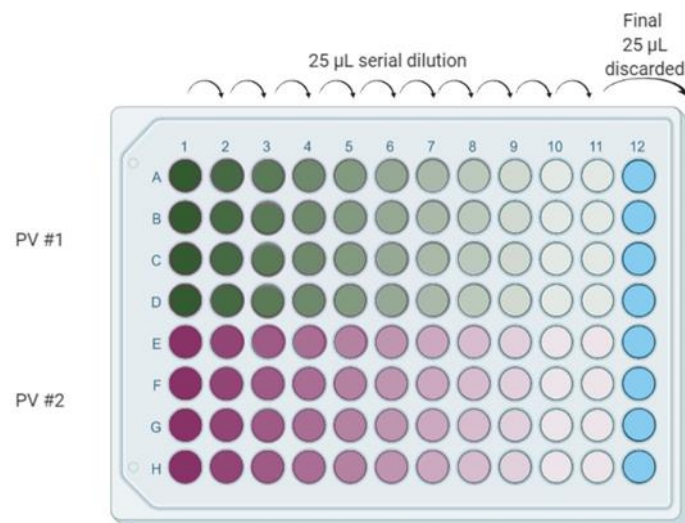


Figure 20: Pseudotype TCID₅₀ titration set-up in 96-well plate. 25 µL of PV s/n is added in quadruplicate to each well of column 1 and serially diluted across the plate till column 11 by taking 25 µL from column 1 to column 2 and so on till column 11. At this point the final 25 µL is discarded. Cell only controls are indicated in blue (column 12). Designed with BioRender.

3.2.7 SDS-Polyacrylamide Gel Electrophoresis

An SDS-PAGE was performed to examine the molecular weight of EHV-1 gB, gC, gD, gH and gL glycoproteins in PV supernatants. PVs were produced as described in Section 3.2.4. Samples were then prepared for SDS-PAGE as described in Section 2.1.13.

3.2.8 Data analysis

To analyse and plot titration data, the method described in Section 2.6. were followed.

3.3 RESULTS

3.3.1 Molecular biology

3.3.1.1 Cloning of EHV-1 gB, gD, gH and gL genes

EHV-1 gB, gD, gH and gL genes (ORF 33, 72, 39 and 62 respectively) were custom synthesised (including specific restriction sites for later subcloning) and inserted into pMX plasmid vectors by GeneArt™ (Thermo Fisher) (Figure 21). pMX-GP genes sizes were first checked by running 500 ng of DNA plasmid on an agarose gel using *XbaI-XhoI* REs strategy (Figure 22). Table 11 shows the length of the GP genes. In order to be subcloned into our in-house pCAGGS plasmid vector, the genes had to first be removed from the pMX plasmids using restriction enzymes. These digests were run on an agarose gel and the gene-containing fragment excised by scalpel for purification (Figure 23).

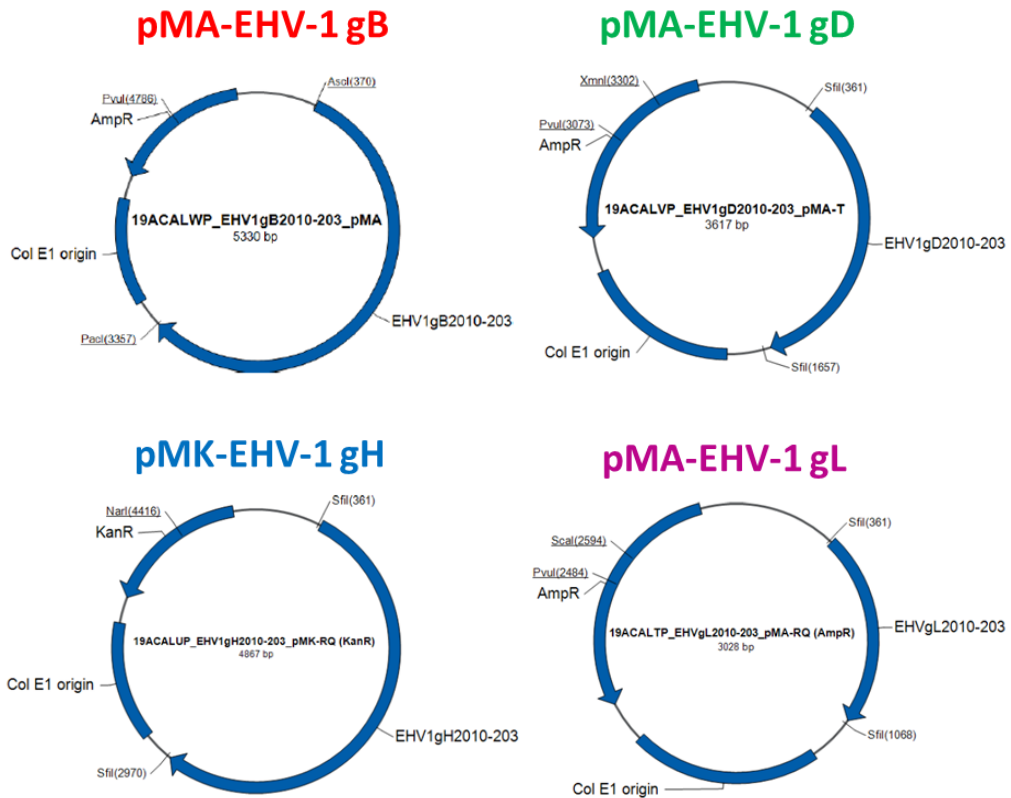


Figure 21: Plasmid maps of pMX-EHV-1 gB, gD, gH and gL. Provided by GeneArt™.

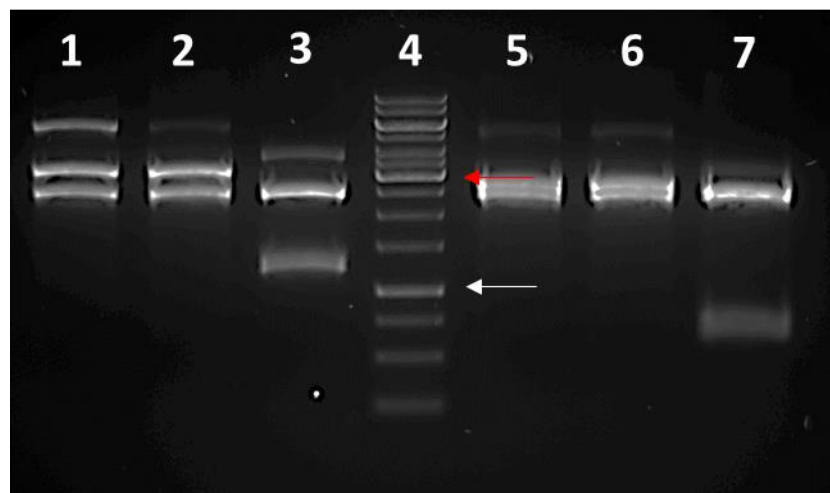


Figure 22: RE digests of EHV-1 GP genes in pMX. Verified on a 1% agarose gel showing vector and gene insert bands. EHV-1 gB (lanes 1 and 2) and gH (lanes 5 and 6) loaded in duplicate. EHV-1 gD (lane 3) and gL (lane 7) loaded once. Fragment sizes estimated by comparison to a GeneRuler 1 kb DNA Ladder (Thermo Scientific™, Thermo Fisher Scientific, #SM0311). White and red arrows indicate 1 kb and 3 kb on DNA ladder. Note the similarity in size between the EHV-1 gB and gH gene fragments and the vector backbone.

| EHV-1 GP gene | Length (bp) |
|---------------|-------------|
| gB | 2973 |
| gD | 1239 |
| gH | 2577 |
| gL | 687 |

Table 11: Length of EHV-1 GP genes.

In order to be subcloned into our in-house pCAGGS plasmid vector, the genes had to first be removed from the pMX plasmids using REs. A detailed subcloning strategy is described in Section 3.2.2. and in the Flow Charts in Appendix Figures 1 and 2 for each EHV-1 GP gene. These digests were run on a 1% low EEO agarose gel (Figure 23) and the gene-containing fragment excised by scalpel for purification as described in Section 3.2.2.

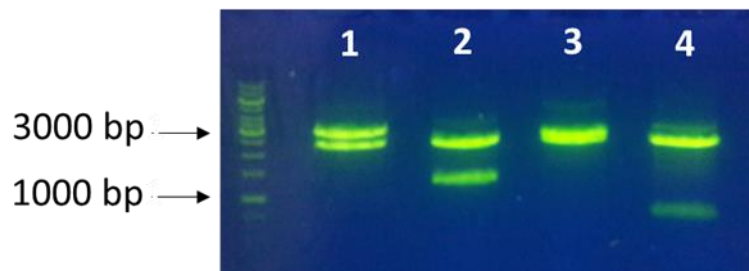


Figure 23: Gel extraction of EHV-1 GP genes from pMX. EHV-1 gB (lane 1), gD (lane 2), gH (lane 3) and gL (lane 4) DNA fragments were run on a 1% low EEO agarose gel for scalpel extraction. Fragment sizes estimated by comparison to a GeneRuler 1 kb DNA Ladder. Note the similarity in size between the EHV-1 gB and gH gene fragments and the vector backbone.

3.3.1.2 Colony screen of EHV-1 gB, gC, gD, gH and gL

Ligation products were transformed into DH5 α competent cells and 50 μ L of SOC/bacteria was plated onto LB Agar plates with the appropriate antibiotic selection (ampicillin) and incubated overnight. The following day, single colonies were picked for colony screening as described in Section 2.1.11. using pCAGGS NT FW and Rev primers for amplification (Table 8). Also, a colony in the vector only plate, if present, was picked as negative control.

The PCR products were visualised on an agarose gel to identify which clones were positive with the gene insertion (Figures 24-28). Positive clone cultures were grown and plasmid clone DNA miniprep purified.

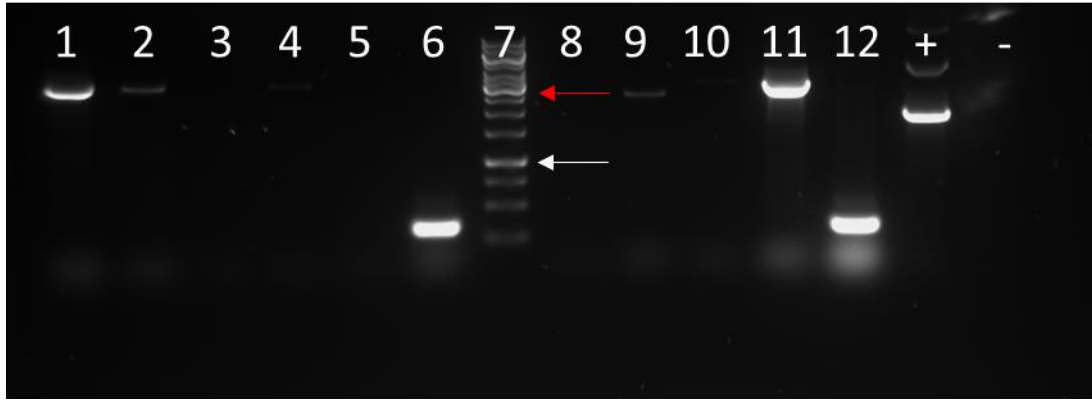


Figure 24: Colony screen of EHV-1 gB clones. Of 10 clones screened, only for clone 1 (lane 1) and 10 (lane 11) a clear band was visible at 2973 bp, showing that the EHV-1 gB insert had ligated into the pCAGGS vector. Fragment sizes estimated by comparison to a GeneRuler 1 kb DNA Ladder. Lane 12 represents the no insert band (pCAGGS empty vector). A positive (+) and negative (-) control were included and represented by pCAGGS-Kz52.HA (different gene insert) and ddH₂O respectively. White and red arrows indicate 1 kb and 3 kb on DNA ladder.

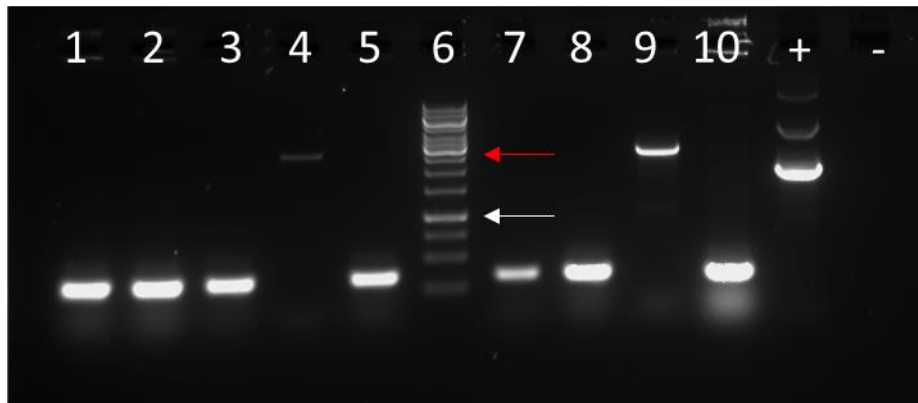


Figure 25: Colony screen of EHV-1 gH clones. Of 8 clones screened, only for clone 4 (lane 4) and 8 (lane 9) a band was visible at 2577 bp, showing that the EHV-1 gH insert had ligated into the pCAGGS vector. Fragment sizes estimated by comparison to a GeneRuler 1 kb DNA Ladder. Lane 10 represents the no insert band (pCAGGS empty vector). A positive (+) and negative (-) control were included and represented by pCAGGS-Kz52.HA and ddH₂O respectively. White and red arrows indicate 1 kb and 3 kb on DNA ladder.

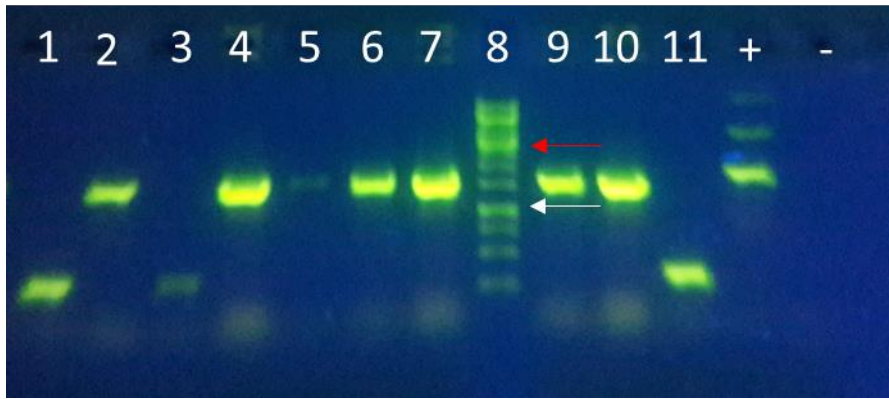


Figure 28: Colony screen of EHV-1 gC clones. Of 9 clones screened, most of the clones (lanes 2, 4, 6, 7, 9 and 10) showed a band visible at 1430 bp, showing that the EHV-1 gC insert had ligated into the pCAGGS vector. Fragment sizes estimated by comparison to a GeneRuler 1 kb DNA Ladder. Lane 11 represents the no insert band (pCAGGS empty vector). A positive (+) and negative (-) control were included and represented by pCAGGS-Kz52.HA and ddH₂O respectively. White and red arrows indicate 1 kb and 3 kb on DNA ladder.

3.3.1.3 Verification of EHV-1 gB, gC, gD, gH and gL genes in pCAGGS

Before sending the DNA plasmid material to be Sanger sequenced, the insert sizes were checked employing FastDigest® REs (Figures 29 and 30). Reactions were set up accordingly using the REs appropriate to the respective the cloning strategies. EHV-1 gB gene was ligated into pCAGGS with a *Sma*I blunt-ligation subsequently filled-in with Klenow fragment at the 5' terminus and XhoI site at the 3' terminus. Therefore, a FastDigest® *Bam*HI was used which is present internally in EHV-1 gB gene sequence.

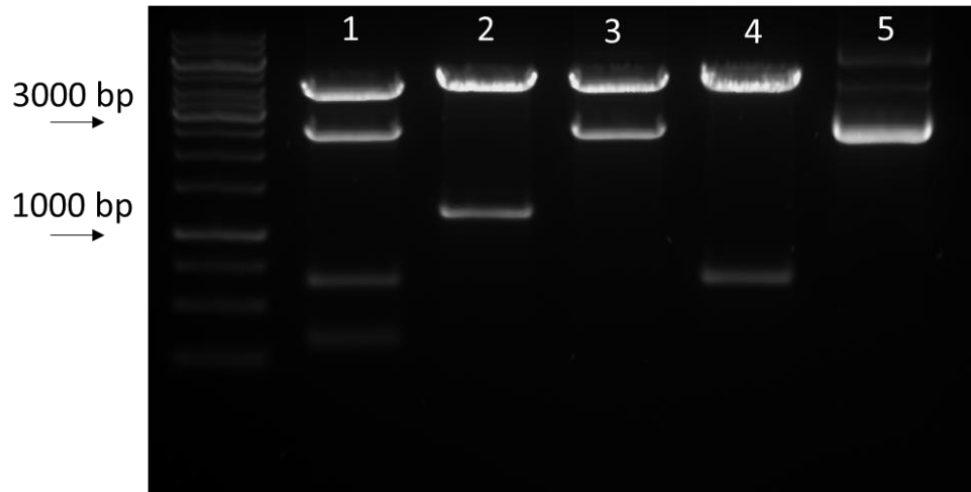


Figure 29: Control digestion of EHV-1 GPs into pCAGGS. Fragment sizes estimated by comparison to a GeneRuler 1 kb DNA Ladder. Cloning of EHV-1 gB (lane 1) to the vector (pCAGGS) was confirmed by BamHI-XhoI restriction digestion. Meanwhile cloning of EHV-1 gD, gH and gL (lanes 2, 3 and 4 respectively) to the vector (pCAGGS) was confirmed by KpnI-XhoI restriction digestion. An empty pCAGGS vector (lane 5) was included as undigested vector (non-linearised, running as supercoiled) and do not run at its actual size.

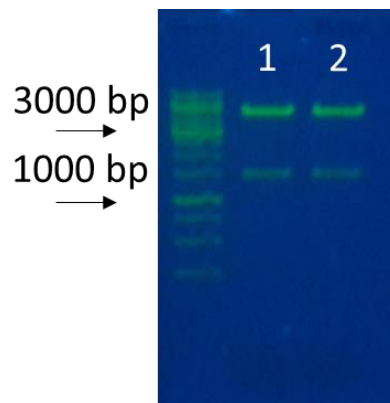


Figure 30: Control digestion of EHV-1 gC into pCAGGS. Fragment sizes estimated by comparison to a GeneRuler 1 kb DNA Ladder. Cloning of EHV-1 gC (lanes 1 and 2) to the vector (pCAGGS) was confirmed by BglII-EcoRI restriction digestion.

3.3.1.4 Sequencing of EHV-1 gB, gC, gD, gH and gL plasmid DNA

Sanger sequencing was performed to verify all cloned gene sequences and particularly check the absence of mutations eventually occurred during the transformation process. pCAGGS FW and Rev primers (Table 7) were employed to verify the 5' and 3' end respectively. To cover the whole length of EHV-1 gB and gH, the corresponding FW and Rev internal gene primers (Table 10) were employed as well. Sequence alignments were analysed on DNADynamo version 1.556 software (BlueTractor) and results are shown below for each EHV-1 GP genes correctly inserted into pCAGGS cloning sites (Figures 31-45).

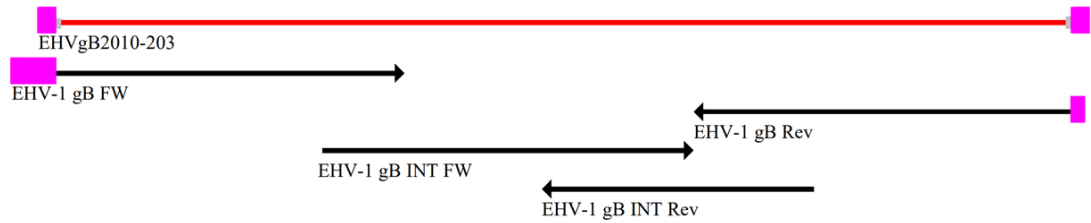


Figure 31: Alignment summary of EHV-1 gB gene sequences. The reference sequence EHVgB2010-203 in red was covered for the whole length by EHV-1 gB FW, gB Rev, gB INT FW and gB INT Rev sequences, with no extra mutation detected.

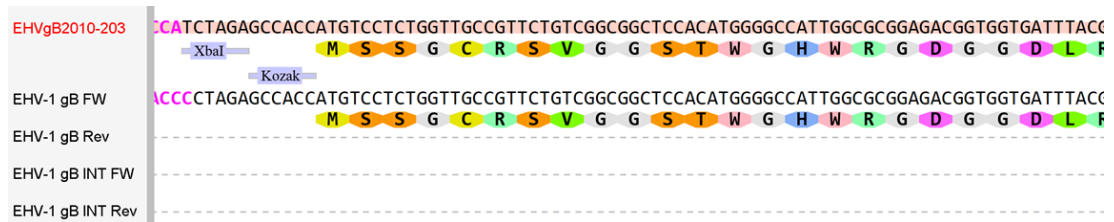


Figure 32: EHV-1 gB gene (strain 2010-203) aligned with EHV-1 gB FW, gB Rev, gB INT FW and gB INT Rev sequences. On the reference sequence, the XbaI site is highlighted to show the cloning site of EHV-1 gB gene used to insert into pCAGGS using a SmaI (CCCGGG) blunt-ligation subsequently filled-in with Klenow fragment followed by the Kozak sequence upstream the ATG start codon.

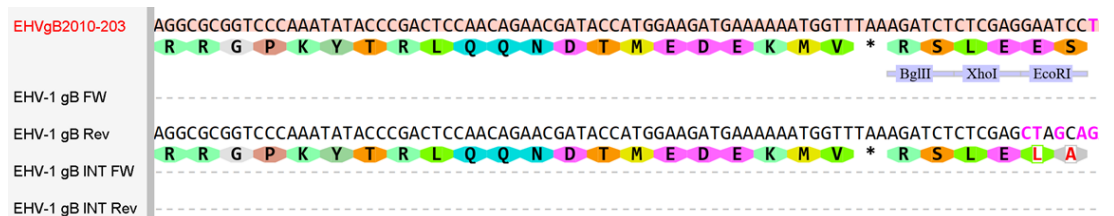


Figure 33: EHV-1 gB gene (strain 2010-203) aligned with EHV-1 gB FW, gB Rev, gB INT FW and gB INT Rev sequences. On the reference sequence, the BglII, XhoI and EcoRI sites downstream the TAA stop codon are highlighted to show the cloning of EHV-1 gB gene used to insert into pCAGGS using XhoI (CTCGAG).

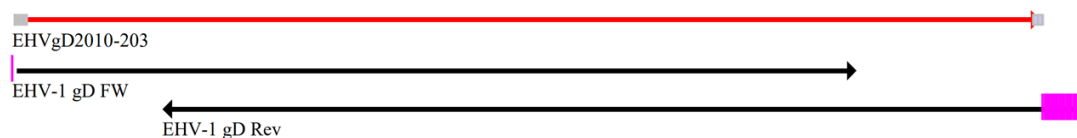


Figure 34: Alignment summary of EHV-1 gD gene sequences. The reference sequence EHVgD2010-203 in red was covered for the whole length by EHV-1 gD FW and gD Rev sequences with no extra mutation detected.

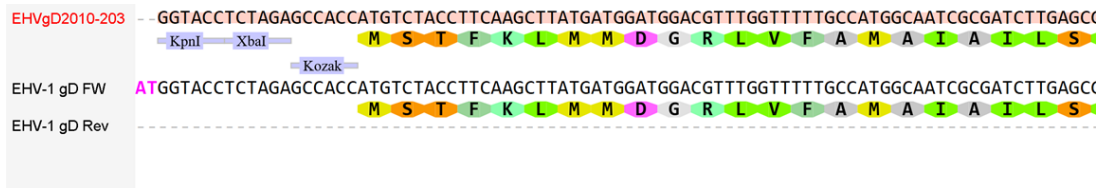


Figure 35: EHV-1 gD gene (strain 2010-203) aligned with EHV-1 gD FW and gD Rev sequences. On the reference sequence, the KpnI and XbaI sites are highlighted to show the cloning site of EHV-1 gD gene used to insert into pCAGGS using KpnI (GGTACC) followed by the Kozak sequence upstream the ATG start codon.

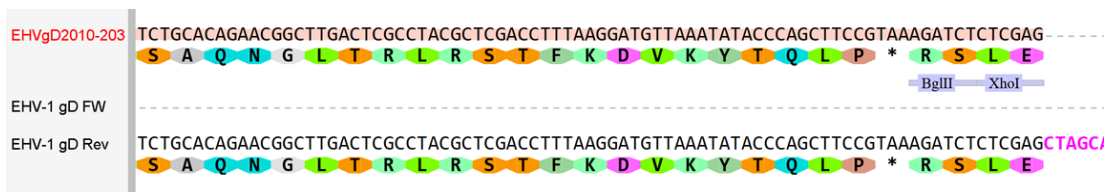


Figure 36: EHV-1 gD gene (strain 2010-203) aligned with EHV-1 gD FW and gD Rev sequences. On the reference sequence, the BglII and XhoI sites downstream of the TAA stop codon are highlighted to show the cloning site of EHV-1 gD gene used to insert into pCAGGS using XhoI (CTCGAG).

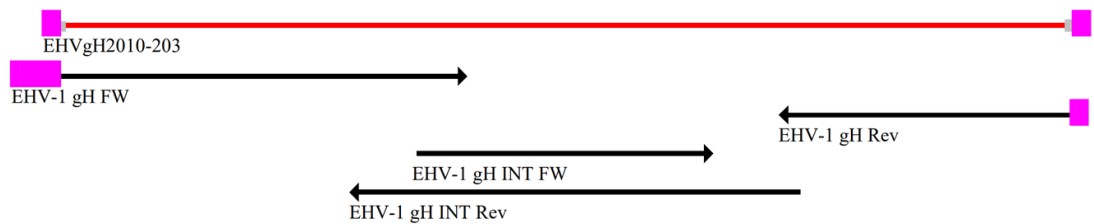


Figure 37: Alignment summary of EHV-1 gH gene sequences. The reference sequence EHVgH2010-203 in red was covered for the whole length by EHV-1 gH FW, gH Rev, gH INT FW and gH INT Rev sequences with no extra mutation detected.



Figure 38: EHV-1 gH gene (strain 2010-203) aligned with EHV-1 gH FW, gH Rev, gH INT FW and gH INT Rev sequences. On the reference sequence, the KpnI and XbaI site are highlighted to show the cloning site of EHV-1 gH gene used to insert into pCAGGS using KpnI (GGTACC) followed by the Kozak sequence upstream the ATG start codon.



Figure 39: EHV-1 gH gene (strain 2010-203) aligned with EHV-1 gH FW, gH Rev, gH INT FW and gH INT Rev sequences. On the reference sequence, the BglII, XhoI and EcoRI sites downstream the TAA stop codon are highlighted to show the cloning site of EHV-1 gH gene used to insert into pCAGGS using XhoI (CTCGAG).



Figure 40: Alignment summary of EHV-1 gL gene sequence. The reference sequence EHVgL2010-203 in red was covered for the whole length by EHV-1 gL FW sequence only with no extra mutation detected.

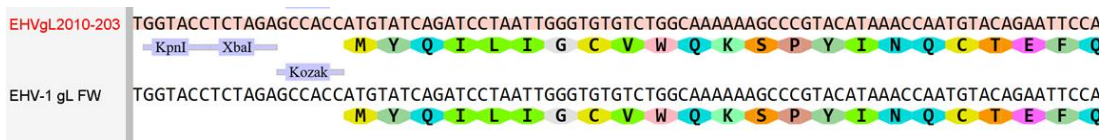


Figure 41: EHV-1 gL gene (strain 2010-203) aligned with EHV-1 gL FW sequence only. The primer is able to cover the whole length of EHV-1 gL gene. On the reference sequence, the KpnI and XbaI sites are highlighted to show the cloning site of EHV-1 gL gene used to insert into pCAGGS using KpnI (GGTACC) followed by the Kozak sequence upstream the ATG start codon.

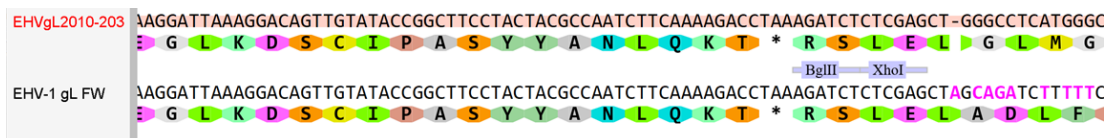


Figure 42: EHV-1 gL gene (strain 2010-203) aligned with EHV-1 gL FW sequence only. On the reference sequence, the BglII and XhoI sites downstream the TAA stop codon are highlighted to show the cloning site of EHV-1 gL gene used to insert into pCAGGS using XhoI (CTCGAG).

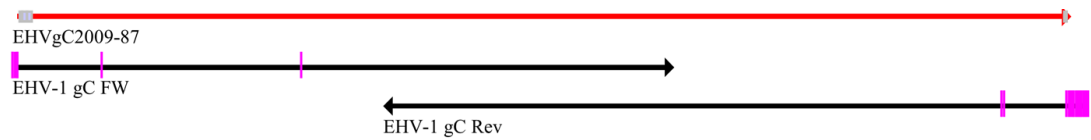


Figure 43: Alignment summary of EHV-1 gC gene sequences. The reference sequence EHVgC2009-87 in red was covered for the whole length by EHV-1 gC FW and gC Rev sequences with no extra mutation detected. The pink lines are highlighting 4 changes which were necessary during the time of synthesis due to the high-GC content. The original EHV-1 gC sequence was optimised using GeneArt™ GeneOptimizer™ tool by changing single nucleotides C120A, C393T, G1350A and G1353A.

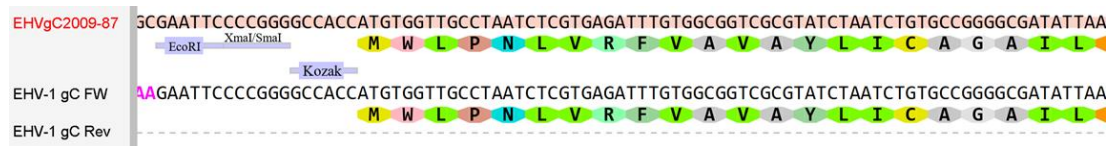


Figure 44: EHV-1 gC gene (strain 2009-87) aligned with EHV-1 gC FW and gC Rev sequences. On the reference sequence, the EcoRI and the neoschizomers XmaI/SmaI sites are highlighted to show the cloning site of EHV-1 gC gene used to insert into pCAGGS using EcoRI (GAATTC) followed by the Kozak sequence upstream the ATG start codon.

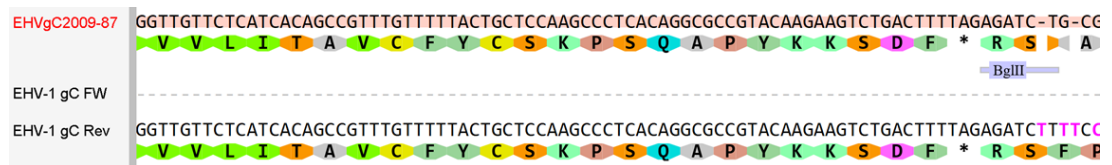


Figure 45: EHV-1 gC gene (strain 2009-87) aligned with EHV-1 gC FW and gC Rev sequences. On the reference sequence, the BglIII site downstream the TAG stop codon is highlighted to show the cloning site of EHV-1 gC gene used to insert into pCAGGS using BglIII (AGATCT).

3.3.2 EHV-1 PV generation

EHV-1 PV generation was attempted using 150 ng, 250 ng or 500 ng amounts of EHV-1 gB, gD, gH and gL gene plasmids in equal proportions and by first using the pCSemGW GFP reporter plasmid and pCSFLW for FLW expression in later experiments, via co-transfection as described in Section 2.3. An EIV PV was generated as a well established positive control to verify the PV production protocol was functioning PV was collected after 48 and 72 hours post-transfection by filtering the supernatant from the transfected cells.

3.3.3 EHV-1 PV titration

A Δenv PV and cell only controls were added to the plate to assess any non-GP mediated transduction of target cells carry over activity and the cells background respectively. GFP and

FLW titration were set up following Section 2.4. instructions. After 48 hours incubation, fluorescently labelled cells were imaged using a fluorescent microscope (ZOE™ Fluorescent Cell Imager; Figure 46) and manually counted to assess relative transduction of PV supernatants and for comparison using the same PV on different target cells (Appendix Table 1).

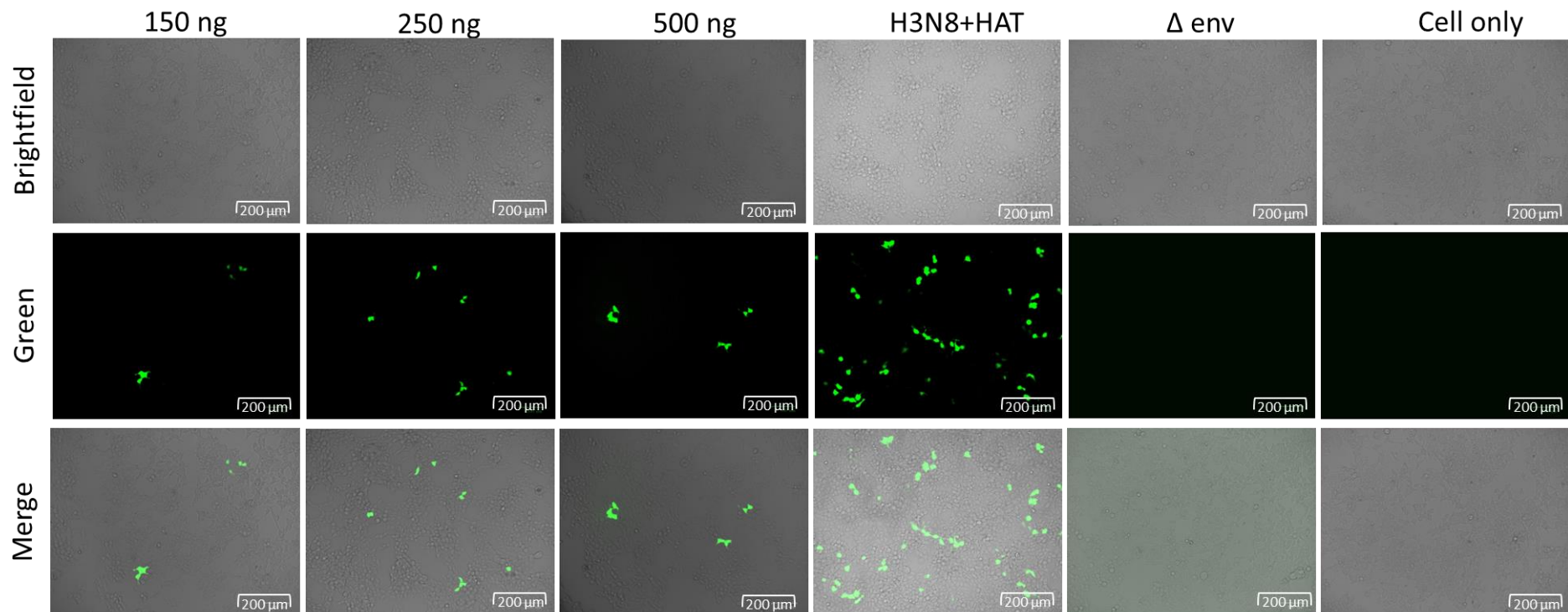


Figure 46: Green HEK293T/17 cells transduced with EHV-1 PV. Transduction was tested with EHV-1 PV generated with either 150 ng, 250 ng or 500 ng of EHV-1 GPs co-transfected with the same amount plasmids. EIV PV (H3N8+HAT) was included as positive control. Δ env PV and cell only controls were included to examine non-specific transduction and morphology/viability of cells. Images were taken at 20x on ZOE™ Fluorescent Cell Imager after 48 hours the GFP titration was set up.

Once PVs containing the GFP reporter gene were evaluated, the FLW reporter PV was employed in PV generation and then titrated by quantifying luminescence in transduced target cells (Figure 47). Interestingly, the highest titre was achieved using 250 ng amount of glycoprotein plasmid. There was no significance difference in titre when using 150 or 250 ng of plasmid (1.75×10^7 RLU/mL and 3.29×10^7 RLU/mL respectively) for the first harvest (Figure 47 Left graph), while the second harvest shows a significant difference ($p=0.0181$; Figure 47 Right graph) for these plasmid amounts. In contrast, 250 ng yielded a significantly higher titre than 500 ng ($p=0.0388$ and $p=0.0006$ for the first and second harvest respectively), suggesting that increasing the amount of plasmid is negatively affecting the production. Surprisingly, no significance difference was reported when comparing titres between the lowest and the highest amount of GP plasmids employed of both 48h and 72h PV harvest. 250 ng of EHV-1 GPs were then employed in co-transfection as optimal amount and in this study the newly generated EHV-1 PV was identified often as BDHL EHV-1 PV.

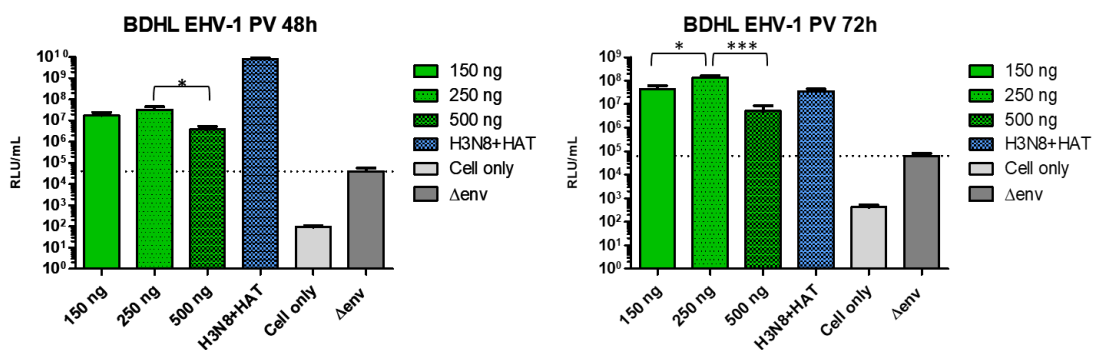


Figure 47: Titration results of EHV-1 PV. EHV-1 PV was generated with either 150 ng, 250 ng or 500 ng of EHV-1 GPs co-transfected with the same amount of plasmids. Controls were included such as an EIV PV, Δenv PV and cell only. **Left graph:** 250 ng yielded a significantly higher titre than 500 ng (* is $p=0.0388$). **Right graph:** a significant difference was reported between 150 ng and 250 ng (* is $p=0.0181$) and between 250 ng and 500 ng (***) is $p=0.0006$). The final titre was the result of the average of duplicates repeated three times.

3.3.4 EHV-1 PV optimisation

Once it had been shown that EHV PVs could be successfully generated using the gB, gD, gH and gL combination, optimisation of the working system was then attempted using different amount combinations of the four EHV-1 GPs (Figure 48). BDHL EHV-1 PV was kept throughout the study as positive control to compare the titre with the newly generated combinations. BDHL compared with a PV generated with 250 ng of pCAGGS-EHV-1 gB and 100 ng of the other GPs plasmids showed a statistically difference ($p=0.0377$ and $p<0.0001$ for 48h and 72h

respectively). The PV titre dropped when generated with 250 ng of pCAGGS-EHV-1 gH and showed a statistical difference when compared with BDHL ($p=0.0082$ and $p<0.0001$ for 48h and 72h respectively; Figure 48 A). BDL(250 ng)H(100 ng) PV showed a statistical difference when compared with BDH(250 ng)L(100 ng) PV ($p<0.0001$ and $p=0.0006$ for 48h and 72h respectively), with BHL(250 ng)D(100 ng) PV ($p<0.0001$ and $p=0.0005$ for 48h and 72h respectively), and with BH(250 ng)DL(100 ng) PV ($p<0.0001$ and $p=0.0004$ for 48h and 72h respectively; Figure 48 B). DL(250 ng)BH(100 ng) PV was compared with HL(250 ng)BD(100 ng) PV ($p=0.0012$ and $p=0.0033$ for 48h and 72h respectively) and with DHL(250 ng)B(100 ng) PV ($p=0.0015$ and $p=0.0070$ for 48h and 72h respectively; Figure 48 C). Interestingly it can be observed that when EHV-1 gH was added in a higher amount (250 ng; Figure 48 A), the titre of the PV decreased significantly ($p=0.0082$ and $p<0.0001$ for first and second harvest respectively). Nevertheless EHV-1 gH is essential in entry as demonstrated in Appendix Table 1. Besides this, EHV-1 gD and gL might also play a crucial role in entry as titre was significantly higher when using 250 ng of both plasmids (1.06×10^8 RLU/mL and 7.87×10^7 RLU/mL for the first and second harvest respectively; Figure 48 A). On the other hand, the titre dropped when using lower amounts of both EHV-1 gD and gL plasmids (1.14×10^6 RLU/mL and 7×10^5 RLU/mL for the first and second harvest respectively; Figure 48 B).

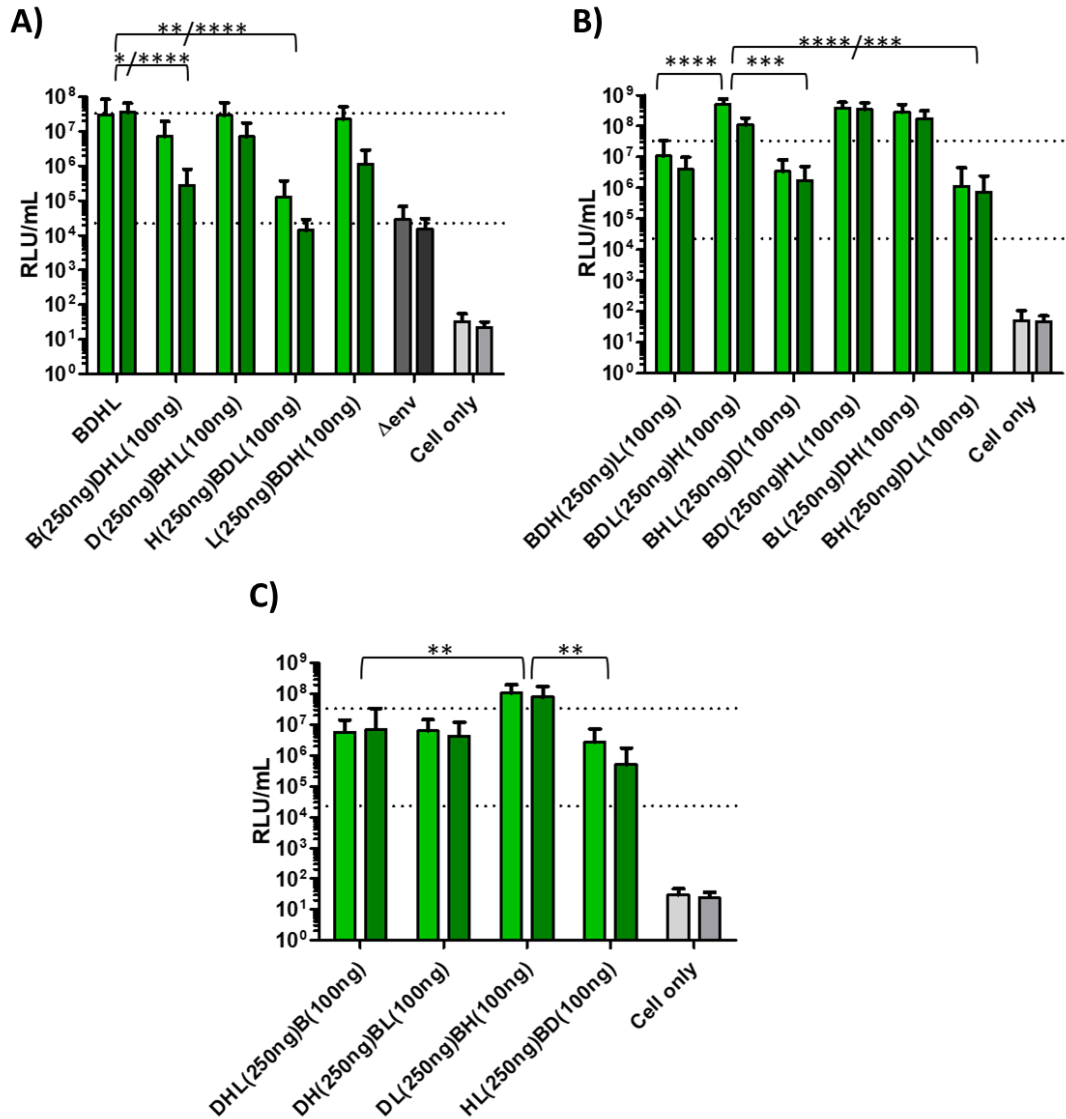


Figure 48: Titration results of EHV-1 PV optimisation. Different amount combination PVs were compared with BDHL using an unpaired t-test. **A):** * is $p=0.0377$ and **** is $p<0.0001$; ** $p=0.0082$ and **** is $p<0.0001$ for 48h and 72h respectively. **B):** **** is $p<0.0001$ and *** is $p=0.0006$; **** is $p<0.0001$ and *** is $p=0.0005$; **** is $p<0.0001$ and *** is $p=0.0004$ for 48h and 72h respectively. **C):** ** is $p=0.0012$ for 48h and $p=0.0033$ for 72h; ** is $p=0.0015$ for 48h and $p=0.0070$ for 72h. The final titre was the result of the average of duplicates repeated three times.

A further optimisation attempt was verified by harvesting the PV at 96 and 120 hours post plasmid transfection (Figure 49). However, titres decreased at these later time points.

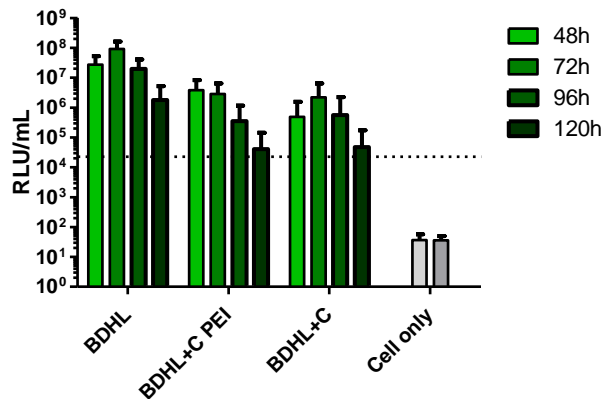


Figure 49: Titration results of EHV-1 PV optimisation. EHV-1 PVs were harvested at 48h, 72h, 96h and 120h post-transfection. Also, the titre of BDHL+C PVs (addition of 250 ng of pCAGGS-EHV-1 gC in co-transfection) and by adjusting the volume for PEI were verified whether an increase would have occurred. BDHL at 72h showed the highest titre achieved (9.13×10^7 RLU/mL). The final titre was the result of the average of duplicates repeated three times.

3.3.5 EHV-1 gC entry function investigation

Further investigation was undertaken to test the contribution of EHV-1 gC to virus particle cell entry by adding or substituting pCAGGS-EHV-1 gC plasmid to the BDHL EHV-1 PV system, and its impact on PV titre. Again, this was done by utilizing the GFP reporter first, before testing PVs produced containing the FLW gene (Figure 50). As observed, the addition of EHV-1 gC to the six-plasmid co-transfection system did not increase the PV titre and interestingly there was significance titre difference between the functional BDHL EHV-1 PV and either adding 250 ng of EHV-1 gC ($p=0.0133$ and $p=0.0049$ for first and second PV harvest respectively) or adding 100 ng ($p=0.0390$ and $p=0.0053$ for first and second PV harvest respectively). Using the GFP reporter, the number of PV-transduced, green cells counted were very low compared with the BDHL counterpart, as recorded in Table 12. Production was also investigated by adding 250 ng of an empty pCAGGS vector only (pCAGGS with no insert) to the BDHL EHV-1 PV system to mimic the insertion of pCAGGS-EHV-1 gC and to verify whether the addition of extra plasmid DNA in co-transfection affected the final titre. The BDHL + empty pCAGGS vector combination PV produced with GFP reporter was able to transduce HEK293T/17 cells more efficiently than BDHL+EHV-1 gC (Table 12). However, no significant difference was detected when the corresponding FLW PV titres were compared. BDHL+empty pCAGGS vector PV was still not as efficient as BDHL EHV-1 PV ($p=0.0203$ and $p=0.0043$ for first and second PV harvest respectively). When 100 ng of EHV-1 gC was added to the BDHL EHV-1 PV system, PEI transfection reagent volume was also adjusted (25 μ L) in proportion to the increasing in DNA plasmid material, but compared with BDHL PV the titre

did not increase. This reinforces the previous hypothesis by which adding an extra plasmid to the system might decrease its potential. When pCAGGS-EHV-1 gC was replacing either pCAGGS-EHV-1 gB, gD, gH or gL in co-transfection, no green cell was appreciated suggesting EHV-1 gC has no role in entry.

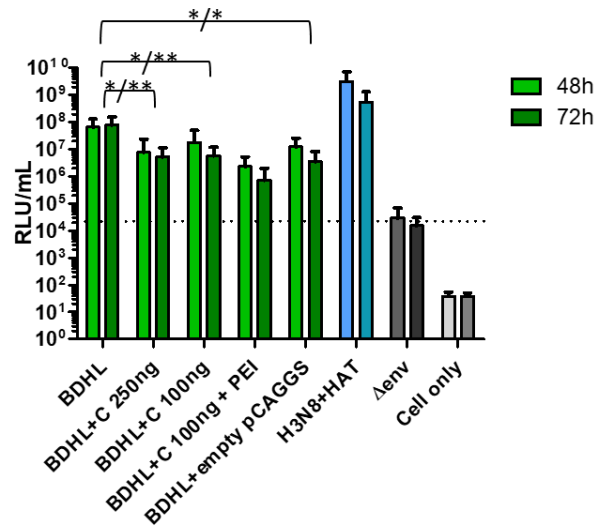


Figure 50: Titration results of EHV-1 PV optimisation. BDHL PV titre was compared with an EHV-1 PV generated by adding 250 ng or 100 ng pCAGGS-EHV-1 gC plasmid. For the latter, an extra PV was generated by adjusting the volume of PEI transfection reagent. A BDHL co-transfected with 250 ng of an empty pCAGGS vector (no insert) was generated as well. Controls were included such as an EIV PV, Δenv PV and cell only. BDHL PV titre was statistically higher than the other PVs: compared to BDHL+C(250 ng) PV (* is $p=0.0133$ and ** is $p=0.0049$), BDHL+C(100 ng) PV (* is $p=0.0390$ and ** is $p=0.0053$), BDHL+C(100 ng) PV (** is $p=0.0098$ and * is $p=0.0142$) and BDHL+empty pCAGGS PV (* is $p=0.0203$ and ** is $p=0.0043$). The final titre was the result of the average of duplicates repeated three times.

| PV | N° Green HEK293T/17 | |
|-------------------|---------------------|-----|
| | 48h | 72h |
| BDHL | 70 | 110 |
| BDHL+C | 2 | - |
| CDHL | - | - |
| BCHL | - | - |
| BDCL | - | - |
| BDHC | - | - |
| BDHL+empty vector | 35 | 30 |
| EIV | 1000 | 200 |

Table 12: Record of green HEK293T/17 cells transduced with EHV-1 PVs. Transduction of EHV-1 PV combinations were tested for both the 48h and 72h harvests. EIV PV is an H3N8 PV included as positive control for both PV production and GFP titration. Green cells were scrutinised under a fluorescent microscope 48 hours post transduction. The numbers reported were visible in the first wells of each PV dilution.

3.3.6 Target cell entry study

Transduction of different target cell lines, detailed in Section 3.2.3., with EHV-1 PVs was assessed (Figure 51). An EIV PV and Δ env PV were included as positive and negative controls respectively. RK13 and E.derm are routinely used in WT EHV-1 diagnostic equine studies (Frampton *et al.*, 2005; Peterson and Goyal, 1988). However, EHV-1 PV was not able to transduce those cell lines as efficiently. The same was observed in FHK despite its equine origin. Interestingly, EIV PV was able to transduce efficiently FHK but not E.derm, both equine cell lines. MDCK I & II are routinely used for influenza studies, while CHO-K1 for Ebola PV. EHV-1 PV was able to transduce these cell lines, but not efficiently (few green cells detected). Vero E6 cells which are permissive to WT EHV-4 but not WT EHV-1 and so were investigated for EHV-1 PV entry. As expected, no green cell was detected because Vero cells restrict HIV-1. Finally, EHV-1 PV entry was also tested on BHK cells. In Appendix Table 1 the number of green cells counted was recorded.

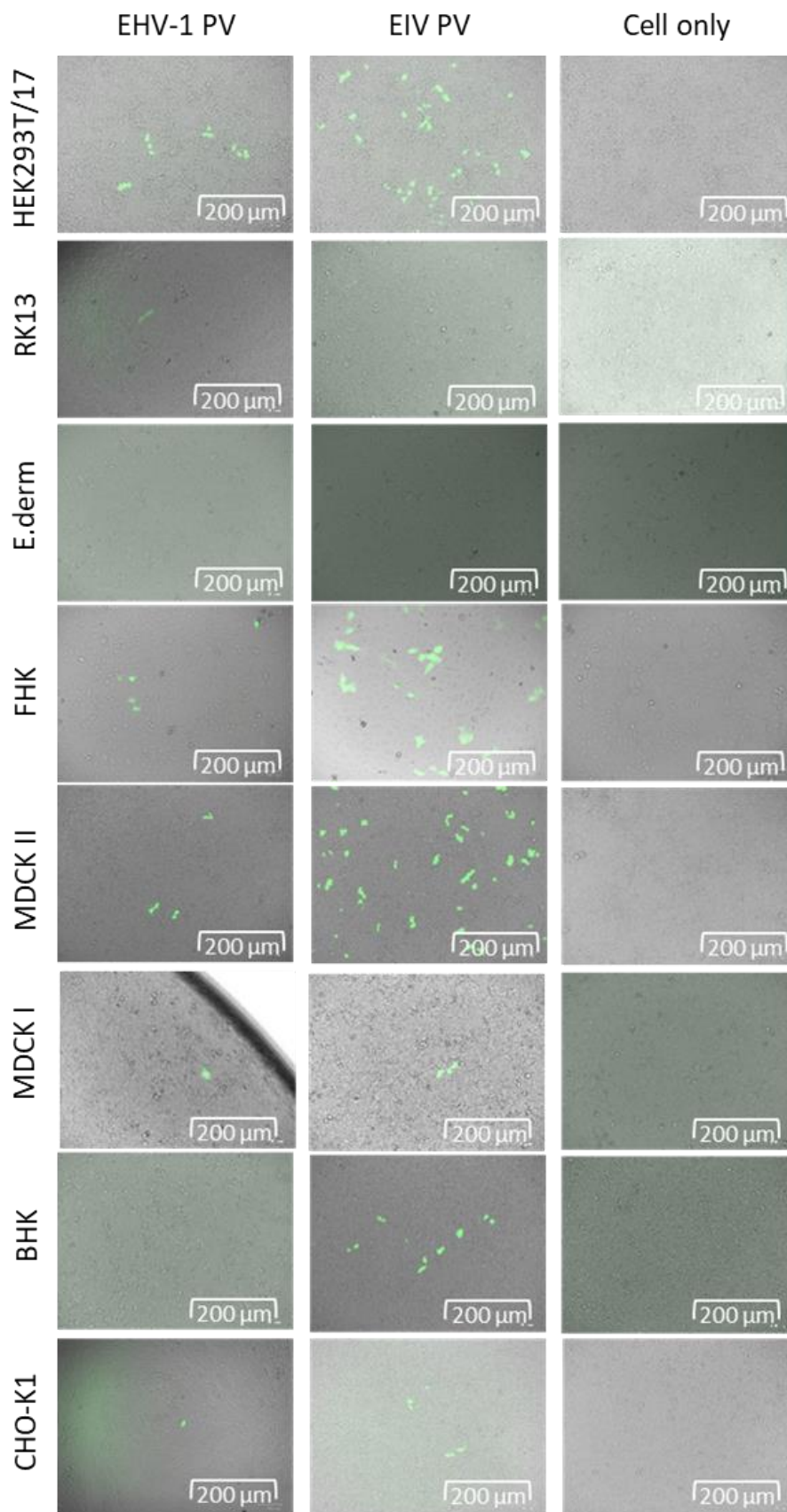


Figure 51: Green target cells transduced with EHV-1 PV and EIV PV. A cell only control was included to examine the morphology of non-transduced target cells. Images were taken at 20x on ZOE™ Fluorescent Cell Imager after 48 hours the GFP titration was set up.

The FLW expressing EHV-1 PV was also employed on the different target cell lines to compensate and confirm the results on the GFP study (Figure 52). Overall, this study shows that HEK293T/17 was the best target cell lines in terms of transduction efficiency and so it was employed for further application (i.e. neutralisation test). This suggests a major binding to cell receptors of the same cell line used for PV production. This might be due to the retention of receptors on the surface during the budding and release of PV particles.

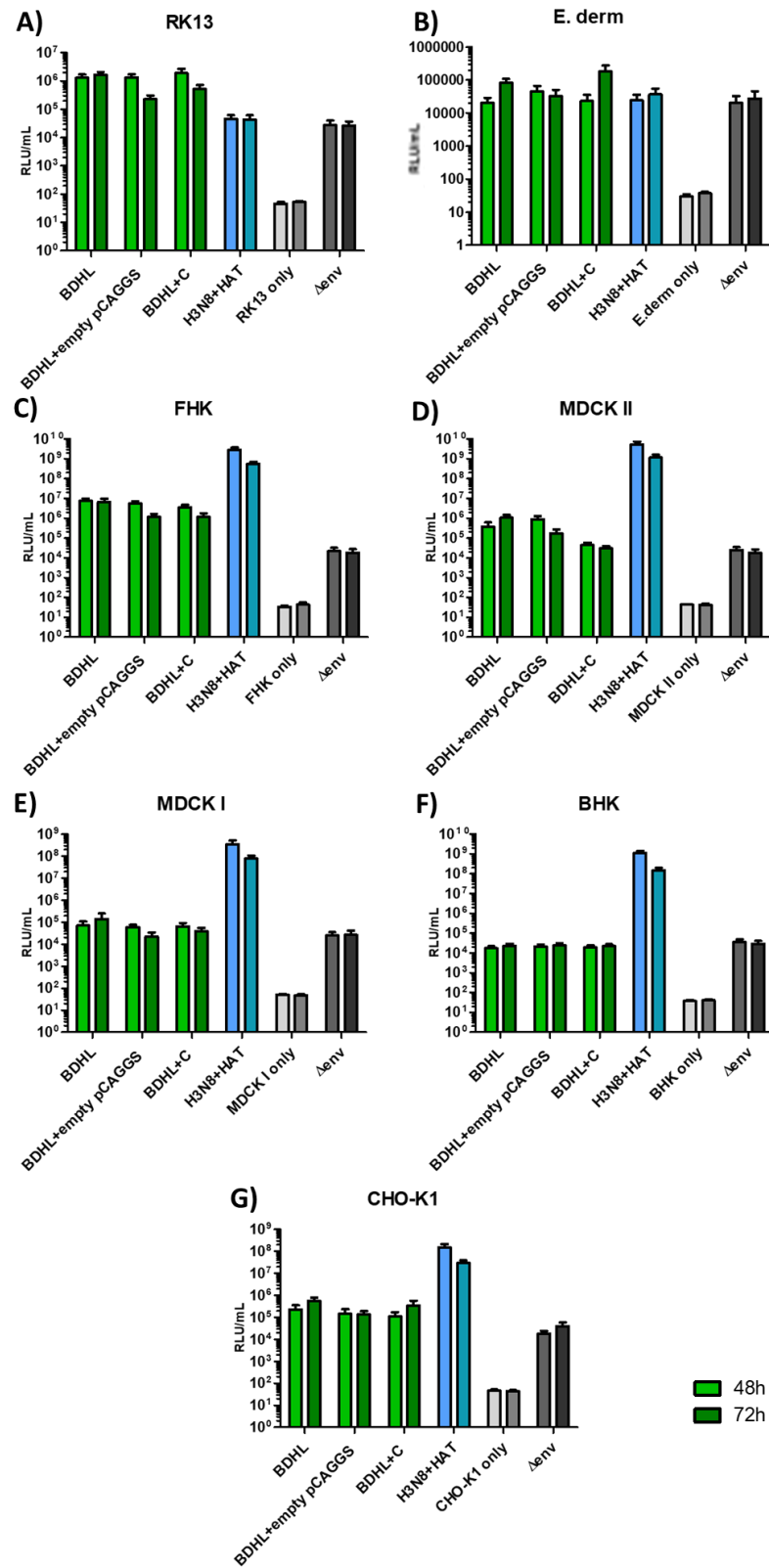


Figure 52: Titration results of target cell entry study. Graphs A-G show combination of EHV-1 PV (BDHL or BDHL added with gC or an empty pCAGGS plasmid) titre on different target cell lines indicated above each graph. Both 48h and 72h PV harvests were titrated. EIV PV (H3N8+HAT) was included as positive control. In addition, Δenv PV and target cell only controls were included to confirm the absence of any transduction activity and cells background. The final titre was the result of the average of duplicates repeated three times.

3.3.7 TCID₅₀

A TCID₅₀ titration was performed to evaluate the virus infectivity and eventually compare the titres in other research lab groups. EHV-1 PV yielded an approximate titre of 1×10^4 TCID₅₀/mL, meanwhile EIV PV titre exceeded 1×10^7 TCID₅₀/mL (Figure 53).

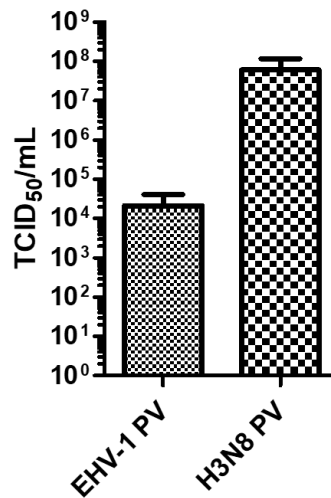


Figure 53: TCID₅₀ titres in HEK293T target cells. EHV-1 and H3N8 (EIV) PV transduction titres are the result of the average of quadruplicates repeated once.

3.3.8 SDS-Polyacrylamide Gel Electrophoresis

An SDS-PAGE was performed including also Kz52 samples (see Figure 186 in Section 7.3.7.). The molecular weight of EHV-1 GPs was hard to interpretate as proteins might not have completed denaturated or p8.91 band might have masked the presence of the glycoprotein polypeptide. Another consideration could be due to the staining method with Coomassie Blue which is widely used for its simplicity binding although not as sensitive compared to alternative stainings.

3.4 DISCUSSION

In this study an EHV-1 pseudotyped lentivirus bearing four glycoproteins gB, gD, gH and gL responsible for target cell entry were successfully generated. Previously there had been only a single report of pseudotyping of a herpesvirus, herpes simplex virus type 1 (HSV-1), using a VSV core and the homologous glycoproteins (Rogalin and Heldwein, 2016). However, prior to the current study it was not known whether the same glycoproteins were essential for EHV-1 entry. Moreover, the recombinant VSVΔG system was applied to create functional HSV-1 PV meanwhile in our case a lentiviral core was used and it was not predictable whether

this technology would have worked out. The VSV core was considered an alternative to attempt generation of EHV-1 vPV in case the lentiviral system failed. To our knowledge, no lentiviral PVs have been created bearing more than three envelope glycoproteins to date. One example is an influenza PV where HA was combined with both NA and M2, and was seen to increase pseudotype yields and infectivity for the PV (Wang *et al.*, 2010). Another was the Human respiratory syncytial virus (hRSV) small hydrophobic protein (hRSV-SH) combined with the hRSV attachment glycoprotein (hRSV-G) and the hRSV fusion protein (hRSV-F) to investigate hRSV cell entry (Haid *et al.*, 2016). However, with our findings we demonstrated that it is possible to create a functional EHV-1 PV by employing four different glycoproteins, expanding the limits of capability of the lentiviral technology. The highest PV titre was achieved employing 250 ng of each glycoprotein encoding plasmid in the co-transfection, implying that lower amounts (150 ng) were not as effective (unpaired t-test; $p=0.0181$ for the second PV harvest) and on the other hand that higher amounts (500 ng) were disrupting ($p=0.0388$ and $p=0.0006$ for the first and second harvest respectively) suggesting that increasing the amount of plasmid is negatively affecting the production. Earlier studies established the importance of gB in EHV-1 penetration and cell-to-cell spread (Wellington 1996; Neubaueur, 1996) and gD in EHV-1 penetration, cell-to-cell spread and endocytic entry (Csellner, 2000; Van de Walle, 2008). The importance of gH mostly complexed with gL in EHV-1 infection was still completely unclear (Robertson, 1991; Stokes, 1996) despite being elucidated for HSV-1 and HSV-2 (Turner, 1998; Muggeridge, 2000). With our findings, the important contributory role of gH and gL in EHV-1 entry was demonstrated.

The current study demonstrated that gB, gD, gH and gL are necessary for EHV-1 PV entry of target cells since if even one of the GP encoding plasmids was excluded in co-transfection (as incomplete GP plasmid sets) the pseudotype particles produced were not able to transduce the target cells. These results were in accordance with VSV Δ G virions where incomplete GP plasmid sets were generated, but particles were not able to enter despite proteins were incorporated into the virions (Rogalin and Heldwein, 2016). Therefore, the initial four HSV-1 homologous entry glycoproteins were required and sufficient for EHV-1 PV entry. However, it is not known the quantity expressed on the surface envelope needed for each glycoprotein to ensure entry and so in which proportion each glycoprotein contribute to this function despite each GP plasmid was added in the same proportion. It was questioned whether the molar ratio of each glycoprotein had an influence in entry. Thus, a combination testing different amounts of GP plasmids during co-transfection was performed. Despite evident differences in the gene sequence length among glycoproteins, the best results were achieved

using the same amount for all four glycoprotein plasmids. It was observed, when the EHV-1 gH plasmid was added in higher amounts the titre dropped significantly. Nevertheless, gH is required for EHV-1 PV entry by complexing with gL, to regulate viral fusion by interacting with gB (Azab, Lehmann and Osterrieder, 2013). Because EHV-1 gH gene is 2577 bp and gL is 687 bp, these findings could imply that the gene sequence length is not correlated to glycoprotein importance and might not influence the amount of glycoprotein expression on the surface envelope. The expression of EHV-1 envelope glycoproteins are not known yet possibly due to the fact that EHV-1 and herpesviruses in general have a very complex envelope. However, Hilterbrand, Daly and Heldwein, 2021 by creating an HSV-1 VSV pseudotype including the four essential entry glycoproteins gB, gD, gH and gL (VSVΔG-BHLD PV) found the levels of gB, gD, gH and gL in VSVΔG-BHLD were in a similar ratio to HSV-1 by Western blotting and densitometry analysis. EHV-1 PV yield was optimised to titres amenable for neutralisation tests, but compared to PV from other virus families generated in-house e.g. SARS-CoV-2-PV (Di Genova *et al.*, 2021) or Influenza PV (Del Rosario *et al.*, 2021), the titre was lower. Consistency during a PVNA is important. Indeed, during the screening of a large sera panel it is preferable to employ a PV from the same batch (PV produced at the same time) to minimise intra-study variability. Therefore, optimisation of EHV-1 PV was necessary to obtain the highest titre possible. Additionally, another factor that could have influenced EHV-1 PV yield was the expression level of the envelope glycoproteins from the plasmid. It has been shown that use of a highly efficient expression vector (e.g. pCAGGS or pI.18) greatly increased the PV titre, along with codon optimisation as reported for instance for expression of SARS spike protein (Nie *et al.*, 2004) or MERS-CoV spike protein (Grehan *et al.*, 2015). Overall, during the optimisation process many packaging conditions should be taken on a case-by-case basis to improve the pseudovirus yield (Sena-Esteves *et al.*, 2004). Further studies should investigate the potential of the VSV system to incorporate EHV-1 glycoproteins as it demonstrated to be a versatile alternative tool to the HIV system (Schnell *et al.*, 1996; Whitt, 2010; Li *et al.*, 2018) and interestingly managed to generate PV while HIV packaging system failed as seen for instance in an hantavirus glycoprotein incorporation study (Brown *et al.*, 2011).

EHV-1 gC is often mentioned as a mediator of EHV-1 entry into cells through direct envelope-plasma fusion (Neubauer *et al.*, 1997; Osterrieder, 1999; Csellner *et al.*, 2000). Consequently, we investigated the inclusion of this GP in our EHV-1 PV particles, and whether it would enhance target cell entry. Despite the working system with four glycoprotein plasmids had been optimised to obtain the higher titres possible, the incorporation of this extra

glycoprotein resulted in a significant decrease in titre using the same or even lower amount of glycoprotein plasmid (250 ng or 100 ng of plasmid added in co-transfection respectively). Thus, the addition of gC, creating five GP PV particles did not result in higher entry performance. Also, the addition of gC plasmid during co-transfection was observed to decrease viability of the producer cell line when compared to the addition of a plasmid only (no insert), suggesting some sort of phenomena of induced toxicity. This might be due to the capacity limit of the lentiviral core, despite EHV-1 gC could drive attachment (Osterrieder, 1999). Osterrieder (1999) demonstrated this by constructing and characterising a gC-negative mutant of EHV-1. Despite the role of gC being found to be important in early steps of EHV-1 infection by attaching to the surface of the target cell via heparan-sulfate containing glycosaminoglycans, it was not an absolute requirement for EHV-1 PV entry.

Optimising the EHV-1 PV titre employing VSV packaging system will be useful not only for further investigation to compare whether it would be a valuable alternative to HIV system, but also to test the capability limits of the VSV packaging system by incorporating more than four GP plasmids as done for the lentiviral system, to better resemble the pseudotype particle to the WT. Incorporation of extra glycoproteins onto the envelope of VSV may be useful to better understand the role of the minor glycoproteins to mediate cellular interactions and to investigate immune responses (Schnell *et al.*, 2006). Especially for this latter consideration, VSV-based pseudotyped system have been demonstrated to be greater in sensitivity, specificity and in correlation with live WT viruses as seen for instance for Ebola virus studies (Steeds *et al.*, 2020). Moreover, in order to investigate EHV-1 gC role in entry, incomplete GP plasmids sets were generated by removing either gB, gD, gH or gL from the combination. In this case, EHV-1 PV was not capable to transduce target cells. Therefore, gC was not essential for EHV-1 PV entry.

Another important variable in our study was represented by the target cells. The PV particles were generated in HEK293T cells employing only four of the total twelve EHV-1 glycoproteins. Once assembled, the pseudotype particles are released from the producer cell by budding. During this stage, the envelope is not only studded with the proteins derived from the study virus but maybe also with residual proteins of the lipid membrane of the producer cell lines. This may explain why HEK293T were found to be the best target cell lines for EHV-1 PV application. The easiness of EHV-1 PV to enter HEK293T might be due to residual HEK293T proteins on its envelope, thus permissive to PV attachment to this particular cell line and further penetration. The host range of cell line which EHV-1 is capable to infect is much wider compared to other EHV-1 or to HSV such as RK13 cells (Whalley *et al.*, 2007). Despite EHV-1

has a tropism for epithelial and endothelial cells, its infectivity is not restricted to these cell types. Indeed, EHV-1 can enter permissive cells either through fusion of its envelope with the host cell membrane or through endocytosis (Frampton *et al.*, 2007). On the other hand, in our study HEK293T proved to be the most transducible with EHV-1 PVs of all the cell line tested. This might be because other minor EHV-1 GPs, that were not included may be involved in cell tropism. This aspect should be further investigated. The study has shown successful EHV-1 PV production for the first time, and this was at a suitable titre for use in subsequent antibody neutralisation, using the best target cell line identified.

4 DEVELOPMENT OF AN EHV-1 PSEUDOTYPE VIRUS NEUTRALISATION ASSAY

4.1 INTRODUCTION

Upon EHV-1 infection, the innate immune system is activated by first releasing cytokines and triggering an inflammatory response at the primary infection site (Kydd *et al.*, 1994; Johnstone *et al.*, 2016). As a consequence, the adaptive immune response is activated to eliminate the viral antigen. Detection of antibodies have been tracked within two weeks after EHV-1 infection and different serotypes have been recognised: IgGa, IgGb, IgGc, IgGd, IgG(T) and IgM (Sugiura *et al.*, 1994; Paillot *et al.*, 2008; Wagner *et al.*, 2015; Perkins *et al.*, 2019), and their response is specific to the viral envelope glycoprotein's epitopes (Allen and Yeargan, 1987; Crabb, Allen and Studdert, 1991; Packiarajah *et al.*, 1998; Perkins *et al.*, 2019). Most likely, mucosal IgA antibodies contribute to reduction of infection in the respiratory tract and viral shedding from the nasopharynx (Hannant *et al.*, 1993; Breathnach *et al.*, 2001). However, their neutralising effect is limited as once the virus establishes cell-associated viremia the antibodies are not able to reach the intracellular level. PCR allows detection of EHV-1 infection by determining the presence of genomic material. However, PCR is not able to determine the viability of the circulating virus. Thus, it is recommended to combine PCR with virus isolation. The latter is considered the gold standard technique to diagnose EHV-1, to observe the CPE as a consequence of infection (OIE Terrestrial Manual, 2018). Diagnosis of EHV-1 is also possible by serology using either virus neutralisation (VN) (Thomson *et al.*, 1976), complement fixation (CF) (Thomson *et al.*, 1976) or enzyme-linked immunosorbent assay (ELISA) (Crabb *et al.*, 1995). EHV-1 can be serologically detected by screening paired serum samples collected during the acute and convalescent stages of infection against type-specific antigens. A four-fold rise in antibody titre implies a positive diagnosis (OIE Terrestrial Manual, 2018). Unfortunately, due to cross-reactivity of antibodies among other EHV-1s especially EHV-4 as a result of prior infections or vaccination, a type-specific diagnosis is difficult to obtain (Balasuriya, Crossley and Timoney, 2015). Furthermore, reproducibility of serological results among laboratories shows some variability, since currently there are no standardised laboratory protocols to perform serological tests or standard reagents recognised internationally (Balasuriya, Crossley and Timoney, 2015). PVNAs offer a potential alternative to current serological assays to detect the presence of functional neutralising antibodies within serum samples for serological screening, vaccine efficacy testing or study the immune host response. Contrary to current serological test, only a small volume of sera (generally 5 μ L) is serially diluted and incubated with a pre-determined amount of PV antigen

(based on titre) to allow antibody binding before target cells are added (usually 1 hour incubation). Neutralisation is measured 48 hours later as the reduction of the reporter gene (e.g. fluorescence/luminescence) compared with an antibody negative control, indicating the presence of antibodies able to inhibit PV transduction (Carnell *et al.*, 2015; Temperton, Wright and Scott, 2015). Taking into account these considerations, an EHV-1 PVNA would use less sample material and less time consuming providing an alternative platform compared to standard EHV-1 serological assay, VN in particular. However, cross-reactivity against EHV-4 might still be an issue. Another aspect to take into consideration is the importance of comparing PVNA with traditional serological assays to assess variability and their use in large studies. Moreover, reproducibility should be investigated as it would give information on the robustness of the assay for standardisation purposes. The aim of the current study was to determine the feasibility of an EHV-1 PVNA by measuring the level of neutralising antibodies from sera samples collected from EHV-1 experimentally infected horses in a longitudinal manner. The antibody titres were then compared with the results obtained from the native virus neutralisation assay.

4.2 MATERIALS AND METHODS

EHV-1 PV was generated and titrated as described in Sections 3.3.2 and 3.3.3. The optimised protocol to produce BDHL EHV-1 PV with FLW as reporter collected at 72 hours post transfection was employed for further applications (i.e. PVNA). HEK293T/17 cells were used as target cells for the PVNA.

4.2.1 Sera samples

A multi-vaccinated pony serum sample was a kind gift from Dr. Janet Daly (University of Nottingham, UK). The subject had been involved in a number of studies at the Animal Health Trust (Newmarket, UK) and the vaccination records state that the pony had been vaccinated not only against various influenza strains but also against EHV-1 using the Duvaxyn® EHV 1,4 Vaccine (Zoetis) first in February 2000 then in March 2000. The serum collected had been heat-inactivated at +56°C for 30 minutes and employed in several influenza vaccine efficacy trials and influenza PVNA validity studies as positive control (Scott *et al.*, 2012; Scott *et al.*, 2016). This serum acted as a positive control throughout the current studies.

The study horse serum panel (also heat inactivated) was kindly provided by Dr. Stéphane Pronost (LABÉO, Saint-Contest, France). In total 52 samples from four 10 month-old male Welsh Mountain ponies (A, B, C and D), which had been raised in a dedicated, specific

pathogen free facility since birth, were experimentally infected by individual nebulisation with C₂₂₅₄ EHV-1 strain (GenBank accession number: MT968035.1) (Sutton *et al.*, 2020). Sample collection occurred on day 0 (A₀, B₀, C₀, D₀) before infection and then daily from day 8 to day 18 (corresponding to sample A₁ to A₁₁, B₁ to B₁₁, C₁ to C₁₁, D₁ to D₁₁) when clinical signs had appeared. 4 extra negative controls were included in the panel represented by sera collected at day 0 from 4 other, non-infected horses (G, I, J and L) (Figure 54).

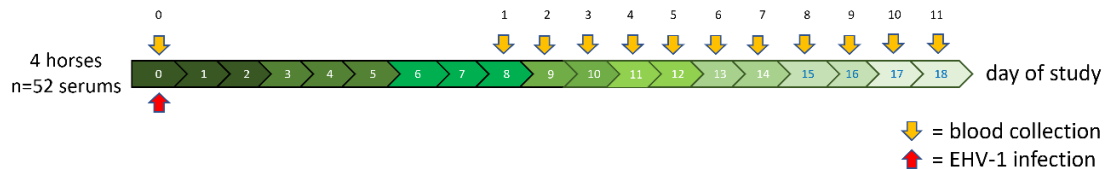


Figure 54: Timeline of study. Infection with EHV-1 on day 0; blood samples were collected at day 0 (sample ID 0) before infection and then daily from day 8 to day 18 (sample ID 1 to 11 respectively) post infection.

4.2.2 EHV-1 PV neutralisation assay

PVNA was carried out as described in Section 2.5. A 1×10^6 RLU/mL input of PV (previously titrated) was added to the wells. FBS is free of EHV-specific antibodies, and thus was used as negative control serum to add to the assay. The positive control serum was that of the multi-vaccinated pony sera described in the previous Section 4.2.1. 5 μ L all the serum samples were serially diluted 2-fold across a 96-well white plate. The plate was incubated for 1 hour at +37°C to allow the binding of any EHV-specific antibodies to EHV surface antigens. After this, 1×10^4 HEK293T/17 cells/well were added to the whole plate. A PV only and cell only control were included in the plate, to represent 0% and 100% neutralisation against the PV respectively. The plate was incubated for 48 hours at +37°C in 5% CO₂ before reading via a GloMax[®] Luminometer.

4.2.3 Data analysis

The raw data files produced by the luminometer were extracted as Microsoft[®] Excel[™] files for initial analysis. The non-linear regression curve fits were then produced using GraphPad Prism[®] following the guidelines in Section 2.6.

4.3 RESULTS

4.3.1 EHV-1 PV neutralisation assay

4.3.1.1 Preliminary EHV-1 PV neutralisation test

The functionality of EHV-1 PV to detect EHV-1 specific antibodies was first assessed in a pilot PV neutralisation test (PVNT) using a multi-vaccinated pony serum (Figure 55). This test was carried out to verify the presence of antibodies and their capability to neutralise EHV-1 PV. Serum was added neat or pre-diluted 1/10 and tested against two different batches of EHV-1 PV produced at different times via the same protocol (Section 3.2.4.). Samples were run in duplicate within each experiment and the test repeated. For both experiments antibodies were able to detect and neutralise the PVs showing a strong neutralisation with IC_{50} values of >40000 (Table 13). The pony had been vaccinated against various influenza strains. Thus, an EIV PV was included as positive control to verify presence of EIV antibodies (Figure 56). For this purpose, serum was added in triplicate as pre-diluted 1/10 and tested against the same batch of EIV PV (Table 14). FBS was included in both assays as a non-virus specific negative control serum, serially diluted and tested against each batch of PV. Another detail to consider was the trend in neutralisation of the PV as the concentration of sera decreased. An expected shift was observed in the gradient of the neutralisation curves for the neat and pre-diluted sera due to the different starting dilution. Direct comparison by statistical analysis was prevented because the neat sera were tested using PV batch 1 meanwhile the pre-diluted 1/10 sera were tested using PV batch 2. However, it seems likely that using different batches of PV starting with pre-diluted serum, the IC_{50} was reduced slightly compared to neat.

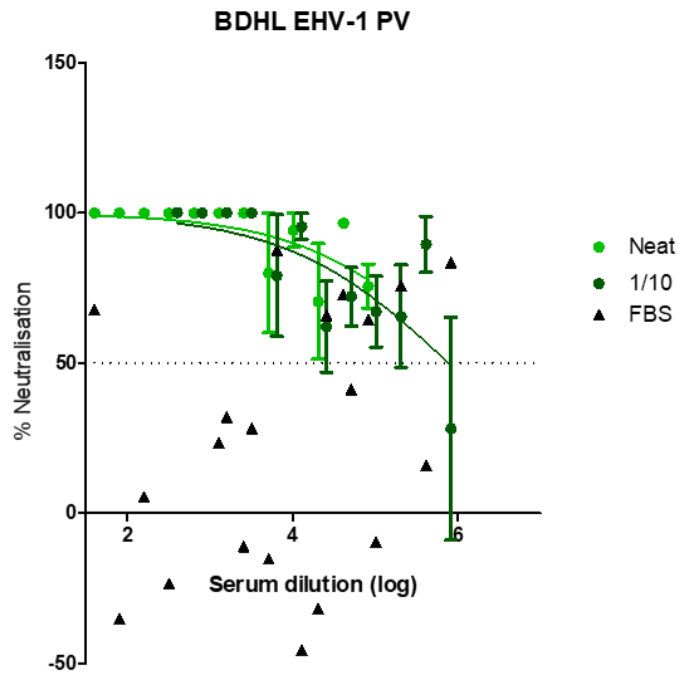


Figure 55: Preliminary PVNT (EHV-1 PV). Neutralisation curves obtained with either neat or pre-diluted serum tested against two different batches of EHV-1 PV. Neat serum was added at a starting dilution of 1/40, while the pre-diluted serum at a starting dilution of 1/400. FBS was included as negative control and no antibodies were detected. Serum was tested in duplicate and experiment carried out once.

| Sera sample | LogIC ₅₀ | IC ₅₀ |
|-----------------|---------------------|------------------|
| Neat | 6.10263 | 1266573 |
| Prediluted 1/10 | 5.847023 | 703109.8 |

Table 13: LogIC₅₀ and IC₅₀ values. Neat or pre-diluted multi-vaccinated pony serum was tested in duplicate against two different batches of EHV-1 PV.

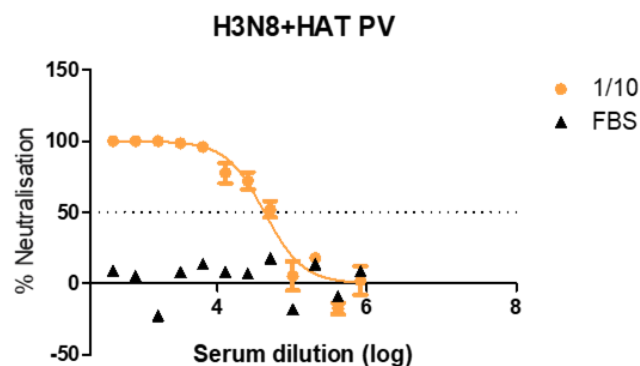


Figure 56: Preliminary PVNT (EIV PV). Neutralisation curve obtained with pre-diluted serum tested against EIV PV to verify the correct performance of the assay. Pre-diluted serum was added at a starting dilution of 1/400. FBS was included as negative control and no antibodies were detected. Serum was added in triplicate and the test was done once.

| Sera sample | LogIC ₅₀ | IC ₅₀ |
|-----------------|---------------------|------------------|
| Prediluted 1/10 | 4.62898 | 42557.860 |

Table 14: LogIC₅₀ and IC₅₀ values. Pre-diluted multi-vaccinated pony serum tested in triplicate against EIV PV.

4.3.1.2 EHV-1 PV in a longitudinal antibody neutralisation study

A larger sera panel from a longitudinal sampling study from horses experimentally infected with EHV-1 was then examined via PVNT (Figure 57). Sera were added neat (in duplicate) at a starting dilution of 1/40 and the assay was repeated twice to verify reproducibility. The first assay was conducted using 2 different batches of PV at the same time because the volume of one PV was not enough to cover the whole panel. The repeat was conducted within 5 months but using one batch of PV. To begin analysis, the threshold of positivity corresponding to detection of neutralising antibodies was defined by averaging the IC₅₀ values of sera samples collected on day 0 (A₀, B₀, C₀, D₀) and of four extra negative sera samples (G, I, J, L) (Section 4.2.1.). An IC₅₀ value of 160 (LogIC₅₀=2.2) was obtained and thus employed as cut-off value for the study. For each assay, the IC₅₀ value of each sample is reported at each time point (from day 0 to day 18) to create a pattern for each individual horse representing the trend of the antibody response throughout the length of the longitudinal study. Each assay included a neat multi-vaccinated pony serum as a positive control and FBS as negative control to verify the correct performance of the assay. Both controls were serially diluted and run against the PV employed. Neutralisation curves were also plotted separately for each horse of the study (A, B, C and D) to observe the trend for each dilution point in time (Figures 58 and 59). Each data point of the two-fold serial dilution was the result of mean of duplicates repeated once. It was interesting to observe how the trend in neutralisation of the PV increased in time for all samples in parallel with the gradient of the neutralisation curves due to the increasing of neutralising antibodies. Statistical analysis was performed using an unpaired t-test between IC₅₀ values of samples tested against different PV batches employed in the assays and it confirmed that there was no significant difference when using different PV batches with the only exception of C₀ (p=0.03; Table 15).

LABÉO SERA PANEL

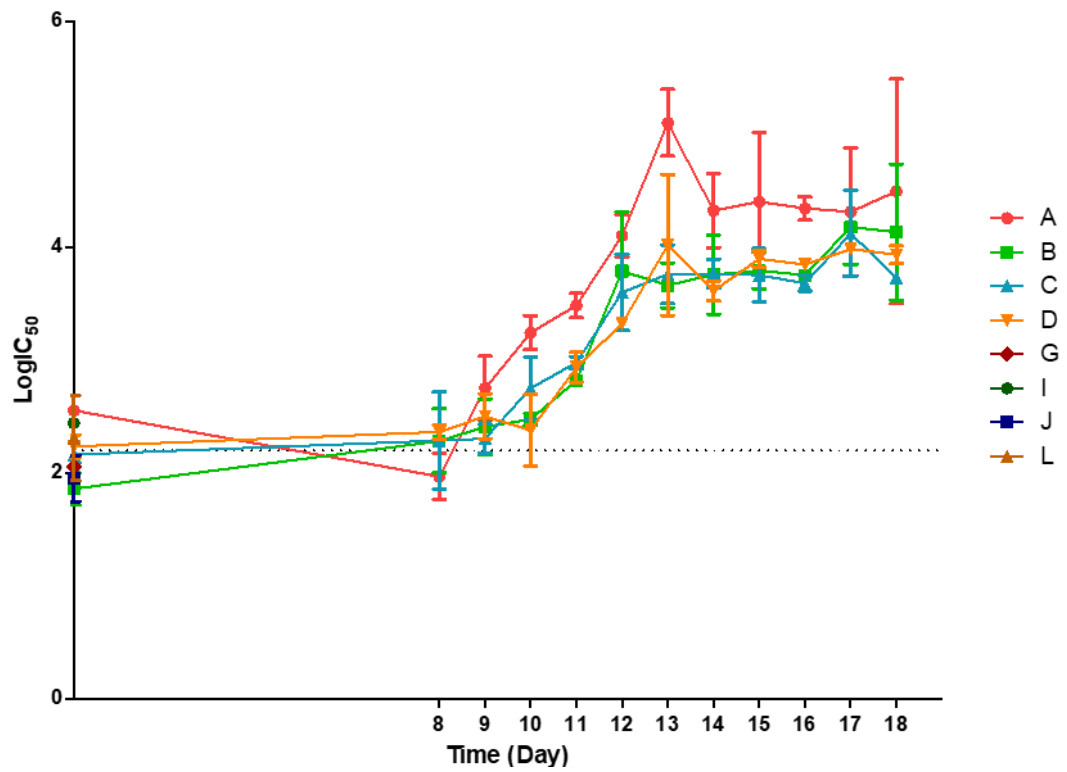


Figure 57: EHV-1 Pseudotype virus neutralisation assay. Longitudinal neutralisation patterns for each individual horse (A, B, C and D) from day 0 to day 18. G, I, J and L were sera collected at day 0 representing the four extra negative samples used to extrapolate the cut-off value (set at $\text{LogIC}_{50}=2.2$) for detection of neutralisation. The LogIC_{50} is reported at each data point represented by the mean with SEM.

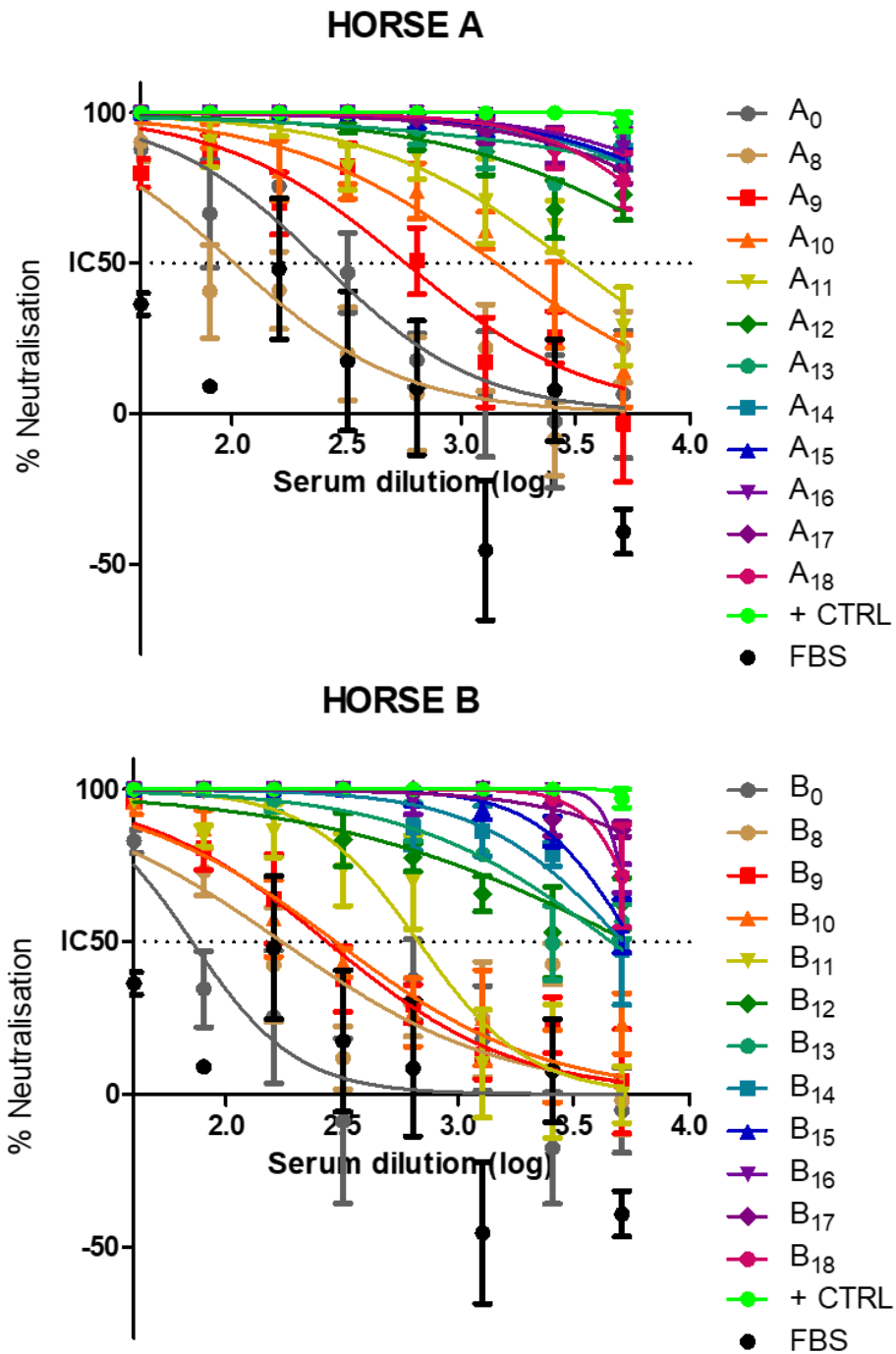


Figure 58: Individual PVNA (A and B). Neutralisation curves obtained separately for horse A and B of the longitudinal study using sample collected on day 0 to day 18 (n=48). Sera were added in duplicate and the test was repeated once. Neat sera were added at a starting dilution of 1/40 (Log of the serial dilution=1.6). The positive control (+ CTRL) was neat multi-vaccinated pony serum. FBS was included as negative control and, as expected, no antibodies were detected. Each data point of the two-fold serial dilution was the result of mean of duplicates repeated once. The % neutralisation is reported at each data point represented by the mean with SEM.

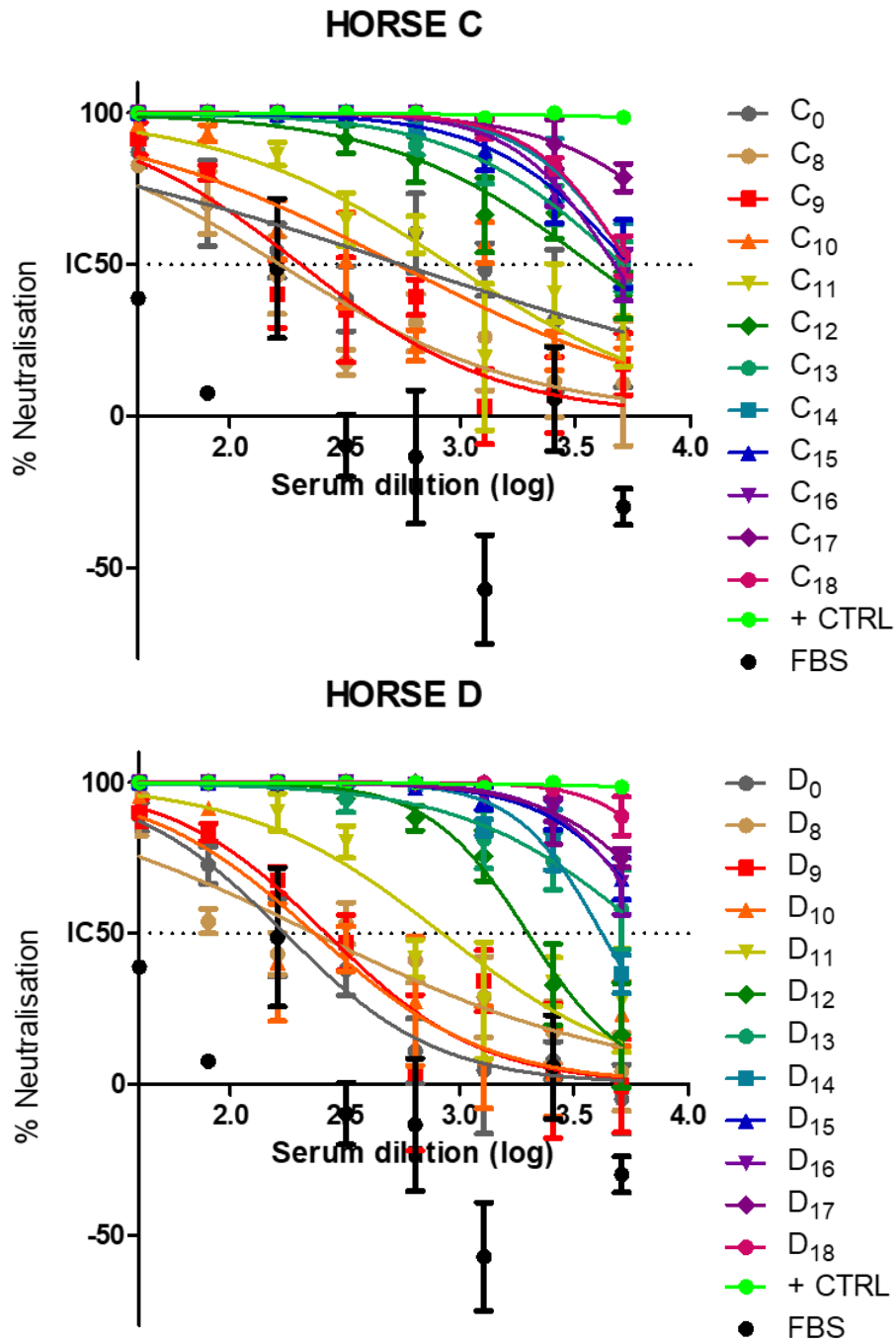


Figure 59: Individual PVNA (C and D). Neutralisation curves obtained separately for horse C and D of the longitudinal study using sample collected on day 0 to day 18 (n=48). Sera were added in duplicate and the test was repeated once. Neat sera were added at a starting dilution of 1/40 (Log of the serial dilution=1.6). The positive control (+ CTRL) was neat multi-vaccinated pony serum. FBS was included as negative control and, as expected, no antibodies were detected. Each data point of the two-fold serial dilution was the result of mean of duplicates repeated once. The % neutralisation is reported at each data point represented by the mean with SEM.

| Horse Sample | A | B | C | D |
|--------------|--------|--------|------------|--------|
| 0 | p=0.31 | p=0.93 | (*) p=0.03 | p=0.83 |
| 8 | p=0.81 | p=0.43 | p=0.11 | p=0.94 |
| 9 | p=0.66 | p=0.35 | p=0.78 | p=0.38 |
| 10 | p=0.58 | p=0.66 | p=0.55 | p=0.43 |
| 11 | p=0.92 | p=0.82 | p=0.88 | p=0.80 |
| 12 | p=0.99 | p=0.26 | p=0.41 | p=0.87 |
| 13 | p=0.97 | p=0.66 | p=0.95 | p=0.52 |
| 14 | p=0.77 | p=0.24 | p=0.97 | p=0.70 |
| 15 | p=0.52 | p=0.84 | p=0.52 | p=0.52 |
| 16 | p=0.43 | p=0.97 | p=0.99 | p=0.76 |
| 17 | p=0.72 | p=0.46 | p=0.72 | p=0.83 |
| 18 | p=0.46 | p=0.45 | p=0.91 | p=0.34 |
| CTRL | p=0.97 | | | |
| FBS | p=0.70 | | | |

Table 15: Statistical analysis of PVNA. Comparison of IC_{50} values of each sample between PV batch 1 (first assay) and PV batch 2 (assay repeat) using an unpaired t-test ($p < 0.05$). P values are reported for all samples compared ($n=48$) and for the positive and negative controls (CTRL and FBS respectively). Only C_0 showed a statistical difference between PV batches (* is $p=0.03$).

4.3.2 Correlation of antibody titres

Once PVNT was successfully performed, it was deemed important to correlate the antibody titres obtained with that from a conventional EHV-1 VN assay using the RK13 cell line (Table 16). Pearson correlation was calculated for all samples collected from day 8 to day 18 ($n=44$) between the EHV-1 VN titres and the reciprocal PVNT IC_{50} values and demonstrated a good correlation ($r=0.82$, $p < 0.0001$; Figure 60). Ab titres of individual horses (A and B) were also measured using xCELLigence kinetics based on Real Time Cell Analysis (RTCA) technology on E.derm (Table 16). To compare the results, Pearson correlation was calculated for A and B samples ($n=22$) between the logarithm IC_{50} values obtained with xCELLigence kinetics and PVNT IC_{50} values and demonstrated a good correlation ($r=0.72$, $p=0.0002$; Figure 61). Both the conventional EHV-1 VN assay and xCELLigence neutralisation assay were performed and analysed by Dr. Gabrielle Sutton (LABÉO, Saint-Contest, France). Reciprocal Ab titres of

horses A and B (n=22) obtained with xCELLigence kinetics were also compared to the conventional EHV-1 VN method ($r=0.87$, $p<0.0001$) (Figure 62).

| Horse A | | | | | | | | | | | |
|---------------------------|------|------|-------|-------|-------|-------|-------|-------|-------|-------|-------|
| Sample | 1 | 2 | 3 | 4 | 5 | 6 | 7 | 8 | 9 | 10 | 11 |
| EHV-1 VN | 2.00 | 2.58 | 3.58 | 6.00 | 6.00 | 7.00 | 8.00 | 8.00 | 5.58 | 7.58 | 8.00 |
| Log ppNT ₅₀ | 7.03 | 8.48 | 11.13 | 11.83 | 13.20 | 16.26 | 15.15 | 13.19 | 14.19 | 13.00 | 17.27 |
| Log xCELLNT ₅₀ | 2.00 | 2.00 | 4.24 | 4.19 | 4.65 | 5.33 | 5.37 | 6.06 | 6.17 | 6.14 | 6.01 |

| Horse B | | | | | | | | | | | |
|---------------------------|------|------|------|------|-------|-------|-------|-------|-------|-------|-------|
| Sample | 1 | 2 | 3 | 4 | 5 | 6 | 7 | 8 | 9 | 10 | 11 |
| EHV-1 VN | 2.58 | 3.58 | 5.58 | 6.58 | 6.58 | 8.00 | 7.58 | 7.58 | 7.58 | 7.00 | 7.58 |
| Log ppNT ₅₀ | 8.26 | 7.43 | 8.10 | 9.32 | 11.35 | 11.71 | 11.67 | 12.23 | 12.47 | 14.65 | 12.32 |
| Log xCELLNT ₅₀ | 2.00 | 3.20 | 3.86 | 4.26 | 5.19 | 6.08 | 6.72 | 7.52 | 6.86 | 7.66 | 2.00 |

| Horse C | | | | | | | | | | | |
|------------------------|------|------|------|------|-------|-------|-------|-------|-------|-------|-------|
| Sample | 1 | 2 | 3 | 4 | 5 | 6 | 7 | 8 | 9 | 10 | 11 |
| EHV-1 VN | 7.58 | 2.00 | 2.00 | 2.58 | 3.00 | 6.58 | 7.00 | 7.00 | 7.00 | 7.58 | 6.58 |
| Log ppNT ₅₀ | 6.59 | 7.36 | 8.49 | 9.78 | 11.17 | 13.10 | 12.82 | 13.02 | 12.40 | 12.80 | 12.36 |

| Horse D | | | | | | | | | | | |
|------------------------|------|------|------|------|-------|-------|-------|-------|-------|-------|-------|
| Sample | 1 | 2 | 3 | 4 | 5 | 6 | 7 | 8 | 9 | 10 | 11 |
| EHV-1 VN | 7.58 | 3.00 | 2.00 | 2.58 | 3.58 | 6.00 | 7.00 | 8.00 | 7.58 | 8.00 | 8.00 |
| Log ppNT ₅₀ | 7.71 | 8.78 | 8.66 | 9.45 | 11.06 | 11.89 | 11.80 | 12.79 | 12.89 | 13.31 | 13.26 |

Table 16: Comparison of EHV-1 PVNA and VN. Antibody titres obtained with a conventional EHV-1 VN assay using the RK13 cell line (EHV-1 VN) and for horse A and B an EHV-1 VN assay performed on E.derm on xCELLigence RTCA (Log xCELLNT₅₀) compared with the reciprocal of the IC₅₀ values with EHV-1 PVNT (Log ppNT₅₀) of sera samples collected from EHV-1 experimentally infected horse A, B, C and D.

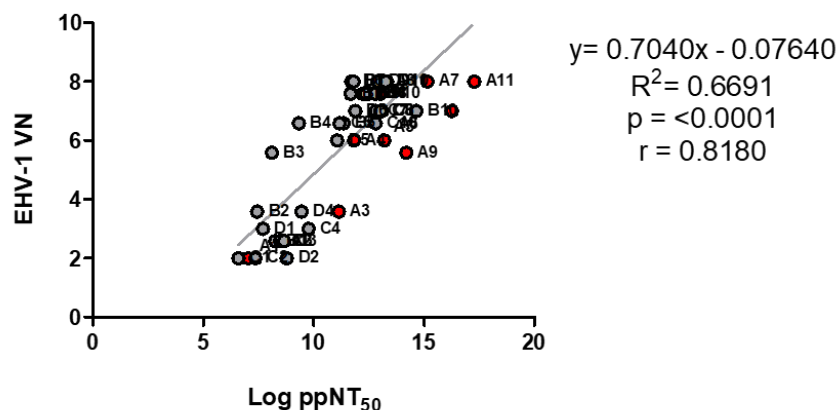


Figure 60: Correlation EHV-1 VN and ppNT50. Correlation of the antibody titres obtained between the conventional EHV-1 VN and the reciprocal of the IC₅₀ values with PVNT (Log ppNT₅₀) and graphed in a Scatter plot. Pearson correlation coefficient $r=0.82$ was calculated for samples collected from day 8 to day 18 (n=44).

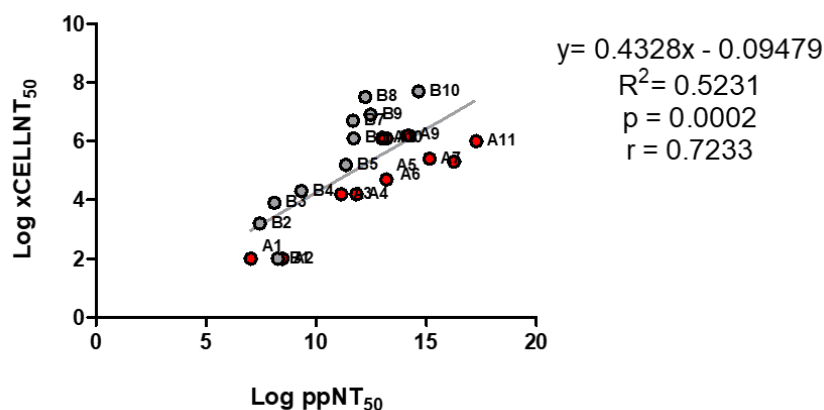


Figure 61: Correlation xCELLNT50 and ppNT50. Correlation of the antibody titres obtained between the logarithm IC_{50} values obtained with xCELLigence kinetics (Log xCELLNT_{50}) and PVNT (Log ppNT_{50}) and graphed in a Scatter plot. Pearson correlation coefficient $r=0.72$ was calculated for samples A and B ($n=22$).

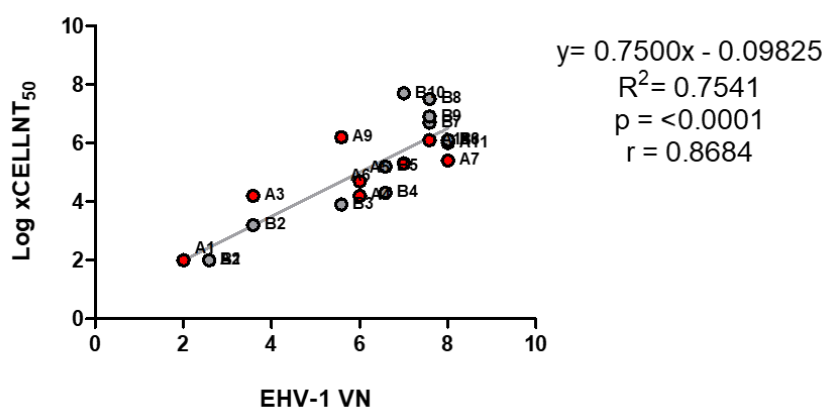


Figure 62: Correlation xCELLNT50 and EHV-1 VN. Correlation of the antibody titres obtained between the logarithm IC_{50} values obtained with xCELLigence kinetics (Log xCELLNT_{50}) and conventional EHV-1 VN and graphed in a Scatter plot. Pearson correlation coefficient $r=0.87$ was calculated for samples A and B ($n=22$).

4.4 DISCUSSION

Before moving to assess neutralisation in large serum panel, EHV-1 PV functionality was first tested against a specific polyvalent vaccinated pony serum sample from the Animal Health Trust (UK) which has been previously employed in several influenza vaccine studies using an EIV H3-pseudotyped lentivirus particles (Scott *et al.*, 2012; Kinsley, Scott and Daly 2016; Kinsley *et al.*, 2020). In the current study this is therefore referred as the positive control serum. Nevertheless, a different type of serum already employed to detect EHV-1 antibodies would have been more appropriate as positive reference control to assess if the EHV-1 PVNA

was able to determine the presence of neutralising antibodies against EHV-1 since the positive control serum chosen in the current study was never tested before. One of the advantages of PVNT is the comparatively small volume of serum sample needed. However, which dilution series range to choose in order to detect the 50% neutralisation level (IC_{50}) is not immediately obvious without preliminary testing. To address this, both neat and pre-diluted sera were tested against EHV-1 PVs. Due to comparatively low titre of EHV PV, two EHV-1 PV batches were employed to complete the test so intra-batch comparison of the IC_{50} values between neat and pre-diluted sera was not possible. However, it seems likely that despite using different batches of PV starting with pre-diluted serum, the IC_{50} was reduced slightly compared to neat. Nevertheless, the main point of the test was to examine antibody reactivity to EHV-1 PVs. The vaccination record history of the pony showed that it was inoculated with Duvaxyn® EHV 1,4 Vaccine (Zoetis) in 2000 (first in February then March) and also experimentally challenged with Ab4 EHV-1 strain in June 2000, August 2001 and November 2005. Serum was collected in January 2012 and despite the long time frame from vaccination and infection to collection of the sample, antibodies in the serum were able to neutralise the PV, inhibiting target cell entry. In addition, one detail to observe was the trend of the inhibition curves. EHV-1 antibody neutralisation curves (Figure 55) were not as well-fitted when compared to the sigmoidal ones obtained with EIV PV (Figure 56). This pattern is often referred to as incomplete neutralisation which occurs when a proportion of the virus particles are resistant to antibody neutralisation depending which region of the glycoprotein is targeted (McCoy *et al.*, 2015). Nevertheless, it was hard to interpret the incomplete slope profile since EHV-1 PV incorporated an incomplete set of the twelve glycoproteins and specificity studies could not be performed. Another aspect to consider was the dynamic and duration of the antibody response. Studies state the antibody responses wanes over time suggesting measurement at early stage of either convalescence or vaccine-induced immunity (Ibarrondo *et al.*, 2020; Iyer *et al.*, 2020; Chia *et al.*, 2021). However, the sigmoidal profile of the positive control (sera tested against EIV PV) is clear. It would be interesting to test if a similar pattern is seen for sera from other horses collected after years after infection (natural or experimental) or vaccination. In the longitudinal PVNT study using a larger sera panel (Section 4.3.1.2.) the neutralisation curves are sigmoidal. Although samples were collected in a short time frame after infection.

Once EHV-1 PV functionality in a PVNT was verified for the positive control pony, it was possible to move to larger studies. The PVNT described above to study the antibody response in experimentally challenged horses in a longitudinal manner was the first of its kind. The

assay was successfully able to measure the neutralising antibody response and observe its trends throughout the whole study. Gradual increase of the neutralising response was observed from day 8 of the study when clinical signs appeared, until reaching the highest values around day 13 before stabilising in a plateau phase. Neutralisation curves of samples collected at the end of the study (plateau phase) resemble more the trend of the internal control, showing higher levels of antibodies detected farther from infection, suggesting a good level of protection. However, correlation of neutralising antibodies induced by experimental or natural infection and protection from infection should be further investigated in future studies. It was first necessary to delimit a threshold of positivity to distinguish positive to negative sera sample in the study. Therefore, a cut-off was set at an IC_{50} value of 160 obtained from the mean value of the negative samples tested ($n=8$; samples collected on day 0). Samples were confirmed negative by VN also. It is important to underline the need to define this threshold this particular since it is hard to find naïve horses who have had no opportunity of being virally infected. EHV-1 is remarkably ubiquitous in the horse population and it has been estimated that by 2 years of age 80-90% is infected (Allen, 2002). The difficulty to prevent the spread of infection to unexposed subjects is mostly due to asymptomatic horses with latent EHV-1 infection (Allen *et al.*, 2004; Paillot *et al.*, 2008). Another aspect to consider was the dilution of serum to employ in the PVNT. For smaller serum samples it is common to use pre-diluted sera to enable multiple tests to be run. But in this PVNT serum was employed neat because of the volumes available from such large animals. Hypothetically, it could have also been employed pre-diluted and eventually compare the final results to investigate consistency between different serum inputs (Carnell *et al.*, 2015). Given the plentiful sera it was also possible to compare whether the use of different batches of PV influenced the results. Based on statistical analysis, the outcome indicates that the assay can be performed employing different batches of PV and achieve comparable results, excluding other variables such as target cell passage number or the time interval in between repeats.

Serological tests such as VN or CF (Thomson *et al.*, 1976) are commonly used to measure levels of antibodies to EHV-1. However, the techniques are not standardised and as a consequence there may be differences in titre determinations among laboratories. Moreover, the serological assay routinely employed are not specific enough to accurately discriminate between EHV-1 and EHV-4 antibodies (Crabb *et al.*, 1995; Lang *et al.*, 2013; Azab *et al.*, 2019). Thus, the development of an assay able to do so would be beneficial. So far, the results obtained with PVNT for EHV-1 were promising after correlating the neutralising

antibody titres with VN ($r=0.82$, $p<0.0001$) considering EHV-1 PV is expressing only four of the total twelve glycoproteins. Further investigation whether other glycoprotein would induce a stronger reaction should be considered. For instance, it has been demonstrated that gG enabled the differentiation between antibodies present in polyclonal sera from mixed cases of infection involving both EHV-1 and EHV-4 by eliciting a type-specific serological response to EHV-4 (Crabb *et al.*, 1992; Crabb *et al.*, 1993; Crabb *et al.*, 1995) thus, inclusion of EHV-1 gG in the pseudotype system might be worth investigating. PVNA resulted to be faster in terms of obtaining neutralisation results (48 hours incubation compared to 4-5 days for VN) and more advantageous especially if there are limited volumes of sera available. VN usually requires at least 50 μL of sera including the duplicate (OIE Terrestrial Manual, 2018) while PVNA would necessitate 1/5 or less of it. Also, it should be considered that in a VN the CPE are examined microscopically by observing the typical morphological changes as a consequence of herpesvirus infection: focal rounding, increase in refractility, and detachment of cells (OIE Terrestrial Manual, 2018). However, this evaluation might lead to non-expertise bias especially due to the fact that there is no standardised criteria. On the other hand, PVNT are readably quantifiable using a plate reader. PVNA specificity has to be further investigated as cross-reactivity with EHV-4 antibodies is not to be ruled out. Immunological assays have reported a strong cross-reactivity when polyclonal serum is employed due to the close antigenic characteristic between EHV-1 and EHV-4 (Allen *et al.*, 2004). Studies employing monoclonal antibodies have demonstrated type-specific and type-common epitopes in both EHV-1 and EHV-4 glycoproteins (Yeargan *et al.*, 1985; Crabb *et al.*, 1991). A PVNA using monoclonal antibodies may be able to differentiate specific antibody response to EHV-1 PV. In a subsequent study of this thesis, an EHV-4 positive sera panel was tested against EHV-1 PV to verify any presence of cross-reactivity, however results were difficult to interpretate. Thus, an EHV-4 PV would be of great aid to better understand the specificity of the assay.

5 EHV-1 PSEUDOTYPE VIRUS LYOPHILISATION AND BIOLOGICAL STABILITY TESTING

5.1 INTRODUCTION

Pseudotyped viruses (PVs) offer a valuable tool for research from basic clinical investigations to high throughput serological investigations such as large sero-surveillance studies and vaccine efficacy testing. Due to their non-replicative genome, they can be manipulated in a low biosafety level environment. PVs are still able to transduce permissible target cell line, but not generate a progeny, thus resulting in a valuable and safer alternative to infectious wildtype viruses (Temperton, Wright and Scott, 2015). Their application can be extended not only to the production laboratory but also to other laboratories as feasible exchangeable material (Mather *et al.*, 2014). However, the stability of PVs in cell culture supernatant relies on low temperature storage (-80°C) and maintenance of cold-chain during transportation. This represents a limit to dissemination of PVs, especially in tropical climate and/or low income countries where the availability of laboratory equipment is very limited. A realistic scenario is represented by the research conducted in Africa to study seroprevalence of Ebola virus and the use of PVNA as serological assay to determine the presence of specific antibodies to EBOV proteins (Steffen *et al.*, 2019). Mather *et al.*, (2014) investigated the possibility of developing a PVNA based kit using lyophilisation suitable for dissemination of the assay globally and at the same time address storage and transportation issues. In the current study, we wished to transport PVs overseas to conduct large studies. The concerns we were facing to export EHV-1 PV to another laboratory were related to the availability of dry ice during the COVID pandemic, and possible transport delays at the customs as a consequence of Brexit. Therefore, lyophilisation was considered as a possible solution to address these issues. Lyophilisation or freeze drying of materials is a common process applied in the pharmaceutical field to produce stable products at a dry state for long term storage. It consists in a first freezing step followed by a drying step at low pressure and temperature. Water is so removed from the sample by sublimation that is the direct passage from solid to vapour state. As such only the solid and dried components from the original liquid are left, resulting as a dry pellet (Tyrrell and Ridgwell, 1965; Wang, 2000; Nireesha *et al.*, 2013; Kraan *et al.*, 2014). Products are pre-treated by adding cryoprotectants to protect their biological components from the lyophilisation process (Wang, 2000). Sucrose has been shown to be a valuable excipient from previous PV lyophilisation assessment studies (Scott and Woodside, 1976; Croyle, Cheng and Wilson, 2001; Wilschut *et al.*, 2007; Shin, Salvay and Shea, 2010; Mather *et al.*, 2014). The aim of this study was to assess EHV-1 PV retention titre

immediately after lyophilisation and reconstitution and following one or four weeks in different storage conditions (-80°C, -20°C, +4°C and RT) and for one week at RT with ice packs to mimic a possible shipping scenario including customs delays. Functionality of lyophilised EHV-1 PV was determined in a PVNA employing a small panel of sera to verify the integrity of the biological function of pseudotyped particles after lyophilisation and reconstitution by detecting antibodies specific to EHV-1. The viability of cells used in the PVNA was also assessed to report any sign of cytotoxic effect from the cryoprotectant. The outcome of these results would determine the best methods of shipment to export EHV-1 PV to other laboratories, and in particular to our research collaborators in France to employ EHV-1 PV in further applications.

5.2 MATERIALS AND METHODS

EHV-1 PV was generated and titrated as described in Sections 3.3.2 and 3.3.3. The optimised protocol to produce BDHL EHV-1 PV with FLW as reporter collected at both 48 hours and 72 hours post transfection was employed for further applications (i.e. concentration, lyophilisation, PV titration and PVNA). HEK293T/17 cells were used as target cells for both PV titration and PVNA.

5.2.1 EHV-1 PV concentration

In order to concentrate and thus increase EHV-1 PV titre, aliquots of 2 mL of both 48h and 72h freshly harvested PVs were low-speed centrifuged at 3000 g at +4°C for 24 hours (Jiang *et al.*, 2015) in a bench top refrigerated microcentrifuge (VWR International Ltd, model: Micro Star 17R, #521-1647). Afterwards, 1.95 mL of supernatant was removed and discarded, making sure not to disrupt the solution at bottom of the tube, and 100 µL of cold OptiMEM® (kept at +4°C) were added to the tube. Samples were incubated overnight at +4°C to permit particle resuspension and further stored at -80°C before further application (i.e. PV titration) or preparing samples for lyophilisation.

5.2.2 EHV-1 PV lyophilisation and storage

100 µL aliquots of EHV-1 PV that had either been concentrated via the above Section 5.2.1. method, or were non concentrated, were lyophilised in a FreeZone 2.5 Liter Benchtop Freeze Dryer (Labconco, model: 7670560). These were then stored at different temperatures (+37°C, RT, +4°C, -20°C, -80°C) for various time periods (1 or 4 weeks). This was in part to mimic

shipment and possible delays during the customs process if sending to other laboratories. At these timepoints, the lyophilised PVs were reconstituted in complete cell culture media and titrated to assess the percentage recovery after lyophilisation and storage. Briefly, 100 µL of PV supernatants were mixed with equal volume of 1 M Sucrose (Sigma-Aldrich®, Merck, #S0389-500G) solution as cryoprotectant in a low binding microtube (Simport, #T330-7LST) to forestall viral glycoprotein binding to the tube material surfaces during the lyophilisation process and so minimise loss of pseudotype titre. Each tube was then covered with a needle-pierced lid to ensure evaporation during the lyophilisation process, and then stored at -80°C overnight prior to freeze drying. During the lyophilisation cycle, the samples undergo low temperature (-40°C to -50°C) and low pressure (< 0.033 mBar) exposure. Lyophilised PV appear as pellets or 'cakes' and the microtube is then sealed with the original intact lid replacing the pierced one. PV pellets were immediately resuspended in cell culture media or stored as mentioned above: +37°C (dry incubator), RT (average of +20°C) with or without ice blocks, +4°C, -20°C and -80°C.

5.2.3 Lyophilised EHV-1 PV titration

After the time periods outlined, lyophilised PVs were titrated in order to assess the potential of lyophilisation to use as an alternative to dry ice for shipment or cold-chain for storage. Lyophilised PVs were reconstituted in 100 µL complete cell culture media, mixed well and incubated for at least 10 minutes at RT before setting up a titration, as previously described in Section 2.4.

5.2.4 Cytotoxicity test

In order to investigate the cytotoxicity effect of the cryoprotectant, a titration was set up on a 96-well clear plate using reconstituted lyophilised PV. Titration was carried out as previously described in Section 2.4. Cells were observed under the light microscope to assess viability. A lyophilised EIV PV was included in parallel to monitor cell viability and compare it to what observed with lyophilised EHV-1 PV.

5.2.5 Lyophilised EHV-1 PV neutralisation assay

A subset (n=4) of the serum panel kindly provided by Dr. Stéphane Pronost (described in Section 4.2.1.) was employed, plus the previous positive control and FBS. Lyophilised PVs were reconstituted in 100 µL complete cell culture media. A PVNA was set up as described

in Section 2.5., but the PV input was reduced to 1×10^5 RLU/mL to reduce the amount of cryoprotectant within the PV sample and as a consequence avoid cytotoxicity. A PVNA was set up in parallel using the EIV PV, similarly lyophilised, as positive control.

5.2.6 Data analysis

The raw data files produced by the luminometer were extracted as Microsoft® Excel™ files for initial analysis. The non-linear regression curve fits were produced using GraphPad Prism® following the guidelines in Section 2.6.

5.3 RESULTS

5.3.1 Impact of lyophilisation on EHV-1 PV titre

PV titre was assessed immediately after lyophilisation to determine the impact of biological activity of PVs (Figure 63). Titre retention was calculated as a percentage value of the absolute titre of the non lyophilised counterpart sample. Overall, the lyophilisation process did not lead to a great loss of titre. There was no significant difference between the lyophilised and non lyophilised PVs, although for the second harvest PV (72h) it appeared that between the lyophilised and non lyophilised sample there was small but significant difference ($p=0.0233$). PV concentration had a significant impact on the titre (up to $p<0.0001$) by increasing approximately 1-log RLU/mL when compared to the non concentrated counterpart sample for both tested conditions (lyophilised and non lyophilised) and PV harvests.

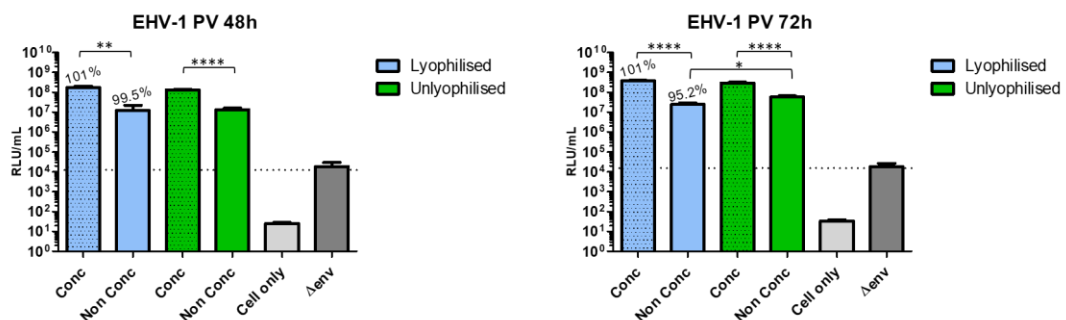


Figure 63: Titration results of EHV-1 PV immediately resuspended after lyophilisation. The PV titre retention value is reported as % on top of each column bar. Δ env PV and cell only were included to determine the cut-off value and cell background. An unpaired t-test was employed for statistical purposes. **Left graph (48h):** ** is $p=0.0026$ and **** is $p<0.0001$. **Right graph (72h):** **** is $p<0.0001$ and * is $p=0.0233$. The final titre was the result of the average of duplicates repeated once.

5.3.2 Impact of storage on lyophilised EHV-1 PV titre

Next, lyophilised samples were stored for 1 or 4 weeks under different temperature conditions. After one week at +37°C (Figure 64 A and B) a significant loss of titre was observed for both PV harvests, while lower temperatures (+4°C and RT; Figure 64 C-F) did not affect titre loss as much. Interestingly after 1 week storage at +37°C titre of lyophilised PV was still rescued compared to the non lyophilised counterpart. (83% and 87% retention average for first and second PV harvest respectively). In addition, PV concentration prior to lyophilisation had increased its titre approximately 1-log RLU/mL for each temperature condition tested compared to the non concentrated counterpart sample. Thus, for the 4 weeks storage study only the concentrated lyophilised PV was assessed for retention (Figure 65). As expected, storage at low temperatures (-80°C up to RT) showed no significant loss in titre while higher temperatures do.

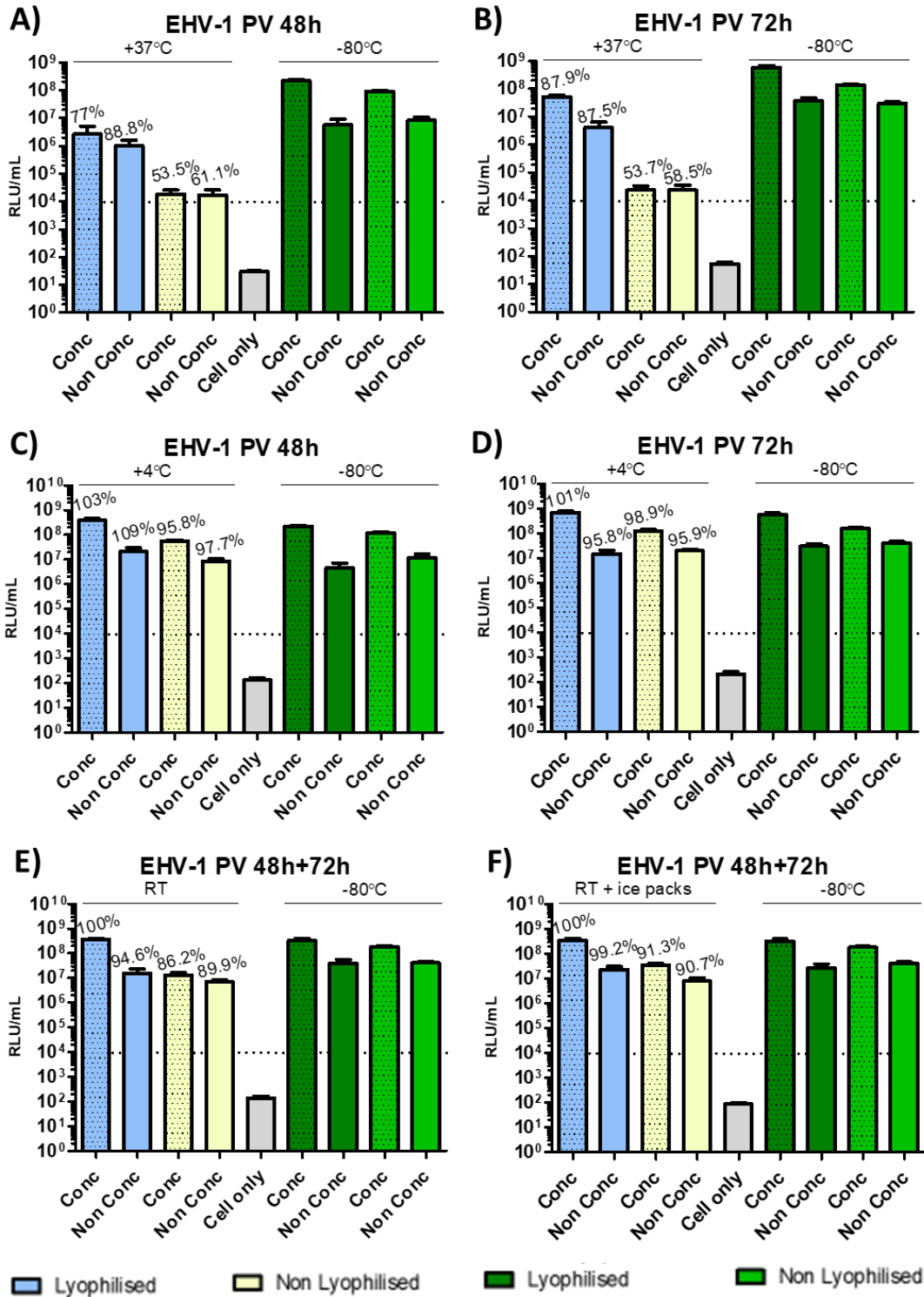


Figure 64: Titration results of impact of storage (1 week) on lyophilised EHV-1 PV. The PV titre retention value is reported as % on top of each column bar. Δ env PV and cell only were included to determine the cut-off value (set at 1.54×10^4 RLU/mL) and cell background. **A) and B):** 1 week storage at +37°C of PV collected at 48h and 72h. **C) and D):** 1 week storage at +4°C of PV collected at 48h and 72h. **E) and F):** 1 week storage at RT with icepacks (F) and without icepacks (E) to mimic shipment conditions. The final titre was the result of the average of duplicates repeated once.

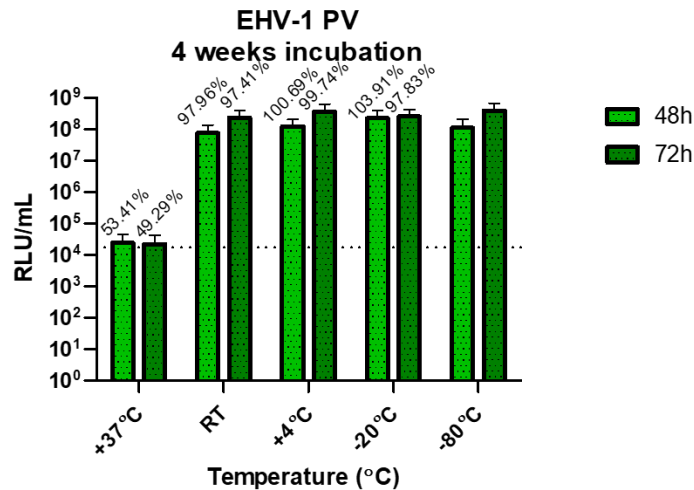


Figure 65: Titration results of impact of storage (4 weeks) on lyophilised EHV-1 PV. The PV titre retention value is reported as % on top of each column bar. Δ env PV and cell only were included to determine the cut-off value (set at 1.72×10^4 RLU/mL) and cell background. The final titre was the result of the average of duplicates repeated once.

5.3.3 Application of lyophilised EHV-1 PV

A PVNA was performed to verify the integrity of the biological function of EHV-1 PV after lyophilisation and binding of specific antibodies to neutralisation epitopes. This was assessed by testing samples (n=4) collected on day 5 of the EHV-1 experimentally vaccinated sera panel (described in Section 4.2.1.). Detection of IC₅₀ was possible only when the PV input was lowered from 10⁶ RLU/mL to 10⁵ RLU/mL (Figure 66). IC₅₀ values are reported in Table 17. Cell viability was assessed under a light microscope. A lyophilised EIV PV was included as control to monitor cell viability and in the PVNA employing a PV input of 10⁶ RLU/mL (Figure 67) and 10⁵ RLU/mL (Figure 68). IC₅₀ values are reported in Table 18. In order to investigate whether the amount of cells added per assay or the PV input chosen would have had an impact on the results, the IC₅₀ values and the gradient of the neutralisation curves were analysed. Statistical analysis confirmed that there was no significant difference between the gradients of the curves if using double amount of target cells despite increasing the IC₅₀ (p=0.60). However, using different PV input might significantly affect the IC₅₀ results (p=0.0139). Interestingly cell viability was not disrupted when testing either 10⁶ RLU/mL or 10⁵ RLU/mL as PV input for lyophilised EIV PV. This observation suggested that cytotoxicity was induced by the cryoprotectant employed for lyophilisation of the PV. As EHV-1 PV has generally a lower titre than EIV PV and in terms of applicability a higher volume of lyophilised PV is needed to add a specific amount of PV, thus a higher amount of cryoprotectant is added per assay well, resulting in increased cytotoxic effect.

Lyophilised EHV-1 PV (INPUT 10^5 RLU/mL)

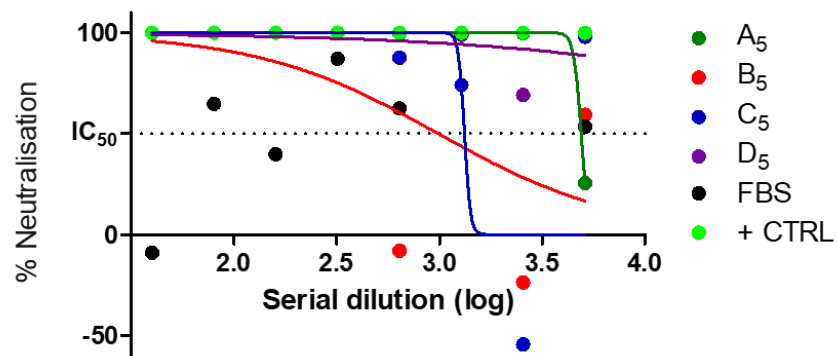


Figure 66: PVNA (lyophilised EHV-1 PV). Neutralisation curves obtained with neat sera added at a starting dilution of 1/40 and tested against a lyophilised EHV-1 PV (PV input of 10^5 RLU/mL). FBS and a multi-vaccinated pony sera (+ CTRL) were included as negative and positive controls.

| Sera sample | LogIC ₅₀ | IC ₅₀ |
|----------------|---------------------|------------------|
| A ₅ | 3.689855 | 4896.150 |
| B ₅ | 2.994381 | 987.1447 |
| C ₅ | 3.122041 | 1324.467 |
| D ₅ | 5.392395 | 246828.200 |
| + CTRL | Not converged | Not converged |
| FBS | Not converged | Not converged |

Table 17: LogIC₅₀ and IC₅₀ values. IC₅₀ was not converged for + CTRL and FBS controls.

Lyophilised EIV PV (INPUT 10^6 RLU/mL)

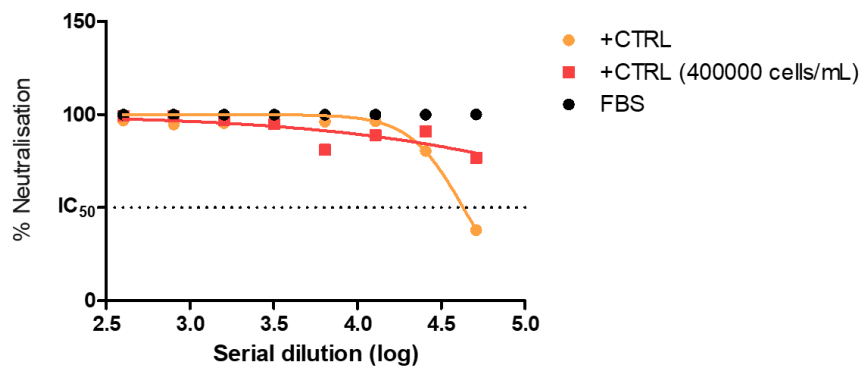


Figure 67: PVNA (lyophilised EIV PV). Neutralisation curves obtained with pre-diluted sera of a multi-vaccinated pony tested against lyophilised EIV PV (PV input 10^6 RLU/mL). Pre-diluted sera were added at a starting dilution of 1/400. FBS was included as negative control. Cells were added as per assay or doubling the amount (400000 cells/mL).

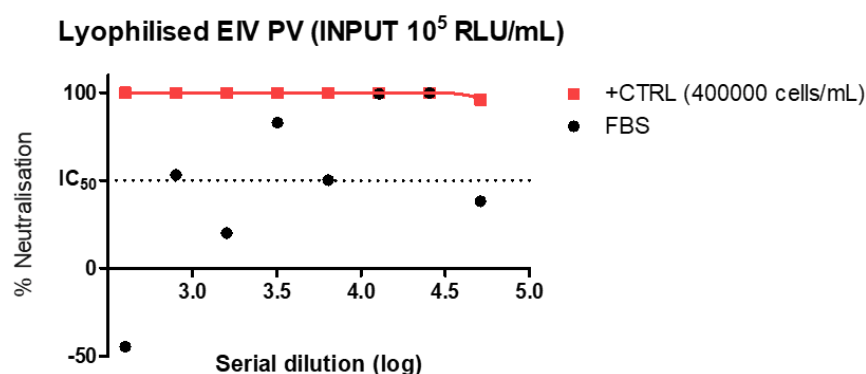


Figure 68: PVNA (lyophilised EIV PV). Neutralisation curve obtained with pre-diluted sera of a multi-vaccinated pony tested against lyophilised EIV PV (PV input 10^5 RLU/mL). Pre-diluted sera were added at a starting dilution of 1/400. FBS was included as negative control. Cells were added as per assay or doubling the amount (400000 cells/mL). Only for the latter condition, neutralisation curves were extrapolated.

| PV INPUT | Sera sample (1/10) | LogIC ₅₀ | IC ₅₀ |
|---------------|-------------------------|---------------------|------------------|
| 10^6 RLU/mL | +CTRL | 4.631583 | 42813.720 |
| | +CTRL (400000 cells/mL) | 5.901023 | 796201.100 |
| 10^5 RLU/mL | +CTRL | Not converged | Not converged |
| | +CTRL (400000 cells/mL) | 4.954741 | 90103.440 |

Table 18: LogIC₅₀ and IC₅₀ values (lyophilised EIV PV). Pre-diluted sera were tested once against lyophilised EIV PV (PV input 10^5 or 10^6 RLU/mL). For the first condition, IC₅₀ was not converged when cells were added as per assay.

5.4 DISCUSSION

The exploitation of PV in serology has revealed it to be a useful tool in understanding the functional neutralising antibody response against viruses. Their flexibility and sensitivity offered a rapid development of the system, especially at low containment level due to their safeness, with effective results (Bentley *et al.*, 2015; Ferrara and Temperton 2018; Toon *et al.*, 2021). Moreover, stability of PVs was reported by maintenance of high titres during cold-chain storage and subsequent freeze-thaw in series (Molesti *et al.*, 2014), offering a reliable tool even in low resource laboratories. The possibility of creating a PV-based serological kit to facilitate the utility and widen PV based neutralisation assay in other laboratories has been investigated (Mather *et al.*, 2014). However, the necessity of a persistent cold-chain of PV containing cell culture supernatants during transport could impede this. Therefore, lyophilisation of PVs has been investigated as an alternative to dry-ice shipments and avoid

its higher costs and potential hold ups through customs. Lyophilisation is a well-established method used for many pharmaceutical products such as vaccines to provide a longer shelf-life of the product and reduce storage and distribution challenges (Orr *et al.*, 2014; Chan, Dutil and Kramer, 2017). During the COVID-19 pandemic there was a lack of dry-ice availability as its usage was prioritized for vaccine storage or COVID research. In the UK Brexit made shipments and exchange of materials more difficult especially presuming long time at customs. Given these issues the possibility of shipping EHV-1 PVs in lyophilised form to LABÉO, our research collaborator in France, was considered to avoid the requirement of cold-chain during transport and possible waiting times for custom clearance. Thus, a stability study on lyophilised PVs was conducted, exposing samples to varying temperatures for various amounts of time, to reflect shipping conditions and times. It was necessary to first assess rescued PV titre retention and recovery by testing storage and stability of lyophilised EHV-1 PV and lastly functionality in serological assay. Sucrose was employed as cryoprotectant as it has been proven to be a valuable excipient from previous studies (Mather *et al.*, 2014; Dr. Martin Mayora-Neto, personal communication). Stability of lyophilised PV was assessed after one-week (short-term) storage to mimic a shipment time frame scenario and also after one month to include possible delays, after exposure to different temperatures. Both concentrated (by centrifuge) and non concentrated PV supernatants were tested at each storage and temperature conditions to verify stability and retain infectivity. A large volume of EHV-1 PV was generated following single scaled-up transfection in order to use a single PV batch. Titre retention was first assessed immediately after the end of the lyophilisation cycle by reconstituting the aliquots of PV pelleted in complete cell culture media to assess whether the process was damaging the glycoprotein functionality. All samples retained infectivity with no major difference when compared to their equivalent non-lyophilised control. However, concentrating the supernatants significantly helps in increasing titres by at least 1 log RLU/mL in both lyophilised and non lyophilised PV controls, from 1×10^7 RLU/mL (as consistent with previous data; Chapter 1.) to 1×10^8 RLU/mL approximately. Concentration of lentiviral particles by low-speed centrifugation has been demonstrated an efficient application to enhance retroviral titre as seen in other studies (Cepko, 1997; Darling *et al.*, 2000). Since good recovery was shown immediately after lyophilisation (overall no significant difference between the lyophilised and non lyophilised PVs; Figure 63), longer storage was assessed at different temperatures. As expected, higher temperatures (+37°C) were deleterious. Interestingly, the lyophilised PVs (both concentrated and non concentrated version) were able to retain more than 77%

and 87% titre recovery respectively after 1 week storage for the first harvest, with less difference range between concentrated and non concentrated PVs showing 87% assessed for the second harvest. This might be explained as observed in previous titre evaluation in which EHV-1 PV titre was slightly higher at the second harvest. Lower temperatures (+4°C and -20°C) were able to maintain titre values closer to the equivalent PVs kept at -80°C with recovery demonstrated at levels starting from 86% and 94% for non lyophilised and lyophilised PVs respectively after 1 week storage. The addition of ice packs to mimic a shipping condition were able to slightly increase titre retention at RT conditions. These first results suggested shipment using a cold-chain would retain most of the PV functionality. Storage was also pushed to one month, although only the concentrated lyophilised PV version was utilised as it resulted to be more stable and gave the best titre retention performance in terms of % titre retention. Indeed, the PVs retained more than 97% of their titres for RT and temperatures below it. However, when stored at +37°C for one month, no titre was detectable. The in-house freeze drying equipment has no secondary drying step able to remove the residual moisture which remains after a lyophilisation cycle as found in an industrial setting (e.g. NIBSC) and probably causing this drastic drop in transduction titres (Nireesha *et al.*, 2013). Promising results were observed when functional titre of lyophilised filovirus PVs was retained even after one month at warmer temperatures by using an industrial freeze drier which included a second drying step (Dr. Martin Mayora-Neto, unpublished data). Once functional titre was assessed, a PVNA was needed to assess function in an antibody neutralisation assay. Therefore, lyophilised EHV-1 PV (and an EIV PV control) was reconstituted and utilised in a PVNA with our standard polyclonal pony serum (vaccinated against both EHV-1 and EIV). It was possible to detect a neutralising response, although results were not as clean as previously observed when the non lyophilised PV was employed (Figure 66). Functionality of the PV was assessed but if the glycoproteins were somehow damaged during the process and their structure compromised to induce less reactivity it was hard to reveal. Further assay should be considered to verify the glycoprotein's structural integrity possibly by testing the glycoprotein binding to mAbs (Telikepalli *et al.*, 2015; Hahn *et al.*, 2020). Moreover, the PV input had to be lowered from 1×10^6 to 1×10^5 RLU/mL to reduce the amount of cryoprotectant within the reconstituted PV which produces cytotoxicity. For the lyophilised EIV PV the conditions were unchanged. Functional titre is essential for the correct performance of a PVNA. Since EHV-1 PV was found to have lower titres from other PVs (e.g. EIV PV), the volume of reconstituted lyophilised PV which needs to be used in an assay is more. Thus, the amount of cryoprotectant is greater,

which could have had effects on cell viability. Indeed, this was observed by testing different PV input on target cells, and also that doubling the dilution is not impacting significantly. Alternative excipients to sucrose should be investigated in the future that would avoid cytotoxicity. Sorbitol has been examined as cryoprotectant in freeze-dried excipient formulation showing less toxicity (Kraan *et al.*, 2014; Mather *et al.*, 2014). However, sucrose obtained higher titre recovery (Mather *et al.*, 2014) while cytotoxicity of sorbitol was not assessed. An alternative disaccharide to sucrose, trehalose, proved to be a successful thermostabiliser of enzymes and increased stability of RNA replicons (Jones, Drane and Gowans, 2007). It has been evaluated as a potential freeze-dryer protective agent candidate in an optimal formulation for lentiviral vectors (Delacroix *et al.*, 2015; Shen *et al.*, 2021). Taken into account all these aspects, it was considered more cautious for the moment to employ non lyophilised EHV-1 PV in a PVNA to obtain the best performance. Thus, it was decided to ship EHV-1 PV in non lyophilised form to our collaborators in France as a frozen stock on dry ice for downstream applications.

6 APPLICATION OF THE PSEUDOTYPE VIRUS NEUTRALISATION ASSAY TO DETERMINE THE IMMUNE STATUS OF HORSES POST EHV-1 VACCINATION AND TRANSDUCTION TESTING OF EHV-1 PSEUDOTYPE VIRUS

6.1 INTRODUCTION

The successful generation of EHV-1 PV and its application in a longitudinal PVNA study to measure the level of neutralising antibodies from EHV-1 experimentally infected horses unlocked the possibility to further exploit the system to detect and measure neutralising antibodies in other larger studies. Therefore, considered the feasibility of the EHV-1 PVNA in the previous study, it was worth investigating if the assay would fit to determine the immune status of horses post EHV-1 vaccination. This study was conducted at LABÉO (France), the host research laboratory. EHV-1 PV batches were produced and titrated at VPU (University of Kent, UK) and shipped to LABÉO (France) in dry ice. The availability of materials and specialised equipment at the host institute tailored the development of the investigations to be undertaken. In order to achieve the principal aim of this study and further test the EHV-1 PV transduction ability, it was necessary to: i) assess EHV-1 PV titre to verify if any loss occurred due to shipment, and to determine the signal sensitivity of the luminometer present at the host laboratory; ii) measure the antibody titres able to neutralise EHV-1 PV using two different panels of equine sera collected either from EHV-1 experimentally infected horses or vaccinated horses against EHV-1. Moreover, in order to further test EHV-1 PV transduction ability, it was necessary to: iii) fine-tune and monitor the evolution of EHV-1 PV transduction onto different target cell lines using the innovative real time cell analysis (RTCA) technology compared to the dynamic of the wild-type; iv) verify the ability of EHV-1 PV to transduce equine PBMCs and differentiate its subpopulations by flow cytometry. Further details of each objective below:

- i. Consistency of results among laboratories is the first step to reduce variabilities. A topical example is represented by the different equipment used to quantify viable pseudotyped particles between laboratories (Carnell *et al.*, 2015). At the host laboratory the luminometer was different from the one at the main laboratory at VPU. As such, it was important to assess what kind of impact this had in terms of RLU output.
- ii. As mentioned previously, PVNAs offer a potential alternative to current serological assays to detect the presence of functional neutralising antibodies within serum samples for serological screening, vaccine efficacy testing or study the immune host response. From the previous study (Section 4.3.1.2.), the PVNA was proven a

valuable serological platform to detect neutralising antibody against EHV-1 PV and measure the humoral immune response from experimentally infected horses in a longitudinal study. Promising results were also obtained by comparing the EHV-1 PVNA titres with a conventional EHV-1 VN assay ($r=0.82$ from Section 4.3.2.). A panel of serum representing a horse population involved in an EHV-1 vaccination campaign was available at LABÉO (France). The different EHV-1 vaccines available on the market provide variable levels of protection by inducing VN antibodies which promote protection of the respiratory upper tract during the initial respiratory infection and reduce the amount and duration of nasopharyngeal viral shedding thus reducing clinical respiratory symptoms (Mumford *et al.*, 1987; Hannant *et al.*, 1993). However, despite the induction of the humoral immune response elicited by vaccination, none of them is able to provide an adequate level of protection against EHV-1 disease or re-infection especially when cell-associated viremia has been registered leading to abortion or EHM (Burrows and Goodridge, 1984; Allen *et al.*, 2004). This suggests that other components of the immune system (e.g. local and/or cell mediated immunity) play a major protection role against EHV-1 (Mumford *et al.*, 1994; Studdert, 1996). Vaccination against EHV-1 is however recommended to help reduce the severity of the clinical symptoms, viral shedding and spread (OIE Terrestrial Manual, 2018). Consequently, we were interested to determine the immune status of horses ($n=13$) post EHV-1 vaccination by exploiting the PVNA system.

- iii. As a consequence to EHV-1 infection, cells appear clustered together, enlarged, rounded and herpetic, detaching easily from the surface (Allen *et al.*, 2004). This typical cytopathic effect (CPE) is exploited to determine viability of EHV-1 in viral isolation for diagnostic purposes. CPE can also be measured indirectly via impedance, an electrical signal/field elicited by cells adhesion to the surface via a novel technology based on RTCA is able to quantify the cell adhesion in a non-invasive way (Fang *et al.*, 2011; Limame *et al.*, 2012). Cells are grown on special plates with a golden electrode array in which impedance is measured and converted into a value called cell index (CI).

$$CI = \frac{\text{Impedance at time point } n - \text{impedance in the absence of cells}}{\text{nominal impedance}}$$

When cells adhere the CI is greater than zero. On the other hand, when alterations of cell adhesion occur (e.g. change in cell morphology or number, such as due to virus infection) the CI decreases. Thereby, the cell status is monitored in real time

and can be exploited to investigate multiple cellular aspects (Solly *et al.*, 2004; Witkowski *et al.*, 2010; Kho *et al.*, 2015). In virological studies, the RTCA system can be employed to better dissect the dynamics of infections and highlight the CPE which would be difficult to observe microscopically. Golke *et al.*, (2012) applied this technology to optimise EHV-1 infection parameters (e.g. cell number, virus input and time of infection) on ED cells and primary murine neurons. Further applications include screening and evaluation of antiviral compounds against EHV-1 (Hue *et al.*, 2016; Thieulent *et al.*, 2019; Sutton *et al.*, 2020). For the purpose of this study, RTCA was fine tuned to monitor EHV-1 PV transduction on different cell lines in parallel with the wild-type virus as control to compare the dynamic of the CI.

- iv. Upon entry, EHV-1 infect epithelial cells of the respiratory upper tract. From the primary infection site, is then able to infect PBMC establishing a cell associated viremia and disseminate to other locations of major clinical importance such as the uterus and the central nervous system. During this phase, EHV-1 is able to evade the host immune system. Despite the high levels of humoral immune levels reported, EHV-1 specific antibodies are not able to recognise PBMC infected cells. The precise mechanism is yet not fully understood, but it seems likely that PBMC infected cells do not present EHV-1 glycoproteins on their surface (van der Meulen, Nauwynck and Pensaert, 2003; van der Meulen, Pensaert and Nauwynck, 2006). Controversially, other studies reported the opposite (Slater *et al.*, 1994a). To better understand the dynamics of early pathogenesis of EHV-1 disease, limited studies *in vitro* addressed to identify which PBMC subpopulations played a more important role in EHV-1 viremia (Scott, Dutta and Myrup, 1983; van Der Meulen *et al.*, 2000). Studies demonstrated the importance of MHC I molecules to mediate EHV-1 entry into equine cells, including PBMC, by interacting with EHV-1 gD (Sasaki *et al.*, 2011). However, EHV-1 tropism might be modulated by other host factors since MHC I is ubiquitously expressed on all cell types (David-Watine, Israël and Kourilsky, 1990). Therefore, to investigate this aspect, EHV-1 PV was employed in a PBMC target study to assess the transduction ability and verify which subpopulation (in this case dendritic cell) was more subject to be infected using antibody staining and flow cytometer analysis.

6.2 MATERIALS AND METHODS

All cell culture procedures were performed in an MSC-SCS Class II Biological Safety Cabinet (Envair, model: SCS 2-4) and using a Forma™ Steri-Cult™ humidified CO₂ Incubator (Thermo Scientific™, Thermo Fisher Scientific, #3308) for incubations at +37°C at 5% CO₂. An InCu-saFe® humidified CO₂ Incubator (PHCbi, model: MCO-170AICUV) was only used for incubation of real-time and live cell assays paired with the InCuCyte® System (Essen BioScience, model: InCuCyte® S3) for incubations at +37°C at 5% CO₂.

6.2.1 Cell lines and maintenance

In order to conduct the study at LABÉO (France) using standard in-house reagents, HEK293T/17 cells were shipped from the VPU (University of Kent, UK) as a frozen stock on dry ice. These cells were used mostly as target cells for PV titration and subsequently PV neutralisation, and were maintained in DMEM (Biowest, #L0104-500) with 10% FBS (Eurobio, #CVFSVF0001) and 1% P/S (Eurobio, #CABPSA000U) in Falcon® T75 flasks (Corning, #353135) at +37°C 5% CO₂. RK13 cells were grown in Minimum Essential Medium with Earle's Balanced Salts (MEM; Eurobio, #CM1MEM1001) added with 10% FBS, 1% P/S and 1% L-glutamine (L-glut; Eurobio, #CSTGLU000U), E.derm and MDCK II cells were grown in Eagle's Minimum Essential Medium (EMEM; ATCC®, #30-2003) with 10% FBS and 1% P/S. Sub-culturing of cells was achieved by removing the media and detaching the cell layer using EDTA-Trypsin (Sigma-Aldrich®, Merck, #T3924). Cells were then resuspended in fresh complete media and seeded at the adequate density for maintenance of the cell line. Equine PBMCs were isolated by Flora Carnet from the whole blood of horses by density gradient using Ficoll® lymphocytes separation media (Eurobio, #CMSMSL01). Briefly, 2 mL of equine blood was left to sediment for 30 minutes at RT in a VACUETTE® Ethylenediaminetetraacetic acid (EDTA) tube (Greiner Bio-One, #455040). After this time, plasma was collected and gently deposited on 4 mL of lymphocyte separation media in a 15 mL falcon tube. Samples were then centrifuged at 400 g for 12 minutes at +20°C with acceleration and deceleration set to 2 in a 2L LISA refrigerated centrifuge (AFI, model: AFI-C200RE). The PBMC layer was gently transferred in a second 15 mL Falcon tube with 10 mL Phosphate Buffered Saline (PBS; Eurobio, #CS1PBS0001) and centrifuged at 300 g for 10 minutes at acceleration and deceleration set to 6. The supernatant was discarded, the pellet was mixed and resuspended in 10 mL PBS and centrifuged at 250 g for 10 minutes. This was repeated once again but then the pellet was resuspended in 1 mL of Roswell Park Memorial Institute 1640 medium (RPMI 1640; Eurobio, #CM1RPM0601) with 1% P/S, 1% L-glut and 1% 4-(2-hydroxyethyl)-1-

piperazineethanesulfonic acid (HEPES; Eurobio, #CSTHEP000P). 20 µL of PBMC were subsequently mixed with 20 µL of Trypan blue and incubated for 5 minutes at RT to assess % viability as well as number before 15 µL were counted on a Malassez Slide. 1×10^7 PBMCs were collected and diluted in 1 mL complete PBMC medium and seeded into a well of a 6-well plate (Corning, #3516) with an extra mL of PBMC media.

6.2.2 EHV-1 PV titration

EHV-1 PV was produced, titrated was measured before shipping from VPU (University of Kent, UK) to LABÉO (France). The PV titre was re-measured in the host lab by performing a titration on a white 96-well microplate (SPL, # 30196) on HEK293T cells as previously described in Section 2.4. and luminescence measured on a SPARK® Microplate Reader (Tecan, model: SPARK® 10M). Δenv PV and cell only controls were added to the plate to identify the PV functionality threshold and the luminescence background respectively. EIV PV was included as positive control to ensure the performance of the assay. Attempts were also made to conduct titrations via two different Real-Time Cell Analysis (RTCA) technologies, described below.

6.2.2.1 EHV-1 PV titration on xCELLigence RTCA

The first approach used an xCELLigence RTCA Instrument (ACEA Biosciences, Agilent, model: MP) positioned in a Forma™ Steri-Cult™ incubator. Briefly, 50 µL of complete cell culture media was first added to RTCA E-Plate 96 PET (Agilent, # 300600900) as a blanking control. Subsequently, 100 µL of target cells per well (Table 19) were added to the E-Plate. 24 hours after the adhesion step, cell culture media was removed and replaced with 50 µL of fresh culture media. On a separate white 96-well microplate, a serial dilution of both the WT EHV-1 Kentucky D (KyD; ATCC®, #VR700) strain and the EHV-1 PV was carried out following the same procedure in Section 6.2.2. and then transferred to the E-Plate on the adherent cells previously added, reaching a total volume of 150 µL. The WT virus was included as positive control for CPE. The E-Plate was positioned on the xCELLigence and incubated for approximately 96 hours at +37°C at 5% CO₂. The program used to run the machine is given below (Table 20).

6.2.2.1.1 Addition of Trypsin (TPCK-treated)

TPCK-trypsin (Thermo Scientific™, Thermo Fisher Scientific, #20233) was added to the titration assay in order to activate and cleave influenza HA of a WT EI

A/equine/Jouars/4/2006 (H3N8, Florida Clade 2 sub-lineage) strain employed as a positive control for CPE (Flora Carnet, unpublished data). The general guidelines reported in the WHO manual (WHO, 2011) were followed. Briefly, 0.25 µg/mL of TPCK-trypsin was mixed in 30 mL of EMEM added with 1% P/S only. In the first row of a white 96-well microplate, 134 µL of media was added to 16 µL of WT EI and then a serial dilution was carried out as previously described in Section 6.2.2.

6.2.2.2 EHV-1 PV titration on Incucyte® RTCA

An Incucyte® Live-Cell Analysis Instrument (Essence Bioscience, model: S3) positioned into an InCu-saFe® incubator. Titration of both the WT and the PV (either GFP or FLW expressing reporter) was performed on a clear Falcon® 96-well Microplate (Corning, #353072) via the same procedure as described for the xCELLigence RTCA technology (Section 6.2.2.1.). The green channel was chosen when PV expressing the GFP reporter was employed. The program used is reported below (Table 20).

| Target cells | Cells/well (100 µL) | Cells/mL |
|--------------|---------------------|----------|
| HEK293T | 20000 | 200000 |
| RK13 | 25000 | 250000 |
| CCL57 | 12000 | 120000 |
| MDCK II | 16000 | 160000 |

Table 19: Target cells per titration assay.

| PROGRAMME: | | | | | |
|-------------|--------------------------|---------------------|----------|-------|--|
| xCELLigence | | | | | Incucyte® |
| N° | Liaison | Step | Interval | Time | |
| 1 | | Base level | 1 min | 1 min | Scan type: Standard Type experience: Virology Channel: <input type="checkbox"/> Phase <input type="checkbox"/> Green <input type="checkbox"/> Red Objective: <input type="checkbox"/> 4X <input type="checkbox"/> 10X <input type="checkbox"/> 20X Images/well: Frequency of acquisition: |
| 2 | <input type="checkbox"/> | Adhesion | 10 min | 10 h | |
| 3 | <input type="checkbox"/> | Proliferation | 10 min | 24 h | |
| 4 | <input type="checkbox"/> | Treatment/Infection | 10 min | 168 h | |

Table 20: RTCA xCELLigence and Incucyte® programmes

6.2.3 EHV-1 PV neutralisation assay

PVNA was carried out as described in Section 2.5. on a white 96-well microplate and read 48 hours on a SPARK® (Tecan) plate reader. Because of the different emittance light sensitivity of detection on SPARK® (Tecan) from GloMax® (Promega) reader, a PV input of 1×10^4 RLU/mL was added to the assay.

6.2.3.1 Sera samples

- 1) Serum samples A₀, B₀, C₀, D₀, G, I, J and L from the previous PVNA study described in Section 4.2.1. were employed to define the threshold of positivity for the SPARK® (Tecan) plate reader.
- 2) Serum samples (n=78) collected from 3 groups of horses for an EHV-1 vaccination campaign with Equip® EHV 1,4 (Zoetis) were screened against the EHV-1 PV. In detail:
 - a. Group 1 (G): pregnant mares (n=3) were vaccinated at the 5th, 7th and 9th month of gestation and sampling occurred every month from the 5th to the 10th month of gestation.
 - b. Group 2 (P): primary-vaccinated foals (n=7) were vaccinated on the 1st, 2nd and 6th month and sampling occurred on the 1st, 2nd, 3rd, 6th, 7th and 8th month of the study.
 - c. Group 3 (R): boosted horses (n=3) were vaccinated on the 1st month of the study and sampling occurred on the 1st, 2nd and 4th month of the study.

6.2.4 Flow cytometry

In order to test whether PBMC can act as potential transduction targets for EHV-1 PV, flow cytometry was employed. 6×10^5 PBMC were infected with 3 mL GFP expressing reporter PV on the 1st, 2nd or 6th day of study and staining and flow analysis occurred on the 3rd, 6th or 8th day. PBMC infected on the 2nd day were analysed on both the next day and after 96 hours to mimic RTCA experiments (Figure 69).

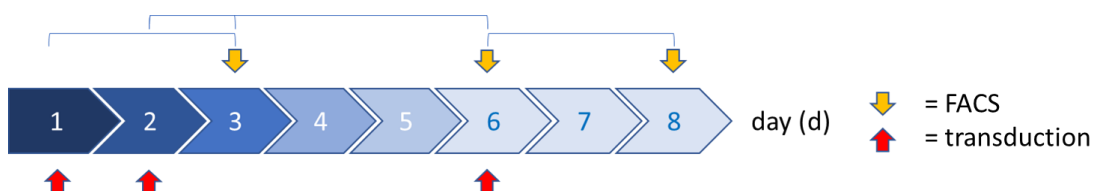


Figure 69: PBMC study design. PBMC transduced on day 1 and 6 were FACS analysed after 48h. Meanwhile PBMC transduced on day 2 were FACS analysed after 24h and 96h.

Cells were seeded in a well of a 6-well plate and incubated at +37°C 5% CO₂ until analysis. A mock control was included by simply adding 3 mL of harvested PV supernatant. A PBMC only control with 3 mL of PBMC culture media was included as well. On the day of analysis, 2×10^5 cells were collected for each condition and transferred in an haemolysis tube (Greiner Bio-One, #115201) then 2 mL of fluorescence-activated single cell sorting (FACS) buffer prepared with PBS with 1% FBS was added. Tubes were centrifuged at 1400 RPM for 3 minutes at +4°C with acceleration and deceleration set to 8. The supernatant was then discarded, the pellet mixed and 100 µL of FACS buffer of 1:10 primary antibody was added and incubated for 20 minutes on ice without exposure to light. Three conditions were considered:

1. The MHC I population was determined by staining cells with anti-MHC I (Thermo Scientific™, Thermo Fisher Scientific, #MA5-16636);
2. The MHC II population was determined by staining cells with anti-MHC II (Thermo Scientific™, Thermo Fisher Scientific, #MA1-81201);
3. A control with no primary antibody representing the whole population of dendritic cells.

After incubation, cells were washed with 2 mL of FACS buffer and centrifuged at 1400 RPM for 3 minutes at +4°C with acceleration and deceleration set to 8, followed by another round of washing and centrifugation. The supernatant was then discarded, the pellet mixed with 100 µL of FACS buffer of 1:100 of Goat anti-Mouse IgG (H+L) Cross-Adsorbed Secondary Antibody, APC (Invitrogen™, Thermo Fisher Scientific, #A865) added to the relevant samples

and incubated for 15 minutes in the dark on ice. Treatment was repeated as above. but this time cells were fixed in 500 µL 0.5% paraformaldehyde (PFA; Sigma-Aldrich®, Merck, #HT-501128) diluted in PBS and incubated for 15 minutes in the dark on ice. After the incubation time, cells were washed twice following the same previous treatment. Finally, cells were resuspended in 200 µL FACS buffer and kept on ice until analysis using a CytoFLEX S Flow Cytometer (Beckman Coulter, model: B75442).

6.2.5 Data analysis

PV titration and PVNA data read on the SPARK® Microplate Reader were analysed using SparkControl™ Magellan™ Software version 1.2 (Tecan). Analysis was carried out using Microsoft® Excel™ and plotted using GraphPad Prism® as previously described in Section 2.6. To monitor any CPE induced by the WT viruses, the xCELLigence RTCA Software 2.0 (ACEA Biosciences, Agilent) and Incucyte® Base Analysis Software (Essen BioScience) were employed to read the impedance as CI. CytExpert Software version 2.2 (Beckman Coulter) Controlled the CytoFLEX instrument operation, data collection and flow cytometry analysis.

6.3 RESULTS

6.3.1 EHV-1 PV titration

6.3.1.1 EIV PV titre comparison on SPARK® (Tecan) and GloMax® (Promega) luminometers

Before measuring EHV-1 PV titres on the SPARK® (Tecan), comparative luminescence was first assessed using a high titre EIV PV. H3 PV was generated with pl.18-H3 (HA) either with or without pl.18-N8 (NA) of A/equine/Richmond/1/2007 (H3N8) and titrated shortly after generation before shipped on dry ice to LABÉO (France) (Figure 70). A canine influenza PV of A/canine/Colorado/30604/2006 (H3N2) was included as control for the correct performance of the PV titration on GloMax® (Promega) luminometer. PV titres were compared using an unpaired t-test and a significant difference was observed between the two luminometers readings ($p=0.0003$ and $p=0.0006$ for the first and second harvest respectively) resulting in 2-log RLU/mL difference. It was questioned if this difference in titre between SPARK® (Tecan) and GloMax® (Promega) might have been due to the fact that the EIV PV batch had been stored at -80°C for a long time at LABÉO (France). However, it was not excluded the idea that this difference was actually due to the reflection of sensitivity of the two luminometers. A comparison of Δenv PVs could not be performed because for one of the test batches Δenv PV was not produced.

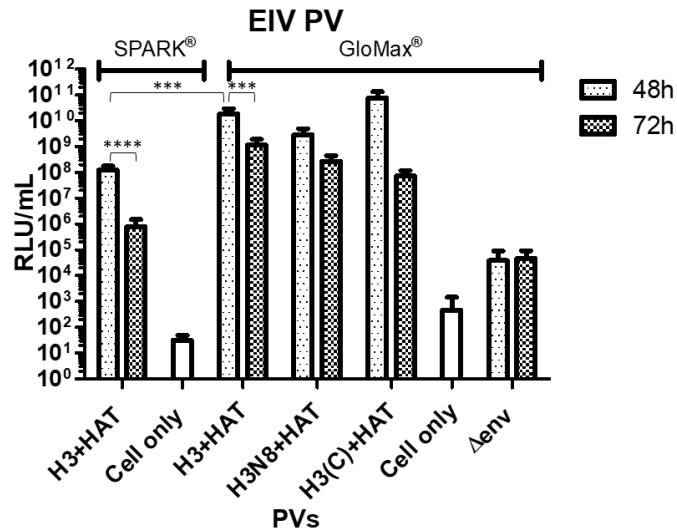


Figure 70: PV titration comparison between GloMax® (Promega) and SPARK® (Tecan) Luminometers. EIV PVs were titrated alongside a canine influenza PV (H3(C)+HAT), Δenv PV and cell only. EIV PVs (H3+HAT) titres were compared and a significant difference was observed between the two luminometers (***) is $p=0.0003$ and $p=0.0006$ for the first and second harvest respectively). A significant difference was reported also between the first (48h) and second (72h) harvest (**** is $p<0.0001$ on SPARK® and *** is $p=0.0005$ and GloMax®). The final titre was the result of the average of duplicates repeated twice.

6.3.1.2 SPARK® (Tecan) luminometer reading mode test

Another test to assess luminescence on SPARK® (Tecan) was the reading mode whether employing an orbital shake of the plate before the actual measure. Plate shaking is often employed to homogenise the mix in each well before start of a measurement. Therefore, EIV PV was titrated on two 96-well plates with the same condition. After 48 hours incubation, luminescence was measured either with shake or no shake reading mode (Figure 71). However, comparing the data between the two readings no significant difference was observed, implying that it is acceptable to use different reading modes as neither affected the titre results. For this reason, plate shaking on SPARK® (Tecan) was excluded to reduce time to collect data and keep the luminescence reading consistent to GloMax® (Promega).

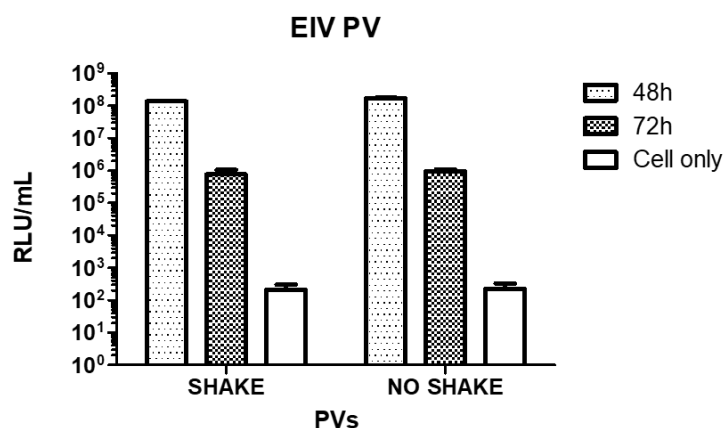


Figure 71: PV titration on SPARK® (Tecan) Luminometer using either an orbital shaking mode or no shaking. EIV PVs harvested at 48h or 72h post-transfection were titrated on two 96-well plates with the same condition. No significant difference was observed. The final titre was the result of the average of duplicates repeated twice.

6.3.1.3 EHV-1 PV titration on SPARK® (Tecan) luminometer

EHV-1 PVs were titrated before and after shipping on dry ice, first on GloMax® (Promega) and then on SPARK® (Tecan) luminometer to assess RLU/mL values (Table 21). As observed, an average of 2-log RLU/mL titre reduction in titre values was reported for the SPARK® (Tecan) machine for all readings, suggesting a significantly lower luminescence sensitivity of the SPARK® (Tecan) than GloMax® (Promega) machine. Thus, extra sensitivity assessment should be performed in different labs before running a PVNA with new samples in order to select a correct PV input.

| PV batch | Harvest (h) | GloMax® (Promega) | Spark® (Tecan) |
|----------|-------------|-------------------|----------------|
| A | 48h | 5.16E+07 | 9.91E+05 |
| | 72h | 1.57E+08 | 1.59E+06 |
| B | 48h | 6.73E+07 | 1.02E+06 |
| | 72h | 1.59E+08 | 1.49E+06 |
| C | 48h | 1.22E+08 | 9.45E+05 |
| | 72h | 3.66E+08 | 1.74E+06 |
| D | 48h | 5.88E+07 | 1.04E+06 |
| | 72h | 2.15E+08 | 2.03E+06 |
| E | 48h | 5.07E+07 | 7.03E+05 |
| | 72h | 2.13E+08 | 1.33E+06 |
| F | 48h | 2.63E+08 | 1.69E+06 |
| | 72h | 3.29E+08 | 2.57E+06 |
| G | 72h | 1.72E+08 | 8.89E+05 |
| H | 72h | 1.85E+08 | 8.32E+05 |
| I | 72h | 6.30E+07 | 1.09E+06 |
| J | 72h | 1.08E+08 | 7.62E+05 |
| K | 72h | - | 5.34E+05 |
| H3N8 | 72h | 2.80E+09 | 3.90E+07 |

Table 21: Record of EHV-1 PVs titre. EHV-1 PV (PV batch A to K) titres obtained on GloMax® (Promega) and SPARK® (Tecan) luminometer. PVs harvested at both 48h and 72h post-transfection were titrated. An EIV PV (H3N8) was included for control purposes.

6.3.1.4 EHV-1 PV titration on xCELLigence and Incucyte® RTCA

Titration were also set up using two different Real-Time Cell Analysis (RTCA) technologies available at LABÉO (France): xCELLigence and Incucyte® RTCA. The evolution of PVs transduction was observed and compared to WT viruses employing a dynamic monitoring of transduction into HEK293T (Figure 72), CCL57 (Figure 73), RK13 (Figure 74) and for EIV PV MDCK II (Figure 75). For xCELLigence, cell adhesion was measured exploiting impedance which reflected the ability of the PV to transduce (or to infect in case of the WT virus). In parallel the same titration conditions were maintained to monitor cytopathic effects on Incucyte® (Appendix Figures 4-7). Both WT EHV-1 KyD and EIV Jouars strains were employed as WT virus controls to verify the known cytopathic effects induced by viral infection for EHV-

1 and EIV respectively. As a consequence, target cell lines were chosen accordingly to which WT reference strain was employed. For instance, titration on MDCK II was performed only for EIV study and not for EHV-1. Although HEK293T are not routinely employed for WT EHV-1 culture experiments, we have shown this to be the best target cell line for EHV-1 PV, a titration was performed on this line to assess viral infectivity. In all graphs (Figures 72-75), a fall of the normalised cell index (CIn) was observed at 24 hours indicating when the titration was performed after the cell adhesion step (0 – 24 hours). From 24 hours, CIn began to be restored for most cases, but not for cells infected with the WT virus (black curves), corresponding to cytopathic effects mediated by the virus. Cytopathic effects on HEK293T were not as evident as observed on CCL57 or RK13. However, cell viabilities were somehow affected suggesting WT EHV-1 KyD was able to infect HEK293T cells. The CIn started to decrease after 50 hours, but values did not reach zero, while for CCL57 and RK13 the CIn started to decrease at earlier stages (30 – 35 hours) and reached zero at 40 and 50 hours respectively. This could imply why EHV-1 PV was efficiently transducing HEK293T because there might be cell surface receptors able to mediate EHV-1 entry which could be enhanced for a simpler virus version such as EHV-1 PV. Due to complications in growing conditions, curves were not so clear for EIV studies on MDCK II. This is probably because optimal cell adhesion levels were not reached in the 24 hours time frame before infection. Overall, PVs did not induce any cytopathic effects on target cells as expected (blue curves). Purple and green curves represented cell responses when transduced with Δ env PV, or cell only respectively. For these conditions the CIn increased after 24 hours (time of infection) and continued until a plateau was reached. This was not the case of HEK293T cells since CIn started to decrease at 70 hours suggesting a delay of cell proliferation.

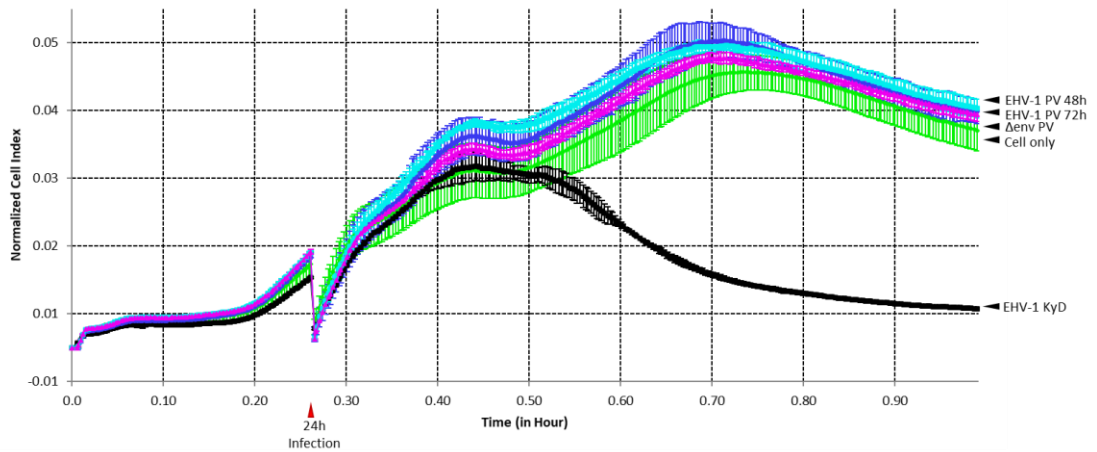


Figure 72: PV titration on xCELLigence RTCA on HEK293T cells. EHV-1 KyD was employed as WT control for cytopathic effects. The Cell Index values was normalised to the last time point before transduction/infection of cells (red arrow) at 24 hours from the beginning of the experiment. The green curve represented the CIn of cell only (not transduced/infected cells) and the purple curve represented the Δenv PV. Blue curves (light and dark) represented the CIn of EHV-1 PV 48h and 72h respectively, while the black curve represented the CIn of EHV-1 KyD infected cells. Each data point indicated the mean SD of one experiment in duplicate, repeated three times.

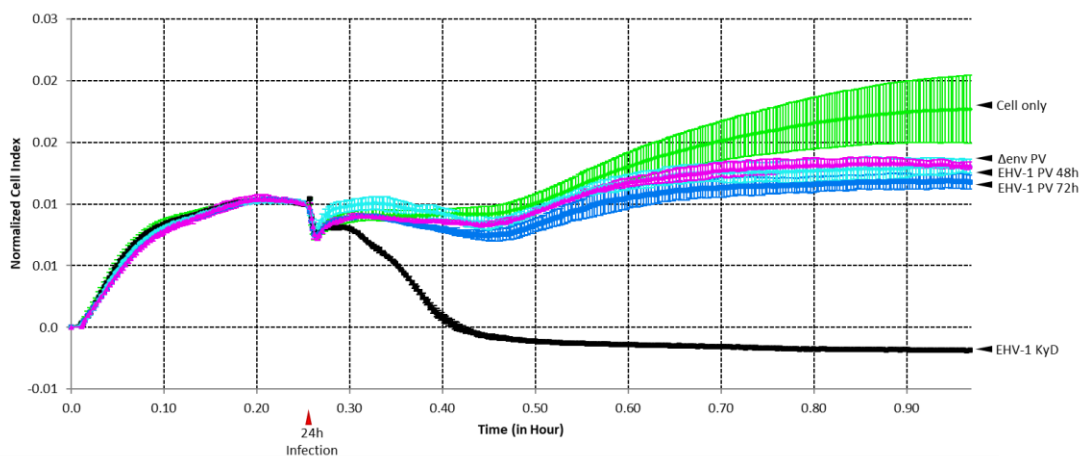


Figure 73: PV titration on xCELLigence RTCA on CCL57 cells. EHV-1 KyD was employed as WT control for cytopathic effects. The Cell Index values was normalised to the last time point before transduction/infection of cells (red arrow) at 24 hours from the beginning of the experiment. The green curve represented the CIn of cell only (not transduced/infected cells) and the purple curve represented the Δenv PV. Blue curves (light and dark) represented the CIn of EHV-1 PV 48h and 72h respectively, while the black curve represented the CIn of EHV-1 KyD infected cells. Each data point indicated the mean SD of one experiment in duplicate, repeated three times.

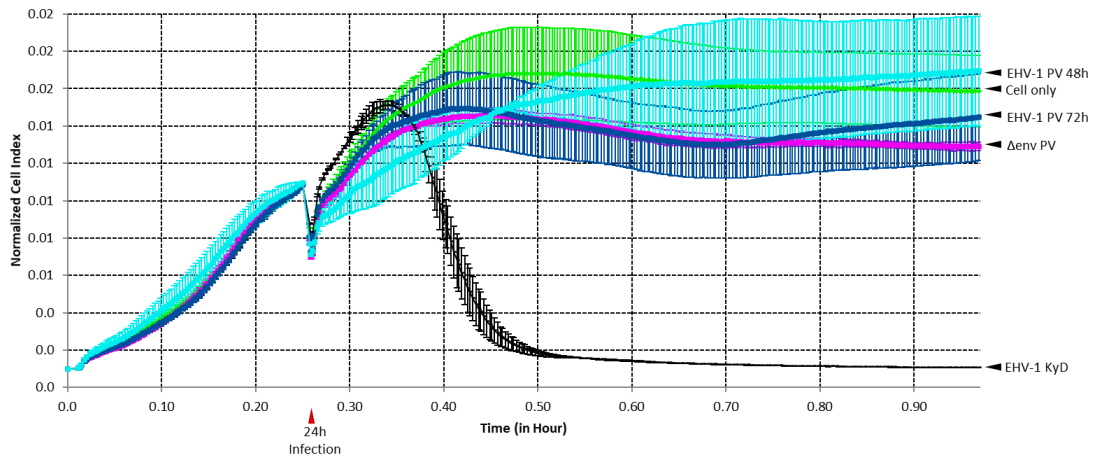


Figure 74: PV titration on xCELLigence RTCA on RK13 cells. EHV-1 KyD was employed as WT control for cytopathic effects. The Cell Index values was normalised to the last time point before transduction/infection of cells (red arrow) at 24 hours from the beginning of the experiment. The green curve represented the CIn of cell only (not transduced/infected cells) and the purple curve represented the Δenv PV. Blue curves (light and dark) represented the CIn of EHV-1 PV 48h and 72h respectively, while the black curve represented the CIn of EHV-1 KyD infected cells. Each data point indicated the mean SD of one experiment in duplicate, repeated three times.

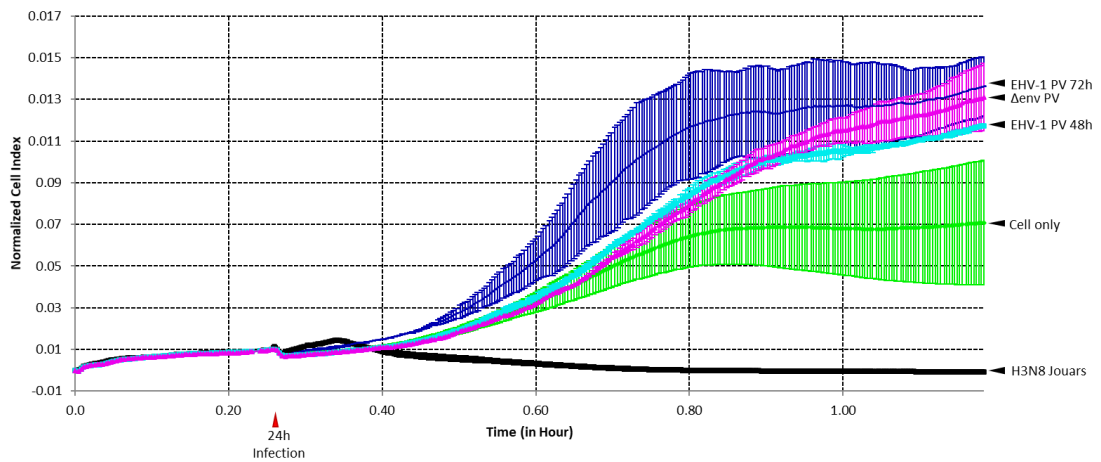


Figure 75: PV titration on xCELLigence RTCA on MDCK II cells. EIV (H3N8 Jouars) was employed as WT control for cytopathic effects. The Cell Index values was normalised to the last time point before transduction/infection of cells (red arrow) at 24 hours from the beginning of the experiment. The green curve represented the CIn of cell only (not transduced/infected cells) and the purple curve represented the Δenv PV. Blue curves (light and dark) represented the CIn of EHV-1 PV 48h and 72h respectively, while the black curve represented the CIn of H3N8 Jouars infected cells. Each data point indicated the mean SD of one experiment in duplicate, repeated three times.

6.3.2 EHV-1 PV transduction assessment by flow cytometry

The transduction ability of EHV-1 PV on PBMC was investigated using flow cytometry. PBMC were transduced and FACS analysed at different stages as illustrated on the schematic representation of the study design (Figure 69 in Section 6.2.4.). Staining of the fraction of the MHC population should have permitted monitoring of EHV-1 PV transduction assessed with GFP detection. GFP fluorescence and MHC staining were plotted on both a histogram overlay (Figure 76) and a dot plot (Figure 77). Antibody staining allowed differentiation of MHC I and MHC II PBMC populations. In the cell only control two distinct peaks were noted especially in the MHC I population, while less evident for MHC II population. Cells were also mock transduced with only culture media (in which PVs were normally harvested) to verify whether components of that particular media were affecting PBMC. Preliminary results suggested EHV-1 PV was not able to transduce PBMC as no GFP was detected and immune response was not altered by comparing transduced conditions with the cell only control, although a broader peak distribution was observed for MHC II, suggesting PBMC were slightly affected by the media PVs were routinely harvested in.

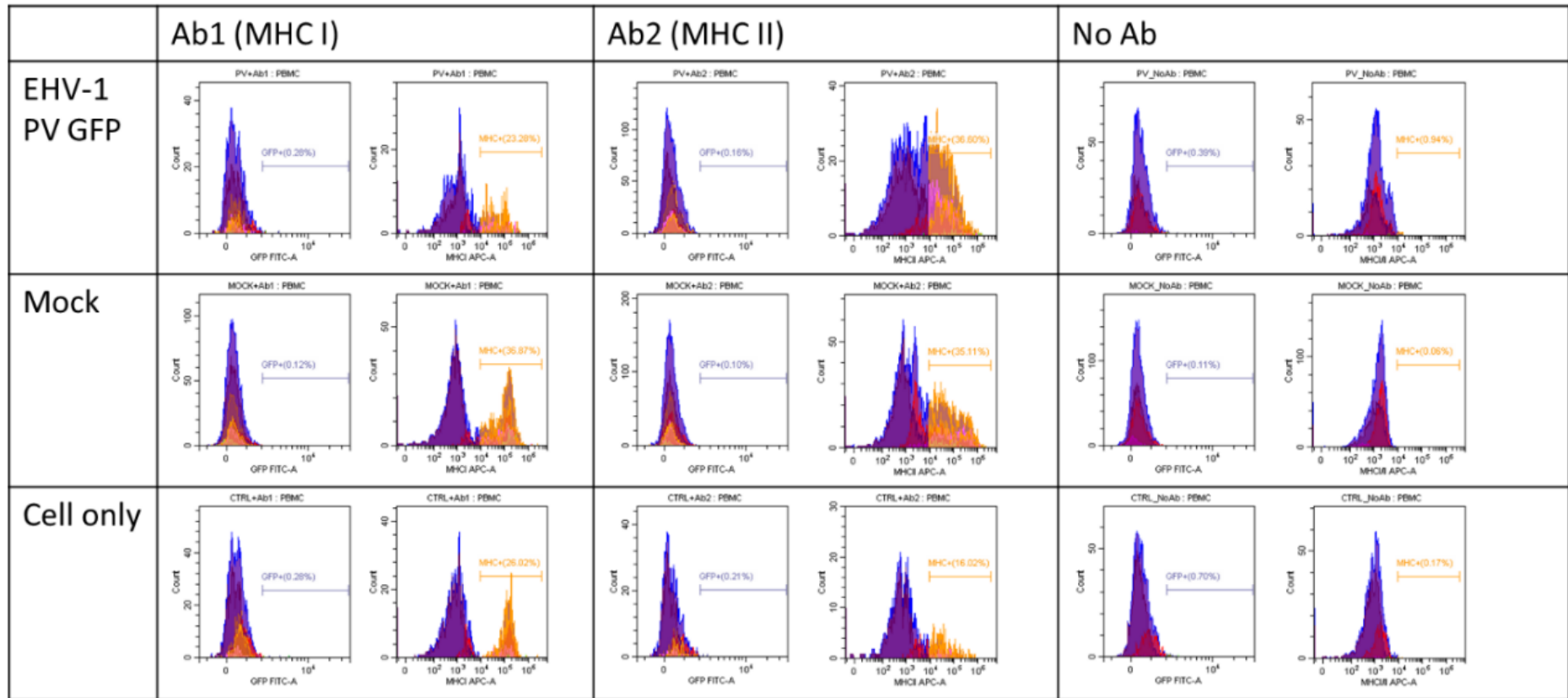


Figure 76: Flow cytometry analysis of equine PBMC. Histograms overlays in a segment gate to analyse the presence of GFP positive equine PBMC cells detected by flow cytometry generated on CytoFLEX. The number of cells sorted (y-axis: count) was interpolated with either GFP fluorescence (X axis: GFP FITC-A) or antibody staining (Y axis: MHC I/II APC-A). MHC I or II class expressing cells were reported as % above the histogram. Two independent experiments were performed.

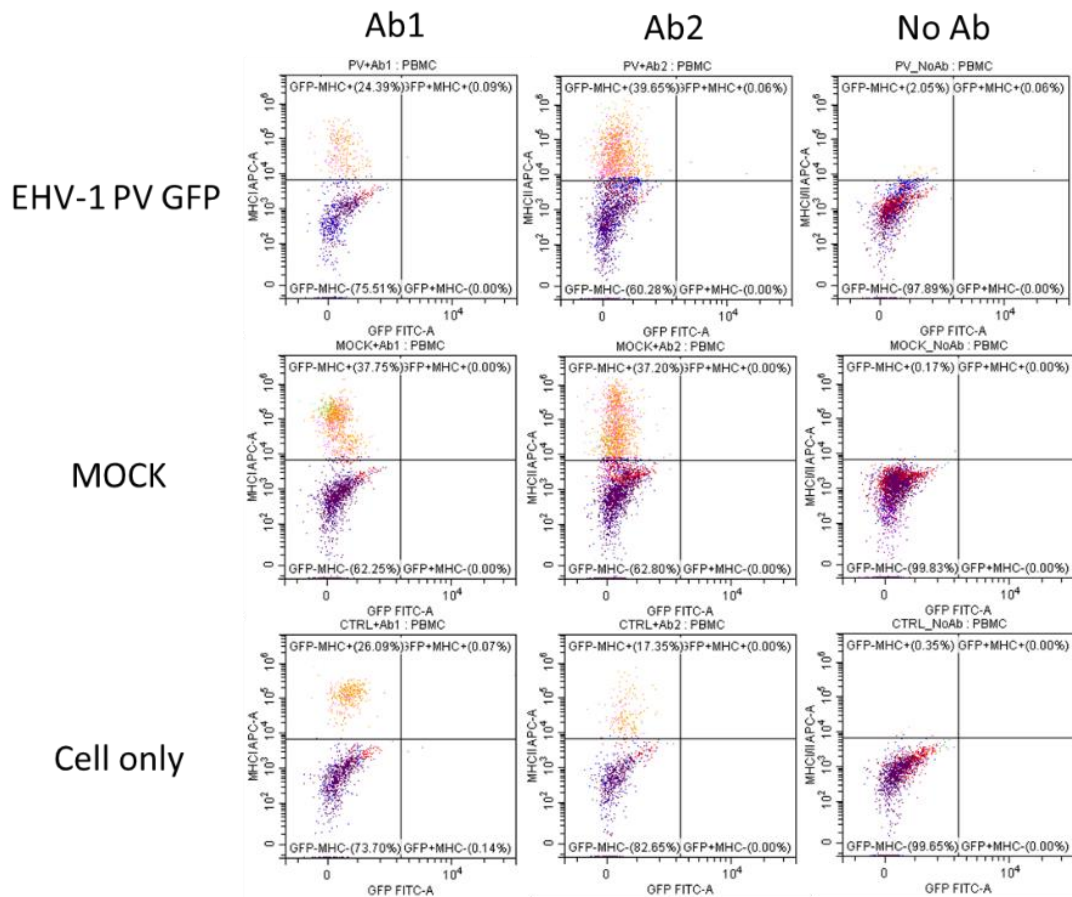


Figure 77: Flow cytometry analysis of equine PBMC. Dot plots in a four-quadrant gate to analyse the presence of GFP positive equine PBMC cells (either MHC I or MHC II) detected by flow cytometry generated on CytoFLEX. Equine PBMC population was gated to differentiate GFP to non GFP cells (X axis: GFP FITC-A) and to differentiate MHC class presented (Y axis: MHC I/II APC-A). MHC I or II positive cells were shown in the upper left quadrant (GFP-MHC+), outdistanced from the main population in the lower left quadrant (GFP-MHC-). Two independent experiments were performed.

As control for GFP detection by flow cytometry and so success of PV transduction, HEK293T cells were transduced with an EIV PV (H3N8 PV). Visual inspections were undertaken on Incucyte® before flow cytometry analysis to confirm EHV-1 and EIV PV successful transduction of HEK293T cells. GFP detection by flow cytometry was possible and interestingly the results obtained were comparable to what was observed on Incucyte®. In both the histograms (Figure 78) and the pseudo colour plots (Figure 79) GFP positive cells were detected at higher levels for EIV PV (+6.19%) than EHV-1 PV (+0.49%). Δenv PV and cell only were employed for control of GFP background and cell morphology respectively.

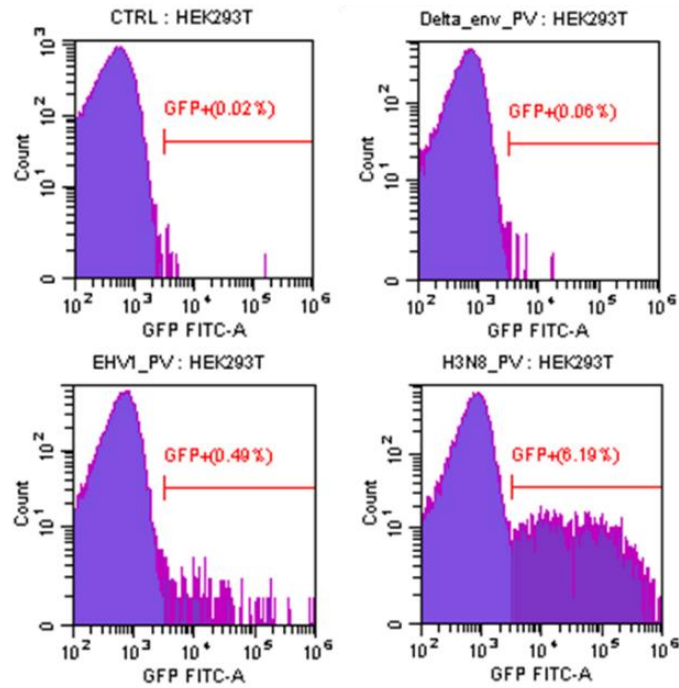


Figure 78: Flow cytometry analysis of HEK293T cells. Histograms in a line segment gate of GFP positive HEK293T cells detected by flow cytometry generated on CytoFLEX. GFP fluorescence (X axis: GFP FITC-A) was interpolated with the number of cells sorted (Y axis: count). GFP positive cells were reported as % above the histogram. Three independent experiments were performed.

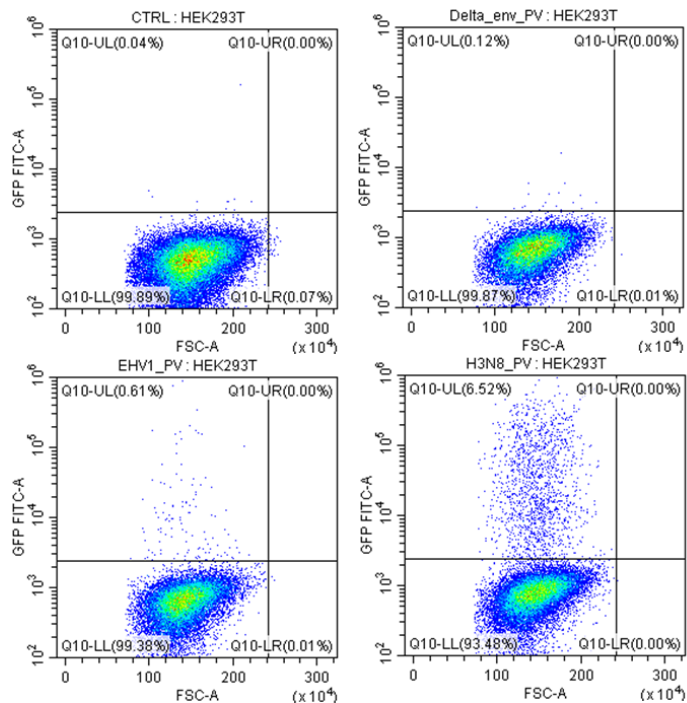


Figure 79: Flow cytometry analysis of HEK293T cells. Pseudo colour plots in a four-quadrant gate of GFP positive HEK293T cells detected by flow cytometry generated on CytoFLEX. GFP fluorescence (Y axis: GFP FITC-A) was interpolated with cell size (X axis: FSC-A). GFP positive cells were shown in the upper left quadrant (Q10-UL), outdistanced from the main population in the lower left quadrant (Q10-LL). Three independent experiments were performed.

6.3.3 EHV-1 PV neutralisation assay

6.3.3.1 EHV-1 PV input assessment

A small number of serum samples ($n=4$) from the EHV-1 experimentally infected study panel (Section 4.2.1.) were tested against EHV-1 PV in a PVNT to assess the PV input to utilise when readings were carried out on the SPARK® (Tecan) luminometer before moving to larger serum panel studies. From the titration findings (Section 6.3.1.3.), 2-log RLU/mL titre difference was reported for all readings on SPARK® (Tecan) compared to GloMax® (Promega). In normal conditions, a PV input of 1×10^6 RLU/mL would have been used for further assay. Therefore, the PV input was lowered of 2-log RLU/mL, from 1×10^6 to 1×10^4 RLU/mL. Neutralisation trend curves (Figure 80) and IC_{50} results (Table 22) obtained from SPARK® (Tecan) were then compared with the results obtained when GloMax® (Promega) luminometer was employed to read luminescence. To verify whether IC_{50} values were affected by the different luminometers, an unpaired t-test was performed for statistical purposes. Interestingly no significant difference was observed between the readings obtained from the two different luminometers. Thus, for further assays a PV input of 1×10^4 RLU/mL was chosen to be employed for the SPARK® (Tecan) luminometer.

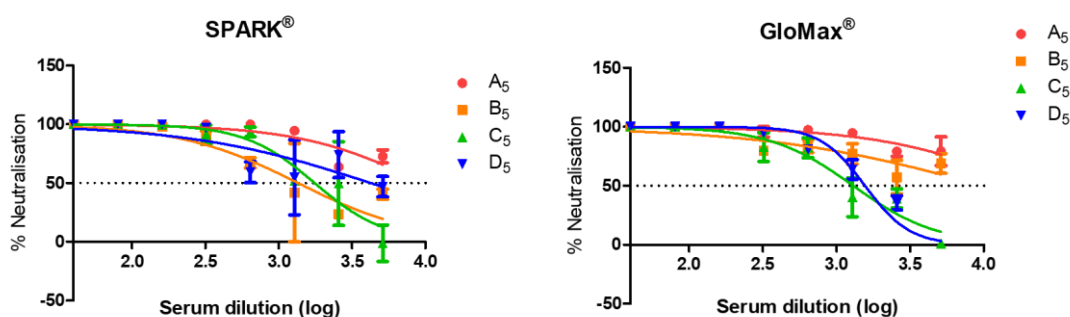


Figure 80: PVNT for PV input assessment. Neutralisation curves of serum sample collected on day 5 from horse A, B, C and D ($n=4$). **Left graph:** results obtained on SPARK® (Tecan). **Right graph:** results obtained on GloMax® (Promega). Neat sera were added at a starting dilution of 1/40 (Log of the serial dilution=1.6). Each data point of the two-fold serial dilution was the result of mean of duplicates repeated twice. The % neutralisation is reported at each data point represented by the mean with SEM.

| Sera sample | SPARK® (Tecan) | | GloMax® (Promega) | |
|----------------|---------------------|------------------|---------------------|------------------|
| | LogIC ₅₀ | IC ₅₀ | LogIC ₅₀ | IC ₅₀ |
| A ₅ | 3.985917 | 9680.934 | 4.305007 | 20184.020 |
| B ₅ | 3.131644 | 1354.078 | 3.996063 | 9909.765 |
| C ₅ | 3.244619 | 1756.384 | 3.112903 | 1296.888 |
| D ₅ | 3.627614 | 4242.429 | 3.193012 | 1559.594 |

Table 22: LogIC₅₀ and IC₅₀ values. Neat sera tested in duplicate against EHV-1 PV obtained from either SPARK® (Tecan) or GloMax® (Promega).

6.3.3.2 IC₅₀ threshold value

The SPARK® (Tecan) luminometer displayed a different sensibility in fluorescence reading when compared to GloMax® (Promega). Therefore, it was essential to establish first a cut-off value to use as threshold of positivity. Negative control sera samples (n=8) from the EHV-1 experimentally infected study panel (Section 4.2.1.) were employed against EHV-1 PV to determine this. Samples were collected on day 0 before infection. It has already been ascertained that seroconversion had not occurred yet from previous PVNA study using the GloMax® (Promega) machine. The threshold for negative samples was obtained from the average of the IC₅₀ of all samples and was set at 300 (IC₅₀pp-NT=300; Figure 81, dotted line). Thus, this threshold was addressed for further PVNT, providing a level to define negative from positive serum samples.

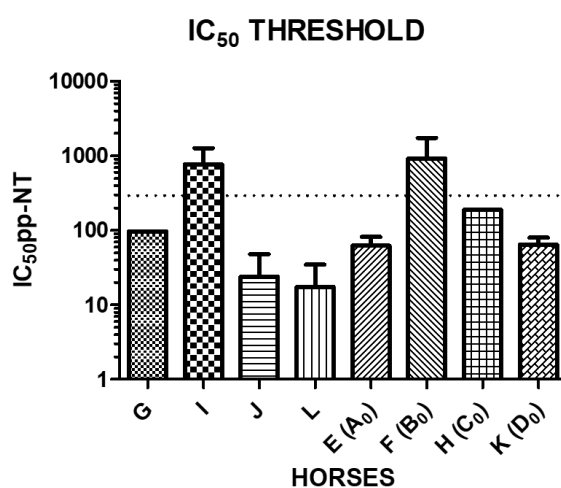


Figure 81: Graphical summary of IC₅₀ values for threshold assessment. Neat sera were added at a starting dilution of 1/40 (Log of the serial dilution=1.6). A dotted line represented the average of the IC₅₀ values. Each column point of the two-fold serial dilution was the result of mean of duplicates repeated twice with SEM.

6.3.3.3 Validation of EHV-1 PV neutralisation assay for the detection of an immune response in vaccinated horses

The presence of EHV-1 antibodies was investigated by screening a large equine sera panel (n=78) which immune response was elicited by vaccination against EHV-1 PV. Three groups of serum samples were characterized based on the status of the horse (pregnant, primary-vaccinated or reboosted) and each group was analysed separately. Extra valuable information is reported in Appendix Table 2 (Sutton *et al.*, 2021). First, the IC₅₀ cut-off value for positivity threshold to determine positive to negative sera samples was set at 300 (IC₅₀pp-NT=300) obtained from the previous study (Section 6.3.3.2.). The cut-off value could have been adjusted employing sera from previously non-vaccinated horses. However, it was unknown whether exposure to EHV-1 had occurred in the past. Antibody reaction against EHV-1 PV was detected for all pregnant mares (Group G) throughout the study, although the IC₅₀ values varied among individuals (Figure 82). Neutralisation started from lower levels at the fifth month of gestation and slightly increased after the first injection. Horse G_A was the only mare not previously vaccinated against EHV-1. Therefore, this might explain why the IC₅₀ levels at the start of the study were closer to the cut-off for positive threshold and subsequently increased. These observations suggested that EHV-1 vaccination schedule stimulated specific antibody production. Neutralisation in the other two mares was detected at earlier stage of the study probably due to previous seroconversion subsequent to EHV-1 vaccination and stayed approximately on the same trend level despite a pick at the 8th or 9th month of gestation.

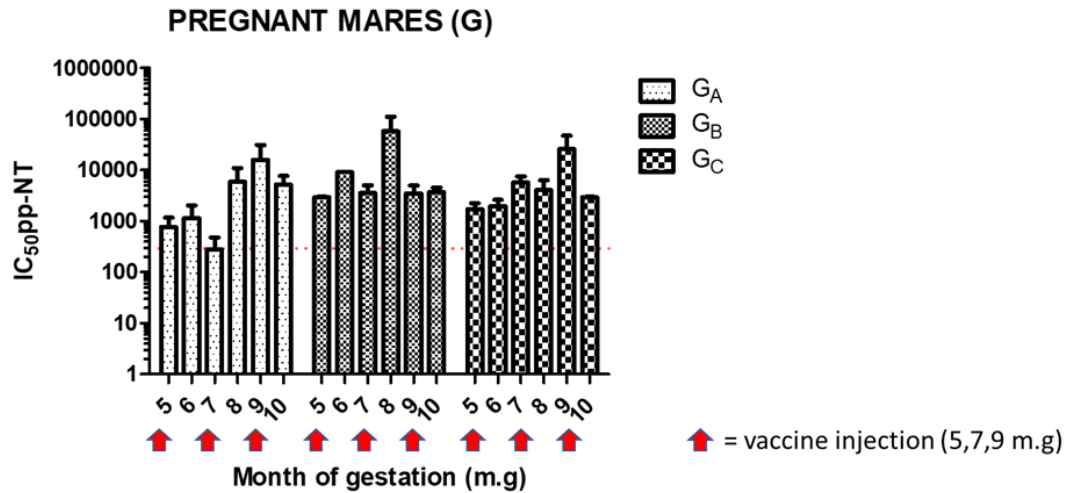


Figure 82: Graphical summary of the IC_{50} values of a panel of sera samples collected from EHV-1 vaccinated pregnant mares (Group G). Neat sera were added at a starting dilution of 1/40 (Log of the serial dilution=1.6) and tested against EHV-1 PV. A dotted line at 300 represented the cut-off value for positive antibody detection. Each column point of the two-fold serial dilution was the result of mean of duplicates repeated twice with SEM.

Sera from primo-vaccinated group (Group P) showed less regular responses among each individual (Figure 83). Samples collected at early stage of the study were found with lower IC_{50} values which increased throughout the study. Some individuals were found to be above the cut-off threshold suspecting an EHV-1 infection exposure previous the start of the vaccination regimen. For these individuals the antibody response was less accentuated compared to those individuals which IC_{50} values were found below the cut-off threshold. These finding once again suggested that EHV-1 vaccination contributed to stimulation of specific antibody production. However, prospective studies whether vaccination contributed to limiting the spread of EHV-1 in the environment and to other susceptible individuals or to manifest symptoms or abortions were not reported.

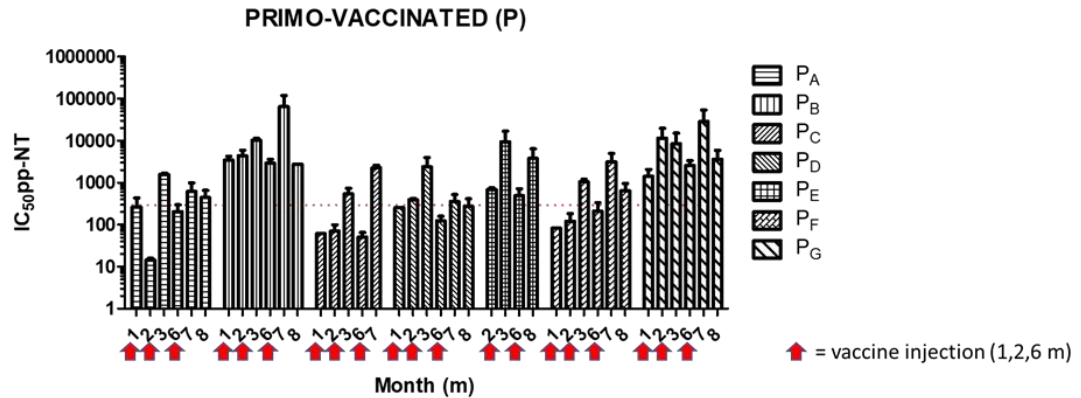


Figure 83: Graphical summary of the IC_{50} values of a panel of sera samples collected from primary EHV-1 vaccinated horses (Group P). Neat sera was added at a starting dilution of 1/40 (Log of the serial dilution=1.6) and tested against EHV-1 PV. A dotted line at 300 represented the cut-off value for positive antibody detection. Each column point of the two-fold serial dilution was the result of mean of duplicates repeated twice with SEM.

Neutralisation of EHV-1 PVs via antibodies in serum samples from boosted horses (Group R) is shown in Figure 84. Most of the IC_{50} levels of Group R were detected above the cut-off value for positivity threshold, with the exception of R_C showing an inexplicable gap between sampling. It was not possible to create the complete picture for horse R_C since serum sample of month 2 had run out. However, it can be observed for the whole length of the sampling (month 1, 2 and 4) of each horse of Group R a slight increase of the IC_{50} levels, although not exceptionally high. This suggests that EHV-1 reboost did not affect neutralisation, but it might have helped in keeping the antibody response high and constant. Another observation taken into consideration was whether EHV-4 cross-reactivity induced a higher antibody response against EHV-1 PV since the horse R_E was found PCR positive to EHV-4 (Appendix Table 2) and the IC_{50} trends were higher compared to the other individuals at the same sampling time.

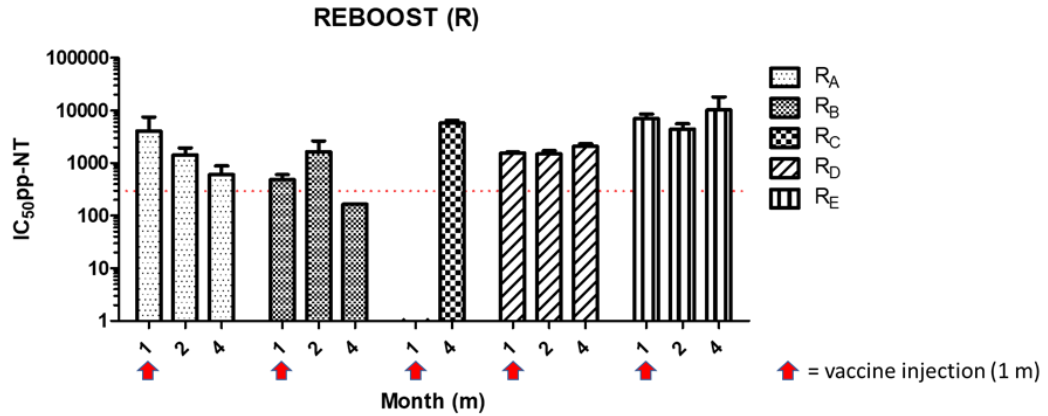


Figure 84: Graphical summary of the IC₅₀ values of a panel of sera samples collected from horses already EHV-1 vaccinated (Group R). Neat sera were added at a starting dilution of 1/40 (Log of the serial dilution=1.6) and tested against EHV-1 PV. A dotted line at 300 represented the cut-off value for positive antibody detection. Each column point of the two-fold serial dilution was the result of mean of duplicates repeated twice with SEM.

6.3.3.3.1 Correlation of antibody titres

Once PVNT was successfully performed, it was of interest to correlate the antibody titres obtained with an EHV-1 VN assay performed on E.derm on xCELLigence RTCA (Table 23). Pearson correlation was calculated to compare the results between the logarithm IC₅₀ values obtained with xCELLigence kinetics and PVNT ($R^2=0.65$, $p<0.0001$; Figure 85). The EHV-1 VN assay on xCELLigence RTCA was performed and analysed by Dr. Gabrielle Sutton (LABÉO, Saint-Contest, France). Moreover, antibody titres measured with the xCELLigence kinetics on E.derm were correlated with the results obtained from a conventional method on RK13 cell line ($R^2=0.83$; Dr. Gabrielle Sutton, unpublished data).

GROUP G

| Horse | G _A | | | | | | G _B | | | | | | G _C | | | | | |
|---------------------------|----------------|-------|------|-------|-------|-------|----------------|-------|-------|-------|-------|-------|----------------|-------|-------|-------|-------|-------|
| Sample | 5 | 6 | 7 | 8 | 9 | 10 | 5 | 6 | 7 | 8 | 9 | 10 | 5 | 6 | 7 | 8 | 9 | 10 |
| Log xCELLNT ₅₀ | 4.79 | 6.02 | 5.42 | 7.64 | 7.55 | 7.96 | 5.25 | 7.57 | 6.4 | 6.43 | 5.81 | 6 | 7.35 | 7.23 | 7.06 | 7.84 | 7.31 | 7.57 |
| Log ppNT ₅₀ | 9.59 | 10.18 | 8.12 | 12.53 | 13.96 | 12.35 | 10.74 | 10.95 | 12.48 | 11.98 | 14.66 | 11.52 | 11.52 | 13.16 | 12.06 | 16.36 | 11.56 | 11.74 |

GROUP R

| Horse | R _A | | | R _B | | | R _C | | | R _D | | | R _E | | |
|---------------------------|----------------|-------|------|----------------|-------|------|----------------|------|-------|----------------|-------|-------|----------------|-------|-------|
| Sample | 1 | 2 | 4 | 1 | 2 | 4 | 1 | 2 | 4 | 1 | 2 | 4 | 1 | 2 | 4 |
| Log xCELLNT ₅₀ | 6.11 | 7.12 | 6.74 | 4.03 | 6.73 | 4.75 | 7.81 | 7.34 | 9 | 5.63 | 5.67 | 5.25 | 7.93 | 8 | 7.82 |
| Log ppNT ₅₀ | 12.00 | 10.48 | 9.24 | 8.92 | 10.69 | 7.37 | - | - | 12.49 | 10.59 | 10.53 | 11.03 | 12.77 | 12.10 | 13.32 |

GROUP P

| Horse | P _A | | | | | | P _B | | | | | | P _C | | | | | |
|---------------------------|----------------|------|-------|------|------|------|----------------|-------|-------|-------|-------|-------|----------------|------|------|------|-------|---|
| Sample | 1 | 2 | 3 | 6 | 7 | 8 | 1 | 2 | 3 | 6 | 7 | 8 | 1 | 2 | 3 | 6 | 7 | 8 |
| Log xCELLNT ₅₀ | 2 | 2 | 5.91 | 3.7 | 7.2 | 5.78 | 5.29 | 6.93 | 8 | 6.47 | 8 | 7.9 | 2.73 | 2 | 3.31 | 2 | - | - |
| Log ppNT ₅₀ | 8.04 | 3.86 | 10.64 | 7.68 | 9.28 | 8.79 | 11.75 | 12.09 | 13.32 | 11.51 | 15.99 | 11.42 | 5.95 | 6.14 | 9.08 | 5.66 | 11.15 | - |

| Horse | P _D | | | | | | P _E | | | | P _F | | | | | | |
|---------------------------|----------------|------|-------|------|------|------|----------------|------|-------|------|----------------|------|------|-------|------|-------|------|
| Sample | 1 | 2 | 3 | 6 | 7 | 8 | 1 | 2 | 3 | 6 | 8 | 1 | 2 | 3 | 6 | 7 | 8 |
| Log xCELLNT ₅₀ | 4.48 | 3.88 | 4.42 | 3.67 | 7.19 | 4.98 | 4.34 | 5.7 | 7.53 | 4.83 | 7.69 | 2 | 3.12 | 6.29 | 3.15 | 7.1 | 6.07 |
| Log ppNT ₅₀ | 8.00 | 8.61 | 11.23 | 6.95 | 8.48 | 7.94 | - | 9.44 | 13.20 | 8.95 | 11.88 | 6.36 | 6.92 | 10.04 | 7.71 | 11.64 | 9.32 |

| Horse | P _G | | | | | |
|---------------------------|----------------|-------|-------|-------|-------|-------|
| Sample | 1 | 2 | 3 | 6 | 7 | 8 |
| Log xCELLNT ₅₀ | 5.05 | 6.5 | 7.46 | 6.55 | 7.48 | 7.82 |
| Log ppNT ₅₀ | 10.48 | 13.50 | 13.04 | 11.32 | 14.81 | 11.83 |

Table 23: Comparison of EHV-1 PVNA and VN. Antibody titres obtained between the logarithm IC₅₀ values obtained with EHV-1 VN assay performed on E.derm on xCELLigence RTCA (Log xCELLNT₅₀) and the reciprocal of the IC₅₀ values with EHV-1 PVNT (Log ppNT₅₀) of sera samples collected from Group G, R and P of the EHV-1 vaccinated horses.

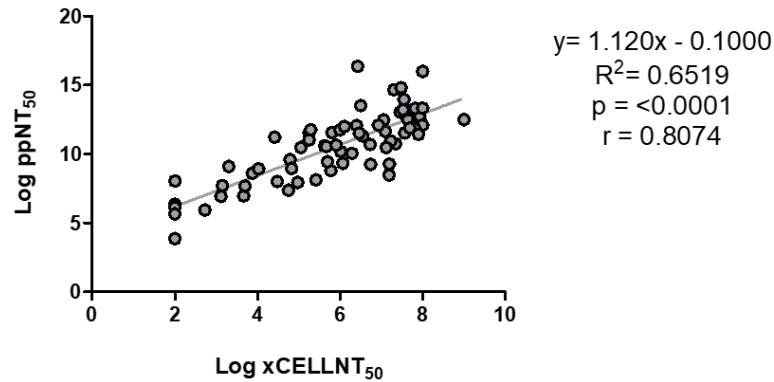


Figure 85: Correlation xCELLNT₅₀ and ppNT₅₀. Correlation of the antibody titres obtained between the logarithm IC₅₀ values obtained with xCELLigence kinetics (Log xCELLNT₅₀) and the reciprocal of the IC₅₀ values with PVNT (Log ppNT₅₀), graphed in a Scatter plot. Pearson correlation coefficient $r=0.81$ was calculated for all samples of all groups (G, P and R; $n=78$).

6.4 DISCUSSION

Firefly luciferase is the primary reporter employed in EHV-1 PV, particularly in PVNT, for quantification of assay data. The signal measured from the luciferase enzyme, obtained by lysis of transduced cells and addition of substrate, is read by a luminometer and output is given as RLU. The RLU readings obtained from titrations can then be used to determine the functional pseudotype particle concentration within a sample (Wright *et al.*, 2009). However, it is well known that RLU readings can be subject to many variables which commonly could occur especially depending on the cell lines used or the plate reading equipment (Carnell *et al.*, 2015). Therefore, reproducibility might be hard to achieve because of these additional variables. Hence the need for internal standards, such as those produced at NIBSC (UK) (e.g. WHO international standards, quality control reagents, *in vitro* diagnostic standards etc). In order to compare data and ensure consistency between laboratories it is important to minimise the introduction of these variables and to approach a more standardised methodology, so that even in the case scenario where different luminometers are used to read the same experiment the results are reproducible (Carnell *et al.*, 2015). Indeed, once EHV-1 PV samples reached the host laboratory (LABÉO, France), the titre had to be first re-measured to measure any titre loss occurred due to shipment. However, at the host platform the luminometer was different from the main laboratory. A 2-log RLU/mL difference was observed between the two luminometers (GloMax® Promega in the UK and SPARK® Tecan in France), and no major loss of viable pseudotype due to shipment was recorded. It was essential to understand the different luminometer signal sensitivity for further PV

application such as neutralisation assay. First, a test to assess the PV input aided to reveal the correct value to employ in a PVNA to guarantee that the antibody titre was independent from the PV input. Subsequently, a negative threshold had to be established to provide a starting point to define negative and positive sera sample, which was set at an IC₅₀ value of 300 from the average of sera collected on day 0 of an EHV-1 experimental infection study. PVNA was applied to quantify the antibody response elicited by vaccination. As expected, each individual horse responded differently depending on many factors such as age, vaccination history or previous exposure to the antigen. However, the information on the vaccination status or whether the horse was previously exposed to the antigen, was hard to find. All three pregnant mares (G_A, G_B and G_C of Group G of the EHV-1 vaccination campaign study; Figure 82) were up to date with EHV-1 vaccination except for G_A. This might explain the slightly different profile to the two other animals (G_B and G_C): after each vaccine injection there is a positive antibody response which is particularly robust after the second dose. Meanwhile mares G_B and G_C did not respond as efficiently to the first injection. It would have been of interest to verify the antibody profile of each of the newborn foal and assess how much the maternal antibody presence induced by vaccination of the mare influenced on its profile. Foote *et al.*, (2002) found a link between the level of antibodies found in foals from their mares depending on how well they responded to vaccination. Seropositive mares did not respond well to vaccination and the levels of antibodies detected in the foals were low. The primary-vaccinated horses group (Group P of the EHV-1 vaccination campaign study; Figure 83) is the most variable as horses were of different ages (from 5 ½ months-old to 24 years-old range; Appendix Table 2) which might have influenced the oldest horses (2 ½ and 24 years old, P_B and P_G) profiles which resulted with the highest titre. The fact that younger foals (e.g. P_A and P_D) showed lower profiles was probably explained by the age (Gilkerson *et al.*, 1998; Wilson *et al.*, 1999; Foote *et al.*, 2002). A typical primo-vaccination profile is best represented by P_F, with increasing peaks after the second and the third dose (Ruitenbergh *et al.*, 2000). Looking at the reboosted horses profiles (Group R of the EHV-1 vaccination campaign study; Figure 84), age might have once again influenced since R_B is the youngest and responded quite well to the first injection showing a higher level on the following month. While the oldest horses (R_C and R_E) showed higher titres. Interestingly, R_E was found to be PCR positive to EHV-4 and showed higher titres of EHV-1 antibodies than R_C, but it is not certain whether this was influenced by cross-reactivity. Seroconversion was detected in all immunised groups (Group G, P and R), indicated by an increase of the neutralising antibody response.

Since the PVNA has not been fully validated as a serological test to monitor response induced from EHV-1 vaccination, it was of interest to compare the results obtained with a conventional VN assay. The results of the conventional VN assay are not reported. However, an EHV-1 VN assay was performed on E.derm on xCELLigence RTCA. Another consideration should be focussed on the sera panel employed in this study to validate the PVNA. It would have been more appropriate to employ sera collected from horses raised in a dedicated, specific pathogen free facility since birth and vaccinated against EHV-1 only. Nevertheless, comparison of the results with the VN are promising ($r=0.81$, $p<0.0001$) with little discordance probably due to the fact that the PVNA is targeting four glycoproteins and not the whole panel as for the VN (Sutton *et al.*, 2021).

An innovative technology to monitor in real time the cytopathic effects induced by viruses in particular EHV-1 was established at our collaborators (Hue *et al.*, 2016; Thieulent *et al.*, 2019; Sutton *et al.*, 2020). It has been assessed as a valid label-free alternative technology to pursue these studies based on the measurement of impedance variations through the aid of golden electrodes (Solly *et al.*, 2004). Viability, growth and any alteration of the adherent cells elicited by viral cytopathic effect is monitored as an impedance signal (Fang *et al.*, 2011; Limame *et al.*, 2012). EHV-1 PV was monitored in real time using the cell analysis technology present by our collaborators in France and compared to the WT. However, despite the fact that PV attach, enter and uncoat in target cells, they did not cause any visible cytopathic effect which appears to be necessary to study the progress of native virus infections. The impedance measurements were also supported by real time imaging on the Incucyte® system which clearly show the cytopathic effects induced by the WT, while the PV has no detrimental effects on the cells despite its capability to transduce. Reliability of RTCA data is mostly assured on cell viability and optimisation (Kho *et al.*, 2015). This latter case could refer to what resulted from the EIV PV study on MDCK cells, as cell growth and proliferation was abnormal (Figure 75).

PBMCs are a key factor in EHV-1 pathogenesis as they are responsible of cell-associated viremia from the primary site of infection to the vascular endothelium in the uterus and central nervous system therefore eliciting the disease (Kydd *et al.*, 1994; Baghi and Nauwynck, 2014). To better understand early pathogenesis of myeloencephalopathy, limited studies *in vitro* tried to identify which PBMC subpopulations played a more important role in EHV-1 viremia (Scott *et al.*, 1983; van Der Meulen *et al.*, 2000). A recent work demonstrated that all major PBMC subpopulations can be infected with EHV-1 *in vivo* with differences among these subpopulations in presence of virus or viral load (Wilsterman *et al.*, 2010).

However, in our study EHV-1 PVs were not able to transduce PBMC as revealed by flow cytometry. It was questioned whether the duration of the study was not enough for EHV-1 PV to transduce PBMC. Viremia has been reported after four days from the primary infection (Pusterla and Hussey, 2014), but Goodman *et al.*, (2007) demonstrated infection of equine PBMC after 48h incubation using a GFP expressing EHV-1. This might answer the limitation of our study, since only four glycoproteins are expressed on the surface of EHV-1 PV. The lack of other viral proteins (besides the four GPs expressed) might restrict the potential of EHV-1 PV to transduce certain cell types such as PBMC. Another factor that might have influenced the ability to infect PBMC is the EHV-1 isolate strain. It has been demonstrated that neuropathogenic and non-neuropathogenic strain exhibited different levels of viremia associated to virulence (Allen *et al.*, 2006; Goodman *et al.*, 2007; Goehring *et al.*, 2009). The fact that our EHV-1 isolate was an abortigenic strain, and as such the glycoprotein expressed on the surface of the PV, might have played a role in difficulties to transduce PBMC. Unfortunately, due to limited PV supernatant this aspect was not investigated further. Nevertheless, there are of many other factors (host or viral) which could influence in this aspect of the EHV-1 cycle (Pavulraj *et al.*, 2020). The use of HIV-1 based pseudotype vectors in gene delivery studies is widely documented as a capable system to transduce non-dividing cells both *in vitro* and *in vivo*, such as PBMC (Schroers *et al.*, 2000; Shuang *et al.*, 2016). Therefore, further optimisation of the transduction process of equine PBMC with EHV-1 lentiviral system is required in order to approach an optimal protocol useful for future investigation. Moreover, a PBMC transduction method would broaden the application of EHV-1 PV as a tool to study early mechanism of viremia and so contributing to limiting the dissemination to the pregnant uterus or the CNS.

7 APPROACHES TO PSEUDOTYPE LENTIVIRUS PARTICLES WITH THE HA OF A NOVEL SUBTYPE OF INFLUENZA VIRUS STRAIN FOR USE AS A TOOL FOR CELL TROPISM AND DIAGNOSTIC STUDIES

7.1 INTRODUCTION

Influenza viruses belong to the *Orthomyxoviridae* family and are segmented RNA viruses that can infect a wide range of avian and mammalian species, including humans (Webster *et al.*, 1992). On the basis of internal protein antigenic and phylogenetic characteristics, four influenza types, A, B, C and D can be distinguished (Centers for Disease Control and Prevention – CDC). Types A and B are associated with seasonal influenza, whereas only A produces pandemics. Type A viruses are further classified into subtypes defined by their envelope glycoproteins haemagglutinin (HA) and neuraminidase (NA). To date there are 16 HA and 9 NA avian influenza subtypes, some of which are also seen in mammals, plus two bat derived subtypes (H17N10 and H18N11, based solely on isolated RNA sequences) (Tong *et al.*, 2012; Tong *et al.*, 2013). The natural reservoir for type A viruses are wild aquatic birds, which are able to spread the pathogens to other avian populations, including domestic poultry (Webster *et al.*, 1992). On the basis of the pathogenicity observed in chickens, influenza A viruses are classified in LPAI and HPAI (OIE Terrestrial Manual, 2021). The outcome of the disease is due to the molecular properties of the HACS. The host proteases recognise and cleave this particular site depending on its amino acids sequence, fundamental for the functional activation of HA permitting entry of the virus into the host cell (Evseev and Magor, 2019). LPAI possess a mono basic cleavage site cleaved by a limited family of proteases mostly trypsin-like proteases of the serine family, thus infection is restricted to certain tissues (Klenk and Garten, 1994). Meanwhile HPAI possess a polybasic cleavage site ubiquitously cleaved by proteases, thus infection is systemic to a wider range of tissues (Thomas, 2002; Horimoto and Kawaoka, 2005). Bacterial infection might also play a role in HA activation since bacterial proteases have been shown ability to cleave HA (Böttcher-Friebertshäuser, Klenk and Garten 2013). Influenza virus is a constantly evolving pathogen with the ability to evade the host adaptive immune response. Antigenic changes mostly affect the two major surface glycoproteins, HA and NA, which are the preferred antibody targets (Virelizier, 1975). The biological mechanism at the basis of this antigenic changes is due to the low fidelity and lack of proofreading ability of the vRNA dependent RNA polymerase enzyme (Steinhauer, Domingo and Holland, 1992). When minor epitope changes occur from introduction of point mutations in the viral genome, this process is referred as

antigenic drift (Both *et al.*, 1983; Kim, Webster and Webby, 2018). Meanwhile when a drastic genetic material exchange of the HA and/or the NA genes occur, this is referred as antigenic shift, which lead to antigenically distinct viruses and potentially contribute to the emergence of new influenza subtypes (Cox and Subbarao, 2000; Kim, Webster and Webby, 2018). Kazakhstan is in a very interesting geographical position as it represents a strategic meeting point of three of the largest migrating bird flyways and plays an important role in the maintenance of the wild aquatic bird populations in Central Asia together with the pathogens they are carrying, such as influenza viruses (Karamendin *et al.*, 2011; Karamendin *et al.*, 2016; Kydyrmanov *et al.*, 2017). As a consequence of this interspecies mixing, virus reassortment events are very frequent and the emergence of new influenza subtypes is most likely to happen (Ito *et al.*, 1998). LPAI are widely distributed among the wild aquatic birds and mostly cause no sign of disease nor harm, and are spread asymptotically to domestic birds (Webster *et al.*, 1992; Taubenberger and Kash, 2010). However, considering the evolutionary ability of influenza viruses, LPAI could mutate into HPAI causing a devastating series of events associated to high mortality of domestic birds and related economic losses to the poultry industry, but also a potential risk to human health (Macken, Webby and Bruno, 2006; Dugan *et al.*, 2008; Capua and Munoz, 2013). Therefore, the importance of constant surveillance of the wild bird population is essential to understand the development of viral variability and evolution and eventually recognise new threats (Fouchier, Osterhaus and Brown, 2003; Sayatov *et al.*, 2007). PVs offer a valuable safe platform for animal sero-surveillance studies (Temperton *et al.*, 2007). The neutralising ability of antibodies targeting the envelope glycoproteins can specifically be assessed and form a robust wild-type virus alternative for serological assay (Mather *et al.*, 2013; Bentley, Mather and Temperton, 2015). Recently, partial genomic RNA sequences from an apparently novel strain (denoted Kz52) closely related to the H9 subtype were isolated from a dead pochard *Aythya farina* duck near the Caspian Sea in Kazakhstan. Extensive database search ascertained whether Kz52 HA was a new variant, strain or subtype. Phylogenetic analysis of Kz52 HA gene by NJ and ML with representative sequences of all AIV subtypes revealed its close relationship to group 1 HAs (subtypes H1, H2, H5, H6, H8, H9, H11, H12, H13, H16 and H17) and together with H9 subtype constitutes a monophyletic clade (Figure 86). Therefore, in accordance with current AIV subtype classification it might be designated as a new H19 subtype renamed A/Common Pochard/Kazakhstan /52/08 HA.

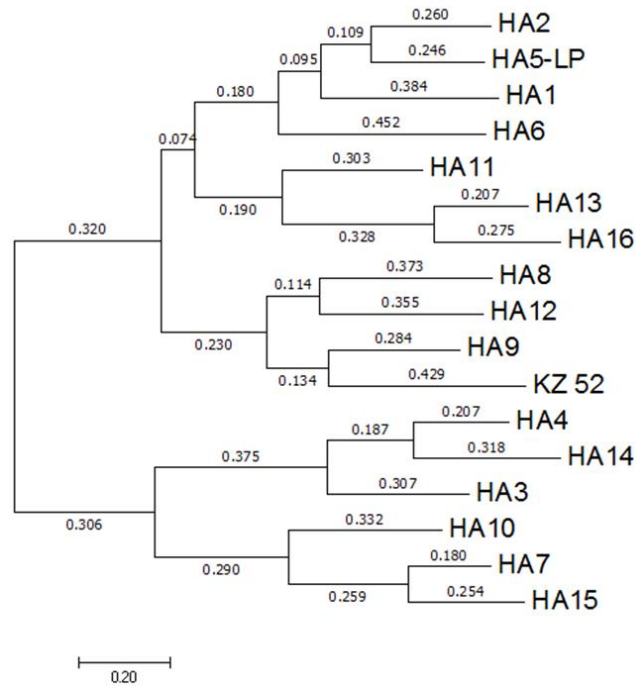


Figure 86: Phylogenetic tree of Kz52 HA. Phylogenetic analysis of Kz52 HA coding region nucleotide sequences and the representative sequences of other AIV subtypes using the NJ method, general time reversible (GTR) model and 1000 bootstrap replicates. Source: Dr. Sasan Fereidouni (unpublished data).

As the virus itself has not been isolated to date, in order to conduct experimental research on the virus (e.g. cell tropism/receptor and develop diagnostic tests) for the purpose of this study, extensive attempts were made to generate HA pseudotyped lentivirus particles. The pseudotype representing Kz52 could find application in a serological assay for screening and sero-surveillance purposes of the wild aquatic bird population (and indeed domestic birds and mammals to assess prior inter-species transmission) in Kazakhstan.

7.2 MATERIALS AND METHODS

7.2.1 Kz52 haemagglutinin (HA) gene sample

A full HA length of Kz52 gene sequence was kindly provided by Dr. Sasan Fereidouni (University of Veterinary Medicine, Vienna, Austria) isolated from a dead Common Pochard (*Aythya ferina*) near the Caspian Sea in Kazakhstan. Phylogenetic analyses were carried out by aligning representative sequences of all AIV subtypes on free MEGA 9 software (Kumar *et al.*, 2018; <https://www.megasoftware.net/>) using neighbour-joining (NJ) method and maximum likelihood (ML) with 1000 bootstrap replicates. Figure 86 reveals the closest

similarity of Kz52 to the H9 influenza subtype based on both HA amino acids and nucleotide sequences (Dr. Sasan Fereidouni, unpublished data). Indeed, comparison of the Kz52 HA amino acids sequence with those of other subtypes (using the online BLAST program) revealed that the nearest related influenza subtype was H9, displaying 68% sequence homology with the H9 HA of the A/Hong Kong/1073/99 strain (H9N2) (GenBank accession number: AJ404626.1).

7.2.2 Recovery project

A second round of sequencing of the HA gene was conducted in collaboration with Virology Research Services (VRS; University College London, UK) and was achieved via two approaches. Firstly, the sequence of the N-terminal 2/3 (~1150 bp) was obtained by one strategy, followed by the C-terminal 1/3 (~600 bp) by an alternative approach. For the former, total extracted RNA was retro-transcribed using random hexamer and influenza HA-specific primers to initiate first round cDNA synthesis via Superscript Reverse Transcriptase (Invitrogen™, Thermo Fisher Scientific) priming at +65°C for 5 minutes, reverse transcribed at +55°C for 10 minutes, then deactivated at +80°C for 10 minutes. HA sequences from this cDNA were then amplified by PCR using HA-specific primers and Phusion Hi-Fidelity DNA Polymerase (Thermo Scientific™, Thermo Fisher Scientific) according to manufacturer's instructions, using the thermal cycling; initially +98°C for 30 seconds, then 25 cycles of +98°C for 10 seconds, +52°C for 30 seconds and +72°C for 30 seconds, with final extension at +72°C for 5 minutes. PCR products (~300-400 bp) were purified by gel electrophoresis and extraction. These products were Sanger sequenced (Source Bioscience, Cambridge, UK) and used to design novel primers to produce further nested PCR products for sequencing. These sequences were assembled into the ~1150 bp consensus. Despite several attempts, it was not possible to extend this sequence further by the same methodology, possibly due to target degradation. Consequently, a second 'gene walking' approach was employed. This involved using PCR primers based on known sequences adjacent to unknown regions to produce ssDNAs from the cDNA above, followed by non-specific binding of reverse primers to generate dsDNAs (single cycle of +98°C for 30 seconds, +45°C for 30 seconds and +72°C for 3 minutes). A second round of nested PCR was conducted (30 cycles, as above) to produce more amplicons that were gel purified and sequenced.

7.2.3 Cloning into expression plasmid

A cloning strategy was devised by adding restriction enzyme recognition sites at both 5' and 3' ends to insert the HA gene in either pl.18 or pCAGGS vector. In addition, Kozak consensus sequence GTCAA was included to initiate the translation process upstream the ATG codon start (Kozak, 1987). A detailed schematic representation of the cloning strategy is described in the Flow Charts in Appendix Figures 8-11. The Kz52 HA gene was synthesised by GeneArt™ as 'Gene Strings' in both codon or non codon optimised forms (denoted as CO Kz52.HA or WT Kz52.HA respectively). Codon Optimisation (CO) was requested in an attempt to enhance the translational efficiency of the gene. In theory, this could increase HA envelope protein expression and consequent pseudotype titres (Carnell *et al.*, 2015).

7.2.4 High-fidelity Polymerase Chain Reaction

A high-fidelity PCR was necessary for cloning purposes. This strategy had to be performed as cloning with RE was problematic due to missing restriction sites in pl.18. Platinum™ SuperFi™ PCR Master Mix (Invitrogen™, Thermo Fisher Scientific, #12358010) was used to amplify CO Kz52 HA gene to be cloned from pl.18 into pCAGGS expression plasmid. A forward (FW) and reverse (Rev) primer pair were designed using the Eurofins PCR primer design tool (<https://eurofinsgenomics.eu/en/ecom/tools/pcr-primer-design/>) to insert a *SmaI* site at the 5' upstream the Kozak sequence and ATG start codon and to amplify the Kz52 HA gene. Primers were synthesised by Eurofins salt free purified in a 10 nmol synthesis scale and delivered lyophilised. Primer sequences are given in Table 24.

| Primer ID | Primer sequence (5' to 3') |
|-----------------------|-------------------------------------|
| <i>SmaI</i> Kz52COFW | FW 5'-acccggggtcaaatgtggaagctggc-3' |
| <i>XhoI</i> Kz52CORev | Rev: 5'-attcctcgagaattcagatg-3' |

Table 24: Primer sequences for CO Kz52 cloning.

A gradient PCR was first carried out to determine the best annealing temperature for the cloning primers using 2X DreamTaq Green PCR Master Mix as described in Section 2.1.11. Briefly, 20 ng of DNA template was added to a PCR mix consisting of 12.5 µL 2X DreamTaq Green PCR Master Mix, 0.5 µL FW and Rev primer (0.2 µM) and adjusted volume of MBG H₂O to make a final volume of 25 µL. Four identical PCR reaction tubes were then placed in a

thermocycler and the following program (Table 25) was run choosing gradient positions representing annealing temperatures of +50°C, +53°C, +57°C and +60°C:

| Step | Temperature | Time | Cycles |
|----------------------------|-------------|--------------------------------|--------|
| Initial denaturation phase | 95°C | 3 minutes | |
| Denaturation | 95°C | 1 minute | 30 |
| Annealing phase | 50-60°C | 1 minute | |
| Extension phase | 72°C | 2 minutes (30 seconds per Kbp) | |
| Final extension | 72°C | 7 minutes | |

Table 25: Gradient PCR program.

Amplification of the PCR product was verified by DNA gel electrophoresis and the best annealing temperature was established before proceeding to the next step. A high-fidelity PCR was set up with the same conditions using Platinum™ SuperFi™ PCR Master Mix for a total volume of 50 µL and run using an annealing temperature of +53°C. 5 µL of this PCR reaction was run on a gel and after verification of the amplified band the remaining PCR product was purified with QIAquick PCR Purification Kit (QIAGEN, #28104) following the manufacturer's instructions and concentration determined by Nanodrop before RE digestion with the appropriate enzymes. A detailed schematic representation of the cloning strategy for CO Kz52 in pCAGGS is described in the Flow Chart in Appendix Figure 11.

7.2.5 3D modelling

A 3D model of the Kz52 HA polypeptide was predicted using the free software Phyre2 (Kelley *et al.*, 2015; www.sbg.bio.ic.ac.uk/phyre2). Modelling compared the novel HA sequence with that of other HAs for which structures have been determined. The best structural alignment was with H16 A/black-headed gull/Sweden/2/99 (H16N3) (GenBank accession number: AY684888.1). Phyre 2 'normal mode' default settings were used to predict the 3D models (Figure 90). The Phyre 2 PDB file was then imported into the PyMOL program (www.pymol.org) in order to highlight specific features on the HA structure.

7.2.6 Plasmids

Plasmids p8.91, pCSFLW and pCSemGW have already been described in Section 2.1.1. pl.18 and pCAGGS plasmids were used to clone Kz52 HA gene. The different proteases used in this study for HA activation were expressed from different expression vectors. The HAT, TMPRSS2 and KLK-5 proteases were cloned in the ampicillin-resistant pCAGGS kindly provided by Prof. Hans Klenk and Dr. Eva Böttcher-Friebertsh (Philipps University Marburg, Germany). The TMPRSS4 protease was expressed from the kanamycin-resistant pCMV-Tag3, while TMPRSS3 and TMPRSS6 were cloned in the ampicillin-resistant pcDNA3.1, were provided by Dr. Stefan Pöhlmann (Infection Biology Unit, German Primate Center, Germany). Several HA and NA expression plasmids were used in this study as controls and were kindly provided by Dr. Nigel Temperton (University of Kent, UK). pl.18-H9 A/Hong Kong/1073/99 (H9N2) (GenBank accession number: AJ404626.1), pHCMV1-H8 A/turkey/Ontario/6118/1968 (H8N4) (GenBank accession number: CY014659.1), pl.18-H3 A/equine/Richmond/1/2007 (H3N8) (GenBank accession number: FJ195395.3), pl.18-H3 A/canine/Colorado/30604/2006 (H3N2) (GenBank accession number: AB537183.1), pl.18-N8 A/equine/Richmond/1/2007 (H3N8) (GenBank accession number: KF559336.1) and pl.18-N2 A/canine/Guangdong/3/2011 (H3N2) (GenBank accession number: JX195360.1).

7.2.7 Site Directed Mutagenesis in-house protocol

SDM was performed in order to alter the Kz52 HA monobasic cleavage site (PIKETR) in a stepwise manner towards the H9 consensous monobasic site (PARSSR). Conversely the monobasic cleavage site in the H9 HA was changed to mimic Kz52 cleavage site sequence (PARSSR→PIKETR). Moreover, SDM was employed to mutate the monobasic cleavage site of both Kz52 and H9 into a polybasic cleavage site (PARSSR→PARKKR). To investigate whether the Kozak sequence was influencing PV generation (via efficiency of the HA translation process), the original Kozak sequence GTCAA designed for cloning purposes was mutated into GCCACC. SDM primers were designed using Agilent Technologies QuikChange™ Site-Directed Mutagenesis Kit primer design program (<http://www.genomics.agilent.com/primerDesignProgram.jsp>) for use in SDM PCR. Primers were synthesised by Eurofins salt free purified in a 10 or 50 nmol synthesis scale and delivered lyophilised. SDM primer sequences are reported in Appendix Tables 3 and 4. The PCR was set up using 25 µL of the proof-reading polymerase, Accuzyme™ mix (Bioline, Meridian Bioscience, #BIO-25028), 140 ng of template DNA, 125 ng of FW and Rev primers and MBG H₂O to a final volume of 50 µL. The DNA mixtures were subsequently placed in a

thermal cycler using the following conditions: +98°C for 3 minutes before commencing 25 cycles of denaturation at +98°C for 20 seconds, annealing at +55°C (temperature defined according to primer design) for 15 seconds, extending the DNA at +72°C for 12 minutes (2 minutes per Kbp) and then further extension at +72°C for 20 minutes to maximise full length products. 5 µL of PCR product was run on a 1% agarose gel to check whether amplification of the DNA band had occurred. If visible, the rest of the PCR product was purified using a Qiagen PCR purification kit and the concentration of the resulting DNA was measured via Nanodrop. SDM was accomplished only when pl.18 clone was used as a template. Subcloning of mutants into the pCAGGS vector was accomplished through RE strategies. At this point it was necessary to digest the DNA with FastDigest® *DpnI* (Thermo Scientific™, Thermo Fisher Scientific, #FD1703) enzyme to remove any remaining parental (methylated) DNA so 700 ng of DNA was digested with 1 µL of *DpnI* enzyme in 1 µL of its FastDigest® buffer and MBG H₂O for a total reaction volume of 10 µL. The digestion reaction was incubated for 20 minutes at +37°C, followed by +80°C for 5 minutes to deactivate the enzyme. The resulting plasmid DNA was transformed into DH5α *Escherichia coli* cells following the methods described in Section 2.1.6. After successful transformation, several colonies were picked and overnight LB cultures were prepared. Plasmid DNA was purified from the bacterial cells using a Qiagen miniprep and was sent for sequencing to verify the correct mutation had been incorporated during SDM.

7.2.8 Site Directed Mutagenesis QuikChange™ protocol

QuikChange™ II XL Site-Directed Mutagenesis Kit (Agilent, #200521) was employed to improve accuracy and minimise unwanted errors during mutagenesis. This was the case when mutation of the non codon optimised monobasic cleavage site of Kz52, codon optimised Kz52 and H9, plus of the KOZAK sequence of H9. The PCR reaction was set up following the manufacturer's instructions. The PCR reaction set up is shown below in Table 26.

| Reagent | Volume |
|--|--|
| 10× reaction buffer | 5 µL |
| dsDNA template | 50 ng |
| SDM FW primer | 125 ng |
| SDM Rev primer | 125 ng |
| dNTP mix | 1 µL |
| QuikSolution | 3 µL |
| MBG H ₂ O | X µL |
| <i>Total reaction volume</i> | <i>50 µL</i> |
| <i>PfuUltra HF DNA polymerase (2.5 U/µL)</i> | <i>1 µL to add after setting up the total reaction</i> |

Table 26: QuikChange™ PCR reaction volumes.

The DNA mixes were subsequently placed in a thermal cycler using the following conditions: +95°C for 1 minute before commencing 18 cycles of denaturation at +95°C for 50 seconds, annealing at +60°C for 50 seconds, extending the DNA at +68°C for 1 minutes per Kbp and then further extension at +68°C for 7 minutes to maximise full length products. 5 µL of PCR product was run on a 1% agarose gel to check whether amplification of the DNA band occurred. If visible, the rest of the PCR product was purified using a Qiagen PCR purification kit and the concentration of the resulting DNA was measured. 700 ng of DNA was digested with 1 µL of *DpnI* enzyme to remove any remaining parental template, 1 µL of its FastDigest® buffer and MBG H₂O for a total reaction volume of 10 µL. The digestion reaction was incubated for 20 minutes at +37°C, followed by +80°C for 5 minutes to deactivate the enzyme. The resulting plasmid DNA was transformed into either One Shot™ TOP10 Chemically Competent *E. coli* (Invitrogen™, Thermo Fisher Scientific, #C404010) or XL10-Gold Ultracompetent Cells (Agilent, #200521) when mutating H9 monobasic cleavage site into a polybasic one (PARSSR→PARKKR) and H9 Kozak sequence (GTCAAA→GCCACC). These competent cells were employed as an alternative to the classic transformation in DH5α Competent Cells when large mutations made cloning difficult. Transformation for cloning purposes was conducted in TOP10 competent cells was carried on as described in Section 2.1.6., while in XL10-Gold cells the manufacturer’s protocol was followed. Briefly, 45 µL of ultracompetent cells were thawed per sample reaction. 2 µL of XL10-Gold β-mercaptoethanol (ME) mix was added to increase transformation efficiency, cells were swirled gently and incubated for 10 minutes on ice. 2 µL of the *DpnI*-treated DNA was

transferred to the aliquot of the ultracompetent cells and incubated for 30 minutes on ice. Subsequently, cells were heat-shocked at +42°C for 30 seconds on a heat block and incubated for 2 minutes on ice before adding 0.5 mL of preheated NZY⁺ broth (Fisher BioReagents™, Thermo Fisher Scientific, #BP2465) to each aliquot tube. Then, cells were incubated at +37°C for 1 hour with shaking at 225 RPM. 50 µL of transformation reaction was spread on LB agar plates containing the appropriate antibiotic for the plasmid vector. Following transformation, colonies were picked and overnight LB cultures were prepared. Plasmid DNA was purified from the bacterial cells using a Qiagen miniprep kit and was sent for sequencing to verify the correct mutation had been incorporated during SDM.

7.2.9 Sequencing of plasmid DNA

Purified plasmid DNA was sent for sequencing to verify the correct mutation had been incorporated during SDM or transformation for plasmid amplification or cloning purposes (i.e. correct orientation of the insert). Samples for sequencing were prepared following the guidelines in Section 2.1.10. using either pI.18 or pCAGGS sequencing primers (Table 7). For the phCMV1-H8 plasmid, the primers reported in Table 27 were employed:

| Primer ID | Primer sequence (5' to 3') | Features | Designed by |
|-----------|-------------------------------|---|--|
| T7 | FW 5'-taatacgactcactataggg-3' | Anneals upstream the MCS of phCMV1 plasmid in position 759-778 | Universal primer (Eurofins) |
| phCMV1 | Rev 5'-tatgttcaggttcaggg-3' | Anneals downstream the MCS of phCMV1 plasmid in position 986-1003 | Dr. Simon Scott (University of Kent, UK) |

Table 27: phCMV1 sequencing primers.

7.2.10 Cell lines and maintenance

HEK293T/17 cells were used for PV production, PV titration and subsequently PV neutralisation. Maintenance of this cell line is described in Section 2.2.1. Other cell lines were employed to test their efficacy as optimal target cells for Kz52 PV entry. MDCK I & II cells and maintenance were previously described in Section 3.2.3. The primary cell lines, duck embryonic fibroblasts (DEF) and chicken embryonic fibroblasts (CEF) were a kind gift of Dr. Janet Daly (University of Nottingham, UK) and were grown in complete DMEM (with 10% FBS and 1% P/S). Unfortunately, CEF were difficult to resuscitate from flask mailed for use in further target cells assays. HEK293T/17 cells expressing the Angiotensin-converting enzyme 2 (ACE2) and Transmembrane protease serine 2 (TMPRSS2) receptors were also tested as target cells for Kz52 PV. HEK293T/17 expressing ACE2 and TMPRSS2 are known to be entry target cells for Severe acute respiratory syndrome coronavirus 2 (SARS-CoV-2) PV. Meanwhile for Influenza virus, the expression of ACE2 might play a role in the development and progression of AIV induced lung pathologies in mice (Yang *et al.*, 2014). pCDNA3.1+-ACE2 plasmid was a kind gift from Dr. Graham Simmons (Vitalant Research Institute, San Francisco, USA). Briefly, 2×10^6 cells were seeded into a 10 cm Nunc™ cell culture dish (Thermo Scientific™, Thermo Fisher Scientific, #150350) and incubated overnight at +37°C in 5% CO₂ in order to achieve 70-90% confluence at the time of transfection. The next day, 100 µL of OptiMEM™ was added with 2 µg of ACE2 plasmid and 150 ng TMPRSS2 plasmids and mixed well. After 5 minutes incubation at RT, 9 µL of FuGENE® HD Transfection Reagent (Promega, #E2311) was directly added just below the surface to the DNA mix-OptiMEM™ and gently mixed during the 20 minutes incubation at RT. In the meantime, cell culture media was removed and replaced with 10 mL of fresh complete cell culture media. After the incubation time, the DNA mix-OptiMEM™-FuGENE® HD solution was added dropwise throughout the total surface area of the dish which was swirled gently before being incubated overnight at +37°C in 5% CO₂ time necessary to overexpress the cell entry receptors. All the cell lines described were maintained at +37°C in 5% CO₂ environment in a humidified incubator.

7.2.11 Influenza PV generation

PVs were generated following the guidelines in Section 2.3.1. via a four-plasmid co-transfection of HEK293T/17 cells using PEI as transfection reagent at 1 mg/mL. Transfections were carried out in a 6-well plate. 500 ng HA surface glycoprotein gene expressed from pl.18 or pCAGGS, 500 ng p8.91-HIV gag-pol retroviral core, 750 ng pCSFLW-firefly luciferase or pCSemGW reporter gene and 125 ng endoprotease expressing plasmid necessary to cleave

the HA were combined with OptiMEM™ whilst a separate PEI-OptiMEM™ mixture was left to incubate at room temperature for 5 minutes. The DNA mix-OptiMEM™ was then added to the PEI-OptiMEM™ mix and incubated at room temperature for 20 minutes. Afterwards, the transfection mix was added to the monolayer of cells (at 70-80% confluence) and incubated at +37°C for 24 hours. 24 hours post-transfection exogenous recombinant neuraminidase from *Clostridium perfringens* (exNA; Sigma-Aldrich®, Merck, #N2876) was added to ensure exit of pseudotyped particles from producer cells. This was not applicable if 125 ng of NA expression plasmid was co-transfected with the other plasmids creating a five-plasmid co-transfection system, as the NA was present on the PV particle surface. The PV was harvested at 48 hours post-transfection through 0.45 µm filters and virus supernatant was stored at -80°C.

7.2.12 Influenza VSV PV generation

The VSV core system was employed as alternative to the lentivirus system in order to generate functional Kz52 VSV PV (vPV). The recombinant VSV (rVSV ΔG) stocks bearing the coccal glycoprotein were kindly provided by Dr. Edward Wright (University of Sussex, UK) and amplified by Dr. Martin Mayora-Neto (University of Kent, UK). Briefly, 2×10^5 HEK293T/17 cells/well were seeded on a 6-well plate and on the next day, cell culture media was replaced and cells were transfected with 500 ng of the HA plasmid of interest, 125 ng of pl.18-N2 and 125 ng of pCMV-Tag3-TMPRSS4. A sole pl.18 or pCAGGS plasmid was included in the transfection as a control. Moreover, a Δenv control was generated as well. The next day, the cell culture media was replaced and cells were infected with amplified rVSV ΔG at a multiplicity of infection (MOI) of 0.2, 1 or 2. Infected cells were incubate at +37°C for 2 hours before washing 3 times with PBS and replacing 2 mL of fresh cell culture media. 0.5U of exNA was added 3 hours later where no NA plasmid was transfected. Cells were incubated at +37°C for 24 hours and vPVs harvested at 24 or 48 hours post infection.

7.2.13 Influenza PV titration

PV titrations were performed as detailed in the Section 2.4. by serially diluting 100 µL of neat supernatant in 1:2 steps across a white or clear 96-well plate (for FLW or GFP expressing PV respectively). A positive control represented by a high titre PV such as H9 or H3 PV was included. A Δenv PV and cell only controls were also included. Next, 1×10^4 target cells were

added in each well and incubated for 48 hours at +37°C. After 48 hours luminescence was assessed using the BG assay system read at GloMax® Luminometer.

7.2.13.1 Addition of Trypsin (TPCK-treated)

L-tosylamido-2-phenyl ethyl chloromethyl ketone treated trypsin (TPCK-trypsin; Sigma-Aldrich®, Merck, #T1426) was added to the titration assay in order to activate and cleave influenza HAs and was thus employed as control and indicator for efficient HA activation. The TPCK-trypsin titration was performed by following the general guidelines reported in the WHO manual (WHO, 2011). Briefly, after serially diluting the PV across the 96-well plate, 50 µL of OptiMEM™ mixed with 1 mg/mL of TPCK-trypsin was added to each well to produce a final concentration of 50 µg/mL. The plate was incubated at +37°C in 5% CO₂ environment in a humidified incubator for 30 minutes and also incubated for 60 minutes, 90 minutes or 120 minutes. After this time, 1x10⁴ target cells were added to each well and incubated for 48 hours at +37°C. No Trypsin Neutralising Solution (TNS) needed to be added to stop the TPCK-trypsin activity since the FBS in the cell culture media was sufficient in doing so. After 48 hours luminescence was assessed using the BG assay system read at GloMax® Luminometer.

7.2.14 Influenza VSV PV titration

vPVs were titrated in a similar set up as for lentiviral PVs titration. Although it is necessary to double the amount of target cells used in the assay. A high titre vPV was included as positive control, represented by a Ravn virus (RAVV) vPV generated by Dr. Martin Mayora-Neto (University of Kent, UK). Plates were incubated at +37°C for 24 hours before luminescence was assessed using the BG assay system read at GloMax® Luminometer.

7.2.15 Influenza PV neutralisation assay

PVNA was performed as previously described in Section 2.5. An H9-like antisera (NIBSC, code: 07/146) was diluted 1/40 and subsequently in a 1:2 dilution across a white 96-well plate. 1x10⁶ RLU/mL of H9 PV was added in each well followed by 1 hour incubation at +37°C to allow neutralisation. Subsequently, 1x10⁴ HEK293T/17 cells were added in each well and incubated for 48 hours at +37°C. Luminescence was once again measured using the BG assay system. A PV only and cell only controls were included on each neutralisation plate representing no neutralisation and complete neutralisation respectively.

7.2.16 SDS-Polyacrylamide Gel Electrophoresis

An SDS-PAGE was performed to verify whether the envelope HA was present on the PV generated. Kz52, H9 (with and without protease) and Δ env PVs were produced as described in Section 7.2.11. Samples were then prepared for SDS-PAGE and loaded on gels as described in Section 2.1.13.

7.2.17 Immunofluorescence

In order to investigate the expression of the HA glycoprotein in the HEK producer cell line, immunofluorescence was undertaken using the H9-like antisera (NIBSC, code: 07/146) as primary antibody and Donkey anti-sheep IgG (H+L) Cross-Adsorbed Alexa Fluor 594 (Invitrogen™, Thermo Fisher Scientific, #A-11016) as secondary antibody. The protocol was optimised using cells transfected with pCAGGS-H9 as positive control and phCMV1-H8 to determine the possibility of antibodies cross-reacting with H8. Poly-D-lysine (PDL; Gibco™, Thermo Fisher Scientific, #A3890401) coated coverslips (Vitrocam, #1290-P01) were placed into wells of a 6-well plate and UV sterilised in a tissue culture cabinet for 30 minutes. 2×10^5 HEK293T/17 cells were then seeded into the 6-well tissue culture plates and placed in a humidified incubator for 24 hours to reach 70-80% confluence, including on the coverslip. Cells were transfected with 500 ng of HA-expressing plasmid using 5 μ L of the 1 mg/mL PEI solution in 100 μ L OptiMEM™, following a protocol similar to the one described to produce influenza PV as described in Section 7.2.11., and incubated in a humidified incubator. After 24 hours, cell culture media was replaced. 48 hours post-transfection (a sufficient duration for expression of the glycoproteins), cells were washed 3 times for 5 minutes each using cold +4°C 1 mL PBS. To fix and permeabilise the transfected cells, 1 mL of 100% methanol (previously stored at -20°C) was added to each well and the plate incubated on ice for 10 minutes. Cells were washed once again 3 times for 5 minutes with cold +4°C 1 mL PBS. Then 500 μ L/well of solutions containing the primary antibody (1:500) was added and the plate incubated overnight at +4°C. The next day, cells were washed 3 times for 5 minutes with 1 mL +4°C PBS. 500 μ L of a secondary antibody solution (1:1000) was added to the cells and incubated for 1 hour at +37°C. Cells were washed again using the previous described washing protocol, and then incubated for 20 minutes at RT with 500 μ L of 2 drops/mL NucBlue™ Live ReadyProbes™ Reagent (Hoechst 33342) (Invitrogen™, Thermo Fisher Scientific, #R37605) in PBS to permit nuclear staining. Cells were washed with +4°C PBS 3 times for 5 minutes one last time before coverslips were mounted on BS 7011 Microscope slides (VWR International Ltd, #631-0906) using MOWIOL® 4-88 (Sigma-Aldrich®, Merck, #475904-100GM-M) solution.

Slides were then stored at +4°C until scrutinised first using a fluorescent microscope (ZOE™ Fluorescent Cell Imager) and then under a confocal Laser Scanning Microscope (LSM; Zeiss, model: LSM880).

7.2.18 SYBR-Green Product-Enhanced Reverse Transcriptase

A SYBR green RT-PCR based assay (SG-PERT) was employed to quantify reverse transcriptase (RT) activity in lentiviral PV samples to identify functional capsids. The assay was first developed by Pizzato *et al.*, (2009) and subsequently revised by Vermeire *et al.*, (2012). The followed protocol was adapted from Dr. Yasu Takeuchi (University College London, UK). RT activity was measured using a recombinant HIV-1 RT (Millipore®, Merck, #382129) to generate the standard curve to use as quality control for PV generation. The standard curve was generated by diluting 1×10^{10} pU/μL recombinant HIV-1 RT (2 ng/μL, 10 mU/μL) in MBG H₂O in a 10-fold serial dilution until 0.5×10^3 pU/μL was achieved to obtain a total of 8 standards. 5 μL of PV supernatant was lysed by adding 5 μL of 2X lysis buffer (100 mM TrisHCl, 50 mM KCl, 0.25% Triton X-100, 40% glycerol) supplemented with 0.8 U/μL RiboLock RNase inhibitor (Thermo Scientific™, Thermo Fisher Scientific, #EO0381) previously diluted in 2X lysis buffer to reach a final concentration of 0.4 U/μL per reaction. The solution mix was incubated at RT for 10 minutes, added with 90 μL of MBG H₂O, mixed and briefly centrifuged. In the meantime, a master mix was set up accordingly to the number of samples using LightCycler® 480 SYBR Green I Master Mix (Roche, #04707516001), μM of MS2 FW and Rev primers (primer sequences are reported in Table 28), 3.5 pmol/mL MS2 RNA (Roche, #10165948001) and 0.02 U/μL Ribolock RNase inhibitor. Subsequently, 12 μL of virus lysate or controls were added. Appropriate volumes are reported in the Table 29 below.

| Primer ID | Primer sequence (5' to 3') |
|-----------|------------------------------------|
| MS2 | FW 5'-tcctgctcaactcctgctcgag-3' |
| | Rev 5'-cacaggtcaaacctcctaggaatg-3' |

Table 28: MS2 primer sequences.

| Reagent | Volume per reaction (µL) |
|--------------------------|--------------------------|
| SYBR Green Master Mix | 12.5 |
| FW primer | 0.125 |
| Rev primer | 0.125 |
| MS2 RNA | 0.125 |
| RiboLock RNase inhibitor | 0.125 |
| <i>Total reaction</i> | <i>13</i> |

Table 29: SG-PERT master mix reaction volumes.

13 µL of Master mix was distributed in each well of a 96-well white LightCycler® 480 Multiwell plates (Roche, #04729692001) plus 12 µL of virus lysate or controls in duplicate. For the RT standards, 10 µL of MBG H₂O was added per reaction to the remaining Master mix and 23 µL aliquoted in each well in duplicates. For the first standard (1 x 10¹⁰ pU/µL), 1 µL of 10 mU/µL HIV-1 RT and 1 µL of MBG H₂O were added in each well in duplicate. Then 2 µL of the subsequent standard was added per well. The plate was film-sealed with LightCycler® 480 Sealing Foil (Roche, #04729757001), inserted in a LightCycler® 480 Instrument (Roche, model: LightCycler® 480) and the SG-PERT cycle run using the following the conditions (Table 30):

| Step | Temperature | Time | Cycles |
|-----------------------------|-------------|------------|--------|
| Reverse transcription | 42°C | 20 minutes | |
| Taq initial heat activation | 95°C | 5 minutes | |
| Denaturation | 95°C | 5 seconds | 40 |
| Annealing phase | 60°C | 5 seconds | |
| Extension phase | 72°C | 15 seconds | |

Table 30: SG-PERT cycle conditions.

7.2.19 Enzyme-Linked Immunosorbent Assay

An in-house ELISA was developed and optimised using purified PVs as antigens to assess antibody binding. The protocol was adapted from Dr. Giada Mattiuzzo (NIBSC, UK). An indirect ELISA with or without a capture antibody was optimised with H9-like antisera (NIBSC, code: 07/146) targeting the HA of H9 as primary antibody, followed by a Peroxidase

AffiniPure Donkey Anti-Sheep IgG (H+L) (Jackson ImmunoResearch, #713-035-003) as secondary antibody. A Δenv PV and cell only s/n (media collected and filtered from non transfected cells) controls were included for assess non-specific antibody binding and used to perform the final calculation by subtracting these background values.

7.2.19.1 Influenza PV concentration and purification

Kz52 PV, H9 PV, Δenv PV and cell only supernatants (Section 7.2.11.) were concentrated following the Lenti-X™ Concentrator Protocol-at-a-Glance (Takara, #PT4421-2). Briefly, PV and controls supernatants were harvested through a 0.45 μm filter and 1 volume of Lenti-X Concentrator (Takara, #631232) was combined with 3 volumes of clarified supernatant. After a gently inversion, the mixture was incubated at +4°C for 30 minutes. Samples were then centrifuged at 1500 g for 45 minutes at +4°C. Supernatant was carefully removed by not disrupting an off-white pellet which was gently resuspended in cold +4°C 1/10 of the original volume of PBS. Protein concentration was subsequently determined using the Pierce™ BCA Protein Assay Kit (Thermo Scientific™, Thermo Fisher Scientific, #23225) following the manufacturer's instructions. Samples were plated on a clear 96-well plate and absorbance was measured at 562 nm on an Infinite® PRO Microplate Reader (Tecan, model: Infinite® PRO).

7.2.19.2 Indirect Enzyme-Linked Immunosorbent Assay

100 μL of 5 μg/mL of purified concentrated PV diluted in PBS was added per well of a Nunc MaxiSorp™ 96 well ELISA plate (Invitrogen™, Thermo Fisher Scientific, #44-2404-21) and incubated overnight at +4°C. The next day, the plate was washed 5 times with 300 μL PBS, blocked using 200 μL/well of 5% (v/v) horse serum in PBS and incubated for 1 hour at 37°C. After this time, the plate was washed 5 times with 300 μL PBS-0.05%Tween® 20 (PBS-T; Sigma-Aldrich®, Merck, #P1379), added with 100 μL/well of 1:100 primary antibody diluted in blocking buffer and incubate for 2 hours at +37°C. The plate was washed again 5 times with 300 μL PBS-T, added with 100 μL/well of 1:5000 secondary antibody in a PBS-10% (v/v) FBS diluent buffer and incubate for 1 hour at +37°C. The plate was washed one last time for 5 times with 300 μL PBS-T, added with 100 μL/well of 1-Step™ Ultra 3,3',5,5'-tetramethylbenzidine (TMB) ELISA Substrate Solution (Thermo Scientific™, Thermo Fisher Scientific, #34028) and incubated at RT in the dark for 20 minutes, sufficient time to develop signal. The reaction was stopped with isovolume of sulphuric acid (H₂SO₄; Sigma-Aldrich®,

Merck, #30743) and the plate read at 450 nm on a Sunrise™ Microplate Reader (Tecan, model: Sunrise™).

7.2.20 Data analysis

PV titres obtained at each of a range of dilution points were expressed as RLU/mL and the arithmetic mean was calculated using Microsoft® Excel™. Subsequently, analysed data was plotted using GraphPad Prism®. To analyse and plot titration data, the guidelines in Section 2.6. were followed. Confocal imaging was carried out using ZEN 2.5 software (Zeiss) and plasmid quantification on ImageJ (<https://imagej.nih.gov/ij/>). SG-PERT data was analysed with the LightCycler® 480 Software version 1.5 (Roche) and then exported to Microsoft® Excel™. A standard curve was first generated based on the recombinant HIV-1 RT in order to interpolate the RT activity reported as either enzyme activity (pU/μL) or total number of PV particles per mL. This estimate is based on each PV supernatant having ~300 pU/μL of RT activity as reported in Vermeire *et al.*, (2012). Optical density (OD) was analysed using SparkControl™ Magellan™ Software version 1.2 (Tecan). Data were subsequently exported on Microsoft® Excel™ and the OD calculated by first subtracting the OD average (blocking buffer only) to the OD value of both PV and PBS coated wells. Subsequently, the OD background (PBS only) was subtracted from the correspondent OD dilution sample.

7.3 RESULTS

7.3.1 Chromatogram and sequence analysis

The amplification of the genomic RNA containing the full length HA coding region was first accomplished by Dr. Sasan Fereidouni and collaborators employing degenerated primers and by assembling the nucleotide sequences (unpublished data). A consensus sequence was sent to the VPU (University of Kent, UK), and this was used to synthesise the gene for cloning into expression vectors and subsequently utilised in attempts to pseudotype lentiviruses with the Kz52 HA. After about a year employing various strategies to achieve this, we requested the original sequence chromatograms for detailed analysis. Upon receiving these chromatograms, analysis using DNADynamo software unfortunately revealed many sequence ambiguities. The original 11 sequences were aligned to the provided HA gene employed as the consensus reference (Figure 87). In order to clarify the sequence, the decision was made to re-sequence the HA coding region. Thus, a second round of sequencing was conducted in collaboration with VRS (University College London, UK). Thanks to the

recovery project, the fragments were assembled and generated a final complete high quality sequence of the HA ORF comprising 1686 nucleotides (Figure 88).

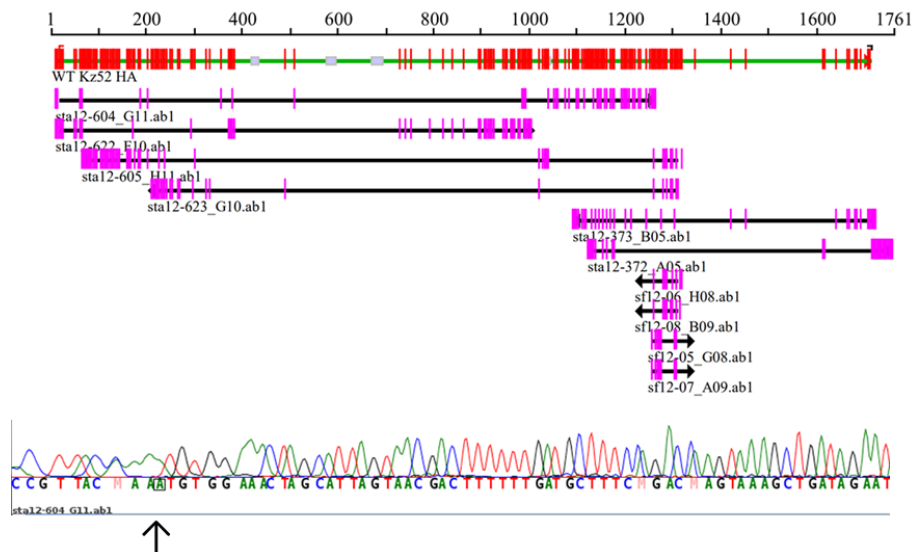


Figure 87: Alignment summary pre-recovery project. Original fragment sequences assembled and aligned to the consensus reference Kz52 HA gene sequence (WT Kz52 HA) on DNADynamo software. Mismatches are reported in red and a chromatogram of the ATG codon start (black arrow) was highlighted below.

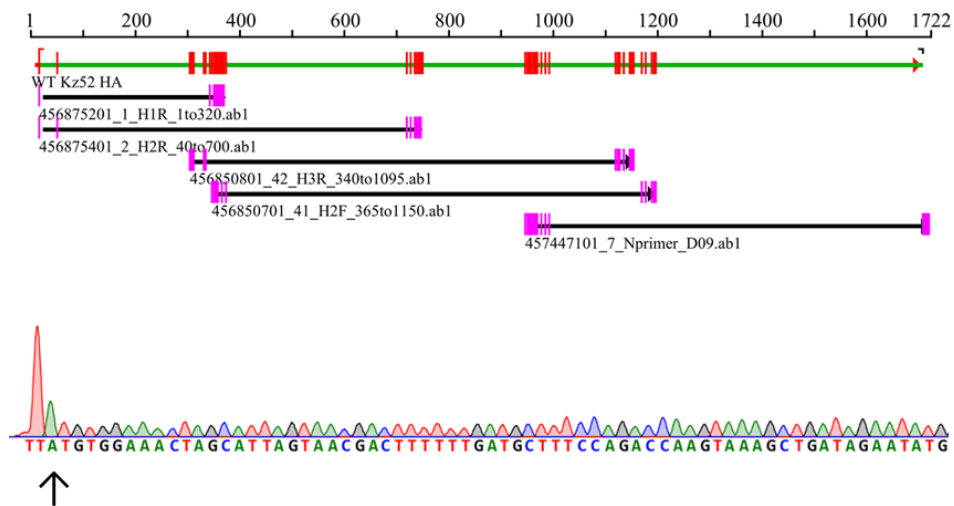


Figure 88: Alignment summary post-recovery project. Recovered fragment sequences assembled and aligned to the consensus reference Kz52 HA gene sequence (WT Kz52 HA) on DNADynamo software. Mismatches are reported in red and a chromatogram of the ATG codon start (black arrow) was highlighted below.

7.3.2 Sequence alignment with H9 haemagglutinin (HA)

A nucleotide basic local alignment search tool (BLASTN) was run by pasting the WT nucleotide sequence of Kz52 HA using the discontinuous megablast program against similar sequences of the H9 subtype revealed to be the closest relative from the phylogenetic analysis (see Figure 86) found in the nucleotide NCBI database. A 69.81% identity was found with A/duck/Malaysia/91/1997 (H9N2) (GenBank accession number: JQ344328.1). A complete BLAST tree view of the distance results is shown in Appendix Figure 13.

When a protein BLAST (BLASTP) was run using the amino acids sequence of Kz52 HA gene against the amino acids sequence of a reference H9 strain A/Hong Kong/1073/99 (H9N2) (GenBank accession number: AJ404626.1) a 68% sequence homology was found (Figure 89). The H9 PV of the same strain was available at VPU (University of Kent, UK) (Ferrara *et al.*, 2017). The same reference sequence was also employed as control throughout this study.

| Score | Expect | Method | Identities | Positives | Gaps |
|----------------|---|------------------------------|--------------|--------------|-----------|
| 844 bits(2180) | 0.0 | Compositional matrix adjust. | 383/565(68%) | 468/565(82%) | 1/565(0%) |
| Query 1 | MWKLALVTTFLMLSRPSKADRICIGYQSTNSTDTVNTLIENEVPVTQSKELLHOEHNGLL | | | | 60 |
| Sbjct 1 | M ++L+T L+++ S AD+ICIG+QSTNST+TV+TL E VPVT +KELLH EHNG+L | | | | 59 |
| Query 61 | CSTSKGSPLELDKCKIEGVIFGNPECDLLLGGRDWSYIIERDTAQEGICYPGNIENVEEL | | | | 120 |
| Sbjct 60 | C+TS G PL LD C IEG+++GNP CDLLLGGR+WSYI+ER +A G CYPGN+EN+EEL | | | | 119 |
| Query 121 | RVLFSSSSSYKRVVMFPDFVWNVYTTTSPACSN SFYRNMRLTQKSNFPTQEAQFKNR | | | | 180 |
| Sbjct 120 | R LFSS+SSY+R+ +FPD WNVYTT TS ACS SFYR+MRWLTQKS +P Q+AQ+ N | | | | 179 |
| Query 181 | ESDPILFMWATHNPSSQSEQEYLYKNLDTTSSVSTEELHRSFKSTFGPNVAIKGIQRMS | | | | 240 |
| Sbjct 180 | ILF+W H+P + +EQ LY DTT+SV+TE+L+R+FK GP + G+QGR+ | | | | 239 |
| Query 241 | YGWGILKPNQTLKIRTNMVMVPHYGHLLRGESHGRILKSAAPLDCLVECQTEKGGFNA | | | | 300 |
| Sbjct 240 | Y W +LKP QTL++R+NGN++ P WYGH+L G SHGRILK+ G+C+V+CQTEKGG N+ | | | | 299 |
| Query 301 | SLPFQNIISKYAFGNCPKYVRTKSLKLAGMRNVPIKETRGLFGAIAAGFIEGGWPGLVAGW | | | | 360 |
| Sbjct 300 | +LPF NISKYAFG CPKYVR SLKLA+G+RNVP + +RGLFGAIAAGFIEGGWPGLVAGW | | | | 359 |
| Query 361 | YGFQHYNSEGTGMAADLASTQRAIDKITSKVNNIIDKMNKQYEVIGHEFSEIETRINMIN | | | | 420 |
| Sbjct 360 | YGFQHSNDQGVGMAADRSTQKAIDKITSKVNNI+DKMKNQYE+I HEFSE+ETR+NMIN | | | | 419 |
| Query 421 | DKIDDDQIQDIWAYNAELLVLENQKTLDEHDSNVRNLYERVKRSLGENAIDEGNGCFELL | | | | 480 |
| Sbjct 420 | +KIDDDQIQD+WAYNAELLVLENQKTLDEHD+NV NLY +VKR+LG NA+++G GCFEL | | | | 479 |
| Query 481 | HKCNNSCMDTIRNGTYSKYQYSEESKLERLRINGIKLESNTVYKVLTIYSTAASSLVLLL | | | | 540 |
| Sbjct 480 | HKC++ CM+TIRNGTY++ +Y EES+LER +I G+KLES YK+LTIYST ASSLVL + | | | | 539 |
| Query 541 | GVTAFMVWAMSNNGSCKCTICISTOP | | 565 | | |
| Sbjct 540 | G AF+ WAMSNNGSC+C ICISTOP | | 564 | | |

Figure 89: BLASTP alignment between Kz52 HA and H9. BLASTP alignment between Kz52 HA (Query) and A/Hong Kong/1073/99 (H9N2) HA (Sbjct) using the blastp (protein-protein) algorithm on the NCBI database revealed a 68% identity. The alignment was created using the NCBI database BLAST® tool.

7.3.3 3D modelling

A 3D model of the Kz52 HA polypeptide was predicted using Phyre2 software which relies on protein homology by comparing the query HA sequence with that of other HAs for which structure modelling has been determined. Of the close phylogenetic relatives tested (including H9), the best structural alignment was with the HA of A/black-headed gull/Sweden/2/99 (H16N3) (GenBank accession number: AY684888.1). The internal control H9 HA structure was also predicted. Interestingly, the software revealed homology with the same H16 model structure, probably due to the fact it was the nearest HA subtype with its complete structure determined. For this reason, only one modelling structure is displayed in Figure 90 since it was difficult to identify differences. Modelling of the Kz52 HA structure allowed antigenic features such as the receptor binding sites (RBS) and the cleavage site of the HA head region to be highlighted (Table 31).

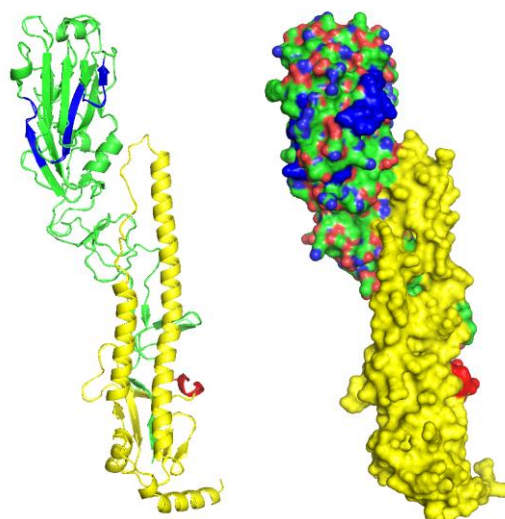


Figure 90: 3D model structures. Predicted 3D model structures of Kz52 HA (and H9) based on the HA of H16 generated using Phyre2 software as ribbon (left) and surface (right) display. The images show the HA1 and HA2 subunits (green and yellow respectively), the cleavage site (red) and receptor binding sites (blue).

| Main antigenic sites | Amino acids position |
|--------------------------|----------------------|
| RBS 130 loop KRVVMF | 131 to 136 |
| RBS 190 helix PILMWA | 184 to 190 |
| RBS 220 loop TEELHRSF | 215 to 222 |
| Cleavage site PIKETR↓GLF | 334 to 339 |

Table 31: Main antigenic sites. Main antigenic sites (RBS and cleavage site) in the HA head of Kz52 amino acids sequence.

7.3.4 Molecular cloning and analysis of the Kz52 haemagglutinin (HA) gene

7.3.4.1 Cloning of Influenza HA genes into pl.18 or pCAGGS

On receiving the Kz52 HA 'gene string' oligonucleotides (either WT or CO), this DNA was resuspended in MBG H₂O to achieve a final concentration of 100 ng/μL as suggested by the manufacturer. WT Kz52 gene was first cloned into the pl.18 vector, then subcloned into pCAGGS (Flow charts in Appendix Figures 8 and 9). Meanwhile, CO Kz52 gene was first cloned into pl.18 and then PCR amplified before being subcloned into pCAGGS (Flow charts in Appendix Figures 10 and 11). For this purpose, cloning primers were designed accordingly (Table 24) and a gradient PCR was first carried out to establish the best annealing temperature (Figure 91). Subsequently, a high-fidelity PCR was performed to amplify CO Kz52 HA gene (Figure 92). A detailed cloning strategy is reported in Section 7.2.3. and depicted as Flow charts in Appendix Figures 8-12. PCR positive clone plasmid DNA was purified. Before sending the DNA plasmid material to be Sanger sequenced, the insert sizes were verified employing FastDigest® REs. Reactions were set up accordingly using the appropriate REs matching to the cloning sites or if this was not possible, an alternative RE was employed. For pl.18-CO Kz52 clones, sequencing was the only reliable method to verify whether correct insertion of the gene into the vector had succeeded (Figures 108-110). Images of the DNA migration patterns were acquired in a G:Box gel imager and GeneSnap software and shown below (Figures 98-101). Sanger sequencing was requested to verify the correct insertion of the HA gene into the plasmid vector and to confirm the absence of mutations which may have occurred during the cloning process. pl.18 or pCAGGS FW and Rev primers (Table 7) were employed for sequencing from the 5' and 3' ends respectively. Sequences were aligned and analysed on DNADynamo software and results are shown below for each HA clone generated (Figures 102-116).

A gradient PCR was performed to determine the best annealing temperature for CO Kz52 cloning primers (Figure 91). pl.18-CO Kz52 was employed as DNA template. 2 pairs of cloning primers were tested: the newly designed cloning primers (Table 24) and SmaIKz52COFW (Table 24) paired with pl.18 internal Rev primer (Table 7). A temperature gradient of +50°C, +53°C, +57°C and +60°C was chosen. The brightest migration patterns were identified at +53°C for both pairs of primer, suggesting the best annealing temperature to employ in the high-fidelity PCR (Section 7.2.4.).

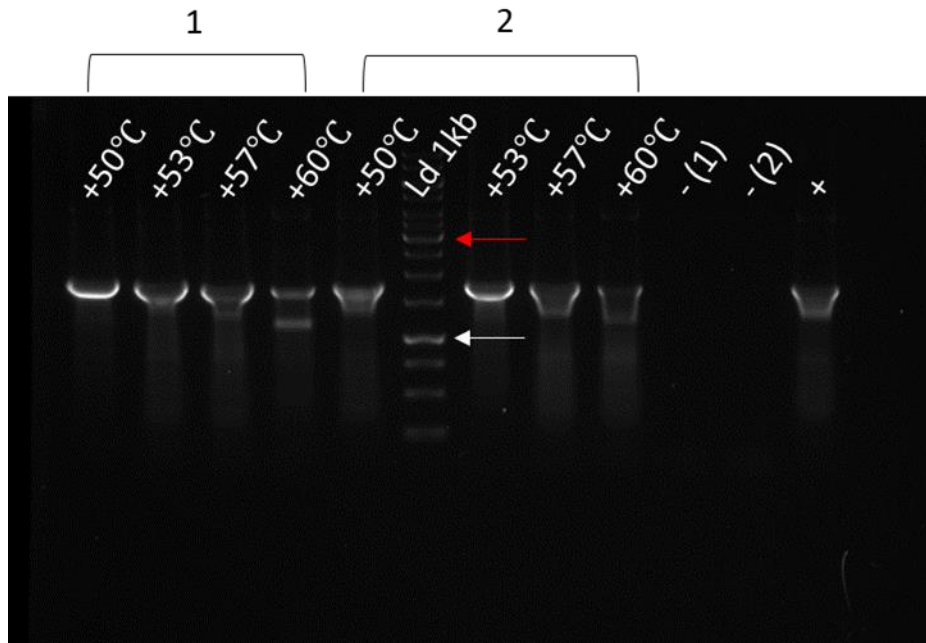


Figure 91: Gradient PCR for CO Kz52 cloning primers. Number 1 represents the newly designed cloning primers, while number 2 represents SmaIKz52COFW paired with pl.18 int Rev. Both pairs of primer were tested for different temperatures. Fragment sizes (1686 bp) were estimated by comparison to a GeneRuler 1 kb DNA Ladder (Ld 1kb). MBG H₂O was combined with either the first (- (1)) or second (- (2)) pair of primers as negative controls, while the DNA template was amplified using pl.18 int FW and Rev primers as positive control (+). White and red arrows indicate 1 kb and 3 kb on DNA ladder.

Once the best annealing temperature was established, a high-fidelity PCR was performed to amplify CO Kz52 HA gene. Amplification product of CO Kz52 was verified on a 1% agarose gel (Figure 92). pl.18-CO Kz52 HA was employed as DNA template and amplified with 2 pairs of cloning primers: either with the newly designed cloning primers (Table 24) or SmaIKz52COFW (Table 24) paired with pl.18 internal reverse primer (Table 7). The PCR product was then purified and inserted into pCAGGS following the methodology in the Flow Chart in Appendix Figure 11.

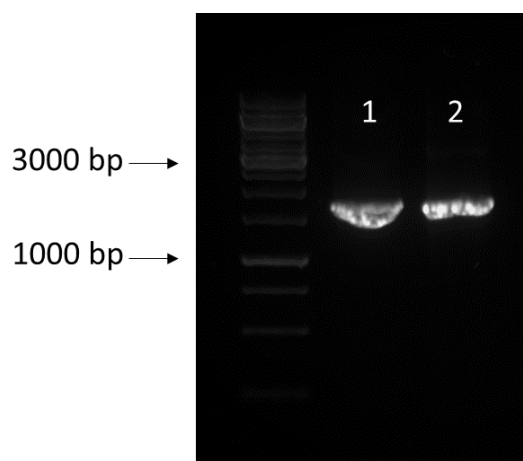


Figure 92: High-fidelity PCR amplification product of CO Kz52. Lane 1 represents the newly designed cloning primers, while lane 2 represents *Sma*I Kz52COFW paired with *pl.18 int Rev*. Fragment sizes (1686 bp) were estimated by comparison to a GeneRuler 1 kb DNA Ladder.

Ligation products were transformed into DH5 α competent cells and 50 μ L of SOC/bacteria was plated onto LB Agar plates with the appropriate antibiotic selection (ampicillin) and incubated overnight. The following day, single colonies were picked for colony screening as described in Section 2.1.11. using *pl.18 internal* (Table 7) or *pCAGGS NT* (Table 8) FW and Rev primers for amplification according to the vector backbone. Also, a colony in the vector only plate, if present, was picked as negative control. The PCR products were visualised on an agarose gel to identify which clones were positive with the gene insertion (Figures 93-97). Positive clone cultures were grown and plasmid clone DNA miniprep purified.

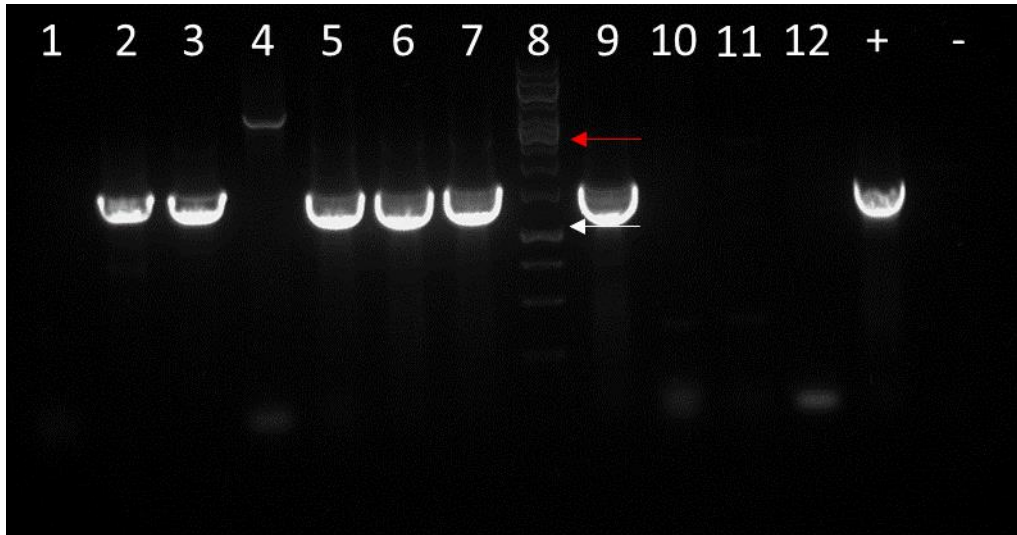


Figure 95: Colony screen of pl.18-CO Kz52 clones. Of 10 clones screened, 6 clones (lanes 2, 3, 5, 6, 7 and 9) showed a clear band was visible at 1686 bp estimated by comparison to a GeneRuler 1 kb DNA Ladder, meaning that Kz52 HA insert had ligated into the pl.18 vector. Lane 12 represents the no insert band (pl.18 empty vector). A positive (+) and negative (-) control were included and represented by an H3N2 canine influenza HA plasmid (pl.18-H3) and ddH₂O respectively. White and red arrows indicate 1 kb and 3 kb on DNA ladder.

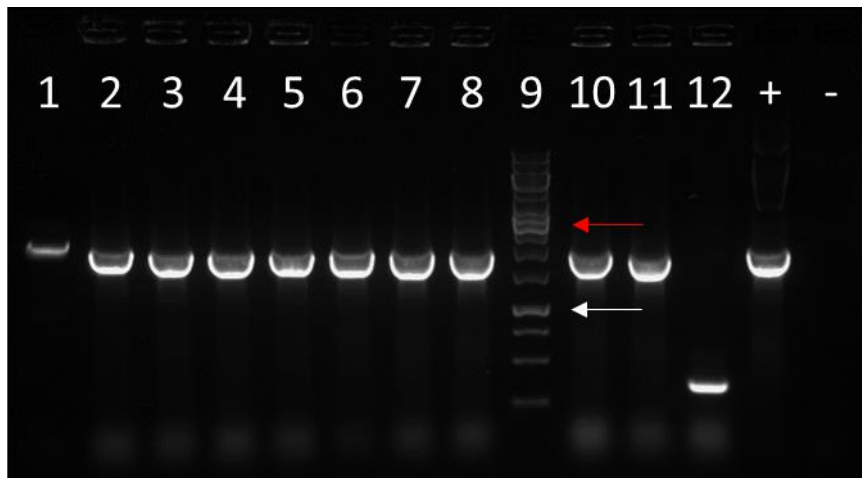


Figure 96: Colony screen of pCAGGS-CO Kz52 clones. Of 10 clones screened, 9 clones (lanes 2-8, 10 and 11) showed a clear band was visible at 1686 bp estimated by comparison to a GeneRuler 1 kb DNA Ladder, meaning that Kz52 HA insert had ligated into the pCAGGS vector. Lane 12 represents the no insert band (pCAGGS empty vector). A positive (+) and negative (-) control were included and represented by a pCAGGS-WT Kz52 and ddH₂O respectively. White and red arrows indicate 1 kb and 3 kb on DNA ladder.

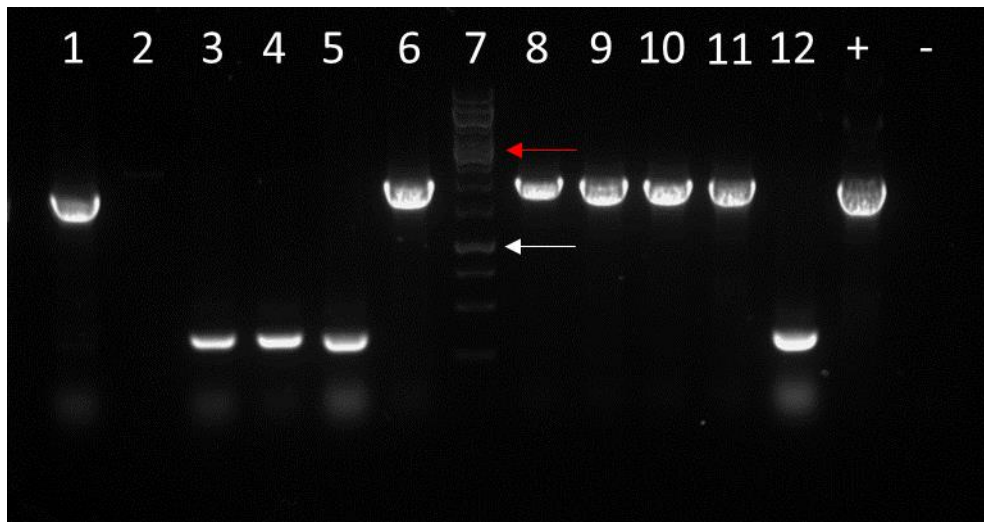


Figure 97: Colony screen of pCAGGS-H9 clones. Of 10 clones screened, 6 clones (lanes 1, 6, 8, 9 10 and 11) showed a clear band was visible at 1683 bp estimated by comparison to a GeneRuler 1 kb DNA Ladder, meaning that H9 HA insert had ligated into the pCAGGS vector. Lane 12 represents the no insert band (pCAGGS empty vector). A positive (+) and negative (-) control were included and represented by a pCAGGS-WT Kz52 and ddH₂O respectively. White and red arrows indicate 1 kb and 3 kb on DNA ladder.

7.3.4.1.1 Restriction enzyme digest of clones DNA

Before sending the DNA plasmid material to be Sanger sequenced, the insert sizes were checked employing FastDigest® REs (Figures 98-101). Reactions were set up accordingly using the REs appropriate to the respective the cloning strategies.

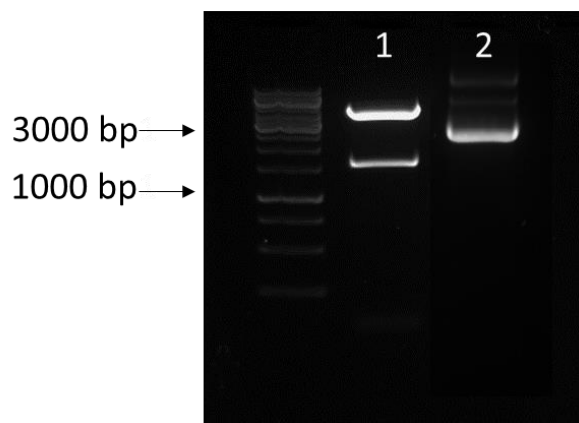


Figure 98: Control digestion of WT Kz52 HA into pl.18. Fragment sizes estimated by comparison to a GeneRuler 1 kb DNA Ladder. Cloning of WT Kz52 HA (lane 1) to the vector (pl.18) was confirmed by KpnI-XhoI restriction digestion. An empty pl.18 vector (lane 2) was included as undigested vector (non-linearised, running as supercoiled) and do not run at its actual size.

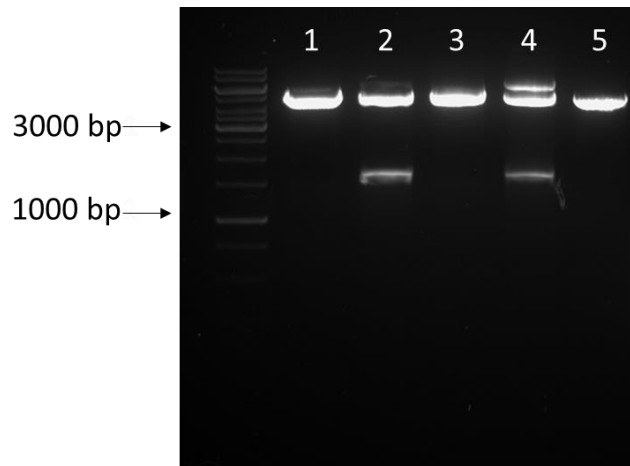


Figure 99: Control digestion of WT Kz52 HA into pCAGGS. Fragment sizes estimated by comparison to a GeneRuler 1 kb DNA Ladder. Cloning of WT Kz52 HA (lanes 1-4) to the vector (pCAGGS) was confirmed by KpnI-XhoI restriction digestion. An empty pCAGGS vector (lane 5) was included as undigested vector (non-linearised, running as supercoiled) and do not run at its actual size.

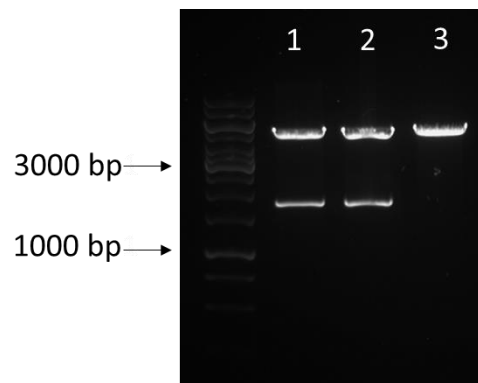


Figure 100: Control digestion of CO Kz52 HA into pCAGGS. Fragment sizes estimated by comparison to a GeneRuler 1 kb DNA Ladder. Cloning of CO Kz52 HA (lanes 1 and 2) to the vector (pCAGGS) was confirmed by KpnI-XhoI restriction digestion. An empty pCAGGS vector (lane 3) was included as digested vector (linearised) and runs as in control digestion.

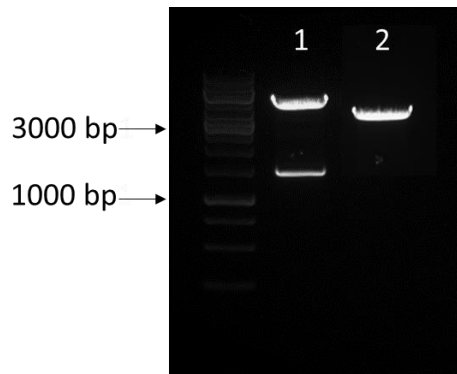


Figure 101: Control digestion of H9 HA into pCAGGS. Fragment sizes estimated by comparison to a GeneRuler 1 kb DNA Ladder. Cloning of H9 (lane 1) to the vector (pCAGGS) was confirmed by *KpnI-XhoI* restriction digestion. An empty pCAGGS vector (lane 2) was included as undigested vector (non-linearised, running as supercoiled) and do not run at its actual size.

7.3.4.1.2 Sequencing of plasmid DNA

Sanger sequencing was performed to verify all cloned gene sequences and particularly check the absence of mutations eventually occurred during the transformation process. pl.18 or pCAGGS FW and Rev primers (Table 7) were employed to verify the 5' and 3' end respectively. Sequencing of pl.18-CO Kz52 HA clone was the only reliable method to verify correct insertion of the HA gene into pl.18 vector (Figures 108-110). This was due to the fact of how the HA gene was inserted into pl.18 at the 5' end. There was no other RE sites upstream of the ATG start codon and in the MCS of pl.18 to allow a digest to excise the cloned fragment for analysis. Sequence alignments were analysed on DNADynamo version 1.556 software (BlueTractor) and results are shown below for each influenza HA genes correctly inserted into pl.18 or pCAGGS cloning sites (Figures 102-116).

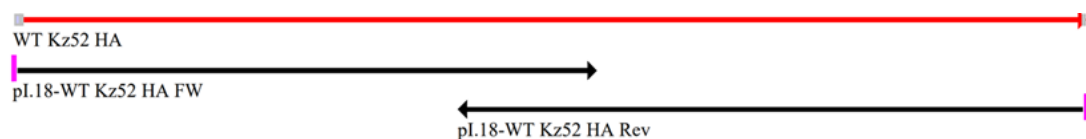


Figure 102: Alignment summary of WT Kz52 HA gene sequences. 5' and 3' sequencing of WT Kz52 HA cloned into pl.18 vector, compared with the consensus reference sequence. No mutation was detected in the clone.

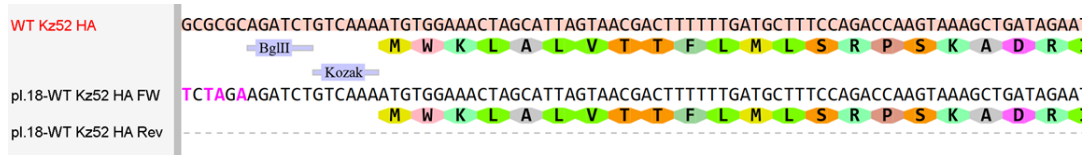


Figure 103: WT Kz52 HA gene clone was sequenced using flanking pl.18 FW primer. On the reference sequence, the 5' BglII cloning site (AGATCT) is highlighted followed by the Kozak sequence (GTCAAA) upstream the ATG start codon.

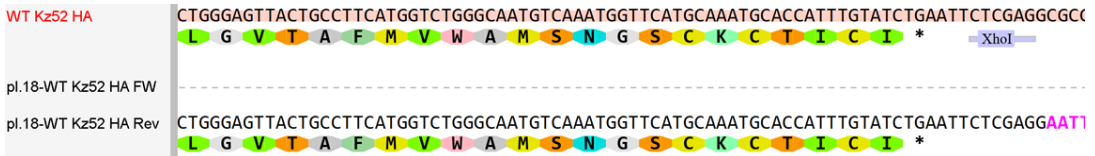


Figure 104: WT Kz52 HA gene clone was sequenced using flanking pl.18 Rev primer. On the reference sequence, the 3' XhoI cloning site (CTCGAG) is highlighted downstream the TGA stop codon.

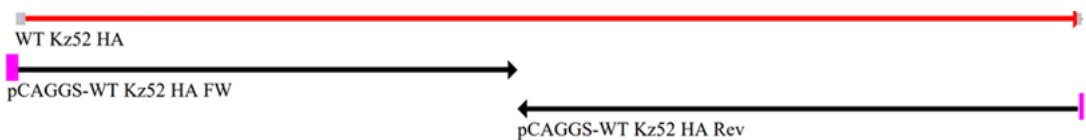


Figure 105: Alignment summary of WT Kz52 HA gene sequences. 5' and 3' sequencing of WT Kz52 HA cloned into pCAGGS vector, compared with the consensus reference sequence. No mutation was detected in the clone.

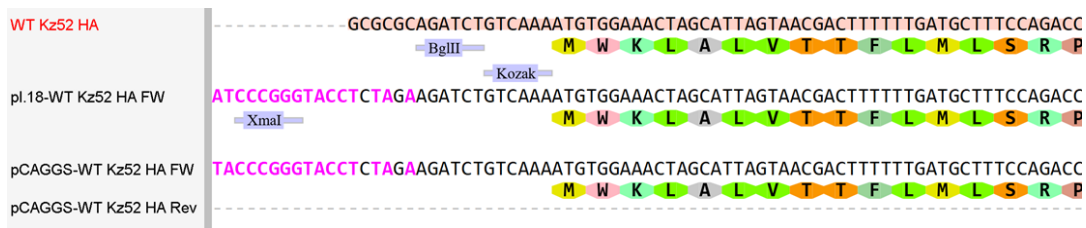


Figure 106: WT Kz52 HA gene clone was sequenced using flanking pCAGGS FW primer. On the reference sequence, the 5' Xmal (ATCCGGG) and BglII (AGATCT) cloning sites are highlighted followed by the Kozak sequence (GTCAAA) upstream the ATG start codon.



Figure 107: WT Kz52 HA gene clone was sequenced using flanking pCAGGS Rev primer. On the reference sequence, the 3' XhoI cloning site (CTCGAG) is highlighted downstream the TGA stop codon.

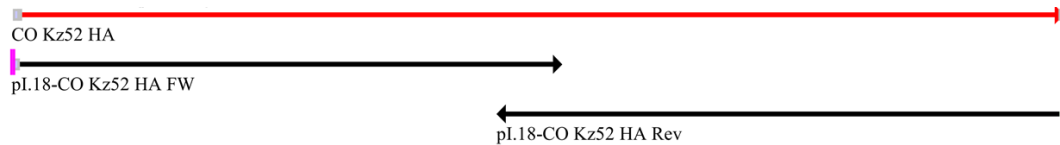


Figure 108: Alignment summary of CO Kz52 HA gene sequences. 5' and 3' sequencing of CO Kz52 HA cloned into pl.18 vector, compared with the consensus reference sequence. No mutation was detected in the clone.

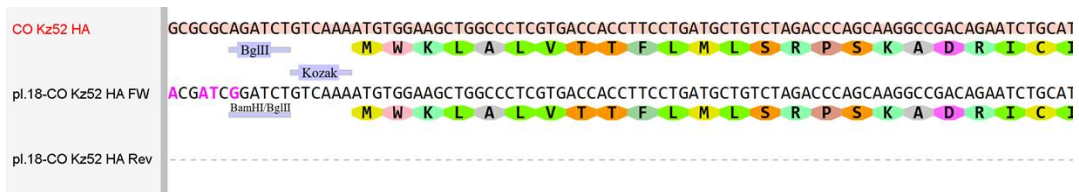


Figure 109: CO Kz52 HA gene clone was sequenced using flanking pl.18 FW primer. On the reference sequence, the 5' BamHI/BglII (GGATCT) and BglII (AGATCT) cloning sites are highlighted followed by the Kozak sequence (GTCAA) upstream the ATG start codon.



Figure 110: CO Kz52 HA gene clone was sequenced using flanking pl.18 Rev primer. On the reference sequence, the 3' XhoI cloning site (CTCGAG) is highlighted downstream the TGA stop codon.

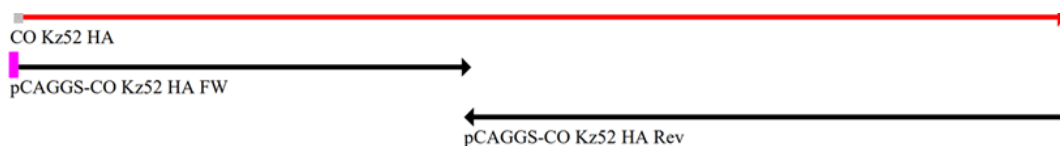


Figure 111: Alignment summary of CO Kz52 HA gene sequences. 5' and 3' sequencing of CO Kz52 HA cloned into pCAGGS vector, compared with the consensus reference sequence. No mutation was detected in the clone.

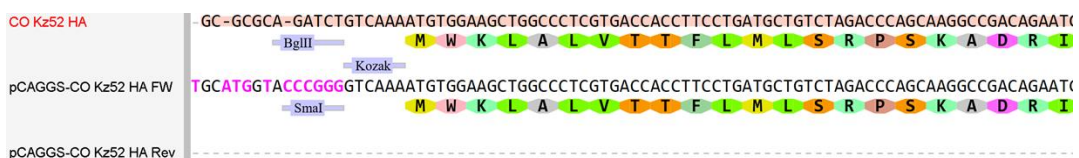


Figure 112: CO Kz52 HA gene clone was sequenced using flanking pCAGGS FW primer. On the reference sequence, the 5' SmaI (CCCGGG) and BglII (AGATCT) cloning sites are highlighted followed by the Kozak sequence (GTCAA) upstream the ATG start codon.

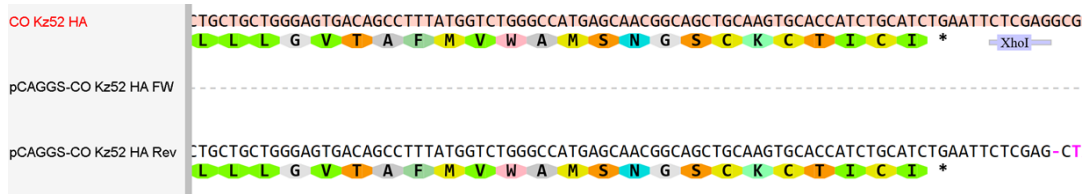


Figure 113: CO Kz52 HA gene clone was sequenced using flanking pCAGGS Rev primer. On the reference sequence, the 3' XhoI cloning site (CTCGAG) is highlighted downstream the TGA stop codon.

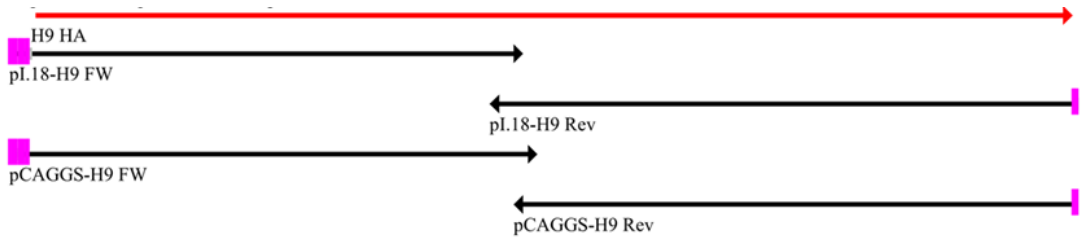


Figure 114: Alignment summary of H9 HA gene sequences. 5' and 3' sequencing of H9 HA cloned into pI.18 and pCAGGS vectors, compared with the consensus reference sequence. No mutation was detected in the clones.

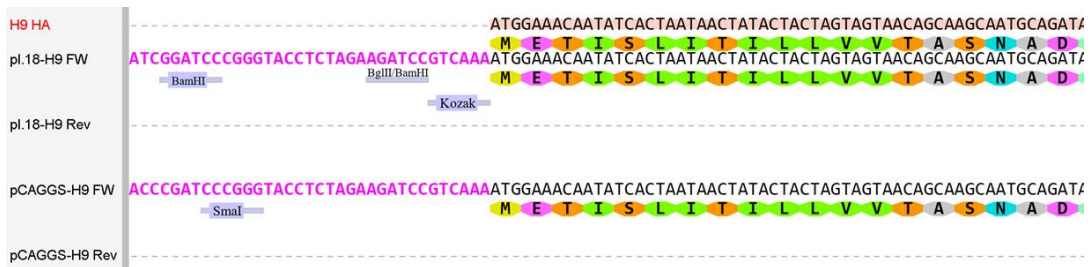


Figure 115: H9 HA gene clone was sequenced using flanking pI.18 and pCAGGS FW primers. The 5' BglII/BamHI (AGATCC) and SmaI (CCCGG) cloning sites are highlighted followed by the Kozak sequence (GTCAAA) upstream the ATG start codon. H9 HA was first cloned into pI.18 by Dr. Francesca Ferrara (St. Jude Children's Research Hospital, USA) and subsequently subcloned into pCAGGS.

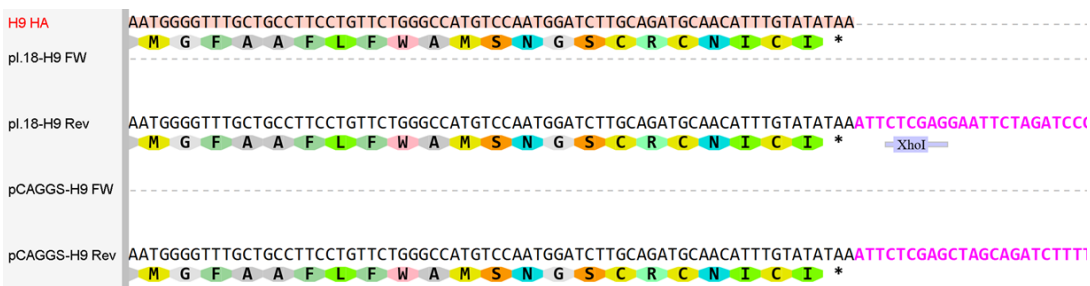


Figure 116: H9 HA gene clone was sequenced using flanking pI.18 and pCAGGS Rev primers. On the reference sequence, the 3' XhoI cloning site (CTCGAG) is highlighted downstream the TGA stop codon.

7.3.4.2 Site Directed Mutagenesis

HA needs protease cleavage to mature (Section 1.2.2.1.1.). These are usually added as plasmids for protease expression during Influenza PV generation. However, the protease plasmids employed so far to attempt production of Kz52 PV were not able to cleave and activate Kz52 HA. If other proteases are able to cleave and activate Kz52 HA it is unknown. On the other hand, proteases able to cleave and activate H9 HA are known. In order to investigate the impact of amino acids changes in Kz52 HA protease cleavage site (PIKETR↓GLF), SDM was performed in a stepwise manner to mimic H9 HA cleavage site (PARSSR↓GLF). First a single amino acid mutation PIKETR→PIKSTR (E337S) was performed, followed by a larger change PIKSTR→PARSSR (I335A, K336R and T338S). On the other hand, H9 HA cleavage site was mutated into the Kz52 HA sequence PARSSR→PIKETR (A334I, R335K, S336E and S337T) to verify its cleavage by several specific proteases. An SDM was also employed to mutate the region of the HA gene which encodes the monobasic cleavage site into one which encodes a polybasic cleavage site PARSSR→PARKKR (S337K and S338K for Kz52 HA, S336K and S337K for H9 HA). Moreover, in order to investigate whether the Kozak sequence was permitting sufficient HA gene translation, the original Kozak sequence recommended by NIBSC and widely included in many HA constructs of various influenza A strains was mutated into the general mammalian Kozak consensus sequence GTCAAA→GCCACC (for both Kz52 and H9 HA). All SDM primers are reported in Appendix Tables 3 and 4 and the procedures were applied to HA clones in pl.18 vector. Subcloning of mutants into the pCAGGS vector was accomplished through RE strategies.

7.3.4.2.1 Mutation of Kz52 HA cleavage site (PIKETR→PIKSTR) in pl.18

7.3.4.2.1.1 Site Directed Mutagenesis

SDM to mutate one single amino acid in both WT and CO Kz52 HA cleavage site E337S was accomplished by PCR following the in-house protocol detailed in Section 7.2.7. employing Accuzyme™ mix and the appropriate SDM primers (Appendix Table 3). 5 µL of PCR product was run on a 1% agarose gel to verify whether amplification of the DNA band occurred (Figures 117 and 118).

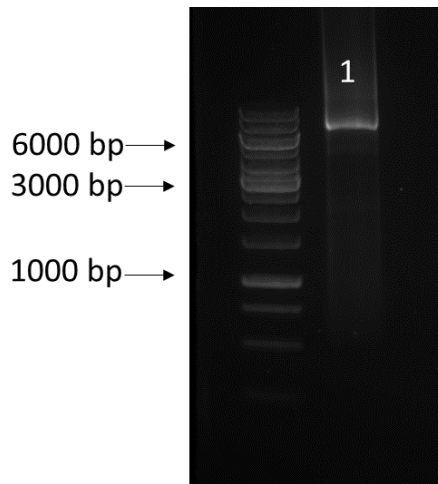


Figure 117: Amplification product of mutant WT Kz52 HA E337 in pl.18. A band is visible at ~6 kb estimated by comparison to a GeneRuler 1 kb DNA Ladder, meaning of successful DNA amplification.

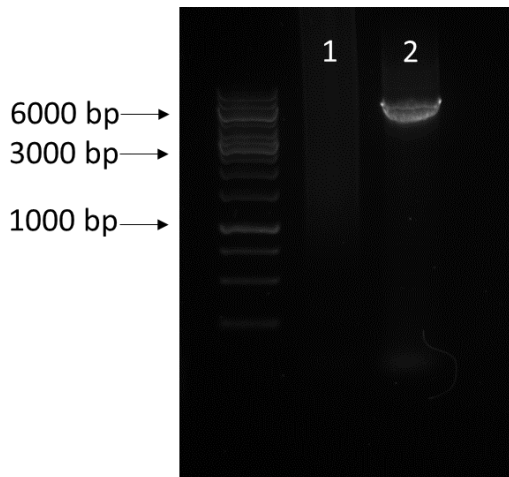


Figure 118: Amplification product of mutant CO Kz52 HA E337 in pl.18. A band (lane 2) is visible at ~6 kb estimated by comparison to a GeneRuler 1 kb DNA Ladder, meaning of successful DNA amplification.

7.3.4.2.1.2 Sequencing

Plasmid clone DNA was subsequently sent for sequencing to verify the correct base substitutions occurred during SDM (Figures 119-122).

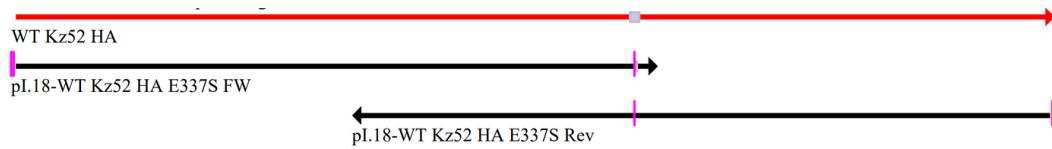


Figure 119: Alignment summary of mutant WT Kz52 HA gene E337S sequences. 5' and 3' sequencing of WT Kz52 HA cloned into pI.18 vector, compared with the consensus reference sequence, to verify whether mutation E337S occurred in the desired position. No extra mutations were detected.

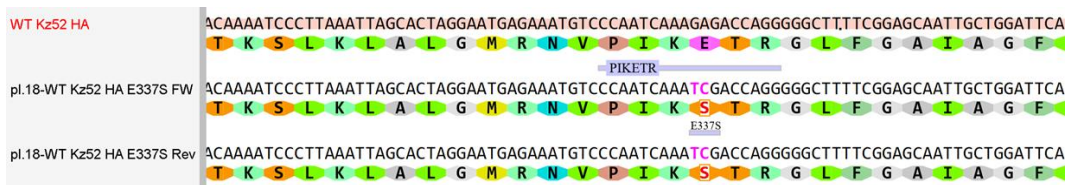


Figure 120: Mutant WT Kz52 HA gene E337S clone was sequenced using flanking pI.18 FW and Rev primers. On the reference sequence, the cleavage site PIKETR was highlighted. The desired mutation E337S was observed on both pI.18 FW and Rev sequences.

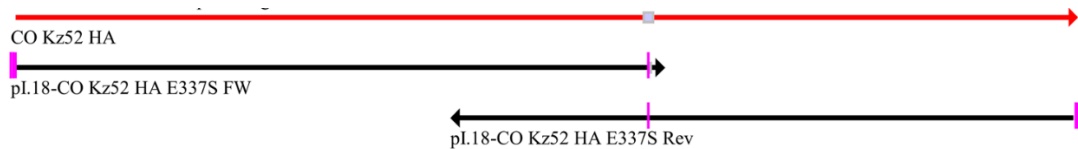


Figure 121: Alignment summary of mutant CO Kz52 HA gene E337S sequences. 5' and 3' sequencing of CO Kz52 HA cloned into pI.18 vector, compared with the consensus reference sequence, to verify whether mutation E337S occurred in the desired position. No extra mutations were detected.

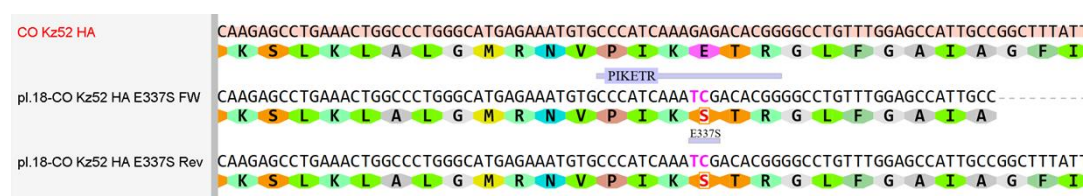


Figure 122: Mutant CO Kz52 HA gene E337S clone was sequenced using flanking pI.18 FW and Rev primers. On the reference sequence, the cleavage site PIKETR was highlighted. The desired mutation E337S was observed on both pI.18 FW and Rev sequences.

7.3.4.2.2 Mutation of Kz52 HA cleavage site (PIKSTR→PARSSR) in pl.18

7.3.4.2.2.1 Site Directed Mutagenesis

SDM to mutate three amino acids in both WT and CO Kz52 HA cleavage site I335A, K336R and T338S was accomplished by PCR following the in-house protocol detailed in Section 7.2.7. employing Accuzyme™ mix and the appropriate SDM primers (Appendix Table 3). 5 µL of PCR product was run on a 1% agarose gel to verify whether amplification of the DNA band occurred (Figure 123).

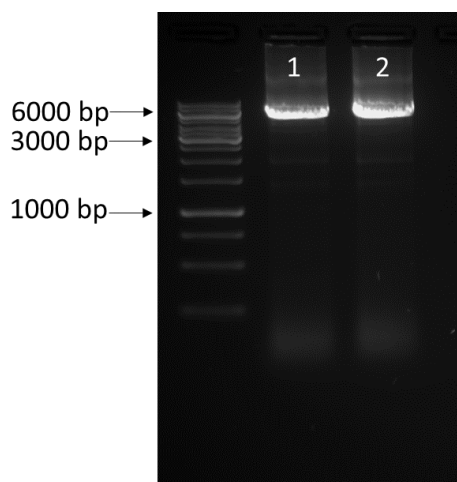


Figure 123: Amplification product of mutants WT and CO Kz52 HA PARSSR in pl.18. Both Kz52 WT (lane 1) and Kz52 CO (lane 2) insert bands are visible at ~6 kb estimated by comparison to a GeneRuler 1 kb DNA Ladder, meaning of successful DNA amplification.

7.3.4.2.2.2 Sequencing

Plasmid clone DNA was subsequently sent for sequencing to verify the correct base substitutions occurred during SDM (Figures 124-127).

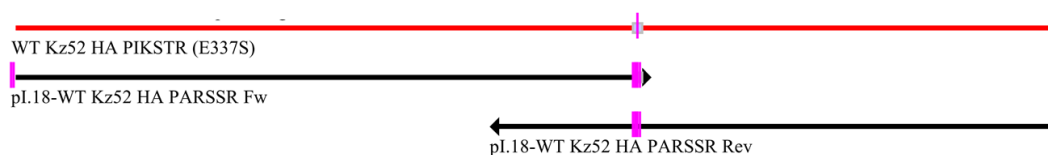


Figure 124: Alignment summary of mutant WT Kz52 HA gene PARSSR sequences. 5' and 3' sequencing of WT Kz52 HA cloned into pl.18 vector, compared with the consensus reference sequence, to verify whether the mutation occurred in the desired position. No extra mutations were detected.

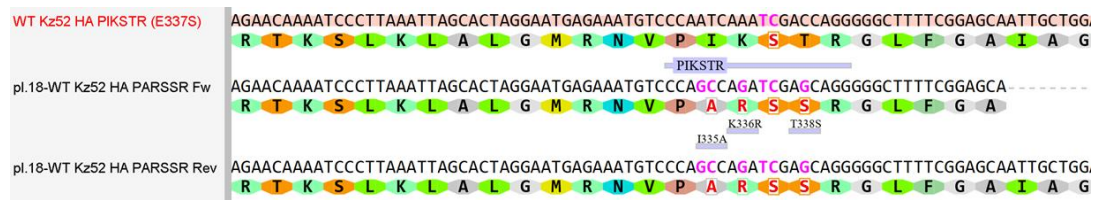


Figure 125: Mutant WT Kz52 HA gene PARSSR clone was sequenced using flanking pl.18 FW and Rev primers. On the reference sequence, the cleavage site PIKSTR was highlighted. The desired mutation I335A, K336R and T338S were observed on both pl.18 FW and Rev sequences.

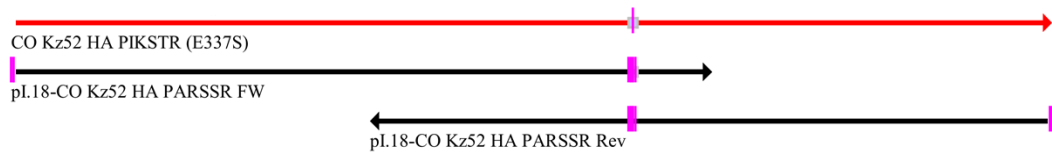


Figure 126: Alignment summary of mutant CO Kz52 HA gene PARSSR sequences. 5' and 3' sequencing of CO Kz52 HA cloned into pl.18 vector, compared with the consensus reference sequence, to verify whether the mutation occurred in the desired position. No extra mutations were detected.

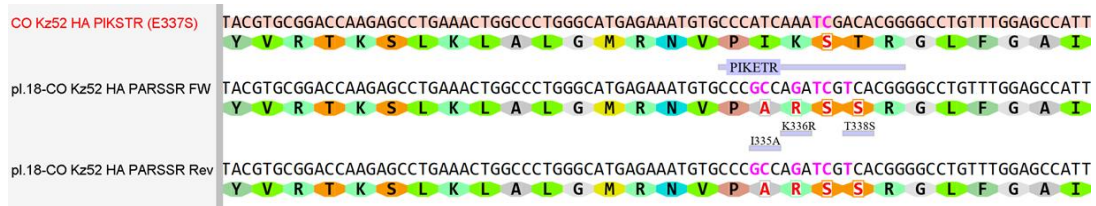


Figure 127: Mutant CO Kz52 HA gene PARSSR clone was sequenced using flanking pl.18 FW and Rev primers. On the reference sequence, the cleavage site PIKSTR was highlighted. The desired mutation I335A, K336R and T338S were observed on both pl.18 FW and Rev sequences.

Subcloning of mutants WT and CO Kz52 HA gene (cleavage site PARSSR) into the pCAGGS vector was accomplished through RE strategies. The strategies are depicted as Flow Charts in Appendix Figures 9 and 11 respectively. The SDM protocols were developed using a pl.18 vector backbone. Therefore, the SDM could not be performed when the HA genes were inserted into pCAGGS probably due to the different length of pCAGGS compared to pl.18.

7.3.4.2.2.3 High-fidelity Polymerase Chain Reaction

A high-fidelity PCR was performed to amplify the mutant CO Kz52 HA gene (cleavage site PARSSR). Amplification product of the mutant gene was verified on a 1% agarose gel (Figure 128). pl.18-CO Kz52 HA (PARSSR) was employed as DNA template and amplified with

SmaIKz52COFW paired with XhoIKz52CORev primer (Table 24). The PCR product was then purified and inserted into pCAGGS following the methodology in in the Flow Chart in Appendix Figure 11.

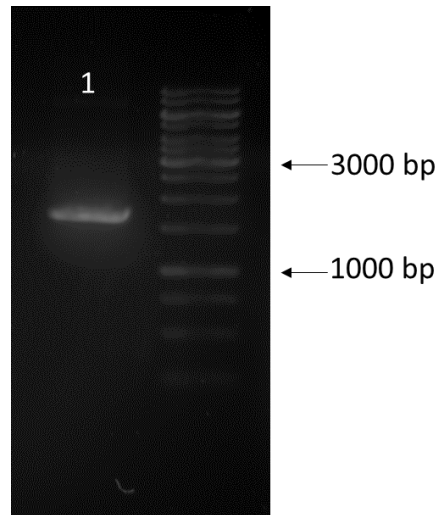


Figure 128: High-fidelity PCR amplification product of mutant CO Kz52 HA (PARSSR). Fragment size was estimated by comparison to a GeneRuler 1 kb DNA Ladder.

7.3.4.2.2.4 Colony screen of mutant HA genes

Ligation products were transformed into DH5 α competent cells and 50 μ L of SOC/bacteria was plated onto LB Agar plates with the appropriate antibiotic selection (ampicillin) and incubated overnight. The following day, single colonies were picked for colony screening as described in Section 2.1.11. using pCAGGS NT FW and Rev primers (Table 8) for amplification. Also, a colony in the vector only plate, if present, was picked as negative control. The PCR products were visualised on an agarose gel to identify which clones were positive with the gene insertion (Figures 129 and 130). Positive clone cultures were grown and plasmid clone DNA miniprep purified.

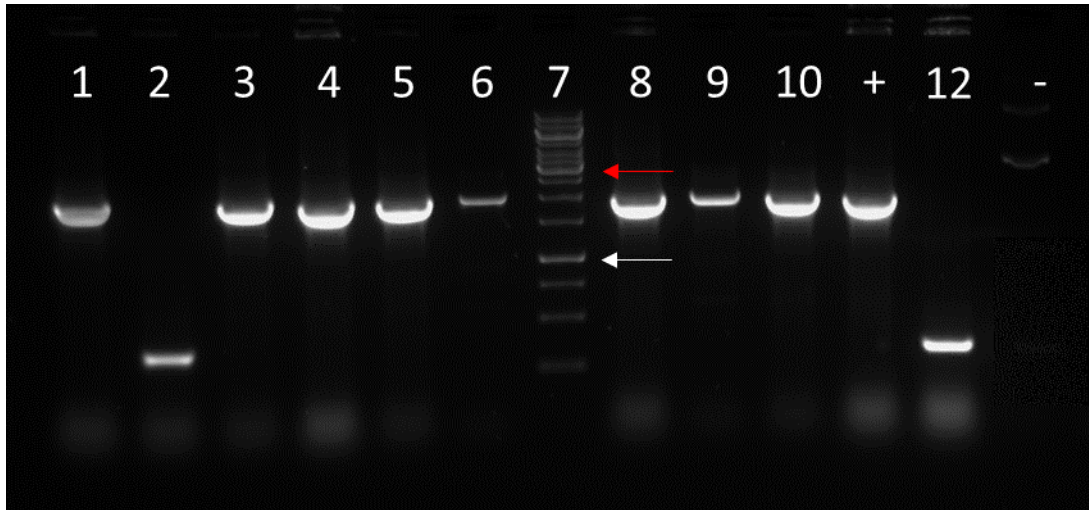


Figure 129: Colony screen of pCAGGS-WT Kz52 mutant clones (PARSSR). Of 9 clones screened, 8 clones (lanes 1, 3, 4, 5, 6, 8, 9 and 10) showed a clear band visible at 1686 bp estimated by comparison to a GeneRuler 1 kb DNA Ladder, meaning that mutant Kz52 HA insert had ligated into the pCAGGS vector. Lane 12 represents the no insert band (pCAGGS empty vector). A positive (+) and negative (-) control were included and represented by a pCAGGS-WT Kz52 and ddH₂O respectively. White and red arrows indicate 1 kb and 3 kb on DNA ladder.

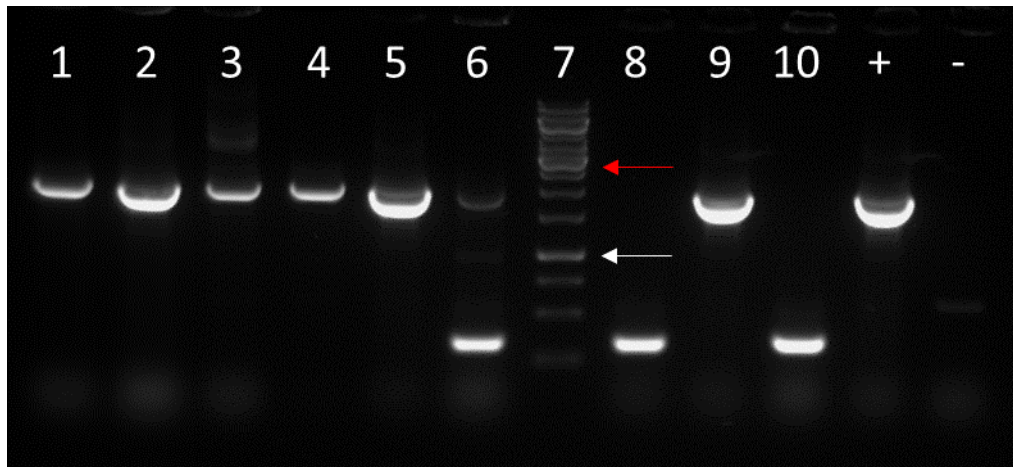


Figure 130: Colony screen of pCAGGS-CO Kz52 mutant clones (PARSSR). Of 8 clones screened, 6 clones (lanes 1-5 and 9) showed a clear band visible at 1686 bp estimated by comparison to a GeneRuler 1 kb DNA Ladder, meaning that mutant Kz52 HA insert had ligated into the pCAGGS vector. Lane 10 represents the no insert band (pCAGGS empty vector). A positive (+) and negative (-) control were included and represented by a pCAGGS-CO Kz52 and ddH₂O respectively. White and red arrows indicate 1 kb and 3 kb on DNA ladder.

7.3.4.2.5 Restriction enzyme digest of mutant clones DNA

Before sending the DNA plasmid material to be Sanger sequenced, the insert sizes were checked employing FastDigest® REs (Figures 131 and 132). Reactions were set up accordingly using the REs appropriate to the respective the cloning strategies.

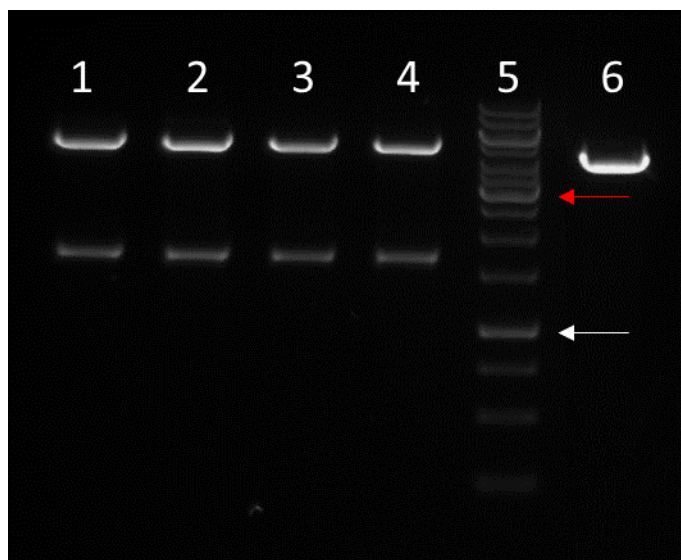


Figure 131: Control digestion of mutant WT Kz52 HA gene (PARRSR) into pCAGGS. Fragment sizes estimated by comparison to a GeneRuler 1 kb DNA Ladder. Cloning of mutant WT Kz52 HA (lanes 1-4) to the vector (pCAGGS) was confirmed by BglII-XhoI restriction digestion. An empty pCAGGS vector (lane 6) was included as undigested vector (non-linearised, running as supercoiled) and do not run at its actual size. White and red arrows indicate 1 kb and 3 kb on DNA ladder.

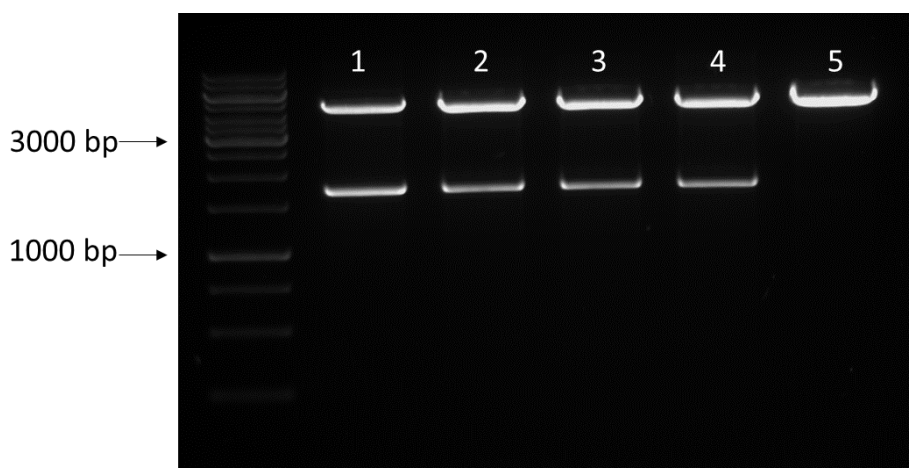


Figure 132: Control digestion of mutant CO Kz52 HA gene (PARRSR) into pCAGGS. Fragment sizes estimated by comparison to a GeneRuler 1 kb DNA Ladder. Cloning of mutant CO Kz52 HA (lanes 1-4) to the vector (pCAGGS) was confirmed by BglII-XhoI restriction digestion. An empty pCAGGS vector (lane 5) was included as digested vector (linearised) and runs as in control digestion.

7.3.4.2.2.6 Sequencing of plasmid DNA

Sanger sequencing was performed to verify all cloned gene sequences and particularly check the absence of mutations eventually occurred during the transformation process (Figures 133-138). pCAGGS FW and Rev primers (Table 7) were employed to verify the 5' and 3' end respectively.

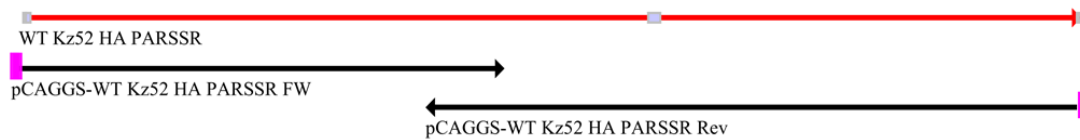


Figure 133: Alignment summary of mutant WT Kz52 HA gene (PARSSR) sequences. 5' and 3' sequencing of WT Kz52 HA cloned into pCAGGS vector, compared with the consensus reference sequence. No mutation was detected in the clone.

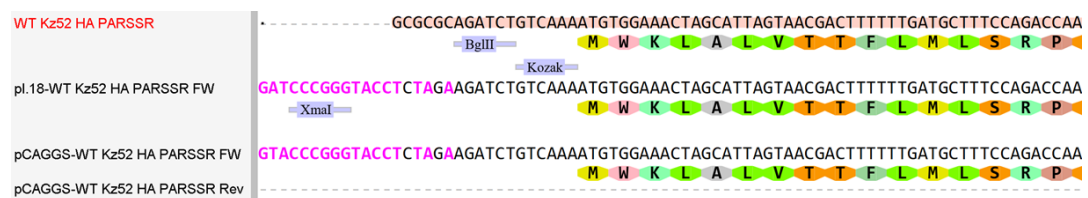


Figure 134: Mutant WT Kz52 HA gene (PARSSR) clone was sequenced using flanking pCAGGS FW primer. On the reference sequence, the 5' XmaI (CCCGGG) and BglII (AGATCT) cloning sites are highlighted followed by the Kozak sequence (GTCAAA) upstream the ATG start codon.

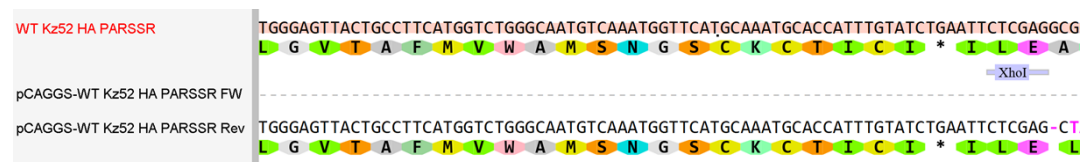


Figure 135: Mutant WT Kz52 HA gene (PARSSR) clone was sequenced using flanking pCAGGS Rev primer. On the reference sequence, the 3' XhoI cloning site (CTCGAG) is highlighted downstream the TGA stop codon.

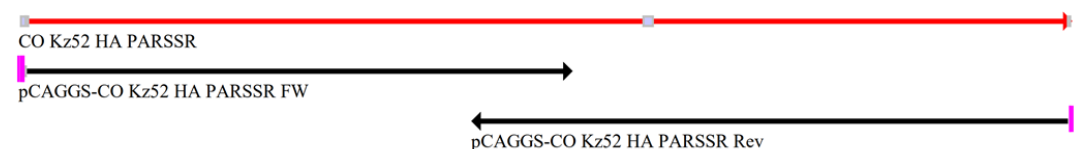


Figure 136: Alignment summary of mutant CO Kz52 HA gene (PARSSR) sequences. 5' and 3' sequencing of CO Kz52 HA cloned into pCAGGS vector, compared with the consensus reference sequence. No mutation was detected in the clone.

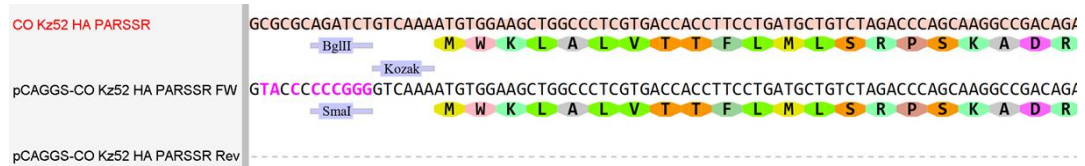


Figure 137: Mutant CO Kz52 HA gene (PARSSR) clone was sequenced using flanking pCAGGS FW primer. On the reference sequence, the 5' SmaI (CCCGGG) and BglII (AGATCT) cloning sites are highlighted followed by the Kozak sequence (GTCAA) upstream the ATG start codon.

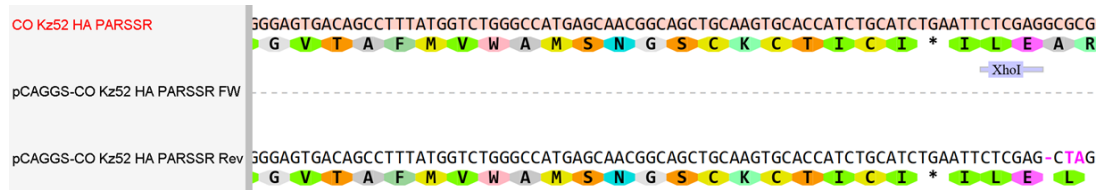


Figure 138: Mutant CO Kz52 HA gene (PARSSR) clone was sequenced using flanking pCAGGS Rev primer. On the reference sequence, the 3' XhoI cloning site (CTCGAG) is highlighted downstream the TGA stop codon.

7.3.4.2.3 Mutation of H9 HA cleavage site (PARSSR→PIKETR) in pl.18

7.3.4.2.3.1 Site Directed Mutagenesis

SDM to mutate four amino acids in H9 HA cleavage site (A334I, R335K, S336E and S337T) was accomplished by PCR following the in-house protocol detailed in Section 7.2.7. employing Accuzyme™ mix and the appropriate SDM primers (H9 PARSSR→PIKETR; Appendix Table 3). 5 µL of PCR product was run on a 1% agarose gel to verify whether amplification of the DNA band occurred (Figure 139).

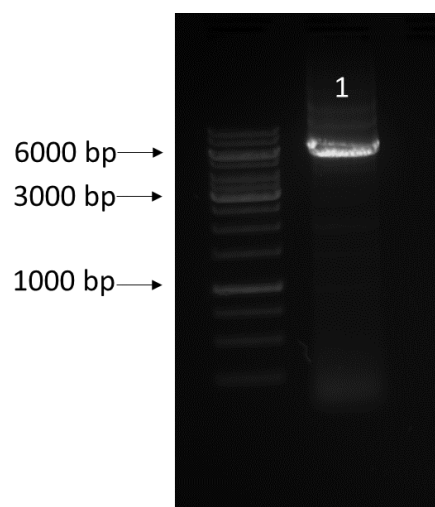


Figure 139: Amplification product of mutants H9 HA PIKETR in pl.18. A band is visible at ~6 kb estimated by comparison to a GeneRuler 1 kb DNA Ladder, meaning of successful DNA amplification.

7.3.4.2.3.2 Sequencing

Plasmid clone DNA was subsequently sent for sequencing to verify the correct base substitutions occurred during SDM (Figures 140 and 141).

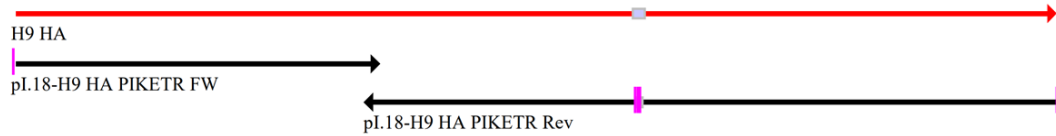


Figure 140: Alignment summary of mutant H9 HA gene PIKETR sequences. 5' and 3' sequencing of H9 HA cloned into pl.18 vector, compared with the consensus reference sequence, to verify whether the mutation occurred in the desired position. No extra mutations were detected.

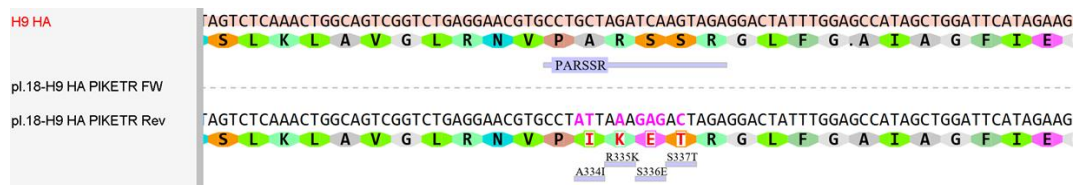


Figure 141: Mutant H9 HA gene PIKETR clone was sequenced using flanking pl.18 FW and Rev primers. On the reference sequence, the cleavage site PIKETR was highlighted. The desired mutation A334I, R335K, S336E and S337T were observed on both pl.18 FW and Rev sequences.

Subcloning of mutant H9 HA gene (cleavage site PIKETR) into the pCAGGS vector was accomplished through RE strategy as described in the Flow Chart in Appendix Figure 12. The SDM protocols were developed using a pl.18 vector backbone. Therefore, the SDM could not be performed when the HA genes were inserted into pCAGGS probably due to the different length of pCAGGS compared to pl.18. Overnight culture of the transformation product resulted in 3 colonies. Therefore, it was thought unnecessary to do a colony screen for such low numbers of clones.

7.3.4.2.3.3 Restriction enzyme digest of mutant clones DNA

Before sending the DNA plasmid material to be Sanger sequenced, the insert sizes were verified employing FastDigest® REs (Figure 142). Reactions were set up accordingly using the REs appropriate to the respective the cloning strategy.

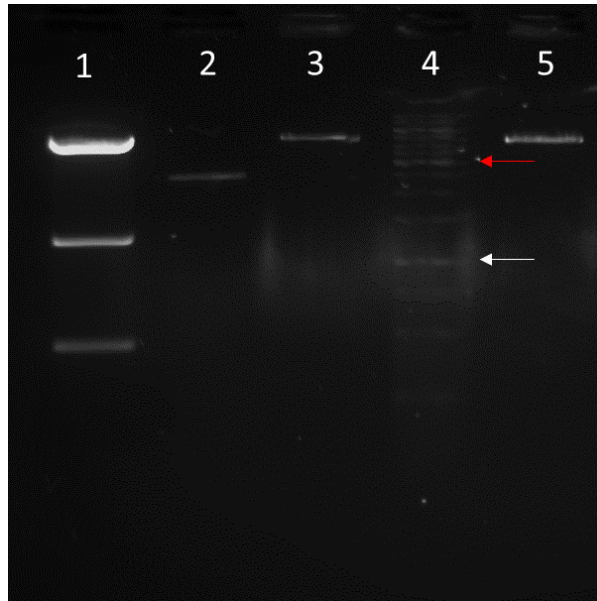


Figure 142: Control digestion of mutant H9 HA gene (PIKETR) into pCAGGS. Fragment sizes estimated by comparison to a GeneRuler 1 kb DNA Ladder. Cloning of the insert to the vector was confirmed by EcoRI-XhoI restriction digestion. In lane 1 two extra fragments were produced from digestion as EcoRI sites internal to H9 HA. An empty pCAGGS vector (lane 5) was included as digested vector (linearised) and runs as in control digestion. White and red arrows indicate 1 kb and 3 kb on DNA ladder.

7.3.4.2.3.4 Sequencing of plasmid DNA

Sanger sequencing was performed to verify all cloned gene sequences and particularly check the absence of mutations eventually occurred during the transformation process. pCAGGS FW and Rev primers (Table 7) were employed to verify the 5' and 3' end respectively (Figures 143-145).

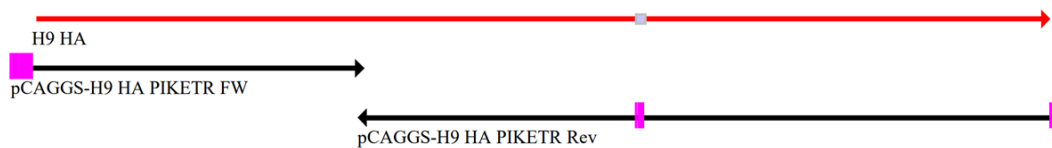


Figure 143: Alignment summary of mutant H9 HA gene (PIKETR) sequences. 5' and 3' sequencing of H9 HA cloned into pCAGGS vector, compared with the consensus reference sequence. No mutation was detected in the clone.

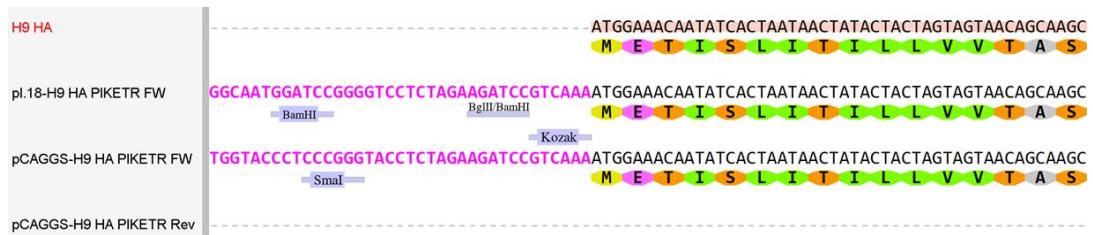


Figure 144: Mutant H9 HA gene (PIKETR) clone was sequenced using flanking pCAGGS FW primer. The 5' BglII/BamHI (AGATCC) and SmaI (CCCGGG) cloning sites are highlighted followed by the Kozak sequence (GTCAAA) upstream the ATG start codon.

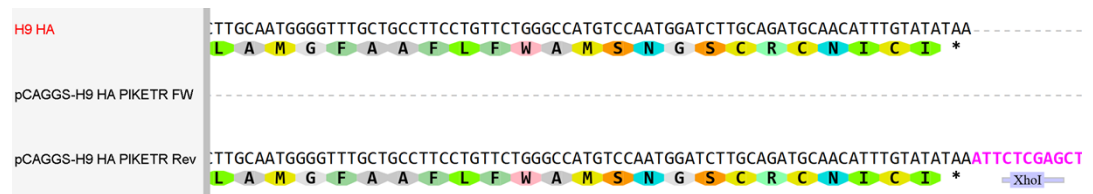


Figure 145: Mutant H9 HA gene (PARSSR) clone was sequenced using flanking pCAGGS Rev primer. On the reference sequence, the 3' XhoI cloning site (CTCGAG) is highlighted downstream the TAA stop codon.

7.3.4.2.4 Mutation of Kz52 and H9 HA cleavage site (PARSSR→PARKKR) in pl.18

7.3.4.2.4.1 Site Directed Mutagenesis

SDM to mutate the monobasic cleavage site into polybasic was accomplished by PCR following the QuikChange™ protocol detailed in Section 7.2.8. employing the appropriate SDM primers PARSSR→PARKKR designed for either WT Kz52, CO Kz52 or H9 HA (Appendix Table 3). 5 µL of PCR product was run on a 1% agarose gel to verify whether amplification of the DNA band occurred (Figure 146).

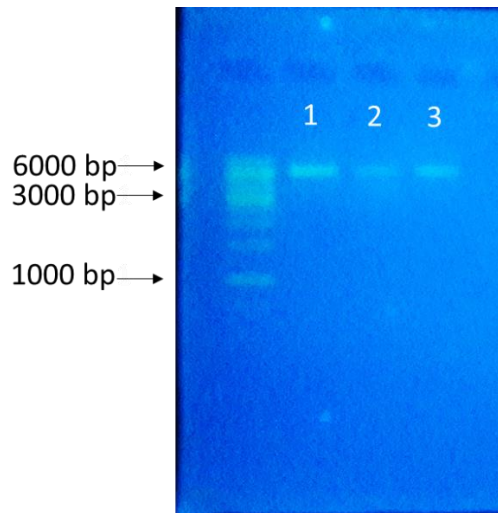


Figure 146: Amplification product of mutants WT and CO Kz52 HA and H9 HA PARKKR in pl.18. A band of Kz52 WT (lane 1), Kz52 CO (lane 2) and H9 (lane 3) are visible at ~6 kb estimated by comparison to a GeneRuler 1 kb DNA Ladder, meaning of successful DNA amplification. Picture was taken with a Samsung A6 camera.

7.3.4.2.4.2 Sequencing

Plasmid clone DNA was subsequently sent for sequencing to verify the correct base substitutions occurred during SDM (Figures 147-152).

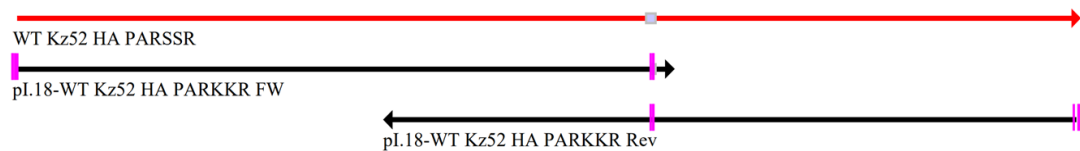


Figure 147: Alignment summary of mutant WT Kz52 HA gene PARKKR sequences. 5' and 3' sequencing of mutant WT Kz52 HA cloned into pl.18 vector, compared with the consensus reference sequence, to verify whether the mutation occurred in the desired position. No extra mutations were detected.

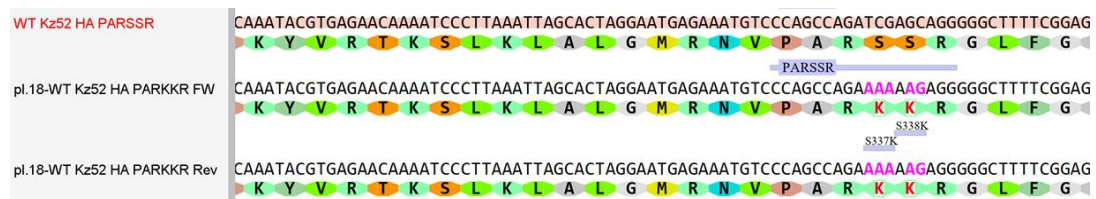


Figure 148: Mutant WT Kz52 HA gene PARKKR clone was sequenced using flanking pl.18 FW and Rev primers. On the reference sequence, the cleavage site PARSSR was highlighted. The desired mutations S337K and S338K were observed on both pl.18 FW and Rev sequences.

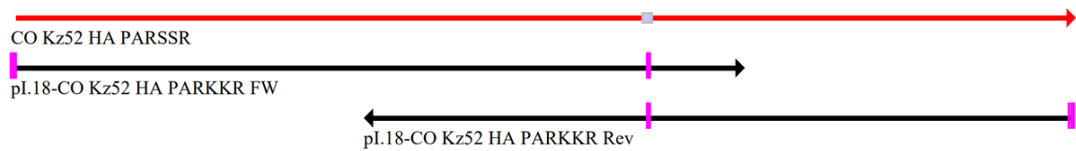


Figure 149: Alignment summary of mutant CO Kz52 HA gene PARKKR sequences. 5' and 3' sequencing of mutant CO Kz52 HA cloned into pI.18 vector, compared with the consensus reference sequence, to verify whether the mutation occurred in the desired position. No extra mutations were detected.



Figure 150: Mutant CO Kz52 HA gene PARKKR clone was sequenced using flanking pI.18 FW and Rev primers. On the reference sequence, the cleavage site PARKKR was highlighted. The desired mutations S337K and S338K were observed on both pI.18 FW and Rev sequences.



Figure 151: Alignment summary of mutant H9 HA gene PARKKR sequences. 5' and 3' sequencing of mutant H9 HA cloned into pI.18 vector, compared with the consensus reference sequence, to verify whether the mutation occurred in the desired position. No extra mutations were detected.

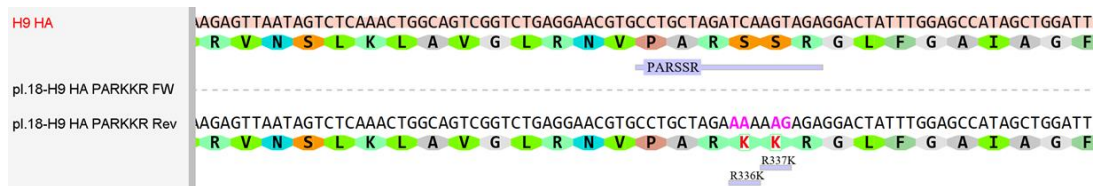


Figure 152: Mutant H9 HA gene PARKKR clone was sequenced using flanking pI.18 FW and Rev primers. On the reference sequence, the cleavage site PARKKR was highlighted. The desired mutations S336K and S337K were observed on both pI.18 FW and Rev sequences.

7.3.4.2.5 Mutation of Kz52 and H9 HA Kozak sequence (GTCAAA→GCCACC) in pl.18

7.3.4.2.5.1 Site Directed Mutagenesis

SDM to mutate the Kozak sequence upstream the ATG start codon was accomplished by PCR following the QuikChange™ protocol detailed in Section 7.2.8. employing the appropriate SDM primers GTCAAA→GCCACC designed for either WT Kz52, CO Kz52 or H9 HA (Appendix Table 4). 5 µL of PCR product was run on a 1% agarose gel to verify whether amplification of the DNA band occurred (Figure 153). Unfortunately, no image showing amplification of the mutant HA HA gene (Kozak) DNA migration pattern was recovered. Moreover, no colony after transformation was rescued due to cloning complications.

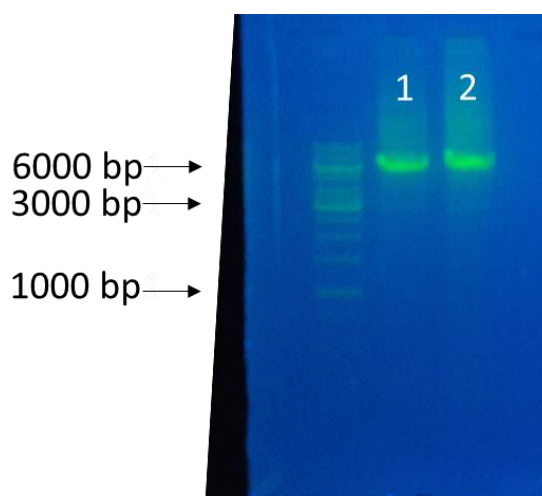


Figure 153: Amplification product of mutants WT and CO Kz52 HA KOZAK in pl.18. A band of Kz52 WT (lane 1) and CO (lane 2) are visible at ~6 kb estimated by comparison to a GeneRuler 1 kb DNA Ladder, meaning of successful DNA amplification. Picture was taken with a Samsung A6 camera.

7.3.4.2.5.2 Sequencing

Plasmid clone DNA was subsequently sent for sequencing to verify the correct base substitutions occurred during SDM (Figures 154-157).

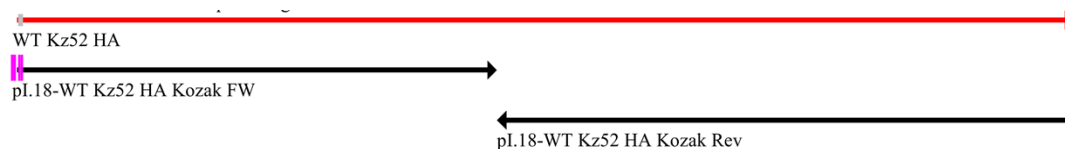


Figure 154: Alignment summary of mutant WT Kz52 HA gene Kozak sequences. 5' and 3' sequencing of mutant WT Kz52 HA cloned into pl.18 vector, compared with the consensus reference sequence, to verify whether the mutation occurred in the desired position. No extra mutations were detected.

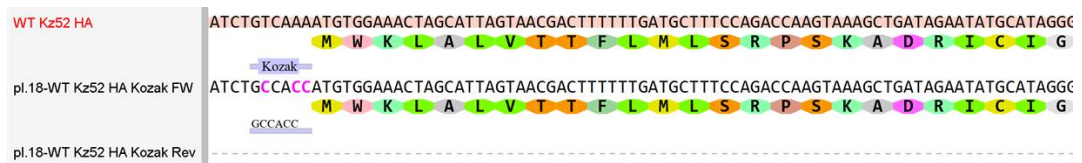


Figure 155: Mutant WT Kz52 HA gene Kozak clone was sequenced using flanking pl.18 FW and Rev primers. On the reference sequence, the cleavage site Kozak was highlighted before (GTCAAA) and after (GCCACC) SDM. The desired mutations to change the Kozak sequence into GCCACC were observed on pl.18 FW sequence only.

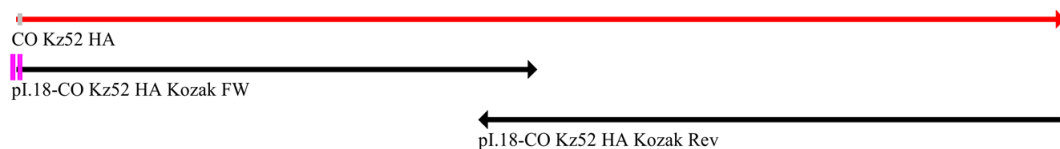


Figure 156: Alignment summary of mutant CO Kz52 HA gene Kozak sequences. 5' and 3' sequencing of mutant CO Kz52 HA cloned into pl.18 vector, compared with the consensus reference sequence, to verify whether the mutation occurred in the desired position. No extra mutations were detected.



Figure 157: Mutant WT Kz52 HA gene Kozak clone was sequenced using flanking pl.18 FW and Rev primers. On the reference sequence, the cleavage site Kozak was highlighted before (GTCAAA) and after (GCCACC) SDM. The desired mutations to change the Kozak sequence into GCCACC were observed on pl.18 FW sequence only.

7.3.5 Attempts to generate functional Kz52 PV particles

Many attempts were performed to generate Kz52 HA PV via different strategies as reported below. The production protocol to generate Kz52 PV was followed as described in Section 7.2.11. In all experiments, appropriate controls were included such as Δ env PV (no surface glycoprotein) and cell only to verify non specific GP binding and cells background respectively. To verify the correct performance of the titration assays, an H3 HA of A/canine/Colorado/30604/2006 (H3N2) was employed as positive control. Moreover, an H9 HA PV was generated as an additional positive control of a different influenza subtype (most closely related to Kz52; Figure 86). Generation of Kz52 PV was first attempted utilising the pCSemGW as the GFP reporter plasmid in transfections, later replaced with the pCSFLW for FLW expression in co-transfection as described in Section 7.2.11. pl.18-WT Kz52 HA and appropriate plasmids controls were employed to generate GFP expressing PVs. Both WT and

the CO Kz52 cloned in pl.18 alongside with pl.18-H9 HA were tested. GFP titration was set up following the instructions in Section 2.4. and after 48 hours incubation, the presence of green cells was visualised under a fluorescent microscope (Figure 158). Despite WT or CO Kz52 PV supernatants not showing HEK cell transduction, a high number of green cells were observed for H9 PV made with TMPRSS4 protease plasmid in transfection. Interestingly, a couple of green cells were detected also for H9 Δ prot PV (no protease plasmid added during co-transfection) suggesting that H9 HA was activated by proteases expressed by the target cells. No cells were detected in Δ env PV and cell only negative controls as suspected.

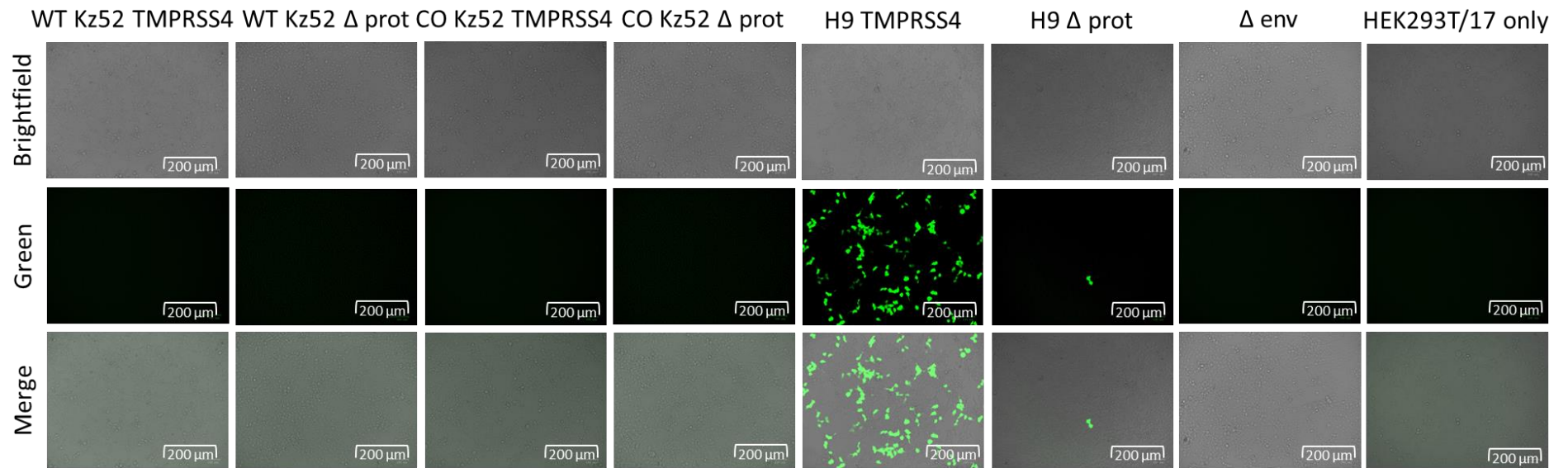


Figure 158: Green HEK293T/17 cells transduced with GFP Kz52 PVs. Transduction efficiency was tested with Kz52 PVs carrying either the WT or CO HA gene and generated either with or without protease plasmid (pCMV-Tag3-TMPRSS4). H9 PV generated with or without the TMPRSS4 protease plasmid (H9 TMPRSS4 or H9 Δ prot respectively), Δ env PV and cell only were included as controls. Images were taken at 20x on ZOE™ Fluorescent Cell Imager.

Following generation of GFP expressing PVs, a FLW version was generated. Again, the same attempts were performed by testing either the WT or CO Kz52 HA and also either cloned in pl.18 or pCAGGS. Different proteases-expressing plasmids (HAT, TMPRSS2 and TMPRSS4) were tested and added in co-transfection. The same strategies were followed to generate H9 and H3 PVs as positive controls for all the different conditions. This was to indicate if successful generation of PV occurred either when using alternative vector plasmids (pl.18 vs pCAGGS) but also to verify the ability of the different proteases to cleave and therefore activate the HA. FLW titrations were performed as previously described and results are reported in RLU/mL (Figures 159 and 160). PVs generated using no protease (Δ prot PVs) were also titrated adding TPCK-trypsin for 30 minutes as described in Section 7.2.13.1. TPCK-trypsin is routinely added in titration assays in order to activate and cleave influenza HAs (WHO, 2011) thus it was employed in this study as control to indicate efficient HA activation. An unpaired t-test was employed for statistical purposes. Interestingly, H9 and H3 TPCK-trypsin PVs yielded a significantly higher titre than PVs produced with protease plasmid ($p=0.0008$ compared to pl.18-H9 TMPRSS4 PV, $p<0.0001$ compared to pl.18-H3 HAT PV; Figure 159 Left graph) ($p=0.0003$ compared to pCAGGS-H3 HAT PV; Figure 159 Right graph) ($p=0.0007$ compared to pl.18-H9 TMPRSS4 PV, $p<0.0001$ compared to pl.18-H3 HAT PV; Figure 160 Left graph) ($p=0.0230$ compared to pCAGGS-H3 HAT PV; Figure 160 Right graph). In some situations, a significant difference between Δ prot PVs and the Δ env PV was reported ($p=0.0001$ for pl.18-H9 PVs; Figure 159 Left graph) ($p=0.0171$ for pl.18-H9 PVs; Figure 159 Left graph). This was proven in the GFP study (Figure 158) regarding H9 Δ prot PV able to transduce HEK293T cells, suggesting the presence of an endogenous protease expressed by the producer cell line able to cleave H9 HA. This was not tested using a GFP H3 Δ prot PV which revealed a significant difference in the FLW studies compared to the Δ env PV ($p=0.0033$ for pl.18-H3 PVs ; Figure 159 Left graph) ($p=0.0077$ for pl.18-H3 PVs; Figure 160 Right graph). To better verify this, a GFP titration could have been carried out by including an H3 Δ prot PV to investigate the ability of transduction.

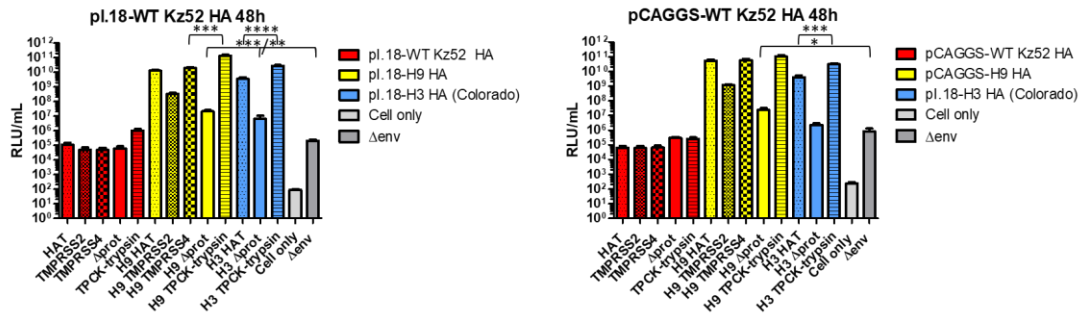


Figure 159: Titration results of WT Kz52 HA in *pl.18* and *pCAGGS*. HAT, TMPRSS2 or TMPRSS4 protease plasmids were included in transfection for HA cleavage. Δ prot PVs were titrated with or without TPCK-trypsin. Controls were included such as Δ env PV and cell only. **Left graph:** titration of Influenza PVs generated from HA genes cloned into *pl.18* vector. TPCK-trypsin PVs showed a significant difference against PV generated with a protease plasmid (** $p=0.0008$ or **** $p<0.0001$ for H9 and H3 respectively). H9 and H3 Δ prot PVs were significantly different than Δ env PV (** $p=0.0001$ and * $p=0.0033$ respectively). **Right graph:** titration of Influenza PVs generated from HA genes cloned into *pCAGGS* vector. A significant difference was observed between H9 Δ prot PV and Δ env PV (* $p=0.0171$) and between H3 TPCK-trypsin treated and H3 HAT PVs (** $p=0.0003$). The final titre was the result of the average of triplicates.

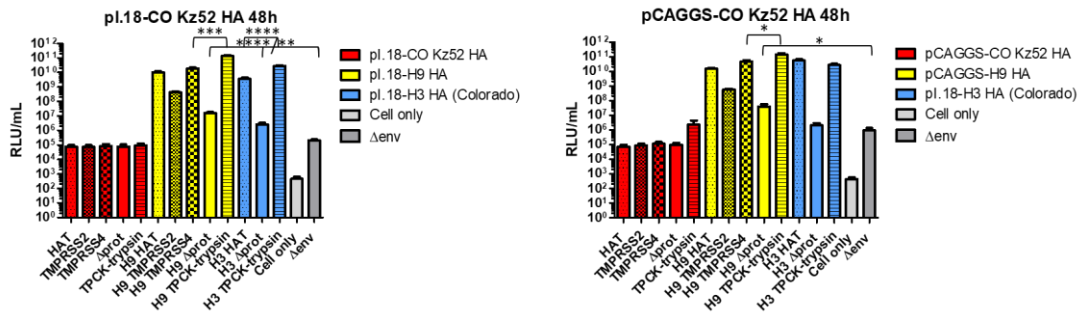


Figure 160: Titration results of CO Kz52 HA in *pl.18* and *pCAGGS*. HAT, TMPRSS2 or TMPRSS4 protease plasmids were included in transfection for HA cleavage. Δ prot PVs were titrated with or without TPCK-trypsin. Controls were included such as Δ env PV and cell only. **Left graph:** titration of Influenza PVs generated from HA genes cloned into *pl.18* vector. TPCK-trypsin PVs showed a significant difference against PV generated with a protease plasmid (** $p=0.0007$ or **** $p<0.0001$ for H9 and H3 respectively). H9 and H3 Δ prot PV was significantly different than Δ env PV (**** $p<0.0001$ and ** $p=0.0077$ respectively). **Right graph:** titration of Influenza PVs generated from HA genes cloned into *pCAGGS* vector. H9 PVs were again successful, unlike all the Kz52 PVs protease combinations. A significant difference was observed between H9 Δ prot PV and Δ env PV (* $p=0.0460$) and between H9 TPCK-trypsin and H9 HAT PVs (* $p=0.0230$). The final titre was the result of the average of triplicates.

7.3.5.1 Effect of Trypsin (TPCK-treated) at different incubation times

TPCK-trypsin treatment was modified by extending the incubation time at 60, 90 and 120 minutes to ascertain if the incubation time had an effect on the HA cleavage (Section

7.2.13.1.). Figures 161 and 162 show all the possible combinations of either WT or CO Kz52 cloned either in pl.18 or pCAGGS. Even extending the time of the TPCK-trypsin treatment we were not able to rescue any Kz52 PVs, as determined by titration. On the other hand, H9 PV titre was constant among all the different treatment time conditions. Thus, it can be assumed that the 30 minutes treatment was enough to rescue the highest PV titre possible. Another interesting observation, H9 Δ prot PV treated with TPCK-trypsin showed a higher titre than the H9 TMPRSS4 PV (Figures 161 and 162 Left graphs) suggesting that TPCK-trypsin more efficiently cleaved the H9 HA than the protease expressed from a plasmid during the transfection protocol.

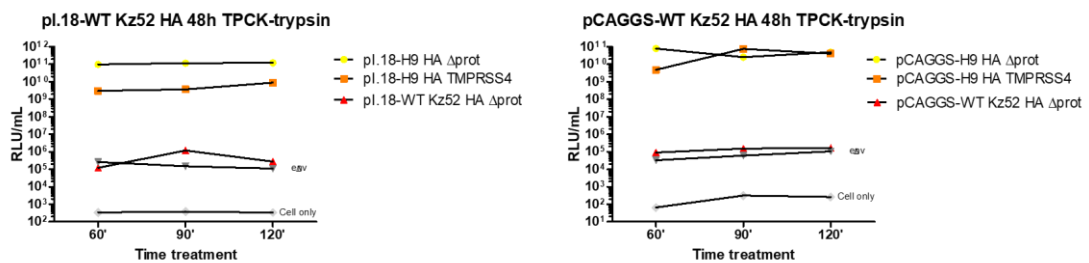


Figure 161: TPCK-trypsin titration of WT Kz52 HA in pl.18 and pCAGGS. Δ prot PVs were titrated with TPCK-trypsin for 60', 90' and 120'. Controls were included such as H9 TMPRSS4, Denv PV and cell only. **Left graph:** titration of Influenza PVs generated from HA genes cloned into pl.18 vector. H9 Δ prot PV was successfully activated with no titre difference among the different incubation times. On the contrary, no titre for Kz52 was rescued. **Right graph:** titration of Influenza PVs generated from HA genes cloned into pCAGGS vector. H9 Δ prot PV was once again successful. The final titre was the result of the average of triplicates.

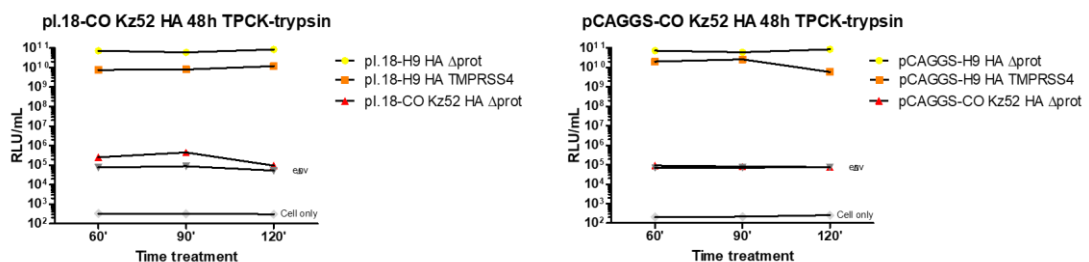


Figure 162: TPCK-trypsin titration of CO Kz52 HA in pl.18 and pCAGGS. Δ prot PVs were titrated with TPCK-trypsin for 60', 90' and 120'. Controls were included such as H9 TMPRSS4, Denv PV and cell only. **Left graph:** titration of Influenza PVs generated from HA genes cloned into pl.18 vector. H9 Δ prot PV was successfully activated with no titre difference among the different incubation times. On the contrary, no titre for Kz52 was rescued. **Right graph:** titration of Influenza PVs generated from HA genes cloned into pCAGGS vector. H9 Δ prot PV was once again successful. The final titre was the result of the average of triplicates.

7.3.5.2 Effect of KLK-5, TMPRSS3 and TMPRSS6 proteases

The different protease-expressing plasmids employed so far (HAT, TMPRSS2 and TMPRSS4) added in co-transfection were not able to efficiently cleave Kz52 HA. Another attempt to generate Kz52 PV was carried on by employing novel protease plasmids: KLK-5, TMPRSS3 and TMPRSS6. PV production was assessed using the WT Kz52 HA either cloned in pl.18 or pCAGGS first (Figure 163). H9 TMPRSS4 PV was used as control of correct performance of the titration assay.

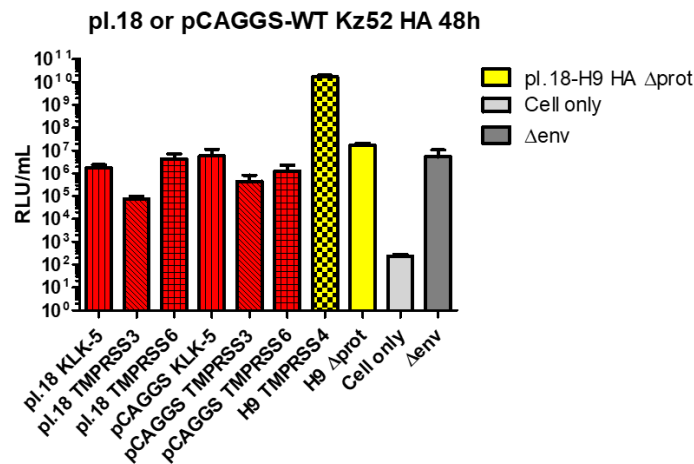


Figure 163: Contribution of KLK-5, TMPRSS3 and TMPRSS6 proteases for WT KZ52 PVs. Titration results of WT Kz52 HA in pl.18 or pCAGGS produced with KLK-5, TMPRSS3 and TMPRSS6 proteases plasmids. Control samples are indicated in the inset key. The final titre was the result of the average of triplicates.

Since no Kz52 significant PV titre was attained using the WT HA sequence, PV production was also assessed employing a CO Kz52 HA cloned either in pl.18 or pCAGGS. In order to assess the ability of the novel proteases to cleave efficiently the HA on the PV during the maturation process. The H9 HA was used as a control in the experiment. Therefore, H9 PV generation was attempted using pl.18 or pCAGGS expression vectors assessed using novel proteases (Figure 164). The H9 PV produced using TMPRSS4 (H9 TMPRSS4 PV) was once again used as control. As depicted in the figures, the novel proteases resulted in no difference in titre when compared to H9 Δprot PV indicating minor or no role of these proteases in the cleavage of H9 HA. Interestingly a significant difference is observed between the H9 PVs produced with the novel proteases and the Δenv PV ($p=0.0003$ for pl.18-H9 KLK-5; Figure 164 Left graph) ($p=0.0002$ for pCAGGS-H9 KLK-5; Figure 164 Right graph). However, this could be independent from of the different proteases to cleave H9 HA but possibly proteases endogenously expressed by the target cell line able to do so. Another way, the expression of

the protease plasmids could be evaluated by confocal microscopy using antibodies against the HA reference antiserum and verify the HA cleavage of H9 PV by the proteases a Western blotting could be performed.

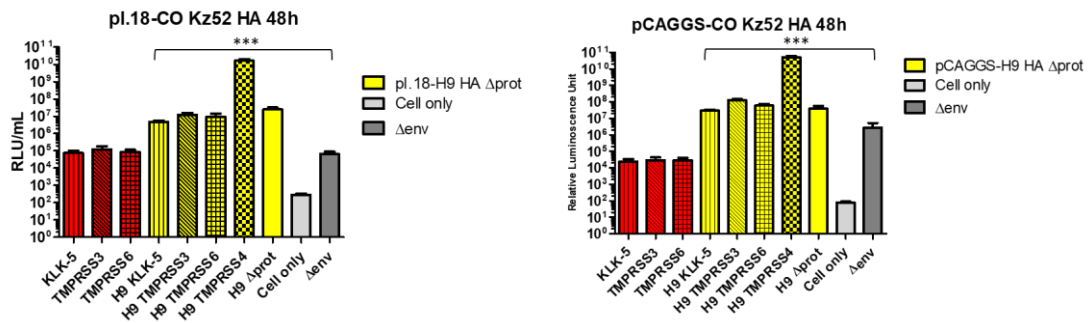


Figure 164: Contribution of KLK-5, TMPRSS3 and TMPRSS6 proteases for CO KZ52 PVs. Control samples are indicated in the inset key. **Left graph:** titre results of CO Kz52 (red columns) and H9 PVs expressed from pl.18 produced with KLK-5, TMPRSS3 and TMPRSS6 protease plasmids. Comparison of the different H9 PVs produced with different proteases compared with H9 Δprot shows no difference. A significant difference was observed between H9 KLK-5 and Δenv PVs (***p*=0.0003) **Right graph:** titre results of CO Kz52 and H9 PVs expressed from pCAGGS produced with KLK-5, TMPRSS3 and TMPRSS6. Again, the different proteases had no impact on H9 PVs production. A significant difference was observed between H9 KLK-5 and Δenv PVs (***p*=0.0002). The final titre was the result of the average of triplicates.

7.3.5.3 Target cell entry study

MDCK I & II are well-established cell lines widely used for the propagation of wild type influenza viruses (WHO, 2011). Therefore, those cell lines were employed as target cells in a FLW titration to investigate the potential for transduction with Kz52 PV, under different conditions. The WT and CO Kz52 HA cloned in pl.18 co-transfected with either HAT, TMPRSS2 or TMPRSS4 protease plasmids or without (Δprot) were employed to generate PVs. H9 TMPRSS4 and Δprot PV were included alongside with controls H3 HAT and Δprot PV as controls. PVs were serially diluted and either MDCK I (Figure 165) or MDCK II (Figure 166) were added to the assay. Δprot PVs were also titrated with TPCK-trypsin treated for 30 minutes as described in Section 7.2.13.1. Results are reported in RLU/mL. Despite no titre being measured for Kz52 PVs, H9 and H3 were successfully produced, as revealed by titration on both/at least one test target cell lines. An unpaired t-test on the MDCK I studies (Figure 165) revealed that there was a significant difference in titre between H9 and H3 TPCK-trypsin PVs and PV produced with protease plasmid (*p*=0.0004 or *p*<0.0001 for H9 and H3 respectively) and between H9 Δprot PV and Δenv PV (*p*=0.0009). In the MDCK II studies

(Figure 166), only H9 PVs yielded a significant titre. Indeed, H9 TPCK-trypsin PV showed a significant difference against H9 TMPRSS4 PV ($p=0.0073$), while H9 Δ prot PV was significantly different than Δ env PV ($p=0.0009$). These findings were confirmed in the GFP study regarding H9 Δ prot PV ability to transduce MDCK II cells, but not MDCK I as seen for the FLW version (Appendix Figure 14).

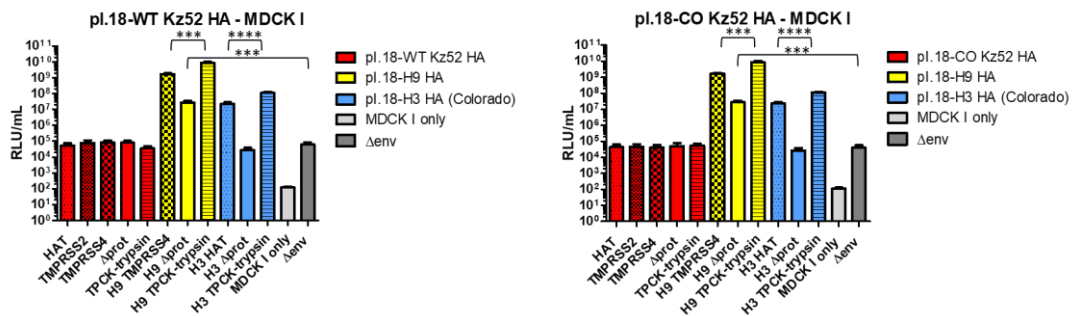


Figure 165: Titration results of WT and CO Kz52 HA in pl.18 on MDCK I. HAT, TMPRSS2 or TMPRSS4 protease plasmids were included in transfection for HA cleavage. Δ prot PVs were titrated with or without TPCK-trypsin. Controls were included such as Δ env PV and cell (MDCK I) only. **Left graph:** titration of WT Kz52 HA PVs. TPCK-trypsin PVs showed a significant difference against PV generated with a protease plasmid (** $p=0.0004$ or **** $p<0.0001$ for H9 and H3 respectively). H9 Δ prot PV was significantly different than Δ env PV (** $p=0.0009$). **Right graph:** titration of CO Kz52 HA PVs. TPCK-trypsin PVs showed a significant difference against PV generated with a protease plasmid (** $p=0.0004$ or **** $p<0.0001$ for H9 and H3 respectively). H9 Δ prot PV was significantly different than Δ env PV (** $p=0.0008$). The final titre was the result of the average of triplicates.

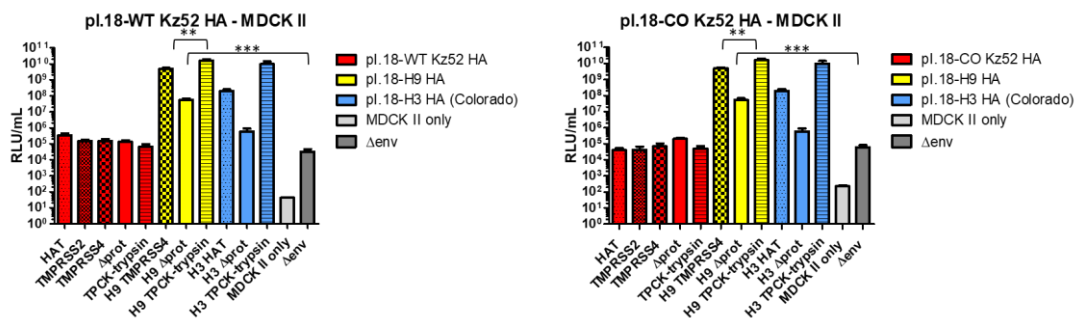


Figure 166: Titration results of WT and CO Kz52 HA in pl.18 on MDCK II. HAT, TMPRSS2 or TMPRSS4 protease plasmids were included in transfection for HA cleavage. Δ prot PVs were titrated with or without TPCK-trypsin. Controls were included such as Δ env PV and cell (MDCK II) only. **Left graph:** titration of WT Kz52 HA PVs. H9 TPCK-trypsin PV showed a significant difference against H9 TMPRSS4 PV (** $p=0.0073$). H9 Δ prot PV was significantly different than Δ env PV (** $p=0.0009$). **Right graph:** titration of CO Kz52 HA PVs. H9 TPCK-trypsin PV showed a significant difference against H9 TMPRSS4 PV (** $p=0.0073$). H9 Δ prot PV was significantly different than Δ env PV (** $p=0.0009$). The final titre was the result of the average of triplicates.

An avian origin cell line (DEF) was investigated for entry of Kz52 PV since the virus itself was first isolated from an *Aythya farina* duck. GFP expressing PVs were produced either with WT or CO Kz52 HA cloned in pl.18 with or without TMPRSS4 protease plasmid. PVs were serially diluted in a GFP titration as previously described in Section 7.2.13. and scrutinised under a fluorescent microscope after 48 hours. An H9 TMPRSS4 and Δ prot PVs were included as controls, plus Δ env PV and cell only for background controls (Appendix Figure 14). Assuming any functional particles produced, Kz52 PV was not able to transduce DEF cell either despite its avian origin. A reasonable number of green cells were observed for H9 PV transduced DEF cells for both TMPRSS4 or Δ prot PV. As expected no green cell was detected in the Δ env PV control. A FLW PV version could have been generated to have a complete picture of this target cell line study, but it was not seemed necessary given the GFP results. Another avian cell line routinely used for WT influenza studies is CEF cells. It would have been an appropriate candidate to test Kz52 PV entry, but unfortunately the primary cell line was problematic to cultivate.

TMPRSS2 is well known to facilitate entry of influenza viruses into host cells by proteolytically cleaving and activating the viral envelope glycoprotein HA. ACE2 has been demonstrated to play a critical role in Influenza A in terms of development and progression of AIV induced lung pathologies in mice (Yang *et al.*, 2014). Thus, HEK293T expressing ACE2 and TMPRSS2 were employed as target to investigate Kz52 PV transduction. Kz52 PVs were generated with either WT or CO Kz52 HA cloned in pl.18 co-transfected with or without TMPRSS4 protease plasmids. H9 TMPRSS4 and Δ prot PV were included as controls. FLW titration was set up as previously described in Section 2.4. and titres read 48 hours post-incubation and reported in RLU/mL (Figure 167). No titre above Δ env PV was noted for Kz52 PVs. A titration with naïve HEK293T should have been performed in parallel for control purposes and to compare attained H9 PV titres.

pl.18-WT or CO Kz52 HA on HEK293T+ACE2+TMPRSS2

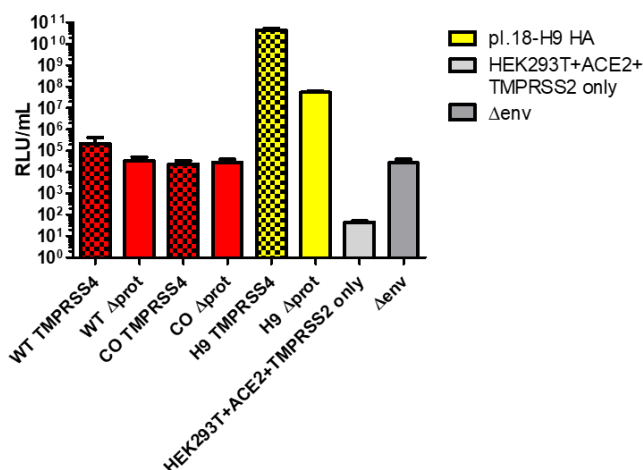


Figure 167: Titration results on HEK293T expressing ACE2 and TMPRSS2. WT or CO Kz52 PVs expressed from pl.18, with or without TMPRSS4 protease plasmid. Control samples are indicated in the inset key. The final titre was the result of the average of triplicates.

7.3.5.4 Site Directed Mutagenesis

7.3.5.4.1 Kz52 PV titre with mutated HA cleavage site (PIKETR→PIKSTR)

None of the strategies above managed to produce a functional Kz52 PV titre. The Kz52 HA possesses a mono-basic cleavage site, which would need to be protease cleaved for maturation of the HA to produced an infectious viral particle. Therefore, it was analysed and by aligning the gene with its closest relative subtype H9 it was recognised to be completely different from that of H9 (PIKETR↓GLF and PARSSR↓GLF respectively as shown in Figure 168). A study by Tse and Whittaker (2015) revealed the amino acids frequency at HA cleavage site of 3,019 H9N2 virus isolate sequences from the NCBI influenza database, showing high conservation and a PARSSR consensus. The WebLogo (Figure 169) showed the amino acid S in position 336 seemed to be highly conserved among the 3,019 isolates. It was then questioned whether changing Kz52 cleavage site to make it more similar to H9 would have helped to produce PV, knowing which proteases could cleave this site. Thus, Kz52 cleavage site was first changed from PIKETR into PIKSTR using a SDM strategy (Figures 119-122 demonstrate the mutation occurred at the desired position). PV production was evaluated by testing WT or CO Kz52 HA only cloned in pl.18 vector, but unfortunately this had no impact on the titre (Figure 170). Δprot PVs were also titrated with the addition of TPCK-trypsin for 30, 60, 90 and 120 minutes (Figure 171). The treatment had no impact either on the titre. On the other hand, high titres for H9 PVs were produced and they were constant among all the

different treatment time conditions. Thus, it can be assumed that the 30 minutes treatment was enough to rescue the highest PV titre possible as previously observed.

| | Cleavage site | Fusion peptide |
|--------------|---------------|----------------------|
| | | P2P1 P1' |
| H9 consensus | -PARRSR | GLFGAIAGFIEGGWPLVAGW |
| Kz52 | .IKET. | GLFGAIAGFIEGGWPLVAGW |

Figure 168: Sequence alignment of H9 HA and Kz52 HA. Cleavage site and fusion peptides are highlighted.

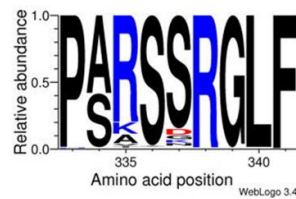


Figure 169: Amino acid motif and conservation of the hemagglutinin cleavage site. WebLogo showing the amino acids frequency at HA cleavage site of 3019 H9N2 virus isolates. Source: Tse and Whittaker, 2015.

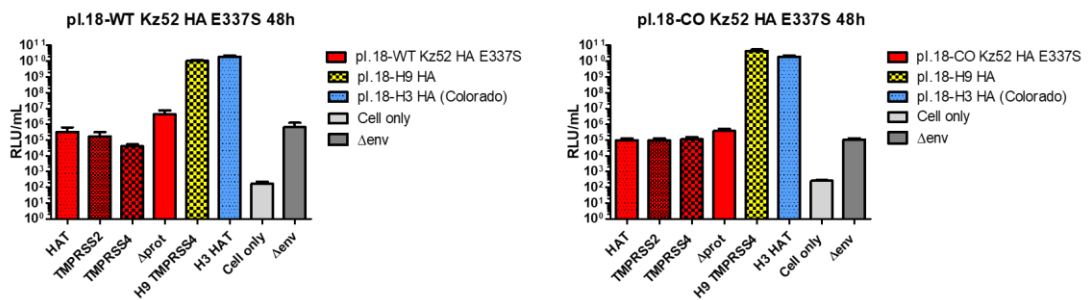


Figure 170: Titration results of mutants WT and CO Kz52 E337S HA in pl.18. Control samples are indicated in the inset key. **Left graph:** titration results of mutant WT Kz52 E337S HA. **Right graph:** titration results of mutant CO Kz52 E337S HA. The final titre was the result of the average of triplicates.

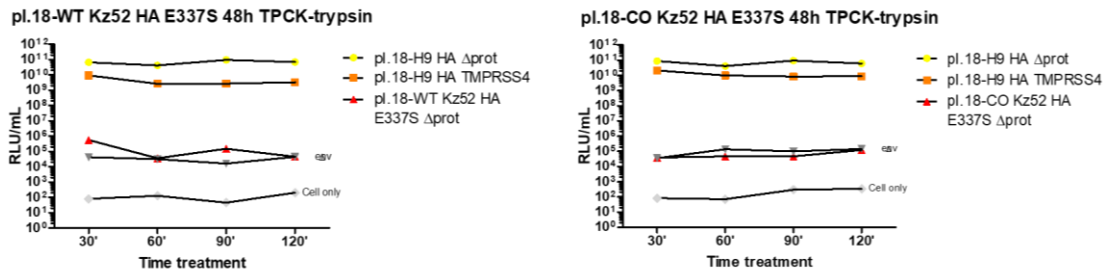


Figure 171: TPCK-trypsin titration of mutants WT and CO Kz52 E337S HA in pl.18. Δ prot PVs were titrated with TPCK-trypsin for 30', 60', 90' and 120'. Controls were included such as H9 TMPRSS4, Δ env PV and cell only. **Left graph:** titration of mutant WT Kz52 E337S Δ prot PV. H9 Δ prot PV was successfully activated with no titre difference among the different incubation times. On the contrary, no titre for Kz52 was rescued. **Right graph:** titration of mutant CO Kz52 E337S Δ prot PV. H9 Δ prot PV was once again successful. The final titre was the result of the average of triplicates.

E337S mutants were also tested on MDCK I & II cell lines since, as stated earlier, these cell lines are widely used for the propagation of influenza viruses. The previous strategies were applied in order to perform a FLW titration of mutant PVs. Although these well-established cell lines were used, no transduction was detected (Figures 172 and 173). H9 and H3 PVs were once again successful in transduction of both MDCK cell lines with higher levels of transduction achieved in MDCK II cells in terms of RLU/mL. Δ prot PVs were also titrated with TPCK-trypsin treated for 30 minutes as described in Section 7.2.13.1. An unpaired t-test on the MDCK I studies (Figure 172) revealed that there was a significant difference in titre between H9 and H3 TPCK-trypsin PVs and PV produced with protease plasmid ($p=0.0004$ or $p<0.0001$ for H9 and H3 respectively) and between H9 Δ prot PV and Δ env PV ($p=0.0009$). In the MDCK II studies (Figure 173), only H9 PVs yielded a significant titre. Indeed, H9 TPCK-trypsin PV showed a significant difference against H9 TMPRSS4 PV ($p=0.0073$), while H9 Δ prot PV was significantly different than Δ env PV ($p=0.0009$). These findings were confirmed in the GFP study regarding H9 Δ prot PV able to transduce MDCK II cells, but not MDCK I as observed for the FLW version (Appendix Figure 14).

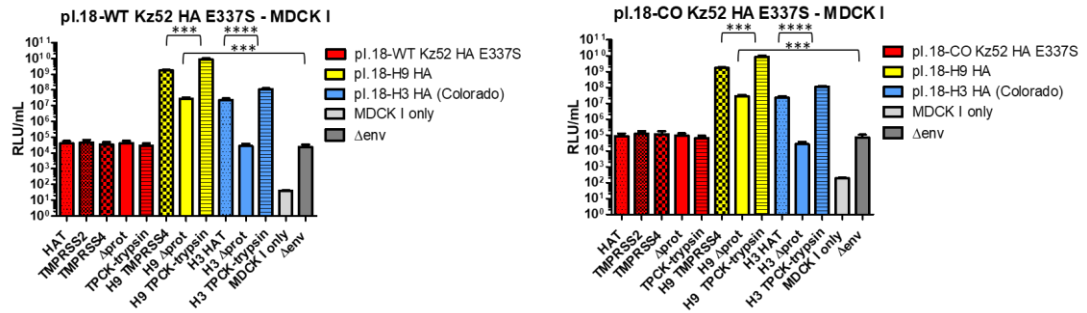


Figure 172: Titration results of mutants WT and CO Kz52 E337S HA in pl.18 on MDCK I. HAT, TMPRSS2 or TMPRSS4 protease plasmids were included in transfection for HA cleavage. Δ prot PVs were titrated with or without TPCK-trypsin. Controls were included such as Δ env PV and cell (MDCK I) only. **Left graph:** titration of mutant WT Kz52 E337S HA PVs. TPCK-trypsin PVs showed a significant difference against PV generated with a protease plasmid (** $p=0.0004$ or **** $p<0.0001$ for H9 and H3 respectively). H9 Δ prot PV was significantly different than Δ env PV (** $p=0.0009$). **Right graph:** titration of mutant CO Kz52 E337S HA PVs. TPCK-trypsin PVs showed a significant difference against PV generated with a protease plasmid (** $p=0.0004$ or **** $p<0.0001$ for H9 and H3 respectively). H9 Δ prot PV was significantly different than Δ env PV (** $p=0.0008$). The final titre was the result of the average of triplicates.

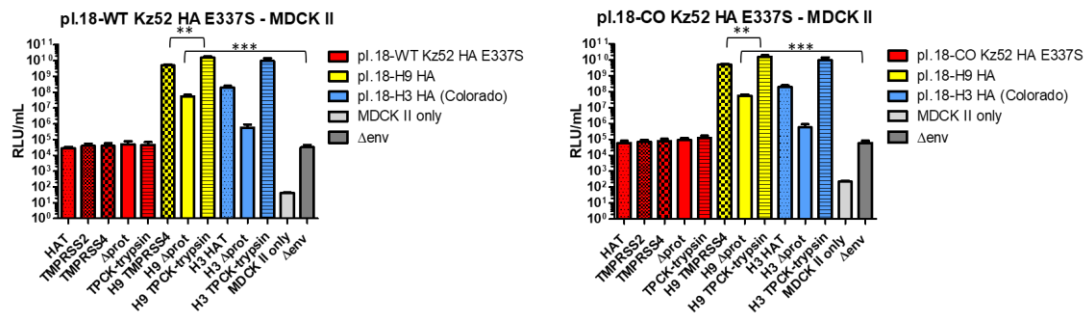


Figure 173: Titration results of mutants WT and CO Kz52 E337S HA in pl.18 on MDCK II. HAT, TMPRSS2 or TMPRSS4 protease plasmids were included in transfection for HA cleavage. Δ prot PVs were titrated with or without TPCK-trypsin. Controls were included such as Δ env PV and cell (MDCK II) only. **Left graph:** titration of WT Kz52 HA PVs. H9 TPCK-trypsin PV showed a significant difference against H9 TMPRSS4 PV (** $p=0.0073$). H9 Δ prot PV was significantly different than Δ env PV (** $p=0.0009$). **Right graph:** titration of CO Kz52 HA PVs. H9 TPCK-trypsin PV showed a significant difference against H9 TMPRSS4 PV (*** $p=0.0073$). H9 Δ prot PV was significantly different than Δ env PV (*** $p=0.0009$). The final titre was the result of the average of triplicates.

7.3.5.4.2 Kz52 PV titre with mutated HA cleavage site (PIKSTR→PARSSR)

Since the single amino acid mutation (E337S) was not effective in rescuing Kz52 PV titre, Kz52 HA cleavage site was completely mutated to make it like H9. Starting from the already mutated clones E337S (PIKETR→PIKSTR) the cleavage site was changed into PARSSR, as

found to be the most frequent amino acids cleavage site in H9N2 virus isolates and in the H9 HA clone sequence employed so far (Figure 169). Only mutants WT and CO Kz52 E337S HA cloned into pl.18 successfully mutated using an in-house SDM protocol as all the PCR conditions tested did not produce the desired mutation when HA genes were cloned into pCAGGS. The new mutants WT or CO Kz52 HA PARSSR (with H9 cleavage site) were subsequently subcloned from pl.18 into pCAGGS using a molecular strategy with REs (depicted as Flow Charts in Appendix Figures 9 and 11). PV production was tested using either the mutant WT or CO version cloned in either pl.18 or pCAGGS employing a similar approach as previously done and Figures 174 and 175 show all the different combinations. Unfortunately, even mutating the whole cleavage site of Kz52 HA to make it identical to the H9 one employed as our positive control did not result in any functional titre.

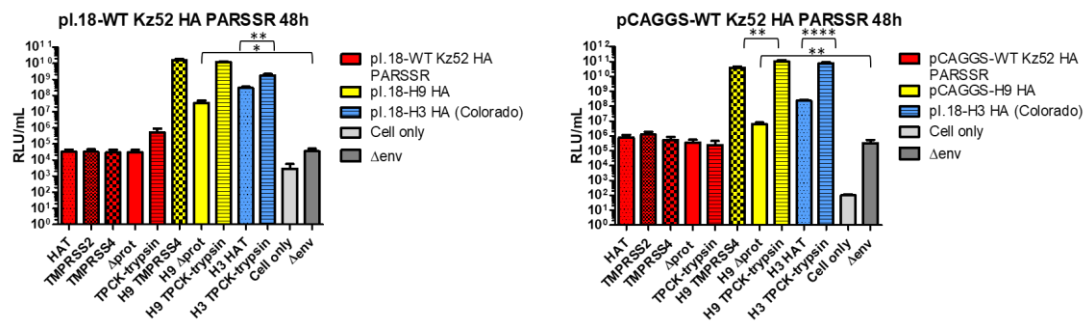


Figure 174: Titration results of mutant WT Kz52 HA PARSSR in pl.18 and pCAGGS. HAT, TMPRSS2 or TMPRSS4 protease plasmids were included in transfection for HA cleavage. Δ prot PVs were titrated with or without TPCK-trypsin. Controls were included such as Δ env PV and cell only. **Left graph:** titration of Influenza HA PVs expressed from pl.18. H3 TPCK-trypsin PV showed a significant difference against H3 HAT PV (** $p=0.0019$). H9 Δ prot PV was significantly different than Δ env PV (* $p=0.0399$). **Right graph:** titration of Influenza HA PVs expressed in pCAGGS (exception of H3 HA). TPCK-trypsin PVs showed a significant difference against PV generated with a protease plasmid (** $p=0.0085$ or **** $p<0.0001$ for H9 and H3 respectively). H9 Δ prot PV was significantly different than Δ env PV (** $p=0.0071$). The final titre was the result of the average of triplicates.

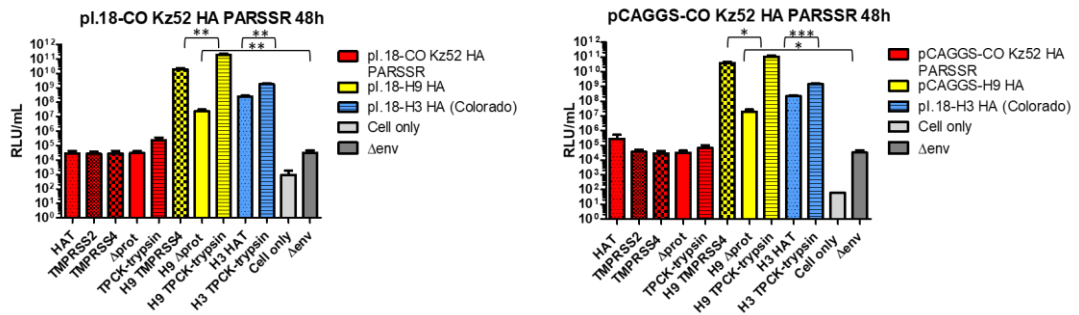


Figure 175: Titration results of mutant CO Kz52 HA PARSSR in pl.18 and pCAGGS. HAT, TMPRSS2 or TMPRSS4 protease plasmids were included in transfection for HA cleavage. Δ prot PVs were titrated with or without TPCK-trypsin. Controls were included such as Δ env PV and cell only. **Left graph:** titration of Influenza HA PVs expressed from pl.18. TPCK-trypsin PVs showed a significant difference against PV generated with a protease plasmid (** $p=0.0029$ or **** $p=0.0010$ for H9 and H3 respectively). H9 Δ prot PV was significantly different than Δ env PV (** $p=0.0053$). **Right graph:** titration of Influenza HA PVs expressed in pCAGGS (exception of H3 HA). TPCK-trypsin PVs showed a significant difference against PV generated with a protease plasmid (* $p=0.0103$ or *** $p=0.0003$ for H9 and H3 respectively). H9 Δ prot PV was significantly different than Δ env PV (* $p=0.0382$). The final titre was the result of the average of triplicates.

7.3.5.4.3 H9 PV titre with mutated HA cleavage site (PARSSR→PIKETR)

In order to investigate whether the proteases employed so far to attempt to generate Kz52 PV were able to cleave its HA cleavage site (PIKETR↓GLF), the H9 HA cleavage site (PARSSR↓GLF) was mutated into the Kz52 HA one (PARSSR→PIKETR) as detailed in Section 7.2.7. and successful mutation was demonstrated in Figures 140 and 141. PVs of the mutant H9 HA PIKETR were generated for both pl.18 and pCAGGS versions and collected at both 48 and 72 hour post-transfection. HAT, TMPRSS2 or TMPRSS4 protease plasmids were included or not (Δ prot) in the co-transfection. A GFP titration was first performed employing PVs generated using pl.18 plasmids and collected at 48 hours post-transfection to verify the ability of the mutant to transduce HEK293T cells before performing a FLW titration. Many green cells were detected under a fluorescent microscope meaning that the common proteases were able to cleave the HA PIKETR↓GLF when present in the H9 backbone (example of mutant H9 HA PIKETR TMPRSS4 and Δ prot PVs in Figure 176 and in Appendix Figure 14).

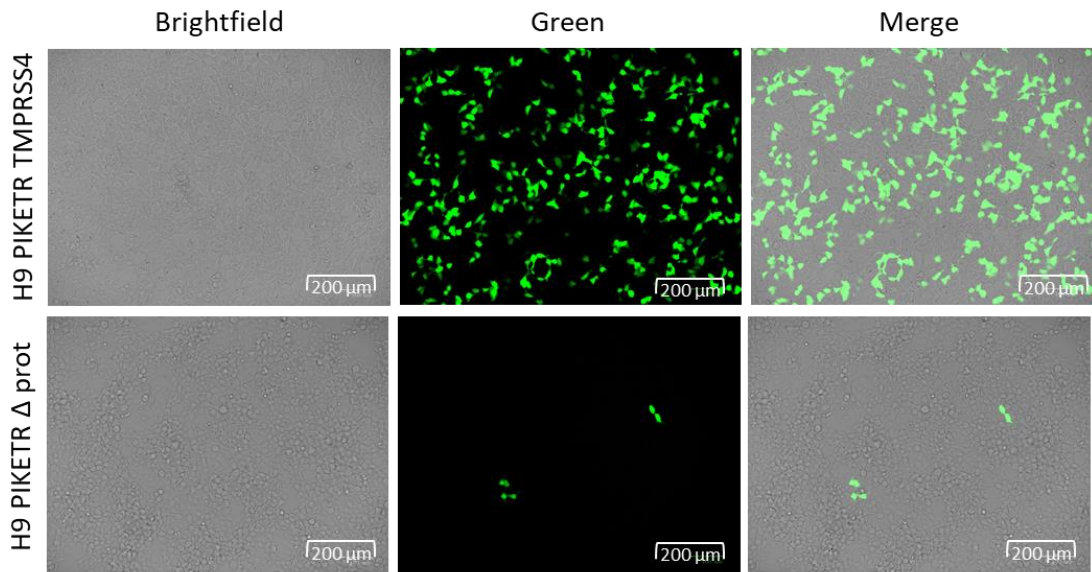


Figure 176: Green HEK293T/17 cells transduced with H9 HA PIKETR PVs. Transduction efficiency was tested with PVs generated either with or without TMPRSS4 protease plasmid (H9 PIKETR TMPRSS4 and H9 PIKETR Δ prot respectively). Images were taken at 20x on ZOE™ Fluorescent Cell Imager.

These results are reinforced by the FLW titration results (Figures 177 and 178). Δ prot PVs were also titrated with TPCK-trypsin treated for 30 minutes as described in Section 7.2.13.1. A significant difference was observed when mutant H9 HA PIKETR (with Kz52 HA cleavage site) PVs expressed in pl.18 were compared to WT H9 PVs ($p=0.0349$ for PVs generated with TMPRSS4 protease plasmid and $p<0.0001$ for TPCK-trypsin PVs collected at 48h; Figure 177 Left graph) ($p=0.0004$ for PVs generated with TMPRSS4 protease plasmid collected at 72h; Figure 177 Right graph) suggesting better transduction of the mutants in DEF cell. However, when mutant H9 HA PIKETR (with Kz52 HA cleavage site) PVs were expressed in pCAGGS, this was less observed, with the exception of PVs generated with TMPRSS4 protease plasmid collected at 72h ($p=0.0001$; Figure 178 Right graph). The outcome of these experiments not only confirmed that PIKETR \downarrow GLF can be cleaved by common proteases, but it reassured that a unique protease was not necessary to be employed to obtain activation. Secondly, it questioned whether Kz52 HA sequence had some other features, other than the precise cleavage site sequence, which did not allow the HA cleavage and activation, in other terms affecting the ability to successfully pseudotype.

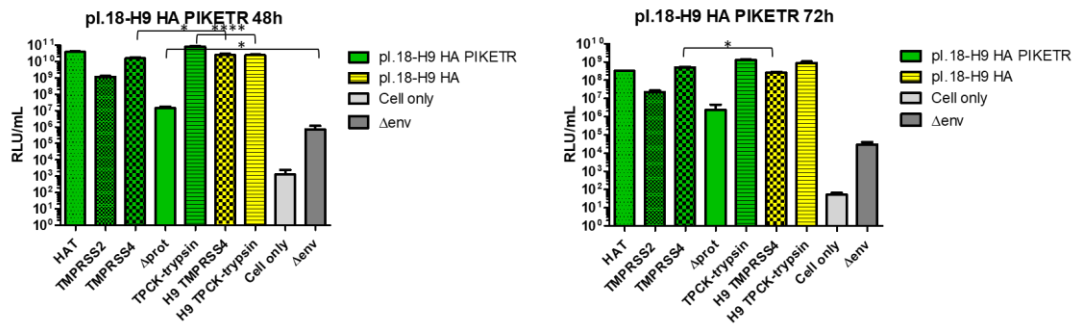


Figure 177: Titration results of mutant H9 HA PIKETR in pl.18. HAT, TMPRSS2 or TMPRSS4 protease plasmids were included in transfection for HA cleavage. Δ prot PVs were titrated with or without TPCK-trypsin. Controls were included such as WT H9 HA PVs, Δ env PV and cell only. **Left graph:** titration of PVs collected at 48h. Mutants H9 TMPRSS4 and TPCK-trypsin PVs showed a significant difference against their WT counterpart (* $p=0.0349$ and **** $p<0.0001$ respectively). Mutant H9 HA PIKETR Δ prot PV was significantly different than Δ env PV (* $p=0.0017$). **Right graph:** titration of PVs collected at 72h. Mutants H9 TMPRSS4 PV showed a significant difference against its WT counterpart (* $p=0.0004$). The final titre was the result of the average of triplicates.

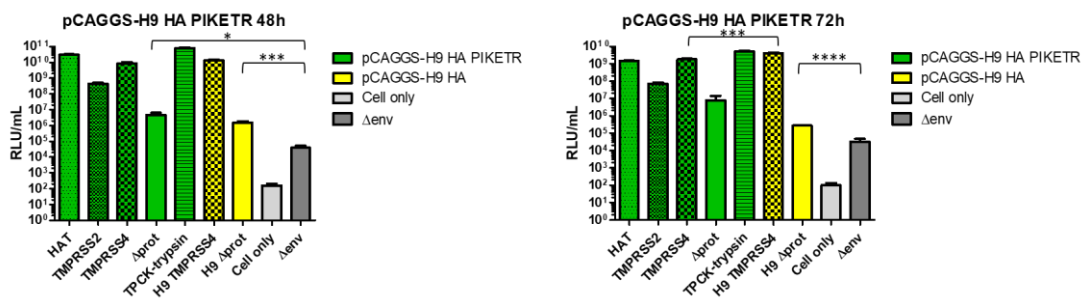


Figure 178: Titration results of mutant H9 HA PIKETR in pl.18. HAT, TMPRSS2 or TMPRSS4 protease plasmids were included in transfection for HA cleavage. Δ prot PVs were titrated with or without TPCK-trypsin. Controls were included such as WT H9 HA PVs, Δ env PV and cell only. **Left graph:** titration of PVs collected at 48h. Both mutant and WT Δ prot PVs showed a significant difference against Δ env PV (* $p=0.0145$ and *** $p=0.0002$ respectively). **Right graph:** titration of PVs collected at 72h. A significant difference was observed between mutant H9 TMPRSS4 PV and its WT counterpart (***) $p=0.0001$ and between WT Δ prot PVs and Δ env PV (**** $p<0.0001$). The final titre was the result of the average of triplicates.

DEF cells were also tested for transduction of the mutant H9 HA PIKETR PV in order to investigate whether DEF cells were able to cleave PIKETR (Kz52 HA cleavage site) via endogenous proteases. The pl.18 and pCAGGS version of H9 mutants were both employed in the FLW titration alongside with WT H9 PVs controls. Both H9 mutant and WT Δ prot PVs were also titrated with TPCK-trypsin treated for 30 minutes as described in Section 7.2.13.1. A Δ env PV and cell only (DEF only) controls were included for background luminescence not

attributed to glycoprotein-specific mediated entry and cells background (Figure 179). The mutant H9 HA PIKETR PV was able to transduce DEF cells in high titres. There was no significant difference among mutants and WT PV titres, with an exception when mutant H9 TPCK-trypsin PV was compared to the WT counterpart ($p=0.0022$ for expression in pl.18 and $p=0.0111$ for expression in pCAGGS). Another interesting finding was the ability of Δ prot PVs to transduce DEF cells suggesting a protease endogenously expressed by that cell line able to activate Kz52 via the HA cleavage site. But only the mutant expressed in pl.18 showed a significant difference when compared to Δ env PV ($p=0.0204$). WT H9 Δ prot PV was significantly different than Δ env PV ($p=0.0122$). Since Kz52 cleavage site (PIKETR) in H9 HA was cleaved easily it might be a possibility that other features in Kz52 HA sequence were not permitting its HA cleavage, and thus need further testing.

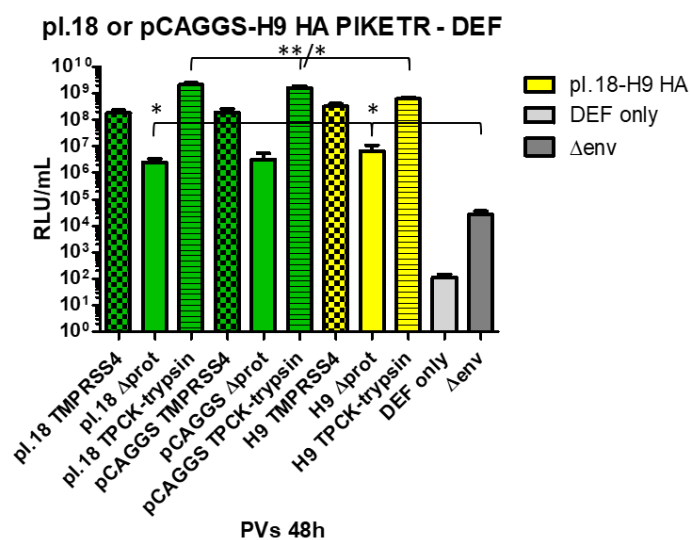


Figure 179: Titration results of mutant H9 HA PIKETR in pl.18 and pCAGGS in DEF cells. TMPRSS4 protease plasmids was included in transfection for HA cleavage. Δ prot PVs were titrated with or without TPCK-trypsin. Control samples are indicated in the inset key. Only mutant H9 Δ prot PV expressed in pl.18 showed a significant difference against Δ env PV ($* p=0.0204$) and between WT H9 Δ prot PV and Δ env PV ($* p=0.0122$). Mutants TPCK-trypsin treated PVs showed a significant difference against their WT counterpart ($** p=0.0022$ and $* p=0.0111$ for expression in pl.18 and pCAGGS respectively). The final titre was the result of the average of triplicates.

7.3.5.4.4 Polybasic cleavage site testing

A final investigation on Kz52 HA cleavage site was performed by mutating the monobasic cleavage site into a polybasic one (PARKKR↓GLF) to investigate whether the PV would have been functional since ubiquitously expressed proteases are able to activate viruses

containing such sites (Böttcher-Friebertshäuser, Garten and Klenk, 2018). The H9 monobasic cleavage site was also mutated into a polybasic one for comparison. Despite successful SDM being achieved for all clones (as previously described and depicted above in Figures 147-152), Kz52 PV titres were not increased compared with previous stocks. On the contrary, mutant H9 HA PARKKR was able to transduce HEK293T cells. The addition in co-transfection of a protease plasmid was not considered since polybasic cleavage sites are activated by ubiquitously expressed proteases. A GFP version was first generated and examined (Figure 180) before FLW expression was investigated (Figure 181). An unpaired t-test was employed to compare mutant H9 HA PARKKR with WT H9 Δ prot PV titres. A significant difference was only found for the first harvest ($p=0.0012$). The GFP study panel can be found in Appendix Figure 14.

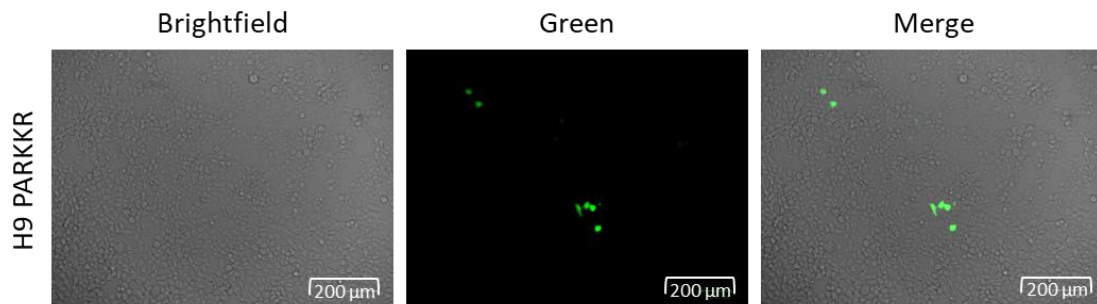


Figure 180: Green HEK293T/17 cells transduced with mutant GFP H9 HA PARKKR PV. Images were taken at 20x on ZOE™ Fluorescent Cell Imager.

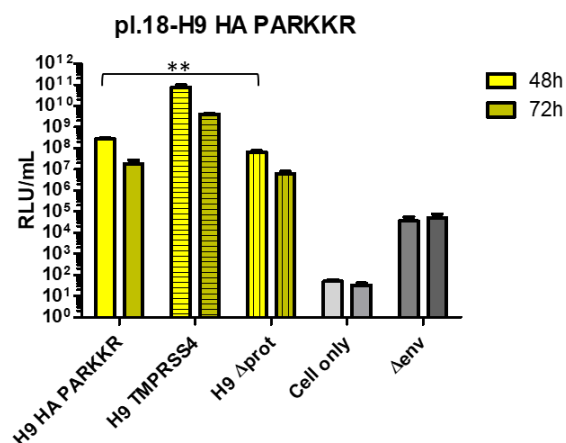


Figure 181: Titration results of mutant H9 HA PARKKR in pl.18. Collection of the first (48h) and second (72h) harvest were tested. Controls were included such as WT H9 TMPRSS4 and Δ prot PVs, Δ env PV and cell only. ** is $p=0.0012$ for the first harvest. The final titre was the result of the average of duplicates.

The mutant H9 HA PARKKR was able to transduce HEK293T cells without the aid of protease plasmids in co-transfection. A statistical analysis confirmed a significant difference between H9 mutant and H9 WT Δ prot PV control ($p=0.0012$). However, an SDM mutation of the cleavage site from monobasic into polybasic should have been carried on a different subtype which titre had no significant difference when compared to the Δ env PV (for instance a canine influenza H3) for further investigations.

7.3.5.4.5 Kozak sequence testing

The Kozak consensus sequence is essential to initiate the translation process together with the ATG starting codon (Kozak, 1987). The plasmids used to attempt production of Kz52 PV contained the sequence GTCAAA which was recommended by NIBSC and widely included in many other HA constructs of various influenza strains (Del Rosario *et al.*, 2021). The Kozak sequence was mutated into the general mammalian GCCACC to investigate the potential to aid functional Kz52 PV production. The Kozak sequence upstream of the H9 HA was mutated as well as control. Despite successful SDM being achieved for all clones (as previously described and depicted above in Figures 154-157), mutants Kz52 GCCACC PV titres were not significant. Unfortunately, due to complications during cloning, no mutant H9 GCCACC clone was rescued. PVs of mutants either WT or CO Kz52 GCCACC were generated also with emGFP plasmid, with or without the TMPRSS4 protease plasmid and tested on HEK293T, MDCK I & II and DEF. No green cells were detected.

7.3.5.5 Influenza PV generated with HA and NA combination

NA is a sialidase that cleaves sialic acid from influenza infected cells to facilitate viral progeny release and also influence viral binding to the receptor (Gottschalk, 1957). For HA only PVs, NA is provided exogenously after transfection of producer cells. Sometimes PVs are made where NA is also present in the envelope. Therefore, generation of influenza PV was investigated by combining either H9 or H3 HA of A/canine/Colorado/30604/2006 (H3N2) with N2 NA of A/canine/Guangdong/3/2011 (H3N2). N2 was cloned into pl.18 expression vector by Dr. Martin Mayora-Neto (University of Kent, UK). pl.18 or pCAGGS-H9 HA plasmids were employed. Δ prot PVs were also titrated with TPCK-trypsin treated for 30 minutes as described in Section 7.2.13.1. An HA only PV (either H9 or H3) should have been included as control for the correct performance of the assay and for statistical purposes. Nevertheless, high titres were rescued for all PVs. PVs collected at 48h (Figure 182 Left graph) showed

higher RLU/mL values than PVs collected at 72h (Figure 182 Right graph). A combination of Kz52 HA with N2 NA should have been attempted as well. However, this was investigated in the vPV study below (Section 7.3.5.6.).

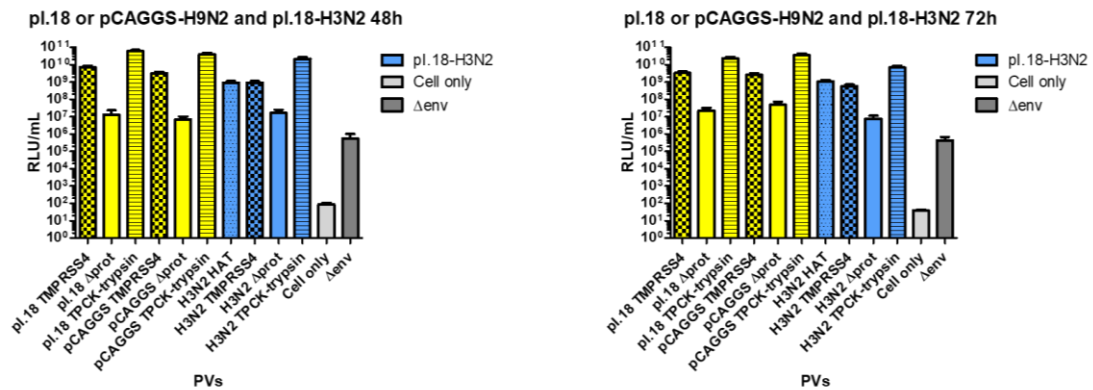


Figure 182: Titration results of HA and NA PV combinations. PVs were generated by combining H9 (yellow column bars) and H3 (blue column bars) HAs with N2 NA with protease plasmids (HAT or TMPRSS4) or not (Δ prot PVs). Δ prot PVs were titrated with or without TPCK-trypsin. Controls were included such as Δ env PV and cell only. **Left graph:** PVs were collected at 48h. **Right graph:** PVs were collected at 72h. The final titre was the result of the average of triplicates.

7.3.5.6 Influenza VSV PV titre

The VSV 'core' system was employed as alternative to the lentivirus core in order to generate functional Kz52 vPV. vPVs were generated either with or without N2 NA plasmid using amplified rVSV Δ G at an MOI of 0.2, 1 or 2 as described in Section 7.2.12. Titrations were carried out as usual. A pCAGGS and pl.18 only were included as controls alongside Δ env PV and cell only. A RAVV vPV was kindly provided by Dr. Martin Mayora-Neto and employed as control. Despite no significant Kz52 vPV titre being measured, high titres for H9 vPVs were recorded (Figure 183). Interestingly, H9 vPVs generated without the NA plasmid showed higher titres ($p=0.0020$, $p=0.0041$ and $p=0.0017$ for MOI 0.2-1-2 respectively). This could be due to either a better sialidase activity of the exNA (*Clostridium perfringens*) or the importance of specificity between NA and HA. Unfortunately, this could not be investigated further since the corresponding N2 for H9 was not available. In addition, it was observed that higher MOI of amplified rVSV Δ G did not improve overall titres. Indeed, a significant difference was only observed between H9 vPVs at MOI 0.2 and 1 ($p=0.0011$ and $p=0.0033$ for vPV generated with or without NA plasmid respectively).

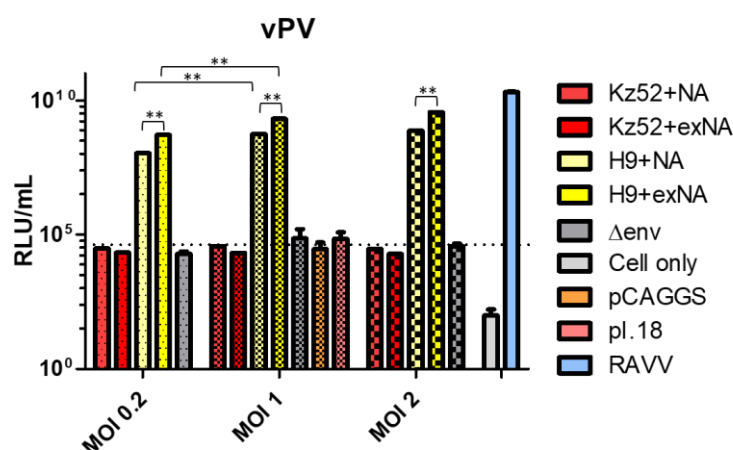


Figure 183: Titration results of vPVs. Kz52 PV and H9 PV produced with N2 or exNA infected with 0.1-1-2 MOI of rVSV Δ G. Controls were included such as RAVV vPV and cell only. An unpaired t-test was employed to compare titres between H9 vPVs generated with or without NA plasmid (** $p=0.0020$, ** $p=0.0041$ and ** $p=0.0017$ for MOI 0.2-1-2 respectively) and rVSV Δ G at different MOI conditions (** $p=0.0011$ and ** $p=0.0033$ for MOI 1 and MOI 0.2 respectively). The final titre was the result of the average of duplicates repeated twice.

7.3.6 Influenza PV neutralisation assay

The ability of antibodies to neutralise H9 PV particles was assessed in a PVNT employing H9-like antisera (Figure 184). Sera was added to the first well of the assay plate either neat or pre-diluted 1/10, and tested against H9 PV generated with Tmprss4 protease plasmid. Specificity of the H9 glycoprotein and antibody interaction was investigated by running the PVNT against an H3 HA of A/canine/Colorado/30604/2006 (H3N2) and an H5 A/Vietnam/1194/2004 (H5N1) (GenBank accession number: ABP51976.1) PV. The H3 PV was generated as previously described, while H5 PV had been previously generated by Dr. Martin Mayora-Neto (University of Kent, UK). No neutralisation was detected in the latter cases, suggesting specific serum antibody binding to H9 glycoprotein only (Table 32). FBS was included as negative control. An expected shift was observed in the gradient of the neutralisation curves for the neat and pre-diluted sera due to the different starting dilution. Despite a decrease of the IC₅₀ values being observed from employing neat to pre-diluted sera, there was no significant difference between the starting dilutions ($p=0.2839$). This suggested that it was acceptable to start a PVNA with either neat or pre-diluted 1/10 sera since the variable won't affect the IC₅₀ results. For the purpose of this study, it would have been interesting to observe whether there was neutralisation of Kz52 PV. However, no Kz52 functional titres were obtained despite the many strategies employed above. Therefore, no PVNA against Kz52 PV was possible.

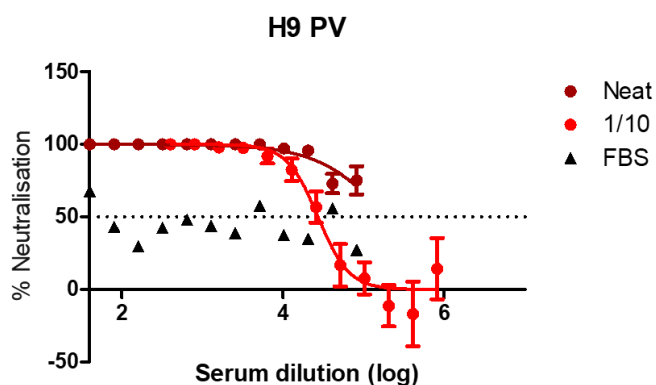


Figure 184: PVNT (H9 PV). Neutralisation curves obtained with either neat or pre-diluted H9-like antisera tested against H9 PV. Neat sera was added at a starting dilution of 1/40, while the pre-diluted at a starting dilution of 1/400. FBS was included as negative control and antibodies were detected. Serum was added in triplicate and the test was done once.

| Sera sample | LogIC ₅₀ | IC ₅₀ |
|-----------------|---------------------|------------------|
| Neat | 5.29966 | 199370.200 |
| Prediluted 1/10 | 4.433575 | 27137.820 |

Table 32: LogIC₅₀ and IC₅₀ values. Neat or pre-diluted H9-like antisera tested in triplicate against H9 PV.

7.3.7 SDS-Polyacrylamide Gel Electrophoresis

Since no functional titre was achieved for Kz52 PV, the expression/presence of the HA was questioned. To verify this, an SDS-PAGE was performed. WT Kz52, H9 (with and without protease) and Δenv PVs were prepared and concentrated according to the protocol described in Section 2.1.13. Concentrated samples were titrated first (Figure 185) alongside with their non concentrated counterpart, before loading onto a gel (Figure 186). The concentrated Δenv PV should have been included as control. Concentrated EHV-1 gB, gC, gD, gH and gL containing PVs were included as well (Section 3.3.8.). The visualisation of proteins was a crucial step. Results were hard to interpretate as proteins might not have completed denaturation or p8.91 plasmid band might have masked the presence of the glycoprotein polypeptide. Another consideration could be due to the staining method with Coomassie Blue which is widely used for its simplicity although not as sensitive compared to alternative stainings (e.g. silver staining).

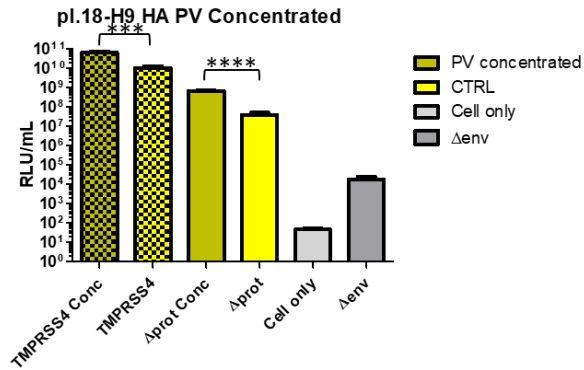


Figure 185: Titration results of concentrated PVs for SDS-PAGE. Controls were included such as Δenv PV and cell only. An unpaired t-test was employed to compare concentrated to non concentrated (CTRL) PV titres (** $p=0.0010$ and **** $p<0.000$ for H9 TMPRSS4 and $\Delta prot$ PV respectively). Samples were run in duplicate.

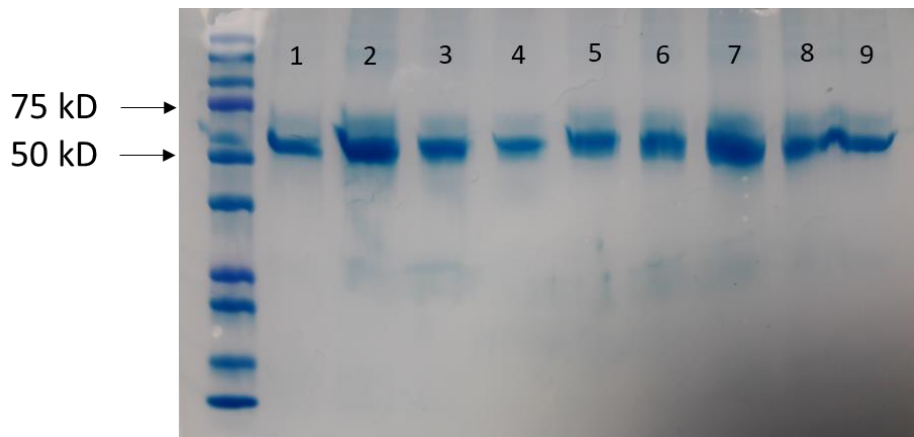


Figure 186: SDS-PAGE results. SDS-PAGE gel to verify the presence of the HA glycoprotein for samples WT Kz52 TMPRSS4, H9 TMPRSS4, H9 $\Delta prot$ and Δenv (columns 6 to 9 respectively). It was also employed to estimate the size of EHV-1 glycoproteins gB, gD, gC, gH and gL (columns 1 to 5 respectively). The molecular weight of proteins is estimated by comparison to a Precision Plus Protein™ Dual Color Standards.

7.3.8 Immunofluorescence of HA in producer cells

In order to investigate the expression of the HA plasmid in the HEK producer cell line, immunofluorescence was performed employing an H9-like antisera because of its proximity to Kz52 HA lineage. The protocol was optimised using pCAGGS-H9 HA as control and phCMV1-H8 HA to investigate cross-reactivity. Immunofluorescence was first investigated under a fluorescent microscope (ZOE™ Fluorescent Cell Imager; Figure 187) and then at confocal microscopy (Zeiss LSM; Figures 188 and 189). Appropriate controls were included to verify whether any non specific primary or secondary antibody binding was taking place

by staining non transfected HEK293T cells with either the second or a combination of the two antibodies. A cell only control was also utilised to verify non transfected unstained cell morphology. Moreover, cells were transfected with either pCAGGS or phCMV1 only (no insert). At this point it was possible to compare the samples stained with both antibodies with the negative controls and thus confirm immunostaining was mediated by specific Ab binding to HA. This was certainly the case for the positive control (cells transfected with pCAGGS-H9 HA) in which a strong immunostaining could be appreciated by red halos on the outside of the individual cell indicating precisely where the HA expression was taking place on the plasma-membrane (Figure 189). These findings confirmed previous successful outcomes and explained why pseudotyping with the H9 envelope glycoprotein was successful. Interestingly, for Kz52 and H8 expression seemed likely cross-reactions occurred. Red halos were visible on the outside part of individual cells. However, they were observed with less intensity and they were not as clear and sharp as on the positive control. This might suggest that Kz52 HA expression was occurring and maybe retroviral particles generated but not able to be released. For H8, cross-reactivity was detected between H8 HA PV and H9N2 reference serum based on IC_{50} (Ferrara *et al.*, 2017). That could explain why immunostaining was observed still in minor frequency as what was happening in the positive control. The number of cells showing HA-Ab staining (plasmid intake) was estimated in percentage for plasmid quantification (Table 33).

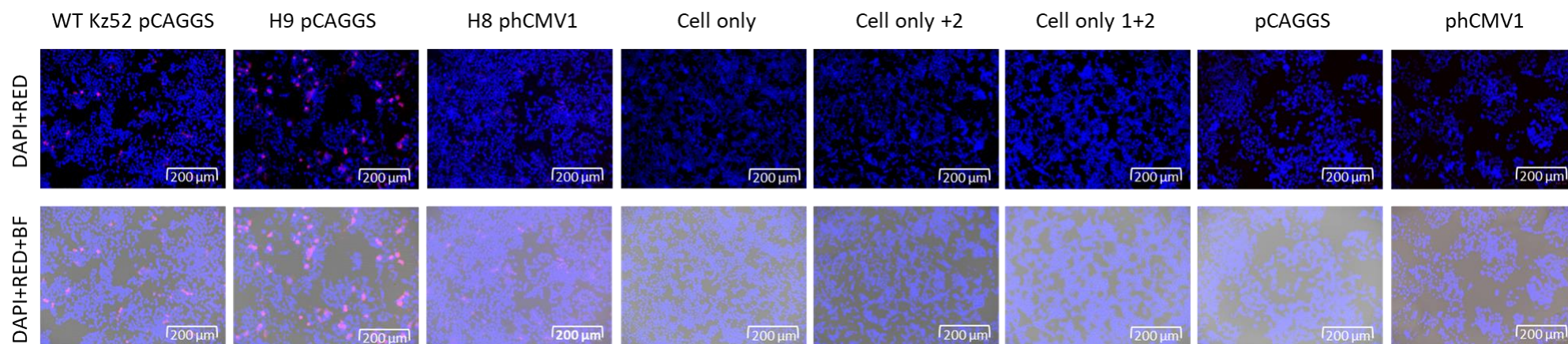


Figure 187: Immunofluorescence at 20x on ZOE™. Cells are HEK293T/17 observed with different channels: DAPI (in blue) marks the nuclei of the cells, RED (in red) marks the fluorescent probes labelling of the cells and BF (brightfield) for general imaging observation. Non transfected HEK293T cells were stained with either secondary (Cell only +2) or a combination of the two antibodies (Cell only 1+2). A cell only control was also utilised to verify non transfected unstained cell morphology. Moreover, cells were transfected with either pCAGGS or phCMV1 only (no insert).

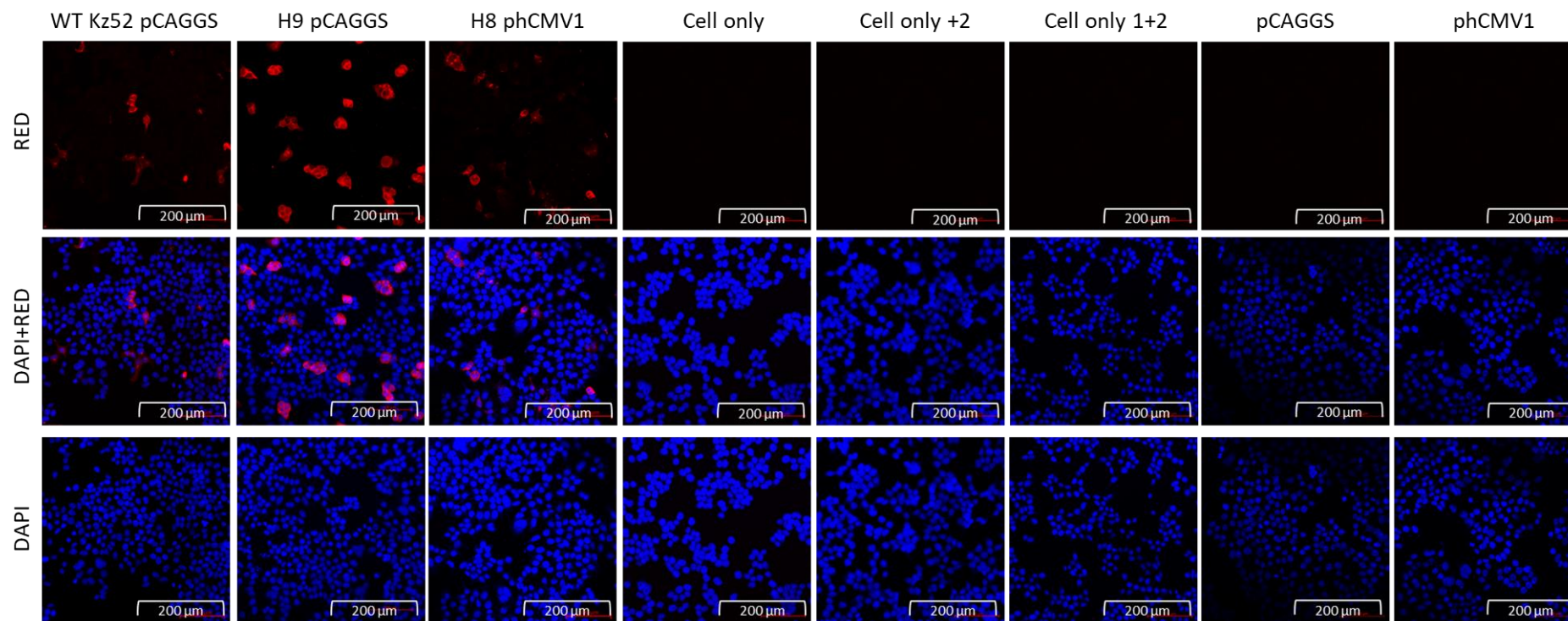


Figure 188: Immunofluorescence at 20x on ZEISS LSM. Cells are HEK293T/17 observed with DAPI channel (in blue) which marks the nuclei of the cells and/or RED channel (in red) which marks the fluorescent probes labelling of the cells. Non transfected HEK293T cells were stained with either secondary (Cell only +2) or a combination of the two antibodies (Cell only 1+2). A cell only control was also utilised to verify non transfected unstained cell morphology. Moreover, cells were transfected with either pCAGGS or phCMV1 only (no insert).

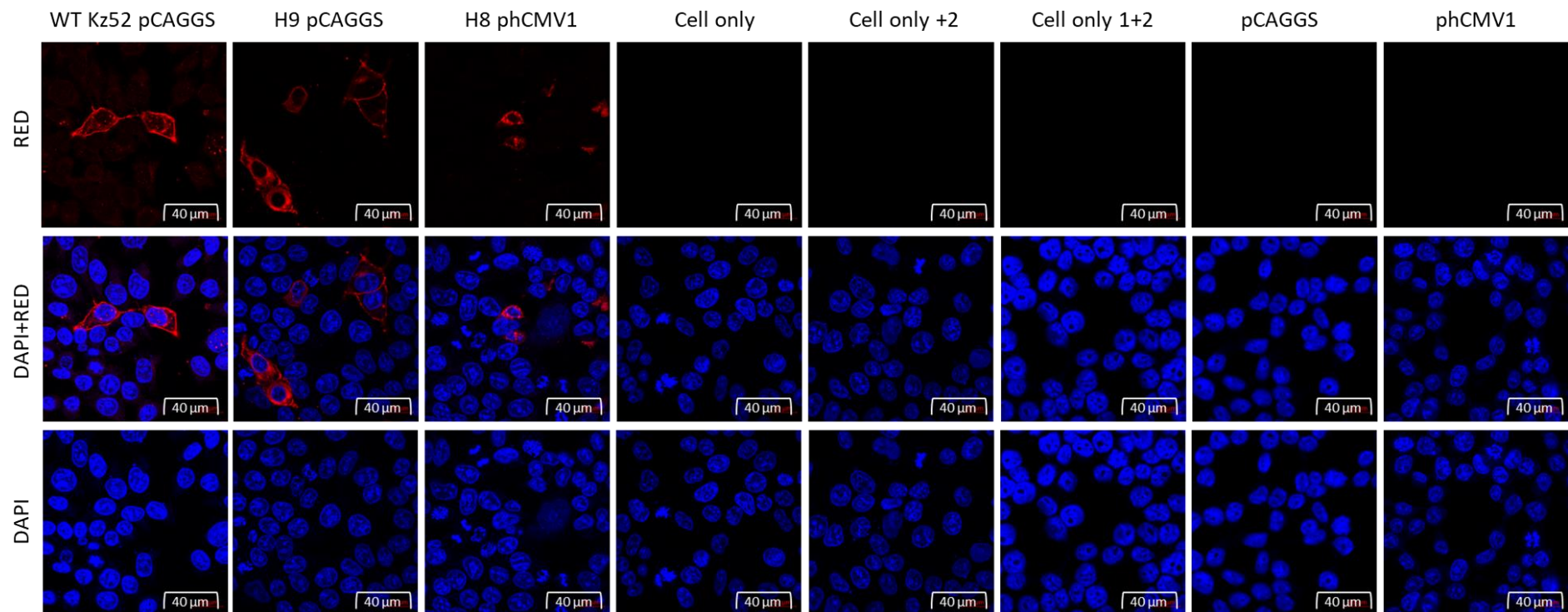


Figure 189: Immunofluorescence at 63x on ZEISS LSM. Cells are HEK293T/17 observed with DAPI channel (in blue) which marks the nuclei of the cells and/or RED channel (in red) which marks the fluorescent probes labelling of the cells. Non transfected HEK293T cells were stained with either secondary (Cell only +2) or a combination of the two antibodies (Cell only 1+2). A cell only control was also utilised to verify non transfected unstained cell morphology. Moreover, cells were transfected with either pCAGGS or phCMV1 only (no insert).

| HA plasmid | % plasmid intake |
|------------|------------------|
| Kz52 | 4 |
| H9 | 10 |
| H8 | 3 |

Table 33: HA plasmid intake. Plasmid quantification measured in % of plasmid intake by manually counting red halos observed in a field area of the sample using ImageJ software.

7.3.9 Influenza PV application in an Enzyme-linked immunosorbent assay

An in-house ELISA was developed and optimised using purified influenza PVs as antigens to assess specific antibody binding. Kz52 and H9 PVs alongside appropriate controls such as Δ env PV and cell only s/n were first concentrated and purified following the Lenti-X™ Concentrator (Takara) Protocol-at-a-Glance before protein concentration was quantified with Pierce™ BCA Protein Assay Kit as described in Section 7.2.19.1. The amount of protein present in each purified PV sample was determined by extrapolating the unknown values from the standard curve generated with known amounts of bovine serum albumin (BSA) using quadratic regression as recommended by the manufacturer's (Figure 190 and Table 34).

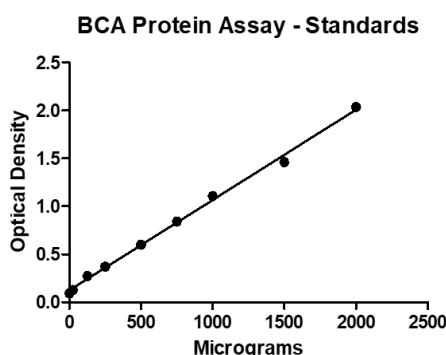


Figure 190: Standard curve obtained with known amounts of BSA.

| PV | OD | μ g/mL |
|--------------|---------|------------|
| Kz52 | 1.5283 | 1490.404 |
| H9 | 1.32405 | 1273.510 |
| Δ env | 1.56245 | 1526.667 |
| Cell only | 1.5534 | 1517.057 |

Table 34: Protein quantification of concentrated purified samples obtained with Pierce™ BCA assay.

Purified concentrated PVs were employed as antigens in an in-house developed indirect ELISA to detect antibody binding against H9-like antisera (Figure 191). H9 PV was employed as positive control since it should have strongly reacted to the sera, as confirmed in the PVNT or immunofluorescence study findings. On the other hand, for Kz52 PV a cross-antibody binding was expected.

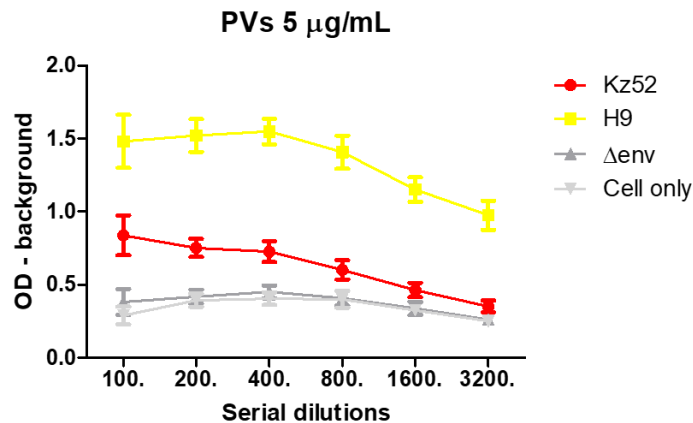


Figure 191: Indirect ELISA results. Indirect ELISA using concentrated purified PV protein at 5 µg/mL in PBS. H9-like antisera was employed as primary antibody at 1:100 dilution. Results from three independent experiments in which each point is the average of duplicates.

Signal from the H9-like antisera was especially noted when observing the H9 PV positive control. Antibody binding was higher at 1:100 dilution and decreased at lower dilutions as expected. However, it seemed there was a slight increase at 1:400 dilution before a decrease was noticeable. This was observed also in the negative controls, although the overall background signal was constantly low throughout the serial dilutions showing a great difference compared to the H9 PV coated wells. Outcome of the negative controls confirmed there was no nonspecific antibody binding to the envelope of pseudotype particles nor residual surface protein receptors from producer cells. Interestingly, signal was detected when Kz52 PV was employed. Whether this was due to cross-antibody binding was not verified since no monoclonal antibodies targeting the H9 glycoprotein in order to increase specificity were not available in that moment. Regardless, the signal was in the range between the positive and negative controls and lowered as dilutions increased. In the future sera collected from confirmed Kz52-positive waterfowl in Kazakhstan might have been the best material to better investigate Kz52 glycoprotein ability to specifically bind to antibodies.

7.3.10 Quality control of lentiviral PV

So far none of the strategies employed were able to produce Kz52 PVs with measurable titres. Because of these difficulties, the lentiviral core activity was questioned. Thus, an SG-PERT assay was employed to measure RT activity in Kz52 PV as quality control of lentiviral PV production (Sweeney and Vink, 2021). A standard curve was first generated on the base of known RT activity of a commercially available recombinant HIV-1 RT in a linear regression (Figure 192). Therefore, the unknown RT activity of samples was extrapolated (Figure 193 Left graph). In all PVs tested RT activity was detected, including in the Δ env PV as expected. From the RT activity levels it was possible to estimate the number of viral particles per mL (VP/mL) (Figure 193 Right graph). However, the values did not correlate with the functional PV titres obtained so far.

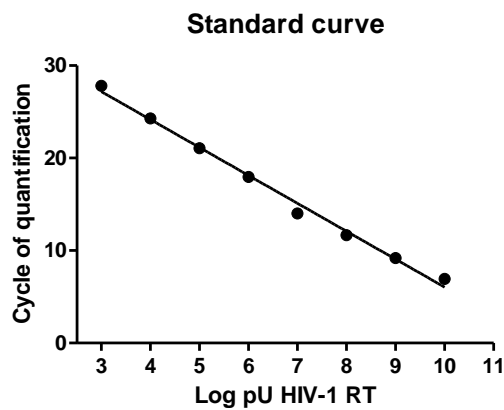


Figure 192: Standard curve obtained with recombinant HIV-1 RT.

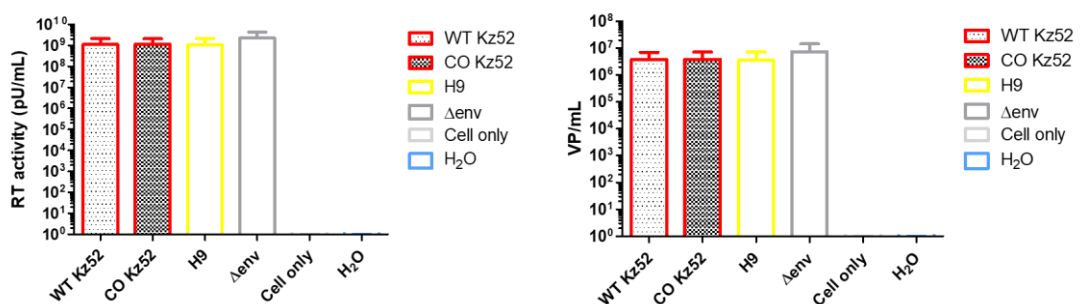


Figure 193: Reverse transcriptase activity RT-activity was measured (left graph) and allowed to estimate the number of VP/mL (right graph). Cell only and H₂O were included as negative controls to ascertain detection of any lentiviral activity from non transfected cells.

7.4 DISCUSSION

In this study, multiple attempts were made to generate a pseudotyped virus based on the HA of a new influenza subtype (temporarily named Kz52), identified by sequencing samples taken from a dead Common Pochard (*Aythya ferina*) duck found near the Caspian Sea in Kazakhstan. This involved applying distinctly different strategies, exploiting the in-house tools available. The history of the sample attracts interest at the evolutionary and genetic level. The geographical position of Kazakhstan makes it an interesting meeting point among the most important flyways for migrating birds and consequently supports a high risk of reassortment of the genetic material and evolution of avian pathogens in particular influenza (Karamendin *et al.*, 2011; Karamendin *et al.*, 2016). Indeed, aquatic birds are the natural reservoir of Influenza A viruses contributing to the maintenance and evolution of the virus population worldwide (Webster *et al.*, 1992; Scholtissek, 1997). Despite there being many influenza strains deemed 'low pathogenicity' (LPAI), attention has to be paid, as they could evolve to high pathogenic (HPAI) strains, which may cross the species barrier and thus represent a potential threat to human health (Ito *et al.*, 1998). A recurring example is represented by the H5 and H7 subtypes, some strains of which have evolved from LPAI to HPAI cause major infections in poultry associated with viral tropism shift thus able to infect human (Dupré *et al.*, 2021). In silico phylogenetic sequence analysis has demonstrated the Kz52 HA could be considered to be a new subtype closely related to H9. H9 has been described as having HPAI potential despite mostly described as LPAI (Carnaccini and Perez, 2020). For this reason, continuous surveillance of wild avian influenza is essential to understand the basis of viral variability and evolution in order to prevent more catastrophic disasters (Animal and Plant Health Agencies; APHA, 2022). Because H9 HA was found to be the closest subtype to Kz52 HA, its nucleotide and amino acids sequences were aligned and compared to H9 HA to highlight its cleavage site, essential to determine HA activation, and the most important RBD sites. The latter characterise the receptor binding specificity determining cell and species tropism and are a hot topic in prevention and development of therapies against influenza (Connaris *et al.*, 2014). Despite Kz52 HA was identified from a Common Pochard (*Aythya ferina*), its cleavage site is identical to a bat H18N11 influenza virus (Tong *et al.*, 2013). For better visualisation of the HA head, 3D modelling of the HA structure of Kz52 was the result of structural alignment of HAs inserted in the database. It turned out that the best structural alignment was with the HA of H16 subtype. Lu *et al.*, (2012) revealed the crystal structure of this H16 subtype and interestingly, the cleavage site presents a peculiar α -helix structure which does not permit the exposure of the cleavage arginine (R239)

making it more difficult for the protease enzyme to reach the site resulting in non maturation of the HA, explaining the low pathogenicity characteristic of the H16 subtype and its species restriction in black-headed gulls. This finding might indicate that amino acids residues close to R329 are involved in determining protease activity and HA activation. In Ferrara (2015), the H16 cleavage site was mutated to resemble H1 HA cleavage site and to verify the role of this α -helix structure. High-titres were rescued from the H16 PV mutant with HAT and TMPRSS4 protease plasmids resembling the H1 PV profiles, but not when TPCK-trypsin was employed suspecting that even by disrupting the α -helical structure is not enough to permit trypsin activity. This points to other factors being involved in HA maturation. Whether cleavage of the HA is subjected to cell specific proteases restricted to a species, future studies might need to answer that. To investigate whether the answer to generating functional Kz52 PVs was residing in the cleavage site, its cleavage site amino acids sequence was mutated to PIKETR→PIKSTR→PARSSR to closer resemble the functional H9 HA cleavage site in a stepwise manner. The H9 HA is efficiently activated by common proteases and trypsin as demonstrated in the profiles (Figures 177 and 178). However, for mutants Kz52 PVs with mutations to the HA cleavage site, this strategy was not successful. Subsequently, insertion of a polybasic cleavage site questioned whether it would have permitted activation of Kz52 HA without the inclusion of protease plasmids. For this reason, the consensus R-K-K-R motif, most frequent amino acids HACS motif in HPAI H5 (Luczo *et al.*, 2015) and H7 (Kido *et al.*, 2012), was introduced into Kz52 HA cleavage site substituting the monobasic one PARSSR→PARKKR. Mutation of H9 HA for control purposes was investigated as well. Pathogenicity of AIV is based on the HACS motif. Indeed, recognition of the polybasic site by ubiquitous proteases found in most cell types determine high pathogenicity of the virus allowing a systematic spread to many tissues and organs (Steinhauer, 1999). It has been shown that mutation at the amino acids level of an H9N2 cleavage site resulted more pathogenic (Soda *et al.*, 2011). For PV generation, addition of a protease plasmid was omitted since HA cleavage is mediated by proteases expressed in the HEK293 producer cell line resulting in a more straight forward production system (Temperton *et al.*, 2007). Despite successful generation of mutant clones, activation of this modified Kz52 HA and thus PVs not rescued. These findings raised whether other amino acids residues distal from the cleavage site might be involved in determining protease specificity. This hypothesis was reinforced when H9 HA cleavage site was mutated to make it like Kz52 and was successfully activated obtaining high PV titres of 1×10^{10} RLU/mL (Figures 177 and 178). These results show that Kz52 HA cleavage site is cleavable by the protease plasmids tested.

The genetic code is degenerate, and most amino acids are encoded by more than one codon. The so-called 'codon usage bias' phenomenon leads to a preference for a particular codon which encodes an amino acid. Protein expression depends on this translation efficiency which can be improved by accommodating codon bias of the host organism (Ikemura, 1985; Sharp, Tuohy and Mosurski, 1986; Comeron, 2004; Plotkin and Kudla, 2011). Therefore, both non codon optimised and codon optimised sequences were attempted to generate functional Kz52 pseudotypes. Better expression is observed when synthetic codon optimised genes are employed in a tRNA-enhanced host cells compared to native genes (Burgess-Brown *et al.*, 2008). Molesti (2014) obtained higher titres using a codon optimised HPAI H7 PV compared to a non codon optimised H7. However, comparison was not exactly comparable since the two H7 HA were not from the same strain. Carnell (2017) described a similar situation was described when a codon optimised type B influenza HA of the B/Florida/4/2006 strain (GenBank accession number: KX058884.1) was successful in producing PVs but not the WT influenza B HA sequence of the B/Brisbane/60/2008 strain (GenBank accession number: EU515992). Despite most of the success in generating influenza A PV from codon optimised HA genes (Del Rosario *et al.*, 2021), codon optimisation was not sufficient to express Kz52 HA.

Expression plasmids represent another variable to create a functional PV. Thus, pI.18 or pCAGGS were employed as alternative expression vectors known to have previously expressed HAs in generating functional PVs (Temperton *et al.*, 2007; Huang *et al.*, 2008). Despite optimised protocols available in house from previous generation of influenza PVs neither pI.18 or pCAGGS permitted successful production of Kz52 HA PVs.

Another question was specific protease was able to cleave the Kz52 HA. The serine proteases available in VPU (University of Kent, UK), which have successfully been used to cleave other influenza HAs to generate functional pseudotypes (Bertram *et al.*, 2010; Ferrara *et al.*, 2012; Scott *et al.*, 2012; Sawoo *et al.*, 2014), were employed in production. TPCK-trypsin treatment can also be used as an alternative to protease plasmids to produce functional PVs (Wang *et al.*, 2008; Yang *et al.*, 2014). However, none of the proteases including TPCK-trypsin were able to activate the Kz52 HA. On the other hand, functional H9 PVs were generated with titres ranging from 1×10^9 to 1×10^{11} RLU/mL (Figures 159-162). Additional proteases of the serine family that are less frequently employed were also tested. However, their functionality was questioned as H9 PV titres rescued were low, comparable to H9 PV produced without protease (Figures 164).

Target cells represent a major factor to quantify PV titres. HEK293T is commonly utilised not only for production but also to for titration and downstream applications, such as antibody assays. However, specialised cells might be required to be able to express particular sialic acids (such as α -2,3 and α -2,6 sialic acids) or other receptors fundamental for viral entry. Thus, many cell lines were employed in Kz52 PV entry experiments. Despite its avian origin, DEF were refractive to measurable entry. MDCK II are highly employed for influenza studies and also susceptible to bat influenza (Giotis *et al.*, 2020) but were not transduced by Kz52 PV. If Kz52 HA cleavage is subjected to cell specific proteases restricted to a species, further studies need to investigate this aspect.

Gene expression is regulated by many factors, one of which is the initiation of the transcription process. The transcription in cells of different species may be impacted by the Kozak consensus sequence (Kozak, 1987). Therefore, investigations were undertaken by mutating the original Kozak consensus sequence inserted during Kz52 HA gene design (GTCAAA) into a general one (GCCACC; the same Kozak sequence inserted during EHV-1 GP genes design for cloning purposes. Ferrara (2015) evaluated the role of two different Kozak sequences upstream of gene promoters by comparing the final PV titres demonstrating equal levels of expression. Moreover, expression of HA was questioned in the absence of a Kozak sequence. Similarly, Mather (2017) attempted to generate JEV PV employing different Kozak candidates, however SDM was unsuccessful and could not be investigated further. However, mutation of the Kozak sequence did not result in Kz52 PV generation. H9 HA with the Kozak sequence mutated (GTCAAA→GCCACC) would have been a valuable control, but unfortunately no colonies after transformation were rescued despite successful SDM.

Another aspect that could not be investigated was the inclusion of the neuraminidase (NA) gene from the same strain as amplification of Kz52 NA gene using a range of sequencing primers previously used for other NAs failed (Dr. Sasan Fereidouni, personal communication). This may indicate that NA was also genetically different from previously identified NAs. Future studies should consider this aspect. ExNA was added in co-transfection for production of Kz52 PV, but this was not rescued, despite other influenza PVs generated with the same protocol managed to pseudotype (Del Rosario *et al.*, 2021). The lack of a Kz52 NA is a limit to this study since combination of precise HA and NA might be essential to release functional PV. This is a similar case to H18 PV which are generated only if the N11 gene is added in co-transfection (Del Rosario *et al.*, 2021). However, N11 together with N10 are bat-origin and distinctly different from the avian NA (Tong *et al.*, 2013) Moreover, NA activity has been recently associated with viral entry when a D151G substitution in the amino

acid sequence of an H3N2 NA was observed and changed NA specificity to binding receptors which were resistant to enzymatic cleavage, suggesting a more direct role of NA in receptor binding (Lin *et al.*, 2010).

The retroviral core (HIV and MLV) is the core most commonly used in house at the VPU (University of Kent, UK) to generate influenza PV (Del Rosario *et al.*, 2021). An alternative system to HIV is VSV which gained popularity for its ability to incorporate a wide range of glycoproteins in an unselective manner (Whitt, 2010). Promising results were obtained in generating influenza PVs of the H5 and H7 subtypes based on VSV system (Cheresiz *et al.*, 2014; Zimmer *et al.*, 2014). Thus, the VSV system was opted as an alternative to the familiar retroviral system in an attempt to generate Kz52 PV. The VSV system is more laborious than the retroviral system as extra steps in production to generate the recombinant core have to be conducted. The resulting rVSV can then be employed to infect the cell line which has been transiently transfected with GP plasmids of interest. In our case HA alone or in combination with NA expressing plasmids. An H9 HA was employed as control, to verify the VSV system was working, and to test the outcome including an NA of A/canine/Guangdong/3/2011 (H3N2) and finally to compare the system to HIV. Despite adopting this system, no functional titre was produced for Kz52 PV. Nevertheless, the VSV was successful when H9 was employed either with or without NA. As for the HIV core, significant titre was seen for H9 PVs when exNA was employed ($p < 0.05$). As an aside, it was noted that a lower input of rVSV MOI in the transient GP transfection producer cells resulted in higher titre compared to increased MOI ($p < 0.05$).

The lack of success at producing Kz52 HA PVs raised the question whether the HA was being expressed at all in producer cells. For this purpose, immunofluorescence was investigated as method to better visualise the cellular expression and localisation of Kz52 HA on the producer cells, and if seen its distribution. Immunofluorescence is a fundamental method for detecting antibody responses (Plotkin *et al.*, 2008). It was decided as a more appropriate technique to show expression and cellular location of the HA expression plasmid rather than SDS-PAGE which would have examined protease-mediated activity of the HACS. Unsurprisingly, there was a lack of sera and monoclonal antibodies specific to Kz52 HA for this study, thus H9-like antisera and H9 HA expression plasmid were employed as positive control. Because of this, it was hoped that the phylogenetic closeness would be manifest in H9 sera cross reactivity. To compare and quantify the potential cross-reactivity with other subtypes, an H8 HA was included for cross-reactivity control chosen on the basis of percentage cross-reactivity (above 60%) between the pseudotype particle and the H9

reference sera (Ferrara *et al.*, 2017), plus to the availability of the HA plasmid and the phylogenetic relationships between the HA subtypes. From the results, qualitative and quantitative evaluation of Kz52 HA expression was determined by detection of immunostaining as 'red halos' on the plasma-membrane of the producer cells (Figure 189). Kz52 HA expression was observed, similar to H8 HA expression but at lower levels than the specific H9 HA-antibody binding present in the reference antiserum. Probably this was a phenomenon of cross-reactivity due to non specificity and binding of the antibodies (Reber and Katz, 2013). It might also suggest Kz52 HA retention and not able to be recruited by the HIV core for its egress.

Promising immunofluorescence findings aroused curiosity of Kz52 HA reactivity to antibodies and guided further investigation. ELISA is to detect the presence of antibodies in serum samples against purified antigens (Plotkin, 2008). This assay has also been highly employed to assess monoclonal antibodies (Glikmann, Mordhorst and Kock, 1995). However, it does not provide information on the neutralisation ability, but more the binding to specific epitopes on the antigen (e.g. HA). For the purpose of this study, PV bearing H9 HA or no envelope (Δ env) were employed as antigens to optimise their use in an ELISA assay to assess HA antibodies binding and to investigate the ability to bind to HA on Kz52 PV particles. Availability of specific serum against Kz52 HA was another weak point despite an available H9 anti-sera which was tested in a PVNA against H9 PV but not Kz52 PV (as no functional titre was achieved with Kz52). Monoclonal antibodies would have been a better material to optimise the ELISA assay using PVs as antigens to minimise potential cross-reactivity and obtain clearer results. However, the use of H9-like antiserum was a ready-available material and the best option for the moment. Antibody binding was assessed including valuable negative controls such as a Δ env PV and cell only to ascertain absence of GPs. Interestingly, binding was detected at lower levels of OD for Kz52 PV compared to H9 suggesting cross-reactivity to Kz52 HA. The binding observed using PVs as antigens also suggests the potential use of PV in ELISA assay. Together with the immunofluorescence results, further strategies should be taken to optimise generation of Kz52 PV and to look further why such difficulties arose.

As a final investigation for quality control purposes, an SG-PERT was performed to verify reverse transcriptase activity was present in the PV particles in the harvested supernatants and to exclude the idea of malfunctioning of the HIV core used to generate PV particles. RT-activity was detected in all samples including in the Δ env PV and the number of viral particles

was found to be in between 10^6 and 10^7 VP/mL (Figure 193) suggesting correct HIV functionality. and arising doubts of release of Kz52 particles, somehow prevented. Multiple approaches were undertaken to generate pseudotype particles representing the new influenza subtype Kz52 with limited success. Despite the system being well established for other influenza A subtypes in the same research group as reported in the latest influenza HA PV library (Del Rosario *et al.*, 2021), the HIV core was not able to produce any infectious PV. The lack of the NA of the same strain represents a potential impediment to the success of the study. A similar situation occurred when a canine influenza HA gene (A/canine/Guangdong/3/2011 (H3N2) was unable to be pseudotyped despite the NA of the same strain (N2) being available (Dr. Rebecca Kinsley, unpublished data). Nevertheless, the impact of this aspect could be of great value for the evolution of this project, thus this should be evaluated in future collaboration works. Other results from this study, showed that the GP expressed on the producer cell line reacted with non-specific antibodies suggesting production but not correctly exposed. Moreover, in the ELISA assay, in which the PV were developed as antigens, Kz52 signal was detected above the level of the negative controls, reinforcing the previous implication. Further 3D analysis should verify if other features in Kz52 HA structure are impeding its release which might contribute to its low pathogenicity and possibly host specificity. Despite the virus has yet to be isolated, the use of a Kz52 PV could enable research, to better understand the entry pathway of the new influenza A subtype and subsequent application in serological assay for screening and sero-surveillance purposes of the wild aquatic wildfowl population in Kazakhstan.

8 CONCLUSIONS AND FUTURE WORK

With the advent of the global SARS-CoV-2 (Severe Acute Respiratory Syndrome Coronavirus 2) pandemic, serology became at the centre of attention in order to investigate antibody dynamics (Post *et al.*, 2020; Xu *et al.*, 2021). PVs offer a safe and effective surrogate to handling wild-type viruses (Bentley *et al.*, 2015; Carnell *et al.*, 2015; Li *et al.*, 2018) and have been used extensively to study the neutralisation of SARS-CoV-2 induced by natural infection or vaccination, the durability of protection and to assess the impact of prior immunity on disease progression and vaccine response (Cantoni, Mayora-Neto and Temperton, 2021; Reynolds *et al.*, 2022).

In this thesis, a wide variety of approaches were attempted to develop a PV system of two veterinary viruses of both animal and human health concern: EHV-1 and a novel avian influenza virus. The PV system could be employed in several downstream application, such as sero-surveillance studies to monitor the virus geographical spread and eventually to enhance serological study and cell entry process of the virus or in vaccine evaluation studies possibly to contribute to determine the level of protection.

EHV-1 is a major equine threat without zoonotic potential, therefore it poses no significant risk to the public health (EFSA, 2022). However, despite non directly posing a risk to human health, the disease lies a huge economic impact for the equine industry concerned (Vandenberghe *et al.*, 2021). In 2021, Europe experienced the most severe EHV-1 epidemic outbreak in the last decades. The EHV-1 outbreak originated at the International Horse Jumping event in Valencia (Spain) in February 2021 and rapidly spread to over 30 premises in various States across Europe, leading to the cancellation of sport horse events in 12 European countries. The magnitude of this event caused at least 18 dead horses as reported by Fédération Équestre Internationale (FEI; FEI Report, 2022) and an increasing awareness and concern to this infection. EHV-1 is latently present in the horse population making prevention of outbreaks difficult because of the carrier status of many asymptomatic horses. When available, an effective measure for preventing equine infectious diseases is the use of proper vaccination. However, their efficacy and effectiveness against the different forms of disease induced by EHV-1 (or EHV-4) are variable. EHV vaccines reduce clinical signs of disease and virus shedding, but may not prevent infection or reactivation (Goodman *et al.*, 2006; Gohering *et al.*, 2010; Goodman *et al.*, 2012). Therefore, biosecurity actions play an important key role in preventing the spread of the disease alongside vaccination and surveillance. PCR and virus isolation are recommended tools to detect and identify EHV-1 by

OIE (OIE Terrestrial Manual, 2018). The clinical outcome of EHV-1 (abortion or EHM) was attributed to the EHV-1 strain either non neuropathogenic (or abortigenic) or neuropathogenic strain respectively (Allen and Breathnach, 2006; Nugent *et al.*, 2006). The presence of a single nucleotide mutation at position 2254 (A→G₂₂₅₄) in ORF30 was associated to the development of EHM (Nugent *et al.*, 2006; Goodman *et al.*, 2007). However, this mutation despite being frequent is not strictly correlated to the outcome of EHM since EHV-1 strains isolated from EHM cases in 2021 were found to carry either mutation (Sutton *et al.*, 2021; Vereecke *et al.*, 2021). Further questions are raised regarding the prognostic importance of the A→G₂₂₅₄ mutation referred as 'neuropathic marker' (Lunn *et al.*, 2009; Pronost *et al.*, 2010; Sutton *et al.*, 2021). Serology gives a valuable effect in longitudinal surveillance. Several serological assays could be used to demonstrate EHV-1 induced seroconversion by screening two blood serum samples collected in a period of 14-21 days (OIE Terrestrial Manual, 2018). A fourfold or greater rise in virus-specific antibody titre by either virus neutralisation (VN) assay, complement fixation (CF) test or ELISA is indicative of recent exposure to EHV-1 (Thomson *et al.*, 1976; Crabb *et al.*, 1995). However, serological assays have limitations due to the prevalence of EHV-1 and most importantly EHV-4 infections in the field that induce detectable levels of EHV-specific antibodies in serum and the lack of type specificity. Moreover, EHV vaccines do not possess DIVA (differentiating infected from vaccinated individuals) ability, which tend to complicate sero-epidemiological surveillance (Goodman *et al.*, 2012). Nonetheless, the OIE recommends VN or ELISA for the prevalence of infection surveillance and they are suitable for this purpose in unvaccinated populations (EFSA, 2022).

For the purpose of this study, we wanted to investigate whether PVs would provide an alternative platform to the serological assays already in use. First of all, it was essential to generate a functional EHV-1 PV able to transduce target cells. The importance of choosing the correct EHV-1 envelope glycoprotein (of the twelve present) was a critical part of this study. Chapter 3 reveals EHV-1 gB, gD, gH and gL are required and sufficient for EHV-1 PV entry and describes a detailed optimisation protocol to generate EHV-1 PV. It was then questioned whether the new PV system would have been able to be neutralised by EHV-1 antibodies. Therefore, feasibility of a PVNA was first tested in Chapter 4 by measuring the level of neutralising antibodies from sera samples collected from EHV-1 experimentally infected horses in a longitudinal manner. The results obtained with the PVNA were compared with the established VN assay ($r=0.82$, $p<0.0001$). Seroconversion is well defined in the established assays as a four-fold or greater increase in titre. Interestingly the neutralising

titres achieved with the PV assay increased concordantly with those detected in the VN assay suggesting that PVNA may be employed as an alternative serological assay to the VN. However, to confirm this observation further studies are required using other sera samples. This was further investigated in Chapter 6 by measuring the antibody titres elicited by vaccination and able to neutralise EHV-1 PV using equine sera collected from vaccinated horses against EHV-1. The results obtained with the PV assay were then compared with a non-conventional VN assay performed on E.derm on xCELLigence RTCA. Nevertheless, correlation of the PVNA results with the VN are promising ($r=0.81$, $p<0.0001$) with neutralising titres increasing concordantly between the two assays, suggesting EHV-1 PVNA could be employed as an alternative serological assay to the established ones. A consideration should be focussed on the sera panel employed in this chapter study as it would have been more appropriate to employ sera collected from horses raised in a dedicated, specific pathogen free facility since birth and vaccinated against EHV-1 to exclude the possibility of previous EHV-1 (or EHV-4) exposure. The specificity of EHV-1 PVNA in differentiating between EHV-1 and EHV-4 elicited response still remains unanswered. Future studies could consider investigating this aspect by exploiting panel of sera ad hoc. Moreover, EHV-1 PV is a 'simplified version' of WT EHV-1 as only four of the total twelve glycoproteins are expressed on its envelope, raising curiosity whether other minor glycoproteins are restricting entry to other target cell lines or have a role in triggering an antibody response.

Avian Influenza is a highly contagious virus of poultry and wild aquatic birds and based on the severity of the disease, influenza viruses are classified into LPAI or HPAI (OIE Terrestrial Manual, 2021). Influenza viruses possess a great zoonotic potential (directly from birds or through an intermediate host such as pigs), posing a public health risk and ability to disrupt the economy and social functions (Mostafa *et al.*, 2018; CDC, NASPH and CSTE, 2022). Since March 2022, Europe is experiencing the largest HPAI epidemic related to H5 subtype in the bird population (poultry, wild and captive birds) posing a potential risk of transmission to mammals, including humans (EFSA, 2022). Response options to this new epidemiological situation include the definition and the rapid implementation of suitable and sustainable HPAI mitigation strategies such as appropriate biosecurity measures and surveillance strategies for early detection in the different poultry production systems. (EFSA, 2022) Moreover, the importance of constant surveillance of the wild bird population is essential to understand the development of viral variability and evolution and eventually recognise new threats (Fouchier, Osterhaus and Brown, 2003; Sayatov *et al.*, 2007). Influenza PV system demonstrated its utility, versatility and ease of employing to enhance surveillance programs

alongside contributing to expanding seasonal influenza prevention and control policies (Del Rosario *et al.*, 2021). The isolation of an apparently novel HA influenza virus (denoted Kz52 in this study) from a dead pochard *Aythya farina* duck near the Caspian Sea in Kazakhstan raised curiosity in terms of geographical spread and seroprevalence of Kz52 HA in the wild aquatic bird population in Kazakhstan. Therefore, in order to conduct experimental research on the virus (e.g. cell tropism/receptor and develop diagnostic tests), attempts were made to generate Kz52 HA pseudotyped lentivirus particles to use in serological assay for screening and sero-surveillance purposes.

Many attempts were conducted to generate a functional Kz52 PV. However, none of them were successful. Generally, the HACS is believed to modulate tissue tropism and affect pathogenicity (Medina and Garcia-Sastre, 2011). For this reason, it was questioned whether Kz52 HA cleavage site was the main obstacle to obtain activation of the HA and so generation of PV particles. Therefore, the cleavage site amino acids sequence was mutated in a step wise manner to resembles the H9 HA one (used as control in this study) in order to facilitate accessibility of protease activity and mediated activation. Failure of these strategies suggests other features in the HA sequence might interfere with activation. Interestingly, the amino acid sequence of Kz52 HA cleavage site was found to be the same as the bat influenza H18 HA one (Tong *et al.*, 2013). More intriguing is the fact that H18 was found to pseudotype only in presence of its corresponding N11 NA (Del Rosario *et al.*, 2021). This raised the question whether the lack of Kz52 NA gene might be a limit to this study as it could be an essential key element in order to pseudotype Kz52. Various studies have also proposed that NA may play other roles in the early stages of the viral life cycle, such as viral attachment and entry, contributing to HA function (Lin *et al.*, 2010; Gulati *et al.*, 2013; Hooper and Bloom, 2013; Mohr, Deng and McKimm-Breschkin, 2015; Ellis *et al.*, 2022). The synthesis of Kz52 NA gene and inclusion in the transfection would be worth investigating in future studies. Kz52 HA expression and binding activity were assessed by immunofluorescence and ELISA which were detected at low levels as a result of cross-reaction against an H9-like antisera. Sera from birds from Kazakhstan would be a valuable resource material to investigate the presence of antibodies against Kz52 HA and as such to question previous exposure to Kz52 antigen. Future studies should focus on both entry and egress mechanism in order to reveal the entry mechanism of this particular subtype and to obtain functional particles able to transduce cells respectively, thus permit the development of a serological assay for screening and surveillance purposes of the wild aquatic fauna.

This thesis focuses on the production and utilisation of PV (EHV-1 and Influenza) in a serological setting. The generation of an EHV-1 PV bearing four glycoproteins was successful and permitted further assessment of the feasibility of PV as surrogate antigens in a neutralisation assay. On the other hand, the generation of a novel Influenza PV resulted more challenging despite the well-known feasibility and use of Influenza PV in surveillance programs and vaccine efficacy studies. Therefore, a few approaches were undertaken in order to better understand the basic biology of this virus, in particular the importance of the cleavage site and the binding ability in cross-reactivity studies. Moreover, it raised the suggestion of a further role of NA possibly involved in entry. Nevertheless, the results presented in this thesis provide additional insight and incentive to optimise, standardise and validate the PV technology as an alternative method to traditional serological assays and as a useful tool to study the biology of viruses, especially when their structure is complicated such as EHV-1.

9 REFERENCES

- Abdelgawad, A., Damiani, A., Ho, S.Y., Strauss, G., Szentiks, C.A., East, M.L., Osterrieder, N. and Greenwood, A.D. (2016) 'Zebra Alpha herpesviruses (EHV-1 and EHV-9): Genetic Diversity, Latency and Co-Infections', *Viruses*, 8(9), pp. 262.
- Abdelgawad, A., Hermes, R., Damiani, A., Lamglait, B., Czirják, G.Á, East, M., Aschenborn, O., Wenker, C., Kasem, S., Osterrieder, N. and Greenwood, A.D. (2015) 'Comprehensive Serology Based on a Peptide ELISA to Assess the Prevalence of Closely Related Equine Herpesviruses in Zoo and Wild Animals', *PloS one*, 10(9), pp. e0138370.
- Abdul-Careem, M.F., Mian, M.F., Yue, G., Gillgrass, A., Chenoweth, M.J., Barra, N.G., Chew, M.V., Chan, T., Al-Garawi, A.A., Jordana, M. and Ashkar, A.A. (2012) 'Critical Role of Natural Killer Cells in Lung Immunopathology During Influenza Infection in Mice', *The Journal of infectious diseases*, 206(2), pp. 167-177.
- Abousenna, M., Khafagy, H., Shafik, N., Abdelmotilib, N. and Yahia, I.S. (2022) 'Detection of humoral immune response induced in horses vaccinated with inactivated Equine Herpes Virus Vaccine', *Revis Bionatura*, 7(1), pp. 21.
- Alberini, I., Del Tordello, E., Fasolo, A., Temperton, N.J., Galli, G., Gentile, C., Montomoli, E., Hilbert, A.K., Banzhoff, A., Del Giudice, G., Donnelly, J.J., Rappuoli, R. and Capocchi, B. (2009) 'Pseudoparticle neutralization is a reliable assay to measure immunity and cross-reactivity to H5N1 influenza viruses', *Vaccine*, 27(43), pp. 5998-6003.
- Alexander, D.J. (2007) 'An overview of the epidemiology of avian influenza', *Vaccine*, 25(30), pp. 5637-5644.
- Aljofan, M., Sganga, M.L., Lo, M.K., Rootes, C.L., Porotto, M., Meyer, A.G., Saubern, S., Moscona, A. and Mungall, B.A. (2009) 'Antiviral activity of gliotoxin, gentian violet and brilliant green against Nipah and Hendra virus in vitro', *Virology Journal*, 6(1), pp. 187.
- Allen, G. (2002) 'Respiratory infections by equine herpesvirus types 1 and 4', *Equine Respiratory Diseases*, Lekeux P. (Eds) *International Veterinary Information Service, Ithaca NY*, 2.
- Allen, G.P. (2006) 'Antemortem detection of latent infection with neuropathogenic strains of equine herpesvirus-1 in horses', *American Journal of Veterinary Research*, 67(8), pp. 1401-1405.

Allen, G.P. (2007) 'Development of a real-time polymerase chain reaction assay for rapid diagnosis of neuropathogenic strains of equine herpesvirus-1', *Journal of veterinary diagnostic investigation: official publication of the American Association of Veterinary Laboratory Diagnosticians, Inc*, 19(1), pp. 69-72.

Allen, G.P. and Breathnach, C.C. (2006) 'Quantification by real-time PCR of the magnitude and duration of leucocyte-associated viraemia in horses infected with neuropathogenic vs. non-neuropathogenic strains of EHV- 1', *Equine veterinary journal*, 38(3), pp. 252-257.

Allen, G.P. and Yeargan, M.R. (1987) 'Use of lambda gt11 and monoclonal antibodies to map the genes for the six major glycoproteins of equine herpesvirus 1', *Journal of virology*, 61(8), pp. 2454-2461.

Allen, G.P., Bolin, D.C., Bryant, U., Carter, C.N., Giles, R.C., Harrison, L.R., Hong, C.B., Jackson, C.B., Poonacha, K., Wharton, R. and Williams, N.M. (2008) 'Prevalence of latent, neuropathogenic equine herpesvirus-1 in the Thoroughbred broodmare population of central Kentucky', *Equine veterinary journal*, 40(2), pp. 105-110.

Allen, G.P., Kydd, J.H., Slater, J.D. and Smith, K.C. (2004) 'Equid Herpesvirus-1 (EHV-1) and -4 (EHV-4) Infections.', in Coetzer, J.A.W. and Tustin, R.C. (eds.) *Infectious Diseases of Livestock*. 2nd Edition edn. Cape Town: Oxford Press, pp. 829-859.

Anderson, K. and Goodpasture, E.W. (1942) 'Infection of Newborn Syrian Hamsters with the Virus of Mare Abortion (Dimock and Edwards)', *The American journal of pathology*, 18(4), pp. 555-561.

Andoh, K., Kai, K., Matsumura, T. and Maeda, K. (2009) 'Further Development of an Equine Cell Line that can be Propagated over 100 Times', *Journal of equine science*, 20(2), pp. 11-14.

Andoh, K., Takasugi, M., Mahmoud, H.Y., Hattori, S., Terada, Y., Noguchi, K., Shimoda, H., Bannai, H., Tsujimura, K., Matsumura, T., Kondo, T. and Maeda, K. (2013) 'Identification of a major immunogenic region of equine herpesvirus-1 glycoprotein E and its application to enzyme-linked immunosorbent assay', *Veterinary microbiology*, 164(1-2), pp. 18-26.

Angeletti, D., Gibbs, J.S., Angel, M., Kosik, I., Hickman, H.D., Frank, G.M., Das, S.R., Wheatley, A.K., Prabhakaran, M., Leggat, D.J., McDermott, A.B. and Yewdell, J.W. (2017) 'Defining B cell immunodominance to viruses', *Nature immunology*, 18(4), pp. 456-463.

Animal and Plant Health Agencies (APHA) (2022) *Avian influenza*. Available at: <https://www.gov.uk/guidance/avian-influenza-bird-flu> (Accessed: 27 March 2022)

Azab, W. and El-Sheikh, A. (2012) 'The role of equine herpesvirus type 4 glycoprotein k in virus replication', *Viruses*, 4(8), pp. 1258-1263.

Azab, W. and Osterrieder, N. (2012) 'Glycoproteins D of equine herpesvirus type 1 (EHV-1) and EHV-4 determine cellular tropism independently of integrins', *Journal of virology*, 86(4), pp. 2031-2044.

Azab, W., Bedair, S., Abdelgawad, A., Eschke, K., Farag, G.K., Abdel-Raheim, A., Greenwood, A.D., Osterrieder, N. and Ali, A.A.H. (2019) 'Detection of equid herpesviruses among different Arabian horse populations in Egypt', *Veterinary Medicine and Science*, 5(3), pp. 361-371.

Azab, W., Dayaram, A., Greenwood, A.D. and Osterrieder, N. (2018) 'How Host Specific Are Herpesviruses? Lessons from Herpesviruses Infecting Wild and Endangered Mammals', *Annual review of virology*, 5(1), pp. 53-68.

Azab, W., Harman, R., Miller, D., Tallmadge, R., Frampton, A.R., Antczak, D.F. and Osterrieder, N. (2014) 'Equid herpesvirus type 4 uses a restricted set of equine major histocompatibility complex class I proteins as entry receptors', *Journal of General Virology*, 95(7), pp. 1554-1563.

Azab, W., Lehmann, M.J. and Osterrieder, N. (2013) 'Glycoprotein H and $\alpha\beta 1$ integrins determine the entry pathway of alphaherpesviruses', *Journal of virology*, 87(10), pp. 5937-5948.

Azab, W., Tsujimura, K., Maeda, K., Kobayashi, K., Mohamed, Y.M., Kato, K., Matsumura, T. and Akashi, H. (2010) 'Glycoprotein C of equine herpesvirus 4 plays a role in viral binding to cell surface heparan sulfate', *Virus research*, 151(1), pp. 1-9.

Azab, W., Zajic, L. and Osterrieder, N. (2012) 'The role of glycoprotein H of equine herpesviruses 1 and 4 (EHV-1 and EHV-4) in cellular host range and integrin binding', *Veterinary research*, 43(1), pp. 61-9716.

Baghi, H.B. and Nauwynck, H.J. (2014) 'Impact of equine herpesvirus type 1 (EHV-1) infection on the migration of monocytic cells through equine nasal mucosa', *Comparative immunology, microbiology and infectious diseases*, 37(5), pp. 321-329.

Baines, J.D. (2011) 'Herpes simplex virus capsid assembly and DNA packaging: a present and future antiviral drug target', *Trends in microbiology*, 19(12), pp. 606-613.

Baker, T.S., Newcomb, W.W., Booy, F.P., Brown, J.C. and Steven, A.C. (1990) 'Three-dimensional structures of maturable and abortive capsids of equine herpesvirus 1 from cryoelectron microscopy', *Journal of virology*, 64, pp. 563.

Balan, P., Davis-Poynter, N., Bell, S., Atkinson, H., Browne, H. and Minson, T. (1994) 'An analysis of the in vitro and in vivo phenotypes of mutants of herpes simplex virus type 1 lacking glycoproteins gG, gE, gI or the putative gJ', *The Journal of general virology*, 75 (Pt 6) (Pt 6), pp. 1245-1258.

Balasuriya, U.B., Crossley, B.M. and Timoney, P.J. (2015) 'A review of traditional and contemporary assays for direct and indirect detection of Equid herpesvirus 1 in clinical samples', *Journal of veterinary diagnostic investigation: official publication of the American Association of Veterinary Laboratory Diagnosticians, Inc*, 27(6), pp. 673-687.

Ballagi-Pordány, A., Klingeborn, B., Flensburg, J. and Belák, S. (1990) 'Equine herpesvirus type 1: detection of viral DNA sequences in aborted fetuses with the polymerase chain reaction', *Veterinary microbiology*, 22(4), pp. 373-381.

Baltimore, D. (1971) 'Expression of animal virus genomes', *Bacteriological Reviews*, 35(3), pp. 235-241.

Bannai, H., Nemoto, M., Tsujimura, K., Yamanaka, T., Kondo, T. and Matsumura, T. (2013) 'Improving a Complement-fixation Test for Equine Herpesvirus Type-1 by Pretreating Sera with Potassium Periodate to Reduce Non-specific Hemolysis', *Journal of equine science*, 24(4), pp. 71-74.

Bannai, H., Tsujimura, K., Nemoto, M., Ohta, M., Yamanaka, T., Kokado, H. and Matsumura, T. (2019) 'Epizootiological investigation of equine herpesvirus type 1 infection among Japanese racehorses before and after the replacement of an inactivated vaccine with a modified live vaccine', *BMC Veterinary Research*, 15(1), pp. 280.

Baron, J., Tarnow, C., Mayoli-Nüssle, D., Schilling, E., Meyer, D., Hammami, M., Schwalm, F., Steinmetzer, T., Guan, Y., Garten, W., Klenk, H.D. and Böttcher-Friebertshäuser, E. (2013) 'Matriptase, HAT, and TMPRSS2 activate the hemagglutinin of H9N2 influenza A viruses', *Journal of virology*, 87(3), pp. 1811-1820.

Bartosch, B., Dubuisson, J. and Cosset, F.L. (2003) 'Infectious hepatitis C virus pseudo-particles containing functional E1-E2 envelope protein complexes', *The Journal of experimental medicine*, 197(5), pp. 633-642.

Basu, A., Antanasijevic, A., Wang, M., Li, B., Mills, D.M., Ames, J.A., Nash, P.J., Williams, J.D., Peet, N.P., Moir, D.T., Prichard, M.N., Keith, K.A., Barnard, D.L., Caffrey, M., Rong, L. and

Bowlin, T.L. (2014) 'New small molecule entry inhibitors targeting hemagglutinin-mediated influenza A virus fusion', *Journal of virology*, 88(3), pp. 1447-1460.

Batterson, W., Furlong, D. and Roizman, B. (1983) 'Molecular genetics of herpes simplex virus. VIII. further characterization of a temperature-sensitive mutant defective in release of viral DNA and in other stages of the viral reproductive cycle', *Journal of virology*, 45(1), pp. 397-407.

Baudin, F., Petit, I., Weissenhorn, W. and Ruigrok, R.W. (2001) 'In vitro dissection of the membrane and RNP binding activities of influenza virus M1 protein', *Virology*, 281(1), pp. 102-108.

Baxi, M.K., Efstathiou, S., Lawrence, G., Whalley, J.M., Slater, J.D. and Field, H.J. (1995) 'The detection of latency-associated transcripts of equine herpesvirus 1 in ganglionic neurons', *The Journal of general virology*, 76 (Pt 12) (Pt 12), pp. 3113-3118.

Bean, W.J., Schell, M., Katz, J., Kawaoka, Y., Naeve, C., Gorman, O. and Webster, R.G. (1992) 'Evolution of the H3 influenza virus hemagglutinin from human and nonhuman hosts', *Journal of virology*, 66(2), pp. 1129-1138.

Becker Y, G.D. (1984) 'Herpes Simplex Virus Type 1 Thymidine Kinase Gene Activity Controls Virus Latency and Neurovirulence in Mice', *Springer*, (Latent Herpes Virus Infections in Veterinary Medicine), pp. 3-19.

Bentley, E.M., Mather, S.T. and Temperton, N.J. (2015) 'The use of pseudotypes to study viruses, virus sero-epidemiology and vaccination', *Vaccine*, 33(26), pp. 2955-2962.

Bertram, S., Glowacka, I., Blazejewska, P., Soilleux, E., Allen, P., Danisch, S., Steffen, I., Choi, S.Y., Park, Y., Schneider, H., Schughart, K. and Pöhlmann, S. (2010) 'TMPRSS2 and TMPRSS4 facilitate trypsin-independent spread of influenza virus in Caco-2 cells', *Journal of virology*, 84(19), pp. 10016-10025.

Beswick, T.S.L. (1962) 'The origin and the use of the word herpes', *Medical history*, 6(3), pp. 214-232.

Biswas, S.K., Boutz, P.L. and Nayak, D.P. (1998) 'Influenza virus nucleoprotein interacts with influenza virus polymerase proteins', *Journal of virology*, 72(7), pp. 5493-5501.

Bloom, D.C. (2016) 'Alpha herpesvirus Latency: A Dynamic State of Transcription and Reactivation', *Advances in Virus Research*, 94, pp. 53-80.

Borchers, K. and Slater, J. (1993) 'A nested PCR for the detection and differentiation of EHV-1 and EHV-4', *Journal of virological methods*, 45(3), pp. 331-336.

Both, G.W., Sleight, M.J., Cox, N.J. and Kendal, A.P. (1983) 'Antigenic drift in influenza virus H3 hemagglutinin from 1968 to 1980: multiple evolutionary pathways and sequential amino acid changes at key antigenic sites', *Journal of virology*, 48(1), pp. 52-60.

Both, L., van Dolleweerd, C., Wright, E., Banyard, A.C., Bulmer-Thomas, B., Selden, D., Altmann, F., Fooks, A.R. and Ma, J.K. (2013) 'Production, characterization, and antigen specificity of recombinant 62-71-3, a candidate monoclonal antibody for rabies prophylaxis in humans', *FASEB journal: official publication of the Federation of American Societies for Experimental Biology*, 27(5), pp. 2055-2065.

Böttcher-Friebertshäuser, E., Freuer, C., Sielaff, F., Schmidt, S., Eickmann, M., Uhlenhorff, J., Steinmetzer, T., Klenk, H.D. and Garten, W. (2010) 'Cleavage of influenza virus hemagglutinin by airway proteases TMPRSS2 and HAT differs in subcellular localization and susceptibility to protease inhibitors', *Journal of virology*, 84(11), pp. 5605-5614.

Böttcher-Friebertshäuser, E., Klenk, H.D. and Garten, W. (2013) 'Activation of influenza viruses by proteases from host cells and bacteria in the human airway epithelium', *Pathogens and disease*, 69(2), pp. 87-100.

Brandenburg, B., Koudstaal, W., Goudsmit, J., Klaren, V., Tang, C., Bujny, M.V., Korse, H.J.W.M., Kwaks, T., Otterstrom, J.J., Juraszek, J., van Oijen, A.M., Vogels, R. and Friesen, R.H.E. (2013) 'Mechanisms of Hemagglutinin Targeted Influenza Virus Neutralization', *PLOS ONE*, 8(12), pp. 1-14.

Brandes, M., Klauschen, F., Kuchen, S. and Germain, R.N. (2013) 'A Systems Analysis Identifies a Feedforward Inflammatory Circuit Leading to Lethal Influenza Infection', *Cell*, 154(1), pp. 197-212.

Brassard, D.L. and Lamb, R.A. (1997) 'Expression of influenza B virus hemagglutinin containing multibasic residue cleavage sites', *Virology*, 236(2), pp. 234-248.

Breathnach, C.C., Soboll, G., Suresh, M. and Lunn, D.P. (2005) 'Equine herpesvirus-1 infection induces IFN-gamma production by equine T lymphocyte subsets', *Veterinary immunology and immunopathology*, 103(3-4), pp. 207-215.

Breathnach, C.C., Yeargan, M.R., Sheoran, A.S. and Allen, G.P. (2001) 'The mucosal humoral immune response of the horse to infective challenge and vaccination with Equine herpesvirus-1 antigens', *Equine veterinary journal*, 33(7), pp. 651-657.

Bresgen, C., Lämmer, M., Wagner, B., Osterrieder, N. and Damiani, A.M. (2012) 'Serological responses and clinical outcome after vaccination of mares and foals with equine herpesvirus type 1 and 4 (EHV-1 and EHV-4) vaccines', *Veterinary microbiology*, 160(1), pp. 9-16.

Brown, D.M., Dilzer, A.M., Meents, D.L. and Swain, S.L. (2006) 'CD4 T Cell-Mediated Protection from Lethal Influenza: Perforin and Antibody-Mediated Mechanisms Give a One-Two Punch', *The Journal of Immunology*, 177(5), pp. 2888-2898.

Brown, J.C. and Newcomb, W.W. (2011) 'Herpesvirus capsid assembly: insights from structural analysis', *Current opinion in virology*, 1(2), pp. 142-149.

Brown, K.S., Safronetz, D., Marzi, A., Ebihara, H. and Feldmann, H. (2011) 'Vesicular stomatitis virus-based vaccine protects hamsters against lethal challenge with Andes virus', *Journal of virology*, 85(23), pp. 12781-12791.

Browning, G.F., Ficorilli, N. and Studdert, M.J. (1988) 'Asinine herpesvirus genomes: comparison with those of the equine herpesviruses', *Archives of Virology*, 101(3-4), pp. 183-190.

Bui, M., Whittaker, G. and Helenius, A. (1996) 'Effect of M1 protein and low pH on nuclear transport of influenza virus ribonucleoproteins', *Journal of virology*, 70(12), pp. 8391-8401.

Bullough, P.A., Hughson, F.M., Skehel, J.J. and Wiley, D.C. (1994) 'Structure of influenza haemagglutinin at the pH of membrane fusion', *Nature*, 371(6492), pp. 37-43.

Burgess-Brown, N.A., Sharma, S., Sobott, F., Loenarz, C., Oppermann, U. and Gileadi, O. (2008) 'Codon optimization can improve expression of human genes in Escherichia coli: A multi-gene study', *Protein expression and purification*, 59(1), pp. 94-102.

Burrows, R. and Goodridge, D. (1984) 'Studies of persistent and latent equid herpesvirus 1 and herpesvirus 3 infections in the Pirbright pony herd', *Latent Herpesvirus Infections in Veterinary Medicine*, pp. 307-319.

Burrows, R., Goodridge, D. and Denyer, M.S. (1984) 'Trials of an inactivated equid herpesvirus 1 vaccine: challenge with a subtype 1 virus', *The Veterinary record*, 114(15), pp. 369-374.

Cai, W.H., Gu, B. and Person, S. (1988) 'Role of glycoprotein B of herpes simplex virus type 1 in viral entry and cell fusion', *Journal of virology*, 62(8), pp. 2596-2604.

Cai, W.Z., Person, S., DebRoy, C. and Gu, B.H. (1988) 'Functional regions and structural features of the gB glycoprotein of herpes simplex virus type 1. An analysis of linker insertion mutants', *Journal of Molecular Biology*, 201(3), pp. 575-588.

Campadelli-Fiume, G. and Menotti, L. (2007) 'Entry of alphaherpesviruses into the cell.', in Arvin A, C.G. (ed.) *Human Herpesviruses: Biology, Therapy, and Immunoprophylaxis*. Cambridge: Cambridge University Press, pp. Chapter 7.

Cantoni, D., Mayora-Neto, M. and Temperton, N. (2021) 'The role of pseudotype neutralization assays in understanding SARS CoV-2', *Oxford Open Immunology*, 2(1).

Capua, I. and Munoz, O. (2013) 'Emergence of influenza viruses with zoonotic potential: open issues which need to be addressed. A review', *Veterinary microbiology*, 165(1-2), pp. 7-12.

Carnaccini, S. and Perez, D.R. (2020) 'H9 Influenza Viruses: An Emerging Challenge', *Cold Spring Harbor perspectives in medicine*, 10(6), pp. a038588.

Carnell, G.W. (2017) *Development of hybrid haemagglutinin pseudotyped lentiviruses to assess heterosubtypic immunity to influenza*. Doctor of Philosophy (PhD) thesis. University of Kent.

Carnell, G.W., Ferrara, F., Grehan, K., Thompson, C.P. and Temperton, N.J. (2015) 'Pseudotype-Based Neutralization Assays for Influenza: A Systematic Analysis', *Frontiers in Immunology*, 6, pp. 161.

Carvalho, R., Oliveira, A.M., Souza, A.M., Passos, L.M. and Martins, A.S. (2000) 'Prevalence of equine herpesvirus type 1 latency detected by polymerase chain reaction', *Archives of Virology*, 145(9), pp. 1773-1787.

Centers for Disease Control and Prevention (CDC) (2021) *Types of Influenza Viruses*. Available at: <https://www.cdc.gov/flu/about/viruses/types.html> (Accessed: 15 March 2022)

Centers for Disease Control and Prevention (CDC), National Association of State Public Health Veterinarians (NASPHV) and Council of State and Territorial Epidemiologists (CSTE) (2022) *Zoonotic Influenza Reference Guide - Detection, Response, Prevention and Control Reference Guide*. Available at: <https://nasphv.org/documentsCompendiaZoonoticInfluenza.html> (Accessed: 22 July 2022)

Cepko, C. (1997) 'Large-Scale Preparation and Concentration of Retrovirus Stocks', *Current Protocols in Molecular Biology*, 37(1), pp. 9.12.1-9.12.6.

Chan, M.Y., Dutil, T.S. and Kramer, R.M. (2017) 'Lyophilization of Adjuvanted Vaccines: Methods for Formulation of a Thermostable Freeze-Dried Product', *Methods in molecular biology (Clifton, N.J.)*, 1494, pp. 215-226.

Chan, S.Y., Speck, R.F., Ma, M.C. and Goldsmith, M.A. (2000) 'Distinct mechanisms of entry by envelope glycoproteins of Marburg and Ebola (Zaire) viruses', *Journal of virology*, 74(10), pp. 4933-4937.

Chang, C.P., New, A.E., Taylor, J.F. and Chiang, H.S. (1976) 'Influenza virus isolations from dogs during a human epidemic in Taiwan', *International journal of zoonoses*, 3(1), pp. 61-64.

Chen, B.J., Leser, G.P., Jackson, D. and Lamb, R.A. (2008) 'The influenza virus M2 protein cytoplasmic tail interacts with the M1 protein and influences virus assembly at the site of virus budding', *Journal of virology*, 82(20), pp. 10059-10070.

Chen, B.J., Leser, G.P., Morita, E. and Lamb, R.A. (2007) 'Influenza virus hemagglutinin and neuraminidase, but not the matrix protein, are required for assembly and budding of plasmid-derived virus-like particles', *Journal of virology*, 81(13), pp. 7111-7123.

Chen, B.J., Takeda, M. and Lamb, R.A. (2005) 'Influenza virus hemagglutinin (H3 subtype) requires palmitoylation of its cytoplasmic tail for assembly: M1 proteins of two subtypes differ in their ability to support assembly', *Journal of virology*, 79(21), pp. 13673-13684.

Chen, C. and Zhuang, X. (2008) 'Epsin 1 is a cargo-specific adaptor for the clathrin-mediated endocytosis of the influenza virus', *Proceedings of the National Academy of Sciences of the United States of America*, 105(33), pp. 11790-11795.

Chen, J., Lee, K.H., Steinhauer, D.A., Stevens, D.J., Skehel, J.J. and Wiley, D.C. (1998) 'Structure of the hemagglutinin precursor cleavage site, a determinant of influenza pathogenicity and the origin of the labile conformation', *Cell*, 95(3), pp. 409-417.

Cheresiz, S.V., Kononova, A.A., Razumova, Y.V., Dubich, T.S., Chepurnov, A.A., Kushch, A.A., Davey, R. and Pokrovsky, A.G. (2014) 'A vesicular stomatitis pseudovirus expressing the surface glycoproteins of influenza A virus', *Archives of Virology*, 159(10), pp. 2651-2658.

Chesters, P.M., Allsop, R., Purewal, A. and Edington, N. (1997) 'Detection of latency-associated transcripts of equid herpesvirus 1 in equine leukocytes but not in trigeminal ganglia', *Journal of virology*, 71(5), pp. 3437-3443.

Chia, W.N., Zhu, F., Ong, S.W.X., Young, B.E., Fong, S., Le Bert, N., Tan, C.W., Tiu, C., Zhang, J., Tan, S.Y., Pada, S., Chan, Y., Tham, C.Y.L., Kunasegaran, K., Chen, M.I., Low, J.G.H., Leo, Y., Renia, L., Bertoletti, A., Ng, L.F.P., Lye, D.C. and Wang, L. (2021) 'Dynamics of SARS-CoV-2 neutralising antibody responses and duration of immunity: a longitudinal study', *The Lancet Microbe*, 2(6), pp. e240-e249.

Chowdary, T.K., Cairns, T.M., Atanasiu, D., Cohen, G.H., Eisenberg, R.J. and Heldwein, E.E. (2010) 'Crystal structure of the conserved herpesvirus fusion regulator complex gH-gL', *Nature structural & molecular biology*, 17(7), pp. 882-888.

Cohen, M., Zhang, X., Senaati, H.P., Chen, H., Varki, N.M., Schooley, R.T. and Gagneux, P. (2013) 'Influenza A penetrates host mucus by cleaving sialic acids with neuraminidase', *Virology Journal*, 10(1), pp. 321.

Comeron, J.M. (2004) 'Selective and mutational patterns associated with gene expression in humans: influences on synonymous composition and intron presence', *Genetics*, 167(3), pp. 1293-1304.

Compans, R.W., Content, J. and Duesberg, P.H. (1972) 'Structure of the Ribonucleoprotein of Influenza Virus', *Journal of virology*, 10(4), pp. 795-800.

Connaris, H., Govorkova, E.A., Ligertwood, Y., Dutia, B.M., Yang, L., Tauber, S., Taylor, M.A., Alias, N., Hagan, R., Nash, A.A., Webster, R.G. and Taylor, G.L. (2014) 'Prevention of influenza by targeting host receptors using engineered proteins', *Proceedings of the National Academy of Sciences*, 111(17), pp. 6401-6406.

Connor, R.J., Kawaoka, Y., Webster, R.G. and Paulson, J.C. (1994) 'Receptor specificity in human, avian, and equine H2 and H3 influenza virus isolates', *Virology*, 205(1), pp. 17-23.

Cooper, G.E., Ostridge, K., Khakoo, S.I., Wilkinson, T.M.A. and Staples, K.J. (2018) 'Human CD49a(+) Lung Natural Killer Cell Cytotoxicity in Response to Influenza A Virus', *Frontiers in immunology*, 9, pp. 1671.

Cooper, P.D. (1961) 'The plaque assay of animal viruses', *Advances in Virus Research*, 8, pp. 319-378.

Cormier Emmanuel G, Fay, T., Francis, K., Durso Robert J, Gardner Jason P and Tatjana, D. (2004) 'CD81 is an entry coreceptor for hepatitis C virus', *Proceedings of the National Academy of Sciences*, 101(19), pp. 7270-7274.

Coulter, L.J., Moss, H.W.M., Lang, J. and McGeoch, D.J. (1993) 'A mutant of herpes simplex virus type 1 in which the UL13 protein kinase gene is disrupted', *Journal of General Virology*, 74(3), pp. 387-395.

Cox, N.J. and Subbarao, K. (2000) 'Global epidemiology of influenza: past and present', *Annual Review of Medicine*, 51, pp. 407-421.

Cox, R.J. (2013) 'Correlates of protection to influenza virus, where do we go from here?', *Human vaccines & immunotherapeutics*, 9(2), pp. 405-408.

Crabb, B.S. and Studdert, M.J. (1993) 'Epitopes of glycoprotein G of equine herpesviruses 4 and 1 located near the C termini elicit type-specific antibody responses in the natural host', *Journal of virology*, 67(10), pp. 6332-6338.

Crabb, B.S., Allen, G.P. and Studdert, M.J. (1991) 'Characterization of the major glycoproteins of equine herpesviruses 4 and 1 and asinine herpesvirus 3 using monoclonal antibodies', *The Journal of general virology*, 72 (Pt 9) (Pt 9), pp. 2075-2082.

Crabb, B.S., MacPherson, C.M., Reubel, G.H., Browning, G.F., Studdert, M.J. and Drummer, H.E. (1995) 'A type-specific serological test to distinguish antibodies to equine herpesviruses 4 and 1', *Archives of Virology*, 140(2), pp. 245-258.

Crabb, B.S., MacPherson, C.M., Reubel, G.H., Browning, G.F., Studdert, M.J. and Drummer, H.E. (1995) 'A type-specific serological test to distinguish antibodies to equine herpesviruses 4 and 1', *Archives of Virology*, 140(2), pp. 245-258.

Crabb, B.S., Nagesha, H.S. and Studdert, M.J. (1992) 'Identification of equine herpesvirus 4 glycoprotein G: a type-specific, secreted glycoprotein', *Virology*, 190(1), pp. 143-154.

Crescenzo-Chaigne, B., Barbezange, C. and van der Werf, S. (2008) 'Non coding extremities of the seven influenza virus type C vRNA segments: effect on transcription and replication by the type C and type A polymerase complexes', *Virology journal*, 5, pp. 132-422X.

Cros, J.F. and Palese, P. (2003) 'Trafficking of viral genomic RNA into and out of the nucleus: influenza, Thogoto and Borna disease viruses', *Virus research*, 95(1-2), pp. 3-12.

Crowhurst, F.A., Dickinson, G. and Burrows, R. (1981) 'An outbreak of paresis in mares and geldings associated with equid herpesvirus 1', *The Veterinary record*, 109(24), pp. 527-528.

Croyle, M.A., Cheng, X. and Wilson, J.M. (2001) 'Development of formulations that enhance physical stability of viral vectors for gene therapy', *Gene therapy*, 8(17), pp. 1281-1290.

Csellner, H., Walker, C., Wellington, J.E., McLure, L.E., Love, D.N. and Whalley, J.M. (2000) 'EHV-1 glycoprotein D (EHV-1 gD) is required for virus entry and cell-cell fusion, and an EHV-1 gD deletion mutant induces a protective immune response in mice', *Archives of Virology*, 145(11), pp. 2371-2385.

Daniels, R.S., Downie, J.C., Hay, A.J., Knossow, M., Skehel, J.J., Wang, M.L. and Wiley, D.C. (1985) 'Fusion mutants of the influenza virus hemagglutinin glycoprotein', *Cell*, 40(2), pp. 431-439.

Darling, D., Hughes, C., Galea-Lauri, J., Gäken, J., Trayner, I.D., Kuiper, M. and Farzaneh, F. (2000) 'Low-speed centrifugation of retroviral vectors absorbed to a particulate substrate: a highly effective means of enhancing retroviral titre', *Gene therapy*, 7(11), pp. 914-923.

David-Watine, B., Israël, A. and Kourilsky, P. (1990) 'The regulation and expression of MHC class I genes', *Immunology today*, 11, pp. 286-292.

Davison AJ (2007) 'Overview of classification.', in Arvin A, C.G. (ed.) *Human Herpesviruses: Biology, Therapy, and Immunoprophylaxis*. Cambridge: Cambridge University Press. Chapter 1 edn.

Davison, A.J. (2002) 'Evolution of the herpesviruses', *Veterinary microbiology*, 86(1), pp. 69-88.

Davison, A.J. and Clements, J.B. (2010) 'Herpesviruses: General Properties' *Topley & Wilson's Microbiology and Microbial Infections* John Wiley & Sons, Ltd.

Davison, A.J., Eberle, R., Ehlers, B., Hayward, G.S., McGeoch, D.J., Minson, A.C., Pellett, P.E., Roizman, B., Studdert, M.J. and Thiry, E. (2009) 'The order Herpesvirales', *Archives of Virology*, 154(1), pp. 171-177.

Davis-Poynter, N., Bell, S., Minson, T. and Browne, H. (1994) 'Analysis of the contributions of herpes simplex virus type 1 membrane proteins to the induction of cell-cell fusion', *Journal of virology*, 68(11), pp. 7586-7590.

Dayaram, A., Seeber, P.A. and Greenwood, A.D. (2021) 'Environmental Detection and Potential Transmission of Equine Herpesviruses', *Pathogens (Basel, Switzerland)*, 10(4), pp. 423.

de Jong, J.C., Rimmelzwaan, G.F., Fouchier, R.A.M. and Osterhaus, A D M E (2000) 'Influenza Virus: a Master of Metamorphosis', *Journal of Infection*, 40(3), pp. 218-228.

de Vries, E., Tscherne, D.M., Wienholts, M.J., Cobos-Jiménez, V., Scholte, F., García-Sastre, A., Rottier, P.J. and de Haan, C.A. (2011) 'Dissection of the influenza A virus endocytic routes reveals macropinocytosis as an alternative entry pathway', *PLoS pathogens*, 7(3), pp. e1001329.

Del Rosario, J.M.M., da Costa, K.A.S., Asbach, B., Ferrara, F., Ferrari, M., Wells, D.A., Mann, G.S., Ameh, V.O., Sabeta, C.T., Banyard, A.C., Kinsley, R., Scott, S.D., Wagner, R., Heeney, J.L., Carnell, G.W. and Temperton, N.J. (2021) 'Establishment of pan-Influenza A (H1-H18) and pan-Influenza B (pre-split, Vic/Yam) Pseudotype Libraries for efficient vaccine antigen selection', *bioRxiv*, pp. 2021.05.20.444964.

Delacroix, N., Mbele, G.O., Deroyer, J., Deplaine, G. and Bauche, C. (2015) 'Development of a Successful Lyophilization Process for Lentiviral Vector Clinical Batches', *Molecular Therapy*, 23, pp. S267.

Demaison, C., Parsley, K., Brouns, G., Scherr, M., Battmer, K., Kinnon, C., Grez, M. and Thrasher, A.J. (2002) 'High-level transduction and gene expression in hematopoietic repopulating cells using a human immunodeficiency [correction of immunodeficiency] virus type 1-based lentiviral vector containing an internal spleen focus forming virus promoter', *Human Gene Therapy*, 13(7), pp. 803-813.

Deng, H.K., Unutmaz, D., KewalRamani, V.N. and Littman, D.R. (1997) 'Expression cloning of new receptors used by simian and human immunodeficiency viruses', *Nature*, 388(6639), pp. 296-300.

Desai, P.J., Schaffer, P.A. and Minson, A.C. (1988) 'Excretion of non-infectious virus particles lacking glycoprotein H by a temperature-sensitive mutant of herpes simplex virus type 1: evidence that gH is essential for virion infectivity', *The Journal of general virology*, 69 (Pt 6) (Pt 6), pp. 1147-1156.

Di Francesco, C.E., Smoglica, C., De Amicis, I., Cafini, F., Carluccio, A. and Contri, A. (2020) 'Evaluation of Colostral Immunity Against Equine Herpesvirus Type 1 (EHV-1) in MartinaFranca's Foals', *Frontiers in Veterinary Science*, 7, pp. 885.

Di Genova, C., Sampson, A., Scott, S., Cantoni, D., Mayora-Neto, M., Bentley, E., Mattiuzzo, G., Wright, E., Derveni, M., Auld, B., Ferrara, B.T., Harrison, D., Said, M., Selim, A., Thompson, E., Thompson, C., Carnell, G. and Temperton, N. (2021) 'Production, Titration, Neutralisation, Storage and Lyophilisation of Severe Acute Respiratory Syndrome Coronavirus 2 (SARS-CoV-2) Lentiviral Pseudotypes', *Bio-protocol*, 11(21), pp. e4236.

Dias, A., Bouvier, D., Crépin, T., McCarthy, A.A., Hart, D.J., Baudin, F., Cusack, S. and Ruigrok, R.W. (2009) 'The cap-snatching endonuclease of influenza virus polymerase resides in the PA subunit', *Nature*, 458(7240), pp. 914-918.

Dimock, W. and Edwards, P.R. (1932) *Infections of fetuses and foals* Kentucky Agricultural Experiment Station, University of Kentucky.

Doll, E., Wallace, E. and Richards, M. (1954) 'Thermal, hematological, and serological responses of weanling horses following inoculation with equine abortion virus: its similarity to equine influenza.', *The Cornell veterinarian*, 44, pp. 181.

Doms, R.W., Lamb, R.A., Rose, J.K. and Helenius, A. (1993) 'Folding and assembly of viral membrane proteins', *Virology*, 193(2), pp. 545-562.

Drake, J.W. (1993) 'Rates of spontaneous mutation among RNA viruses', *Proceedings of the National Academy of Sciences of the United States of America*, 90(9), pp. 4171-4175.

Dugan, V.G., Chen, R., Spiro, D.J., Sengamalay, N., Zaborsky, J., Ghedin, E., Nolting, J., Swayne, D.E., Runstadler, J.A., Happ, G.M., Senne, D.A., Wang, R., Slemons, R.D., Holmes, E.C. and Taubenberger, J.K. (2008) 'The evolutionary genetics and emergence of avian influenza viruses in wild birds', *PLoS pathogens*, 4(5), pp. e1000076.

Dunowska, M., Gopakumar, G., Perrott, M.R., Kendall, A.T., Waropastrakul, S., Hartley, C.A. and Carslake, H.B. (2015) 'Virological and serological investigation of Equid herpesvirus 1 infection in New Zealand', *Veterinary microbiology*, 176(3), pp. 219-228.

Dunuwille, W.M.B., YousefiMashouf, N., Balasuriya, U.B.R., Pusterla, N. and Bailey, E. (2020) 'Genome-wide association study for host genetic factors associated with equine herpesvirus type-1 induced myeloencephalopathy', *Equine veterinary journal*, 52(6), pp. 794-798.

Dupré, G., Hoede, C., Figueroa, T., Bessière, P., Bertagnoli, S., Ducatez, M., Gaspin, C. and Volmer, R. (2021) 'Phylogenetic study of the conserved RNA structure encompassing the hemagglutinin cleavage site encoding region of H5 and H7 low pathogenic avian influenza viruses', *Virus Evolution*, 7(2).

Dutta, S.K. and Myrup, A.C. (1983) 'Infectious center assay of intracellular virus and infective virus titer for equine mononuclear cells infected in vivo and in vitro with equine herpesviruses', *Canadian journal of comparative medicine: Revue canadienne de médecine comparée*, 47(1), pp. 64-69.

Dutta, S.K., Talbot, N.C. and Myrup, A.C. (1983) 'Detection of equine herpesvirus-1 antigen and the specific antibody by enzyme-linked immunosorbent assay', *American Journal of Veterinary Research*, 44(10), pp. 1930-1934.

ECCD European Community Commission Directive (2006) *Commission Decision 2006/437/EC of 4 August 2006 approving a Diagnostic Manual for avian influenza as provided for Council Directive 2005/94/EC*.

Edington, N. And Bridges, C.G. (1990) 'One way protection between equid herpesvirus 1 and 4 in vivo', *Research in veterinary science*, 48(2), pp. 235-239.

Edington, N., Bridges, C.G. and Griffiths, L. (1989) 'Equine interferons following exposure to equid herpesvirus-1 or -4', *Journal of interferon research*, 9(4), pp. 389-392.

Edington, N., Bridges, C.G. and Huckle, A. (1985) 'Experimental reactivation of equid herpesvirus 1 (EHV 1) following the administration of corticosteroids', *Equine veterinary journal*, 17(5), pp. 369-372.

Edington, N., Bridges, C.G. and Patel, J.R. (1986) 'Endothelial cell infection and thrombosis in paralysis caused by equid herpesvirus-1: equine stroke', *Archives of Virology*, 90(1-2), pp. 111-124.

Edington, N., Smyth, B. and Griffiths, L. (1991) 'The role of endothelial cell infection in the endometrium, placenta and foetus of equid herpesvirus 1 (EHV-1) abortions.', *Journal of comparative pathology*, 104 4, pp. 379-387.

Edington, N., Welch, H.M. and Griffiths, L. (1994) 'The prevalence of latent Equid herpesviruses in the tissues of 40 abattoir horses', *Equine veterinary journal*, 26(2), pp. 140-142.

EDQM European Directorate for the Quality of Medicines and Healthcare (2017) *European Pharmacopoeia monograph 249 Equine Influenza Vaccine (Inactivated)*.

EFSA (European Food Safety Authority), ECDC (European Centre for Disease Prevention and Control) (2022) 'Scientific report: Avian influenza overview March–June 2022. ', *EFSA Journal*, 20(6):7415, 67 pp.

Efstathiou, S. and Preston, C.M. (2005) 'Towards an understanding of the molecular basis of herpes simplex virus latency', *Virus research*, 111(2), pp. 108-119.

Efstathiou, S., Kemp, S., Darby, G. and Minson, A.C. (1989) 'The role of herpes simplex virus type 1 thymidine kinase in pathogenesis', *The Journal of general virology*, 70 (Pt 4) (Pt 4), pp. 869-879.

Eisenberg, R.J., Atanasiu, D., Cairns, T.M., Gallagher, J.R., Krummenacher, C. and Cohen, G.H. (2012) 'Herpes Virus Fusion and Entry: A Story with Many Characters', *Viruses*, 4(5), pp. 800-832.

El Brini, Z., Fassi Fihri, O., Paillot, R., Lotfi, C., Amraoui, F., El Ouadi, H., Dehhaoui, M., Colitti, B., Alyakine, H. and Piro, M. (2021) 'Seroprevalence of Equine Herpesvirus 1 (EHV-1) and Equine Herpesvirus 4 (EHV-4) in the Northern Moroccan Horse Populations', *Animals: an open access journal from MDPI*, 11(10), pp. 2851.

Ellis, D., Lederhofer, J., Acton, O.J., Tsybovsky, Y., Kephart, S., Yap, C., Gillespie, R.A., Creanga, A., Olshefsky, A., Stephens, T., Pettie, D., Murphy, M., Sydeman, C., Ahlrichs, M., Chan, S., Borst, A.J., Park, Y.J., Lee, K.K., Graham, B.S., Veessler, D., King, N.P. and Kanekiyo, M. (2022) 'Structure-based design of stabilized recombinant influenza neuraminidase tetramers', *Nature communications*, 13(1), pp. 1825-022.

EMA European Medicines Agency (2014) *Guideline on data requirements for changes to the strain composition of authorised equine influenza vaccines in line with OIE recommendations EMA/CVMP/IWP/97961/2013.*

EMA European Medicines Agency (2016) *Guideline on influenza vaccines. Non-clinical and Clinical Module EMA/CHMP/VWP/457259/2014.*

European Food Safety Authority (EFSA), Carvelli, A., Nielsen, S.S., Paillot, R., Broglia, A. and Kohnle, L. (2022) 'Clinical impact, diagnosis and control of Equine Herpesvirus-1 infection in Europe', *EFSA Journal*, 20(4), pp. e07230.

Evseev, D. and Magor, K.E. (2019) 'Innate Immune Responses to Avian Influenza Viruses in Ducks and Chickens', *Veterinary sciences*, 6(1), pp. 5.

Fang, Y., Ye, P., Wang, X., Xu, X. and Reisen, W. (2011) 'Real-time monitoring of flavivirus induced cytopathogenesis using cell electric impedance technology', *Journal of virological methods*, 173(2), pp. 251-258.

Fédération Équestre Internationale (FEI) (2022) *EHV-1 Report*. Available at: <https://inside.fei.org/fei/your-role/veterinarians/biosecurity-movements/biosecurity/ehv-1/report> (Accessed: 22 July 2022)

Ferrara, F. (2015) *Using Pseudotypes To Study Heterosubtypic Antibody Responses Elicited By Seasonal Influenza Vaccination*. Doctor of Philosophy (PhD) thesis. University of Kent.

Ferrara, F. and Temperton, N. (2018) 'Pseudotype Neutralization Assays: From Laboratory Bench to Data Analysis', *Methods and protocols*, 1(1), pp. 8.

Ferrara, F., Molesti, E., Böttcher-Friebertshäuser, E., Cattoli, G., Corti, D., Scott, S.D. and Temperton, N.J. (2012) 'The human Transmembrane Protease Serine 2 is necessary for the production of Group 2 influenza A virus pseudotypes', *Journal of molecular and genetic medicine: an international journal of biomedical research*, 7, pp. 309-314.

Ferrara, F., Molesti, E., Scott, S., Cattoli, G. and Temperton, N. (2017) 'The Use of Hyperimmune Chicken Reference Sera Is Not Appropriate for the Validation of Influenza Pseudotype Neutralization Assays', *Pathogens (Basel, Switzerland)*, 6(4), pp. 45.

Field, H.J. and Wildy, P. (1978) 'The pathogenicity of thymidine kinase-deficient mutants of herpes simplex virus in mice', *The Journal of hygiene*, 81(2), pp. 267-277.

Flowers, C.C. and O'Callaghan, D.J. (1992) 'Equine herpesvirus 1 glycoprotein D: mapping of the transcript and a neutralization epitope', *Journal of virology*, 66(11), pp. 6451-6460.

Fodor, E. (2013) 'The RNA polymerase of influenza A virus: mechanisms of viral transcription and replication', *Acta virologica*, 57(2), pp. 113-122.

Foote, C.E., Love, D.N., Gilkerson, J.R. and Whalley, J.M. (2002) 'Serological responses of mares and weanlings following vaccination with an inactivated whole virus equine herpesvirus 1 and equine herpesvirus 4 vaccine', *Veterinary microbiology*, 88(1), pp. 13-25.

Forrester, A., Farrell, H., Wilkinson, G., Kaye, J., Davis-Poynter, N. and Minson, T. (1992) 'Construction and properties of a mutant of herpes simplex virus type 1 with glycoprotein H coding sequences deleted', *Journal of virology*, 66(1), pp. 341-348.

Fouchier, R.A., Munster, V., Wallensten, A., Bestebroer, T.M., Herfst, S., Smith, D., Rimmelzwaan, G.F., Olsen, B. and Osterhaus, A.D. (2005) 'Characterization of a novel influenza A virus hemagglutinin subtype (H16) obtained from black-headed gulls', *Journal of virology*, 79(5), pp. 2814-2822.

Fouchier, R.A., Osterhaus, A.D. and Brown, I.H. (2003) 'Animal influenza virus surveillance', *Vaccine*, 21(16), pp. 1754-1757.

Frampton, A.R., Goins, W.F., Cohen, J.B., von Einem, J., Osterrieder, N., O'Callaghan, D.J. and Glorioso, J.C. (2005) 'Equine herpesvirus 1 utilizes a novel herpesvirus entry receptor', *Journal of virology*, 79(5), pp. 3169-3173.

Frampton, A.R., Stolz, D.B., Uchida, H., Goins, W.F., Cohen, J.B. and Glorioso, J.C. (2007) 'Equine herpesvirus 1 enters cells by two different pathways, and infection requires the activation of the cellular kinase ROCK1', *Journal of virology*, 81(20), pp. 10879-10889.

Fujii, Y., Goto, H., Watanabe, T., Yoshida, T. and Kawaoka, Y. (2003) 'Selective incorporation of influenza virus RNA segments into virions', *Proceedings of the National Academy of Sciences of the United States of America*, 100(4), pp. 2002-2007.

Fukushi, H., Tomita, T., Taniguchi, A., Ochiai, Y., Kirisawa, R., Matsumura, T., Yanai, T., Masegi, T., Yamaguchi, T. and Hirai, K. (1997) 'Gazelle herpesvirus 1: a new neurotropic herpesvirus immunologically related to equine herpesvirus 1', *Virology*, 227(1), pp. 34-44.

Fukushi, H., Yamaguchi, T. and Yamada, S. (2012) 'Complete genome sequence of equine herpesvirus type 9', *Journal of virology*, 86(24), pp. 13822-12.

Funke, S., Maisner, A., Mühlebach, M.D., Koehl, U., Grez, M., Cattaneo, R., Cichutek, K. and Buchholz, C.J. (2008) 'Targeted cell entry of lentiviral vectors', *Molecular therapy: the journal of the American Society of Gene Therapy*, 16(8), pp. 1427-1436.

Galdiero, S., Falanga, A., Vitiello, M., Raiola, L., Fattorusso, R., Browne, H., Pedone, C., Isernia, C. and Galdiero, M. (2008) 'Analysis of a membrane interacting region of herpes simplex virus type 1 glycoprotein H', *The Journal of biological chemistry*, 283(44), pp. 29993-30009.

Gamblin, S.J. and Skehel, J.J. (2010) 'Influenza hemagglutinin and neuraminidase membrane glycoproteins', *The Journal of biological chemistry*, 285(37), pp. 28403-28409.

Garcia, J.M. and Lai, J.C. (2011) 'Production of influenza pseudotyped lentiviral particles and their use in influenza research and diagnosis: an update', *Expert review of anti-infective therapy*, 9(4), pp. 443-455.

García-Sastre, A. (2012) 'The neuraminidase of bat influenza viruses is not a neuraminidase', *Proceedings of the National Academy of Sciences of the United States of America*, 109(46), pp. 18635-18636.

Garko-Buczynski, K.A., Smith, R.H., Kim, S.K. and O'Callaghan, D.J. (1998) 'Complementation of a replication-defective mutant of equine herpesvirus type 1 by a cell line expressing the immediate-early protein', *Virology*, 248(1), pp. 83-94.

Garvey, M., Lyons, R., Hector, R.D., Walsh, C., Arkins, S. and Cullinane, A. (2019) 'Molecular Characterisation of Equine Herpesvirus 1 Isolates from Cases of Abortion, Respiratory and Neurological Disease in Ireland between 1990 and 2017', *Pathogens*, 8(1).

Gerl, M.J., Sampaio, J.L., Urban, S., Kalvodova, L., Verbavatz, J.M., Binnington, B., Lindemann, D., Lingwood, C.A., Shevchenko, A., Schroeder, C. and Simons, K. (2012) 'Quantitative analysis of the lipidomes of the influenza virus envelope and MDCK cell apical membrane', *The Journal of cell biology*, 196(2), pp. 213-221.

Gilkerson, J., Love, D. And Whalley, J. (2000) 'Incidence of equine herpesvirus 1 infection in Thoroughbred weanlings on two stud farms', *Australian Veterinary Journal*, 78(4), pp. 277-278.

Gilkerson, J., Love, D., Drummer, H., Studdert, M. and Whalley, J. (1998) 'Seroprevalence of equine herpesvirus 1 in Thoroughbred foals before and after weaning', *Australian Veterinary Journal*, 76(10), pp. 677-682.

Gilkerson, J.R., Whalley, J.M., Drummer, H.E., Studdert, M.J. and Love, D.N. (1999) 'Epidemiological studies of equine herpesvirus 1 (EHV-1) in Thoroughbred foals: a review of studies conducted in the Hunter Valley of New South Wales between 1995 and 1997', *Veterinary microbiology*, 68(1-2), pp. 15-25.

Giotis, E.S., Carnell, G., Young, E.F., Ghanny, S., Soteropoulos, P., Wang, L.F., Barclay, W.S., Skinner, M.A. and Temperton, N. (2019) 'Entry of the bat influenza H17N10 virus into mammalian cells is enabled by the MHC class II HLA-DR receptor', *Nature microbiology*, 4(12), pp. 2035-2038.

Glikmann, G., Mordhorst, C.H. and Koch, C. (1995) 'Monoclonal antibodies for the direct detection of influenza-A virus by ELISA in clinical specimens from patients with respiratory infections', *Clinical and diagnostic virology*, 3(4), pp. 361-369.

Goehring, L.S., Maanen, C.v., Berendsen, M., Cullinane, A., Groot, R.J.d., Rottier, P.J.M., Wesselingh, Jeroen J C M and Oldruitenborgh-Oosterbaan, Marianne M. Sloet van (2010) 'Experimental infection with neuropathogenic equid herpesvirus type 1 (EHV-1) in adult horses', *The Veterinary Journal*, 186(2), pp. 180-187.

Goehring, L.S., van Winden, S.C., van Maanen, C. and Sloet van Oldruitenborgh-Oosterbaan, M M (2006) 'Equine herpesvirus type 1-associated myeloencephalopathy in The Netherlands:

a four-year retrospective study (1999-2003)', *Journal of veterinary internal medicine*, 20(3), pp. 601-607.

Gohrbandt, S., Veits, J., Breithaupt, A., Hundt, J., Teifke, J.P., Stech, O., Mettenleiter, T.C. and Stech, J. (2011) 'H9 avian influenza reassortant with engineered polybasic cleavage site displays a highly pathogenic phenotype in chicken', *The Journal of general virology*, 92(Pt 8), pp. 1843-1853.

Golke, A., Cymerys, J., Słoińska, A., Dzieciatkowski, T., Chmielewska, A.M., Tucholska, A. and Bańbura, M.W. (2012) 'The xCELLigence system for real-time and label-free analysis of neuronal and dermal cell response to equine herpesvirus type 1 infection.', *Polish journal of veterinary sciences*, 15 1, pp. 151-153.

Goodman, L.B., Loregian, A. (2007) 'A Point Mutation in a Herpesvirus Polymerase Determines Neuropathogenicity', *PLOS Pathogens*, 3(11), pp. 1-10.

Goodman, L.B., Wagner, B., Flaminio, M J B F, Sussman, K.H., Metzger, S.M., Holland, R. and Osterrieder, N. (2006) 'Comparison of the efficacy of inactivated combination and modified-live virus vaccines against challenge infection with neuropathogenic equine herpesvirus type 1 (EHV-1)', *Vaccine*, 24(17), pp. 3636-3645.

Goodman, L.B., Wimer, C., Dubovi, E.J., Gold, C. and Wagner, B. (2012) 'Immunological Correlates of Vaccination and Infection for Equine Herpesvirus 1', *Clinical and Vaccine Immunology*, 19(2), pp. 235-241.

Görlich, D., Henklein, P., Laskey, R.A. and Hartmann, E. (1996) 'A 41 amino acid motif in importin-alpha confers binding to importin-beta and hence transit into the nucleus', *The EMBO journal*, 15(8), pp. 1810-1817.

Gottschalk, A. (1957) 'Neuraminidase: the specific enzyme of influenza virus and *Vibrio cholerae*', *Biochimica et biophysica acta*, 23(3), pp. 645-646.

Granzow, H., Klupp, B.G., Fuchs, W., Veits, J., Osterrieder, N. and Mettenleiter, T.C. (2001) 'Egress of Alphaherpesviruses: Comparative Ultrastructural Study', *Journal of virology*, 75(8), pp. 3675-3684.

Gray, W.L., Baumann, R.P., Robertson, A.T., Caughman, G.B., O'Callaghan, D.J. and Staczek, J. (1987a) 'Regulation of equine herpesvirus type 1 gene expression: characterization of immediate early, early, and late transcription', *Virology*, 158(1), pp. 79-87.

Gray, W.L., Baumann, R.P., Robertson, A.T., O'Callaghan, D.J. and Staczek, J. (1987b) 'Characterization and mapping of equine herpesvirus type 1 immediate early, early, and late transcripts', *Virus research*, 8(3), pp. 233-244.

Greenwood, A.D., Tsangaras, K., Ho, S.Y., Szentiks, C.A., Nikolin, V.M., Ma, G., Damiani, A., East, M.L., Lawrenz, A., Hofer, H. and Osterrieder, N. (2012) 'A potentially fatal mix of herpes in zoos', *Current biology: CB*, 22(18), pp. 1727-1731.

Grehan, K., Ferrara, F. and Temperton, N. (2015) 'An optimised method for the production of MERS-CoV spike expressing viral pseudotypes', *MethodsX*, 2, pp. 379-384.

Grinde, B. (2013) 'Herpesviruses: latency and reactivation - viral strategies and host response', *Journal of oral microbiology*, 5:1.

Gryspeerd A.C., Vandekerckhove, A. (2010) 'Differences in replication kinetics and cell tropism between neurovirulent and non-neurovirulent EHV1 strains during the acute phase of infection in horses', *Veterinary microbiology*, 142, pp. 242-253.

Guan, Y. and Smith, G.J.D. (2013) 'The emergence and diversification of panzootic H5N1 influenza viruses', *Virus research*, 178(1), pp. 35-43.

Guilligay, D., Tarendeau, F., Resa-Infante, P., Coloma, R., Crepin, T., Sehr, P., Lewis, J., Ruigrok, R.W., Ortin, J., Hart, D.J. and Cusack, S. (2008) 'The structural basis for cap binding by influenza virus polymerase subunit PB2', *Nature structural & molecular biology*, 15(5), pp. 500-506.

Gulati, S., Smith, D.F., Cummings, R.D., Couch, R.B., Griesemer, S.B., St George, K., Webster, R.G. and Air, G.M. (2013) 'Human H3N2 Influenza Viruses Isolated from 1968 To 2012 Show Varying Preference for Receptor Substructures with No Apparent Consequences for Disease or Spread', *PloS one*, 8(6), pp. e66325.

Guo, Y.J., Jin, F.G., Wang, P., Wang, M. and Zhu, J.M. (1983) 'Isolation of influenza C virus from pigs and experimental infection of pigs with influenza C virus', *The Journal of general virology*, 64 (Pt 1) (Pt 1), pp. 177-182.

Hahn, W.H., Bae, S.P., Song, S., Park, S., Lee, J., Seo, J.B. and Kang, N.M. (2020) 'The freeze-drying does not influence the proteomic profiles of human milk', *The journal of maternal-fetal & neonatal medicine: the official journal of the European Association of Perinatal Medicine, the Federation of Asia and Oceania Perinatal Societies, the International Society of Perinatal Obstetricians*, 33(12), pp. 2069-2074.

Haid, S., Grethe, C., Bankwitz, D., Grunwald, T., Pietschmann, T. and Lyles, D.S. (2016) 'Identification of a Human Respiratory Syncytial Virus Cell Entry Inhibitor by Using a Novel Lentiviral Pseudotype System', *Journal of virology*, 90(6), pp. 3065-3073.

Hamilton, B.S., Whittaker, G.R. and Daniel, S. (2012) 'Influenza virus-mediated membrane fusion: determinants of hemagglutinin fusogenic activity and experimental approaches for assessing virus fusion', *Viruses*, 4(7), pp. 1144-1168.

Hammond, G.W., Smith, S.J. and Noble, G.R. (1980) 'Sensitivity and specificity of enzyme immunoassay for serodiagnosis of influenza A virus infections', *The Journal of infectious diseases*, 141(5), pp. 644-651.

Hannant, D., Jessett, D.M., O'Neill, T., Dolby, C.A., Cook, R.F. and Mumford, J.A. (1993) 'Responses of ponies to equid herpesvirus-1 ISCOM vaccination and challenge with virus of the homologous strain', *Research in veterinary science*, 54(3), pp. 299-305.

Hartlaub, J., von Arnim, F., Fast, C., Mirazimi, A., Keller, M. and Groschup, M.H. (2021) 'Experimental Challenge of Sheep and Cattle with Dugbe Orthonairovirus, a Neglected African Arbovirus Distantly Related to CCHFV', *Viruses*, 13(3).

Hartley, C.A., Wilks, C.R., Studdert, M.J. and Gilkerson, J.R. (2005) 'Comparison of antibody detection assays for the diagnosis of equine herpesvirus 1 and 4 infections in horses', *American Journal of Veterinary Research*, 66(5), pp. 921-928.

Hartley, J.W. and Rowe, W.P. (1963) 'Tissue culture cytopathic and plaque assays for mouse hepatitis viruses', *Proceedings of the Society for Experimental Biology and Medicine. Society for Experimental Biology and Medicine (New York, N.Y.)*, 113, pp. 403-406.

Harty, R.N., Colle, C.F., Grundy, F.J. and O'Callaghan, D.J. (1989) 'Mapping the termini and intron of the spliced immediate-early transcript of equine herpesvirus 1', *Journal of virology*, 63(12), pp. 5101-5110.

Hause, B.M., Collin, E.A., Liu, R., Huang, B., Sheng, Z., Lu, W., Wang, D., Nelson, E.A. and Li, F. (2014) 'Characterization of a novel influenza virus in cattle and Swine: proposal for a new genus in the Orthomyxoviridae family', *mBio*, 5(2), pp. e00031-14.

Hause, B.M., Ducatez, M., Collin, E.A., Ran, Z., Liu, R., Sheng, Z., Armien, A., Kaplan, B., Chakravarty, S., Hoppe, A.D., Webby, R.J., Simonson, R.R. and Li, F. (2013) 'Isolation of a novel swine influenza virus from Oklahoma in 2011 which is distantly related to human influenza C viruses', *PLoS pathogens*, 9(2), pp. e1003176.

He, X., Draghi, M., Mahmood, K., Holmes, T.H., Kemble, G.W., Dekker, C.L., Arvin, A.M., Parham, P. and Greenberg, H.B. (2004) 'T cell–dependent production of IFN- γ by NK cells in response to influenza A virus', *The Journal of clinical investigation*, 114(12), pp. 1812-1819.

Hebert, D.N., Zhang, J.X., Chen, W., Foellmer, B. and Helenius, A. (1997) 'The number and location of glycans on influenza hemagglutinin determine folding and association with calnexin and calreticulin', *The Journal of cell biology*, 139(3), pp. 613-623.

Heggeness, M.H., Smith, P.R., Ulmanen, I., Krug, R.M. and Choppin, P.W. (1982) 'Studies on the helical nucleocapsid of influenza virus', *Virology*, 118(2), pp. 466-470.

Heldwein, E.E. and Krummenacher, C. (2008) 'Entry of herpesviruses into mammalian cells', *Cellular and molecular life sciences: CMLS*, 65(11), pp. 1653-1668.

Henry, B.E., Robinson, R.A., Dauenhauer, S.A., Atherton, S.S., Hayward, G.S. and O'Callaghan, D.J. (1981) 'Structure of the genome of equine herpesvirus type 1', *Virology*, 115(1), pp. 97-114.

Hensley, S.E., Das, S.R., Bailey, A.L., Schmidt, L.M., Hickman, H.D., Jayaraman, A., Viswanathan, K., Raman, R., Sasisekharan, R., Bennink, J.R. and Yewdell, J.W. (2009) 'Hemagglutinin Receptor Binding Avidity Drives Influenza A Virus Antigenic Drift', *Science*, 326(5953), pp. 734-736.

Herfst, S., Schrauwen, E.J., Linster, M., Chutinimitkul, S., de Wit, E., Munster, V.J., Sorrell, E.M., Bestebroer, T.M., Burke, D.F., Smith, D.J., Rimmelzwaan, G.F., Osterhaus, A.D. and Fouchier, R.A. (2012) 'Airborne transmission of influenza A/H5N1 virus between ferrets', *Science (New York, N.Y.)*, 336(6088), pp. 1534-1541.

Highlander, S.L., Cai, W.H., Person, S., Levine, M. and Glorioso, J.C. (1988) 'Monoclonal antibodies define a domain on herpes simplex virus glycoprotein B involved in virus penetration', *Journal of virology*, 62(6), pp. 1881-1888.

Hill, N.J., Ma, E.J., Meixell, B.W., Lindberg, M.S., Boyce, W.M. and Runstadler, J.A. (2016) 'Transmission of influenza reflects seasonality of wild birds across the annual cycle', *Ecology Letters*, 19(8), pp. 915-925.

Hilterbrand, A.T., Daly, R.E., Heldwein, E.E. and Shenk, T. (2021) 'Contributions of the Four Essential Entry Glycoproteins to HSV-1 Tropism and the Selection of Entry Routes', *mBio*, 12(2), pp. e00143-21.

Hirst, G.K. (1941) 'The Agglutination of Red Cells by Allantoic Fluid of Chick Embryos Infected with Influenza Virus', *Science (New York, N.Y.)*, 94(2427), pp. 22-23.

Holsinger, L.J. and Alams, R. (1991) 'Influenza virus M2 integral membrane protein is a homotetramer stabilized by formation of disulfide bonds', *Virology*, 183(1), pp. 32-43.

Hong, M. and DeGrado, W.F. (2012) 'Structural basis for proton conduction and inhibition by the influenza M2 protein', *Protein science: a publication of the Protein Society*, 21(11), pp. 1620-1633.

Hongwei S., Minghao L. (2021) 'Preparation and stability study of lyophilized lentiviral vector', *Journal of East China Normal University (Natural Science)*, 2021(3), pp. 114.

Hooper, K.A. and Bloom, J.D. (2013) 'A mutant influenza virus that uses an N1 neuraminidase as the receptor-binding protein', *Journal of virology*, 87(23), pp. 12531-12540.

Horimoto, T. and Kawaoka, Y. (2005) 'Influenza: lessons from past pandemics, warnings from current incidents', *Nature reviews. Microbiology*, 3(8), pp. 591-600.

Hu, S., Mohan Kumar, D., Sax, C., Schuler, C. and Akkina, R. (2016) 'Pseudotyping of lentiviral vector with novel vesiculovirus envelope glycoproteins derived from Chandipura and Piry viruses', *Virology*, 488, pp. 162-168.

Huang, I., Li, W., Sui, J., Marasco, W., Choe, H. and Farzan, M. (2008) 'Influenza A Virus Neuraminidase Limits Viral Superinfection', *Journal of virology*, 82(10), pp. 4834-4843.

Hue, E.S., Fortier, C.I., Suzanne, P., Zientara, S., Hans, A., Munier-Lehmann, H., Fortier, G., Pitel, P.H., Vidalain, P.O. and Pronost, S.L. (2016) 'Real-time monitoring of Equid herpesviruses infectivity in equine dermal cell based on impedance measurements', *Journal of Equine Veterinary Science*, 39, pp. S69-S70.

Huff, V., Cai, W., Glorioso, J.C. and Levine, M. (1988) 'The carboxy-terminal 41 amino acids of herpes simplex virus type 1 glycoprotein B are not essential for production of infectious virus particles', *Journal of virology*, 62(11), pp. 4403-4406.

Hussey, G.S., Ashton, L.V., Quintana, A.M., Walle, Gerlinde R Van de, Osterrieder, N. and Lunn, D.P. (2014) 'Equine herpesvirus type 1 pUL56 modulates innate responses of airway epithelial cells', *Virology*, 464-465, pp. 76-86.

Hussey, G.S., Hussey, S.B., Wagner, B., Horohov, D.W., Van de Walle, Gerlinde R, Osterrieder, N., Goehring, L.S., Rao, S. and Lunn, D.P. (2011) 'Evaluation of immune responses following

infection of ponies with an EHV-1 ORF1/2 deletion mutant', *Veterinary research*, 42(1), pp. 23.

Hutchinson, L., Browne, H., Wargent, V., Davis-Poynter, N., Primorac, S., Goldsmith, K., Minson, A.C. and Johnson, D.C. (1992) 'A novel herpes simplex virus glycoprotein, gL, forms a complex with glycoprotein H (gH) and affects normal folding and surface expression of gH', *Journal of virology*, 66, pp. 2240-2250.

Hwang, I., Scott, J.M., Kakarla, T., Duriancik, D.M., Choi, S., Cho, C., Lee, T., Park, H., French, A.R., Beli, E., Gardner, E. and Kim, S. (2012) 'Activation mechanisms of natural killer cells during influenza virus infection', *PloS one*, 7(12), pp. e51858.

Ibarrondo, F.J., Fulcher, J.A., Goodman-Meza, D., Elliott, J., Hofmann, C., Hausner, M.A., Ferbas, K.G., Tobin, N.H., Aldrovandi, G.M. and Yang, O.O. (2020) 'Rapid Decay of Anti-SARS-CoV-2 Antibodies in Persons with Mild Covid-19', *The New England journal of medicine*, 383(11), pp. 1085-1087.

Ikemura, T. (1985) 'Codon usage and tRNA content in unicellular and multicellular organisms', *Molecular biology and evolution*, 2(1), pp. 13-34.

Ito, T., Couceiro, J.N., Kelm, S., Baum, L.G., Krauss, S., Castrucci, M.R., Donatelli, I., Kida, H., Paulson, J.C., Webster, R.G. and Kawaoka, Y. (1998) 'Molecular basis for the generation in pigs of influenza A viruses with pandemic potential', *Journal of virology*, 72(9), pp. 7367-7373.

Javier, R.T., Stevens, J.G., Dissette, V.B. and Wagner, E.K. (1988) 'A herpes simplex virus transcript abundant in latently infected neurons is dispensable for establishment of the latent state', *Virology*, 166(1), pp. 254-257.

Jiang, W., Hua, R., Wei, M., Li, C., Qiu, Z., Yang, X. and Zhang, C. (2015) 'An optimized method for high-titer lentivirus preparations without ultracentrifugation', *Scientific Reports*, 5(1), pp. 13875.

Johnson, D.C. and Baines, J.D. (2011) 'Herpesviruses remodel host membranes for virus egress', *Nature reviews. Microbiology*, 9(5), pp. 382-394.

Johnson, D.C. and Ligas, M.W. (1988) 'Herpes simplex viruses lacking glycoprotein D are unable to inhibit virus penetration: quantitative evidence for virus-specific cell surface receptors', *Journal of virology*, 62(12), pp. 4605-4612.

Johnstone, S., Barsova, J., Campos, I. and Frampton, A.R. (2016) 'Equine herpesvirus type 1 modulates inflammatory host immune response genes in equine endothelial cells', *Veterinary microbiology*, 192, pp. 52-59.

Jones, K.L., Drane, D. and Gowans, E.J. (2007) 'Long-term storage of DNA-free RNA for use in vaccine studies', *BioTechniques*, 43(5), pp. 675-681.

Jorba, N., Coloma, R. and Ortín, J. (2009) 'Genetic trans-complementation establishes a new model for influenza virus RNA transcription and replication', *PLoS pathogens*, 5(5), pp. e1000462.

Joseph, U., Su, Y.C.F., Vijaykrishna, D. and Smith, G.J.D. (2017) 'The ecology and adaptive evolution of influenza A interspecies transmission', *Influenza and Other Respiratory Viruses*, 11(1), pp. 74-84.

Jung, H.E. and Lee, H.K. (2020) 'Host Protective Immune Responses against Influenza A Virus Infection', *Viruses*, 12(5), pp. 504.

Karakus, U., Thamamongood, T., Ciminski, K., Ran, W., Günther, S.C., Pohl, M.O., Eletto, D., Jeney, C., Hoffmann, D., Reiche, S., Schinköthe, J., Ulrich, R., Wiener, J., Hayes, M.G.B., Chang, M.W., Hunziker, A., Yángüez, E., Aydillo, T., Krammer, F., Oderbolz, J., Meier, M., Oxenius, A., Halenius, A., Zimmer, G., Benner, C., Hale, B.G., García-Sastre, A., Beer, M., Schwemmler, M. and Stertz, S. (2019) 'MHC class II proteins mediate cross-species entry of bat influenza viruses', *Nature*, 567(7746), pp. 109-112.

Karamendin, K., Kydyrmanov, A., Seidalina, A., Asanova, S., Daulbayeva, K., Kasymbekov, Y., Khan, E., Fereidouni, S., Starick, E., Zhumatov, K. and Sayatov, M. (2016) 'Circulation of avian paramyxoviruses in wild birds of Kazakhstan in 2002-2013', *Virology journal*, 13, pp. 23-016.

Karamendin, K., Kydyrmanov, A., Zhumatov, K., Asanova, S., Ishmukhametova, N. and Sayatov, M. (2011) 'Phylogenetic analysis of avian influenza viruses of H11 subtype isolated in Kazakhstan', *Virus genes*, 43(1), pp. 46-54.

Katz, J.M., Hancock, K. and Xu, X. (2011) 'Serologic assays for influenza surveillance, diagnosis and vaccine evaluation', *Expert review of anti-infective therapy*, 9(6), pp. 669-683.

Kawano, J., Onta, T., Kida, H. and Yanagawa, R. (1978) 'Distribution of antibodies in animals against influenza B and C viruses', *The Japanese journal of veterinary research*, 26(3-4), pp. 74-80.

Kawaoka, Y., Yamnikova, S., Chambers, T.M., Lvov, D.K. and Webster, R.G. (1990) 'Molecular characterization of a new hemagglutinin, subtype H14, of influenza A virus', *Virology*, 179(2), pp. 759-767.

Kelley, L.A., Mezulis, S., Yates, C.M., Wass, M.N. and Sternberg, M.J. (2015) 'The Phyre2 web portal for protein modeling, prediction and analysis', *Nature protocols*, 10(6), pp. 845-858.

Kemenesi, G., Tóth, G.E., Mayora-Neto, M., Scott, S., Temperton, N., Wright, E., Mühlberger, E., Hume, A.J., Zana, B., Boldogh, S.A., Görföl, T., Estók, P., Lanszki, Z., Somogyi, B.A., Nagy, Á, Pereszlényi, C.I., Dudás, G., Földes, F., Kurucz, K., Madai, M., Zeghib, S., Maes, P., Vanmechelen, B. and Jakab, F. (2021) 'Reservoir host studies of Lloviu virus: first isolation, sequencing and serology in Schreiber's bats in Europe', *bioRxiv*, , pp. 2021.08.10.455806.

Khanna, M., Saxena, L., Gupta, A., Kumar, B. and Rajput, R. (2013) 'Influenza pandemics of 1918 and 2009: a comparative account', *Future Virology*, 8(4), pp. 335-342.

Kho, D., MacDonald, C., Johnson, R., Unsworth, C.P., O'Carroll, S.J., du Mez, E., Angel, C.E. and Graham, E.S. (2015) 'Application of xCELLigence RTCA Biosensor Technology for Revealing the Profile and Window of Drug Responsiveness in Real Time', *Biosensors*, 5(2), pp. 199-222.

Kida, H., Yoden, S., Kuwabara, M. and Yanagawa, R. (1985) 'Interference with a conformational change in the haemagglutinin molecule of influenza virus by antibodies as a possible neutralization mechanism', *Vaccine*, 3(3 Suppl), pp. 219-222.

Kido, H., Okumura, Y., Takahashi, E., Pan, H., Wang, S., Yao, D., Yao, M., Chida, J. and Yano, M. (2012) 'Role of host cellular proteases in the pathogenesis of influenza and influenza-induced multiple organ failure', *Biochimica et Biophysica Acta (BBA) - Proteins and Proteomics*, 1824(1), pp. 186-194.

Kido, H., Okumura, Y., Takahashi, E., Pan, H.Y., Wang, S., Chida, J., Le, T.Q. and Yano, M. (2008) 'Host envelope glycoprotein processing proteases are indispensable for entry into human cells by seasonal and highly pathogenic avian influenza viruses', *Journal of molecular and genetic medicine: an international journal of biomedical research*, 3(1), pp. 167-175.

Kim, C.U., Lew, W., Williams, M.A., Liu, H., Zhang, L., Swaminathan, S., Bischofberger, N., Chen, M.S., Mendel, D.B., Tai, C.Y., Laver, W.G. and Stevens, R.C. (1997) 'Influenza Neuraminidase Inhibitors Possessing a Novel Hydrophobic Interaction in the Enzyme Active

Site: Design, Synthesis, and Structural Analysis of Carbocyclic Sialic Acid Analogues with Potent Anti-Influenza Activity', *Journal of the American Chemical Society*, 119(4), pp. 681-690.

Kim, C.W., Yoo, H.J., Park, J.H., Oh, J.E. and Lee, H.K. (2019) 'Exogenous Interleukin-33 Contributes to Protective Immunity via Cytotoxic T-Cell Priming against Mucosal Influenza Viral Infection', *Viruses*, 11(9).

Kim, H., Webster, R.G. and Webby, R.J. (2018) 'Influenza Virus: Dealing with a Drifting and Shifting Pathogen', *Viral immunology*, 31(2), pp. 174-183.

Kim, S.K., Holden, V.R. and O'Callaghan, D.J. (1997) 'The ICP22 protein of equine herpesvirus 1 cooperates with the IE protein to regulate viral gene expression', *Journal of virology*, 71(2), pp. 1004-1012.

Kinsley, R., Pronost, S., De Bock, M., Temperton, N., Daly, J.M., Paillot, R. and Scott, S. (2020) 'Evaluation of a Pseudotyped Virus Neutralisation Test for the Measurement of Equine Influenza Virus-Neutralising Antibody Responses Induced by Vaccination and Infection', *Vaccines*, 8(3), pp. 466.

Kirisawa, R., Endo, A., Iwai, H. and Kawakami, Y. (1993) 'Detection and identification of equine herpesvirus-1 and -4 by polymerase chain reaction', *Veterinary microbiology*, 36(1-2), pp. 57-67.

Klenk H D and Garten W (1994) 'Activation cleavage of viral spike proteins by host proteases' Wimmer E, editor. *Cellular Receptors for Animal Viruses* Cold Spring Harbor, NY: Cold Spring Harbor Press, pp. 241-280.

Kozak, M. (1987) 'An analysis of 5'-noncoding sequences from 699 vertebrate messenger RNAs', *Nucleic acids research*, 15(20), pp. 8125-8148.

Kraan, H., van Herpen, P., Kersten, G. and Amorij, J. (2014) 'Development of thermostable lyophilized inactivated polio vaccine', *Pharmaceutical research*, 31(10), pp. 2618-2629.

Krammer, F., Smith, G.J.D., Fouchier, R.A.M., Peiris, M., Kedzierska, K., Doherty, P.C., Palese, P., Shaw, M.L., Treanor, J., Webster, R.G. and García-Sastre, A. (2018) 'Influenza', *Nature Reviews Disease Primers*, 4(1), pp. 3.

Kreijtz, J H C M, Fouchier, R.A.M. and Rimmelzwaan, G.F. (2011) 'Immune responses to influenza virus infection', *Virus research*, 162(1), pp. 19-30.

Kukhanova, M.K., Korovina, A.N. and Kochetkov, S.N. (2014) 'Human herpes simplex virus: life cycle and development of inhibitors', *Biochemistry.Biokhimiia*, 79(13), pp. 1635-1652.

Kumagai, Y., Takeuchi, O., Kato, H., Kumar, H., Matsui, K., Morii, E., Aozasa, K., Kawai, T. and Akira, S. (2007) 'Alveolar Macrophages Are the Primary Interferon- α Producer in Pulmonary Infection with RNA Viruses', *Immunity*, 27(2), pp. 240-252.

Kumar, S., Stecher, G., Li, M., Niyaz, C. and Tamura, K. (2018) 'MEGA X: Molecular Evolutionary Genetics Analysis across Computing Platforms', *Molecular biology and evolution*, 35(6), pp. 1547-1549.

Kurtz, B.M., Singletary, L.B., Kelly, S.D. and Frampton, A.R. (2010) 'Equus caballus Major Histocompatibility Complex Class I Is an Entry Receptor for Equine Herpesvirus Type 1', *Journal of virology*, 84, pp. 9027.

Kydd, J.H., Hannant, D. and Mumford, J.A. (1996) 'Residence and recruitment of leucocytes to the equine lung after EHV-1 infection', *Veterinary immunology and immunopathology*, 52(1-2), pp. 15-26.

Kydd, J.H., Smith, K.C., Hannant, D., Livesay, G.J. and Mumford, J.A. (1994) 'Distribution of equid herpesvirus-1 (EHV-1) in respiratory tract associated lymphoid tissue: implications for cellular immunity', *Equine veterinary journal*, 26(6), pp. 470-473.

Kydyrmanov, A., Sayatov, M., Karamendin, K., Zhumatov, K., Asanova, S., Daulbayeva, K., Starick, E. and Fereidouni, S. (2017) 'Monitoring of influenza A viruses in wild bird populations in Kazakhstan in 2002-2009', *Archives of Virology*, 162(1), pp. 147-155.

Lakadamyali, M., Rust, M.J., Babcock, H.P. and Zhuang, X. (2003) 'Visualizing infection of individual influenza viruses', *Proceedings of the National Academy of Sciences of the United States of America*, 100(16), pp. 9280-9285.

Lamb, R.A. and Lai, C.J. (1982) 'Spliced and unspliced messenger RNAs synthesized from cloned influenza virus M DNA in an SV40 vector: expression of the influenza virus membrane protein (M1)', *Virology*, 123(2), pp. 237-256.

Lamb, R.A. and Lai, C.J. (1984) 'Expression of unspliced NS1 mRNA, spliced NS2 mRNA, and a spliced chimera mRNA from cloned influenza virus NS DNA in an SV40 vector', *Virology*, 135(1), pp. 139-147.

Lamb, R.A., Zebedee, S.L. and Richardson, C.D. (1985) 'Influenza virus M2 protein is an integral membrane protein expressed on the infected-cell surface', *Cell*, 40(3), pp. 627-633.

Lang, A., Vries, M.d., Feineis, S., Müller, E., Osterrieder, N. and Damiani, A.M. (2013) 'Development of a peptide ELISA for discrimination between serological responses to equine herpesvirus type 1 and 4', *Journal of virological methods*, 193(2), pp. 667-673.

Laver, W.G. and Kilbourne, E.D. (1966) 'Identification in a recombinant influenza virus of structural proteins derived from both parents', *Virology*, 30(3), pp. 493-501.

Lawrence, G.L., Gilkerson, J., Love, D.N., Sabine, M. and Whalley, J.M. (1994) 'Rapid, single-step differentiation of equid herpesviruses 1 and 4 from clinical material using the polymerase chain reaction and virus-specific primers', *Journal of virological methods*, 47(1-2), pp. 59-72.

Le Deuff, R., Nicolas, J., Renault, T. and Cochennec, N. (1994) 'Experimental transmission of a herpes-like virus to axenic larvae of Pacific oyster, *Crassostrea gigas*', *Bulletin of the European Association of fish Pathologists*, 14(2), pp. 69-72.

Lee, D.H., Bertran, K., Kwon, J.H. and Swayne, D.E. (2017) 'Evolution, global spread, and pathogenicity of highly pathogenic avian influenza H5Nx clade 2.3.4.4', *Journal of veterinary science*, 18(S1), pp. 269-280.

Lee, J.Y., Irmiere, A. and Gibson, W. (1988) 'Primate cytomegalovirus assembly: Evidence that DNA packaging occurs subsequent to B capsid assembly', *Virology*, 167(1), pp. 87-96.

Li, Q., Liu, Q., Huang, W., Li, X. and Wang, Y. (2018) 'Current status on the development of pseudoviruses for enveloped viruses', *Reviews in medical virology*, 28(1), pp. e1963.

Ligas, M.W. and Johnson, D.C. (1988) 'A herpes simplex virus mutant in which glycoprotein D sequences are replaced by beta-galactosidase sequences binds to but is unable to penetrate into cells', *Journal of virology*, 62(5), pp. 1486-1494.

Limame, R., Wouters, A., Pauwels, B., Fransen, E., Peeters, M., Lardon, F., De Wever, O. and Pauwels, P. (2012) 'Comparative analysis of dynamic cell viability, migration and invasion assessments by novel real-time technology and classic endpoint assays', *PloS one*, 7(10), pp. e46536.

Lin, Y.P., Gregory, V., Collins, P., Kloess, J., Wharton, S., Cattle, N., Lackenby, A., Daniels, R. and Hay, A. (2010) 'Neuraminidase receptor binding variants of human influenza A(H3N2) viruses resulting from substitution of aspartic acid 151 in the catalytic site: a role in virus attachment?', *Journal of virology*, 84(13), pp. 6769-6781.

Linster, M., van Boheemen, S., de Graaf, M., Schrauwen, E.J.A., Lexmond, P., Mänz, B., Bestebroer, T.M., Baumann, J., van Riel, D., Rimmelzwaan, G.F., Osterhaus, A D M E, Matrosovich, M., Fouchier, R.A.M. and Herfst, S. (2014) 'Identification, characterization, and natural selection of mutations driving airborne transmission of A/H5N1 virus', *Cell*, 157(2), pp. 329-339.

Lu, X., Shi, Y., Gao, F., Xiao, H., Wang, M., Qi, J. and Gao, G.F. (2012) 'Insights into avian influenza virus pathogenicity: the hemagglutinin precursor HA0 of subtype H16 has an alpha-helix structure in its cleavage site with inefficient HA1/HA2 cleavage', *Journal of virology*, 86(23), pp. 12861-12870.

Luczo, J.M., Stambas, J., Durr, P.A., Michalski, W.P. and Bingham, J. (2015) 'Molecular pathogenesis of H5 highly pathogenic avian influenza: the role of the haemagglutinin cleavage site motif', *Reviews in medical virology*, 25(6), pp. 406-430.

Lunn, D.P., Davis-Poynter, N., Flaminio, M.J., Horohov, D.W., Osterrieder, K., Pusterla, N. and Townsend, H.G. (2009) 'Equine herpesvirus-1 consensus statement', *Journal of veterinary internal medicine*, 23(3), pp. 450-461.

Ma, G., Azab, W. and Osterrieder, N. (2013) 'Equine herpesviruses type 1 (EHV-1) and 4 (EHV-4)—masters of co-evolution and a constant threat to equids and beyond', *Veterinary microbiology*, 167(1-2), pp. 123-134.

Ma, G., Feineis, S., Osterrieder, N. and Van de Walle, G R (2012) 'Identification and characterization of equine herpesvirus type 1 pUL56 and its role in virus-induced downregulation of major histocompatibility complex class I', *Journal of virology*, 86(7), pp. 3554-3563.

Macken, C.A., Webby, R.J. and Bruno, W.J. (2006) 'Genotype turnover by reassortment of replication complex genes from avian influenza A virus', *The Journal of general virology*, 87(Pt 10), pp. 2803-2815.

Mackie, J.T., MacLeod, G.A., Reubel, G.H. and Studdert, M.J. (1996) 'Diagnosis of equine herpesvirus 1 abortion using polymerase chain reaction', *Australian Veterinary Journal*, 74(5), pp. 390-391.

Maclachlan, N. (2017) 'Chapter 9 - Herpesvirales', in N James MacLachlan and Edward J Dubovi (eds.) *Fenner's Veterinary Virology (Fifth Edition)*. Fifth Edition edn. Boston: Academic Press, pp. 189-216.

Madrid, P.B., Chopra, S., Manger, I.D., Gilfillan, L., Keepers, T.R., Shurtleff, A.C., Green, C.E., Iyer, L.V., Dilks, H.H., Davey, R.A., Kolokoltsov, A.A., Carrion, R., Patterson, J.L., Bavari, S., Panchal, R., Warren, T., Wells, J.B., Moos, W.H., Burke, R.L. and Tanga, M.J. (2013) 'A Systematic Screen of FDA-Approved Drugs for Inhibitors of Biological Threat Agents', *PLoS ONE*, 8.

Mahmoud, H.Y., Andoh, K., Hattori, S., Terada, Y., Noguchi, K., Shimoda, H. and Maeda, K. (2013) 'Characterization of glycoproteins in equine herpesvirus-1', *The Journal of veterinary medical science*, 75(10), pp. 1317-1321.

Manninger R (1949) 'Studies on infectious abortion in mares due to a filterable virus', *Acta Veterinaria Academiae Scientiarum Hungaricae*, 1, pp. 62-69.

Manninger R and Csontos J (1941) 'Virusabortus der Stuten', *Dtsch Tierarztl Wschr*, 49, pp. 105-111.

Marenzoni, M.L., Stefanetti, V., Danzetta, M.L. and Timoney, P.J. (2015) 'Gammaherpesvirus infections in equids: a review', *Veterinary medicine (Auckland, N.Z.)*, 6, pp. 91-101.

Martin, K. and Helenius, A. (1991) 'Nuclear transport of influenza virus ribonucleoproteins: the viral matrix protein (M1) promotes export and inhibits import', *Cell*, 67(1), pp. 117-130.

Mather, S., Scott, S., Temperton, N., Wright, E., King, B. and Daly, J. (2013) 'Current progress with serological assays for exotic emerging/re-emerging viruses', *Future Virology*, 8(8), pp. 745-755.

Mather, S.T. (2017) *Development of pseudotyped virus assays for the serological study of Japanese encephalitis flavivirus*. Doctor of Philosophy (PhD) thesis. University of Kent.

Mather, S.T., Wright, E., Scott, S.D. and Temperton, N.J. (2014) 'Lyophilisation of influenza, rabies and Marburg lentiviral pseudotype viruses for the development and distribution of a neutralisation -assay-based diagnostic kit', *Journal of virological methods*, 210, pp. 51-58.

Matrosovich, M., Stech, J. and Klenk, H.D. (2009) 'Influenza receptors, polymerase and host range', *Revue scientifique et technique (International Office of Epizootics)*, 28(1), pp. 203-217.

Matrosovich, M.N., Matrosovich, T.Y., Gray, T., Roberts, N.A. and Klenk, H.D. (2004) 'Neuraminidase is important for the initiation of influenza virus infection in human airway epithelium', *Journal of virology*, 78(22), pp. 12665-12667.

Matsumura, T., Kondo, T., Sugita, S., Damiani, A.M., O'Callaghan, D.J. and Imagawa, H. (1998) 'An equine herpesvirus type 1 recombinant with a deletion in the gE and gI genes is avirulent in young horses', *Virology*, 242(1), pp. 68-79.

McCoy, Laura E and Falkowska (2015) 'Incomplete Neutralization and Deviation from Sigmoidal Neutralization Curves for HIV Broadly Neutralizing Monoclonal Antibodies', *PLOS Pathogens*, 11(8), pp. 1-19.

Medina, R.A. and García-Sastre, A. (2011) 'Influenza A viruses: new research developments', *Nature Reviews Microbiology*, 9(8), pp. 590-603.

Mettenleiter, T.C. (2002) 'Herpesvirus Assembly and Egress', *Journal of virology*, 76(4), pp. 1537-1547.

Mettenleiter, T.C. (2006) 'Intriguing interplay between viral proteins during herpesvirus assembly or: the herpesvirus assembly puzzle', *Veterinary microbiology*, 113(3-4), pp. 163-169.

Mettenleiter, T.C., Klupp, B.G. and Granzow, H. (2006) 'Herpesvirus assembly: a tale of two membranes', *Current opinion in microbiology*, 9(4), pp. 423-429.

Mettenleiter, T.C., Klupp, B.G. and Granzow, H. (2009) 'Herpesvirus assembly: an update', *Virus research*, 143(2), pp. 222-234.

Minson, A.C. (2000) 'Family Herpesviridae', in Van Regenmortel, M H V (ed.) *Virus Taxonomy* San Diego: Academic Press, pp. 203–225.

Mohr, P.G., Deng, Y.M. and McKimm-Breschkin, J.L. (2015) 'The neuraminidases of MDCK grown human influenza A(H3N2) viruses isolated since 1994 can demonstrate receptor binding', *Virology journal*, 12, pp. 67-015.

Molesti, E. (2014) *The development and application of influenza pseudotype-based neutralisation assays*. Doctor of Philosophy (PhD) thesis. University of Kent.

Molesti, E., Cattoli, G., Ferrara, F., Böttcher-Friebertshäuser, E., Terregino, C. and Temperton, N. (2012) 'The production and development of H7 Influenza virus pseudotypes for the study of humoral responses against avian viruses', *Journal of molecular and genetic medicine: an international journal of biomedical research*, 7, pp. 315-320.

Molesti, E., Milani, A., Terregino, C., Cattoli, G. and Temperton, N.J. (2013) 'Comparative Serological Assays for the Study of H5 and H7 Avian Influenza Viruses', *Influenza Research and Treatment*, 2013, pp. 286158.

Molesti, E., Wright, E., Terregino, C., Rahman, R., Cattoli, G. and Temperton, N.J. (2014) 'Multiplex evaluation of influenza neutralizing antibodies with potential applicability to in-field serological studies', *Journal of immunology research*, 2014, pp. 457932.

Mostafa, A., Abdelwhab, E.M., Mettenleiter, T.C. and Pleschka, S. (2018) 'Zoonotic Potential of Influenza A Viruses: A Comprehensive Overview', *Viruses*, 10(9).

Mould, J.A., Li, H., Dudlak, C.S., Lear, J.D., Pekosz, A., Lamb, R.A. and Pinto, L.H. (2000) 'Mechanism for Proton Conduction of the M2 Ion Channel of Influenza A Virus', *Journal of Biological Chemistry*, 275(12), pp. 8592-8599.

Muggeridge, M.I. (2000) 'Characterization of cell-cell fusion mediated by herpes simplex virus 2 glycoproteins gB, gD, gH and gL in transfected cells', *Journal of General Virology*, 81(8), pp. 2017-2027.

Mumford, J., Hannant, D. (1994) 'Abortigenic and neurological disease caused by experimental infection with equid herpesvirus-1', in H Nakajima and W Plowright (ed.) *Equine infectious diseases*. Proceedings of the Seventh International Conference on Equine Infectious Diseases edn. Newmarket, United Kingdom: R&W Publications.

Mumford, J.A. and Bates, J. (1984) 'Trials of an inactivated equid herpesvirus 1 vaccine: challenge with a subtype 2 virus', *The Veterinary record*, 114(15), pp. 375-381.

Mumford, J.A. and Rossdale, P. (1980) 'Virus and its relationship to the "poor performance" syndrome', *Equine veterinary journal*, 12, pp. 3-9.

Mumford, J.A., Rossdale, P.D., Jessett, D.M., Gann, S.J., Ousey, J. and Cook, R.F. (1987) 'Serological and virological investigations of an equid herpesvirus 1 (EHV-1) abortion storm on a stud farm in 1985', *Journal of reproduction and fertility.Supplement*, 35, pp. 509-518.

Munster, V.J., Wallensten, A., Baas, C., Rimmelzwaan, G.F., Schutten, M., Olsen, B., Osterhaus, A.D. and Fouchier, R.A. (2005) 'Mallards and highly pathogenic avian influenza ancestral viruses, northern Europe', *Emerging infectious diseases*, 11(10), pp. 1545-1551.

Naldini, L., Blömer, U., Gallay, P., Ory, D., Mulligan, R., Gage, F.H., Verma, I.M. and Trono, D. (1996) 'In vivo gene delivery and stable transduction of nondividing cells by a lentiviral vector', *Science (New York, N.Y.)*, 272(5259), pp. 263-267.

- Neu, K.E., Dunand, C.J.H. and Wilson, P.C. (2016) 'Heads, stalks and everything else: how can antibodies eradicate influenza as a human disease?', *Current opinion in immunology*, 42, pp. 48-55.
- Neubauer, A. and Osterrieder, N. (2004) 'Equine herpesvirus type 1 (EHV-1) glycoprotein K is required for efficient cell-to-cell spread and virus egress', *Virology*, 329(1), pp. 18-32.
- Neubauer, A., Beer, M., Brandmüller, C., Kaaden, O.R. and Osterrieder, N. (1997a) 'Equine herpesvirus 1 mutants devoid of glycoprotein B or M are apathogenic for mice but induce protection against challenge infection', *Virology*, 239(1), pp. 36-45.
- Neubauer, A., Braun, B., Brandmüller, C., Kaaden, O.R. and Osterrieder, N. (1997b) 'Analysis of the contributions of the equine herpesvirus 1 glycoprotein gB homolog to virus entry and direct cell-to-cell spread', *Virology*, 227(2), pp. 281-294.
- Newcomb, W.W., Brown, J.C., Booy, F.P. and Steven, A.C. (1989) 'Nucleocapsid mass and capsomer protein stoichiometry in equine herpesvirus 1: scanning transmission electron microscopic study', *Journal of virology*, 63(9), pp. 3777-3783.
- Nicoll, M.P., Proença, J.T. and Efstathiou, S. (2012) 'The molecular basis of herpes simplex virus latency', *FEMS microbiology reviews*, 36(3), pp. 684-705.
- Nie, Y., Wang, P., Shi, X., Wang, G., Chen, J., Zheng, A., Wang, W., Wang, Z., Qu, X., Luo, M., Tan, L., Song, X., Yin, X., Chen, J., Ding, M. and Deng, H. (2004) 'Highly infectious SARS-CoV pseudotyped virus reveals the cell tropism and its correlation with receptor expression', *Biochemical and biophysical research communications*, 321(4), pp. 994-1000.
- Nireesha, G., Divya, L., Sowmya, C., Venkateshan, N., Babu, M.N. and Lavakumar, V. (2013) *Lyophilization/Freeze Drying - A Review*.
- Niwa, H., Yamamura, K. and Miyazaki, J. (1991) 'Efficient selection for high-expression transfectants with a novel eukaryotic vector', *Gene*, 108(2), pp. 193-199.
- Noda, T., Sagara, H., Yen, A., Takada, A., Kida, H., Cheng, R.H. and Kawaoka, Y. (2006) 'Architecture of ribonucleoprotein complexes in influenza A virus particles', *Nature*, 439(7075), pp. 490-492.
- Nugent, J. (2003) *DNA polymerase sequence variation is a marker of virulence for equine herpesvirus type 1 (abstract)*, Proc. 3rd Int. Vet. Vaccine Diagnostics Conf edn.

Nugent, J. and Paillot, R. (2009) 'Equine herpesvirus myeloencephalopathy: unravelling the enigma', *Veterinary journal (London, England: 1997)*, 180(3), pp. 271-272.

Nugent, J., Birch-Machin, I., Smith, K.C., Mumford, J.A., Swann, Z., Newton, J.R., Bowden, R.J., Allen, G.P. and Davis-Poynter, N. (2006) 'Analysis of equid herpesvirus 1 strain variation reveals a point mutation of the DNA polymerase strongly associated with neuropathogenic versus nonneuropathogenic disease outbreaks', *Journal of virology*, 80(8), pp. 4047-4060.

Nuwarda, R.F., Alharbi, A.A. and Kayser, V. (2021) 'An Overview of Influenza Viruses and Vaccines', *Vaccines*, 9(9).

Obenauer, J.C., Denson, J., Mehta, P.K., Su, X., Mukatira, S., Finkelstein, D.B., Xu, X., Wang, J., Ma, J., Fan, Y., Rakestraw, K.M., Webster, R.G., Hoffmann, E., Krauss, S., Zheng, J., Zhang, Z. and Naeve, C.W. (2006) 'Large-scale sequence analysis of avian influenza isolates', *Science (New York, N.Y.)*, 311(5767), pp. 1576-1580.

Ohwada, K., Kitame, F., Sugawara, K., Nishimura, H., Homma, M. and Nakamura, K. (1987) 'Distribution of the antibody to influenza C virus in dogs and pigs in Yamagata Prefecture, Japan', *Microbiology and immunology*, 31(12), pp. 1173-1180.

OIE (2018) 'Equine rhinopneumonitis (Infection with equid herpesvirus-1 and -4)', *Manual of Diagnostic Tests and Vaccines for Terrestrial Animals*, pp. 1320-1332.

OIE (2021) 'Avian influenza (including infection with high pathogenicity avian influenza viruses)', *Manual of Diagnostic Tests and Vaccines for Terrestrial Animals*, pp. 1-26.

Ojala, P.M., Sodeik, B., Ebersold, M.W., Kutay, U. and Helenius, A. (2000) 'Herpes simplex virus type 1 entry into host cells: reconstitution of capsid binding and uncoating at the nuclear pore complex in vitro', *Molecular and cellular biology*, 20(13), pp. 4922-4931.

Okuno, Y., Tanaka, K., Baba, K., Maeda, A., Kunita, N. and Ueda, S. (1990) 'Rapid focus reduction neutralization test of influenza A and B viruses in microtiter system', *Journal of clinical microbiology*, 28(6), pp. 1308-1313.

Oladunni, F.S., Horohov, D.W. and Chambers, T.M. (2019) 'EHV-1: A Constant Threat to the Horse Industry', *Frontiers in microbiology*, 10, pp. 2668.

Olguin-Periglione, C., Vissani, M.A., Alamos, F., Tordoya, M.S. and Barrandeguy, M. (2020) 'Multifocal outbreak of equine influenza in vaccinated horses in Argentina in 2018: Epidemiological aspects and molecular characterisation of the involved virus strains', *Equine veterinary journal*, 52(3), pp. 420-427.

Olsen, B., Munster, V.J., Wallensten, A., Waldenström, J., Osterhaus, A.D. and Fouchier, R.A. (2006) 'Global patterns of influenza A virus in wild birds', *Science (New York, N.Y.)*, 312(5772), pp. 384-388.

O'Neill, R.E., Jaskunas, R., Blobel, G., Palese, P. and Moroianu, J. (1995) 'Nuclear import of influenza virus RNA can be mediated by viral nucleoprotein and transport factors required for protein import', *The Journal of biological chemistry*, 270(39), pp. 22701-22704.

O'Neill, T., Kydd, J.H., Allen, G.P., Watrang, E., Mumford, J.A. and Hannant, D. (1999) 'Determination of equid herpesvirus 1-specific, CD8+, cytotoxic T lymphocyte precursor frequencies in ponies', *Veterinary immunology and immunopathology*, 70(1-2), pp. 43-54.

Orr, M.T., Kramer, R.M., Barnes, L.S., Dowling, Q.M., Desbien, A.L., Beebe, E.A., Laurance, J.D., Fox, C.B., Reed, S.G., Coler, R.N. and Vedvick, T.S. (2014) 'Elimination of the cold-chain dependence of a nanoemulsion adjuvanted vaccine against tuberculosis by lyophilization', *Journal of controlled release: official journal of the Controlled Release Society*, 177, pp. 20-26.

Osterhaus, A.D.M.E., Rimmelzwaan, G.F., Martina, B.E.E., Bestebroer, T.M. and Fouchier, R.A.M. (2000) 'Influenza B Virus in Seals', *Science*, 288(5468), pp. 1051-1053.

Osterrieder, N. (1999) 'Construction and characterization of an equine herpesvirus 1 glycoprotein C negative mutant', *Virus research*, 59(2), pp. 165-177.

Osterrieder, N. and Van de Walle, G.R. (2010) 'Pathogenic potential of equine alpha herpesviruses: The importance of the mononuclear cell compartment in disease outcome', *Veterinary microbiology*, 143(1), pp. 21-28.

Osterrieder, N., Holden, V.R., Brandmüller, C., Neubauer, A., Kaaden, O.R. and O'Callaghan, D.J. (1996a) 'The equine herpesvirus 1 IR6 protein is nonessential for virus growth in vitro and modified by serial virus passage in cell culture', *Virology*, 217(2), pp. 442-451.

Osterrieder, N., Neubauer, A., Brandmüller, C., Braun, B., Kaaden, O.R. and Baines, J.D. (1996b) 'The equine herpesvirus 1 glycoprotein gp21/22a, the herpes simplex virus type 1 gM homolog, is involved in virus penetration and cell-to-cell spread of virions', *Journal of virology*, 70(6), pp. 4110-4115.

Ostlund, E.N. (1993) 'The equine herpesviruses', *The Veterinary clinics of North America. Equine practice*, 9(2), pp. 283-294.

Ouchi, A., Nerome, K., Kanegae, Y., Ishida, M., Nerome, R., Hayashi, K., Hashimoto, T., Kaji, M., Kaji, Y. and Inaba, Y. (1996) 'Large outbreak of swine influenza in southern Japan caused by reassortant (H1N2) influenza viruses: its epizootic background and characterization of the causative viruses', *Journal of General Virology*, 77(8), pp. 1751-1759.

Packiarajah, P., Walker, C., Gilkerson, J., Whalley, J.M. and Love, D.N. (1998) 'Immune responses and protective efficacy of recombinant baculovirus-expressed glycoproteins of equine herpesvirus 1 (EHV-1) gB, gC and gD alone or in combinations in BALB/c mice', *Veterinary microbiology*, 61(4), pp. 261-278.

Paillot, R., Case, R., Ross, J., Newton, R. and Nugent, J. (2008) 'Equine Herpes Virus-1: Virus, Immunity and Vaccines', *The Open Veterinary Science Journal*, 2, pp. 68-91.

Paillot, R., Daly, J.M., Juillard, V., Minke, J.M., Hannant, D. and Kydd, J.H. (2005) 'Equine interferon gamma synthesis in lymphocytes after in vivo infection and in vitro stimulation with EHV-1', *Vaccine*, 23(36), pp. 4541-4551.

Paillot, R., Daly, J.M., Luce, R., Montesso, F., Davis-Poynter, N., Hannant, D. and Kydd, J.H. (2007) 'Frequency and phenotype of EHV-1 specific, IFN-gamma synthesising lymphocytes in ponies: the effects of age, pregnancy and infection', *Developmental and comparative immunology*, 31(2), pp. 202-214.

Paillot, R., Ellis, S.A., Daly, J.M., Audonnet, J.C., Minke, J.M., Davis-Poynter, N., Hannant, D. and Kydd, J.H. (2006) 'Characterisation of CTL and IFN-gamma synthesis in ponies following vaccination with a NYVAC-based construct coding for EHV-1 immediate early gene, followed by challenge infection', *Vaccine*, 24(10), pp. 1490-1500.

Palese, P. and Compans, R.W. (1976) 'Inhibition of influenza virus replication in tissue culture by 2-deoxy-2,3-dehydro-N-trifluoroacetylneuraminic acid (FANA): mechanism of action', *The Journal of general virology*, 33(1), pp. 159-163.

Palese, P., Tobita, K., Ueda, M. and Compans, R.W. (1974) 'Characterization of temperature sensitive influenza virus mutants defective in neuraminidase', *Virology*, 61(2), pp. 397-410.

Patel, J.R. and Heldens, J. (2005) 'Equine herpesviruses 1 (EHV-1) and 4 (EHV-4) – epidemiology, disease and immunoprophylaxis: a brief review', *Veterinary journal (London, England: 1997)*, 170(1), pp. 14-23.

Patel, J.R., Edington, N. and Mumford, J.A. (1982) 'Variation in cellular tropism between isolates of equine herpesvirus-1 in foals', *Archives of Virology*, 74(1), pp. 41-51.

Pavulraj, S., Kamel, M., Stephanowitz, H., Liu, F., Plendl, J., Osterrieder, N. and Azab, W. (2020) 'Equine Herpesvirus Type 1 Modulates Cytokine and Chemokine Profiles of Mononuclear Cells for Efficient Dissemination to Target Organs', *Viruses*, 12(9), pp. 999.

Pegu, A., Yang, Z.Y., Boyington, J.C., Wu, L., Ko, S.Y., Schmidt, S.D., McKee, K., Kong, W.P., Shi, W., Chen, X., Todd, J.P., Letvin, N.L., Huang, J., Nason, M.C., Hoxie, J.A., Kwong, P.D., Connors, M., Rao, S.S., Mascola, J.R. and Nabel, G.J. (2014) 'Neutralizing antibodies to HIV-1 envelope protect more effectively in vivo than those to the CD4 receptor', *Science translational medicine*, 6(243), pp. 243ra88.

Perdue, M.L., Cohen, J.C., Randall, C.C. and O'Callaghan, D.J. (1976) 'Biochemical studies of the maturation of herpesvirus nucleocapsid species', *Virology*, 74(1), pp. 194-208.

Perdue, M.L., Kemp, M.C., Randall, C.C. and O'Callaghan, D.J. (1974) 'Studies of the molecular anatomy of the L-M cell strain of equine herpes virus type 1: proteins of the nucleocapsid and intact virion', *Virology*, 59(1), pp. 201-216.

Perkins, G., Babasyan, S., Stout, A.E., Freer, H., Rollins, A., Wimer, C.L. and Wagner, B. (2019) 'Intranasal IgG4/7 antibody responses protect horses against equid herpesvirus-1 (EHV-1) infection including nasal virus shedding and cell-associated viremia', *Virology*, 531, pp. 219-232.

Peterson, R.B. and Goyal, S.M. (1988) 'Propagation and quantitation of animal herpesviruses in eight cell culture systems', *Comparative immunology, microbiology and infectious diseases*, 11(2), pp. 93-98.

Pflug, A., Lukarska, M., Resa-Infante, P., Reich, S. and Cusack, S. (2017) 'Structural insights into RNA synthesis by the influenza virus transcription-replication machine', *Virus research*, 234, pp. 103-117.

Pinto, L.H. and Lamb, R.A. (2006) 'The M2 proton channels of influenza A and B viruses', *The Journal of biological chemistry*, 281(14), pp. 8997-9000.

Pinto, L.H., Holsinger, L.J. and Lamb, R.A. (1992) 'Influenza virus M₂ protein has ion channel activity', *Cell*, 69(3), pp. 517-528.

Pizzato, M., Erlwein, O., Bonsall, D., Kaye, S., Muir, D. and McClure, M.O. (2009) 'A one-step SYBR Green I-based product-enhanced reverse transcriptase assay for the quantitation of retroviruses in cell culture supernatants', *Journal of virological methods*, 156(1-2), pp. 1-7.

Plotch, S.J., Bouloy, M., Ulmanen, I. and Krug, R.M. (1981) 'A unique cap(m7GpppXm)-dependent influenza virion endonuclease cleaves capped RNAs to generate the primers that initiate viral RNA transcription', *Cell*, 23(3), pp. 847-858.

Plotkin, J.B. and Kudla, G. (2011) 'Synonymous but not the same: the causes and consequences of codon bias', *Nature reviews. Genetics*, 12(1), pp. 32-42.

Plotkin, S.A. (2008) 'Vaccines: correlates of vaccine-induced immunity', *Clinical infectious diseases: an official publication of the Infectious Diseases Society of America*, 47(3), pp. 401-409.

Plummer, G. and Waterson, A. (1963) 'Equine herpes viruses.', *Virology*, 19, pp. 412-416.

Post, N., Eddy, D., Huntley, C., van Schalkwyk, May C I, Shrotri, M., Leeman, D., Rigby, S., Williams, S.V., Bermingham, W.H., Kellam, P., Maher, J., Shields, A.M., Amirthalingam, G., Peacock, S.J. and Ismail, S.A. (2021) 'Antibody response to SARS-CoV-2 infection in humans: A systematic review', *PLOS ONE*, 15(12), pp. e0244126.

Pronost, S., Léon, A., Legrand, L., Fortier, C., Mischczak, F., Freymuth, F. and Fortier, G. (2010) 'Neuropathogenic and non-neuropathogenic variants of equine herpesvirus 1 in France', *Veterinary microbiology*, 145(3), pp. 329-333.

Pusterla, N. and Hussey, G.S. (2014) 'Equine herpesvirus 1 myeloencephalopathy', *The Veterinary clinics of North America. Equine practice*, 30(3), pp. 489-506.

Pusterla, N., Barnum, S., Miller, J., Varnell, S., Dallap-Schaer, B., Aceto, H. and Simeone, A. (2021) 'Investigation of an EHV-1 Outbreak in the United States Caused by a New H(752) Genotype', *Pathogens (Basel, Switzerland)*, 10(6), pp. 747.

Pusterla, N., Hatch, K., Crossley, B., Wademan, C., Barnum, S. and Flynn, K. (2020) 'Equine herpesvirus-1 genotype did not significantly affect clinical signs and disease outcome in 65 horses diagnosed with equine herpesvirus-1 myeloencephalopathy', *Veterinary journal (London, England: 1997)*, 255, pp. 105407.

Pusterla, N., Mapes, S. and Wilson, W.D. (2010) 'Prevalence of equine herpesvirus type 1 in trigeminal ganglia and submandibular lymph nodes of equids examined postmortem', *The Veterinary record*, 167(10), pp. 376-378.

Pusterla, N., Mapes, S., Madigan, J.E., Maclachlan, N.J., Ferraro, G.L., Watson, J.L., Spier, S.J. and Wilson, W.D. (2009) 'Prevalence of EHV-1 in adult horses transported over long distances', *The Veterinary record*, 165(16), pp. 473-475.

Quast, M., Sreenivasan, C., Sexton, G., Nedland, H., Singrey, A., Fawcett, L., Miller, G., Lauer, D., Voss, S., Pollock, S., Cunha, C.W., Christopher-Hennings, J., Nelson, E. and Li, F. (2015) 'Serological evidence for the presence of influenza D virus in small ruminants', *Veterinary microbiology*, 180(3-4), pp. 281-285.

Racaniello, V. *Influenza microneutralization assay*. Available at: <https://www.virology.ws/2009/05/28/influenza-microneutralization-assay/> (Accessed: 6 July 2022)

Radoshitzky, S.R., Abraham, J., Spiropoulou, C.F., Kuhn, J.H., Nguyen, D., Li, W., Nagel, J., Schmidt, P.J., Nunberg, J.H., Andrews, N.C., Farzan, M. and Choe, H. (2007) 'Transferrin receptor 1 is a cellular receptor for New World haemorrhagic fever arenaviruses', *Nature*, 446(7131), pp. 92-96.

Ran, Z., Shen, H., Lang, Y., Kolb, E.A., Turan, N., Zhu, L., Ma, J., Bawa, B., Liu, Q., Liu, H., Quast, M., Sexton, G., Krammer, F., Hause, B.M., Christopher-Hennings, J., Nelson, E.A., Richt, J., Li, F. and Ma, W. (2015) 'Domestic pigs are susceptible to infection with influenza B viruses', *Journal of virology*, 89(9), pp. 4818-4826.

Randall, C.C., Ryden, F.W., Doll, E.R. and Schell, F.S. (1953) 'Cultivation of equine abortion virus in fetal horse tissue in vitro', *The American journal of pathology*, 29(1), pp. 139-153.

Reber, A. and Katz, J. (2013) 'Immunological assessment of influenza vaccines and immune correlates of protection', *Expert review of vaccines*, 12(5), pp. 519-536.

Reid, A.H., Fanning, T.G., Slemons, R.D., Janczewski, T.A., Dean, J. and Taubenberger, J.K. (2003) 'Relationship of Pre-1918 Avian Influenza HA and NP Sequences to Subsequent Avian Influenza Strains', *Avian Diseases*, 47(s3), pp. 921.

Reignier, T., Oldenburg, J., Noble, B., Lamb, E., Romanowski, V., Buchmeier, M.J. and Cannon, P.M. (2006) 'Receptor use by pathogenic arenaviruses', *Virology*, 353(1), pp. 111-120.

Ren, Y., Bell, S., Zenner, H.L., Lau, S.K. and Crump, C.M. (2012) 'Glycoprotein M is important for the efficient incorporation of glycoprotein H-L into herpes simplex virus type 1 particles', *The Journal of general virology*, 93(Pt 2), pp. 319-329.

Reynolds, C.J., Gibbons, J.M., Pade, C., Lin, K., Sandoval, D.M., Pieper, F., Butler, D.K., Liu, S., Otter, A.D., Joy, G., Menacho, K., Fontana, M., Smit, A., Kele, B., Cutino-Moguel, T., Maini, M.K., Noursadeghi, M., null, n., Brooks, T., Semper, A., Manisty, C., Treibel, T.A., Moon, J.C.,

null, n., McKnight, Á, Altmann, D.M. and Boyton, R.J. (2022) 'Heterologous infection and vaccination shapes immunity against SARS-CoV-2 variants', *Science*, 375(6577), pp. 183-192.

Riaz, A., Murtaz-ul-Hasan, K. and Akhtar, N. (2017) 'Recent understanding of the classification and life cycle of herpesviruses: a review', *Sci.Letters*, 5(2), pp. 195-207.

Rixon, F.J., Cross, A.M., Addison, C. and Preston, V.G. (1988) 'The products of herpes simplex virus type 1 gene UL26 which are involved in DNA packaging are strongly associated with empty but not with full capsids', *The Journal of general virology*, 69 (Pt 11) (Pt 11), pp. 2879-2891.

Robertson, G.R., Scott, N.A., Miller, J.M., Sabine, M., Zheng, M., Bell, C.W. and Whalley, J.M. (1991) 'Sequence characteristics of a gene in equine herpesvirus 1 homologous to glycoprotein H of herpes simplex virus', *DNA Sequence*, 1(4), pp. 241-249.

Robertson, J.S., Schubert, M. and Lazzarini, R.A. (1981) 'Polyadenylation sites for influenza virus mRNA', *Journal of virology*, 38(1), pp. 157-163.

Rodriguez-Boulan, E., Paskiet, K.T. and Sabatini, D.D. (1983) 'Assembly of enveloped viruses in Madin-Darby canine kidney cells: polarized budding from single attached cells and from clusters of cells in suspension', *The Journal of cell biology*, 96(3), pp. 866-874.

Rogalin, H.B. and Heldwein, E.E. (2016) 'Characterization of Vesicular Stomatitis Virus Pseudotypes Bearing Essential Entry Glycoproteins gB, gD, gH, and gL of Herpes Simplex Virus 1', *Journal of virology*, 90(22), pp. 10321-10328.

Rogers, G.N. and Paulson, J.C. (1983) 'Receptor determinants of human and animal influenza virus isolates: differences in receptor specificity of the H3 hemagglutinin based on species of origin', *Virology*, 127(2), pp. 361-373.

Röhm, C., Zhou, N., Süss, J., Mackenzie, J. and Webster, R.G. (1996) 'Characterization of a novel influenza hemagglutinin, H15: criteria for determination of influenza A subtypes', *Virology*, 217(2), pp. 508-516.

Roizman, B. (1996) 'Herpesviridae', *Fields virology*, pp. 2221-2230.

Roizmann, B., Desrosiers, R.C., Fleckenstein, B., Lopez, C., Minson, A.C. and Studdert, M.J. (1992) 'The family Herpesviridae: an update. The Herpesvirus Study Group of the International Committee on Taxonomy of Viruses', *Archives of Virology*, 123(3-4), pp. 425-449.

- Roop, C., Hutchinson, L. and Johnson, D.C. (1993) 'A mutant herpes simplex virus type 1 unable to express glycoprotein L cannot enter cells, and its particles lack glycoprotein H', *Journal of virology*, 67(4), pp. 2285-2297.
- Rosenthal, P.B., Zhang, X., Formanowski, F., Fitz, W., Wong, C.H., Meier-Ewert, H., Skehel, J.J. and Wiley, D.C. (1998) 'Structure of the haemagglutinin-esterase-fusion glycoprotein of influenza C virus', *Nature*, 396(6706), pp. 92-96.
- Rossman, J.S., Jing, X., Leser, G.P. and Lamb, R.A. (2010) 'Influenza Virus M2 Protein Mediates ESCRT-Independent Membrane Scission', *Cell*, 142(6), pp. 902-913.
- Roy, A.M., Parker, J.S., Parrish, C.R. and Whittaker, G.R. (2000) 'Early stages of influenza virus entry into Mv-1 lung cells: involvement of dynamin', *Virology*, 267(1), pp. 17-28.
- Rubin, H. (1965) 'Genetic Control of Cellular Susceptibility to Pseudotypes of Rous Sarcoma Virus', *Virology*, 26, pp. 270-276.
- Rudolph, J. and Osterrieder, N. (2002) 'Equine herpesvirus type 1 devoid of gM and gp2 is severely impaired in virus egress but not direct cell-to-cell spread', *Virology*, 293(2), pp. 356-367.
- Rudolph, J., Seyboldt, C., Granzow, H. and Osterrieder, N. (2002) 'The gene 10 (UL49.5) product of equine herpesvirus 1 is necessary and sufficient for functional processing of glycoprotein M', *Journal of virology*, 76(6), pp. 2952-2963.
- Ruigrok, R.W.H. and Baudin, F. (1995) 'Structure of influenza virus ribonucleoprotein particles. II. Purified RNA-free influenza virus ribonucleoprotein forms structures that are indistinguishable from the intact influenza virus ribonucleoprotein particles', *Journal of General Virology*, 76(4), pp. 1009-1014."
- Ruitenbergh, K.M., Love, D.N., Gilkerson, J.R., Wellington, J.E. and Whalley, J.M. (2000) 'Equine herpesvirus 1 (EHV-1) glycoprotein D DNA inoculation in horses with pre-existing EHV-1/EHV-4 antibody', *Veterinary microbiology*, 76(2), pp. 117-127.
- Runstadler, J., Hill, N., Hussein, I.T., Puryear, W. and Keogh, M. (2013) 'Connecting the study of wild influenza with the potential for pandemic disease', *Infection, genetics and evolution: journal of molecular epidemiology and evolutionary genetics in infectious diseases*, 17, pp. 162-187.

Rusli, N.D., Mat, K.B. and Harun, H.C. (2014) 'A Review: Interactions of Equine Herpesvirus-1 with Immune System and Equine Lymphocyte', *Open Journal of Veterinary Medicine*, Vol.04No.12, pp. 14.

Russell, S.M., McCahon, D. and Beare, A.S. (1975) 'A single radial haemolysis technique for the measurement of influenza antibody', *The Journal of general virology*, 27(1), pp. 1-10.

Rybachuk, G.V. (2009) 'Antiviral chemotherapeutic agents against equine herpesvirus type 1: the mechanism of antiviral effects of porphyrin derivatives', *LSU Doctoral Dissertations*, 2545.

Sakaguchi, T., Leser, G.P. and Lamb, R.A. (1996) 'The ion channel activity of the influenza virus M2 protein affects transport through the Golgi apparatus', *The Journal of cell biology*, 133(4), pp. 733-747.

Salem, E., Cook, E.A.J., Lbacha, H.A., Oliva, J., Awoume, F., Aplogan, G.L., Hymann, E.C., Muloi, D., Deem, S.L., Alali, S., Zouagui, Z., Fèvre, E.M., Meyer, G. and Ducatez, M.F. (2017) 'Serologic Evidence for Influenza C and D Virus among Ruminants and Camelids, Africa, 1991-2015', *Emerging infectious diseases*, 23(9), pp. 1556-1559.

Sant, A.J., Chaves, F., Krafcik, F.R., Lazarski, C.A., Menges, P.R., Richards, K.A. and Weaver, J.M. (2007) 'Immunodominance in CD4 T-cell responses: implications for immune responses to influenza virus and for vaccine design', *Expert Review of Vaccines*, 6, pp. 357.

Sasaki, M., Hasebe, R., Makino, Y., Suzuki, T., Fukushi, H., Okamoto, M., Matsuda, K., Taniyama, H., Sawa, H. and Kimura, T. (2011) 'Equine major histocompatibility complex class I molecules act as entry receptors that bind to equine herpesvirus-1 glycoprotein D', *Genes to cells: devoted to molecular & cellular mechanisms*, 16(4), pp. 343-357.

Sawoo, O., Dublineau, A., Batéjat, C., Zhou, P., Manuguerra, J.C. and Leclercq, I. (2014) 'Cleavage of hemagglutinin-bearing lentiviral pseudotypes and their use in the study of influenza virus persistence', *PloS one*, 9(8), pp. e106192.

Sayatov M.Kh., Kydyrmanov, A. (2007) *Influenza A virus surveillance in wild birds in Northern and Eastern Caspian in 2002–2006. Proceedings of International Conference Preparedness to the influenza pandemic—an international outlook*, Saint- Petersburg, Russia, March 15–17, 2007, pp. 79-80.

Schild, G.C., Pereira, M.S. and Chakraverty, P. (1975) 'Single-radial-hemolysis: a new method for the assay of antibody to influenza haemagglutinin. Applications for diagnosis and

seroepidemiologic surveillance of influenza', *Bulletin of the World Health Organization*, 52(1), pp. 43-50.

Schmidt, M.E. and Varga, S.M. (2018) 'The CD8 T Cell Response to Respiratory Virus Infections', *Frontiers in immunology*, 9, pp. 678.

Schnell, M.J., Buonocore, L., Kretzschmar, E., Johnson, E. and Rose, J.K. (1996) 'Foreign glycoproteins expressed from recombinant vesicular stomatitis viruses are incorporated efficiently into virus particles', *Proceedings of the National Academy of Sciences*, 93(21), pp. 11359-11365.

Scholtissek, C. (1997) *Molecular epidemiology of influenza*. Vienna: Springer Vienna, pp. 99.

Schroers, R., Sinha, I., Segall, H., Schmidt-Wolf, I.G.H., Rooney, C.M., Brenner, M.K., Sutton, R.E. and Chen, S. (2000) 'Transduction of Human PBMC-Derived Dendritic Cells and Macrophages by an HIV-1-Based Lentiviral Vector System', *Molecular Therapy*, 1(2), pp. 171-179.

Scott, E.M. and Woodside, W. (1976) 'Stability of pseudorabies virus during freeze-drying and storage: effect of suspending media', *Journal of clinical microbiology*, 4, pp. 1.

Scott, J.C., Dutta, S.K. and Myrup, A.C. (1983) 'In vivo harboring of equine herpesvirus-1 in leukocyte populations and subpopulations and their quantitation from experimentally infected ponies', *American Journal of Veterinary Research*, 44(7), pp. 1344-1348.

Scott, S., Molesti, E., Temperton, N., Ferrara, F., Böttcher-Friebertshäuser, E. and Daly, J. (2012) 'The use of equine influenza pseudotypes for serological screening', *Journal of molecular and genetic medicine: an international journal of biomedical research*, 6, pp. 304-308.

Scott, S.D., Kinsley, R., Temperton, N. and Daly, J.M. (2016) 'The Optimisation of Pseudotyped Viruses for the Characterisation of Immune Responses to Equine Influenza Virus', *Pathogens (Basel, Switzerland)*, 5(4), pp. 68.

Sedarati, F., Izumi, K.M., Wagner, E.K. and Stevens, J.G. (1989) 'Herpes simplex virus type 1 latency-associated transcription plays no role in establishment or maintenance of a latent infection in murine sensory neurons', *Journal of virology*, 63(10), pp. 4455-4458.

Sena-Esteves, M., Tebbets, J.C., Steffens, S., Crombleholme, T. and Flake, A.W. (2004) 'Optimized large-scale production of high titer lentivirus vector pseudotypes', *Journal of virological methods*, 122(2), pp. 131-139.

Seyboldt, C., Granzow, H. and Osterrieder, N. (2000) 'Equine herpesvirus 1 (EHV-1) glycoprotein M: effect of deletions of transmembrane domains', *Virology*, 278(2), pp. 477-489.

Sharma, P.C., Cullinane, A.A., Onions, D.E. and Nicolson, L. (1992) 'Diagnosis of equid herpesviruses -1 and -4 by polymerase chain reaction', *Equine veterinary journal*, 24(1), pp. 20-25.

Sharp, P.M., Tuohy, T.M. and Mosurski, K.R. (1986) 'Codon usage in yeast: cluster analysis clearly differentiates highly and lowly expressed genes', *Nucleic acids research*, 14(13), pp. 5125-5143.

Shelton, H., Roberts, K.L., Molesti, E., Temperton, N. and Barclay, W.S. (2013) 'Mutations in haemagglutinin that affect receptor binding and pH stability increase replication of a PR8 influenza virus with H5 HA in the upper respiratory tract of ferrets and may contribute to transmissibility', *The Journal of general virology*, 94(Pt 6), pp. 1220-1229.

Shin, S., Salvay, D.M. and Shea, L.D. (2010) 'Lentivirus delivery by adsorption to tissue engineering scaffolds', *Journal of biomedical materials research. Part A*, 93(4), pp. 1252-1259.

Sieczkarski, S.B. and Whittaker, G.R. (2002) 'Influenza virus can enter and infect cells in the absence of clathrin-mediated endocytosis', *Journal of virology*, 76(20), pp. 10455-10464.

Skehel, J.J. and Wiley, D.C. (2000) 'Receptor binding and membrane fusion in virus entry: the influenza hemagglutinin', *Annual Review of Biochemistry*, 69, pp. 531-569.

Slater J, B.M. (1994a) 'Experimental infection of specific pathogen-free ponies with equid herpesvirus-1: detection of infectious virus and viral DNA.', VII: 255-260.

Slater, J.D., Borchers, K., Thackray, A.M. and Field, H.J. (1994b) 'The trigeminal ganglion is a location for equine herpesvirus 1 latency and reactivation in the horse', *The Journal of general virology*, 75 (Pt 8) (Pt 8), pp. 2007-2016.

Smith, D.J., Iqbal, J., Purewal, A., Hamblin, A.S. and Edington, N. (1998) 'In vitro reactivation of latent equid herpesvirus-1 from CD5+/CD8+ leukocytes indirectly by IL-2 or chorionic gonadotrophin', *The Journal of general virology*, 79 (Pt 12) (Pt 12), pp. 2997-3004.

Smith, K.C., Whitwell, K.E., Mumford, J.A., Hannant, D., Blunden, A.S. and Tearle, J.P. (2000) 'Virulence of the V592 isolate of equid herpesvirus-1 in ponies', *Journal of comparative pathology*, 122(4), pp. 288-297.

Smith, K.L., Li, Y., Breheny, P., Cook, R.F., Henney, P.J., Sells, S., Pronost, S., Lu, Z., Crossley, B.M., Timoney, P.J. and Balasuriya, U.B.R. (2012) 'New Real-Time PCR Assay Using Allelic Discrimination for Detection and Differentiation of Equine Herpesvirus-1 Strains with A₂₂₅₄ and G₂₂₅₄ Polymorphisms', *Journal of clinical microbiology*, 50(6), pp. 1981-1988.

Soboll, G., Breathnach, C.C., Kydd, J.H., Hussey, S.B., Mealey, R.M. and Lunn, D.P. (2010) 'Vaccination of ponies with the IE gene of EHV-1 in a recombinant modified live vaccinia vector protects against clinical and virological disease', *Veterinary immunology and immunopathology*, 135(1-2), pp. 108-117.

Soboll, G., Hussey, S.B., Whalley, J.M., Allen, G.P., Koen, M.T., Santucci, N., Fraser, D.G., Macklin, M.D., Swain, W.F. and Lunn, D.P. (2006) 'Antibody and cellular immune responses following DNA vaccination and EHV-1 infection of ponies', *Veterinary immunology and immunopathology*, 111(1), pp. 81-95.

Soda, K., Asakura, S., Okamatsu, M., Sakoda, Y. and Kida, H. (2011) 'H9N2 influenza virus acquires intravenous pathogenicity on the introduction of a pair of di-basic amino acid residues at the cleavage site of the hemagglutinin and consecutive passages in chickens', *Virology journal*, 8, pp. 64-422X.

Sodeik, B., Ebersold, M.W. and Helenius, A. (1997) 'Microtubule-mediated transport of incoming herpes simplex virus 1 capsids to the nucleus', *The Journal of cell biology*, 136(5), pp. 1007-1021.

Solly, K., Wang, X., Xu, X., Strulovici, B. and Zheng, W. (2004) 'Application of real-time cell electronic sensing (RT-CES) technology to cell-based assays', *Assay and drug development technologies*, 2(4), pp. 363-372.

Spear, P.G. (2004) 'Herpes simplex virus: receptors and ligands for cell entry', *Cellular microbiology*, 6(5), pp. 401-410.

Spickler, A.R., Trampel, D.W. and Roth, J.A. (2008) 'The onset of virus shedding and clinical signs in chickens infected with high-pathogenicity and low-pathogenicity avian influenza viruses', *Avian pathology: journal of the W.V.P.A.*, 37(6), pp. 555-577.

Stallknecht, D.E. and Shane, S.M. (1988) 'Host range of avian influenza virus in free-living birds', *Veterinary research communications*, 12(2-3), pp. 125-141.

Staring, J., Raaben, M. and Brummelkamp, T.R. (2018) 'Viral escape from endosomes and host detection at a glance', *Journal of cell science*, 131(15), pp. jcs216259.

Stauffer, S., Feng, Y., Nebioglu, F., Heilig, R., Picotti, P. and Helenius, A. (2014) 'Stepwise priming by acidic pH and a high K⁺ concentration is required for efficient uncoating of influenza A virus cores after penetration', *Journal of virology*, 88(22), pp. 13029-13046.

Steeds, K., Hall, Y., Slack, G.S., Longet, S., Strecker, T., Fehling, S.K., Wright, E., Bore, J.A., Koundouno, F.R., Konde, M.K., Hewson, R., Hiscox, J.A., Pollakis, G. and Carroll, M.W. (2020) 'Pseudotyping of VSV with Ebola virus glycoprotein is superior to HIV-1 for the assessment of neutralising antibodies', *Scientific Reports*, 10(1), pp. 14289.

Steffen, I., Lu, K., Yamamoto, L.K., Hoff, N.A., Mulembakani, P., Wemakoy, E.O., Muyembe-Tamfum, J.J., Ndembi, N., Brennan, C.A., Hackett, J., Stramer, S.L., Switzer, W.M., Saragosti, S., Mbensa, G.O., Laperche, S., Rimoin, A.W. and Simmons, G. (2019) 'Serologic Prevalence of Ebola Virus in Equatorial Africa', *Emerging infectious diseases*, 25(5), pp. 911-918.

Steiner, I., Spivack, J.G., Lirette, R.P., Brown, S.M., MacLean, A.R., Subak-Sharpe, J.H. and Fraser, N.W. (1989) 'Herpes simplex virus type 1 latency-associated transcripts are evidently not essential for latent infection', *The EMBO journal*, 8(2), pp. 505-511.

Steinhauer, D.A. (1999) 'Role of Hemagglutinin Cleavage for the Pathogenicity of Influenza Virus', *Virology*, 258(1), pp. 1-20.

Steinhauer, D.A., Domingo, E. and Holland, J.J. (1992) 'Lack of evidence for proofreading mechanisms associated with an RNA virus polymerase', *Gene*, 122(2), pp. 281-288.

Stokes, A., Alber, D.G., Greensill, J., Amellal, B., Carvalho, R., Taylor, L.A., Doel, T.R., Killington, R.A., Halliburton, I.W. and Meredith, D.M. (1996) 'The expression of the proteins of equine herpesvirus 1 which share homology with herpes simplex virus 1 glycoproteins H and L', *Virus research*, 40(1), pp. 91-107.

Studdert MJ (1996) 'Virus infections of Equines', in Horzinek MC (ed.) *Virus Infections of Vertebrates* Amsterdam: Elsevier.

Su, C.Y., Wang, S.Y., Shie, J.J., Jeng, K.S., Temperton, N.J., Fang, J.M., Wong, C.H. and Cheng, Y.S. (2008) 'In vitro evaluation of neuraminidase inhibitors using the neuraminidase-dependent release assay of hemagglutinin-pseudotyped viruses', *Antiviral Research*, 79(3), pp. 199-205.

Suarez, D.L. (2010) 'Avian influenza: our current understanding', *Animal health research reviews*, 11(1), pp. 19-33.

Subramanian, R.P. and Geraghty, R.J. (2007) 'Herpes simplex virus type 1 mediates fusion through a hemifusion intermediate by sequential activity of glycoproteins D, H, L, and B', *Proceedings of the National Academy of Sciences of the United States of America*, 104(8), pp. 2903-2908.

Sugahara, Y., Matsumura, T., Kono, Y., Honda, E., Kida, H. and Okazaki, K. (1997) 'Adaptation of equine herpesvirus 1 to unnatural host led to mutation of the gC resulting in increased susceptibility of the virus to heparin', *Archives of Virology*, 142(9), pp. 1849-1856.

Sugiura T, Kondo, T. (1994) 'IgG subclass responses in equid herpesvirus-1 infected horses', in Nakajima H and Plowright W Ed (ed.), *Proceedings of Seventh International Conference on Equine Infectious Diseases* edn. Newmarket: R & W Publications Ltd, pp. 350.

Sugiura, T., Kondo, T., Matsumura, T., Imagawa, H., Kamada, M. And Ihara, T. (1997) 'Evaluation of Enzyme-Linked Immunosorbent Assay for Titration of Antibody to Equine Herpesvirus Type 1', *Journal of Equine Science*, 8(3), pp. 57-61.

Sun, X., Shi, Y., Lu, X., He, J., Gao, F., Yan, J., Qi, J. and Gao, G.F. (2013) 'Bat-Derived Influenza Hemagglutinin H17 Does Not Bind Canonical Avian or Human Receptors and Most Likely Uses a Unique Entry Mechanism', *Cell Reports*, 3(3), pp. 769-778.

Sun, Y., MacLean, A.R., Aitken, J.D. and Brown, S.M. (1996) 'The role of the gene 71 product in the life cycle of equine herpesvirus 1', *Journal of General Virology*, 77(3), pp. 493-500.

Sutton, G., Carnet, F., Normand, C., Thieulent, C., Hue, E., Fortier, C., Pléau, A., Deslis, A., Guitton, E., Buisson, B., Pronost, S. and Paillot, R. (2021) 'Development of an assay using real time cell analysis for the measurement of equid herpesvirus 1 specific neutralizing antibody in horses after experimental infection or field vaccination', *Equine veterinary journal*, 53(S56), pp. 54-55.

Sutton, G., Thieulent, C., Fortier, C., Hue, E.S., Marcillaud-Pitel, C., Pléau, A., Deslis, A., Guitton, E., Paillot, R. and Pronost, S. (2020) 'Identification of a New Equid Herpesvirus 1 DNA Polymerase (ORF30) Genotype with the Isolation of a C(2254)/H(752) Strain in French Horses Showing no Major Impact on the Strain Behaviour', *Viruses*, 12(10), pp. 1160.

Suzuki, Y., Ito, T., Suzuki, T., Holland, R.E., Chambers, T.M., Kiso, M., Ishida, H. and Kawaoka, Y. (2000) 'Sialic acid species as a determinant of the host range of influenza A viruses', *Journal of virology*, 74(24), pp. 11825-11831.

Sweeney, N.P. and Vink, C.A. (2021) 'The impact of lentiviral vector genome size and producer cell genomic to gag-pol mRNA ratios on packaging efficiency and titre', *Molecular Therapy - Methods & Clinical Development*, 21, pp. 574-584.

Szpara, M.L., Kobilier, O. and Enquist, L.W. (2010) 'A common neuronal response to alphaherpesvirus infection', *Journal of neuroimmune pharmacology: the official journal of the Society on NeuroImmune Pharmacology*, 5(3), pp. 418-427.

Tamura, S. and Kurata, T. (2004) 'Defense mechanisms against influenza virus infection in the respiratory tract mucosa', *Japanese journal of infectious diseases*, 57(6), pp. 236-247.

Tashiro, M., Ciborowski, P., Klenk, H.D., Pulverer, G. and Rott, R. (2011) 'Role of Staphylococcus protease in the development of influenza pneumonia', *Nature*, 325(6104), pp. 536-537.

Tashiro, M., Ciborowski, P., Reinacher, M., Pulverer, G., Klenk, H.D. and Rott, R. (1987) 'Synergistic role of staphylococcal proteases in the induction of influenza virus pathogenicity', *Virology*, 157(2), pp. 421-430.

Taubenberger, J.K. and Kash, J.C. (2010) 'Influenza virus evolution, host adaptation, and pandemic formation', *Cell host & microbe*, 7(6), pp. 440-451.

Taubenberger, J.K. and Morens, D.M. (2006) '1918 Influenza: the mother of all pandemics', *Emerging infectious diseases*, 12(1), pp. 15-22.

Tearle, J.P., Smith, K.C., Platt, A.J., Hannant, D., Davis-Poynter, N.J. and Mumford, J.A. (2003) 'In vitro characterisation of high and low virulence isolates of equine herpesvirus-1 and -4', *Research in veterinary science*, 75(1), pp. 83-86.

Telford, E.A., Watson, M.S., McBride, K. and Davison, A.J. (1992) 'The DNA sequence of equine herpesvirus-1', *Virology*, 189(1), pp. 304-316.

Telford, E.A., Watson, M.S., Perry, J., Cullinane, A.A. and Davison, A.J. (1998) 'The DNA sequence of equine herpesvirus-4', *The Journal of general virology*, 79 (Pt 5) (Pt 5), pp. 1197-1203.

Telikepalli, S., Kumru, O.S., Kim, J.H., Joshi, S.B., O'Berry, K.B., Blake-Haskins, A.W., Perkins, M.D., Middaugh, C.R. and Volkin, D.B. (2015) 'Characterization of the physical stability of a lyophilized IgG1 mAb after accelerated shipping-like stress', *Journal of pharmaceutical sciences*, 104(2), pp. 495-507.

Temperton, N.J., Hoschler, K., Major, D., Nicolson, C., Manvell, R., Hien, V.M., Ha, D.Q., De Jong, M., Zambon, M., Takeuchi, Y. and Weiss, R.A. (2007) 'A sensitive retroviral pseudotype assay for influenza H5N1-neutralizing antibodies', *Influenza and Other Respiratory Viruses*, 1(3), pp. 105-112.

Temperton, N.J., Wright, E. and Scott, S.D. (2015) 'Retroviral Pseudotypes – From Scientific Tools to Clinical Utility' *eLS* John Wiley & Sons, Ltd, pp. 1-11.

Thieulent, C.J., Hue, E.S., Fortier, C.I., Dallemagne, P., Zientara, S., Munier-Lehmann, H., Hans, A., Fortier, G.D., Pitel, P., Vidalain, P. and Pronost, S.L. (2019) 'Screening and evaluation of antiviral compounds against Equid alpha-herpesviruses using an impedance-based cellular assay', *Virology*, 526, pp. 105-116.

Thomas, G. (2002) 'Furin at the cutting edge: from protein traffic to embryogenesis and disease', *Nature reviews. Molecular cell biology*, 3(10), pp. 753-766.

Thomson, G.R., Mumford, J.A., Campbell, J., Griffiths, L. and Clapham, P. (1976) 'Serological detection of equid herpesvirus 1 infections of the respiratory tract', *Equine veterinary journal*, 8(2), pp. 58-65.

Tong, S., Li, Y., Rivaller, P., Conrardy, C., Castillo, D.A., Chen, L.M., Recuenco, S., Ellison, J.A., Davis, C.T., York, I.A., Turmelle, A.S., Moran, D., Rogers, S., Shi, M., Tao, Y., Weil, M.R., Tang, K., Rowe, L.A., Sammons, S., Xu, X., Frace, M., Lindblade, K.A., Cox, N.J., Anderson, L.J., Rupprecht, C.E. and Donis, R.O. (2012) 'A distinct lineage of influenza A virus from bats', *Proceedings of the National Academy of Sciences of the United States of America*, 109(11), pp. 4269-4274.

Tong, S., Zhu, X., Li, Y., Shi, M., Zhang, J., Bourgeois, M., Yang, H., Chen, X., Recuenco, S., Gomez, J., Chen, L.M., Johnson, A., Tao, Y., Dreyfus, C., Yu, W., McBride, R., Carney, P.J., Gilbert, A.T., Chang, J., Guo, Z., Davis, C.T., Paulson, J.C., Stevens, J., Rupprecht, C.E., Holmes, E.C., Wilson, I.A. and Donis, R.O. (2013) 'New world bats harbor diverse influenza A viruses', *PLoS pathogens*, 9(10), pp. e1003657.

Tønnessen, R.A.H. (2013) 'Host Restrictions of Avian Influenza Viruses: In Silico Analysis of H13 and H16 Specific Signatures in the Internal Proteins', *PLOS ONE*, 8(4), pp. 1-7.

Toon, K., Bentley, E.M. and Mattiuzzo, G. (2021) 'More Than Just Gene Therapy Vectors: Lentiviral Vector Pseudotypes for Serological Investigation', *Viruses*, 13(2), pp. 217.

Trapnell, B.C. and Whitsett, J.A. (2002) 'GM-CSF Regulates Pulmonary Surfactant Homeostasis and Alveolar Macrophage-Mediated Innate Host Defense', *Annual Review of Physiology*, 64(1), pp. 775-802.

Tse, L.V. and Whittaker, G.R. (2015) 'Modification of the hemagglutinin cleavage site allows indirect activation of avian influenza virus H9N2 by bacterial staphylokinase', *Virology*, 482, pp. 1-8.

Tsujimura, K., Shiose, T., Yamanaka, T., Nemoto, M., Kondo, T. and Matsumura, T. (2009) 'Equine herpesvirus type 1 mutant defective in glycoprotein E gene as candidate vaccine strain', *The Journal of veterinary medical science*, 71(11), pp. 1439-1448.

Tumová, B. and Schild, G.C. (1972) 'Antigenic relationships between type A influenza viruses of human, porcine, equine, and avian origin', *Bulletin of the World Health Organization*, 47(4), pp. 453-460.

Turner, A., Bruun, B., Minson, T. and Browne, H. (1998) 'Glycoproteins gB, gD, and gHgL of herpes simplex virus type 1 are necessary and sufficient to mediate membrane fusion in a Cos cell transfection system', *Journal of virology*, 72(1), pp. 873-875.

Tyrrell, D.A.J. and Ridgwell, B. (1965) 'Freeze-drying of Certain Viruses', *Nature*, 206(4979), pp. 115-116.

Van de Sandt, C.E., Kreijtz, J.H.C.M. and Rimmelzwaan, G.F. (2012) 'Evasion of Influenza A Viruses from Innate and Adaptive Immune Responses', *Viruses*, 4(9), pp. 1438-1476.

Van de Walle, G R, Peters, S.T., VanderVen, B.C., O'Callaghan, D.J. and Osterrieder, N. (2008) 'Equine herpesvirus 1 entry via endocytosis is facilitated by alphaV integrins and an RSD motif in glycoprotein D', *Journal of virology*, 82(23), pp. 11859-11868.

Van de Walle, G.R., Goupil, R., Wishon, C., Damiani, A., Perkins, G.A. and Osterrieder, N. (2009) 'A Single-Nucleotide Polymorphism in a Herpesvirus DNA Polymerase Is Sufficient to Cause Lethal Neurological Disease', *The Journal of infectious diseases*, 200(1), pp. 20-25.

van der Meulen, K., Pensaert, M. and Nauwynck, H. (2006) 'Absence of viral envelope proteins in equine herpesvirus 1-infected blood mononuclear cells during cell-associated viremia', *Veterinary microbiology*, . 113(3-4), pp. pp. 265-2006 v.113 no.3.

van der Meulen, K.M, Nauwynck, H.J., Buddaert, W. and Pensaert, M.B. (2000) 'Replication of equine herpesvirus type 1 in freshly isolated equine peripheral blood mononuclear cells

and changes in susceptibility following mitogen stimulation', *Journal of General Virology*, 81(1), pp. 21-25.

van der Meulen, K.M., Favoreel, H.W., Pensaert, M.B. and Nauwynck, H.J. (2006) 'Immune escape of equine herpesvirus 1 and other herpesviruses of veterinary importance', *Veterinary immunology and immunopathology*, 111(1-2), pp. 31-40.

van der Meulen, K.M., Nauwynck, H.J. and Pensaert, M.B. (2003) 'Absence of viral antigens on the surface of equine herpesvirus-1-infected peripheral blood mononuclear cells: a strategy to avoid complement-mediated lysis', *Journal of General Virology*, 84(1), pp. 93-97.

van Galen, G., Leblond, A., Tritz, P., Martinelle, L., Pronost, S. and Saegerman, C. (2015) 'A retrospective study on equine herpesvirus type-1 associated myeloencephalopathy in France (2008-2011)', *Veterinary microbiology*, 179(3-4), pp. 304-309.

van Lint, A.L. and Knipe, D.M. (2009) 'Herpesviruses', in Moselio Schaechter (ed.) *Encyclopedia of Microbiology (Third Edition)*. Third Edition edn. Oxford: Academic Press, pp. 376-390.

van Maanen, C., de Boer-Luijtz, E. and Terpstra, C. (2000) 'Development and validation of a monoclonal antibody blocking ELISA for the detection of antibodies against both equine herpesvirus type 1 (EHV1) and equine herpesvirus type 4 (EHV4)', *Veterinary microbiology*, 71(1-2), pp. 37-51.

Vandekerckhove, A.P., Glorieux, S., Gryspeerdt, A.C., Steukers, L., Duchateau, L., Osterrieder, N., Van de Walle, G R and Nauwynck, H.J. (2010) 'Replication kinetics of neurovirulent versus non-neurovirulent equine herpesvirus type 1 strains in equine nasal mucosal explants', *Journal of General Virology*, 91(8), pp. 2019-2028.

Vandenberghe, E., Boshuizen, B., Delesalle, C.J.G., Goehring, L.S., Groome, K.A., van Maanen, K. and de Bruijn, C. (2021) 'New Insights into the Management of an EHV-1 (Equine Hospital) Outbreak', *Viruses*, 13(8), pp. 1429.

Varghese, J.N., Laver, W.G. and Colman, P.M. (2011) 'Structure of the influenza virus glycoprotein antigen neuraminidase at 2.9 Å resolution', *Nature*, 303(5912), pp. 35-40.

Vasin, A.V., Temkina, O.A., Egorov, V.V., Klotchenko, S.A., Plotnikova, M.A. and Kiselev, O.I. (2014) 'Molecular mechanisms enhancing the proteome of influenza A viruses: an overview of recently discovered proteins', *Virus research*, 185, pp. 53-63.

Veckman, V., Österlund, P., Fagerlund, R., Melén, K., Matikainen, S. and Julkunen, I. (2006) 'TNF- α and IFN- α enhance influenza-A-virus-induced chemokine gene expression in human A549 lung epithelial cells', *Virology*, 345(1), pp. 96-104.

Veit, M. and Schmidt, M.F. (1993) 'Timing of palmitoylation of influenza virus hemagglutinin', *FEBS letters*, 336(2), pp. 243-247.

Venkataraman, P., Lamb, R.A. and Pinto, L.H. (2005) 'Chemical Rescue of Histidine Selectivity Filter Mutants of the M2 Ion Channel of Influenza A Virus*', *Journal of Biological Chemistry*, 280(22), pp. 21463-21472.

Vereecke, N., Carnet, F., Pronost, S., Vanschandevijl, K., Theuns, S. and Nauwynck, H. (2021) 'Genome Sequences of Equine Herpesvirus 1 Strains from a European Outbreak of Neurological Disorders Linked to a Horse Gathering in Valencia, Spain, in 2021', *Microbiology resource announcements*, 10(20), pp. e00333-21.

Verhagen, J.H., Herfst, S. and Fouchier, R.A. (2015) 'Infectious disease. How a virus travels the world', *Science (New York, N.Y.)*, 347(6222), pp. 616-617.

Verhagen, J.H., Lexmond, P. (2017) 'Discordant detection of avian influenza virus subtypes in time and space between poultry and wild birds; Towards improvement of surveillance programs', *PLOS ONE*, 12(3), pp. 1-21.

Vermeire, J., Naessens, E., Vanderstraeten, H., Landi, A., Iannucci, V., Van Nuffel, A., Taghon, T., Pizzato, M. and Verhasselt, B. (2012) 'Quantification of reverse transcriptase activity by real-time PCR as a fast and accurate method for titration of HIV, lenti- and retroviral vectors', *PloS one*, 7(12), pp. e50859.

Virelizier, J.L. (1975) 'Host defenses against influenza virus: the role of anti-hemagglutinin antibody', *Journal of immunology (Baltimore, Md.: 1950)*, 115(2), pp. 434-439.

von Einem, J., Schumacher, D., O'Callaghan, D.J. and Osterrieder, N. (2006) 'The alpha-TIF (VP16) homologue (ETIF) of equine herpesvirus 1 is essential for secondary envelopment and virus egress', *Journal of virology*, 80(6), pp. 2609-2620.

von Einem, J., Smith, P.M., Van de Walle, G R, O'Callaghan, D.J. and Osterrieder, N. (2007) 'In vitro and in vivo characterization of equine herpesvirus type 1 (EHV-1) mutants devoid of the viral chemokine-binding glycoprotein G (gG)', *Virology*, 362(1), pp. 151-162.

Voorhees, I.E.H., Glaser, A.L., Toohey-Kurth, K., Newbury, S., Dalziel, B.D., Dubovi, E.J., Poulsen, K., Leutenegger, C., Willgert, K.J.E., Brisbane-Cohen, L., Richardson-Lopez, J.,

Holmes, E.C. and Parrish, C.R. (2017) 'Spread of Canine Influenza A(H3N2) Virus, United States', *Emerging infectious diseases*, 23(12), pp. 1950-1957.

Wagner, B., Goodman, L.B., Babasyan, S., Freer, H., Torsteinsdóttir, S., Svansson, V., Björnsdóttir, S. and Perkins, G.A. (2015) 'Antibody and cellular immune responses of naïve mares to repeated vaccination with an inactivated equine herpesvirus vaccine', *Vaccine*, 33(42), pp. 5588-5597.

Wagner, W.N., Bogdan, J., Haines, D., Townsend, H.G. and Misra, V. (1992) 'Detection of equine herpesvirus and differentiation of equine herpesvirus type 1 from type 4 by the polymerase chain reaction', *Canadian journal of microbiology*, 38(11), pp. 1193-1196.

Walker, P.J., Siddell, S.G., Lefkowitz, E.J., Mushegian, A.R., Adriaenssens, E.M., Alfenas-Zerbini, P., Davison, A.J., Dempsey, D.M., Dutilh, B.E., García, M.L., Harrach, B., Harrison, R.L., Hendrickson, R.C., Junglen, S., Knowles, N.J., Krupovic, M., Kuhn, J.H., Lambert, A.J., Łobocka, M., Nibert, M.L., Oksanen, H.M., Orton, R.J., Robertson, D.L., Rubino, L., Sabanadzovic, S., Simmonds, P., Smith, D.B., Suzuki, N., Van Doerslaer, K., Vandamme, A., Varsani, A. and Zerbini, F.M. (2021) 'Changes to virus taxonomy and to the International Code of Virus Classification and Nomenclature ratified by the International Committee on Taxonomy of Viruses (2021)', *Archives of Virology*, 166(9), pp. 2633-2648.

Wang, B., Russell, M.L., Brewer, A., Newton, J., Singh, P., Ward, B.J. and Loeb, M. (2017) 'Single radial haemolysis compared to haemagglutinin inhibition and microneutralization as a correlate of protection against influenza A H3N2 in children and adolescents', *Influenza and other respiratory viruses*, 11(3), pp. 283-288.

Wang, P., Chen, J., Zheng, A., Nie, Y., Shi, X., Wang, W., Wang, G., Luo, M., Liu, H., Tan, L., Song, X., Wang, Z., Yin, X., Qu, X., Wang, X., Qing, T., Ding, M. and Deng, H. (2004) 'Expression cloning of functional receptor used by SARS coronavirus', *Biochemical and biophysical research communications*, 315(2), pp. 439-444.

Wang, W. (2000) 'Lyophilization and development of solid protein pharmaceuticals', *International journal of pharmaceutics*, 203(1-2), pp. 1-60.

Wang, W., Butler, E.N., Veguilla, V., Vassell, R., Thomas, J.T., Moos, M., Ye, Z., Hancock, K. and Weiss, C.D. (2008) 'Establishment of retroviral pseudotypes with influenza hemagglutinins from H1, H3, and H5 subtypes for sensitive and specific detection of neutralizing antibodies', *Journal of virological methods*, 153(2), pp. 111-119.

Wang, W., Xie, H., Ye, Z., Vassell, R. and Weiss, C.D. (2010) 'Characterization of lentiviral pseudotypes with influenza H5N1 hemagglutinin and their performance in neutralization assays', *Journal of virological methods*, 165(2), pp. 305-310.

Warda, F.F., Ahmed, H.E.S., Shafik, N.G., Mikhael, C.A., Abd-ElAziz, H.M.G., Mohammed, W.A. and Shosha, E.A. (2021) 'Application of equine herpesvirus-1 vaccine inactivated by both formaldehyde and binary ethylenimine in equine', *Veterinary world*, 14(7), pp. 1815-1821.

Wareing, M.D., Lyon, A., Inglis, C., Giannoni, F., Charo, I. and Sarawar, S.R. (2007) 'Chemokine regulation of the inflammatory response to a low-dose influenza infection in CCR2^{-/-} mice', *Journal of leukocyte biology*, 81(3), pp. 793-801.

Wareing, M.D., Lyon, A.B., Lu, B., Gerard, C. and Sarawar, S.R. (2004) 'Chemokine expression during the development and resolution of a pulmonary leukocyte response to influenza A virus infection in mice', *J Leukoc Biol*, 76(4), pp. 886-95.

Webster, R.G. (1999) 'Influenza Viruses (Orthomyxoviridae) | General Features', in Allan Granoff and Robert G Webster (eds.) *Encyclopedia of Virology (Second Edition)*. Second Edition edn. Oxford: Elsevier, pp. 824-829.

Webster, R.G. and Laver, W.G. (1967) 'Preparation and Properties of Antibody Directed Specifically Against the Neuraminidase of Influenza Virus', *The Journal of Immunology*, 99(1), pp. 49-55.

Webster, R.G. and Rott, R. (1987) 'Influenza virus a pathogenicity: The pivotal role of hemagglutinin', *Cell*, 50(5), pp. 665-666.

Webster, R.G., Bean, W.J., Gorman, O.T., Chambers, T.M. and Kawaoka, Y. (1992) 'Evolution and ecology of influenza A viruses', *Microbiological reviews*, 56(1), pp. 152-179.

Webster, R.G., Laver, W.G. and Kilbourne, E.D. (1968) 'Reactions of antibodies with surface antigens of influenza virus', *The Journal of general virology*, 3(3), pp. 315-326.

Weis, W., Brown, J.H., Cusack, S., Paulson, J.C., Skehel, J.J. and Wiley, D.C. (1988) 'Structure of the influenza virus haemagglutinin complexed with its receptor, sialic acid', *Nature*, 333(6172), pp. 426-431.

Welch, H.M., Bridges, C.G., Lyon, A.M., Griffiths, L. and Edington, N. (1992) 'Latent equid herpesviruses 1 and 4: detection and distinction using the polymerase chain reaction and co-cultivation from lymphoid tissues', *The Journal of general virology*, 73 (Pt 2) (Pt 2), pp. 261-268.

Wellington, J.E., Love, D.N. and Whalley, J.M. (1996) 'Evidence for involvement of equine herpesvirus 1 glycoprotein B in cell-cell fusion', *Archives of Virology*, 141(1), pp. 167-175.

Whalley, J.M., Robertson, G.R. and Davison, A.J. (1981) 'Analysis of the Genome of Equine Herpesvirus Type 1: Arrangement of Cleavage Sites for Restriction Endonucleases EcoRI, BglII and BamHI', *Journal of General Virology*, 57(2), pp. 307-323.

Whalley, J.M., Ruitenbergh, K.M., Sullivan, K., Seshadri, L., Hansen, K., Birch, D., Gilkerson, J.R. and Wellington, J.E. (2007) 'Host cell tropism of equine herpesviruses: glycoprotein D of EHV-1 enables EHV-4 to infect a non-permissive cell line', *Archives of Virology*, 152(4), pp. 717-725.

Whitbeck, J.C., Peng, C., Lou, H., Xu, R., Willis, S.H., Ponce de Leon, M., Peng, T., Nicola, A.V., Montgomery, R.I., Warner, M.S., Soulika, A.M., Spruce, L.A., Moore, W.T., Lambris, J.D., Spear, P.G., Cohen, G.H. and Eisenberg, R.J. (1997) 'Glycoprotein D of herpes simplex virus (HSV) binds directly to HVEM, a member of the tumor necrosis factor receptor superfamily and a mediator of HSV entry', *Journal of virology*, 71(8), pp. 6083-6093.

White, J., Helenius, A. and Gething, M.J. (1982) 'Haemagglutinin of influenza virus expressed from a cloned gene promotes membrane fusion', *Nature*, 300(5893), pp. 658-659.

White, S.K., Ma, W., McDaniel, C.J., Gray, G.C. and Lednicky, J.A. (2016) 'Serologic evidence of exposure to influenza D virus among persons with occupational contact with cattle', *Journal of clinical virology: the official publication of the Pan American Society for Clinical Virology*, 81, pp. 31-33.

Whitley, R.J. and Gnann, J.W. (1993) 'The epidemiology and clinical manifestation of herpes simplex virus infections', in Roizman, B. (ed.) *The Human Herpesviruses* New York: Raven Press, pp. 69-105.

Whitt, M.A. (2010) 'Generation of VSV pseudotypes using recombinant Δ G-VSV for studies on virus entry, identification of entry inhibitors, and immune responses to vaccines', *Journal of virological methods*, 169(2), pp. 365-374.

Whittaker, G.R. and Helenius, A. (1998) 'Nuclear import and export of viruses and virus genomes', *Virology*, 246(1), pp. 1-23.

Whittaker, G.R., Taylor, L.A., Elton, D.M., Giles, L.E., Bonass, W.A., Halliburton, I.W., Killington, R.A. and Meredith, D.M. (1992) 'Glycoprotein 60 of equine herpesvirus type 1 is a

homologue of herpes simplex virus glycoprotein D and plays a major role in penetration of cells', *Journal of General Virology*, 73(4), pp. 801-809.

WHO (1980) 'A revision of the system of nomenclature for influenza viruses: a WHO memorandum', *Bulletin of the World Health Organization*, 58(4), pp. 585-591.

WHO (2011) *Manual for the laboratory diagnosis and virological surveillance of influenza*. World Health Organization.

Wilschut, J., de Jonge, J., Huckriede, A., Amorij, J.P., Hinrichs, W.L. and Frijlink, H.W. (2007) 'Preservation of influenza virosome structure and function during freeze-drying and storage', *Journal of Liposome Research*, 17(3-4), pp. 173-182.

Wilson, D.W., Davis-Poynter, N. and Minson, A.C. (1994) 'Mutations in the cytoplasmic tail of herpes simplex virus glycoprotein H suppress cell fusion by a syncytial strain', *Journal of virology*, 68(11), pp. 6985-6993.

Wilson, I.A., Skehel, J.J. and Wiley, D.C. (1981) 'Structure of the haemagglutinin membrane glycoprotein of influenza virus at 3 Å resolution', *Nature*, 289(5796), pp. 366-373.

Wilson, W. and Rosedale, P. (1999) 'Effect of age on the serological responses of Thoroughbred foals to vaccination with an inactivated EHV-1/EHV-4 vaccine', *Equine infectious diseases VIII. Newmarket: R & W Publications*, 428.

Wilson, W.D. (1997) 'Equine herpesvirus 1 myeloencephalopathy', *The Veterinary clinics of North America: Equine practice*, 13(1), pp. 53-72.

Wilsterman, S., Soboll-Hussey, G., Lunn, D.P., Ashton, L.V., Callan, R.J., Hussey, S.B., Rao, S. and Goehring, L.S. (2011) 'Equine herpesvirus-1 infected peripheral blood mononuclear cell subpopulations during viremia', *Veterinary microbiology*, 149(1), pp. 40-47.

Witkowski, P.T., Schuenadel, L., Wiethaus, J., Bourquain, D.R., Kurth, A. and Nitsche, A. (2010) 'Cellular impedance measurement as a new tool for poxvirus titration, antibody neutralization testing and evaluation of antiviral substances', *Biochemical and biophysical research communications*, 401(1), pp. 37-41.

Wood, J.M., Gaines-Das, R.E., Taylor, J. and Chakraverty, P. (1994) 'Comparison of influenza serological techniques by international collaborative study', *Vaccine*, 12(2), pp. 167-174.

- Wool-Lewis, R.J. and Bates, P. (1998) 'Characterization of Ebola virus entry by using pseudotyped viruses: identification of receptor-deficient cell lines', *Journal of virology*, 72(4), pp. 3155-3160.
- Wright, E., McNabb, S., Goddard, T., Horton, D.L., Lembo, T., Nel, L.H., Weiss, R.A., Cleaveland, S. and Fooks, A.R. (2009) 'A robust lentiviral pseudotype neutralisation assay for in-field serosurveillance of rabies and lyssaviruses in Africa', *Vaccine*, 27(51), pp. 7178-7186.
- Wu, Y., Wu, Y., Tefsen, B., Shi, Y. and Gao, G.F. (2014) 'Bat-derived influenza-like viruses H17N10 and H18N11', *Trends in microbiology*, 22(4), pp. 183-191.
- Xu, X., Nie, S., Wang, Y., Long, Q., Zhu, H., Zhang, X., Sun, J., Zeng, Q., Zhao, J., Liu, L., Li, L., Huang, A., Hou, J. and Hou, F.F. (2021) 'Dynamics of neutralizing antibody responses to SARS-CoV-2 in patients with COVID-19: an observational study', *Signal transduction and targeted therapy*, 6(1), pp. 197.
- Yamagishi, H., Nagamine, T., Shimoda, K., Ide, S., Igarashi, Y., Yoshioka, I. and Matumoto, M. (1982) 'Comparative measurement of equine influenza virus antibodies in horse sera by single radial hemolysis, neutralization, and hemagglutination inhibition tests', *Journal of clinical microbiology*, 15(4), pp. 660-662.
- Yang, J., Li, W., Long, Y., Song, S., Liu, J., Zhang, X., Wang, X., Jiang, S. and Liao, G. (2014) 'Reliability of pseudotyped influenza viral particles in neutralizing antibody detection', *PLoS one*, 9(12), pp. e113629.
- Yang, K., Homa, F. and Baines, J.D. (2007) 'Putative terminase subunits of herpes simplex virus 1 form a complex in the cytoplasm and interact with portal protein in the nucleus', *Journal of virology*, 81(12), pp. 6419-6433.
- Yang, P., Gu, H., Zhao, Z., Wang, W., Cao, B., Lai, C., Yang, X., Zhang, L., Duan, Y., Zhang, S., Chen, W., Zhen, W., Cai, M., Penninger, J.M., Jiang, C. and Wang, X. (2014) 'Angiotensin-converting enzyme 2 (ACE2) mediates influenza H7N9 virus-induced acute lung injury', *Scientific reports*, 4, pp. 7027.
- Yang, W., Schountz, T. and Ma, W. (2021) 'Bat Influenza Viruses: Current Status and Perspective', *Viruses*, 13(4), pp. 547.
- Yeargan, M.R., Allen, G.P. and Bryans, J.T. (1985) 'Rapid subtyping of equine herpesvirus 1 with monoclonal antibodies', *Journal of clinical microbiology*, 21(5), pp. 694-697.

- Yoshimura, A. and Ohnishi, S. (1984) 'Uncoating of influenza virus in endosomes', *Journal of virology*, 51(2), pp. 497-504.
- Yu, X., Sainz, B., Petukhov, P.A. and Uprichard, S.L. (2012) 'Identification of hepatitis C virus inhibitors targeting different aspects of infection using a cell-based assay', *Antimicrobial Agents and Chemotherapy*, 56(12), pp. 6109-6120.
- Yuan, P., Bartlam, M., Lou, Z., Chen, S., Zhou, J., He, X., Lv, Z., Ge, R., Li, X., Deng, T., Fodor, E., Rao, Z. and Liu, Y. (2009) 'Crystal structure of an avian influenza polymerase PA(N) reveals an endonuclease active site', *Nature*, 458(7240), pp. 909-913.
- Zambon M (1998) 'Laboratory diagnosis of influenza. ', in Webster RG, H.A. (ed.) *Textbook of Influenza* Oxford Blackwell, Oxford, UK, pp. 291–313.
- Zaraket, H., Bridges, O.A. and Russell, C.J. (2013) 'The pH of activation of the hemagglutinin protein regulates H5N1 influenza virus replication and pathogenesis in mice', *Journal of virology*, 87(9), pp. 4826-4834.
- Zebedee, S.L. and Lamb, R.A. (1988) 'Influenza A virus M2 protein: monoclonal antibody restriction of virus growth and detection of M2 in virions', *Journal of virology*, 62(8), pp. 2762-2772.
- Zhao, G., Du, L., Ma, C., Li, Y., Li, L., Poon, V.K.M., Wang, L., Yu, F., Zheng, B., Jiang, S. and Zhou, Y. (2013) 'A safe and convenient pseudovirus-based inhibition assay to detect neutralizing antibodies and screen for viral entry inhibitors against the novel human coronavirus MERS-CoV', *Virology Journal*, 10(1), pp. 266.
- Zhou, G., Juang, S.W.W. and Kane, K.P. (2013) 'NK cells exacerbate the pathology of influenza virus infection in mice', *European journal of immunology*, 43(4), pp. 929-938.
- Zhu, X., Yu, W., McBride, R., Li, Y., Chen, L., Donis, R.O., Tong, S., Paulson, J.C. and Wilson, I.A. (2013) 'Hemagglutinin homologue from H17N10 bat influenza virus exhibits divergent receptor-binding and pH-dependent fusion activities', *Proceedings of the National Academy of Sciences*, 110(4), pp. 1458-1463.
- Zimmer, G., Locher, S., Berger Rentsch, M. and Halbherr, S.J. (2014) 'Pseudotyping of vesicular stomatitis virus with the envelope glycoproteins of highly pathogenic avian influenza viruses', *The Journal of general virology*, 95(Pt 8), pp. 1634-1639.

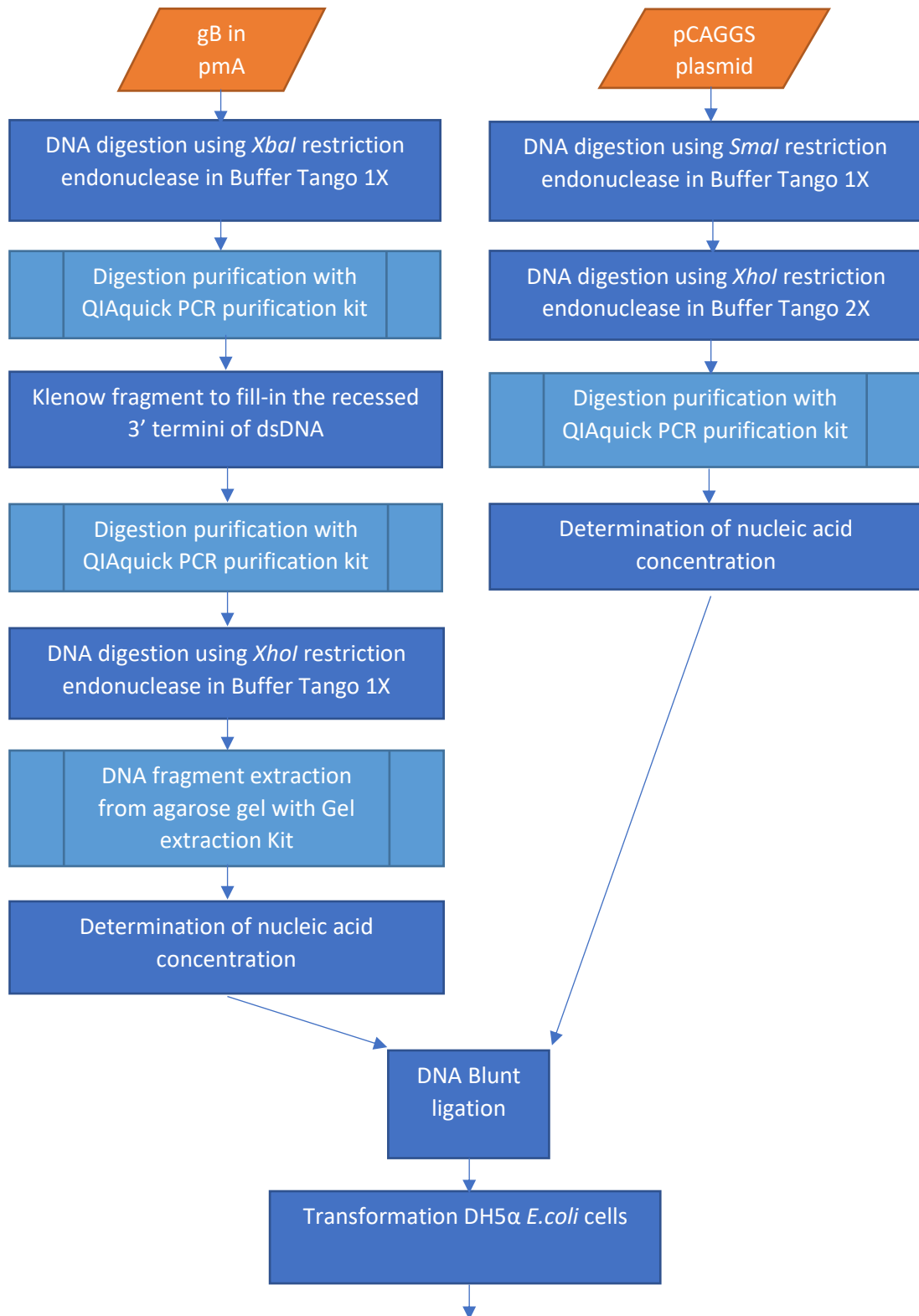
Zmora, P. and Pöhlmann, S. (2014) ' Microscopy as a useful tool to study the proteolytic activation of influenza viruses', in Méndez-Vilas, A.e. (ed.) *Microscopy: Advances in Scientific Research and Education* Formatex Research Center, pp. 725-731.

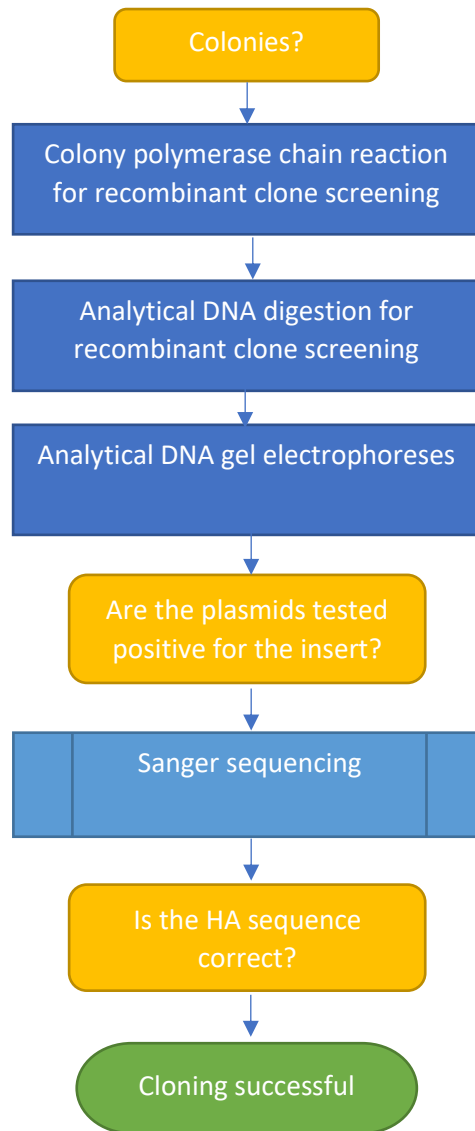
Zohari, S., Neimanis, A., Härkönen, T., Moraeus, C. and Valarcher, J.F. (2014) 'Avian influenza A(H10N7) virus involvement in mass mortality of harbour seals (*Phoca vitulina*) in Sweden, March through October 2014', *Euro surveillance: bulletin Europeen sur les maladies transmissibles = European communicable disease bulletin*, 19(46), pp. 20967.

Zufferey, R., Nagy, D., Mandel, R.J., Naldini, L. and Trono, D. (1997) 'Multiply attenuated lentiviral vector achieves efficient gene delivery in vivo', *Nature biotechnology*, 15(9), pp. 871-875.

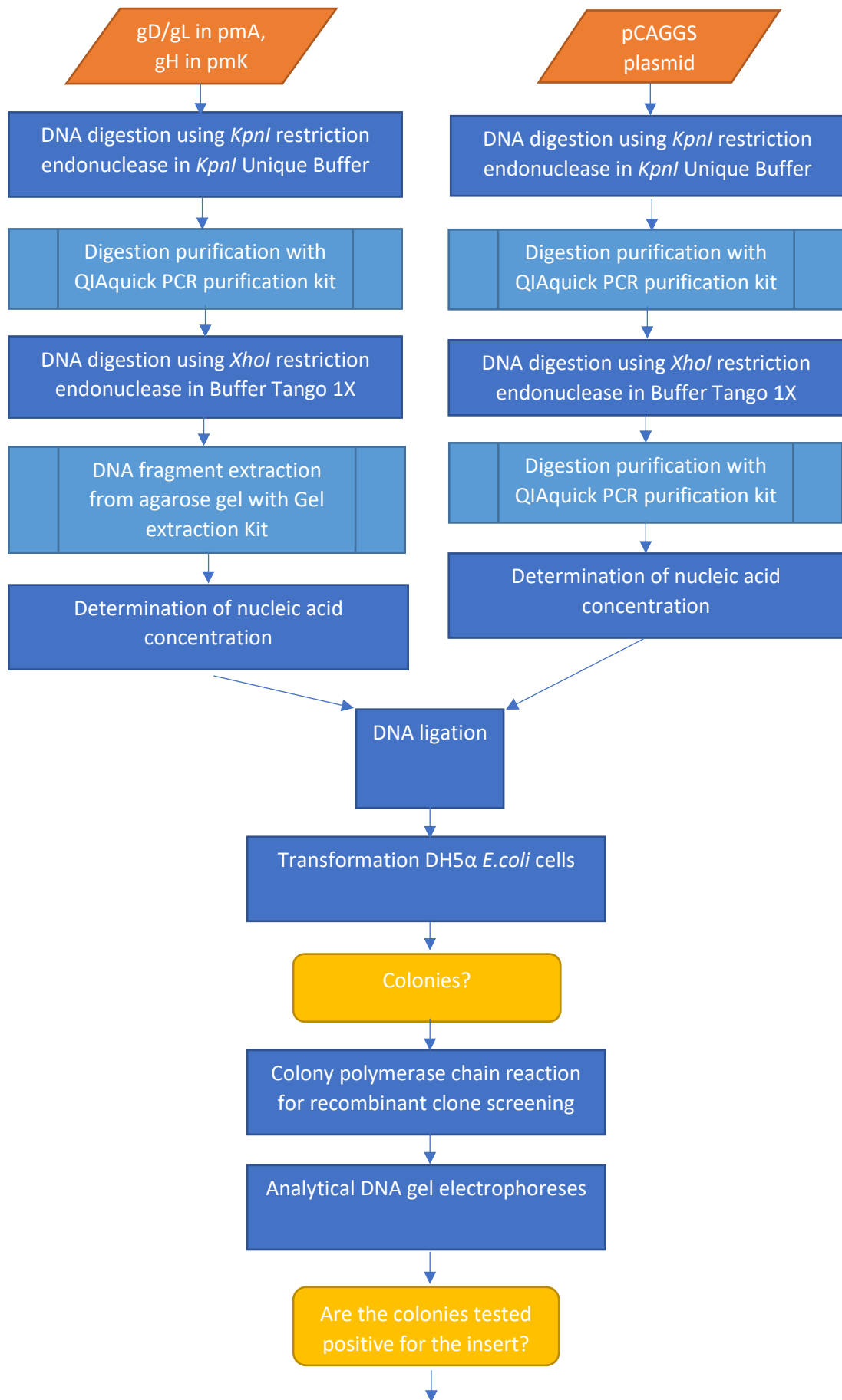
10 APPENDIX

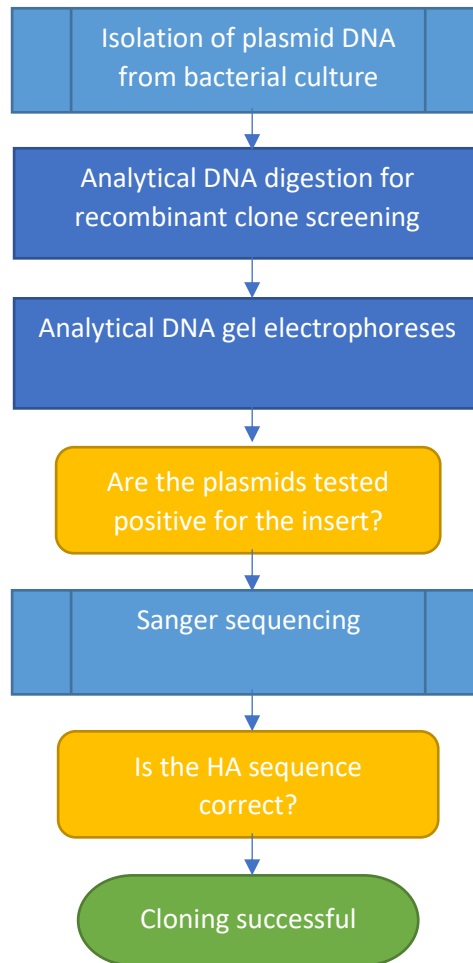
10.1 APPENDIX CHAPTER 3



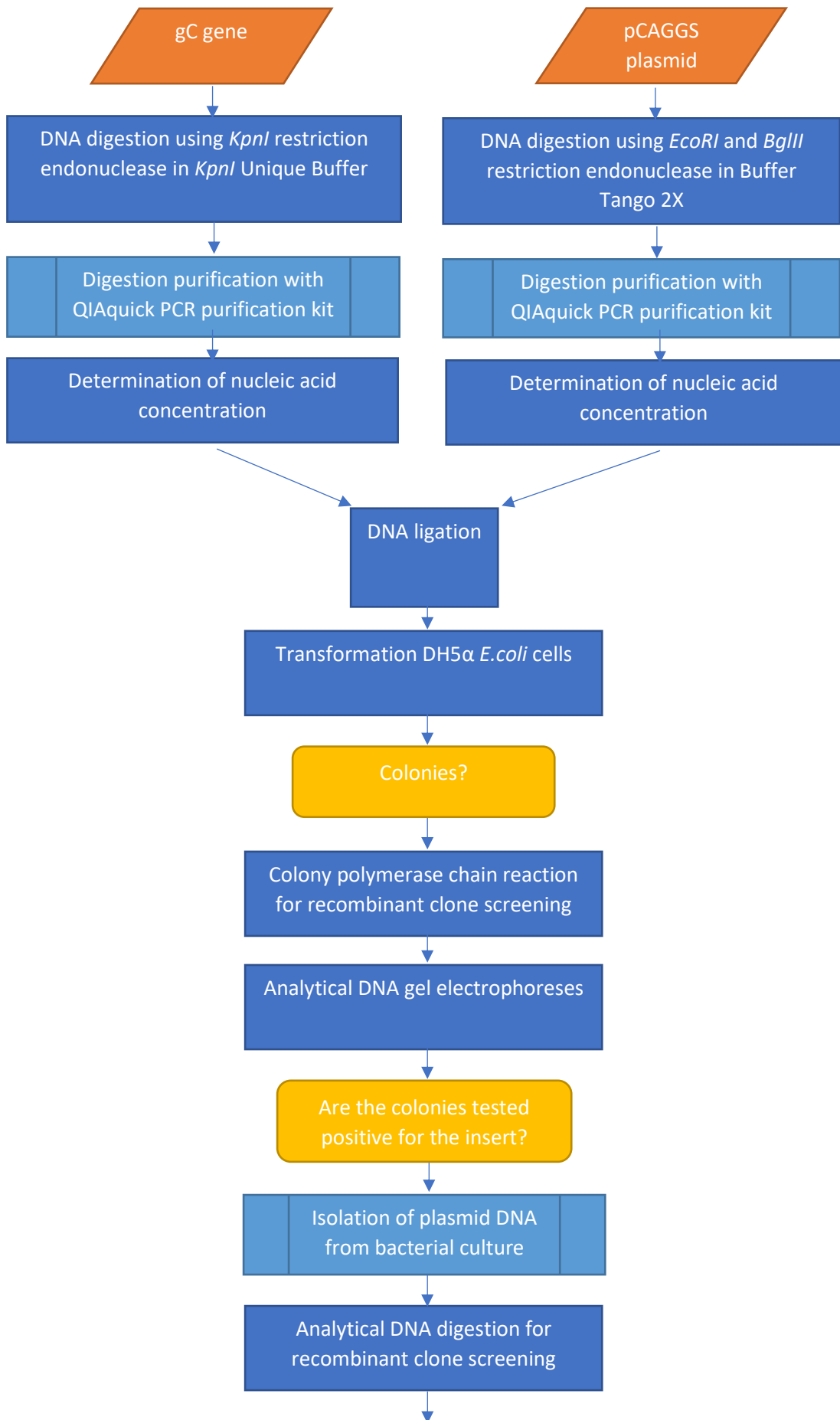


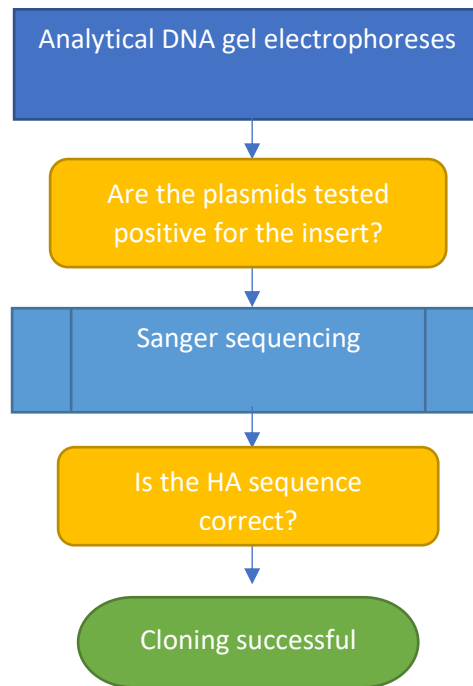
Appendix Figure 1: Flow chart - Subcloning gB from pMA in pCAGGS. This flow chart represents all the steps that were undertaken to subclone EHV-1 gB from pMA into pCAGGS. gB was cloned into pMA with XbaI restriction site designed at the 5' previous the start codon ATG. Since pCAGGS had no XbaI site, SmaI was chosen as restriction endonuclease. SmaI restriction site is represented by a blunt end so it was necessary to fill-in the recessed 3' termini in gB at the XbaI site using the Klenow fragment (Thermo Scientific™, Thermo Fisher Scientific, #EP0051) to make it blunt. Once completed, a blunt end ligation was necessary to complete the cloning.





Appendix Figure 2: Flow chart - Subcloning of gD and gL from pMA and gH from pMK in pCAGGS. This flow chart represents the cloning strategies and of all the steps followed in the absence of experimental issues. EHV-1 glycoprotein genes were extracted from pMA or pMK first and then subcloned into pCAGGS vector. KpnI and XhoI restriction endonucleases were chosen since their restriction sites were present in MCS pCAGGS and absent in the glycoprotein gene sequences. Thus EHV-1 glycoproteins were first extracted from pMA or pMK and then cloned into pCAGGS using KpnI-XhoI at 5' and 3' end respectively.



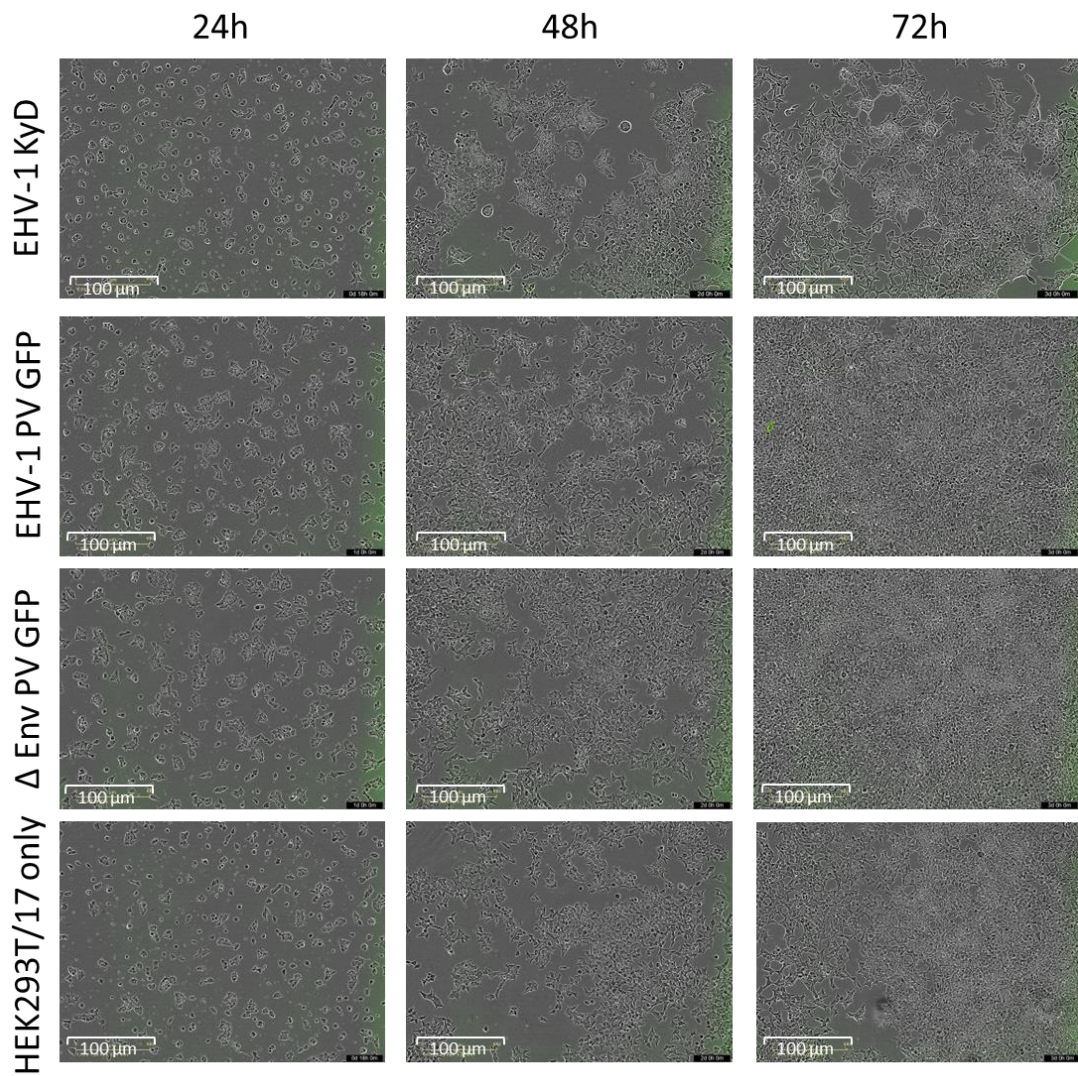


Appendix Figure 3: Flow chart - Cloning of gC in pCAGGS. All the steps were followed in the absence of experimental issues. EHV-1 gC gene was successfully cloned into pCAGGS using EcoRI-BglII at 5' and 3' end respectively.

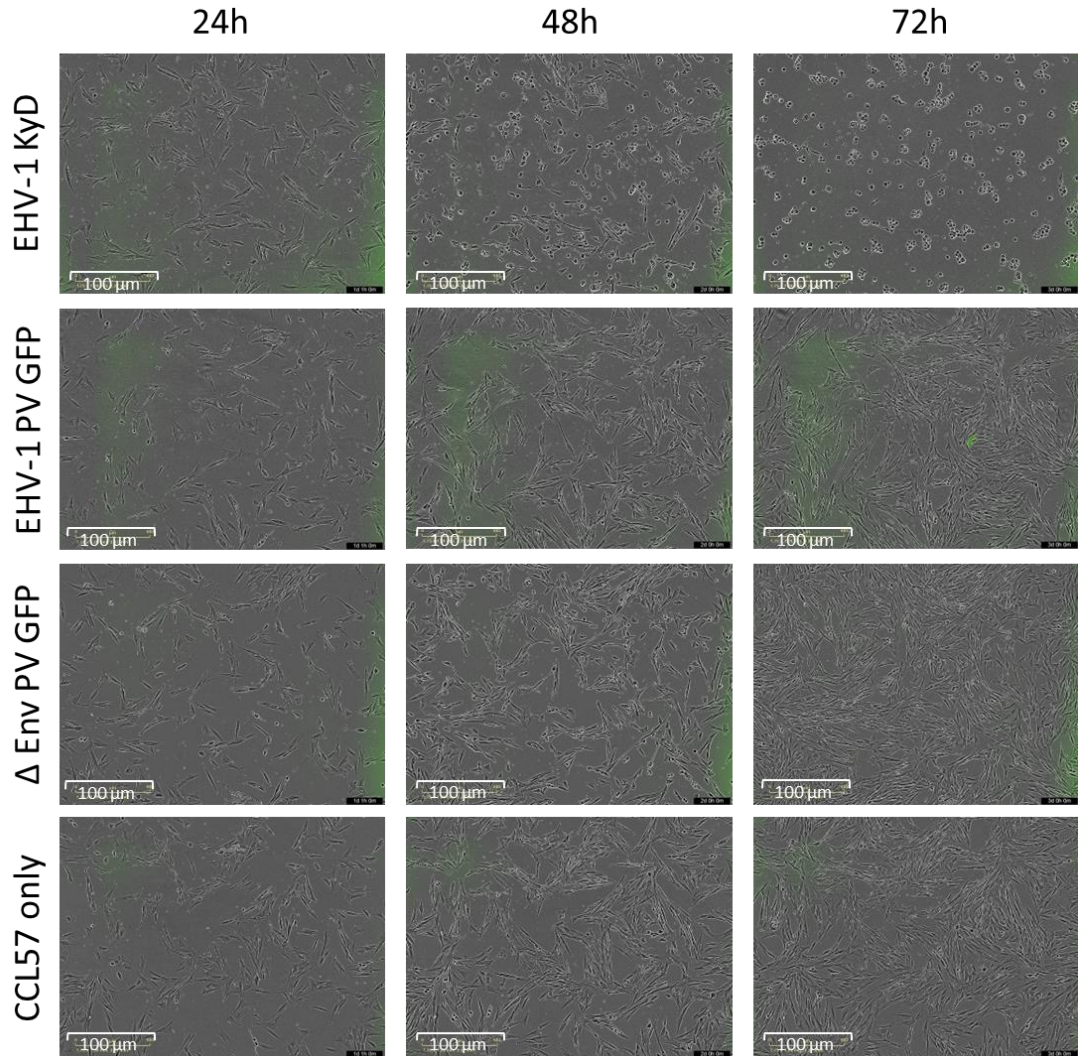
| | Green HEK293T | | Green VERO | Green RK13 | | Green CHO-K1 | | Green BHK | | Green FHK | | Green MDCK I | | Green MDCK II | | Green E.derm | |
|-------------------|---------------|-----|------------|------------|-----|--------------|-----|-----------|-----|-----------|-----|--------------|-----|---------------|-----|--------------|-----|
| | 48h | 72h | 48h | 48h | 72h | 48h | 72h | 48h | 72h | 48h | 72h | 48h | 72h | 48h | 72h | 48h | 72h |
| B | - | - | | | | | | | | | | | | | | | |
| D | - | - | | | | | | | | | | | | | | | |
| BD | - | - | | | | | | | | | | | | | | | |
| BDH | - | - | | | | | | - | - | | | - | - | | | | |
| BDL | - | - | | | | | | - | - | | | - | - | | | | |
| BHL | - | - | | | | | | - | - | | | - | - | | | | |
| DHL | - | - | | | | | | - | - | | | - | - | | | | |
| BDHL | 70 | 110 | - | - | 7 | - | 1 | - | - | 5 | 15 | - | 1 | 3 | 20 | - | |
| BDHL+C | 2 | - | | - | 3 | - | - | - | - | 4 | 4 | - | - | 2 | 4 | - | |
| CDHL | - | - | | | | | | - | - | | | - | - | | | | |
| BCHL | - | - | | | | | | - | - | | | - | - | | | | |
| BDCL | - | - | | | | | | - | - | | | - | - | | | | |
| BDHC | - | - | | | | | | - | - | | | - | - | | | | |
| BDHL+empty pCAGGS | 35 | 30 | | - | - | - | - | - | - | - | 1 | - | - | 6 | 1 | - | |
| H3N8+HAT | 1000 | 200 | - | - | - | 15 | 1 | 80 | 10 | 1000 | 200 | 10 | - | 1000 | 400 | - | |

Appendix Table 2: Record of green target cells transduced with combination of EHV-1 PVs. Transduction of EHV-1 PV combinations were tested for both the 48h and 72h harvests. EIV PV (H3N8+HAT) was included as positive control for both PV production and GFP titration. Green cells were scrutinised under a fluorescent microscope 48 hours post transduction. The numbers reported were visible in the first wells of each PV dilution.

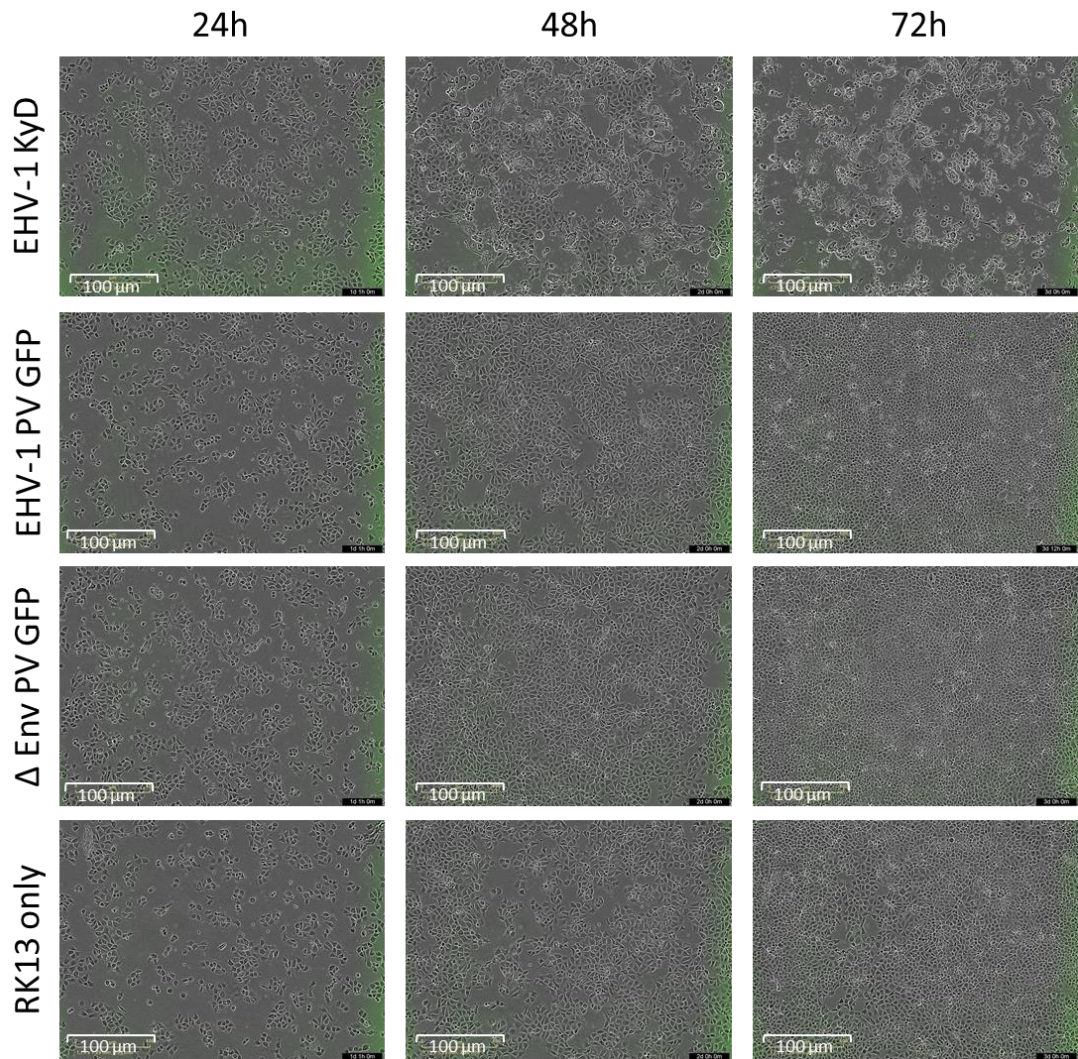
10.2 APPENDIX CHAPTER 6



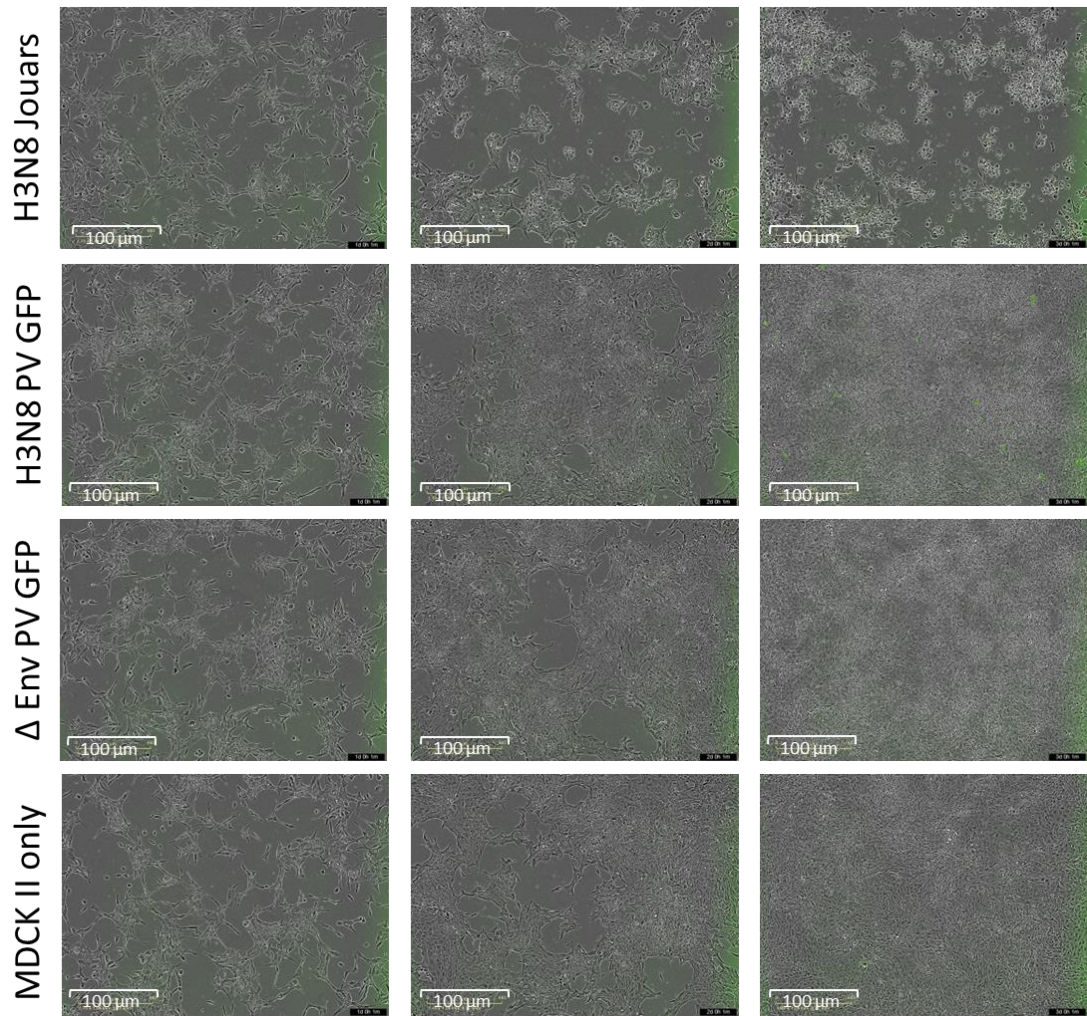
Appendix Figure 4: RTCA PV titration on HEK293T/17 cells. Microscopic observation of HEK293T/17 cells infected with either EHV-1 PV or WT virus at 24 h (time of infection), 48 h and 72 h. Cells were also infected with Δ env PV or not for cell background control. Photos were taken at 10x on Incucyte®.



Appendix Figure 5: RTCA PV titration on CCL57 cells. Microscopic observation of CCL57 cells infected with either EHV-1 PV or WT virus at 24 h (time of infection), 48 h and 72 h. Cells were also infected with Δ env PV or not for cell background control. Photos were taken at 10x on Incucyte®.



Appendix Figure 6: RTCA PV titration on RK13 cells. Microscopic observation of RK13 cells infected with either EHV-1 PV or WT virus at 24 h (time of infection), 48 h and 72 h. Cells were also infected with Δ env PV or not for cell background control. Photos were taken at 10x on Incucyte®.



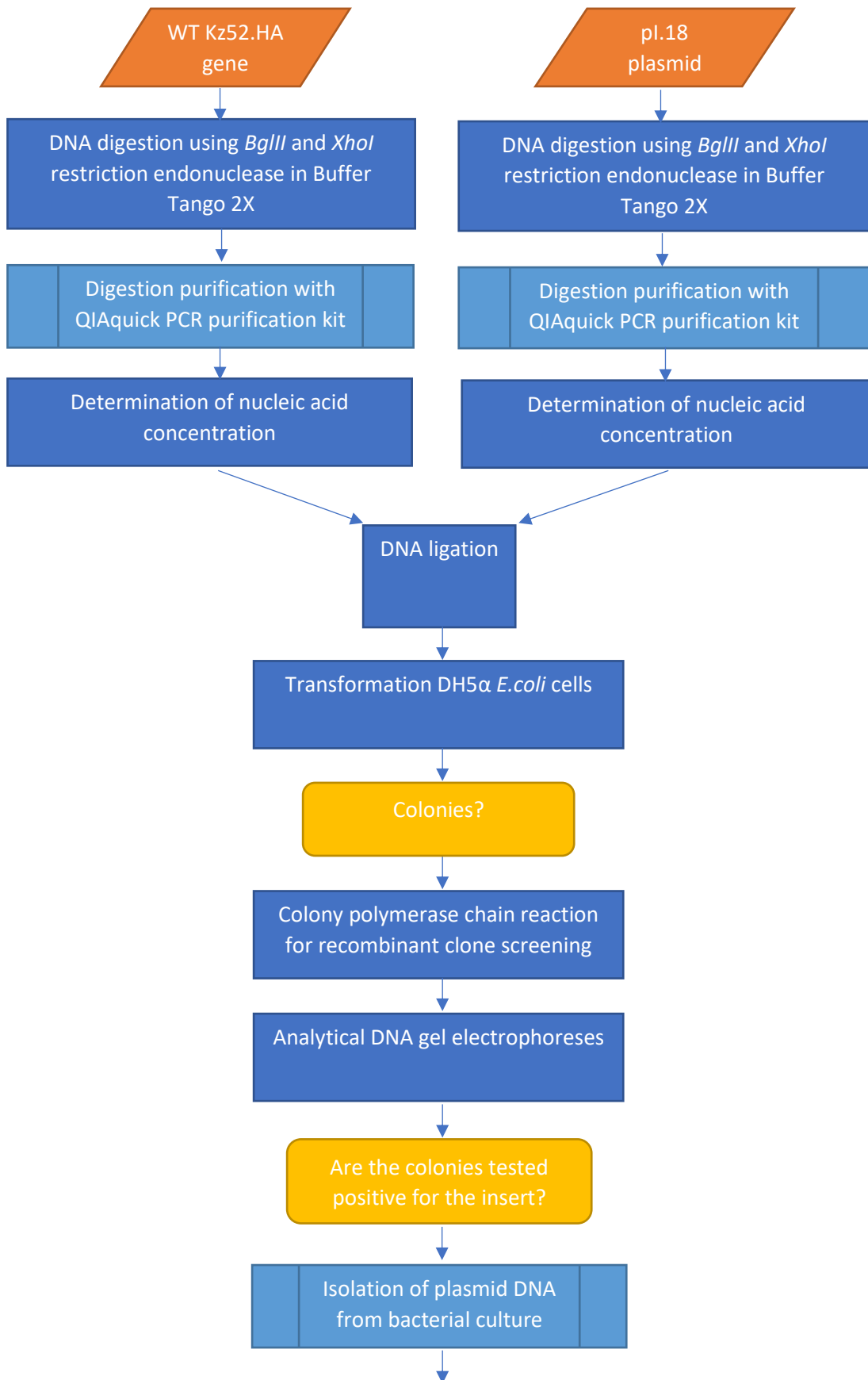
Appendix Figure 7: RTCA PV titration on MDCK II cells. Microscopic observation of MDCK II cells infected with either H3M8 PV or WT virus at 24 h (time of infection), 48 h and 72 h. Cells were also infected with Δ env PV or not for cell background control. Photos were taken at 10x on Incucyte®.

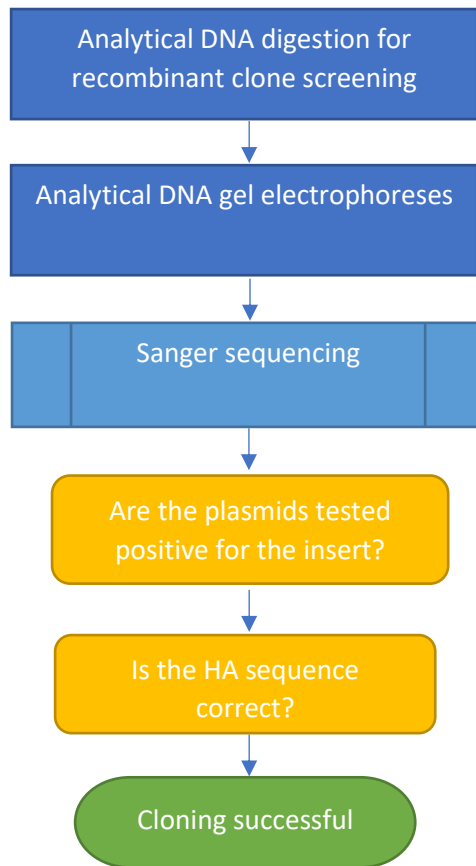
| Identification | Set of serums in the study | Gender | Breed | Age | Vaccination group | Vaccination protocol | Sampling point | Premises | Vaccination history | Additional information |
|----------------|----------------------------|-------------------|-------------------|------------------|-------------------|---|--------------------------------------|------------|--|--|
| P _D | Vaccination Set#3 | Female | Origine constatée | 6 months-old | Primo-vaccinated | 1 st , 2 nd and 6 th month of the campaign | M1, M2, M3, M6, M7, M8 | Premises 2 | No previous vaccination | Foal of Horse 15 |
| P _A | Vaccination Set#3 | Male | Selle Français | 5 1/2 months-old | Primo-vaccinated | 1 st , 2 nd and 6 th month of the campaign | M1, M2, M3, M6, M7, M8 | Premises 1 | No previous vaccination | |
| P _G | Vaccination Set#3 | Gelding | Selle Français | 24 years-old | Primo-vaccinated | 1 st , 2 nd and 6 th month of the campaign | M1, M2, M3, M6, M7, M8 | Premises 2 | Up-to-date EIV vaccination, no or very ancient EHV1,4 vaccination | |
| P _F | Vaccination Set#3 | Female | Selle Français | 1 1/2 years-old | Primo-vaccinated | 1 st , 2 nd and 6 th month of the campaign | M1, M2, M3, M6, M7, M8 | Premises 1 | Up-to-date EIV vaccination, no EHV1,4 vaccination | |
| P _B | Vaccination Set#3 | Female | Connemara | 2 1/2 years-old | Primo-vaccinated | 1 st , 2 nd and 6 th month of the campaign | M1, M2, M3, M6, M7, M8 | Premises 1 | Up-to-date EIV vaccination, no EHV1,4 vaccination | |
| R _D | Vaccination Set#3 | Stalion | Selle Français | 7 years-old | Reboost | 1 st month of the campaign | M1, M2, M4 | Premises 3 | Up-to-date EIV and EHV1,4 vaccination | Vaccinated every year as required for breeding |
| R _E | Vaccination Set#3 | Female | KWPN | 16 years-old | Reboost | 1 st month of the campaign | M1, M2, M4 | Premises 4 | Received EIV+EHV1,4 pregnancy protocol during the previous breeding season (2017/2018) | Positive EHV-4 PCR test in May 2018 |
| R _B | Vaccination Set#3 | Female | Selle Français | 1 1/2 years -old | Reboost | 1 st month of the campaign | M1, M2, M4 | Premises 2 | Up-to-date EIV and EHV1,4 vaccination | |
| R _A | Vaccination Set#3 | Gelding | Selle Français | 9 years-old | Reboost | 1 st month of the campaign | M1, M2, M4 | Premises 2 | Up-to-date EIV and EHV1,4 vaccination | |
| R _C | Vaccination Set#3 | Mare | Selle Français | 16 years-old | Reboost | 1 st month of the campaign | M1, M2, M4 | Premises 2 | Received EIV+EHV1,4 pregnancy protocol during the previous breeding season (2017/2018) | |
| G _A | Vaccination Set#3 | Female (Pregnant) | Thoroughbred | 14 years-old | Pregnant mares | 5 th , 7 th and 9 th month of pregnancy | M1 ¹ , M2, M3, M4, M5, M6 | Premises 1 | Up-to-date EIV ² vaccination, no EHV1,4 ³ vaccination | |
| G _C | Vaccination Set#3 | Female (Pregnant) | Selle Français | 15 years-old | Pregnant mares | 5 th , 7 th and 9 th month of pregnancy | M1, M2, M3, M4, M5, M6 | Premises 2 | Up-to-date EIV and EHV1,4 vaccination | |
| G _B | Vaccination Set#3 | Female (Pregnant) | Selle Français | 18 years-old | Pregnant mares | 5 th , 7 th and 9 th month of pregnancy | M1, M2, M3, M4, M5, M6 | Premises 1 | Up-to-date EIV and EHV1,4 vaccination | |

¹M1=Month 1, ²EIV= equine influenza virus, ³EHV1,4= equid herpesvirus 1 and 4.

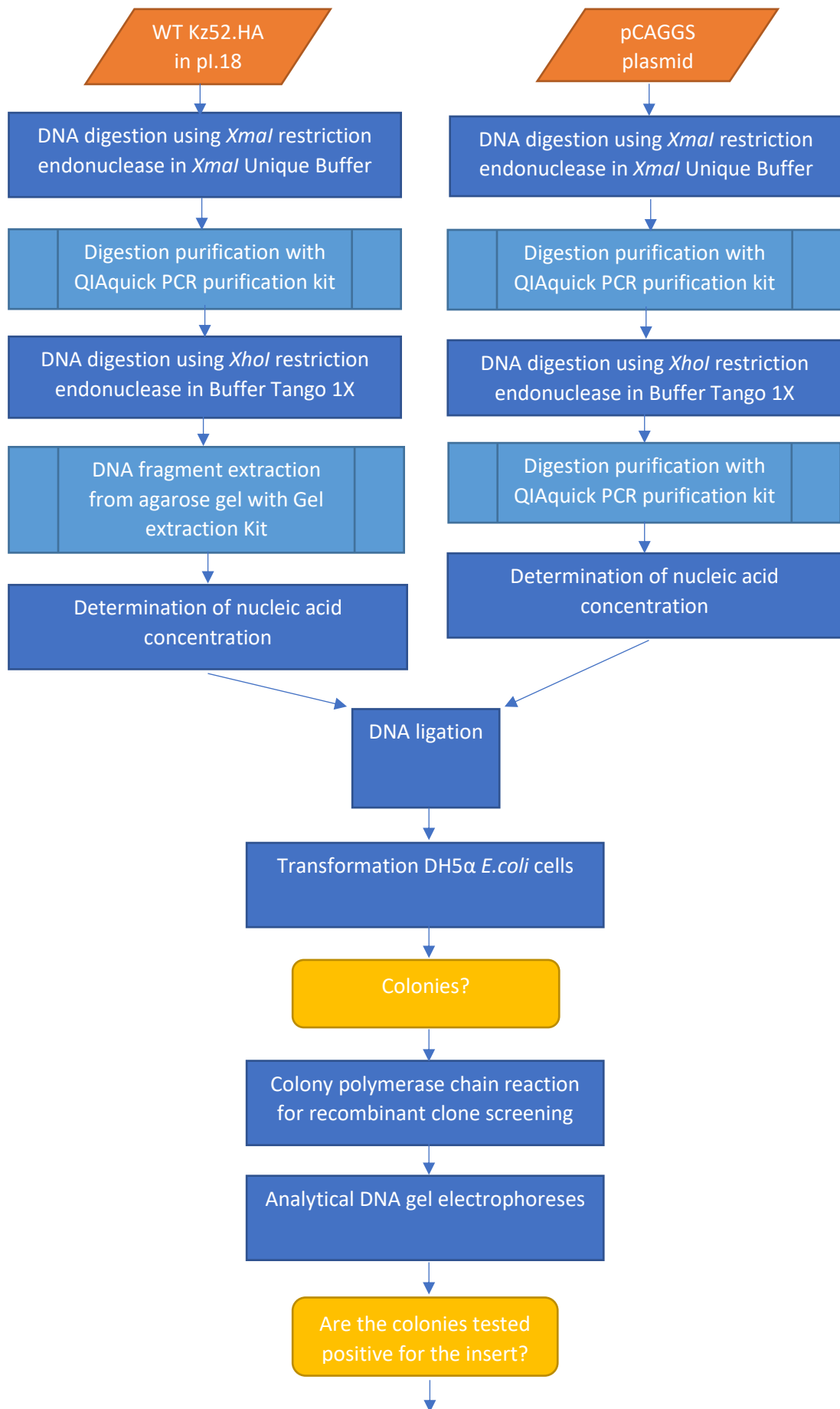
Appendix Table 4: Supplementary information. Identification, general information, vaccination protocol, sampling points, and history of vaccination/infection of horses from Group G, P and R of the EHV-1 vaccination campaign study. Source: Sutton et al., 2021.

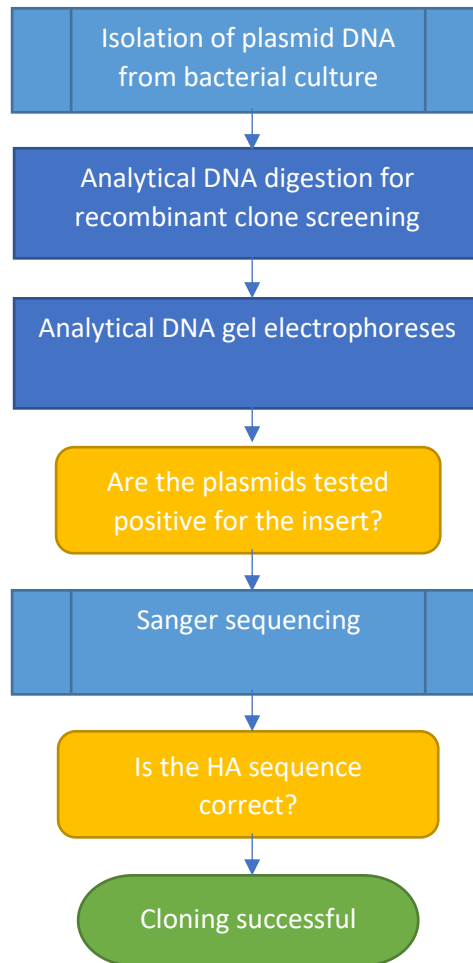
10.3 APPENDIX CHAPTER 7



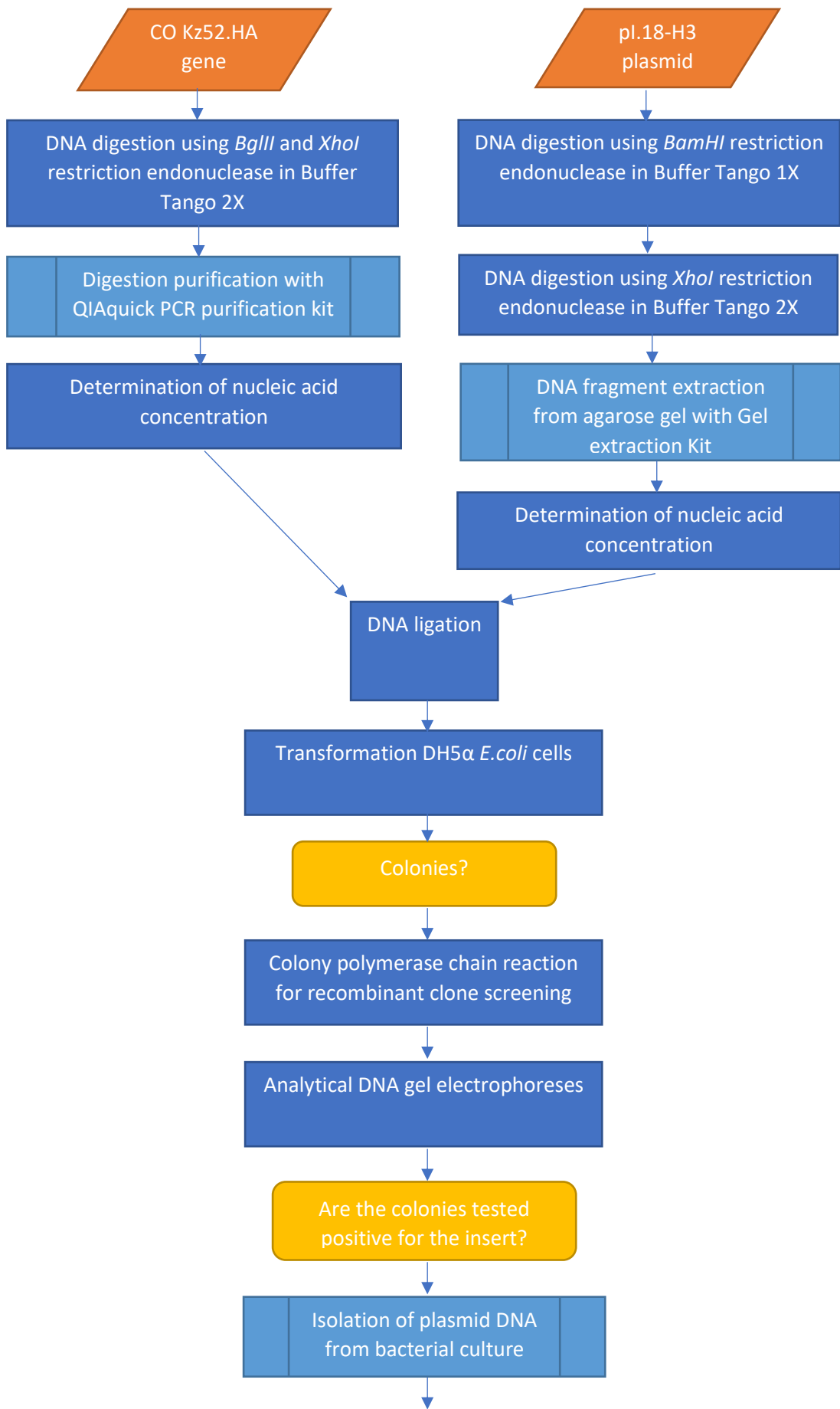


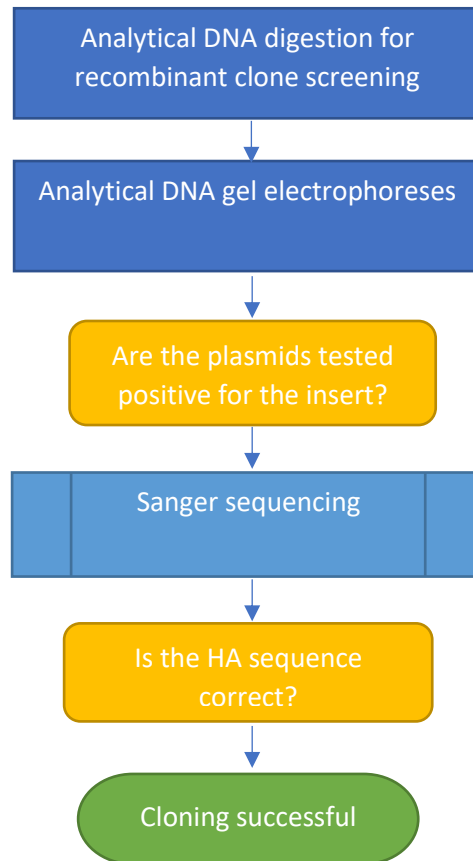
Appendix Figure 8: Flow chart – Cloning of WT Kz52 HA gene into pl.18 vector. All the steps were followed in the absence of experimental issues. Kz52 HA gene was successfully cloned into pl.18 using BglII-XhoI at 5' and 3' termini respectively.



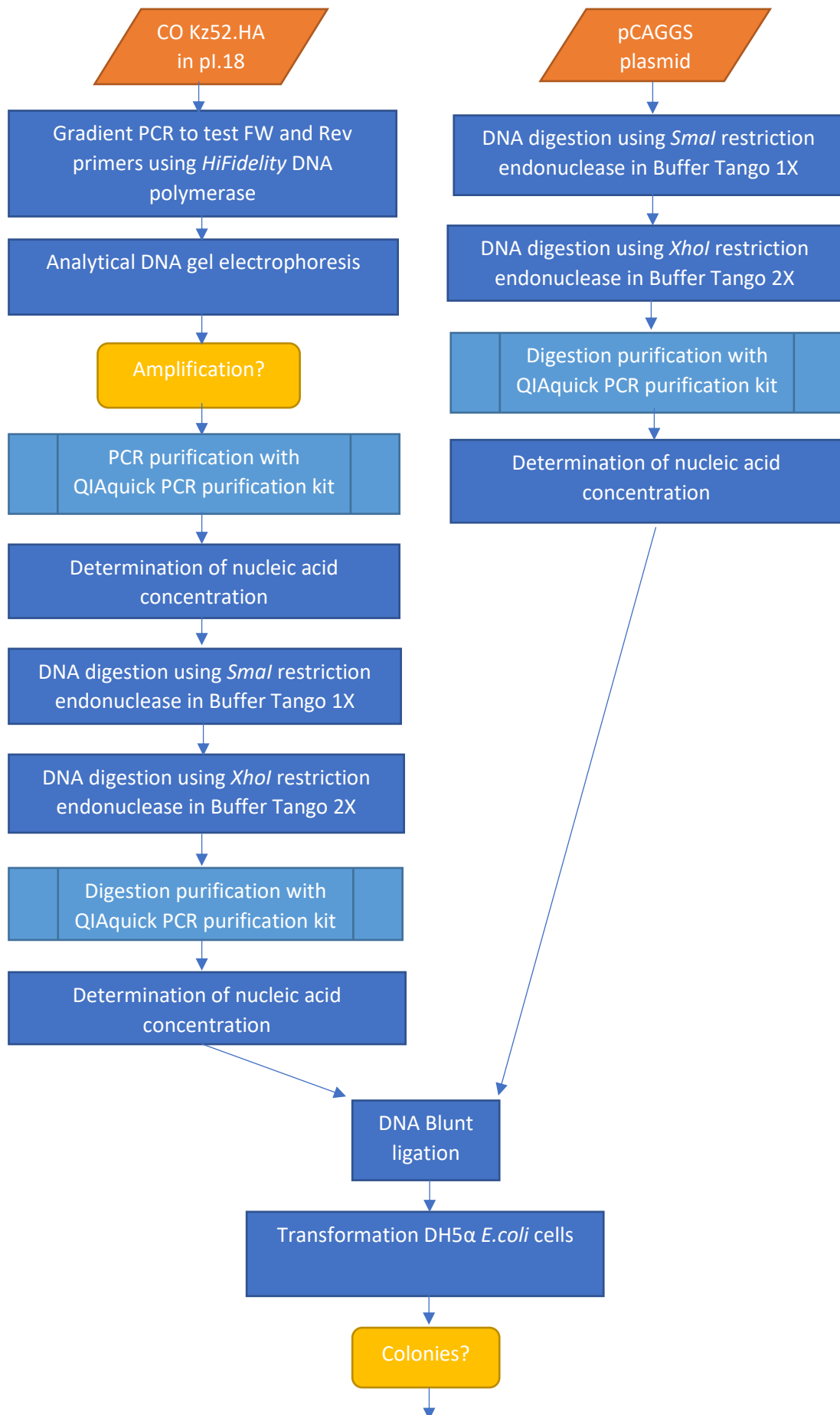


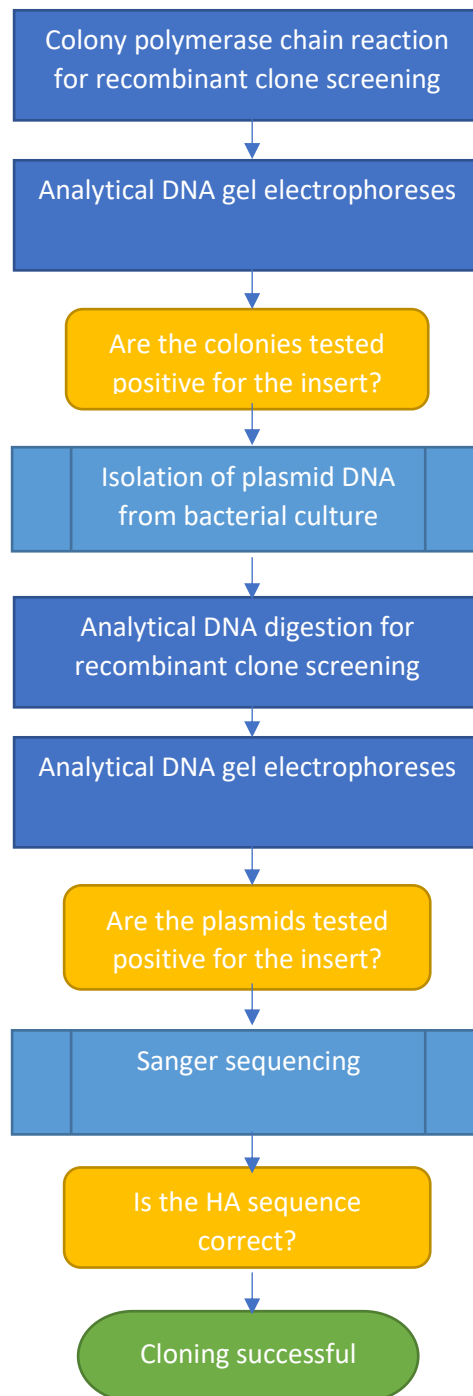
Appendix Figure 9: Flow chart – Subcloning of WT Kz52 HA gene into pCAGGS vector. All steps followed in the absence of experimental issues. Kz52 HA gene was subcloned from pl.18 into pCAGGS vector. Since pCAGGS had no BglII restriction site, it was necessary to use a different restriction endonuclease to clone Kz52 HA in pCAGGS. XmaI restriction endonuclease was chosen since its restriction site was present both in pCAGGS and in pl.18. Thus, Kz52 HA was first extracted from pl.18 and then cloned into pCAGGS using XmaI-XhoI at 5' and 3' termini respectively.



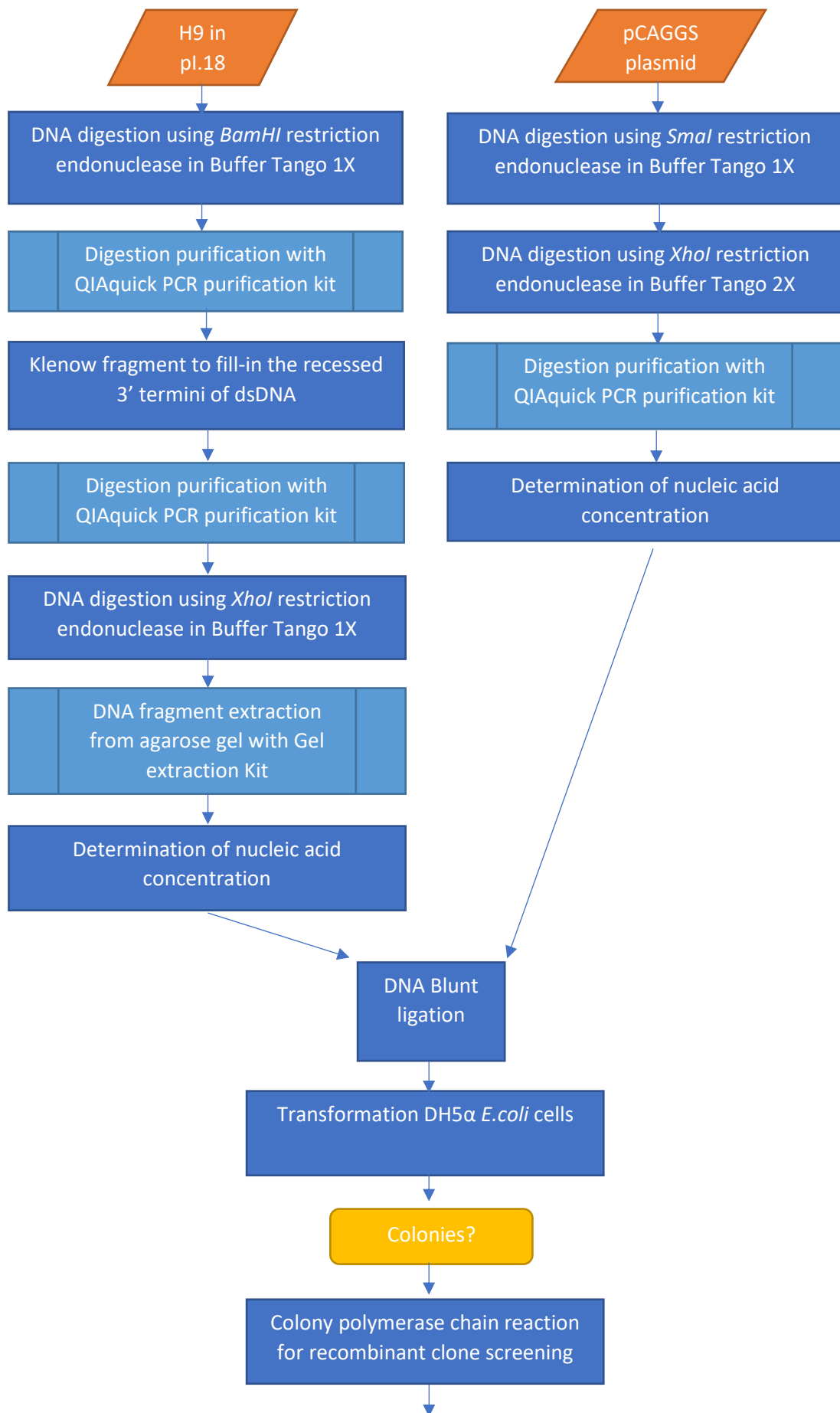


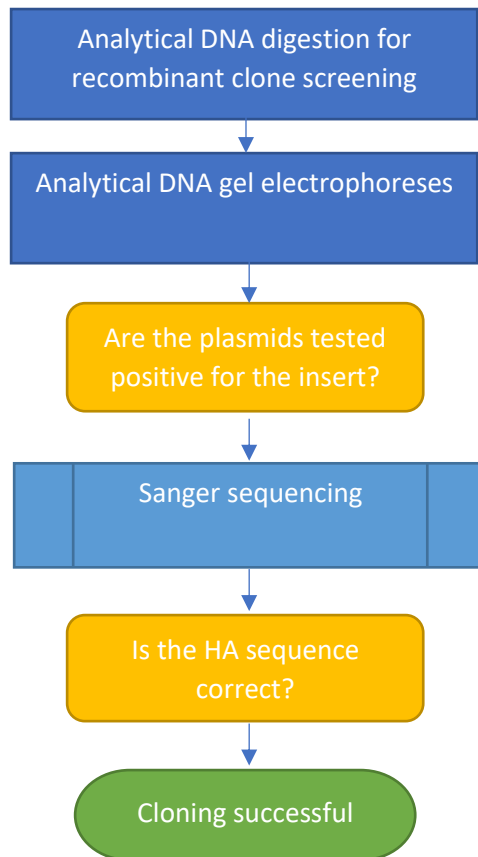
Appendix Figure 10: Flow chart – Cloning of CO Kz52 HA gene into pl.18 vector. All steps were followed in the absence of experimental issues. The pl.18 vector was chosen due to previous success with this vector. It was necessary to extract pl.18 first and separate it from H3 (A/equine/Richmond/1/2007) insert using BamHI and XhoI restriction endonucleases. Then, CO Kz52 HA was successfully cloned into pl.18 using a BamHI/BglII strategy at the 5' and XhoI was used at the 3' terminus.



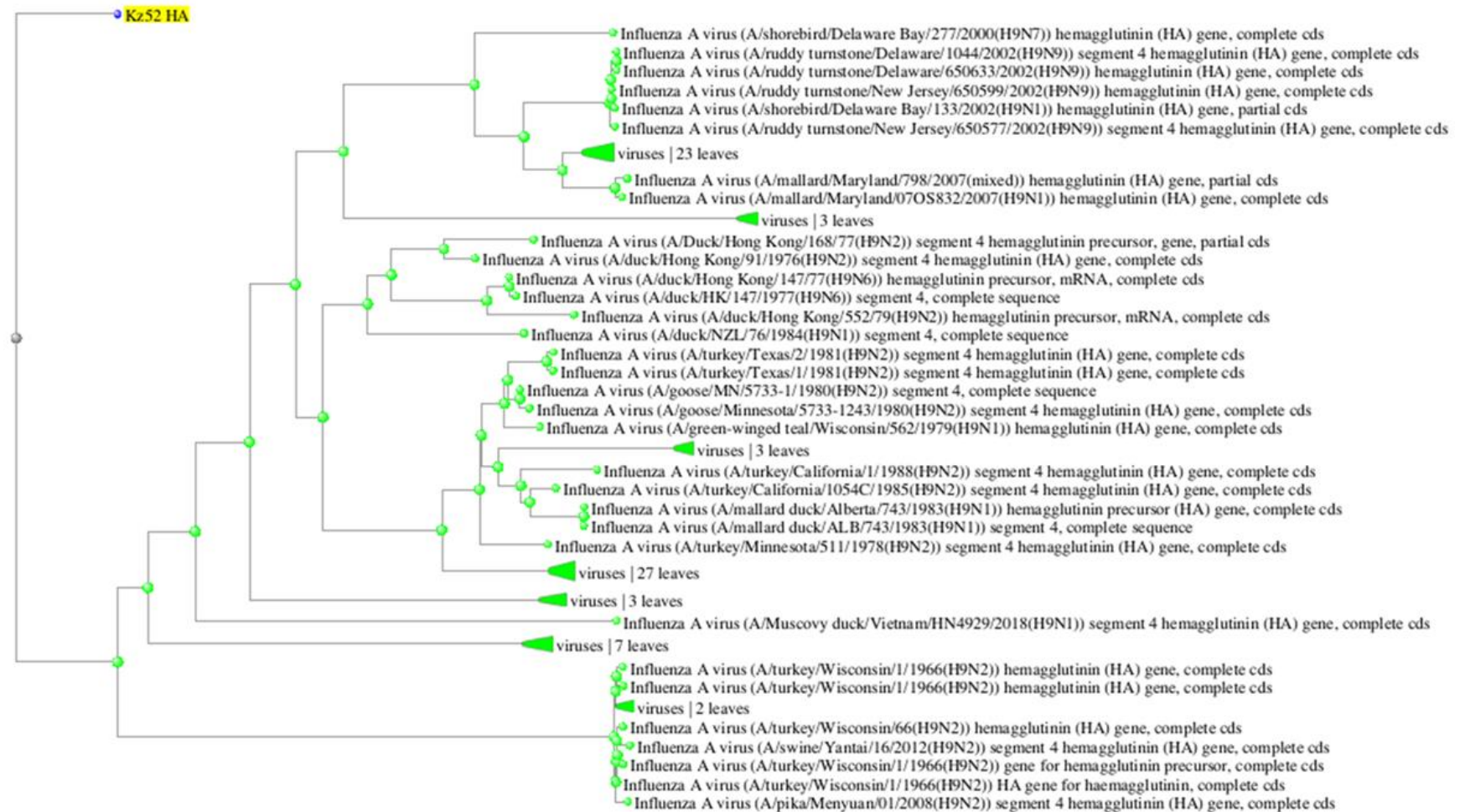


Appendix Figure 11: Flow chart – Subcloning of CO Kz52 HA gene into pCAGGS vector. All the steps followed in the absence of experimental issues. FW and Rev primers were designed including a *Sma*I and *Xho*I restriction site respectively at the 5'. Primers were first tested using a gradient PCR (annealing temperature range +50 °C to +60 °C). Subsequently, the PCR product was amplified using a HiFidelity DNA polymerase and PCR purified using QIAquick PCR kit. CO Kz52 HA gene was then extracted out of pl.18 using *Sma*I and *Xho*I restriction endonucleases and successfully cloned into pCAGGS.





Appendix Figure 12: Flow chart – Subcloning of H9 HA gene into pCAGGS vector. H9 was cloned into pl.18 using a BglII/BamHI strategy. Since pCAGGS had no BglII site, SmaI was chosen as restriction endonuclease. SmaI restriction site is represented by a blunt end so it was necessary to fill-in the recessed 3' termini in H9 at the BamHI site using the Klenow fragment (Fermentas, Klenow #EP0051) to make it blunt. Once completed, a blunt end ligation was necessary to complete the cloning.



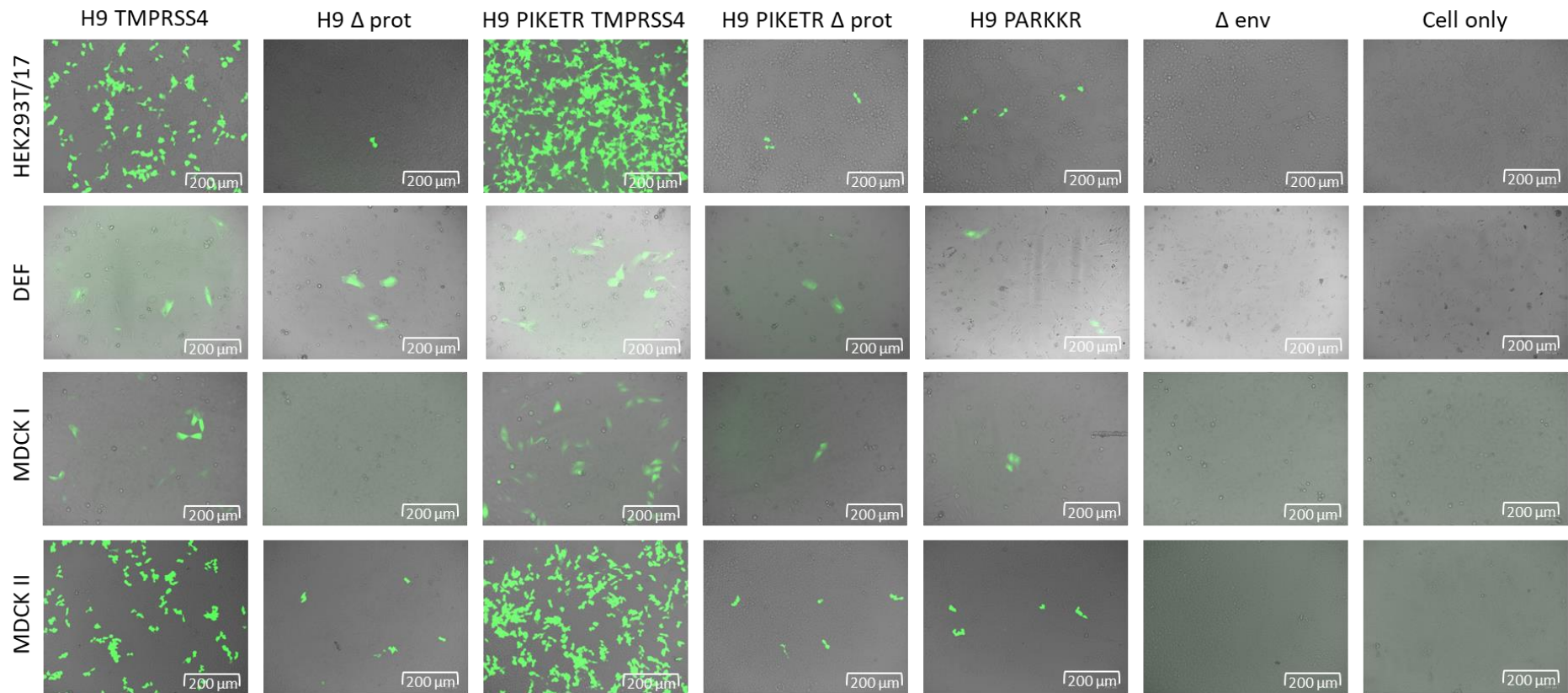
Appendix Figure 13: BLASTN tree. Nucleotide sequence alignment of WT Kz52 HA with H9 HA sequences on the NCBI database. The distance tree was created using the NCBI database BLAST® tool.

| Primer ID | Mutation | Primer sequence (5'to 3') |
|-----------------------------|----------------------------|--|
| Kz52 non CO PIKETR → PIKSTR | E337S | FW 5'-gcaattgctccgaaaagccccctgctcgatctggctgggacatttctcattcctagtgc-3' |
| | | Rev 5'-gcactaggaatgagaaatgtcccagccagatcgagcagggggcttttcggagcaattgc-3' |
| Kz52 CO PIKETR → PIKSTR | E337S | FW 5'-tggctccaaacaggccccgtgacgatctggcgggcacatttctcatgccag-3' |
| | | Rev 5'-ctgggcatgagaaatgtgcccgccagatcgtcacggggcctgtttggagcca-3' |
| Kz52 non CO PIKSTR → PARSSR | I335A, K336R, T338S | FW 5'-gctccgaaaagccccctgctcgatctggctgggacatttctcattcc-3' |
| | | Rev 5'-ggaatgagaaatgtcccagccagatcgagcagggggcttttcggagc-3' |
| Kz52 CO PIKSTR → PARSSR | I335A, K336R, T338S | FW 5'-ctccaaacaggccccgtgacgatctggcgggcacatttctcatgcc-3' |
| | | Rev 5'-ggcatgagaaatgtgcccgccagatcgtcacggggcctgtttggag-3' |
| H9 PARSSR → PIKETR | A334I, R335K, S336E, S337T | FW 5'-ccagctatggctccaaatagtctctagtctctttaataggcacgttctcagaccgactgccag-3' |
| | | Rev 5'-ctggcagtcggtctgaggaacgtgcctattaaagagactagaggactatttgagccatagctgg-3' |
| Kz52 non CO PARSSR → PARKKR | S337K, S338K | FW 5'-agcactaggaatgagaaatgtcccagccagaaaaaagagggggcttttcggag-3' |
| | | Rev 5'-ctccgaaaagccccctctttttctggctgggacatttctcattcctagtgc-3' |
| Kz52 CO PARSSR → PARKKR | S337K, S338K | FW 5'-ccctgggcatgagaaatgtgcccgccagaaaaaagcggggcctgtttgga-3' |
| | | Rev 5'-tccaaacaggccccgctttttctggcgggcacatttctcatgccaggg-3' |
| H9 PARSSR → PARKKR | S336K, S337K | FW 5'-gtcggctgaggaacgtgctgtagaaaaaagagaggactatttgag-3' |
| | | Rev 5'-ctccaaatagtcctctctttttctagcaggcacgttctcagaccgac-3' |

Appendix Table 5: Primers sequences used for SDM PCR (cleavage site). Primers for WT or CO Kz52 HA PIKETR to mutate first into PIKSTR, then into PARSSR; H9 HA PARSSR to mutate into PIKETR; WT and CO Kz52 HA and H9 HA monobasic cleavage site to mutate into polybasic cleavage site (PARKKR).

| Primer ID | Mutation | Primer sequence (5'to 3') |
|---------------------------|----------|---|
| Kz52 non CO GTCAAA→GCCACC | KOZAK | FW 5'-ccgggtacctctagaagatctgccaccatgtggaaactagcattagtaa-3' |
| | | Rev 5'-ttactaatgctagtttccacatggtggcagatcttctagaggtaccgg-3' |
| Kz52 CO GTCAAA→GCCACC | KOZAK | FW 5'-ttgacacgatcggatctgccaccatgtggaagctggcctc-3' |
| | | Rev 5'-gagggccagcttccacatggtggcagatccgatcgtgtcaa-3' |
| H9 GTCAAA→GCCACC | KOZAK | FW 5'-cccgggtacctctagaagatccgccaccatggaacaatatcactaataact-3' |
| | | Rev 5'-agttattagtgatattgtttccatggtggcggatcttctagaggtaccggg-3' |

Appendix Table 6: Primers sequences used for SDM PCR (Kozak sequence). Primers for WT and CO Kz52 HA and H9 HA to mutate the Kozak sequence originally designed (GTCAAA) into a general one (GCCACC).



Appendix Figure 14: Green HEK293T/17, DEF, MDCK I & II cells transduced with Influenza H9 PVs. A cell only control was included to examine the morphology of non-transduced target cells. Images were taken at 20x on ZOE™ Fluorescent Cell Imager after 48 hours the GFP titration was set up.